Foredune Blowout Sediment Transport: Event Scale Dynamics and Meso-Scale Geomorphic Change.

Nicholas James O'Keeffe

Thesis submitted to Edge Hill University in partial fulfilment of the requirements for the degree of Doctor of Philosophy

November 2021

Nicholas O'Keeffe

Presented for the degree of Doctor of Philosophy

Foredune Blowout Sediment Transport: Event Scale Dynamics and Meso-scale Geomorphic Change.

Abstract

Blowouts are dune landforms associated with high relative levels of sediment transport. Conceptual models of morphodynamics explain system behavior, through cross-shore transfers of energy and materials (Short and Hesp, 1982). Further, the seminal model of evolution, (Psuty, 1988) denotes beach-foredune sediment exchanges to be of paramount importance to meso-scale change. Therefore, foredune blowouts, recognised for heightened sediment transport activity, and located in a critical cross-shore position, may be landforms of particular significance. Whilst in a period of prolonged sea level rise, as coastal dunes act a natural buffer against storms and flooding, this thesis addresses the need for better understanding of foredune blowout transport events, and their implications to longer term evolution.

The research examines event scale airflow and transport dynamics at a foredune blowout location. Synchronous, high frequency airflow and instantaneous sediment transport were measured using ultra-sonic anemometry, and laser particle counters respectively. Meso-scale geomorphic change was assessed along a transgressive coastline which is characterised by frequent foredune blowouts, using a LiDAR time-series of an unprecedented duration (19 years).

Longshore transport across the foredune was identified as a principle pathway for sediment delivery to the blowout. At the landform scale, wind approach angle relative to foredune orientation, governed airflow enhancements within the blowout, which were a primary control on transport. The spatial clustering of trough sensors demonstrated an inverse relationship between wind speed and transport intensity. Sediment input from the far field and directional divergence of airflow and transport vectors exerted strong control on event dynamics. Novel analytical techniques are introduced which offer improvements to conventional methods.

At the meso-scale, foredune blowouts were confirmed to enhance the rates and magnitude of geomorphic change. Blowouts, formed and maintained by visitor pressure, made significant direct contributions to coastline recession and indirectly augment trends of retreat.

Keywords: Foredune, Blowout, Aeolian, Sediment Transport, Beach-Dune, Sediment Budget, LiDAR, Sefton.

Declaration: Publications

This thesis is written and presented in an unpublished manuscript format. Original interpretations, data processing, analyses, presentation, and writing was conducted by N O'Keeffe. Supervisors assisted with field data collection (Delgado-Fernandez and Jackson, short-term experiment) and/or editing the final drafts. Chapters are to be submitted as journal articles following the submission of the thesis.

The manuscript was solely prepared by N. O'Keeffe; I Delgado-Fernandez, Paul Aplin, and Derek Jackson provided guidance throughout the thesis.

Additional to conference presentations, the following publications are directly linked with this thesis:

DELGADO-FERNANDEZ, I., O'KEEFFE, N. and DAVIDSON-ARNOTT, R.G., 2019. Natural and human controls on dune vegetation cover and disturbance. *Science of the Total Environment.* (672) pp. 643-656.

RODGERS, S., O´KEEFFE, N. and DELGADO-FERNANDEZ, I., 2019. Factors affecting dune mobility in Newborough, Wales. In: DURÁN, R., GUILLÉN, J. and SIMARRO, G., (Eds.). Libro de Comunicaciones de las *X Jornadas de Geomorfología Litoral*, Sociedad Geológica de España. pp. 129. (Conference oral presentation accompanied this publication).

SANROMUALDO-COLLADO, A., O'KEEFFE, N., GALLEGO-FERNÁNDEZ, J.B., DELGADO-FERNANDEZ, I., MARTÍNEZ, M.L., HESP, P., FERRER-VLERO, N. and HERNANDEZ-CALVENTO, L., 2019. Resultados preliminares del análisis de relaciones entre variables ecológicas y sedimentológicas en la duna costera (foredune) de un sistema de dunas árido. In: DURÁN, R., GUILLÉN, J. and SIMARRO, G., (Eds.). Libro de Comunicaciones de las *X Jornadas de Geomorfología Litoral*, Sociedad Geológica de España. pp. 141.

Acknowledgements

I gratefully acknowledge my supervisory team and was fortunate to benefit from having three outstanding mentors; Professors Irene Delgado-Fernandez, Paul Aplin and Derek Jackson. Their knowledge, sage advice, and support throughout the preparation of this thesis has been invaluable. In particular, that of my Director of Studies, an inspirational scientist, and exceptional human being to boot. The endless enthusiasm afforded to the research by Irene, has been a continual source of energy at every step along the way.

I must further recognise the genuine togetherness of the aeolian and coastal research community. My development as a researcher has benefitted from much practical advice, fieldwork support, loans of equipment, frequent ‘pearls of wisdom’, and also even the occasional beer from colleagues. In this, I’m especially thankful to Nye O’Neil, Susana Costas, Thom Smyth, Robin Davidson-Arnott, Eugene Farrell, Colin Anderson, Chris Marston, Ruairí Flood, and Susan Rodgers. Additionally, the rigorous review and constructive criticism provided by Dr Kevin Lynch brought many welcome improvements to the final thesis.

In the moment, submission of the final thesis has the feel of being the last step of a long and eventful journey, (with a good few highs and lows). This sent the mind right back to the point of setting out. I remain indebted to Dr Nigel Richardson, who helped me take the very first step, in offering me a place on the undergraduate Geography degree course at Edge Hill, and has continued to be supportive right through to the final stages of the PhD.

Above all else, I am deeply grateful to my parents. Reaching this point would not have been possible without their limitless love, unwavering support, and great patience throughout the journey.

CHAPTER 3 – STATISTICAL RELATIONSHIPS BETWEEN SEDIMENT TRANSPORT AND WIND FORCING UNDER COMPLEX AIRFLOW SCENARIOS.

CHAPTER 4 – MESO-SCALE GEOMORPHIC CHANGE AT A RETREATING COASTLINE IN THE PRESENCE OF FOREDUNE BLOWOUTS.

List of figures

List of tables

CHAPTER 1 – INTRODUCTION

1.1. Scientific context of the thesis.

Whilst this thesis contains elements which touch on a number of geographical disciplines, geomorphology is the principle field of study in which the research is positioned, (a branch of physical geography). The etymology of *geomorphology* remains useful in summarising the substance of the discipline. The name can be broken down into three components of ancient Greek origin: γεω or *geo* (the Earth), μορφή or *morph* (form), and λογία or *ology* (the scientific study, or discourse of). Allaby (2020, p.196) defines the discipline as the "scientific study of the land-forms on the Earth's surface and of the processes that have fashioned them". Although initially specific to the land surface of the Earth, many scholars now consider geomorphology in its broadest sense to also encompass the study of both submarine, and inter-planetary landforms (Huggett, 2017).

1.1.2. Fundamentals of geomorphology.

Regardless of the many sub-disciplines in existence, there is an accepted consensus that in its simplest form, geomorphology is the study of landforms. Individually, landforms can be described as discrete features, or geomorphic units, on the Earth's surface. They are typically classified, or delimited by various physical attributes of their surface form, and sometimes alternatively, or additionally, by their location in association with surrounding units of the continual land surface (Gregory and Lewin, 2014, p.31). They exist within a hierarchy of diverse spatial scales, from small ripples on a sandy surface, and features of comparable scale, right up to 'continental' sized mountain ranges or plateaux (Evans, 2012).

In geomorphology, the word landscape is typically used as a collective noun. As individual landforms exist within the landscape, and in often defining landforms as geomorphic ‘units’, it follows that the term landscape can be thought of as a larger scale entity, or whole, composed of any number of landforms. The landscape can therefore be considered as a system, with Kemp (1998, p.391) defining a system being ‘an assemblage of interrelated objects organised as an integrated whole’. Thus, landforms are the building blocks of landscape systems (Gregory and Lewin, 2014, p.33). Following early seminal works within the discipline (Strahler, 1950, 1952, 1980; Chorley, 1962), adoption of a systems approach is now deeply rooted in geomorphological landscape studies.

Irrespective of any specific type or classification, an individual landform, or landscape system, can be described as the product of two factors; 1) the geo-materials of which it is composed, and 2) the morphological processes which are acting upon it (Ahnert, 1998; Huggett, 2017). Beyond this, the three primary morphological processes which shape the land surface are weathering, erosion and deposition. Slaymaker (2009) identified a number of key themes into which all geomorphological works typically fall. The research presented here includes elements of three of these themes, namely;

1) Process-form response, in the case of this thesis, based principally in physics.

2) Characterisation of landforms, or systems of landforms, grounded in geo-spatial science.

3) Landform or landscape evolution over time.

The landforms upon which this thesis is focused are *foredune blowouts,* and the landscape systems of which they form a component part, are *coastal dunes*.

Aeolian Geomorphology and Coastal Geomorphology are the two branches of the discipline in which the research is primarily positioned.

1.1.3. Importance of the coast and coastal research

For a multitude of reasons, and since the beginning of civilisation, populations throughout the world have chosen to establish settlements at the coast. An accurate assessment of the current global population which lives within the coastal zone is in itself a challenge, not least because the number is highly dynamic, it varies with the method of quantification, and is also dependent on the chosen definition of 'coastal'. Martínez, *et al.* (2007) estimated that 41% of the world's population currently live within 100km of the coast. In addition to the absolute number, coastal zones often also exhibit relatively high population densities. Of the current 31 global *megacities*, 20 are located at the coast (Brown, *et al.* 2013), and with this, so too are relatively higher levels of infrastructure and economic assets. Beyond the considerable total numbers, coastal populations are also experiencing rapid and disproportionate growth (Small and Nicholls, 2003). Between 1992 -2005, the world's coastal population grew by 56%, significantly higher than the global population growth rate of just 14% (Hattam, *et al.* 2010).

Whilst there are many socio-economic benefits linked both to settlement at the coast, and commercial development of it, a number natural hazards associated with coastal zones are persistent. Perhaps the most acknowledged are coastal flooding, coastal storms, and coastal erosion (Keller, *et al.* 2019; Masselink, 2012). As a result of climate change induced, global warming, it is believed these hazards are being exacerbated. For over a century, the Earth has been experiencing an extended period of SLR (sea level rise), with approximately a third of the total rise occurring over the last three decades (Lindsey, 2021). Accelerated SLR over recent decades is largely attributed to the combined effects of thermal expansion

of the oceans, together with increased ice loss in Greenland (Frederiske, *et al*. 2020). This well documented SLR is of course bringing about relative increases in coastal flooding.

Additionally, although the melting of polar ice also leads to relative global increases in atmospheric water vapour, (a factor of relevance to storm genesis, storm severity, and influential to macro-weather systems), the case that climate change is leading to enhanced storminess is currently less well substantiated and certain (e.g., Haarsma, *et al*. 2013; Feser, *et al*. 2014; Sun, *et al*. 2017; Rädler, *et al*. 2019). Regardless of this ongoing debate, it is clear that even if only considering a rising but 'planar' sea level, coastal flooding is increasing in frequency, as are the magnitude of its impacts (e.g., Vitousek, *et al*. 2017; Taherkhani, *et al*. 2020).

Sustained, incremental rises to mean sea have long been recognised to be a cause of coastal erosion (Bruun, 1962), and during the 20th century, over two-thirds of coastlines globally are identified as having been experiencing erosion (Bird, 1985). Over the past three decades, Mentaschi, *et al*. (2018) quantified the global land area lost to coastal erosion to be more than double the land surface gained via accretion, and that this trend is likely to be accelerated in line with the estimated trend in global warming. SLR for the current century varies dependent on GHG (Green House Gas) emissions but is projected to be significant, and 44% of experts forecast it to be in excess of 1 m, by 2100 (Horton, *et al*. 2020). This coincidence of increasing coastal hazards, and concentrations of people in the coastal zone presents many challenges to mankind. Kirezci, *et al*. (2020) offer the wholly plausible suggestion that by 2100, 52% of the Earth's population, and 46% of its assets, will be at risk of flooding. Concerns such as these are a leading

motivation for the continued growth in coastal related research over the past century.

1.2.1. Coastal environments and beach-dune systems

Coastal systems in their entirety are considered the most dynamic zones of the planet, bringing together the processes of the Earth's four major spheres; the hydrosphere, the lithosphere, the atmosphere, and the biosphere (Davidson-Arnott, *et al*. 2019). Geographical location, geological setting, natural processes, and anthropogenic activities all combine to result in a great diversity of coastlines worldwide. This research focuses on 'soft', sedimentary coastlines, comprising sandy beaches and dunes. Of primary interest are aeolian (wind driven) processes operating in close proximity to the beach-dune interface, and the morphological form of the coastal dune system over time. Of all the Earth's geo-materials, sand, due to its granular, porous, and frequently loose structure, is perhaps the least stable (Nickling, 1994). As a result, landscapes comprised primarily of sand, experience heightened levels of morphological change, and are typically more responsive to the physical processes acting upon them, relative to landscapes composed of more stable materials (Ahnert, 1998). Further, levels of geomorphic processes in coastal zones typically exhibit great diversity, and much higher relative frequencies, and magnitudes, than for non-coastal environments. As a consequence of this, compression of meanings associated with spatio-temporal scale related terminology is customary in coastal studies, if compared to other geomorphological disciplines (Sherman, 1995). For example, whilst for other environments, 'meso-scale' may be considered most appropriately measured in centuries, time units of decades better represent the 'coastal' understanding of the term (Walker, *et al*. 2017).

Beach-dune systems have long been valued for their function as a natural and mobile, protective buffer against SLR, storms, and coastal flooding (Nordstrom, *et al*. 1990; Carter, *et al*. 1992; Masselink, *et al*. 2011; Anthony, 2013). Given the outlined implications of climate change on coastal hazards, there exists a growing need to better understand the geomorphic processes operating, and the strongly coupled responses in form, occurring within these environments. Beyond their morphological and protective function, coastal dune systems are also frequently of high ecological, economic, and recreational value (Delgado-Fernandez, *et al*. 2019b).

1.2.2. Coastal Dunes

In geomorphological terminology, sand dunes fall under a category of landform known as *bedforms*. A bedform being the shape of the surface of a bed of granular sediment, produced by fluid flow over the sediment (Allaby, 2020, p.48). In plain language, dunes can be described as ‘mound’ or ‘ridge’ shaped accumulations of sand. Although not exclusively, the vast majority of dune landforms are *aeolian* in nature, having been formed by *wind action*. Their fundamental existence depends on the erosion, transport, and deposition of sand by the wind. Dunes form in locations where sand is deposited due to flow having insufficient energy to maintain transport. Dune initiation, and subsequent growth, at any specific location is the result of the deposition of sediment exceeding that which is eroded. The physical barrier they present to fluid flow, often also creates a positive feedback by promoting further deposition of sediment, and thus further growth.

The formation of any sand dune is dependent on two key requirements. An ample supply of sediment, and a wind regime capable of sediment transport. Categorisation as coastal relates solely to their geographic location. Most often, coastal dune formation is strongly associated with vegetation, however examples

can be found where un-vegetated dunes occur at the land-sea boundary (e.g. La Guajira, Caribbean coast of Colombia; Atlantic coast of Namibian Desert). Due to the requirement for a sufficient supply of sediment, extensive coastal dune systems are most frequent in locations adjacent to previously glaciated areas, in proximity to river outlets, or downwind of large ocean basins, as environments such as these are typically sediment rich in character (Masselink, *et al*. 2011, p.267).

An endless diversity of local conditions may contribute to coastal dune formation at any individual site. What follows here is the basic but most commonplace mechanisms leading to coastal dune development. Countless similar examples can be found across a multitude of texts (e.g., Masselink, *et al*. 2011; Haslett, 2016; Davidson-Arnott, *et al*. 2019).

1.2.3. Coastal dune initiation/growth

Initially, tidal currents and/or wave action deliver sediment from the nearshore to the beach face. Accumulations of this sediment may manifest as a single, back-beach berm, or as is often the case, become organised into the form of, quasi-shore parallel, intertidal bars on the beach face. The sporadic landward migration of these bars introduces sediment to the back-beach area, which then becomes available for aeolian transport. When dry beach sediments are exposed to wind action of sufficient energy, typically but not exclusively onshore, sand will become entrained by airflow, and transported landwards.

Subsequent to this, and typically just landward of the reach of normal wave action, pioneer vegetation colonising the back-beach area will remove or ‘trap’ sediment from airflow, or reduce flow to below the velocity required for transport to be maintained, resulting in sediment deposition, and embryo dune formation (small

scale mounds of sand associated with patches of vegetation). As vegetation grows, and further sand is introduced, these features may coalesce to develop into foredunes, often in the form of linear ridges, and frequently orientated broadly parallel to the coast. To varying degrees, the composition, and coverage of vegetation present, will fix this sediment in place by reducing susceptibility of the foredune surface to erosion. Ultimately, the changing morphology of the dune system will depend on the spatio-temporal variability of sediment input by deposition, and sediment output by erosion. Coverage of the evolution of beach-dune systems in greater detail, and including prominent conceptual models within the discipline are returned to in section 1.6.

1.3. Aeolian processes

The word *aeolian* is derived from Aeolus, the 'keeper of the winds' in Greek mythology, and aeolian processes and landforms are the focus of this research (Leeming, 2006, p.2). *Aeolian* means anything relating to, or arising from, the action of the wind. Dunlop (2008, p.103) describes wind as the movement of air across the surface of the Earth, with this being the result primarily of horizontal pressure gradients associated with regional variability in atmospheric air pressure. The basic aeolian processes that give rise to geomorphic responses in the form of dune environments are erosion, sediment transport, and deposition.

1.3.1. Wind erosion and sediment transport

Wind erosion of sand from the land surface, (sometimes termed *deflation*) is complex, and influenced by a plethora of environmental conditions. Before expanding on some of the potential additional factors of most relevance in coastal settings, it is worth considering the fundamental principles of aeolian sediment transport in their simplest form. The erosion of an individual sand grain from the land surface into airflow, (or its *entrainment*), occurs when the forces exerted on

the grain promoting movement, exceed those resisting it. *Shear stress* is the 'movement promoting' force the surface is subjected to, which imparts both drag and lift forces onto individual grains. The forces resisting movement are gravity, and any cohesion which exists between grains at the surface. The point of entrainment, at which forces promoting movement exceed those resisting, is often termed the *threshold velocity*. This comes from the fact that shear stress at the bed is problematic to measure, but through experiment, for known grain sizes and densities, shear stress can be related to wind velocity at a specified height above the bed (Livingstone and Warren, 1996).

1.3.2. Modes of aeolian sediment transport

There are four main classes of aeolian sediment transport; creep, suspension, saltation and retaption, (or modified saltation). In beach-dune locations, primarily composed of medium-fine grained sand, saltation is the dominant mode of transport. Creep involves the downwind motion of particles, which largely remain in contact with the bed. Suspension, as the name implies involves the transport of grains suspended in airflow, which are seldom in contact with the bed. Whilst suspension is a very common mode of sediment transport in water, as water has a fluid density approximately 1000 times greater than air, air is far less capable of entraining sediment, and maintaining transport in this way. This difference in fluid density means that the specific density of grains in aeolian transport are more than three orders of magnitude greater than those in water (Bauer, *et al*. 2013). As a result, in sandy environments, aeolian transport via suspension is infrequent, and saltation is dominant. Aeolian transport via suspension most typically relates to sediment sizes much finer than sand, and is therefore rare in beach-dune settings.

Saltation describes the aeolian transport of sediment in which particles follow a 'hopping' motion. Grains are lifted vertically from the surface, and then propelled

downwind in airflow. Individual grains then follow ballistic trajectories for between just a few centimetres, up to several metres, with gravity providing the downward force for grains to return to the surface. The length of each saltation trajectory is controlled by a number of factors, most notably grain size, grain density, wind speed, and the height of initial lift from the bed (Davidson-Arnott, *et al*. 2019). This saltation process also introduces a positive feedback into the transport regime. As saltating grains return to the bed at some point downwind, their impact can result in further grains being ejected into airflow. As momentum from impacting grains is transferred to the surface, in addition to wind related shear stress, the threshold velocity to initiate further grains into motion is lower. This kinetic energy within the transport system effectively means that relatively lower wind velocities are required for the maintenance of transport, in comparison to initiation. It is estimated that the impact threshold to entrain grains via this mechanism is approximately 80% that of the initial flow velocity threshold (Livingstone and Warren, 1996; Masselink, *et al*. 2011).

The final mode of aeolian transport, retaption, (or alternatively, modified saltation), refers to grains ejected from the surface in a splash like motion via grain impact. Retapting grains typically make much shorter hops that those in saltation, and their direction is less influenced by near surface wind direction (Davidson-Arnott, *et al*. 2019). Although the vector of grains ejected from the surface via retaption may be in any direction, influence of the near surface wind direction will produce a downwind tendency to varying degrees.

1.3.3. Factors influencing transport

Potential factors which may influence aeolian sediment transport, are vast in number. Comprehensive coverage of research concerning these factors is beyond the scope of this review, not least because strong inter-dependencies exist

between many, and the nature of how any number of these variables can combine, gives rise to a multitude of complex effects. Many of these effects are yet to be fully understood. Although considerable overlap exists, they can be broadly split into those relating to the wind, those to the sediment, and those to the surface. A concise summary covering factors considered to be of most importance follows. The relative importance of contributing factors at foredune blowout locations is considered in the research chapters to follow).

1.3.3.1. Wind properties

Speed is a fundamental property of the wind which exerts a strong control on aeolian sediment transport. In idealised conditions of a level, dry, sandy surface, a strong positive relationship exists between wind speed and sediment transport, with increasing wind speed resulting in higher magnitude transport. As surface shear stress is a function of wind velocity, the threshold for sediment transport is often expressed in terms of a wind velocity at some height above the bed. Of the many deterministic models for aeolian transport, wind speed together with grain size and density are largely the most influential variables on the rate of transport (e.g. Bagnold, 1941; Chapman, 1990; Anderson, *et al*. 1991; McEwan and Willets, 1994; Sherman, *et al*. 1996; Sherman, *et al*. 2013; Baas, *et al*. 2020).

Although not incorporated into deterministic transport models, for many decades, turbulence within wind flow has been known to be a critical wind property of influence to aeolian sediment transport (Jackson, 1976; Grass, 1983). Turbulence can be described as the degree to which airflow across a surface deviates from laminar fluid flow. In addition to the inherent gustiness of the wind, the general frictional drag associated with the co-planar flow of wind over the land surface (Kline, *et al*. 1967; Livingstone and Warren, 1996), together with slope (Sweet and

Kocurek, 1990; Sherman, *et al*. 1996), topographic complexity or variance (Walker and Nickling, 2002; Lynch, *et al*. 2010; Bauer, *et al*. 2013), and the presence of vegetation (Sterk, *et al*. 1998; Mayaud, *et al*. 2016; Walker, *et al*. 2006), or anthropogenic structures/obstacles (Garcia-Romero, *et al*. 2019; Grilliot, *et al*. 2019), are common surface related factors which can increase turbulence in wind flow.

In beach-dune environments, bursts of sediment transport typically manifest, and can be visually observed as episodic, sinuous, near-surface, saltation 'clouds', termed *streamers*. Although strongly associated with turbulence in boundary layer airflow (Baas and Sherman, 2005; Baas, 2006; Caneiro, *et al*. 2015; Huang, 2020), the chaotic nature of these structures are yet to be fully resolved. Whilst traditionally, relationships between wind speed and saltation remain standard practice, it has been found that measures of high frequency aeolian transport can sometimes be more strongly associated with those of high frequency turbulence (Smyth, *et al*. 2014). Turbulence within airflow has also been used to explain the maintenance of sediment transport at below threshold velocity wind speeds, such as in the windward area of the dune toe, which is characteristically a zone of flow stagnation (Wiggs, *et al*. 1996; Chapman, *et al*. 2013).

Finally on wind parameters which may contribute to levels of transport, the density of air is a factor incorporated into most aeolian sediment transport models. Atmospheric temperature, pressure, and humidity, can all influence air density, and thus transport capacity. As air expands, and so its density decreases with relative increases in temperature, cooler air is more efficient in sediment transport than warmer air (Masselink, *et al*. 2011, p.280).

1.3.3.2. Sediment Characteristics

Grain size and grain density are the two sediment related factors of greatest importance to aeolian transport. As entrainment occurs when the forces promoting movement exceed those resisting it, grain size in combination with density are both functions of the gravitational force resisting movement, they directly contribute to threshold velocity, and thus play a fundamental role in the occurrence of transport (Sherman and Hotta, 1990). Sediment mineralogy therefore, also has influence on transport through controlling density. On entrainment, grain size will also strongly influence the nature of transport as relatively finer grains are both lifted higher from the surface, and fall slower, resulting in their ballistic trajectories during saltation being of greater relevant distances (Arens, *et al*. 2002).

The fluid density of water is orders of magnitude greater than that of air. As a result, airflow is much less transport capable fluid flow than water, and therefore aeolian transport is far more selective in terms of grain size (Davidson-Arnott, *et al*. 2019). This selectivity in entrainment, and that grain size variability influences saltation trajectory distances, are two important factors which contribute to aeolian sediments being characteristically well sorted in comparison to those deposited by other fluids (Blott and Pye, 2001; Masselink, *et al*. 2011). In coastal environments it also contributes to the commonplace trends of grain size becoming finer, and the degree of sediment sorting increasing, moving landwards along a cross-shore beach-dune profile (e.g., Aduodha, 2003; Preoteasa and Vespremeaunu-Stroe, 2010).

This great disparity between the fluid density of air and water contributes to saltation being the principal mode of aeolian transport, rather than suspension, which is far more commonplace in water. In water, whilst the speed of sediment in suspension closely mirrors that of the fluid flow, the speed of grains in saltation,

following ballistic trajectories, is markedly lower than that of the airflow. This has the effect of grains in transport extracting momentum from the fluid flow of air. Relatively coarser grain sizes are known to have greater influence on fluid flow during saltation 'hops', through this mechanism, and additionally have an increased influence on the magnitude of retaption due to higher grain impacts (McEwan and Willetts, 1994; Dong, *et al*. 2003). The 'drag' influence on airflow of saltating, or retapting grains, through extraction of momentum, is positively correlated with grain size. As both processes occur in the very near-surface, their effects can also create sharp gradients in the vertical wind profile. Bauer, *et al*. (2013) theorised that this in itself may be sufficient to initiate secondary, turbulent structures within airflow. That grain size has the potential to modify fluid forcing, and thus also the transport regime, provides a useful example of the complexity of the system, and the strong inter-dependencies of many factors which may influence the nature of aeolian transport.

Beyond directly impacting the fundamental physics of aeolian transport, in both natural settings, and idealised wind tunnel environments, grain size introduces multiple indirect consequences to aeolian processes. Grain size relationships which concern the presence of surface moisture, or vegetation are of greatest significance, as both are typically major inhibitors of sediment transport. In coastal locations, the inter-tidal beach is the principle source of sediment for landward dune fields. In exerting a primary control on porosity and permeability, grain size strongly influences beach surface moisture content, and also the rate at which the beach surface dries out on becoming exposed by a receding tide (Jackson and Nordstrom, 1997; Davidson-Arnott, *et al*. 2005; Baas and Sherman, 2006; Anthony, *et al*. 2009). Spatial variability in grain size has also been recognised to be a controlling factor on the distribution, composition, and structure of coastal

vegetation (Musila, 1998; Bertoni, *et al*. 2014), all of which can significantly impact aeolian processes.

Finally in relation to sediment, although secondary to grain size, the surface texture, and the shape of individual grains, are two important characteristics recognised as contributing to transport dynamics. Both factors have the capacity to influence cohesion between grains on the surface. Additionally, during transport, these characteristics have been found to exert control on ballistic trajectories, time in flight (or settling velocities), and the frequency of collisions between saltating grains (e.g. Williams, 1964; Willetts, *et al*. 1982; Mazzullo, *et al*. 1986; Farrell and Sherman, 2015).

1.3.3.3. Surface properties

The most frequent and fundamental surface related factors which influence aeolian sediment transport can be broadly catagorised as those relating to, surface form, surface moisture, and surface vegetation.

1.3.3.4. Surface form

Aeolian sediment transport is dependent on a threshold in critical shear stress being exceeded, and is therefore strongly associated with airflow parameters, primarily wind speed. Even over an idealised, near-planar, and aerodynamically smooth terrain, the land surface imparts a frictional drag on airflow, reducing its speed. The lowest vertical portion of the regional wind field, where flow is modified through interaction with the surface is termed the *boundary layer*, and typically exhibits a wind speed profile where flow is slowest nearest the surface, and increases with elevation (Davidson-Arnold, *et al*. 2019). Airflow modifications within this boundary layer increase with surface complexity. In a beach-dune environment, perhaps two of the simplest examples of divergence from an

idealised surface, are beach slope, and beach surface roughness, (associated with grain size variability). Relative increases in either of these parameters imparts a greater resistance to airflow, thus reducing wind speed, and likely also increasing turbulence (Sherman and Bauer, 1993). Short and Hesp (1982) identified three static-state beach typologies as being dissipative, intermediary, and reflective. With dissipative beaches being characterised as generally wider, flatter, and composed of finer sediment, they have the greatest potential for aeolian transport. Irrespective of their greater availability of sediment, their finer grain size has a lower critical shear stress threshold, and near surface winds speeds experience less surface slope, or roughness induced deceleration of flow. Conversely, at the opposite end of the spectrum, the steeper profile, and most often, coarser sediment of reflective beaches, retard wind speeds to a greater extent, in addition to their coarser sediment also directly raising the shear stress threshold for entrainment (Short and Hesp, 1982; Sherman and Bauer, 1993). These seminal works concerning beach-dune and cross-shore categorisations are expanded on in section 1.6, in relation to characterising the nature of beach-dune interactions and morphodynamics.

‘Soft’ coastlines are characterised by pronounced levels of landscape dynamism. The frequent occurrence of processes capable of geomorphic work, together with their sedimentary composition, give rise to continual responses in form, even over the shortest of temporal scales (King, 1972; Haslett, 2016). Beach-dune landscapes comprise a high diversity of landforms, which exist across a wide range of nested, spatial scales. The nature of discrete landscape components range from ephemeral to quasi-permanent, with their stability in form, and/or residence time normally being positively correlated with their spatial scale (Sherman, 1995; Walker, *et al*. 2017). At the micro, spatial and temporal scales, sand ripples are undoubtedly the most ubiquitous of bedforms in beach-dune

systems, and most other aeolian landscapes. In creating minor modifications to near surface airflow, micro-topography such as ripples are frequently cited as a cause for high spatio-temporal variability in aeolian sediment transport (e.g., Baas and Sherman, 2005; Nield and Wiggs, 2011).

As coastal dune systems are frequently associated with extensive beaches, their coincidence with relatively wider inter-tidal beaches is frequent. The occurrence of 'ridge and runnel' (or alternatively termed, 'bar and trough') topography on such beaches is commonplace (Biausque, *et al*. 2020). With the amplitude in relief from trough minimum, to bar crest maximum sometimes being as much as 1.5 m, such topographic variability has the potential to exert significant variability to cross-shore boundary layer flow, and thus impact sediment transport (Masselink and Anthony, 2001). In addition to increasing the purely topographic influence on airflow, these bedforms typically exhibit marked variability in grain size (e.g. Thornton, *et al*. 1996; Gunaratna, *et al*. 2019), thus also adding potentially to the aerodynamic roughness of the surface, to further impact flow, and therefore transport. The most documented impact of bar and trough bedforms however, comes from the strong association of topographic variability with moisture, to be detailed in section 1.3.3.5.

A significant body of research concerning interactions between airflow and complex dune topography is to be summarised in section 1.4.4. (on 'secondary airflow'). For now, the topographic modification to flow and thus sediment transport, which is arguably of greatest consequence, occurs at what is typically the most pronounced change in relief in the cross-shore profile of a beach-dune system, the interface of these two sub-units. Embryo dune formation is most often associated with increased roughness and/or sediment trapping, at the landward extent of the back-beach, in association with vegetation or beach debris (e.g.,

Bauer, *et al*. 1990; Arens, 1996; Hesp, 1999; Nordstrom, *et al*. 2011; Grilliot, *et al*. 2019). A positive feedback is recognised to occur here, as increased topographic roughness extracts momentum from flow, thereby inducing sediment deposition. The increasing slope gradient associated with this deposition causes further flow stagnation, to then promote further deposition as a consequence (Davidson-Arnold, *et al*. 2019).

1.3.3.5. Surface Moisture

In coastal environments, moisture is recognised to often be a dominant control on aeolian sediment transport. Capillary water in surficial sediment produces a strong tension force between grains, increasing the forces resisting movement, the shear stress threshold for entrainment, and thus the critical shear wind velocity required to initiate transport (Belly, 1964; Fecan, *et al*. 1999). A substantial body of research exists concerning the influence of surface moisture on transport, and a number of studies have sought to incorporate its effect within aeolian sediment flux models (e.g., Hotta, *et al*. 1984; McKenna-Neuman and Nickling, 1989; Cornelis, *et al*. 2004). Wiggs, *et al*. (2004) determined that surface moistures levels of just ≈5 per cent can be sufficient to completely inhibit entrainment.

Whilst precipitation is an important consideration in temperate climates, the effects of continual submergence/exposure of the inter-tidal beach by tidal water has received frequent attention. In such environments, surface water typically exhibits high spatio-temporal variability, which along with grain size variability, and micro-topography is considered one of the primary factors reflected in the high spatio-temporal variability of beach sediment transport (e.g., Davidson-Arnott, *et al*. 2003; Baas and Sherman, 2005, 2006). A multitude of factors can combine to influence the rate at which the inter-tidal beach surface dries following the recession of tidal waters, and the inherent variability within this drying process. Wind speed, wind

steadiness, wind direction, grain size variability, air temperature, relative humidity, sediment compaction, antecedent moisture conditions, and beach topography offer a non-exhaustive list of examples (e.g., Sherman, *et al*. 1996; Jackson and Nordstrom, 1997; Davidson-Arnott, *et al*. 2003; 2005; Wiggs, *et al*. 2004; Yang and Davidson-Arnott, 2005; Bauer, *et al*. 2009; Anthony, *et al*. 2009; Delgado-Fernandez and Davidson-Arnott, 2009; 2011; Nield, *et al*. 2011). Although a rarity, occasional field studies include examples of moisture presence, sometimes enhancing transport. Nield and Wiggs (2011), for instance noted that harder surfaces, associated with higher relative moisture content, can induce greater saltation heights and distances, particularly during high intensity transport events.

Fetch distance is a well acknowledged factor controlling sediment transport, particularly so for beach-dune systems which encompass bar and trough topography, across the inter-tidal zone. Here, fetch refers to the continuous length of surface, saltation can occur across uninterrupted. Minimum fetch distance thresholds exist in order that airflow may become fully saturated by saltating grains, with these distances varying due to factors such as fluid forcing, grain size, moisture, and surface topography (Chepil and Milne, 1939; Davidson-Arnott and Law, 1990; Masselink, *et al*, 2011). Beach troughs, within a barred, inter-tidal system, vary in drying time, and can in many instances, also remain partially, or completely submerged for the full duration of tidal cycles. These moist, or submerged surfaces may completely inhibit aeolian transport, or result in saltation being highly intermittent over the cross-shore beach profile. Whilst sediment characteristics and beach topography are important controlling variables in the occurrence of such events, the presence of moisture is the dominant factor which prevents or disrupts aeolian transport, with such systems being described as ‘fetch-limited’.

Coastline orientation and wind direction can therefore have significant impacts on the extent to which beach transport is 'fetch-limited', with increasing obliquity of the wind approach angle, away from shore normal, typically resulting in marked increases in sediment flux (Udo, *et al*. 2008; Bauer, *et al*. 2012). Beyond this impact of moisture during individual transport events, as sediment supply from the back-beach is a fundamental control on the evolution of coastal dunes, the cumulative effect of this impact can be considerable. Multiple papers have sought to incorporate beach moisture effects on the medium to longer term evolution of dune fringed coasts, and also highlighted that this makes the dune sediment supply highly non-linear, thus prohibiting accurate modelling, or the up-scaling of measured transport events (e.g., Aagaard, *et al*. 2004; Anthony, *et al*. 2009; Houser, 2009; Delgado-Fernandez and Davidson-Arnott, 2009; 2011; Miot da Silva and Hesp, 2010).

1.3.3.6. Surface Vegetation

There are two principle mechanisms by which the physical presence of surface vegetation has a considerable direct consequence to sediment in transport. Firstly, vegetation cover itself provides a protective barrier between surficial sediment and fluid flow, in addition to typically having a binding effect, thereby increasing cohesion between adjacent surface grains (Dupont, *et al*. 2014). Both of these factors reduce the erodibility of the surface by increasing the forces resisting movement, and thus increase the critical shear stress threshold required for entrainment (Chepil and Woodruffe, 1963; Hesp, 1981; Wolfe and Nickling, 1993). Secondly, during periods of aeolian transport activity, vegetation obstructs the transport vector of saltating grains, and directly 'traps' sediment, removing it from airflow (Hesp, 1989; Suter-Burri, *et al*. 2013; Lindell, *et al*. 2017).

Indirectly, vegetation has the capacity to induce substantial modifications to airflow. Predominately, vegetation protruding from the ground surface into the lower boundary layer may increase surface roughness and extract momentum from the wind to cause flow stagnation. This may serve to decelerate flow to below the threshold velocity required to initiate transport, or equally reduce it to a velocity insufficient for the maintenance of saltating grains in motion, resulting in deposition (Pye, 1983; Hesp, 2002). The composition and structure of surface vegetation are important factors with regard to the nature of flow modifications, as they control vegetation density, and therefore the porosity of vegetation by airflow (Hesp, 1983; 1989; Sherman and Hotta, 1990). The nature of boundary layer flow modifications are complex and multi-variant dependent. Although considerable attention has been paid to relationships between vegetation structure, distribution, plant type, underlying topography, wind speed, turbulence, and direction, a much wider evidence base is required to fully resolve biological factors impacting aeolian transport (Walker, *et al*. 2006; Davidson-Arnott, *et al*. 2012; Bauer, *et al*. 2012). At present, density of the vegetation canopy is considered to be a primary factor, as porosity exerts control on the degree to which the turbulent inner boundary layer is displaced vertically, relative to momentum extraction from 'bleed' flow passing through the canopy (Dong, *et al.* 2008). In the case of low porosity canopies, the nature of secondary flow modifications, such as near surface turbulence, flow stagnation, compression or separation are strongly controlled by the geometry of vegetation assemblages (e.g. Hesp, 1983; Walker, *et al*. 2006; Hesp and Smyth, 2017).

Two positive feedback mechanisms related to aeolian sedimentation in association with vegetation are of particular consequence to beach-dune systems. Firstly, in addition to vegetation inducing deceleration of the wind, the resultant deposition increases relief to then cause further flow stagnation, and enhance further

deposition. This process is most often reflected in the development of incipient foredunes at the beach-dune interface (Arens, 1996; Sarre, 1989; Hesp, 1989; 2002; Luna, *et al*. 2011; Keijsers*, et al*. 2015). Secondly, the most seaward extent of the dune field is typically colonised by particularly hardy, or saline tolerant, vegetation pioneer species. A number of these species thrive on burial, with sedimentation accelerating plant growth to promote further, enhanced levels of deposition (Hesp, 1991; Maun, 1994).

The absence, existence, and nature of vegetation at coastal dune systems is strongly linked with the presence of moisture. At greater spatial scales, (regional or continental), climatic conditions, in combination with vegetation, play an important role in controlling the behavior, and evolution of dune systems, (which are discussed further in section 1.6.3.).

1.4. Deterministic models: Aeolian sediment transport and landscape evolution.

In its simplest form, the mechanics of aeolian sediment transport is rooted in classic Newtonian physics. The occurrence, or not, of entrainment is governed by Newton's first law of motion, or more appropriately, of 'inertia', (this being fundamentally comparable with the theories of Galileo). These principles determine that an object will remain at rest, or continue to be in motion at a constant speed and direction, unless a force is exerted upon it. As mass is essentially a measure of inertia, grain size together with density can be directly related to the motion promoting force necessary to initiate movement (Chatterjee, 2013). In attempting to understand this process, and to explain levels of transport, a British army officer, Ralph Bagnold, laid down the foundations to which almost all modern aeolian research refers back. His seminal work, *The Physics of Blown Sand,* provided and explained what remains the benchmark equation for sediment

mass flux, which bases transport levels on a critical shear stress at the surface, which in turn can be related to wind velocities at given heights above the surface (Bagnold, 1941). The model of Bagnold is rooted in the findings of von Karman's (1931) fluid dynamics 'Law of the Wall' theories, concerning boundary layer flow. These theories determined that the vertical velocity profile of non-laminar fluid flow, could be explained by the logarithmic distance of a given height to the 'wall', (in the case of airflow, the ground surface).

Fueled by the motivation of being able to explain historic, or forecast the future evolution of sedimentary landscapes, extensive work has been devoted to the subject of aeolian sediment mass flux models over the past century. With this, multiple alternative, or preferential models to that of Bagnold have been proposed (e.g., Kawamura, 1951; Zingg, 1953; Owen, 1964; Hsu, 1971). The most frequent feature of such deterministic equations is to express proportional relationships between sediment mass flux, and the cube of wind shear velocity (Baas, *et al*. 2020). Whilst the most elementary models are based on idealised conditions, of dry, level surfaces composed of homogenous sediment, numerous developments have sought to introduce, and parameterise important additional factors. Examples include threshold velocity, slope, and moisture (e.g., Belly, 1964; Lettau and Lettau, 1977; Hotta, et al. 1984). Beyond the models themselves, studies concerning their theoretical or numerical structure, the testing of their results against empirical wind tunnel and field data, or seeking to optimise their performance through re-calibration of specific component parts, have been recurring themes within the discipline (e.g., Anderson, *et al*. 1991; McEwan and Willetts, 1994; Lancaster, 1995; Sherman, *et al*. 1996; Dong, *et al*. 2003; Baas and Sherman, 2006; Liu, *et al*. 2006; Ellis, *et al*. 2009; Sherman, *et al*. 2013).

Recognition of strong relationships which exist between wind characteristics and aeolian sediment transport has led to extensive methodologies which employ wind records to resolve and/or forecast aeolian landscape evolution. The most noteworthy development in the use of wind regime data for process-form response analysis, and on which further landscape evolution studies have been based, came from Fryberger and Dean (1979). Their method uses both wind speed and direction, within time averaged historic records, used to determine sand transport vectors. Using the Lettau and Lettau (1977) model, (modified to incorporate the duration of the wind averaging period), sand drift potentials, (essentially transport capacity) could be calculated. The frequency and magnitude of transport capacity in each of the 16 (inter)cardinal compass directions could then provide transport as a vector unit, or RDP (Resultant Drift Potential). Although a number of shortcomings are associated with the Fryberger and Dean method (1979), model simplicity, wind data availability, and the lack of suitable alternatives have resulted in multiple applications for landscape evolution studies (e.g., Panario and Pineiro, 1997; Olivier and Garland, 2003; Käyhkö, 2007; Hesp, *et al*. 2007; Miot de Silva, *et al*. 2013).

1.4.1. Criticism of aeolian transport models.

Since their initial introduction, aeolian geomorphic research has remained heavily reliant on sediment mass flux models. Despite this, the use of these deterministic equations for quantifying transport are persistently criticised. A decade has now passed since Sherman, *et al*. (2011:p.1) described there now being ‘overwhelming evidence’ against their suitability. Similar and explicit statements can be found in a multitude of publications (e.g. Baas and Sherman, 2006; Houser, 2009; Delgado-Fernandez and Davidson-Arnott, 2011; Bauer, *et al*. 2013; Baas, *et al*. 2020).

Following Fryberger and Dean (1979), the use of transport models in combination with time averaged wind records, (invariably sourced from local weather stations), was a commonplace method employed to explain medium to long term landscape evolution. Fundamental limitations associated with this practice were recognised from outset, and many more have been acknowledged since;

1.4.2. Averaged wind parameters are unrepresentative of 'real' flow

Firstly, when dealing with extended periods of time, average winds speeds provide a very poor representation of the inherent gustiness of wind. For clarity, the simplest example of this concept is that, for a given location, average wind speed over a fixed period of time may be below the threshold wind speed necessary to initiate aeolian transport of sand. In reality of course, other than in the highly unlikely event that wind speed has remained constant for an extended period of time, say a day, a month or a year, this average speed will include shorter periods of time, when wind speeds were well below the threshold, resulting in no transport events, and also periods of time where wind speeds were significantly above the threshold, and transport may have been considerable. In this example, changes in the morphology of the landscape cannot be explained by an average wind speed which has 'remained' below the speed required for transport. The same is also true of wind direction which historically has been divided into arbitrary compass directions of 16 or 32 points, which again will be unrepresentative of the real nature in which the wind exhibits high temporal variability, and will lead to bias in direction based on the number of directional classes chosen.

With the aim of overcoming constraints related to averaging periods, and further promoted by technological advancements, there has been exponential growth in the prominence of process based aeolian research. A primary motivation has been to capture the intermittent and highly variable nature of both wind flow, and

transport response (Sherman and Hotta, 1990; Bauer, *et al.* 2012). There now exists a huge body of work detailing high frequency measurement of aeolian processes in both laboratory and field settings. With regard to wind direction, irrespective of frequency, it is also intrinsically under-represented in deterministic models. Although in reality both fluid forcing and sediment transport are truly vector properties, they are invariably treated as scalar. As wind speed is exclusively the dominant factor of all models, wind direction is routinely disregarded in determining flux, and transport direction is then typically assumed to mirror that of the flow vector, which is frequently not the case (Bauer, *et al*. 2013).

1.4.3. Surface controls on transport and supply limiting factors

The vast number of process based field studies conducted over recent decades bring with them an ever expanding appreciation of the great diversity of factors which may influence, and often restrict aeolian transport. Deterministic models are based on the premise that higher wind speeds translate to higher levels of shear stress at the surface, and thus greater levels of sediment transport. In addition to the most simplistic of models being based on steady airflow over an idealised, clean, dry and flat surface, they also crucially encompass the assumption of an unlimited supply of sediment. In field environments, and almost exclusively for coastal settings, multiple factors typically combine to limit sediment availability (Nickling and Davidson-Arnott, 1990). As a result, the many deterministic models which assume idealised conditions, invariably over-predict sediment transport to varying degrees (Sarre, 1987; Sherman, *et al*. 2013; de Vries, *et al*. 2014).

The two principle supply limiting factors in coastal beach-dune settings, surface moisture and vegetation were discussed in sections 1.3.3.5 and 1.3.3.6 respectively. A plethora of other potential, observed, or measured factors exist. A

non-exhaustive list includes, coarse lags such as shells or pebbles (Davidson-Arnott, *et al*. 1997; van der Wal, 1998), salt crusts (Davidson-Arnott, *et al*. 2019), slope gradient (de Vries, *et al*. 2012), snow/ice cover (Delgado-Fernandez and Davidson-Arnott, 2011), surface roughness or topography (Davidson-Arnott, *et al*. 2005), woody debris (Grilliot, *et al*. 2019), and fetch (Bauer and Davidson-Arnott, 2002; Davidson-Arnott, *et al*. 2005; Bauer, *et al*. 2009). In some cases, adjustments or additions to deterministic sediment flux models have been applied with the aim of accounting for limiting factors such as moisture (e.g. Belly, 1964; Hotta, *et al*. 1984), or fetch (Davidson-Arnott and Law, 1996; Bauer and Davidson-Arnott, 2002). A key motivation in doing so is that their effects can be validated using transport data from short term field experiments, with the intention of then incorporating impacts over increasing time scales. A major issue associated with this approach is that supply limiting factors typically exhibit pronounced spatio-temporal variability, both during field studies, and of between them over the medium to longer term. This has the effect of constraining our ability apply, calibrations made and validated using field measurements, to longer term wind records (Sherman, 1995; Aagaard, *et al*. 2004; Houser, 2009; Barrineau and Ellis, 2013; Walker, *et al*. 2017).

1.4.4. Secondary airflow and transport

Finally, as the body of field based datasets for quasi-instantaneous, high frequency measurements (of both airflow and transport) have increased, so too has recognition that near-surface airflow can be significantly different to that of the regional wind field. These differences in flow are most pronounced nearest to the surface (within the zone that transport occurs), and reduce with height through the boundary layer, to become aligned with regional wind vectors. Although there remains much to learn, diversions in near-surface flow, away from that of the upper wind field most frequently relate to topography, surface conditions

(roughness or moisture), and vegetation (e.g., Chepil and Woodruff, 1963; Walker, 1999, Walker and Nickling, 2002; Schatz and Hermann, 2006; Walker, *et al.* 2006; Lynch, *et al.* 2008). A multitude and variety of near-surface flow diversions can occur, including acceleration, deceleration, topographic steering, flow attachment or separation, flow reversals and turbulent eddies (e.g. Beyers, *et al.* 2010; Parsons, *et al.* 2004; Wakes, *et al.* 2010; Jackson, *et al.* 2011).

As beach-dune systems are characterised by complex topography, which exhibits high spatio-temporal variability, near-surface airflow is typically unrepresentative of the regional wind field. This questions the validity of using regional wind records to predict or resolve sediment transport, and also the approaches which have been adopted in the past when doing so. Whilst countless relevant scenarios exist, for dune fringed coasts, the occurrence of offshore wind provides a very simple example. Sediment supply from the upper beach is widely recognised to exert a strong control on the evolution of coastal foredunes (Sherman and Bauer, 1993). In this knowledge, when seeking to determine beach-dune sediment flux, the exclusion of periods of offshore flow from a regional wind time-series is customary, (based on the assumption that transport vectors align with those of flow), and will therefore not contribute to dune sediment input. The findings from recent studies at Magilligan Strand, (NI), documented onshore directed transport during offshore directed wind, as a result of foredune induced flow reversals (Lynch, *et al*. 2008; Jackson, *et al*. 2011).

As near-surface flow varies both spatially and temporally across beach-dune topography, so too does shear stress at the bed. Therefore, in order to expand our knowledge and understanding of sediment transport events, we must first seek to fully understand wind flow dynamics over the beach and dunes. Finally on air flow modifications it is useful to also mention the frequent occurrence of sediment flux

being ‘transport-limited’. This term refers to transport being restricted as a result of the capability of fluid forcing to initiate, or maintain sediment transport, as opposed to supply limiting factors which refer to surface controls on sediment availability (Masselink, *et al*. 2011). Numerous factors such a slope, surface roughness or vegetation can induce reduced flow velocities relative to that of regional wind. Additionally, as grains in saltation have the effect of extracting momentum from flow, transport itself has the capacity to reduce wind speed. Again, such factors are highly challenging to accurately incorporate within deterministic models. As such, in settings where their effects are likely to be considerable, this strongly questions our continued reliance on their use.

1.4.5. Limitations of sediment flux model structure and validation

In depth review of the structure, application and validity of sediment flux models is beyond the scope or requirement of this chapter, not least because their inclusion was ruled out at an early stage of the PhD project. Although the host of additional challenges concerning their use could be labelled in a number of ways, beyond the three generic categories above, recognised limitations can most often be classified as those regarding model variables in relation to reality, or those associated with our ability to accurately validate their performance through measurement. Frequently cited drawbacks concerning model structure are that equations do not always incorporate a threshold velocity, and do not account for the effects of turbulence, or grain size variability (Chapman, 1990; Sherman, *et al*. 1998; Sherman, *et al*. 2013). That models make the assumption of wind flow being steady, further, and importantly guarantees that some level of error is intrinsic (Sherman, *et al*. 1996).

With regard to model validation through field experiments, suitable measurement of high frequency sediment transport is impacted by multiple constraints. Chaotic

lag times between fluid forcing and transport response, variable sediment trap efficiency, sensor performance varying dependent on transport intensity, and an inability to accurately measure quasi-instantaneous grain size variability, or effectively calibrate 'count' data to mass flux offer few examples (e.g., Jackson, 1996; Dong, *et al*. 2003; Ellis, *et al*. 2009; Hugenholtz and Barchyn, 2011 Sherman, *et al*. 2013; Bauer, *et al*. 2012; Duarte-Campos, *et al*. 2021).

1.5. Blowout Landforms

The primary motivations of this project are to improve understanding of aeolian processes associated with foredune blowout sediment transport, and to examine the implications of these processes, and landforms, with respect to longer term coastal evolution. This section provides an introduction to blowout landforms and an overview of the most relevant research to date.

Gaining scientific acceptance during the mid-twentieth century (Bagnold, 1941; Laing, 1954, Olson, 1958, Cooper, 1958), the term blowout defines, generally saucer, bowl or trough shaped hollows in sand based surfaces (Carter, *et al.* 1990; Hesp, 2002; Hesp and Walker, 2013). They are formed by deflation, the removal of sediment by wind action (Smyth, *et al*. 2014). Blowouts are common landforms found in both coastal (Gares and Nordstrom, 1995; Bate and Ferguson, 1996; González-Villanueva, *et al.* 2011; Smyth *et al*, 2014; Abhar, *et al.* 2015) and continental dune systems (Hugenholtz and Wolfe, 2006; Wang, *et al.* 2007; Sun, *et al.* 2016), throughout a wide range of latitudes (Barbosa and Dominguez, 2004; Käyhkö, 2007).

Typically classified as erosional features within dune landscapes (e.g., Carter, *et al*. 1990), the morphology of the landforms themselves, could more accurately be described as manifestations of aeolian sediment transport. In their entirety,

blowouts most often comprise an upwind area of erosion, the deflation basin or trough, together with a downwind zone of deposition, termed a depositional lobe or apron, and generally also considered to be a component part of the landform (Carter, *et al.* 1990; Hesp, 2002). Their form is thus symptomatic of sediment transport. Largely through interpretations of form, and numerous observations of the propensity of their topography to modify airflow sufficiently to encourage the entrainment or continued transport sediment, they are often described as highly efficient transport corridors (Carter, *et al.* 1990; Hesp, 2002; Anderson and Walker, 2006; Hesp and Walker, 2013). Although blowouts can occur in a diversity of evolutionary phases in beach-dune systems, they are most frequently associated with stretches of coastline experiencing a negative sediment budget (Carter, *et al.* 1990). In addition to commonly being classified as erosive features, they are also perceived as smaller scale landforms within an eroding landscape, as opposed to a fundamental cause of the erosion of the coastline itself.

1.5.1. Blowout Genesis

In essence, blowout initiation is caused by the occurrence of either, or both, an increased susceptibility of the surface to erode, and localised acceleration of airflow. There exists a multitude of environmental and/or anthropogenic processes which may combine to produce either of these events. The former is predominantly associated with removal or reduced coverage of vegetation, through a variety of causes including increased aridity, fire, grazing, pedestrian pressure, nutrient depletion, sand mining, off-road vehicles, and direct management interventions (e.g., Marston, 1986; Jungerius, *et al.* 1991; Cooke, *et al*. 1993; Thom, *et al.* 1994; Seppala, 1995; Blanco, *et al.* 2008; Mir-Gual and Pons, 2011; Mir-Gual, *et al.* 2013; Barchyn and Hugenholtz, 2013; Jewell, *et al*. 2014; Burkley, *et al*. 2014). In addition to these generic dune field factors, initiation

within foredunes is often attributed to accelerated airflow over existing topography, or via confined alongshore slumps following wave scarping events (Carter *et al*, 1990; Gares and Nordstrom, 1995; Hesp, 2002; Sawakuchi, *et al.* 2008; Jewell, *et al.* 2014).

1.5.2. Blowout processes, evolution, and classifications

Localised accelerations of airflow in the lower boundary layer are fundamentally associated with variability in topography and surface roughness. In aeolian environments, countless studies include commentaries detailing how such surface complexities may give rise to flow acceleration, through either streamline compression, or reduced frictional drag (Walker and Nickling, 2002; Lynch, *et al*, 2010; Burri, *et al*. 2011; Wiggs and Weaver, 2012; Bauer, *et al*. 2013). During initiation, and early stage, blowout evolution, an intrinsic positive feedback exists as a result of form-flow interactions. At the micro-scale, even small topographic depressions or variance can induce flow accelerations associated with compression, which thus induces further deflation, and therefore potentially, further subsequent enhancements to flow.

Post-initiation, through continued deflation, blowouts develop and enlarge via three principle mechanisms. Firstly, vertical expansion to deepen the hollow occurs as a result of basal scouring, the extent of which may be ultimately limited by vegetation growth, the development of a course lag, or the height of the water table relative to the blowout floor (Ritchie, 1972; Gares, 1992; Gares and Nordstrom, 1995, Hesp, 2002). Secondly, expansion laterally through the erosion of side walls. In addition to direct scouring of the blowout side walls, over-steepening can also result in slope process related changes to form. Mass movements associated with under-cutting and slumping being the most common (Carter, *et al*. 1990). These events introduce further available sediment to the

basin or trough floor for future deflation. Thirdly, longitudinal growth occurs as material eroded from the upwind sub-unit is deposited downwind. Additional to this, the stoss slope of the depositional lobe may also directly experience deflation. Both sediment inputs and airflow may result in extension or downwind migration of the depositional sub-unit (Carter, *et al.* 1990; Hesp, 2002). One final growth mechanism receiving occasional mention is the development of rim dunes, most frequently along the blowout side walls as a result of sediment being ejected laterally from the basin or trough to be then rapidly deposited on flow expansion(e.g. Gares and Nordstrom, 1995; Hesp and Hyde, 1996).

There has been little advancement over the decades concerning blowout classification based on morphological form. An early paper by Ritchie (1972) offered the four alternatives of cigar shaped, v-shaped, scooped hollow, or cauldron and corridor. In recent times, saucer, trough and bowl are in most frequent use, and as no standardised metrics exist to aid identification, there is some degree of subjectivity involved. Beyond classifications based on shape, a systems approach allows blowouts to also be categorised as either ‘open’ or ‘closed’. The geometric form of an ‘open’ blowout encompasses a topographic opening, ordinarily termed a *throat*. This provides connectivity between the interior and the surrounding land surface external to the blowout, thereby greatly enhancing potential for the introduction of further sediment. For ‘closed’ system blowouts, in the absence of a throat, blowout evolution is ultimately controlled by the size, shape and position of the host dune in which it forms. The research in this thesis focuses on foredune blowouts, with this terminology referring to their topographic setting. In bisecting the foredune (frontal/primary dune), foredune blowouts are intrinsically ‘open’ as they have a throat at their seaward extent providing connectivity with the beach, and the adjacent, seaward foredune slopes, thus offering significant potential for additional sediment supply. Figure 1.1

displays a foredune blowout in Sefton viewed from both within the blowout, looking seaward, and from the beach looking landwards to the east.

Figure 1.1: Annotated example of a foredune blowout in Sefton.

Examples of blowout development within the literature include instances of both cyclical and progressive evolution. Over time, the continued erosion of the deflation basin or trough, together with the transfer of sediment to the downwind depositional area may eventually lead to parabolic dune formation (Melton, 1940; Verstappen, 1968; Hesp, 2002; Anderson and Walker, 2006; McKenna, 2007; Hesp and Walker, 2013). In this instance, the depositional lobe of the blowout develops into a downwind migrating dune, with the side walls of the deflation basin, or trough, becoming the trailing arms of the parabolic dune. Gares and Nordstrom (1995) detailed a cyclical model of blowout evolution, albeit on a leeward coast, but the cycle proposed could equally be of relevance independent of wind regime, or geographical setting. In their model, deposition at the seaward extent led to blowout closure, whilst side wall slumping resulted in gentler slopes within the blowout interior, thereby reducing the potential for flow compression, and therefore also both the frequency and magnitude of subsequent deflation events. Again, a feedback mechanism may promote this process once initiated, as the gradual reduction in relief may lead to flow expansion, along with further deposition.

In reality, numerous environmental and anthropogenic factors can influence the nature of blowout evolution, whether that be cyclical, episodic, or progressive. The progressive development of foredune blowouts with throats allowing the input of additional beach sediment may become constrained on becoming 'closed' systems through a tendency for sedimentation around the throat (Bitton and Byrne, 2002), or on incipient foredune development (Hesp, 2002). Many examples can be found of blowout initiation, evolution, or their orientation being associated with storm events, or the longer term wind regime (e.g., Lancaster, 1986; Jungerius, *et al.* 1991; Hugenholtz and Wolfe, 2006; Käyhkö, 2007). Just as storm events, or an energetic wind regime may contribute to their initiation, equally a general calming of the wind regime over time may reduce or cease blowout activity.

Limitations on basal scouring, and therefore blowout depth, together with sediment supply to the downwind depositional area may exert a strong control on evolution. Whilst development of a coarse lag across the basin floor can inhibit vertical erosion (Carter, *et al*. 1990), it is often the case that scouring continues until a level is reached were the blowout floor is permanently, or seasonally affected by the water table. Both basin floor submergence, and persistent high moisture can be completely prohibitive of sediment transport for extended periods of time. On this occurrence, continued morphological change may potentially become controlled by oscillations in the water table due to intermittent periods of expansion or contraction to blowouts areas affected by ponding, or excessive moisture content (Luna, *et al.* 2012; Mountney and Russell, 2009). As was the case for the Devil's Hole *blowout* in Sefton dunes, deflation to the water table invariably results in rapid colonisation by dune slack flora (Smith and Lockwood, 2013: Smith, 2014), with the nature of this vegetation typically exerting significant control over

aeolian processes. The implications of vegetation on dune field dynamics are expanded further in section 1.6.3.

Blowout orientations are often found to be aligned with the most frequently occurring dominant winds (Gresswell, 1937; Jungerius, *et al.* 1991; Hesp, 2002). This in turn can be linked to the assertions of Smyth, *et al.* (2012), who state that the central axis of blowouts are frequently corridors of high wind speed, which would thereby promote enhanced deflation along this axis. A number of authors have also observed the windward stoss slope of depositional lobes to be areas of high erosion (Lancaster, 1986; Byrne, 1997), with this also potentially enhancing longitudinal extension in line with prevailing winds as deflated sediment is transported downwind. It should be noted that Jungerius, *et al*. (1981) found this is not always the case, with other factors including storm events or human impacts affecting blowout orientation. More recently, there has been increasing recognition of existing topography, in particular the steep lateral walls of trough blowouts, exerting a strong control on the regional wind field. Topographic steering of incident winds typically results in winds from a wide range of approach angles becoming, central axis aligned on entering the blowout (Hesp and Pringle, 2001; Hesp, 2002; Hansen, *et al*. 2009; Smyth and Hesp, 2016; Delgado-Fernandez, *et al*. 2018; Smyth, *et al*. 2020b). This topographic modification often resolves many recorded instances of non-alignment of blowouts with dominant wind vectors.

In relation to blowout configuration, extensive research of the Manawatu dune fields of New Zealand by Hesp (2001; 2002) identified potential relationships between various aspects of blowout geometry. The lengths of blowout deflation basins were found to correlate almost perfectly on a 1:1 ratio with the lengths of their depositional lobes. For trough blowouts it was suggested the ratio between width and the length of the depositional lobe was approximately 1:4. Jungerius, *et*

al. (1991), whilst researching blowouts in De Blink, Holland, noted that a correlation may also exist between blowout depth and width. They were further able to conclude that upon downward deflation ceasing, width continued to grow independently of depth. As a caveat to these findings, Carter, *et al.* (1990) highlighted that there is a greater likelihood of such relationships being apparent in more isolated, 'closed' systems, as 'open' system blowouts may act as transport corridors. The potential for significant throughput of sediment in 'open' blowouts can therefore create considerable 'noise' if attempting to establish relationships which essentially concern sediment transfers between component parts of the landform.

Early research on blowouts was largely dominated by studies regarding form, modes of initiation, and resolution of their progressive evolution. Over recent decades however, in line with the trend of 'reductionism' (Bauer and Sherman, 1999), together with technological advancements, research has become heavily focused on processes, resulting in our knowledge of the dynamic, and often complex patterns of airflow associated with these landforms greatly improving (e.g., Hesp, 1996; Hesp and Hyde, 1996; Hesp and Pringle, 2001; Hesp and Walker, 2012; Smyth, *et al.* 2012, 2013, 2014; Pease and Gares, 2013; Delgado-Fernandez, *et al.* 2018). The variety of modifications to incident wind characteristics identified include increased turbulence, areas of both flow acceleration and stagnation, flow reversals and separation, topographic steering, and the formation of helicoidal vortices (Hesp and Hyde, 1996; Smyth, *et al.* 2012; 2013; Hesp and Walker, 2012; Hesp, *et al.* 2016; Smyth and Hesp, 2016). In respect of topographic flow modifications, the influence of incident wind speed has been found to be of negligible impact, with blowout configuration and incident wind approach angle being identified as dominant controls on the nature of secondary airflow structures generated (Smyth, *et al.* 2013; Pease and Gares, 2013).

Increased turbulence and wind velocities are two principle flow modifications associated with blowouts which may enhance levels of aeolian sediment transport. Hesp and Pringle (2001) recognised that the steep lateral walls of trough blowouts promote the topographic steering of incident flow, and that there can be pronounced acceleration across the walls. In addition to acceleration along blowout walls, as airflow mass entering blowouts increases, the resultant compression of flow produces marked increases in wind speed, this being the primary mechanism by which transport capacity may be enhanced. It should also be noted here that whilst turbulence can sometimes resolve levels of transport which cannot be adequately explained by wind speed, pronounced flow compression can also serve to suppress turbulence, resulting in relatively steadier, stronger, and less chaotic airflow, thereby also enhancing transport. They further asserted that oblique winds with higher degrees of incidence to that of the main blowout axis, typically result in both greater turbulence, and enhanced levels of topographic steering. Beyond flow compression within the blowout interior, they additionally theorised that incident winds are likely drawn, or *sucked* into blowouts due to the pressure gradient which exists, with blowout topography creating localised areas of low pressure. This point is of particular significance, as in addition to blowout form often inducing airflow enhancements, and thereby increased transport capacity, that their topography is capable of promoting incident winds to enter the blowout, also increases the frequency of this occurrence.

In dune landscapes, blowouts are acknowledged to be zones of high sediment transport, and therefore play an important role in dune field evolution. As a consequence, they are customarily described in such terms as being sediment pathways, or efficient transport corridors (e.g. Gares, 1992; Hesp, 2002; Smyth and Hesp, 2016; Delgado-Fernandez, *et al*. 2018). Evidence supporting this perception comes from a variety of sources, not least that their morphology

comprises zones of both erosion and deposition, providing strong cumulative evidence of frequent transport events. In coastal dune systems, which are to varying degrees, most often characterised by vegetation cover, active blowouts are typically not, or only sparsely vegetated, relative to their surroundings, and with being less impacted by this supply limiting factor, usually exhibit higher relative levels of transport activity.

As detailed, numerous studies centred on the internal airflow dynamics of blowouts, have in turn also described the topographically induced flow enhancements they identify as being likely to promote sediment transport (e.g. Smyth, *et al.* 2012; Pease and Gares, 2013). Despite this, there remains a scarcity of research including actual measurement of quasi-instantaneous transport, and no more so than for foredune blowouts, where the nature of transport events are yet to be characterised. A summary of what is known about high frequency, blowout sediment transport is included in section 1.8.2., to contextualise the knowledge gaps and the original contributions being targeted, in association with this element of the thesis.

1.6. Coastal dune evolution

As landscape change is fundamentally governed by spatio-temporal patterns of erosion and deposition, it follows that aeolian sediment transport in coastal dune settings is a contributing factor to the evolution of such environments. Further, given that in these settings, blowouts are dune landforms acknowledged for their high relative levels of transport, a reasonable expectation may be for higher magnitude aeolian geomorphic change to be associated with their locations. Additional to this, sediment exchanges between the foredune and beach ‘sub-units’ of the cross-shore profile, are known to be a primary control on the evolution of beach-dune systems. It may therefore also be the case that the influence of

foredune blowout landforms, on the evolution of the larger scale coastal landscape, may be further enhanced in association with their position in the foredune. This section details the dynamics of beach-dune systems with reference to conceptual models of geomorphic evolution and behaviour.

1.6.1. Foredunes

It is first useful to define foredunes within the coastal, beach-dune system. Sometimes, alternatively referred to as *primary dunes,* foredunes are those existing at the most seaward extent of dune fringed coastlines. Bauer and Sherman (1999) identified the foredune as being distinct to all other dune bedforms, whether in coastal or continental settings, as by definition, they are intermittently, but directly influenced by nearshore processes, (in particular, wave action). Independent of their comparable volume, or size, relative to that of the landward dune field, being the most seaward dunes, *foredunes* are exclusively defined as *primary*. Beyond this essential criteria associated with marine processes, it should also be noted that the development, form, and behaviour of foredunes is invariably, (but not exclusively), strongly controlled by the presence, and nature of coastal vegetation (Hesp, 1983; Hesp, 2002). Although foredunes frequently exist, and are most easily recognised as a continuous shore parallel ridge (Davidson-Arnott, et al. 2019), collections of discrete, individual nebkha dunes, which at a larger scale, collectively form a linear ‘unit’ of dunes along the backshore, are also classed as primary foredunes. García-Romero, *et al*. (2019) provide a useful, three category system in which foredunes are considered either as continuous ridges, discontinuous, or comprised of nebkha. In respect of their vegetative state, the coverage, seasonality, structure, density, and species of vegetation are all recogonised as factors influencing foredune configuration (Arens, 1996; Hesp, 2002). Regardless of this, pioneer species in the most seaward extent of beach-dune systems that are associated with foredune

development, almost exclusively possess adaptions which are advantageous to colonising these most hostile environments (Jefferies, *et al*. 1979; Davidson-Arnott, *et al*. 2019). The most commonplace being, a higher relative tolerance of salinity, rhizomatous roots, and enhancements to growth in association with sand burial, via adventitious buds (Hesp, 1991; MacLachlin, 1991; Maun, 2009). Further validating the frequently dominant role of vegetation on foredune evolution and character, at a global scale, Hesp, *et al*. (2021) also drew links with continental scale variability in precipitation, as this exerts a primary control on the vegetative state of coastal beach-dune systems.

1.6.2. Foredune Evolution: Conceptual models and coastal morphodynamics

With a multitude of academic texts covering generic, process-form descriptions of coastal dune development, the most common elements are widely recognised (e.g. Masselink, *et al*. 2011; Davidson-Arnott, *et al*. 2019). Typically, the initial phase in such commentaries is focused on pioneer vegetation trapping sand to form ‘embryo’ dunes, immediately seaward of the established dune field. Of course, (predominately, but not exclusively) landward directed, aeolian transport of beach sediment is a prerequisite to its deposition in the back shore area. Processes operating in the nearshore, delivery of sediment to the foreshore, and beach development may sometimes contextualise this initial dune building phase. An early, site specific, New South Wales model by Hesp (1983), offers a notable diversion from this in describing the offshore directed transport of seedlings, which initiate dune building, as a result of germinating in beach sediments.

In examining foredune evolution, at any fixed point in their existence, sediment erosion or deposition, by any mechanism, results in a guaranteed change to their ‘static’ state morphology. With this, consideration of changes in foredune total volume, (termed their sediment budget), provides a popular method by which

foredune geomorphic change can be better understood (e.g. Carter and Wilson, 1990; Carter, *et al*. 1990). Although the sediment budget approach can be fundamental when accounting for any given geometric change in form, and often also highly informative for explaining the foredune character, coastal dune evolution cannot be fully resolved by sediment budget analysis in isolation. That a foredune sediment budget theoretically could remain perfectly constant for many decades, whilst its configuration has exhibited significant adjustment, or equally, foredune geometry and character may have persisted, whilst its geographic position migrated, are two, albeit aberrant examples which highlight potential limitations associated with dependency on budget analysis exclusively.

As foredune sediment gains and losses exert a primary control on morphology, the sediment budget concept is frequently utilised to either explain historic, or to predict future geomorphic change. Instances of wholly progressive foredune evolution are not only unlikely, but to the knowledge of the author, as yet undocumented. It is also infrequent but not unheard of, that established foredunes experience complete destruction, for instance via high magnitude washover events (e.g. Mathew, *et al*. 2009). Ordinarily, over extended time frames, geomorphic behaviour leans towards an equilibrium. Across temporal scales ranging from minutes and hours, to years and decades, continual fluctuations in budget are characteristic, with foredune form at any given time being an expression of repeated cycles of sediment erosion and deposition. Although considerable alterations in configuration and geographic position may come about from such changes, they are often regarded, simply as oscillations within a longer term, steady state of equilibrium (Davidson-Arnott, *et al*. 2019, p.296).

Historically, a clear divide has been evident within coastal geomorphology, often between studies, or researchers, that were focussed on the wave dominated

beach and nearshore zone, and those concerned with the subaerial, wind dominated dunes (Sherman and Bauer, 1993). With so many unknowns remaining about each of these 'sub-units' of the coastal zone, this division still remains valid for many studies, and is often also necessary, particularly for logistical purposes. One of the overarching motivations of the wider discipline however, is improving our ability to forecast future, or resolve past coastal evolution, across macro spatio-temporal scales. For many decades now, there has been increasing recognition of the limitations associated with treating specific zones of the cross-shore profile as individual systems.

Holistically, large scale coastal systems are characterised as environments where large volumes of energy are dissipated across relatively short areas, with this occurring in coincidence with near-continuous, multi-directional transfers of geo-materials (Masselink, *et al*. 2011). As such, advancements in understanding, when treating specific sections of the coastal profile as discrete, and effectively 'closed' systems, is often highly constrained, or frequently over reliant on including assumptions concerning the flow-flux dynamics of adjacent, proximal sub-units. The beach and foredune components of the coast are now wholly acknowledged to be deeply coupled. As such, the changes in form, composition, and energy regimes of both sub-units occur bilaterally, through mutual adjustment, whilst additionally being subject to a diversity of both positive, and negative feedbacks which add even further layers of complexity (Sherman and Bauer, 1993).
In comparison to non-coastal environments, beach-dune systems experience relatively high levels of processes capable of geomorphic work, and the quasi-unconsolidated structure of sedimentary coastlines results in relatively greater morphological responsiveness, with higher frequency geomorphic change being the norm. Fluid flow, and therefore the forcing of such changes, whether by wind or water, are in turn also adjusted as a consequence. These types of process-form

relationships, occurring across a broad range of spatio-temporal scales are described as *morphodynamics*, a term first coined by Wright and Thom (1977). With a diversity of intimate, and pronounced relationships existing, especially between sections of the cross-shore profile, morphodynamics are most strongly associated with coastal landscapes, relative to other environment types. Further, within coastal morphodynamics, beach-dune interactions have received the greatest attention, as the dynamics of these two sub-units are known to strongly influence both the character of the coast in its entirety, and to exert significant control on longer term evolution (e.g. Bauer and Sherman, 1999). A number of influential review papers over recent decades have highlighted the pressing need to improve our rate of progression concerning the resolution of beach-dune dynamics, and the great value in understanding to be gained from such advancement, together with the persistent logistical issues which continue to constrain doing so (Sherman and Bauer, 1993; Sherman, 1995; Bauer and Sherman, 1999; Houser, 2009; Walker, *et al*. 2017).

A seminal, heavily cited, and widely applied text, which details beach-dune dynamics in southeastern Australia came from Short and Hesp (1982). Although largely descriptive and theoretical in nature, identification of three broad categories of beach ‘stage’, namely dissipative, intermediate, and reflective, has proved to be of considerable value. This model describes the strong coupling, and inter-dependencies existing between the nearshore, beach, and foredunes, with the nearshore energy regime having significant influence on beach-dune morphodynamics. In relation to dune building, dissipative beaches were identified as having the greatest potential for aeolian sediment transport, and therefore typically exhibit higher magnitude foredunes. Their characteristically wider beach, lower gradient profile, and relatively finer grained composition, all potentially offer contributions towards relative enhancements in aeolian transport and dune

building. Further, beach width and slope also combine to reduce the frequency, and magnitude of dune scarping, through greater capacity for dissipating wave energy.

An occasional criticism of this model is it being most applicable to the high wave energy, stable coastline, micro-tidal setting of its study site, with variability of foredune configuration also being regular in the longshore. Despite this, in providing a framework by which commonplace, highly evident, multi-variant links, between the nearshore energy regime, beach slope, grain characteristics, and foredune configuration, the model is widely applicable throughout a diversity of physical settings (Sherman and Bauer, 1993; Bauer and Sherman, 1999). For example, Miot da Silva, *et al*. (2010; 2012) found the model suitable for predicting dune evolution in a micro-tidal setting, and regardless of there being longshore variability in both coastline stability, and foredune characteristics. Frequently, the model has also been validated in macro-tidal, unstable settings, with beach slope and width often being strongly associated with longshore variability between the balance of dune growth and wave scarping (Saye, *et al*. 2005; Pye and Blott, 2008; Anthony, *et al*. 2009, 2013).

At the other end of the spectrum, reflective beaches are most often characterised by a steeply sloping profile, narrower beach, coarser sediment, and strongly erosional trends, with therefore limited dune building potential. Individually, any or all of these features are frequently used to support suggestions of beach type and behaviour, often solely based on initial visual inspections. Between the two, intermediate beach types are associated with medium frequency, foredune erosion events, foredune blowouts, and in some instances, to landward parabolic dune development (Bauer and Sherman, 1993). Beyond the fundamentally geomorphic parameters included by Short and Hesp (1982), over time, numerous additional

factors such as vegetation (Hesp, 2002), moisture (Miot da Silva, *et al*. 2010), fluctuations in sea level (Pye and Bowman, 1984; Pye, *et al*. 2007; Hesp, 2002), and anthropogenic factors (Pye, 1990) have been more prominently incorporated within the context of this framework.

The morphodynamics discussed within the Short and Hesp model (1982) provide great insight into beach-dune interactions, and are widely applied to explain coastal character and system behaviour. Ultimately the morphodynamics at play for any given setting bring about sediment exchanges between distinct sub-units of the cross-shore profile, which in turn govern geomorphic change. Psuty (1988) provided a heavily utilised, conceptual model of beach-dune interaction, where foredune morphology and character, could be explained by comparing the relative sign and magnitude of the beach sediment budget, with that of the foredune. Disregarding the beach budget for a moment, all things being equal, if a foredune has a positive sediment budget, it can be expected to experience growth. This may manifest in the form of increasing height, and/or width, with such expansion often also leading to foredune progradation. Alternatively, should the primary dune have a negative budget, foredune attenuation will occur, through either or both, losses in height and/or width, with this typically resulting in landward transgression of the foredune toe. In any given period, the sign of the foredune sediment budget, and its relative magnitude, is governed by the balance between sediment gains, primarily via aeolian deposition, and sediment losses, most often via wave scarping.

The application of the Psuty (1988) model is particularly useful for resolving evolution as it benefits from the simplicity of being based exclusively on the beach and the foredune sediment budgets, and the premise that foredune morphology is dependent on sediment exchanges with the nearshore beach. This differentiates it

from the Short and Hesp (1982) model which explains beach-dune evolution through consideration of a number of key elements influencing morphodynamics, and therefore also sediment exchanges.

Whilst the Short and Hesp (1982) model is frequently found to be applicable in locations which do not possess all the characteristics of the original study setting, in adopting this singular 'sediment budget only' approach, the Psuty (1988) model better avoids site specific variables, and can be tested or applied in any beach-dune system (Davidson-Arnott, *et al*. 2019). Given this simplicity, a notable assumption made by the Psuty (1988) model is that the combined beach-dune sediment volume is quasi-constant, and therefore sediment exchanges between the foredune, and landward secondary dunes are in the main disregarded (Masselink, *et al*. 2011). Foredune blowouts however are known to provide a potential pathway for the landward transfer of significant volumes of sediment to the dune field. Within the initial framework proposed by Psuty (1988), such features were assumed, in the main to be short lived. It considered that blowout development occurred rapidly as a result of a negative budget, even if only temporary, and the foredune could return to a steady state of equilibrium, equally quickly, should the dune sediment budget recover at a similar rate (Sherman and Bauer, 1993). In assuming away landward transfers to the secondary dunes, foredune geomorphic change in this model depends on beach-dune sediment exchanges, and is a result of a proportion of the total system budget being repeatedly cycled between the two, cross-shore sub-units. A final shortfall of the Psuty (1988) model is that it assumes the influence of vegetation on foredune development to be secondary (Sherman and Bauer, 1993).

Although this conceptual model has been developed by others to include a number of additional, and more specific evolutionary stages, or conditions, (e.g.,

Sherman and Bauer, 1993; Hesp, 2002; Nickling and Davidson-Arnott, 1990). Psuty (1988) elaborated four primary beach-dune states in the initial theory proposed. Namely, a positive budget in both the nearshore beach, and the foredune, with this resulting in coastal progradation, and usually the presence of multiple dune ridge topography. Secondly, both sub-units having negative budgets, and this being associated with a transgressive coastal system, with high potential for washover events, blowouts, parabolics, and hummock dune features. Thirdly, a negative dune budget coinciding with a positive beach budget, and this combination typically giving rise to beach ridge topography. Finally, and of note, the balance considered to provide maximum foredune growth, was a positive dune budget, with a neutral, (or marginally negative) beach budget.

Whilst solely concerning beach-dune sediment exchange and the resultant sediment budgets, the Psuty (1988) model is intrinsically related to beach-dune interactions more generally, and the numerous relationships which exist between the sub-units in the cross-shore profile. Although it assumes foredune sediment inputs are largely via aeolian deposition, it is worthy of mention that marine processes may sometimes deliver some relatively small proportion of sediment inputs to the foredune (Cohn, *et al*. 2018). Equally, sediment losses from the foredune in reality are not exclusively via wave scarping/marine processes, and sediment may be removed from the foredune by a diversity of other mechanisms, (for example by mass movements and/or direct deflation). Any and all, beach-dune sediment exchanges, occurring in either cross-shore direction, are the fundamental components of the Psuty (1988) model, and this highlights another point of note. Foredunes, and coastal dune fields more broadly are routinely considered as sediment sinks, and of course, their function as a protective buffer against coastal flooding is a ubiquitous comment in generic descriptions of beach-dune environments. Something referred to less often is that foredunes also

provide a buffer to the seaward beach. They may do this by acting as a sediment source for the beach during periods of negative budget, and/or low sediment supply to the beach from the offshore zone (Ruz, *et al*. 2005).

Foredune growth being the result of net sediment gains, and foredune attenuation resulting from net sediment losses are two widely recognised facets concerning the evolution of beach-dune systems. In being taken as a given, although these actualities have been formalised as elements of the Psuty (1988) model, it is often not explicitly expressed in many papers examining beach-dune geomorphic change, or sediment supply to coastal dunes. Nethertheless, a multitude of studies, detailing both measured and modelled beach-dune geomorphic change, do explicitly apply the Psuty (1988) model, and frequently also make use of the theories of Short and Hesp (1982) to support explanations of the sediment related, geomorphic changes which occur. Delgado-Fernandez and Davidson-Arnott (2011) and Strypsteen, *et al*. (2019), are two examples were greater insights into meso-scale dune evolution have been gained through its application. At the Sefton coast, the physical setting of this PhD research project, Dissanayake, *et al*. (2010; 2015) used X-Beach, a software specifically designed to model beach-dune interactions and sediment exchanges, to improve understanding of storm impacts on the coastline. In addition to the beach-dune sediment exchanges and budgets of Psuty's model, Pye and Blott (2008) also incorporated characteristics from Short and Hesp's (1982) model to better resolve actual evolution at Sefton. They found that dune erosion was greater in longshore sections of the coast where the inter-tidal beach was relatively narrower and/or steeper in gradient.

As a final example, the Psuty (1988) model was strongly validated by Aagaard, *et al*. (2004) whilst researching coastal dunes on the Skallingen peninsula, Denmark. In their study, they were able to identify that over time, volumetric foredune growth

mirrored very closely, the size and landward migration rates of inter-tidal bars. That the extent of the cross-shore profile under investigation appeared effectively to be a ‘closed’ system, with the total, combined sediment budget of the nearshore beach and foredune remaining near constant during the study undoubtedly strengthened the relationships they identified in cross-shore sediment exchanges. This suggests either, that there were negligible sediment inputs or losses to the total system, or alternatively, that sediment loss from the foredune to the landward dune field, and any potential input of additional sediment to the nearshore beach from the offshore zone, were closely matched. Although foredune losses associated with aeolian transport of sediment to secondary dunes, landward of their position, had minimal influence in this case, the Psuty (1988) model routinely disregarding this possibility remains a constraint. No more so than for coastlines characterised by foredune blowouts, as their presence may, theoretically enhance the frequency and the magnitude of transport events, which contribute to the total system loss during the period. That this model limitation exists, and that the influence of potentially enhanced sediment transfer to the landward dune field, have up to this point been viewed as a secondary consideration in relation to longer term evolution at Sefton, were two motivating factors in the design of this project. Further comment on this is provided in section 1.8.5.

1.6.3. Dune field dynamics in relation to climate and vegetation

The two principle themes of this PhD both concern aeolian sediment transport associated with foredune blowouts. (Further expanded in section 1.8.). The first will be focused on event scale, quasi-instantaneous transport, and the second, on assessing the influence such transport events may have on longer term, coastal dune field evolution. Both these research pathways could be categorised under the theme of ‘dune field mobility’, as this mobility is fundamentally driven by transport events. Detailed in sections 1.3.3.5 and 1.3.3.6 respectively, weather

conditions, and dune vegetation cover, exert significant influence over aeolian sediment transport. Further, section 1.5.1 detailed that changes in the levels of vegetation are also strongly associated with blowout genesis and evolution. Over large spatial scales, climate conditions are known to be a primary control on vegetation. For many years now, the inter-dependencies which exist between dune field mobility, regional climate, and coastal dune vegetation have attracted considerable attention. To compliment the details to this point on factors which influence the physics of sediment transport at the micro-scale, coverage of dune field mobility over greater spatio-temporal scales is briefly discussed here.

The character of regional dune fields throughout the world is highly diverse. At the local level, variability in the nature of vegetation is an important driver for this diversity, and in turn, regional climate conditions have an overarching control over this vegetation (Davidson-Arnott, *et al*. 2019). As levels of vegetation cover typically have an inverse relationship with levels of aeolian sediment transport, regional climates strongly influence the nature of coastal dune field evolution. In very broad terms, arid regions are associated with a scarcity of vegetation which promotes greater mobility in dunes, whilst levels of precipitation in temperate or tropical zones, ordinarily promote much higher vegetation cover, which in turn serves to reduce mobility/increase stability (Hesp, 2013). A number of studies have employed climate variables to establish deterministic models of dune field mobility, or as they are commonly termed, dune mobility indices (Delgado-Fernandez, *et al*. 2019b).

As fluid forcing and vegetation are two essential factors for levels of aeolian sediment transport, such indices invariably rely on wind and precipitation data, with the latter being recognised as the dominant control on vegetation cover (Hesp, 2002). Wind data is typically used to produce an annual figure for average

‘wind power’, or alternatively is expressed as a percentage of the average, with the purpose of calibrating the annual mean value to account for the number of days when wind speeds were above the threshold for sediment transport to occur (Tsoar, 2005). In addition to wind power, the influence of precipitation on vegetation can be further refined with the use of temperature data to encompass potential evapotranspiration (Lancaster, 1988). The indices have since been employed to determine mobility for dune fields in numerous locations globally (e.g., Ash and Wassen, 1983; Lancaster, 1988; McTainsh, *et al*. 1990; Muhs and Maat, 1993; Bullard, *et al*. 1997; Kocurek and Lancaster, 1999; Delgado-Fernandez, *et al*. 2019b).

Lancaster (1988) further denoted qualitative descriptors for dune fields, dependent on the resultant M (mobility) value derived from his mobility index. Dune systems with M values < 50 were identified as being fully inactive, and fully active dunes were associated with M values > 200. M indices of 50 - 100 generally resulted in vegetated dunes, with some active dune crests, while between 100 to 200 M, dune systems were described as being mostly active but with some vegetated inter-dunes, and/or lower slopes. Various nomenclature continues to be used describe the degree to which geomorphic change in dune systems is constrained by their vegetative state. Terms for heavily vegetated systems for which dune mobility is restricted by vegetation coverage fixing sand in place include fixed, vegetated, stabilised, inactive, impeded, and sealed. Most frequently, those for which geomorphic change is unconstrained by vegetation are described as free, mobile, active, or dynamic. Individually, dunes which are fixed in place to some degree by vegetation are sometimes termed impeded or anchored, and generically, the level of vegetation cover is acknowledged to result in differing dune forms (Davidson-Arnott, *et al*. 2019). Pye (1983) devised a series of descriptors for coastal dunes which included the typical dune forms associated with differing levels of mobility,

related to a spectrum surface vegetation, ranging from completely bare sand, up to fully vegetated. In general, blowout landforms are commonly associated with a sparsity of vegetation cover.

In addition to dune mobility at any given geographical location being an expression of the vegetative state associated with their regional climate, dune systems typically exhibit a high responsiveness to temporal variability in climate. Numerous case studies have explored the links between, dune field mobility or evolution, in relation to climatic conditions and vegetation cover (e.g., Seppälä, 1995; Hesp, 2001; Catto, *et al*. 2002; Gutiėrrez-Elorza, *et al*. 2005; Hugenholtz and Wolfe, 2005; Clemmensen, *et al*. 2009; Miot da Silva, *et al.* 2013). Studies which examine contemporary change over periods of decades invariably make use of time-series aerial photography, or satellite imagery, time-series LiDAR, or repeat, ground based topographic surveys, together with historic weather data sourced from proximal meteorological stations (e.g., Hugenholtz and Wolfe, 2005). Those seeking to establish phases of historic dune activity and stabilisation over geological time frames largely employ sediment coring or GPR (Ground Penetrating Radar) to examine dune stratigraphy (e.g., Clemmensen, *et al*. 2009; González-Villanueva, *et al*. 2011). The presence of paleosols are then routinely used to identify periods of dune stabilisation, as highly vegetated systems are associated with soil development. Radiocarbon dating and OSL (Optically Stimulated Luminescence) are common methods employed to date stratigraphic layers.

1.6.4. Recent trend of coastal dune stabilisation

Over the last century, and particularly for the past few decades, there has been growing recognition of an increasing trend in the rapid stabilisation of coastal dunes, through association with vegetation. Numerous studies have identified or

assessed the extent of this trend throughout a range of locations globally. These include, northern or western Europe (e.g., Rhind*, et al*. 2001; Jackson and Cooper, 2011; Provoost, *et al*. 2011; Pye, *et al*. 2014), the Americas (e.g. Seeliger, *et al*. 2000; Darke, *et al*. 2013), and Africa (Avis, 1989). This macro scale stabilisation is usually associated with climate change, relating particularly to conditions of increasing precipitation, increasing temperatures, and also the resultant longer duration of growing seasons (Jackson and Cooper, 2011). A non-exhaustive list of other factors cited as contributing to the stabilisation, or 'scrubbing up' of coastal dunes in many locations globally, include reduced windiness, the spread of invasive species, decreasing grazing activity (especially in connection with the impact of myxomatosis on rabbit populations), increasing atmospheric nitrogen deposition, and also the legacy relating to many decades of coastal dune management practices targeted at reducing mobility (Pye, *et al*. 2014).

From a purely ecological standpoint, coastal dune managers have largely viewed this 'over' stabilisation negatively, as it is typically associated with reduced biodiversity in absolute terms, and is additionally attributed to losses in a number of rare species of flora or fauna, which rely on bare sand habitats (van Boxel, *et al*. 1997; Houston, *et al*. 2001; Leege and Kilgore, 2014). In coastal dunes specifically, a confounding issue of foredune stabilisation by vegetation is marked reductions in the levels of sand transferred from the seaward beach, to the landward dune field. As a consequence of beach sand generally containing higher levels of shell content, it is relatively more calcareous, and therefore acts as a buffer to acidity. In the absence of such sand, which would otherwise serve to raise pH, soil in the secondary dunes rapidly acidifies, promoting further growth of scrubby vegetation (van Boxel, *et al*. 1997).

1.6.5. Dynamic restoration and foredune 'notching'

With the aim of increasing coastal dune biodiversity, and creating habitat for specialist, bare sand biota, a suite of management interventions have been introduced which promote sand dune mobility (Pye, *et al*. 2014; Cooper and Jackson, 2020). A range of practices which fall under the broad umbrella of dune 'restoration', or 'rejuvenation', are aimed at increasing levels of bare sand, aeolian dune dynamics, and often, sand supply to secondary dunes from the seaward beach area. Removal of dune vegetation, and the 'notching' of foredunes, which is essentially the creation of artificial, foredune trough blowouts, are the two most common practices (Arens, *et al*. 2004; Riksen, *et al*. 2016; Ruessink, *et al*. 2017; Cooper and Jackson, 2020). To date the success of such interventions has been mixed. Marked increases in biodiversity are often countered by temporal limitations associated with the rapid re-growth of vegetation.

With as yet, only a limited evidence base available to fully assess the implications of dynamic restoration, the relative merits, and particularly the long term effects of such interventions remain poorly understood. A number of researchers within the earth science community have criticised what appears to be prioritisation of the potential, or proven, ecological benefits, at the expense of geomorphological considerations (e.g. Cooper and Jackson, 2020). The intentional creation of instability within coastal dune systems, which are widely valued for their function as a protective barrier against coastal flooding is an obvious concern (De Jong, *et al*. 2014; Delgado-Fernandez, *et al*. 2019b). Something that has received less attention is a comprehensive discourse on the implications with regard to beach-dune interactions and sediment exchange, which are acknowledged to be the primary factors governing longer term coastal evolution (Psuty, 1988; Sherman and Bauer, 1993). The findings of the research presented here, and the theoretical context which underpins it, may therefore be timely in providing new,

and welcome insights into the current, ongoing debate (e.g., Delgado-Fernandez, *et al*. 2019a; Pye, *et al*. 2020; Creer, *et al*. 2020; Arens, *et al*. 2020).

1.6.6. Anthropogenic controls on coastal dune vegetation

In fully natural environments, coastal dune mobility/evolution is largely controlled by climatic conditions, and the associated vegetative state of individual dune systems. In a recent paper by Delgado-Fernandez, *et al*. (2019b), the mobility index of Lancaster (1988) was utilised to identify human disturbance on coastal dune vegetation. Using climate data for the region, an M index, and therefore the expected vegetation cover associated with the value was derived for Sefton dunes. At reduced spatial scales, comparison between observed vegetation cover, and expected cover proved successful in identifying dune field localities where human impacts rather than climate were the primary control on vegetation. Benefitting from a rich dataset which detailed spatio-temporal variability in land use, management practices, and visitor pressure, information was gained about the probable causes of divergence away from the expected vegetation cover at numerous locations along the coast.

Overall, since 1945, Sefton dunes exhibited a general trend towards stabilisation by vegetation, which was in line with the expected M value, (and the associated vegetative state), based on regional climate data. Despite this, a number of locations showed a pronounced divergence from the trend, with some having experienced expansion of bare sand areas. These locations were situated in the area of Formby Point, on National Trust land, and concentrated within the cross-shore zone accommodating the foredunes. Coincidence with primary beach access points/carparks, and peak visitor densities, bare sand was attributed to vegetation trampling by beach visitors. As the locations of the majority of current, discrete, bare sand patches are known to be foredune blowouts, the influence of

these landforms on longer term evolution can therefore also be directly linked to human impact. In Sefton, a primary mechanism of vegetation disturbance, and thus promotion of dune mobility, is through blowouts being initiated and maintained by visitor pressure. Supported by the findings of this paper, insights into the influence of human impact on coastal dune evolution can therefore also be gauged through assessment of the geomorphic change associated with the blowouts explored in this thesis, (as they are intrinsically linked).

1.7. Thesis Aims, Research Questions and Objectives

1.7.1. Aims

The overall aim of this thesis is to broaden understanding of aeolian sediment transport, and of geomorphic change, associated with foredune blowouts. Addressing the scarcity of knowledge with regard to instantaneous sediment transport at the event scale is a principle aim, as is understanding the implications of foredune blowout transport events to the evolution of coastal dune fields over extended time frames.

1.7.2. Research Questions

The project seeks to address the following four questions;

1) What are the characteristics of event scale, aeolian sediment transport and airflow dynamics in foredune blowouts?

2) Can improvements be made in respect of traditional analytical approaches for event scale, aeolian sediment transport data?

3) What influence do foredune blowout transport events have on the medium to longer term evolution of coastal dune systems?

4) Which environmental factors appear to be of primary importance to the frequency or magnitude of foredune blowout transport events?

1.7.3. Objectives

Objectives aimed at responding to the research questions and advancement of the project included;

1) Measure, analyse, and characterise instantaneous sediment transport in conjuncture with airflow dynamics, at the beach-dune interface of a foredune blowout.

2) Identify potential improvements to the analysis of high frequency airflow and transport data recorded in complex topography (as current methodologies limit the extent to which such data can be fully resolved).

3) Assess geomorphic change over the meso-scale at a retreating coastal dune field where foredune blowouts are frequent, and quantify changes in dune sediment budgets for retreating sections of the dune field where blowouts are present.

4) Identify factors which appear to exhibit control on transport activity at foredune blowout locations, and discuss their implications to dune managers.

1.7.4. Temporal Scale Terminology

The term *event* scale appears frequently throughout the thesis. This adjective delimits the temporal scale referred to by the duration of something happening, in the case of this research, a geomorphic event. Such events ordinarily occur over the short temporal scale and typically have duration ranges lasting for seconds, minutes, or hours. As their durations are determined by the start and end time of a geomorphic process being active, or a quasi-discrete piece of geomorphic work having occurred, their boundaries are ‘fuzzy’ and open to interpretation. Examples of such events in a beach-dune setting might include a quasi-discrete period of aeolian transport being active, or the duration for which a high tide is interacting with a foredune. That the start and end time of individual events can vary dependent on a multitude of factors including human perception, visual

observation, or sensitivity of measuring instruments, results in their 'fuzzy' boundaries. Negligible value is gained through achieving high levels of precision in delimiting such events, and arbitrary, rule of thumb decisions are the acceptable norm for geomorphic studies of this nature.

Research question 3 refers to 'medium to longer' term coastal evolution. Longer term, medium term, and additionally 'meso-scale' or decadal are used interchangeably throughout the thesis. For some readers, long term coastal evolution might be considered as occurring over temporal units of centuries, whilst other would assert that long term should more accurately refer to geological time frames. Meso-scale in the context of this research broadly relates to changes occurring over periods of several years, or on occasions being exactly a decade. Making in-text distinctions for instances when data did not permit use of exact 10 year units of time was deemed unnecessary and inconsequential to the meaning being conveyed. The findings of 'meso-scale' research are of particular relevance to coastal managers as significant management decisions, reviews of strategy, or assessment of intervention driven, bio-geomorphic change, typically occur over comparable time scales.

1.8. Knowledge Gaps, Motivations, Project Design and Relevance

The growing importance of coastal zones globally, and with associated research concerning coastal change was discussed in the early pages of this chapter. The decision to focus on coastal dune blowouts for this PhD, did in part come from a personal research interest. Frequent, high magnitude, foredune blowouts existing along my local coastline in Sefton was of course a factor in sparking my initial curiosity. Engagement with coastal/aeolian academic literature over time, and involvement with coastal dune research external to the PhD further developed

both my interest, and recognition of the critical role blowouts likely play in coastal evolution generically, and beyond my local coastline. The benefits gained from having a natural laboratory PhD study site, with several advantageous logistical features, simply ‘on the doorstep’, over time, and in all honesty, became a less heavily weighted factor.

That blowouts are recognised as areas of high relative, sediment transport activity, enhances their potential importance to longer term evolution. Knowledge gaps associated with event scale dynamics and regarding the influence they have on longer term evolution further validated the research.

1.8.1. Scale Related Issues and Approaches: Constructivism vs. Reductionism

Inclusion of both event scale and meso-scale elements within this project is an important facet of the research. The interplay between beaches and coastal dune fields over extended time scales have long been recognised. Strong adjustment between the sub-aqueous and sub-aerial environments (coastal winds and wave climatology) have been conceptualised in a variety of heuristic models which were discussed in section 1.6.2. (e.g., Short and Hesp, 1982; Psuty, 1988; Sherman and Bauer, 1993). These have provided explanations of foredune behaviour as part of overall systems comprising the nearshore, beach and dune field zones. Constructivist approaches such as these centre on theoretical models and allow a holistic understanding of beach-dune interactions over periods of months and years, to decades and centuries. The theories which underpin them are based on sediment budgets, cross-shore morphodynamics, beach types, and coastal cycles (Carter, 1988). These conceptualisations encompass well-reasoned explanations of coastal evolution, and typically do so across macro spatio-temporal scales.

Their descriptive nature relies heavily on interpretation, and on comprehensive knowledge of the geomorphic process-form responses in operation. Nethertheless, they are considered to be lacking in empirical evidence. Although providing valuable insights into large scale, and/or, longer term evolution, there remains an underlying dissatisfaction with their limitations. Like all scientific models, in character they essentially represent a simplified version of reality. As such, they depend on inherent assumptions about the nature and cumulative effects of geomorphic processes, which are known to exhibit pronounced variability across very small spatial scales and time frames.

As a consequence, there has been a resultant shift in the nature of investigations undertaken by the research community, towards an approach of reductionism. A principle driver in this being a consensus of belief that in order to understand longer term coastal evolution, or changes over greater spatial scales, the beach – foredune – dune field system must be broken down into smaller and smaller component parts. The motivation being, to first fully understand the workings of these components in fine detail, and subsequently seek to ‘upscale’ the findings over greater temporal and/or spatial scales. Not only have field experiments been scaled down to focus on specific landscape features, but often simplified wherever possible, in order to remove complicating factors, and to allow a better understanding of how individual controlling variables impact on specific processes. Hesp (2002) likens the project design of such research to tuning a radio, where if each major factor were a frequency control dial, all but one should be set as near as possible to constant. The objective being that the remaining variable can be altered or measured a number of times in order that, through experiment, the impact of this remaining variable can be more fully understood. These trends in research have been both facilitated and fuelled by the emergence of new

technologies, including the relatively recent availability of high-resolution, wind and sediment transport sensors (e.g., 3D ultrasonic anemometers, Laser Particle Counters, etc.), which are capable of measuring aeolian processes at increasingly finer temporal frequencies.

Potential outcomes sought from the growing evidence base of smaller scale, higher frequency measurements, of event scale processes include, the validation of conceptual models, assessment of the degree to which assumptions can be made about the contributions of specific variables, and seeking to parameterise specific variables for incorporation within improved evolutionary models. Progression towards these valuable outcomes has been hindered by numerous methodological/logistical shortcomings, as has extensive application of event scale results, due to a number of significant scale related constraints (Sherman, 1995; Bauer and Sherman, 1999; Aagaard *et al.* 2004; Davidson-Arnott, 2010; Masselink, *et al*. 2011; Bauer, *et al.* 2012; Walker, *et al*. 2017). Despite this, significant progress has been achieved through the growing evidence base. There now exists a much deeper understanding of event scale dynamics, and the inherent complexities within the beach-dune system. The nature of events have been found to be non-linear in character, with both airflow and transport dynamics typically exhibiting high spatio-temporal variability. Multiple positive and negative feedbacks, together with changeable degrees of hysteresis impacting a range of system variables further contribute the stochastic nature of individual field studies (Aagaard, *et al.* 2004; Houser, 2009). Along with this progress there has also been a growing appreciation of the numerous spatial and temporal scale discontinuities in existence (Sherman, 1995; Bauer and Sherman, 1999). These fundamental challenges strongly question the value in, or validity of, ‘up-scaling’ empirical

results from short-term field studies, with the aim of resolving evolution over much greater spatial and temporal scales (Walker, *et al*. 2017).

This project benefits from procurement of both, high resolution, event scale, process data, alongside a meso-scale, multi-epoch time-series of landscape scale geomorphic change. It is hoped that in the case of foredune blowouts, initial steps can be made in mitigating some of the scale related limitations, through identification of links, between any characteristics of the ‘event’ and ‘landform’ scale, field study, which are also expressed in some way within the longer term, landscape scale data.

Although such insights are of course highly desirable, they were not an explicit research aim of the design stage. That the project comprises two substantial, (and quasi-discrete) elements, which are most readily distinguishable by their respective, spatio-temporal scale, was unintended. Fundamentally this came as a consequence of prioritising the many blowout related knowledge gaps which exist. In the opinion of the author, it would be challenging to identify, and also difficult to then validate, alternative research problems, which are more pressing to the discipline than those selected (section 1.8.2 and 1.8.4).

Sections 1.3, 1.3.3, and 1.4 discussed the physics of aeolian sediment transport, together with a diversity of wind, sediment or surface controls, which may exert control over instantaneous transport, their relative importance, and a number of prominent inter-dependencies which exist between individual factors. Understanding of which factors are of primary importance, and which might be considered secondary, during individual events, and over extended time frames, is heavily constrained by the context of scale. Critically, because their relative

contributions to sediment transport exhibit pronounced spatio-temporal variability, both within discrete events, and between them. This characteristic has long been recognised as confounding realistic attempts to ‘up-scale’ empirical field data, into longer term models of evolution (Sherman and Bauer, 1993; Sherman, 1995). The complexity of the aeolian transport system, specifically in coastal environments, and our limited capacity to measure all the relevant parameters during individual events, means this particular issue persists, and for the time being has to be accepted (Walker, *et al*. 2017).

Sherman (1995) made a number of generalised suggestions as to which variables might be considered as critical to instantaneous, at-a-point, aeolian transport, during the event scale. The specific controls related to the wind system for instance, were limited to only speed, and direction. Over the past few decades however, much greater appreciation of the potential influences from the full diversity of wind parameters has been achieved (section 1.3.3). Likewise, the potential for, local environmental factors, such as moisture, vegetation or topographic airflow modifications, to significantly enhance, or retard sediment transport, is much better understood (Walker, *et al*. 2017). Given their composite effects to transport limiting conditions, and to sediment supply limiting conditions, are in character, highly variable between individual events, any level of confidence in predictive models of longer term evolution, decreases greatly at the point such event scale data is introduced. Additionally, effective measurement of numerous controls within the transport system, or parameterisation of their resultant influence is yet to be achieved. In this, Walker, *et al*. (2017) postulate that the bridging of spatio-temporal scales, continues to remain largely confined to identifying which controls appear to have been dominant, either during short field studies, or equally over extended periods. In doing so, technological advancements, and bespoke

field study designs, will in time allow the effects of those identified, to be truly quantified and characterised. The event scale, and the meso-scale components of this research, were formulated due to clear voids in knowledge concerning their explicit objectives. It must therefore be acknowledged from outset, that any insights gained in respect of the scale-discontinuities existing between the two discrete research elements, come from only the very first, and primitive steps.

1.8.2. Event Scale: Foredune blowout sediment transport: knowledge gaps

Two lines of enquiry have dominated research concerning blowouts. The first, largely during the early years of blowout related research, was dominated by studies regarding form, modes of initiation and progressive evolution. Most frequently, these form related papers proposed interpretative theories on initiation, and subsequently analysing evolution in relation to environmental settings.

The second, over more recent decades, and in line with the trend of 'reductionism' has been strongly focused on geomorphic processes. With the exception of a handful which make use of CFD (Computational Fluid Dynamics) modelling (e.g. Beyers, *et al*. 2010; Jackson, *et al*. 2011; Smyth, *et al*. 2012), the majority of these studies rely heavily on field measurements. In turn, the central theme of these event scale, process based investigations, concern airflow characteristics, and the dynamics of flow-form relationships. Technological advancements which introduced sensors capable of measuring airflow in three dimensions, and at very high frequency partly fuelled this shift in research focus. The cumulative contributions of these studies has also benefitted greatly by encompassing a diversity of blowout configurations, and a variety of incident wind approach angles. Incremental progress along this pathway has resulted in our knowledge and understanding of the dynamic and often complex patterns of airflow associated

with these landforms greatly improving (e.g. Hesp, 1996; Hesp and Hyde, 1996; Hesp and Pringle, 2000; Hesp and Walker, 2012; Smyth, *et al.* 2012, 2013, 2014; Pease and Gares, 2013; Delgado-Fernandez, *et al.* 2018). A brief synopsis of development in the understanding of airflow dynamics were covered earlier in the chapter (section 1.4.4.).

Whilst blowout airflow dynamics have been well characterised, this is not the case for transport. Although a by-product of many studies is often the inclusion of commentaries relating to sediment transport, they are typically based solely on field observations or topographic inference, and blowout studies including the synchronous measurement of quasi-instantaneous transport are rare. To date, the majority of studies which examine, or offer commentaries on sediment transport within blowouts, have based interpretations on geomorphic change measured using erosion/depth of deposition pins, and/or repeat topographic surveys (e.g. Gares and Nordstrom, 1988; Jungerius and van der Meulen, 1989; Jungerius, *et al.* 1991; Byrne, 1997; Bitton and Byrne, 2002; Hugenholtz and Wolfe, 2006; Käyhkö, 2007; Hugenholtz, *et al*. 2009), and the first early attempts at measuring actual transport in relation to wind speed were conducted over extended periods of time (Pluis, 1992; Hesp and Hyde, 1996).

As yet, very few investigations have measured quasi-instantaneous, near surface wind characteristics in synchronicity with transport (e.g. Anderson and Walker, 2006; Smyth, *et al*. 2014; Sun, *et al.* 2016; Hesp, *et al.* 2017; Delgado-Fernandez, *et al.* 2018). Of these, the only study to capture the synchronous transfer of beach sediment to the landward dune field via a blowout was Walker and Anderson (2006), albeit with very limited transport activity occurring due to continuous rain. Hesp, *et al.* (2017) provided further advancements with their study of a ‘cauldron and corridor’ foredune blowout, but the use of a roving anemometer limited

insights for potential landform scale flow, and resultant patterns (or pathways) of sediment transport. In contrast to this research project, the remaining three studies concerned relatively ‘closed’ blowout systems. Smyth, *et al.* (2014) did detail a coastal blowout, however it was situated in the lee of the foredune. For the blowout-parabolic study of Delgado-Fernandez, *et al.* (2018), the site was within a vegetated dune field, and finally, the field setting for Sun, *et al.* (2016) was a continental grassland environment.

As a result of only limited research, the dynamics of event scale, aeolian sediment transport in blowouts remains poorly understood, and no more so than in respect of foredune blowouts, (which occur at the beach-dune interface). In this project, the measurement, and in depth analysis of event scale, synchronous, high frequency flow and transport dynamics at a foredune blowout, provides the first step in addressing this knowledge gap. That the validity of deterministic models used to predict transport is highly questionable in topographically complex, coastal settings, supports the methodological direction chosen. Making an initial contribution to the comprehensive base of empirical evidence which will be needed to fully resolve this phenomenon further validates the approach.

1.8.3. Event Scale: Methodological Approach and Rationale

Early geomorphological science was strongly focused on the form of the land surface, classification of features, and theoretical work around landscape/landform evolution. In growing recognition of the limitations and uncertainty associated with this constructivist approach, reductionism has revolutionised the discipline. Spanning several decades now, there has been huge growth in studies exploring the geomorphic processes which shape the land surface. Whilst descriptive and interpretive discourse might offer explanations of landscape dynamics, (often over extended time frames), process based geomorphology inherently concerns

geomorphic process-form dynamics occurring over reduced spatial and temporal scales. The new contributions to knowledge gained incrementally with each study conducted, invariably also highlight new gaps requiring further investigation. As a consequence, and fuelled by continual advancements in technology, organic development in the nature of process based coastal geomorphology continues. Field based studies typically measure geomorphic processes (and more recently, on occasion, also morphological response) over confined spatial scales. These may concern pre-defined spatial domains of the land surface, be designed to provide spatial coverage at the individual landform scale, or even be specifically focussed upon a discrete landform feature/point location(s). The duration of such studies are invariably constrained by the logistic necessity of instrument deployment in the field for the measurement of processes. The frequency at which measurements are taken have also greatly increased, and advancements in sensor capabilities have led to sub-second sampling now being customary.

For many decades, and to some extent still, dogged efforts to resolve, validate or improve deterministic models of sediment flux, controlled experiment design. A large body of work to this end involved the use of wind tunnels to modulate fluid forcing (e.g. Wiggs, *et al*. 1996; Nickling and McKenna-Neuman, 1997; Goossens, *et al*. 2000; Dong, *et al*. 2003; Barchyn, *et al*. 2014). Despite many successes, it is acknowledged that natural conditions cannot be truly replicated in laboratory conditions. In being inherently unrepresentative of the natural environment, the application of their findings are relatively more constrained, leading to the use of this methodological approach being less frequent than in the past.

The characteristic complexity of coastal and aeolian geomorphic systems is also associated with a multitude of technological and logistical issues. The vast number

of factors influencing flow and transport, being prohibitive of comprehensive measurement of all variables is fundamental. Acute spatio-temporal variability in processes adds further complexity. Typically, choices are required in experiment design, and multiple playoffs are involved in these choices. The focus, or purpose of each study informs the decisions taken. A very limited set of examples include, simplicity or otherwise of the field setting, which variables to measure, the density of the instrument array, choices around the most appropriate instruments to be used, and if horizontal, or vertical variability in airflow and/or transport can be encompassed. Further, time and resources have overarching controls on these decisions.

As a discipline, there remains complete acceptance that multiple limitations persist in all studies of this nature (e.g. Sherman, 1995; Bauer, *et al*. 2013; Walker, *et al*. 2017). As a rule, a variety of assumptions have to be made, and unavoidable constraints acknowledged. Wherever possible, the extent to which this is the case needs consideration, justification, and ideally, attempts made to mitigate the resultant implications in respect of any findings. Specifically, with regard to sediment transport measurement, the capabilities of individual instrument types, and whether they can be used effectively in specific environmental settings/conditions, exerts significant control over the decisions made. Problems associated with lag times between instantaneous transport and its measurement, an inability to accurately account for grain size variability, generally having to treat transport as a scalar rather than vector property, and differences in sensor accuracy, and/or sensitivity are all important issues to be managed (Sherman and Bauer, 1993). As improving our knowledge of the relationships between fluid forcing and transport response, are of primary interest, a persistent inability to

measure airflow in the very near-surface zone in which transport occurs, places further constraints on contemporary methods.

The event scale investigation in this research makes use of state of the art technology. Early experiments of this type which included measurement of airflow, employed much more rudimentary sensors than are available today. Mechanically based cup anemometers for speed, in conjunction with wind vanes for direction provide one example of traditional instruments which have been used extensively (e.g. Bauer, *et al*. 1990; Arens, *et al*. 1995; Hesp and Hyde, 1996; Sherman, *et al*. 1996). The research presented here benefits from, multi-dimensional, ultra-sonic anemometry. The instruments used are capable of recording airflow at high frequency and precision. In allowing measurement of flow in the streamwise, spanwise, and vertical, the direction of airflow vectors can be more truly represented, and levels of flow turbulence also parameterised. Facilitating inclusion of these wind properties, in high resolution, is recognised to greatly improve the understanding of events. Although not within the primary transport zone, instrument design allowing measurement of near-surface flow, and comparison of synchronous flow at multiple point locations also permits well-reasoned interpretations of topographically induced flow modifications, a factor known to be of great importance to aeolian dynamics in complex coastal dune terrain. The value of ultra-sonic anemometry is now heavily documented, and its use considered standard practice in studies of this nature (e.g. Walker, 2005; Jackson, *et al*. 2011). The instrument deployment for airflow measurement used in this study replicates the generic methods of numerous similar experiments (e.g. Smyth, *et al*. 2012, 2014; Delgado-Fernandez, *et al*. 2018), with available resources, and the individual physical setting simply informing the specific layout providing optimal benefits. (Details of which are covered in chapter 2). Finally regarding airflow, in less complex topographic settings, many studies make use of

quadrant and Reynolds stress analysis to optimise instrument deployment, and to gain further insights into transport activity (e.g. Chapman, *et al*. 2013). In acknowledgement that airflow would be complex and non-logarithmic, no attempt was made to employ these methodologies, or to align sensors with local streamlines.

Accurate measurement of aeolian sediment transport at high frequencies is achievable through a range of acoustic, laser based, or piezo-electric particle counters, or with weight based sediment traps (Ellis, *et al.* 2009, 2012; Sherman, *et al.* 2011). Deterministic models of aeolian transport (section 1.4), predict sediment flux in volume, based on (quasi), near-surface airflow, and in the main, idealised conditions. The acute complexity of the study location therefore guaranteed there would be very little value in exploring event scale, measured transport, with any equation based model forecast. Quantification of mass transport would however have been informative, as would calibration of grain count data, with absolute volume. This can be achieved through the co-location of a weight based sediment trap, with a sensor which records grain counts (e.g. Barchyn, *et al*. 2014). The topographic complexity of the site in this study was however prohibitive of the use of sediment traps, as their deployment relies on planar, quasi-uniform terrain. This focussed the investigation of sediment flux on the variability in transport intensity, quantified by grain counts per unit time.

Transport intensity is this study was measured with Wenglor© Laser Particle Counters. Access to these instruments was the most significant factor in their selection. The reason for this pre-determined choice however strongly justifies their partly enforced selection. Resources used in the event scale element of this PhD were highly dependent on their procurement from the niche research community that myself, and my supervisory team form a part. Experimentation

with a variety of alternative instruments over the last two decades has brought to light the numerous logistical, and precision limitations of other potential sensors. Reducing sensor accuracy over experiment duration, quasi-instantaneous variability in sensor accuracy being dependent on transport intensity, and variability in sensitivity between instruments, offer some of the most important (Davidson-Arnott, *et al*. 2009; Ellis, *et al.* 2009,2012; Sherman, *et al.* 2011). This has led to a gradual shift towards the sensors employed now being widely considered as the optimal choice. Ease of deployment in complex topography, acknowledged quality of measurement, and very limited relative variance between sensors being their three important advantages (Davidson-Arnott, *et al*. 2009, 2012; Barchyn, *et al*. 2014).

As secondary airflow modifications are characteristic of complex topography (such as that of foredune blowouts), it was acknowledged pre-experiment that this was an important consideration. In seeking to understand transport dynamics, and in the knowledge that acute modifications to fluid forcing would exert a strong control on transport, accurate representation of site topography was also highly desirable. Regular airborne LIDAR surveys are undertaken at the site as part of the Environment Agency's national monitoring program. As dune topography experiences geomorphic change over very short times scales, and that the DEMs, Digital Elevation Models, derived from the most recent surveys had a spatial resolution of 1m, a finer resolution terrain model would provide closer representation of topography during the event. With this, interpretation of potential airflow modifications occurring in real time are also improved, and more strongly supported. To allow rapid capture of high resolution topography, topographic surveys were acquired through the use of a TLS (Terrestrial Laser Scanner). This methodology is the most advantageous method available. TLS surveys are far less time consuming than the alternative method of DGPS Differential Global

Positioning Systems survey, and of course than other, even less favourable survey options (e.g. Nield and Wiggs, 2011; James and Quinton, 2014; Gillies, *et al.* 2014). They also offer the highest potential resolution, together with the optimal accuracy, providing best practice survey procedures are followed (Smith, 2015).

Although the norm for almost all short term, process based aeolian experiments is to limit field measurements to airflow and sediment transport, pre and post event topography proved to be a highly valuable additional dataset in a recent similar study (Delgado-Fernandez, *et al*. 2018). The primary generic objective of event scale studies of this type is to address knowledge gaps concerning instantaneous geomorphic processes. Beyond the value of this in itself, gaining improved understanding of relationships between event scale processes and longer term morphological change is an overarching motivation. As coastal dunes have high relative responsiveness to such geomorphic processes, dependent on event magnitude, and the scale of the study site, there is some potential to assess geomorphic change, specifically related to its respective individual event. Quantifying the process-form response over a short duration obviously has advantages over making interpretations of longer term dune evolution, solely through the use of process based, time-series data. Pre and post event TLS surveys were therefore undertaken based on the potential of gaining an additional, and informative layer of evidence.

A key limitation of both wind and sediment flux instrumentation is that they provide only ‘at a point’ measurements, and as both airflow and transport typically demonstrate acute spatio-temporal variability it remains a challenge to understand their characteristics fully (Baas and Sherman, 2006; Ellis, *et al.* 2009; Bauer, *et al.* 2012). This limitation however, can be greatly mitigated through the deployment of grid based instrument arrays such as that selected for the event scale

investigation in this study. In addition to quantification of this variability, interpretation of the flow and transport record at a specific point location can potentially be improved through comparison with the records of proximal sensor locations. Interpretation of the event could also be further improved through relating variability in flow and transport dynamics to the topographic setting and expected topographic modifications that may be characteristic of individual sensor locations.

Discussion of the most important additional factors which influence aeolian sediment transport were given concise coverage earlier in the chapter. Sediment characteristics, the presence of moisture, and the presence of vegetation are all known to be important considerations.

No grain size analysis was conducted as part of this research. This was also the case for a very recent study, comparable in character, and also conducted at Sefton dunes. As grain size (and variability therein), are vital components of deterministic sediment flux models, they are typically only assessed for studies which seek to compare measured transport, with model predicted transport. In knowing predictive transport models are wholly unsuitable for use in complex topographic settings, there use in this study had already been excluded prior to experiment design. An awareness of sediment characteristics in Sefton further supported the exclusion of grain size analysis. The Sefton coast is composed of medium to fine, quartz rich sand. In absolute terms, as variability within this size fraction is only marginal, it was considered inconsequential, and deemed of insufficient value for inclusion.

No survey of vegetation was conducted for the event scale investigation. As is customary for studies of this nature, assessment of vegetation coverage, and

density was limited to recording visual observations, and the procurement of photographic evidence. All instruments were positioned in field locations with zero, or only immaterial, trace levels of vegetation in their immediate surroundings. Based on this information, the influence of spatial variability in vegetation coverage was also considered, and discussed within the analysis.

Finally, the presence of moisture has the potential to exert a primary control on event scale sediment transport, and particularly its spatio-temporal variability. In the days leading up to the experiment, only trace levels of precipitation had occurred, and high tides had not reached the back-beach or foredune line. Surficial sediment in the back-beach area, across the foredunes, and within the blowout were therefore completely dry. Sediment transport across the inter-tidal beach had been initiated shortly before commencement of data recording. Irrespective of incident winds being directly onshore, or as they were at this time, onshore-oblique, the fetch length of the inter-tidal beach where transport was active, was many hundreds of metres in distance. The swash line immediately prior to launching the data loggers was of such distance, that it was not clearly visible to the naked eye.

Although highly dynamic, the character of this extensive beach system is persistently that of three dimensional, bar and trough topography. In its seaward extent, complete drying of beach troughs is rare. Typically, multiple patches of beach surface within trough areas maintain high levels of moisture, and patches being affected by the ponding of surface water for the duration of tidal cycles is also common. The daily distribution of such patches is stochastic, in part reflecting the high dynamism of micro beach topography. Given the length of fetch, and the nature of aeolian streamers, to the naked eye, cross-shore transport appeared to

be active throughout the entire beach width. Although imperceptible, in reality, cross-shore transport activity will have been intermittent, and interrupted by areas of high water content. As a consequence, levels of sediment arriving to the back-beach from the inter-tidal zone would have certainly included some degrees of temporal variability. Further irregularity will have also been introduced by spatio-temporal variability in the rate at which the beach surface was drying.

Understanding the influence of moisture on beach transport has been disregarded in this event scale study. A finite number of data loggers, limited personnel, the logistics of time limited instrument deployment during the falling tide, and the inability to achieve systematic coverage across the extent of the inter-tidal zone, provide just a few of the factors which contributed to this decision. As measurement of transport dynamics in the area of the beach-dune interface was the principle knowledge gap to be addressed, incorporation of beach transport analysis, and the impact of beach moisture on this transport, could not be included, or justified. A multitude of research gaps around the moisture variability associated with bar-trough topography, and resultant fetch-limited beach transport patterns remain unanswered. The author, together with, Delgado-Fernandez and Jeff Ollerhead (Mount Allison University) undertook some preliminary field experiments in Sefton a few years prior to this study. Further investigations across a range of locations remains a research opportunity for the future. The scope of work necessary to make any reasonable assessments of the potential implications of beach moisture to blowout transport for inclusion here, validated its omission. Beach transport intensity, and therefore delivery of sediment to the back-beach over the short experiment duration was essentially treated as being steady.

1.8.4. Meso-scale: Geomorphic change and the role of foredune blowouts in coastal evolution: Knowledge gaps

Dune blowout evolution has been a relatively common research theme, particularly so in early studies. Most often, such studies have described the evolution of individual, or small collections of dune blowouts, frequently with reference to the potential, site specific, environmental controls identified as being of greatest importance. To the knowledge of the author, no study has quantified meso-scale, foredune blowout, geomorphic change with any detail, nor performed coastal dune sediment budget analysis, in direct association with these landforms. Importantly, very little is known about the influence that foredune blowouts may have on the evolution of coastal dune fields at the landscape scale.

1.8.5. Meso-scale: Theoretical Background

Generically, a desirable outcome of short duration, process based, coastal field studies, is that comprehensive understanding of such events may allow longer term geomorphic change to be better explained, together with gaining an improved ability to predict future coastal evolution. Whilst investigating the dynamics of foredune blowout transport at the event scale addresses the scarcity of knowledge regarding how instantaneous sediment transport occurs, understanding the implications with respect to longer term evolution is no doubt of equal importance. Multiple threads within established, coastal geomorphology theory point towards such events being of significant consequence to meso-scale trends. Despite the rationale for this research being strongly supported by wholly acknowledged concepts in coastal science, as yet, surprisingly little attention has been paid to the influence of foredune blowout, sediment transports, on longer term, landscape scale evolution.

Irrespective of a continental or coastal setting, dune blowouts generically are recognised as zones of high relative sediment transport, and thus a key role in the dynamism of dune landscapes. Even in ‘closed’ blowout systems, this facet can be attributed to the occurrence of either, or both of, the physical characteristics associated with blowout genesis. These being, an increased susceptibility of the surface to deflation, and local topographically induced enhancements to airflow which promote aeolian transport. Commonly used descriptive terms for these landforms, such as ‘highly efficient or effective, sediment transport pathways, or corridors’ highlights their second characteristic of potentially great importance. In addition to ordinarily experiencing higher relative deflation of *in situ* sediment, their frequent association with the significant ‘throughput’ of sediment, derived externally to that available from their host dune, may result in disproportionate levels of geomorphic change. Regardless of absolute sediment transport in volume, that the total quantity of sediment flux for any individual blowout may include a major additional contribution associated with throughput, offers noteworthy potential enhancements to geomorphic change over time.

With foredune blowouts being fronted by the substantial additional sediment source of the seaward beach, in all probability, irregularly high contributions to total flux that are associated with sediment throughput will likely be relatively more frequent, than is the case for blowouts in non-foredune locations. Beyond these characteristics, the topographic setting of foredune blowouts within the larger beach-dune system is of critical importance to their role in longer term, landscape scale evolution. Long standing and accepted conceptual models (Psuty, 1988, Sherman and Bauer, 1993) identify sediment exchanges between the beach and the foredune as overriding controls on the evolution of dune fringed coasts. As landforms associated with heightened transport activity, it follows that blowouts positioned within foredunes may provide relative enhancements to beach-dune

sediment exchange, and therefore be of great significance to landscape evolution. Despite these assertions being in no way novel, any exploration of the nature of their contribution to evolution, or attempts to quantify them are absent. This represents a glaring and specific void in current understanding.

Given their associations with sediment transport and their critical position in the cross-shore profile, a working hypothesis of this study is that the presence of blowouts within a foredune may promote and enhance coastal erosion. The rationale for this research project therefore falls within the context of extensively applied conceptual models of beach-dune sediment exchange (e.g. Psuty, 1988). Figure 1.2 summarises some of the key aspects of these principles, and Figure 1.3 provides the conceptual framework supporting the need for investigation. Sediment input to foredunes is primarily in the form of aeolian transport (Bauer and Davidson-Arnott, 2002; Delgado-Fernandez and Davidson-Arnott, 2011). Although marine processes can also deliver relatively small quantities of sand to coastal dunes (Cohn, *et al.* 2018), coastal waters are in the main responsible for the large majority of foredune losses, through the mechanism of wave scarping and sediment removal during storm surges (Fig. 1.2 (A)).

The balance between sediment inputs and outputs over a particular period determines the foredune sediment budget, and hence changes to the volume of sand stored in these coastal sinks (Fig. 1.2 (B)). Under positive sediment budget scenarios, foredune volume has experienced growth. This can be translated in either coastal progradation and/or increases in foredune height and width. That is, foredunes can both accrete in size whilst holding their position, and/or prograde seawards by embryo dunes forming seaward of the foredune toe, and subsequently welding onto the foredune, so that the position of the beach-dune boundary migrates in an offshore direction. This process occurs when aeolian

sediment input to the foredunes exceeds any sediment losses through episodic marine processes, such as wave scarping, or potentially washover, (with the latter being negligible at the study location in Sefton due to foredune amplitude and a large, dissipative, inter-tidal zone).

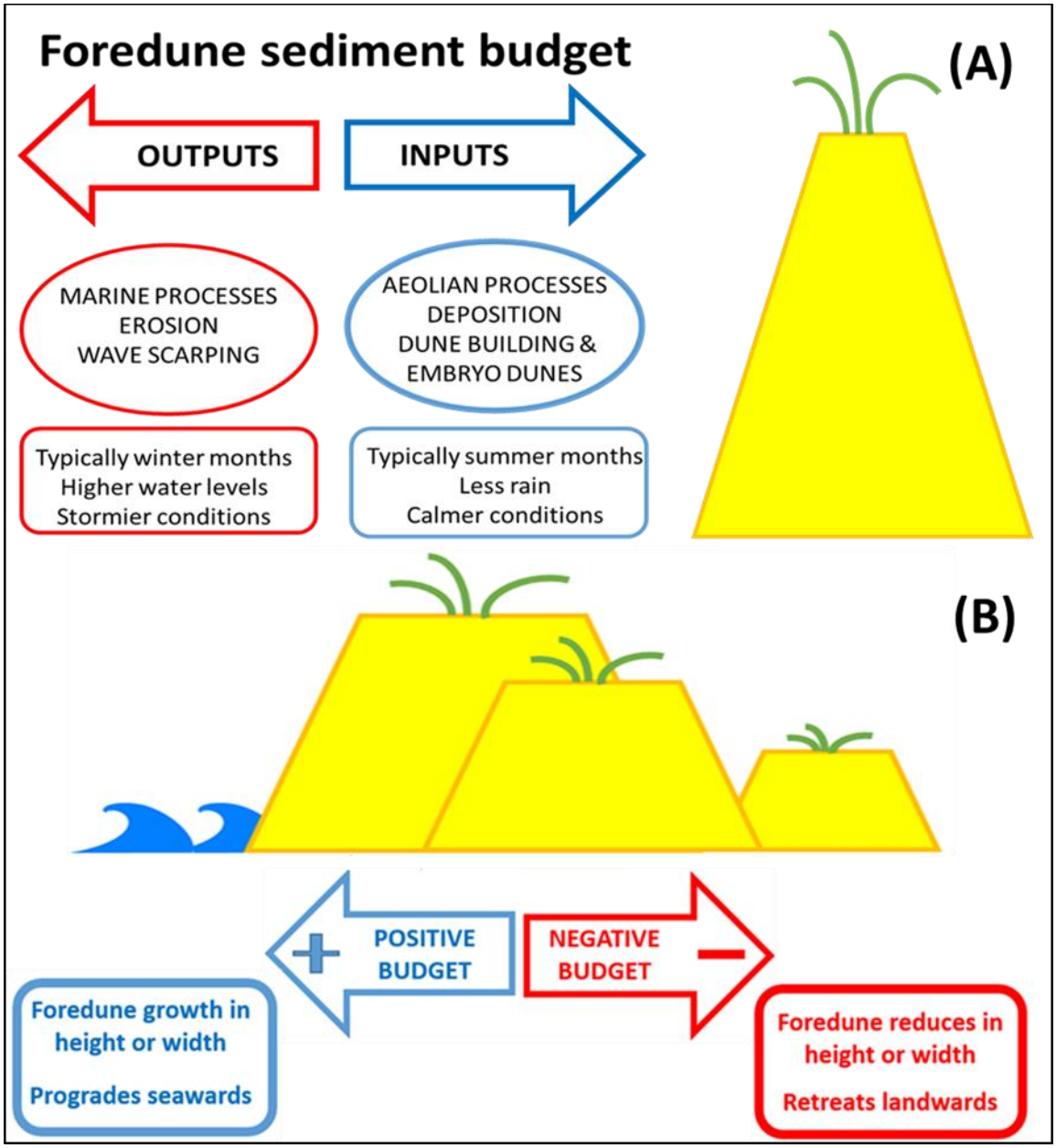

Figure 1.2: Beach-dune sediment exchange and geomorphic responses to changes in foredune sediment budget.

If however, in a given period of time, the amount of sediment being input to the foredune is reduced, the probability of a net negative balance over a given period of sediment exchanges increases, and as a consequence, so too does the likelihood of coastline retreat. That is, under negative sediment budget scenarios, the amount of sediment removed by marine processes would be a relatively higher

proportion of the total dune sediment budget, and if this proportion exceeded inputs, the foredune would erode. This erosion can manifest as coastal retreat, or decreases in foredune height and/or width.

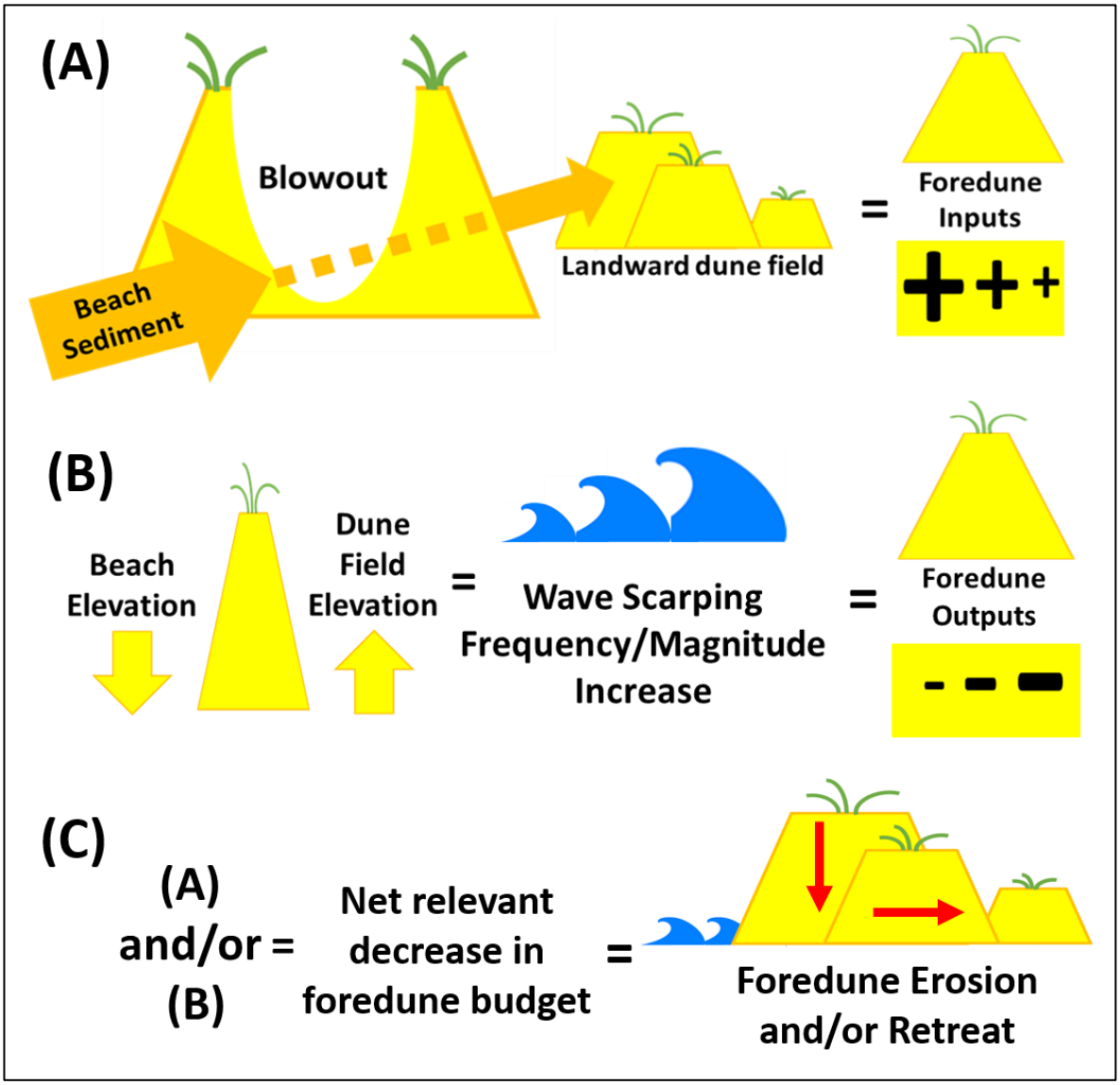

Figure 1.3: Impacts of foredune blowouts on beach-dune sediment exchange and resultant geomorphic responses.

An underlying hypothesis of the research is that the presence of foredune blowouts interfere with beach-dune sediment exchanges, thereby exerting an inordinate degree of control on foredune sediment budgets and evolutionary trends (Fig. 1.3). As foredune blowouts are transport corridors, sand delivered by wind from the beach, can bypass the foredune via blowout ‘corridors’, to be ‘directly’ transferred and deposited deep within the landward dune field. In the

absence of blowouts, subsequent to wave scarping events, this sand would ordinarily aid foredune recovery.

Since sediment bypasses the frontal dunes rather than being deposited within them, the presence of blowouts leads to a relative reduction of sediment input to the foredune itself, increasing the probability of a negative foredune sediment budget (Fig. 1.3 (A)). In turn, this increases the probability of foredune erosion (expressed as retreat or a reduction in foredune size), as the amount of sediment the foredunes receive in a given time period will have foregone the amount that was transferred quasi-directly through the blowout ‘corridors’ to the landward dune field.

Additional to this, sediment output from the foredunes in the presence of blowouts is also likely to show relative increases. As blowouts promote the landward transport of sediment, over time a proportion of the sediment that would ordinarily be repeatedly cycled between the beach and the foredune, is transferred via blowouts to the landward dune field (Fig. 1.3 (A)). As a consequence, all things being equal, this will also result in a relative decrease to beach elevations, at the expense of an overall increase in the mean elevation of the dune field. Decreasing beach elevations have the mutual effect of reducing the inter-tidal beach width, and both of these geomorphic changes lead to increases in the frequency and/or magnitude of wave scarping to the foredune (Fig. 1.3. (B)). Decreases in foredune inputs (Fig. 1.3 (A)), and increases in foredune outputs (Fig. 1.3. (B)) both increase the probability of a negative foredune sediment budget, likely resulting in reductions in foredune amplitude and/or coastline retreat (Fig. 1.3 (C)).

Two other theoretical points of note regarding the potential for foredune blowouts to enhance coastline retreat further motivated the project. The first is largely

anecdotal, yet to be supported by studies, and therefore lacks an evidence base of empirical findings. It is however reasonable to assume that a continuous, well vegetated, linear foredune would be more robust to the effects of wave scarping, than one which is heavily fragmented by the presence of blowouts. That blowouts are associated with 'bare' or sparsely vegetated dune topography also means that linear foredunes characterised by frequent blowouts are intrinsically less well conserved by vegetation, than foredunes with an absence of blowouts. As vegetation is wholly accepted to protect surficial sediment from erosion, and to promote dune stability by the binding, or 'fixing' of sediment in place, it follows that foredunes with a high frequency of blowouts are likely to enhance coastal dune erosion simply by being more susceptible to sediment losses by both marine and aeolian processes. Equally, as vegetation is also recognised to play an important role in dune accretion, by trapping windblown sediment, the scarcity of vegetation in blowout locations undoubtedly reduces foredune resilience by inhibiting post storm recovery, thus further promoting longer term trends of retreat.

Finally, beyond visitor pressure being involved in the initiation and maintenance of foredune blowouts, vegetation trampling is often also reflected in a sparsity of vegetation cover across the seaward face of the foredunes themselves. The erosion of sediment by longshore deflected winds, directly from foredunes flanking individual blowouts therefore becomes a process of higher probability. There is now a significant body of literature suggesting the occurrence of alongshore, foredune deflected wind is an event of high frequency (e.g. Walker, 1999; Walker, *et al.* 2006; Bauer, *et al.* 2012). Studies which encompass measurement of transport however remain limited. In addition to the direct transfer of beach sediment, this deflected airflow may entrain sediment from the foredune itself, which is transferred longshore until blowouts are reached, facilitating landward directed transport. Longshore transport and the vegetative state of the seaward

foredune slopes, may therefore also be important factors in promoting coastline retreat associated with blowouts.

1.8.6. Meso-scale Motivations and Rationale

Whilst foredune blowouts are typically classed as erosional landforms, they are generally considered to be a symptom of coastal erosion rather than a principle root cause. Psuty (1988) considered their initiation simply reflected a temporary deficit in sediment supply. He surmised their presence to be short lived, with blowout longevity being aligned with the passing of a limited period of time prior to the balance of beach-dune sediment exchanges being restored to a quasi -'steady state' of equilibrium (Sherman and Bauer, 1993). In having the capacity to limit, post-storm dune recovery, to significantly alter the nature of beach-dune sediment exchanges, and to reduce the overall beach-foredune budget through allowing the landward transfer of sediment to secondary dunes, they have potential to enhance erosional trends. This function of facilitating total system (nearshore beach/foredune) budget losses via sediment transfer to the landward dune field is essentially disregarded in the Psuty model (1988). This does represent a clear shortcoming in a heavily utilised, and frequently effective model of coastal evolution. Quantification in this study, of the extent to which this mechanism may influence geomorphic change, offers a potential enhancement to the model, and opportunities for improved validity when applied to coastal systems which are characterised by blowouts in the frontal dunes.

At the landscape scale, and over extended time frames, the evolution of coastal dune systems is an expression of the cumulative effect of a multitude of smaller scale, short duration geomorphic events occurring during the intervening period. Gregory and Lewin (2014) described landforms as being the building blocks, (and therefore smaller scale geomorphic units) of landscape systems. It is hypothesised

in this research that as foredune blowouts may strongly influence fundamental sediment exchanges, they may equally exert enhanced control on the rate and direction of evolutionary trends. Assessment of the nature and extent of geomorphic changes associated with these landforms over the meso-scale will inform on their relative importance in to evolution. Through this potential enhanced influence, it is proposed that short duration, landform scale, foredune blowout transport events, may strongly impact, landscape scale, longer term change. To date, although a widely accepted process, evidence of foredune blowouts being involved in the transfer of beach and/or foredune sediment to the landward dune field is largely anecdotal, descriptive, and lacking in empirical evidence.

Despite this, and motivated by ecological benefits, the creation of artificial foredune blowouts (‘notching’), is a dune management intervention experiencing rapid growth in popularity. One of a suite of practices which are collectively termed ‘dynamic restoration’, the desired effect of ‘notching’ is to promote sediment transfer from the seaward beach to the secondary dunes, landward of the foredune. Additionally, in stripping vegetation from the foredune, and often also in landward areas, it is hoped that heightened aeolian activity may be sustained naturally, and these geomorphic processes will reduce rates of vegetation recolonisation/re-stabilisation. Multiple choices have to be made pre-intervention with a view to optimising the desired effects, and to mitigate any potential negative impacts. As yet, only a very limited evidence base is available to inform managers on the most important controls. This constrains the effectiveness of how such choices are prioritised. As an example, a few obvious decisions from the multitude that might be considered include, optimal longshore position, ‘notch’ configuration, foredune geometry, and coastline orientation relative to prevailing winds. Research concerning blowouts, whether detailing event scale sediment transport

dynamics, or longer term geomorphic change in foredune blowouts, and resultant dune field evolution could therefore greatly inform dynamic intervention management strategies.

As a consequence of the complexity of aeolian sediment transport dynamics, and the diverse array of local environmental factors, many of which have strong inter-dependencies, the extent to which knowledge gained from individual field studies can be broadly applied is often limited. A frequent comment in the concluding remarks of such papers is to suggest the need for further studies, with similar instrument deployments, but which encompass a change to one of the environmental variables which appears to have exerted strong control on the reported event. Differing wind approach angles, levels of vegetation cover, and alternative landform configurations are common. The frequency, magnitude, locations, and characteristics of foredune blowouts likely all have potential implications on aeolian activity, sediment transport pathways, and dune field evolution. Research evaluating coastal evolution in the presence of foredune blowouts is extremely scarce and therefore a specific gap the thesis seeks to address. This study assesses geomorphic change associated with foredune blowouts over the meso-scale, that which is of most relevance to coastal managers. Quantification of sediment transfers and characterisation of geomorphic change over the extended time frame used in this study offers an empirical evidence base to inform both the management of coastal dunes where blowouts occur *naturally*, and to those considering artificial creation via 'notching'.

1.8.7. Motivations and rationale specific to the Sefton Coast study location

The Sefton Coast, NW England is the study site for all research presented in the thesis. The longshore section of Sefton dunes, which is retreating at a rate of up to ≈4 m pa is characterised by a high frequency of foredunes blowouts, making it an

ideal natural laboratory for the research. A specific objective of the thesis is to measure event scale, aeolian sediment transport dynamics in a foredune blowout location. Whilst Pye and Blott (2016) have previously observed this occurrence at the study site, empirical evidence supporting their observations is required. As events of this nature directly promote the landward transfer of sediment, and therefore dune field treat associated with foredune blowouts, empirical evidence detailing the extent to which this may be the case is needed. Quantification and characterisation of this process over the meso-scale, (that which is of most relevance to managers), is a direct route to impact for the research.

At Sefton explicitly, and also more generally, coastal erosion is often linked exclusively to marine processes, with limited information on the role played by aeolian processes or the presence of foredune blowouts fragmenting coastal dunes (Pye and Neal, 1994; Esteves, *et al*. 2012; Mir-Gual, *et al.* 2015; Pye and Blott, 2016). Coastal erosion, or more specifically foredune retreat in the vicinity of Formby Point at Sefton is strongly associated with marine processes. The principle mechanism of incremental retreat has been identified as continual wetting of the dune toe which leads to ‘slumping’ or slope failure of the foredune face (Pye and Blott, 2016). Lower frequency, but high magnitude dune scarping has been linked to a variety of marine related conditions. Although the list in not exhaustive, these include; the coincidence of spring high tides with storm surge, the combination of wave run up and tide height exceeding specified elevation thresholds, the duration water levels remain above a specified threshold, total water levels exceeding a specified threshold on concurrent tides, and the width of the ‘back-shore’ falling below a minimum distance (Pye and Neal, 1994; Esteves, *et al*. 2012; Dissanayake, *et al*. 2015; Pye and Blott, 2016).

To date, the contribution of aeolian processes to coastline retreat at the study site is treated only as a secondary factor and considered to be of minor significance. A potential influence on this perception is that aeolian transport events involving the transfer of beach and foredune sediment landwards via blowout pathways, are most often relatively short in duration, and individual, high magnitude events are rare. This suggestion regarding magnitude is however in the main, simply a perception, and one that may also be influenced by human bias. As marine erosion events are strongly focussed within the confined spatial extent of the dune toe, at beach-dune interface, their effects are highly visible, and in the immediate days following a storm, a reasonable view on their relative magnitude is feasible through human observation with the naked eye. Aeolian transport events have the potential also to transfer significant volumes of sediment landwards, but both the zones of erosion and of deposition tend to be extensive. As a result, changes in surface elevations are frequently imperceptible, post-event. To validate the dismissal of the role of aeolian processes to 'bigger picture', coastal change, there is a pressing need for measurement.

Short duration, aeolian geomorphic events of low to moderate magnitude, ordinarily occur with greater frequency than those of relatively higher magnitudes. Their observation by the author, on multiple occasions annually, and for many years supports this view, albeit subjectively. The time frame over which these frequent events have occurred is therefore a major factor in assessing their net, cumulative effect. Intimate knowledge of the site and through many written or verbal accounts, further highlights their potential importance. The vast majority of foredune blowouts present at Sefton have been identified as having existed in some form comparable with the current state, from upwards of 50 years. Analysis of dune vegetation disturbance by Delgado-Fernandez, *et al*. (2019b) further identified that vegetation tramping in association with visitor pressure has

maintained their existence, and therefore also transport activity. In concerning high frequency events which have persisted over such an extended time frame, quantification of their effects offers the only route to fully understanding their influence on longer term evolution at Sefton. Empirical evidence from the meso-scale investigation in this thesis allows assessment of the contribution of aeolian processes, blowout transport events to long term erosional trends, (and therefore also anthropogenic disturbance as they are intrinsically linked). Should findings identify landward transfers of sediment via blowouts to be significant, with their mutual effect of lowering beach elevations, and therefore widths, this could only indicate they have also produced relative enhancements to the frequency, and the magnitude of marine erosion. Currently, coastal retreat at the site is exclusively attributed to marine processes. The scientific dissatisfaction of the author concerning the dismissal of contributions relating to aeolian processes, and specifically blowout transport, was a strong personal motivation for the meso-scale element of the investigation.

1.8.8. Meso-scale methodological rationale

Large scale, longer term research concerning changes to the land surface rely heavily on remotely sensed data. The logistical, economic, time, and labour costs associated with field measurements dictate this. Aerial photography has been the most extensively utilised resource within coastal science, is widely available, and offers large volumes of visual data, for analysis in two-dimensional, horizontal format (Andrews, *et al*. 2002). Whilst satellite imagery can be valuable to national, continental, or global analysis, as coastal environments exhibit an exceptionally high degree of spatial variability, other than over very recent years, the relatively coarse resolution of satellite imagery, typically constrains its application within regional or local studies. Using aerial photography, changes in the locations of

geographical features, horizontal distances, areal coverage, or land type classifications, are all readily available for analysis (e.g. Dolan, *et al.* 1978; DeKimpe, *et al.* 1991; Mashhadi, *et al.* 2007; Kish and Donoghue, 2013).

The use of aerial photography, in conjunction with GIS (Geographical Information Systems) software has allowed significant advancements in many disciplines of physical science. As coastal environments in character experience high relative levels of geomorphological processes, they customarily also exhibit pronounced degrees of landscape dynamism, with perceptible changes to the land surface occurring frequently, and often over short durations. As a result, data of this type is of particularly high value for coastal research, in comparison to other more stable environments, where meaningful geomorphic change occurs over much longer time frames. As the acquisition of aerial imagery only became semi-regular during the mid to late 20th century, its application is therefore of limited value in respect of environments with much lower landscape dynamism, as the earliest datasets do not provide a sufficient time-series duration for significant changes to be detectable.

Although aerial photography can offer a diversity of information for longer term geomorphological research, its two dimensional format is a key limitation, particularly within geomorphology. In offering spectral data in plan form, analysis of landform or landscape evolution relies heavily on human interpretation of changes in land cover. The findings from such research therefore have inherent limitations, or need to be supplemented with three dimensional data which provides information on ground surface elevations. Three dimensional elevation data permits individual landforms to be delimited, changes in the landscape to be quantified, the migration of features to be tracked, and of specific importance for

sedimentary environments, the movement of geo-materials to be calculated in volume.

Comprehensive understanding and quantification of landform, or landscape evolution therefore depends on analysis of repeat topographic surveys. Historically, a key limitation in this regard has been the labour intensive nature of ground based survey techniques. Topographic surveys covering only limited spatial extents, or which include very few epochs within a given time-series are the most common constraints. The Sefton coast benefits from a long history of systematic environmental monitoring, and this has included extensive ground based topographic surveying, for many decades now. Although a rich suite of historic elevation data exists, the nature of this data is extremely variable over time. An assessment of available topographic data for Sefton was conducted during the initial stages of the project. Multiple issues regarding the format, content, coverage, point uncertainty values, and diversity in detail between individual surveys, rendered the data unfit for the requirements of the project. To offer just a few examples, complications or limitations associated with its application included; a predominance of either discrete point, or transect only data, insufficient sampling for creation of surface models, variability in survey accuracies dependent on instrument/method of acquisition, patchy spatial coverage, and very few surveys containing sufficient points landward of the beach-dune interface to provide even rough estimations of cross-shore sediment transfers via blowouts. Many surveys also included data points which were identified as specific landscape features, (such as the dune toe), thereby also encompassing additional levels of point uncertainty and accuracy. As subjective selection and measurement in the field depends on both the survey technique and operator, the level of confidence associated with specific landscape features varies, year on year. The cumulative outcome of these issues was a time-series with exceptionally high

survey frequency, but which was composed of discrete, individual surveys which too often contained incomparable information, or were lacking in spatial coherence. Desirable characteristics of the time-series under construction for this research, included optimal levels of temporal consistency for survey information, and minimal levels of point uncertainty. These requirements informed the decision to limit the use of ground based survey data wherever possible.

Since the birth of airborne LiDAR (Light Detection and Ranging) remote sensing, research on coastal evolution has experienced an explosion in the availability of topographic datasets (Andrews, *et al*. 2002; Brock and Purkis, 2009). The relatively low cost and short acquisition time of this remote sensing technique has resulted in increases to both the frequency, and spatial extent of coastal topographic surveys. Sefton dunes, the location of this investigation benefits from a multi-epoch suite of LiDAR surveys, which also spans the maximum temporal range available for any coastline in the UK. The temporal range of available LiDAR for Sefton, and the consistency brought to the research project via exclusive use of a single type/format of elevation data, were influential in the decision making process.

Relatively more contemporary remote sensing techniques which directly capture ground surface elevations were discounted from the project. No SAR (Synthetic Aperture Radar) or UAV (Unmanned Aerial Vehicle) acquired survey data is in existence for the study site, with sufficient temporal duration, spatial coverage, or appropriate resolution. The only other potential alternative source of remotely sensed data from which topography could be derived was the extensive set of aerial ortho-photographs. Photogrammetry techniques could have theoretically been utilised to produce three dimensional terrain models of the Sefton coast (Fryer, *et al*. 2007). Although the temporal range of the study could have been

extended, multiple constraints validated quickly discounting this option in the preliminary stages of constructing a topographic dataset. Contributing factors included ‘patchy’ availability of stereo images, some epochs not being fully ‘at nadir’, and the acknowledged uncertainties associated with elevation values for landscapes such as the Sefton coast, where vegetation coverage and elevations exhibit high spatio-temporal variability (Aber, *et al*. 2019).

The LiDAR data available for Sefton offered unprecedented temporal coverage for any UK coastal dune system and validated its selection. That the time-series benefitted from multiple epochs, and also offered consistent use of a single data, type further justified its selection. Specifics on the best practice methods used in its application are detailed in chapter 4.

1.9. Structure of the thesis

The thesis is comprised of five chapters, with this first chapter initially positioning and contextualising the work within the broader research discipline. An extensive literature review provides coverage of the scientific knowledge to date, which is of most relevance, and the theoretical background which supports the aims of the project. Knowledge gaps are identified, together with research questions and objectives, designed to address them. Motivations and rationale for project design and methodological approaches are then discussed. Methodological decisions are further specified, explained, or validated in the subsequent research chapters where necessary.

Chapter 2 details and discusses event scale, instantaneous airflow and transport dynamics, at a foredune blowout location. The event is characterised with a particular focus on the spatio-temporal variability of geomorphic processes, with discussion also of potential environmental factors contributing to this variability.

Chapter 3 accords detailed statistical analysis of event scale processes at a foredune blowout, to enhance understanding of sediment transport and airflow dynamics, together with additional evidence to support the initial interpretation, and allow for further expansion. Novel analytical approaches which improved resolution of the event, and which can be more broadly applied within the discipline are additionally introduced.

Chapter 4 is focused on geomorphic change associated with foredune blowouts over the meso-temporal scale. A range of GIS techniques are applied to characterise and quantify geomorphic change at a variety of spatio-temporal scales. Measured and theoretical contributions made by foredune blowouts to coastline retreat are discussed. Implications of the findings, and environmental factors which appear to exert important control on coastal dune field evolution are discussed.

Finally, Chapter 5 summarises research findings with reference to the knowledge gaps, research questions, and project objectives specified in the first chapter. The implications of foredune blowouts to coastal dune managers are discussed. Concise, critical evaluation of the research project is offered, and points of departure for future studies aimed at further advancing the research themes are identified.

CHAPTER 2 – HIGH RESOLUTION AIRFLOW AND SEDIMENT TRANSPORT AT THE BEACH-DUNE INTERFACE OF A FOREDUNE TROUGH BLOWOUT

2.1. Introduction

This chapter is the first of two which directly address research question 1 of the thesis (section 1.7.2.). The discussion section of the chapter (section 2.5), additionally makes contributions in respect of research question 4. The aim of this chapter is to make initial steps towards characterising event scale, aeolian sediment transport and airflow dynamics, at a foredune blowout. To achieve this, and in line with objective 1 of the thesis (section 1.7.3.), the chapter details the measurement and analysis of high frequency, instantaneous, sediment transport and airflow, at a foredune trough blowout location.

Aeolian processes are explored by use of a grid based instrument array within a confined topographic area. Throughout the study site, sediment transport intensity and transport activity are quantified during an 84 minute event. Characterisation of transport dynamics benefits from comparison with the synchronous measurement of wind speed, direction, turbulence, and steadiness. The study took place during alongshore, and obliquely onshore, incident winds.

2.2 Study Site

The Sefton Coast, NW England, borders the eastern Irish Sea and is situated between the Mersey and Ribble estuaries (Figure 2.1). The Sefton Dunes represent the largest coastal dune field in England and Wales, extending 16 km alongshore, up to 4 km inland at their widest point, and covering an area of 2,100 ha, which contains dunes exceeding 30 m in height (Esteves, *et al.* 2012). The

coast experiences a semi-diurnal, macro-tidal regime, with a mean spring tidal range in excess of 8 m (Plater and Grenville, 2008). Fronting the dunes, during low tide, an extensive, multiple-barred beach system is exposed, which is primarily composed of fine grained, quartz rich sand.

The coastline holds a number of national and international conservation designations including Ramsar sites, NNRs (National Nature Reserves), SSSIs (Sites of Special Scientific Interest), and one SAC (Special Area of Conservation). Anthropogenic influence at the site has been significant, with notable activities including agriculture, silviculture, sand mining, and intense visitor pressure/recreational use, the latter having intensified since the early 1900's through the removal of access restrictions following land purchases by local authorities (Smith, 2009; Delgado-Fernandez, *et al*. 2019b). In the central zone of the coastline, focused around Formby Pont, the beach-dune boundary has been retreating landwards at an average rate of ≈ 4 m pa. This is largely attributed to continual slumping of the dune face following regular wetting of the dune toe during high tides, wave energy converging on this section of the coastline, and isolated high magnitude wave scarping, on the coincidence of extreme high tides with storm events (Esteves, *et al.* 2012; Dissanayake, *et al*. 2015; Pye and Blott, 2016). In Ainsdale, to the north of the erosion zone, and to the south, near Hightown, the foredunes are accreting seawards. The blowout examined in this study is located on Natural England land towards the northern extent of the erosion zone, in the least accessible longshore section of the foredunes, broadly equidistant to carpark access at Victoria Road, Formby, to the S (south), and Shore Road, Ainsdale, to the N (north), (Figure 2.1.1). As a result, visitor pressure, evidenced in other parts of the coastline via significant vegetation trampling and high densities of footprints, is less pronounced (Delgado-Fernandez, *et al*. 2019b).

A contributing factor in selecting the blowout to be examined in this study was the relative simplicity of its throat area.

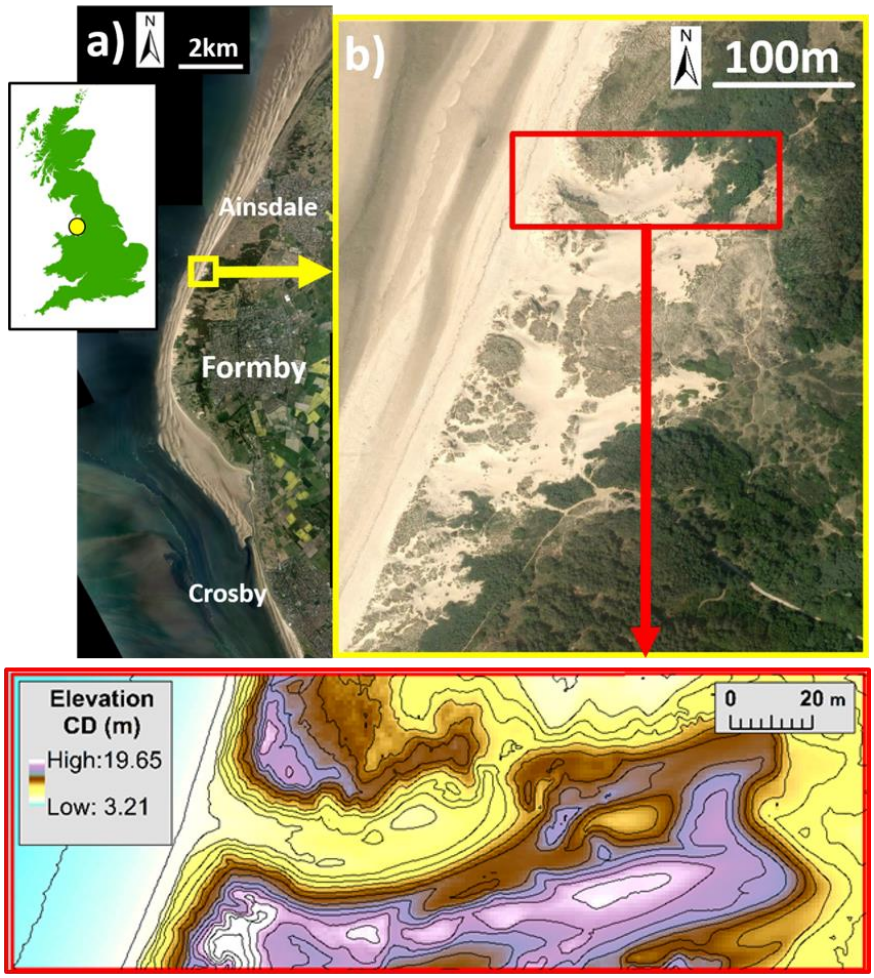

Figure 2.1: Location of study site (a), Sefton Coast, NW England, Aerial photograph showing orientation of the coastline and trough blowout (b) examined as a feature within a larger erosional system, and Digital elevation model (c), including 1m contours to highlight the throat and provide topographic context.

Figure 2.1.1: Study location relative to principle beach access points.

The blowout throat is comparatively narrow, measuring approximately 10 m longshore, and is flanked to the north and south by steep foredunes, with dune crests approximately 15 m above the dune toe elevation. The throat extends landwards for approximately 25 m at a constant width before expanding to a wider trough which skews in a north-easterly direction, from the throat which is broadly orientated north-west to south-east. The relatively flat basin floor extends 65 m landwards of the beach. The foredune itself along this stretch of the coast is orientated broadly SSW to NNE (Figure 2.1).

2.3. Methodology

2.3.1. Field data collection

Airflow and sediment transport data were recorded at the study site on the afternoon of 27th October 2016, during a moderate SW wind event. Data presented here has a total duration of 84 minutes, the period for which all anemometers and transport sensors recorded synchronously (15:49 to 17:12). A grid of instruments consisting of 12 3D Ultrasonic Anemometers (UAs), and 10 Wenglor Laser Particle Counters (LPCs) were deployed at the back-beach, beach-dune interface, and blowout trough (Figure 2.2).

The grid of instruments covered an area of approximately 300 m^2 (20 m longshore, by 15 m cross-shore, Figure 2.3). Airflow dynamics were measured with 3D Gill HS-50 ultrasonic anemometers, mounted at an elevation of 0.4 m above the surface, with their UV plane positioned horizontally. The UAs have a recording range of 0-45 ms^{-1} for speed, and 0-359° for direction. Data was recorded at 50 Hz. As airflow dynamics were expected to be complex, and vertical profiles, non-logarithmic, no attempt was made to align sensors with potential local streamlines, and no quadrant or Reynolds stress analysis was conducted (Lee and Baas, 2012; Chapman, *et al.* 2013).

Figure 2.2: Sensor locations, pictured from the crest of the northern foredune (positions numbered black include UAs co-located with LPCs, and red, UAs only).

Near surface sediment transport was measured with 10 LPCs (Laser Particle Counters), including 8 Wenglor models YH08PCT8 and 2 TH03PCT8, with fork widths of 80 mm and 30 mm, respectively. Each LPC was co-located directly beneath a UA with the beam positioned horizontally 20 mm above the surface (Figure 2.4). The sensors measure transport intensity, emitting pulses on the event of suspended or saltating grains partially blocking the 0.6 mm laser path, and are well suited for use in complex beach-dune topography (Davidson-Arnott, *et al*. 2009, 2012; Barchyn, *et al*. 2014). Data were recorded using Onset HOBO data loggers at a sampling frequency of 1 Hz.

Sensors were positioned into four, shore normal rows, with three positions in each row moving landwards cross-shore. Throughout the paper, all measured flow and transport descriptions are made with reference to their respective sensor location within the array (A1 to A12). The first row (A1, A2, and A3) was located on the back-beach, and the final two rows, within the blowout trough (Figure 2.3). During

setup, significant transport was observed, with multiple streamers moving northwards across the surface of the S (south/southern) foredune stoss slope, immediately upwind of the blowout. In this second row, two sensors were located in line with the approximate beach-dune interface, with the third being positioned on the S foredune stoss itself (Figure 2.4).

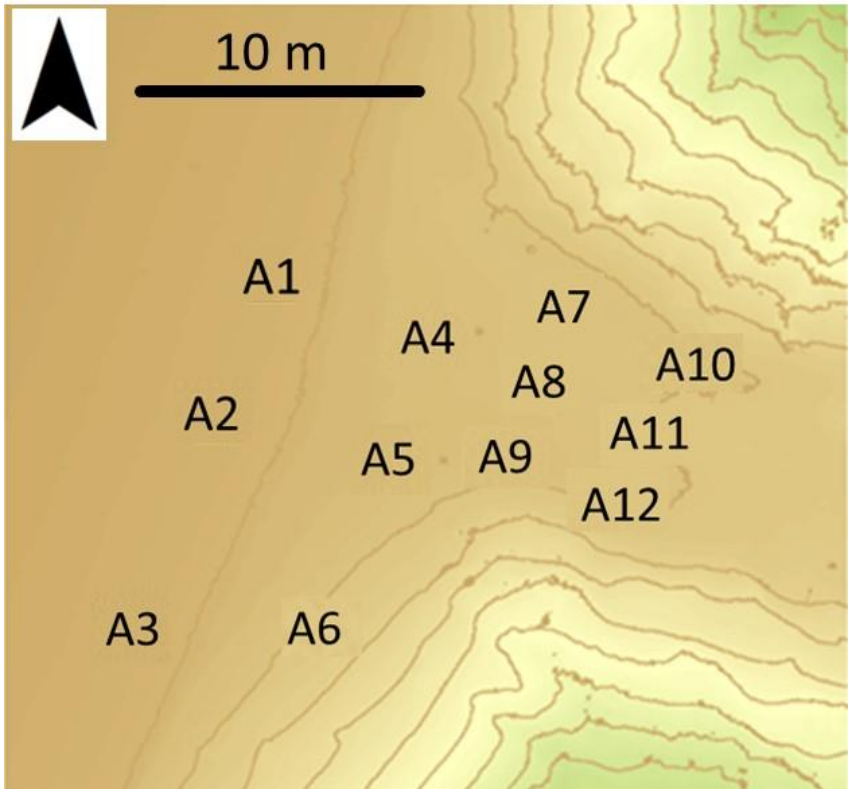

Figure 2.3: Digital elevation model of the site and instrument locations.

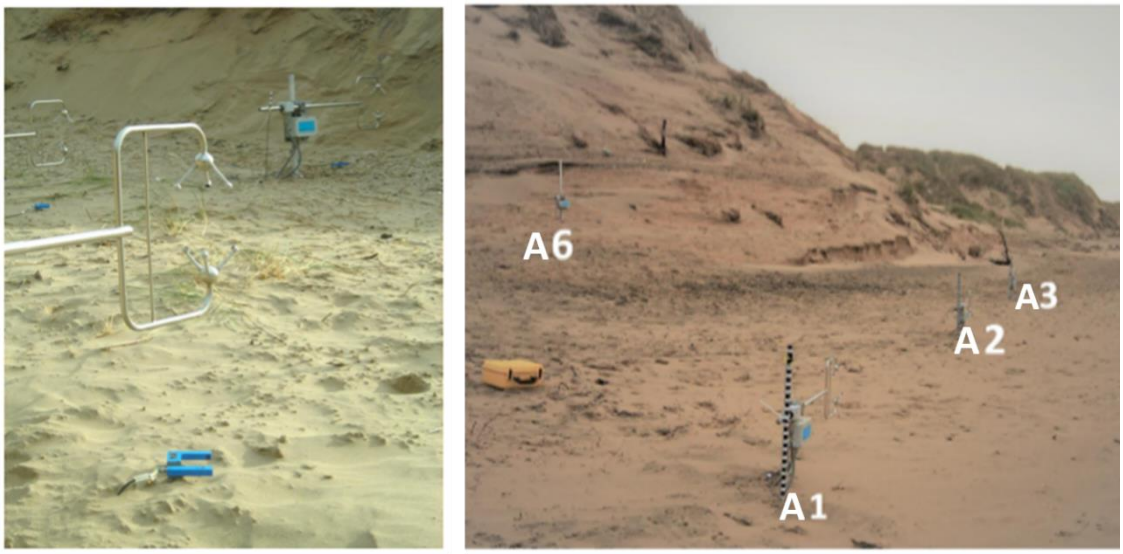

Figure 2.4: Left - UAs 8, 11 and 12 within the blowout, co-located with LPCs; Right - UAs positioned at back-beach and on the upwind stoss slope of the S foredune. UA 2 and UA6 are co-located with LPCs.

The locations of all sampling points were captured via a Terrestrial Laser Scanner survey (TLS), model FARO Focus 3D x 330. This system operates a single return laser with a scanning range of up to 330 m, and a ranging error of ±2 mm. The scanner was set to a measurement speed of 976,000 points s. Multiple overlaying scans were undertaken using a network of spherical targets. The geographic coordinates of each target were recorded with a Trimble 5800 DGPS, which allowed for scans to be subsequently registered into a single point cloud.

TLS scans of the terrain immediately surrounding the instrument grid and extending landwards, through the blowout towards the crest of the depositional lobe were performed pre and post data recording. Their primary intended purpose was to quantify the geomorphic response to airflow and transport measurements during the 'event'. As transport capable winds were low magnitude, 'event' duration short (84 min), and blowout scale relatively large, detected elevation changes were extremely low in magnitude albeit often extending across relatively large spatial areas. Although TLS offers 'high' precision measurements (± 2 mm), terrain 'roughness' and the most advantageous interpolation method of DEM (Digital Elevation Model) creation both contribute to the total error of each individual DEM. When propagated into a DoD (DEM of Difference), the total DoD 'uncertainty', (assumed to be spatially uniform), was slightly greater than the large majority of detected change. As only elevation changes above DoD uncertainty can be attributed as 'real' geomorphic change, DoD analyses were omitted from further exploration. The first TLS derived DEM was however of great value in providing a high precision representation of site topography during the event.

Finally, a 2D sonic anemometer was mounted on a 6 m mast and deployed at the crest of the depositional lobe, approximately 90 m landwards of the beach-dune interface, in order to provide details of the regional wind field. The data logger

associated with this instrument failed to record, and has thus been omitted from the remainder of the article. Hourly averages of wind speed and direction were available from a local Met station in Crosby, 9 km south of the study site, and provided an estimate of the regional wind field during the experiment.

2.3.2 Data Analysis

Total wind speed was derived from the three components of flow measured by the UAs using equation (1):

$$\text{Total wind speed } (U) = \sqrt{u^2 + v^2 + w^2} \quad (1)$$

where u is horizontal streamwise flow, v is horizontal spanwise flow, and w is the vertical component of flow. To calculate wind direction (a) the horizontal streamwise component is first aligned with geographical north for each instrument location. Direction was then calculated, using equation (2), as the opposite (-180°) of the horizontal flow vector using the arctangent function (Jackson, *et al.* 2011).

$$\text{Wind direction (a)} = \text{atan2}(u,v) - 180° \quad (2)$$

The standard deviation (SD) of wind speed is an accepted concept indicative of fluctuations in wind characteristics (Smyth, *et al.* 2014). Coefficient of variation (CV) can be used to normalise the SD of wind speed recorded by each UA, and thus allow comparison between sensor locations. Equation (3) was used to calculate CV of wind speed for each instrument, expressed as a percentage scale:

$$CV = (\sigma \text{ wind speed} / \text{mean wind speed}) \times 100 \quad (3)$$

Turbulent kinetic energy (TKE) defines the level to which flow deviates from the mean, and is hence an indicator of airflow turbulence intensity. A number of studies have found TKE to be a valuable parameter to compare with sediment

transport, particularly in locations where transport is not well associated with total wind speed (Wiggs and Weaver, 2012; Lynch, *et al.* 2013; Smyth, *et al.* 2014, Delgado-Fernandez, *et al.* 2018). TKE was calculated at 1 min averages using equation (4):

$$TKE = ½ ((\sigma u^2) + (\sigma v^2) + (\sigma w^2)) \quad (4)$$

Sediment transport intensity recorded by each LPC at a frequency of 1 Hz was expressed as counts (c) at 1 minute averages, in addition to the absolute count number being given in reference to specific time durations within the event. To allow transport intensity (which often differed greatly in absolute terms) to also be compared between sensors at a comparable scale, (c) per minute was also normalised (ntt), with 1 min mean values expressed as a percentage of the total counts recorded at each LPC location over the 84 minute measuring period.

The Activity Parameter (AP) for each LPC was also calculated (using 1 min intervals). AP values vary between 0.0 (no transport), up to 1.0 (continuous transport). This parameter allows quantification of the proportion of time sediment transport was active at different locations of the site during the study period (Davidson-Arnott, *et al.* 2012).

As is customary, and in line with Smyth, *et al.* (2014), the 1 minute averaging interval employed throughout, was used to help mitigate short term fluctuations in airflow dynamics and transport intensity, and thus improves suppression of any temporal lags between wind forcing and transport response (Baas and Sherman, 2006; Davidson-Arnott, *et al.* 2012; Smyth, *et al.* 2014).

2.4. Results

2.4.1 General description of the event and incident winds

During the week leading up to data collection a ‘blocking anticyclone’ persisted over the UK. In Sefton conditions were calm, only trace levels of rainfall were experienced, and winds had been predominately offshore and below the threshold for aeolian sediment transport. Over the 24 hours preceding the experiment the prevailing winds began to shift from the south to south westerlies and average speeds increased. The local met station in Crosby registered average hourly wind speeds of 10.8 m s^{-1} and 10.3 m s^{-1} from 3-4pm and 4-5pm, respectively, with a steady wind direction of 250°. Wind speeds decreased to 4.6 m s^{-1} from 5-6pm, coinciding with the end of data recording at the study site.

Due to the failure of the 2D UA at the top of the depositional lobe dune crest, high frequency data of the regional wind was not recorded. Thus the UA positioned at A3 was used as a reference anemometer with its airflow record used as a proxy for near surface incident wind at the site. The A3 sensor location was positioned on the back beach approximately 6 m seaward of the dune toe, and in the furthest upwind position of the instrument grid (Figure 2.3). Although it is likely that A3 airflow was significantly modified relative to the regional wind field, it provided a high frequency record of the near-surface airflow approaching the blowout and permitted interpretation of topographic modification expressed in the records of downwind locations.

Wind direction recorded at A3 was relatively stable at around 210° (i.e. alongshore to slightly onshore) from 15:49 to ca. 16:49. Incident flow of ≈ 200° would be perfectly aligned with the S to N orientation of the S foredune line in this section of the coastline. From this point, whilst remaining highly oblique, wind direction

became more onshore directed, peaking at 225° at 17:08. Wind speed remained relatively constant throughout the study period with a range of just 1.29 m s^{-1} and an average of 6.5 m s^{-1} (Figure 2.5).

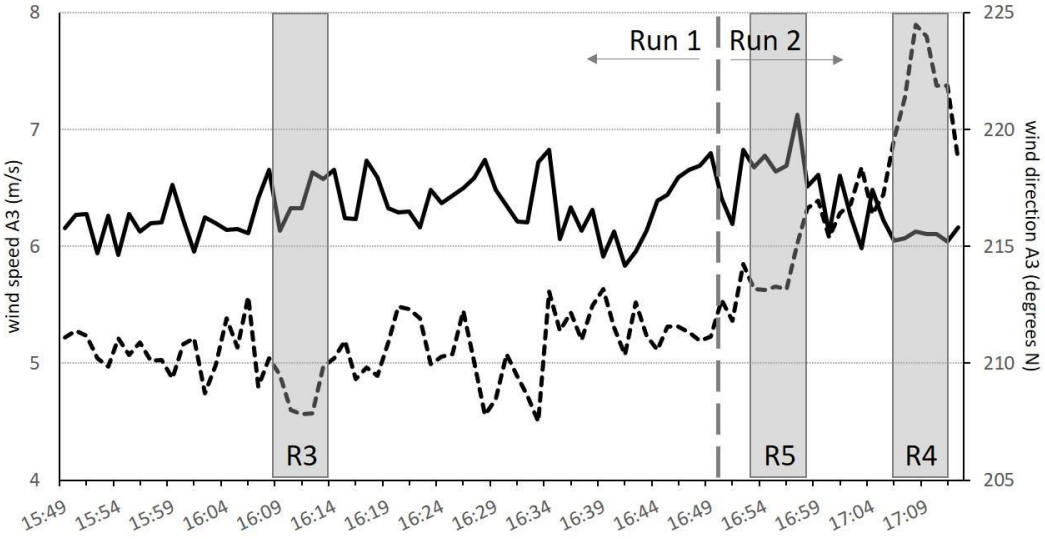

Figure 2.5: UA3 wind time-series: full 84 min duration (solid line is wind speed).

The time-series was sub-divided into two long runs (R), covering the first 61 min of the data collection (R1), and the last 23 min of data collection (R2). The majority of instrument positions recorded a characteristically different wind and transport regime during these two time periods (cut off time at 16:50). With a range of 12.7° during the final 23 minutes of the UA3 time-series, absolute variability in wind direction was more than twice that of the 5.7° range during the preceding 61 minutes (R2), with fluctuations trending in an increasingly onshore direction.

Additionally, three 5 min ‘runs’ representative of different wind directions were selected for further analysis. R3, which occurred within the longer R1, had the lowest 5 minute average of wind direction relative to geographical N, with direction perfectly aligned with the S foredune orientation of 210° (± 2°); R4 covered the period from 17:06-17:10, which coincided with the maximum orientation of direction relative to geographical north; and R5, covering the transition from

alongshore to onshore oblique incident winds, whilst also representing the maximum 5 min average A3 wind speed (Table 2.1).

Table 2.1 Average values for local incident winds at A3 for the 5 runs investigated.

RUN	Start	End (inc.)	Duration (min)	U (m/s)	Dir (°)	TKE (m/s)	CV (%)
R1	15:49	16:49	61	6.33	211	0.64	13.7
R2	16:50	17:12	23	6.38	217	0.65	13.5
R3	16:09	16:13	5	6.40	209	0.70	14.3
R4	17:07	17:11	5	6.09	223	0.67	14.1
R5	16:53	16:57	5	6.78	214	0.67	13.1

2.4.2 Response to change in approach of wind direction (R1 *vs* R2)

Wind patterns

R1

Average spatial patterns during R1 are included in Figure 2.6. Strongest winds were recorded at A6, A5, A9 and A12, all located towards the southern foredune stoss slope and along the interior south wall of the blowout. Wind direction at A6 was slightly offshore and in contrast to all other locations. A7, A8, A9, A10, A11, and A12 show considerable steering of wind direction and a gradual adjustment towards onshore directed, and hence greater alignment with the orientation of the blowout trough. In general, there is a spatial trend in wind direction variability of increasing values relative to geographical north that become more pronounced with landwards progression into the trough, with a direction shift ranging between 40 and 69°. A7 against the N wall recorded the lowest R1 mean wind speed of all UAs, with an average of 4.17 m s^{-1}. A5 recorded the highest average speed of 6.68 m s^{-1}, slightly over (0.35 m s^{-1} increase) the R1 mean recorded at A3 (Fig 2.6, top-left).

There is a general trend for TKE to increase with proximity to elevated dune topography (Fig 2.6, top-right). A7 recorded the second highest level of turbulence, with a R1 average TKE value of 1.25 $m^2 s^{-2}$, whilst also experiencing the lowest mean wind speed of all locations. TKE values recorded at all three UAs on the back-beach were approximately half this level. All three UAs in the most landward, (and topographically confined area of the trough), recorded high levels of TKE, with A12 showing the maximum mean value of 1.51 $m^2 s^{-2}$.

Mean CV of wind speed across the 12 locations was 15.59%. A5 and A9, both in close proximity to the S blowout wall have the two lowest CV, with mean values of 12.74% and 12.6% respectively. The next three lowest CV values are for A2, A3 and A6, the two back-beach sensors closest to the S foredune and the sensor on the foredune slope itself. Within each of the first three rows of sensors, the location furthest from the S foredune has the highest CV. A7, at the foot of the N wall is the maximum mean CV at 22.95%, an outlier with a CV 7.36% above the overall average, and 10.36% above the A9 minimum. A10 and A12, both in the most landward row of sensors have the second and third highest CV.

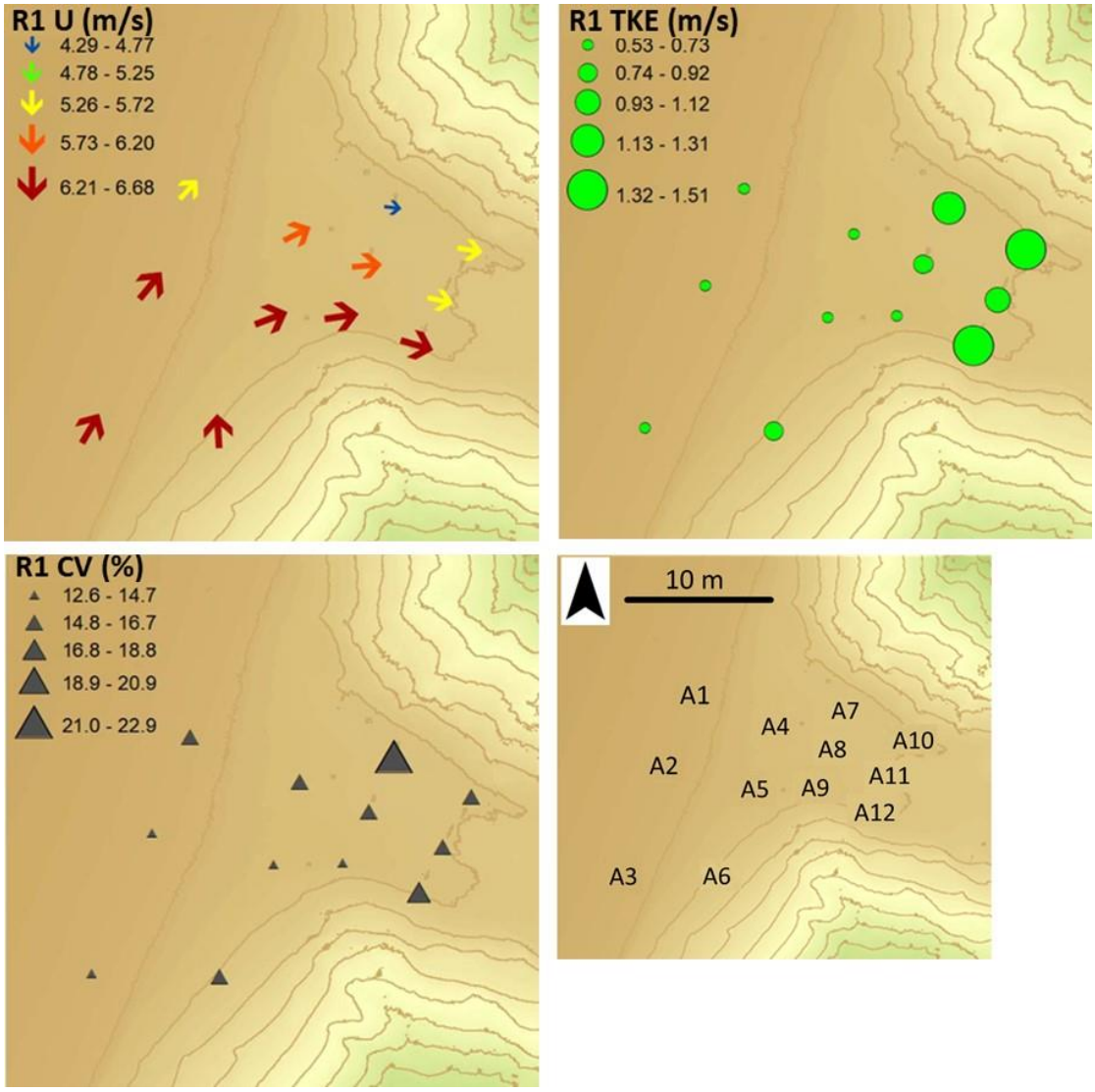

Figure 2.6: R1 wind patterns. Top-left: average wind speed and direction; Top-right: TKE; Bottom-left: CV. Inset with instruments locations.

R2

A3 reference mean wind speed during R2 shows negligible difference to that recorded in R1 (+ 0.05 m s^{-1}) but though extremely oblique, direction is slightly more onshore directed (+ 6.6°). As in R1, A1, the back-beach UA furthest distance from the upwind foredune shows the lowest average speed of the three back-beach locations (Figure 2.7). All UAs within the blowout again show marked difference in wind direction, to become more aligned with the orientation of the trough axis. Noticeable steering occurs in relation to the A3 reference anemometer, with wind direction also becoming more strongly aligned with the trough axis in more landward positions. Despite similar incoming wind speed at the A3 reference anemometer, the slight change in A3 wind direction leads to marked

increases in speed within the trough. Wind speeds along the S wall, were again the strongest, this time with A9 recording the highest R2 average of 7.68 m s^{-1}. During R4, a 5 min period within R2, at 8.14 m s^{-1}, A12 experienced the highest mean wind speed of all locations during any 5 min period, and was > 2 m s^{-1} higher than that recorded at A3. Similar to R1, A7 had the lowest mean wind speed of those instruments located within the trough (Figure 2.7, top-left).

TKE values during R2 (Figure 2.7, top-right) at the back-beach were marginally higher for all three UAs located here than in R1. Again, locations in proximity to topography generally showed relatively higher TKE values than those locations in more 'open' surroundings. Despite this, during the R4, 5 min period within R2, with an average TKE of 0.57 m^2 s^{-2}, A8 recorded the lowest value of all instruments. In the same 5 minute period, A12 provided a mean TKE of 4.45 m^2 s^{-2}. This level equalling 348% of the highest R1 mean, and 481% of the next highest value calculated during R2.

With the exception of A12, CV of wind speed reduces at all locations during R2. The two locations with the lowest CV are again A5 and A9 with mean values of 11.25% and 11.47% respectively. The pattern of higher CV values with increasing distance from the upwind S foredune in each of the first three rows is again exhibited. Although switching rank, A7 and A12 have the two highest CV values at 19.76% and 21.39% respectively. In contrast to all other locations, A12 CV increased during R2 to produce the highest value of 21.39% (up by 3.76%). Despite a 3.19% decrease, and excluding A12, CV at A7 was notably higher than all other locations. A8, positioned within the trough on the central axis has the highest reduction in mean CV between R1 and R2 of 3.9%.

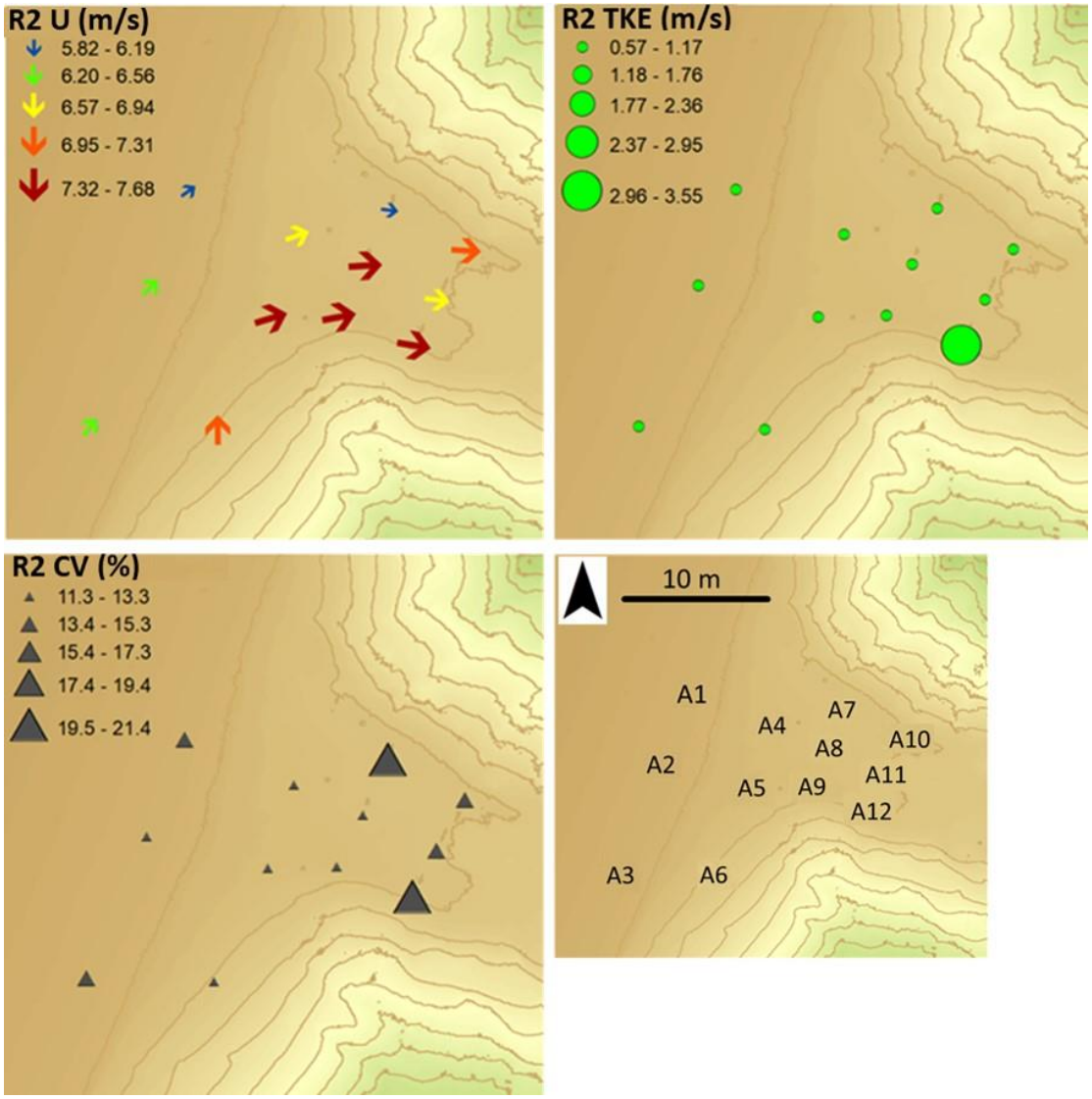

Figure 2.7: R2 wind patterns. Top-left: average wind speed and direction; Top-right: TKE; Bottom-left: CV. Inset with instruments locations.

Airflow on the back-beach was influenced by topographically induced modifications associated with proximity to the foredune. The three back-beach sensors are aligned parallel to the orientation of the foredune, with A3 being the most upwind, A1 furthest downwind and aligned seawards of the blowout central axis, and A2 in between, broadly seaward of the juncture of the S foredune and the S wall of the blowout (Figure 2.3). Their longshore positions, relative to the foredune/blowout throat, led to variability in magnitude of topographic airflow modifications. A general trend of reducing wind speed and increasingly onshore direction, from A3 to A1, was exhibited throughout the experiment. This likely being indicative of reducing topographically induced modifications to airflow, as

proximity to the S foredune reduced. A3 was located approximately 5 m upwind of the throat, with the landward foredune stretching longshore in both directions. Airflow at this location is therefore influenced more heavily by the presence of the foredune, with both longshore deflected winds and incoming oblique onshore regional winds contributing to its resultant vector. A2 is broadly seaward of the S foredune terminus, at the foredune-throat juncture, with the foredune face and toe having already begun to trend landwards. Longshore deflection of the regional wind field by, and compression against the foredune ceases in this locality, (as deflected flow effectively 'runs out' of foredune topography, with airflow then being steered into the trough as the dune topography trends landwards. At A1, broadly aligned with the trough central axis, and approximately 5 m longshore beyond the S foredune terminus, expansion of airflow reduces wind speed, and the marked reduction in contribution of longshore foredune deflected flow to the A1 vector, relative to regional flow, results in a more onshore directed vector. Relative flow direction differences between these 3 back-beach locations remained constant throughout the experiment, with all sensors also consistently reflecting the general changes in wind direction towards the end of the experiment (Figure 2.8).

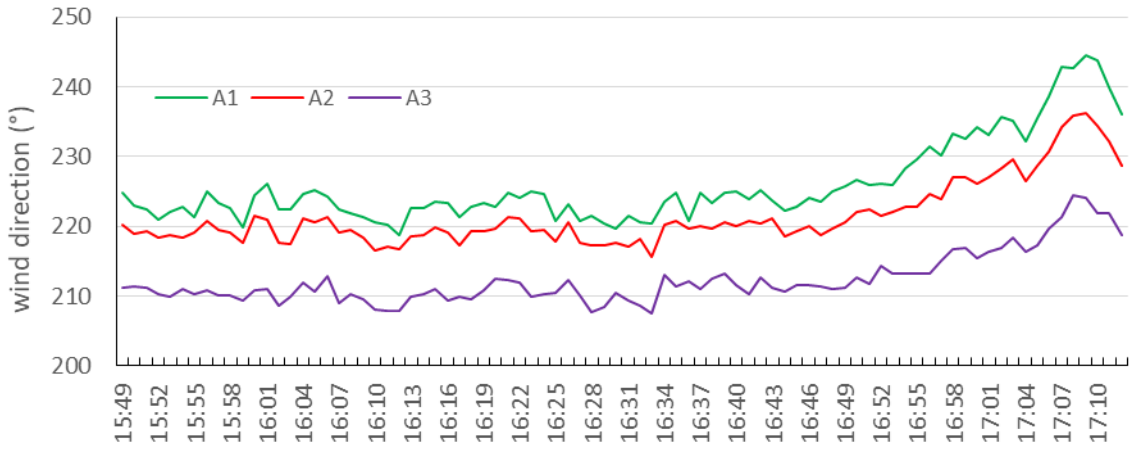

Figure 2.8: Back-beach wind direction, showing changes from alongshore, to oblique onshore during the final 23 minutes of measurement, (in R2).

Transport patterns

Table 2.2 provides a summary of transport recorded for each location. Highest magnitude transport was at A6, on the lower foredune slope.

Table 2.2 Summary of transport data (average counts per min and total counts) recorded at all LPC locations for R1 and R2.

	R1 ***(61 min)***		**R2** ***(23 min)***		***R1 & R2***
LPC	**counts per min**	**total**	**counts per min**	**total**	**total**
2	585	35,695	753	17,320	53,015
4	299	18,225	1,680	38,638	56,863
5	142	8,667	210	4,827	13,494
6	5,040	307,436	7,050	162,147	469,583
7	995	60,687	3,810	87,619	148,306
8	218	13,321	1,977	45,466	58,787
9	18	1,104	337	7,757	8,861
10	306	18,655	941	21,653	40,308
11	59	3,582	1,132	26,045	29,627
12	4	230	158	3,628	3,858

To allow for visual comparisons, Figure 2.9 displays total counts for all sensors other than A6. Despite much shorter duration (ca. a quarter of the time), marked increases in transport intensities for all locations led to multiple sensors recording significantly higher total counts in R2 compared to R1. This highlights that even small changes in incident wind direction can generate marked differences in the sediment transport intensity.

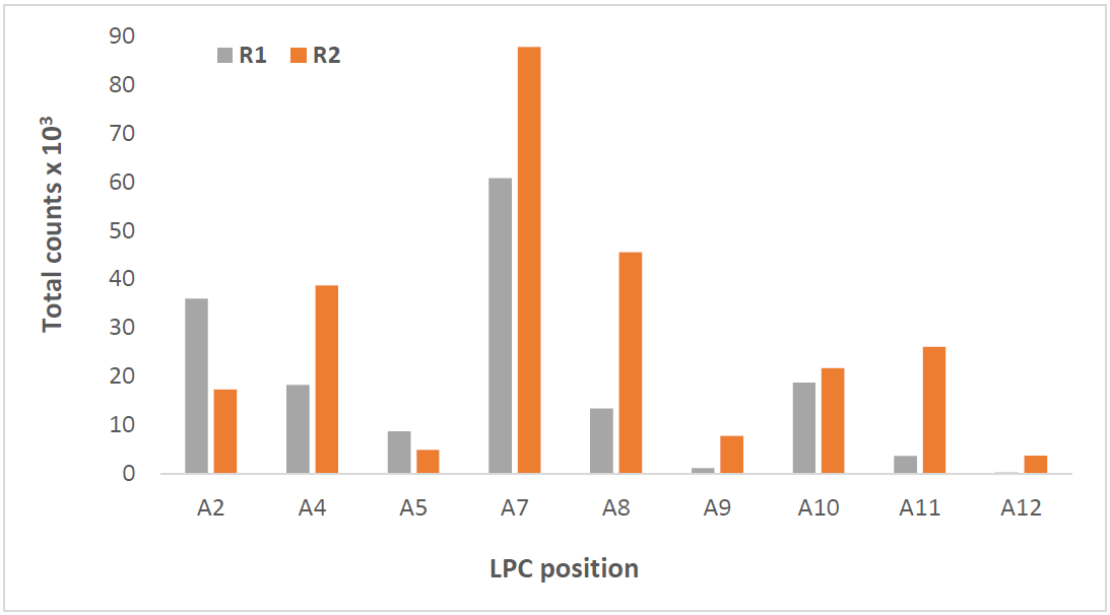

Figure 2.9: Total counts during R1 and R2

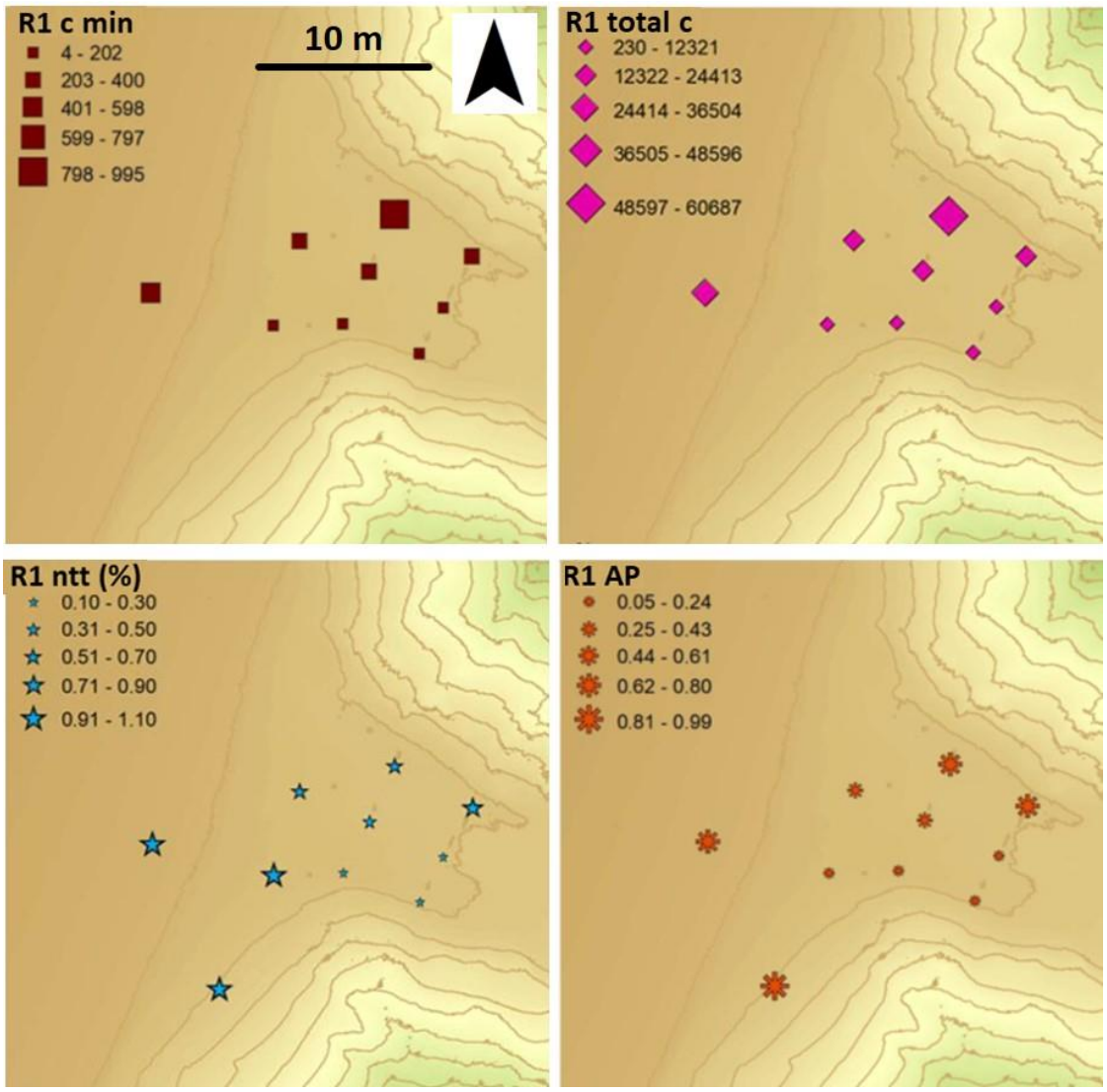

Figure 2.10: Transport patterns during R1.

The lowest amount of transport was recorded at A12, the most landward sensor along the S wall. During R1 only intermittent and trace levels of transport were

recorded, these slightly increasing in R2 when the regional winds became more onshore oblique.

Figure 2.10 shows spatial patterns of sediment transport during R1. The average counts recorded per minute (top-left), was higher towards the northern blowout wall, with the second highest value (excluding that of A6, on the seaward facing, foredune stoss slope) observed at A7. Cumulative counts were also higher towards the northernmost section of the study site (top-right), with AP values following a similar trend.

Trends were similar for R2 (Figure 2.11), with absolute averages per minute increasing at all locations, but broadly maintaining the same relative differences observed during R1. It is worth stressing that transport intensity was markedly greater during R2 despite negligible difference in incoming, mean wind speed at A3 between R1 and R2 (+0.05 m/s), with wind speeds increasing inside the blowout in coincidence with a slight change in incident direction. It is also worth pointing out that transport intensity and wind speed inside the blowout are inverse to this, with locations of relatively low velocities displaying strong transport, and vice versa (section 2.5.1).

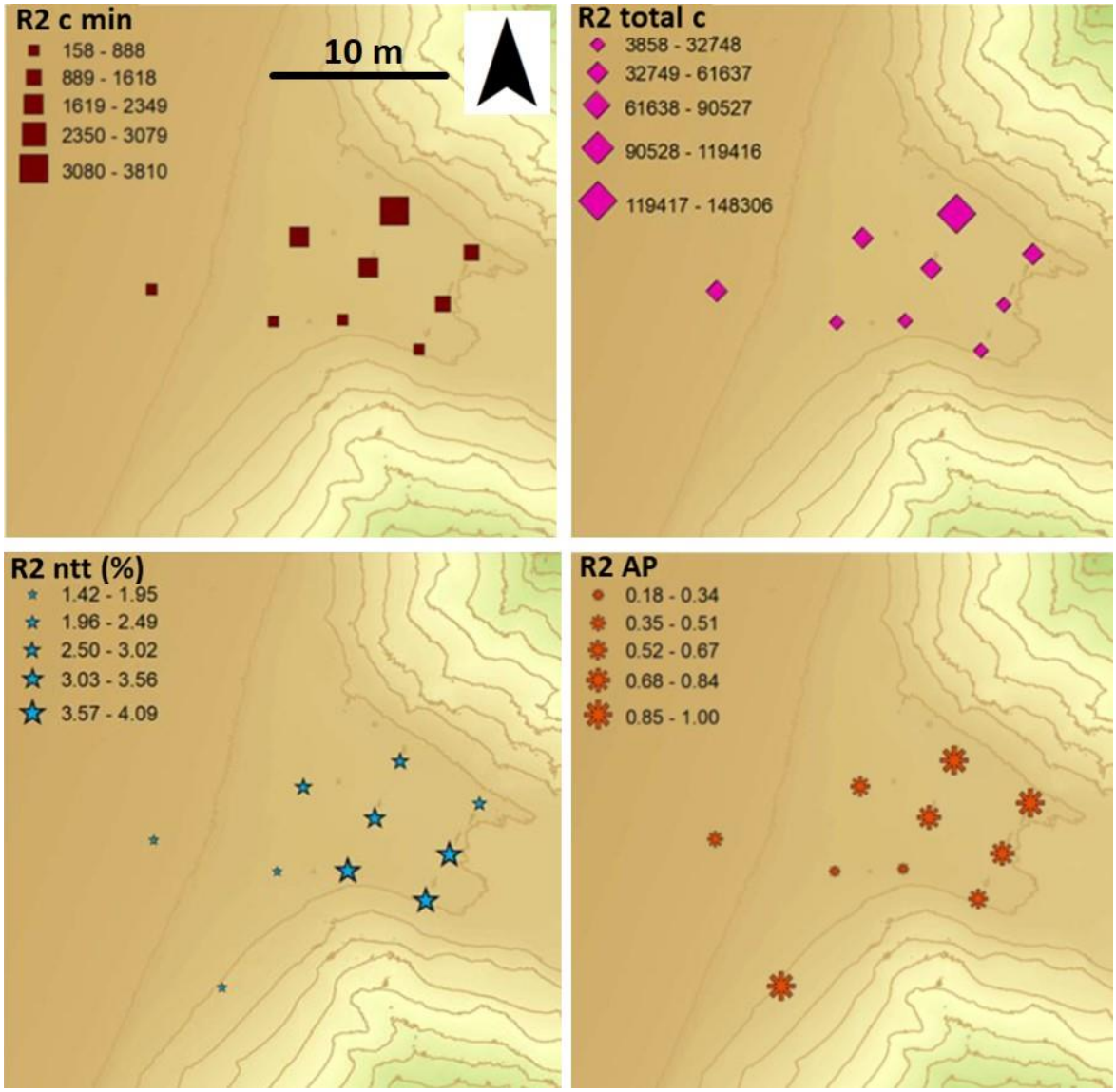

Figure 2.11: Transport patterns during R2.

Average AP values were consistent with general spatial trends shown in Figures 2.10 and 2.11. The AP oscillates between 0 and 1 and is independent of count magnitude, as it simply describes how many seconds within each minute, grain counts were registered. It thus provides an extra layer of information about the nature of transport (Figure 2.12).

A6 AP was the highest of all locations and strongly agrees with visually observed and measured transport on the foredune, which was high magnitude, and appeared near constant throughout. The absolute grain count on the foredune slope was orders of magnitude beyond that of all other sensors. There were only

54 seconds within the 5,040 second duration when grain counts were not recorded.

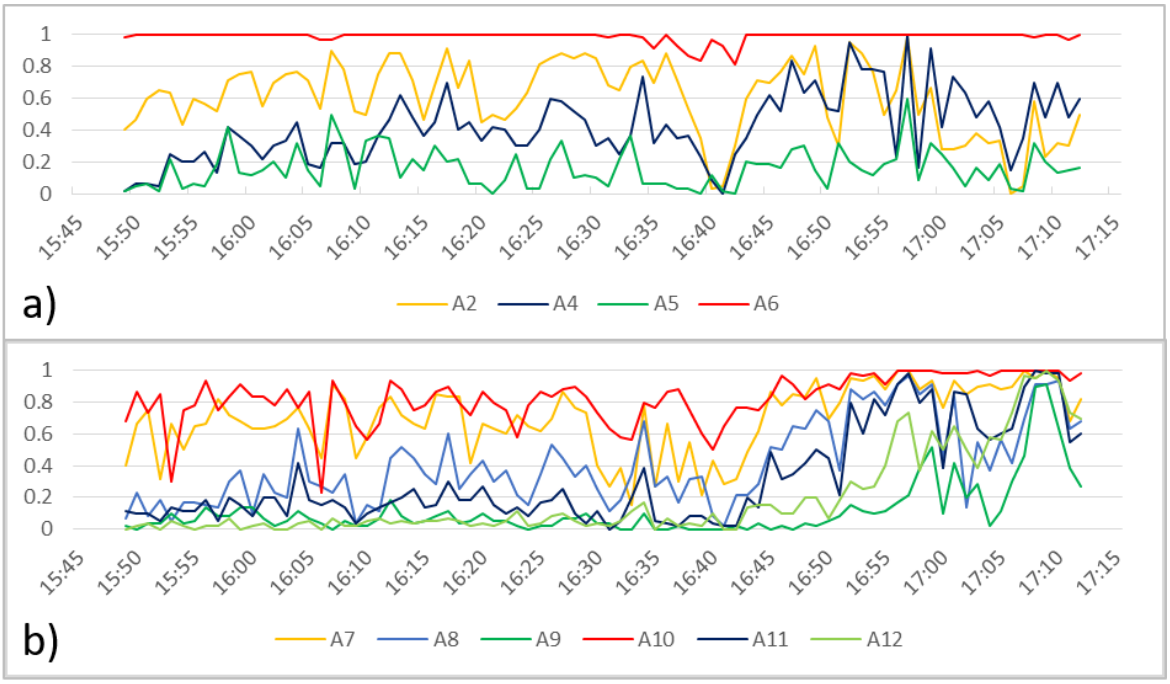

Figure 2.12: Activity parameter (AP) time-series for (a) back-beach and beach-dune interface locations, and (b) blowout trough locations.

A2 on the back-beach was the most seaward of all LPCs. It was therefore the least susceptible to topographic modifications to both flow and transport vectors, and had the second highest mean AP for locations outside of the blowout. Statistical analyses in Chapter 3 show that its measured transport had one of the highest correlations of all locations with wind speed. The AP of A5 is substantially lower than that of its two adjacent sensors (A6 and A4), and also of A2 on the back-beach. Sediment supply/transport at A5 was particularly constrained due to both complex ballistic sand grain trajectories, and potential limitations in the LPC's 'field of view' or degree of alignment with dominant transport vectors (section 2.5.1 and 2.5.6).

Although A4 showed a slightly higher, mean AP towards the end of the experiment, it was landward locations within the blowout itself, that clearly showed marked increases to AP during R2 (Figure 2.12, b), likely evidencing increases in

wind speed and steadiness attributed to flow compression. In particular, A7 and A10 showed AP values that were of considerably higher magnitude than other trough locations. The A7 total count just for R2 was greater than the total study of all other sensors combined, with the exception of A6. Despite having only the fourth highest total R2 count, A10 transport was near continuous as reflected by the highest mean AP value of all trough locations at 0.98.

2.4.3 Spatial complexities in wind and transport responses (R3-5)

Figures 2.13-2.15 show results for the three 5-min wind and transport runs selected from the time-series to provide further insights. Matching R3, R4 and R5 durations allows comparison of wind and transport values for runs with comparable mean incident wind speed but gradually changing wind direction from alongshore (R3) to highly oblique but most strongly onshore directed (R4) and during a transition period between the two (R5). Although A3 wind speeds are similar between the three runs, R5 represents the 5 minute period of maximum mean wind speed throughout the full 84 minute study duration. This allows an enhanced understanding of the relative importance of incident wind speed and incident direction on blowout sediment transport.

Wind characteristics (left column) and aeolian transport (right column) for alongshore winds at the beach (R3) are displayed in Figure 2.13. R3 represents the 5 min period for which reference wind direction at A3 had the lowest mean value relative to geographical N, and gave near perfect alignment of flow with the S foredune orientation. Wind speed decreased by > 1 m s^{-1} towards the N of the back-beach (between A3 and A1). Flow veered landwards around the S foredune edge and into the blowout leading to relatively stronger winds towards the S wall, and lower winds towards the N wall. A6, A5, A9 and A12 speeds were all

marginally higher than incident flow at A3, whilst all other locations were lower. TKE increased northwards and landwards, and the highest mean CV was recorded at A7 towards the N wall.

In terms of absolute counts, transport at all locations within the trough during R3 were at minimal levels and of negligible magnitudes relative to respective R4 and R5 values. In relation to flow parameters, A7 and A10, the locations of both lowest wind speeds and highest TKE, coincided with the strongest transport intensity values (excluding those recorded at A6). Markedly high relative AP values at A2, A7 and A10 likely contributed to these locations experiencing relatively high transport albeit at low absolute levels. Despite the strongest winds occurring along the S wall of the blowout, A9 and A12 recorded the lowest transport intensities and transport activity. Only two locations, (A2 and A5) experienced higher normalised transport intensities (ntt) during R3 than when A3 reference flow was more strongly onshore directed. This may reflect both their transport records being dominated by incoming streamers across the beach and optimal alignment with these transport vectors during this period.

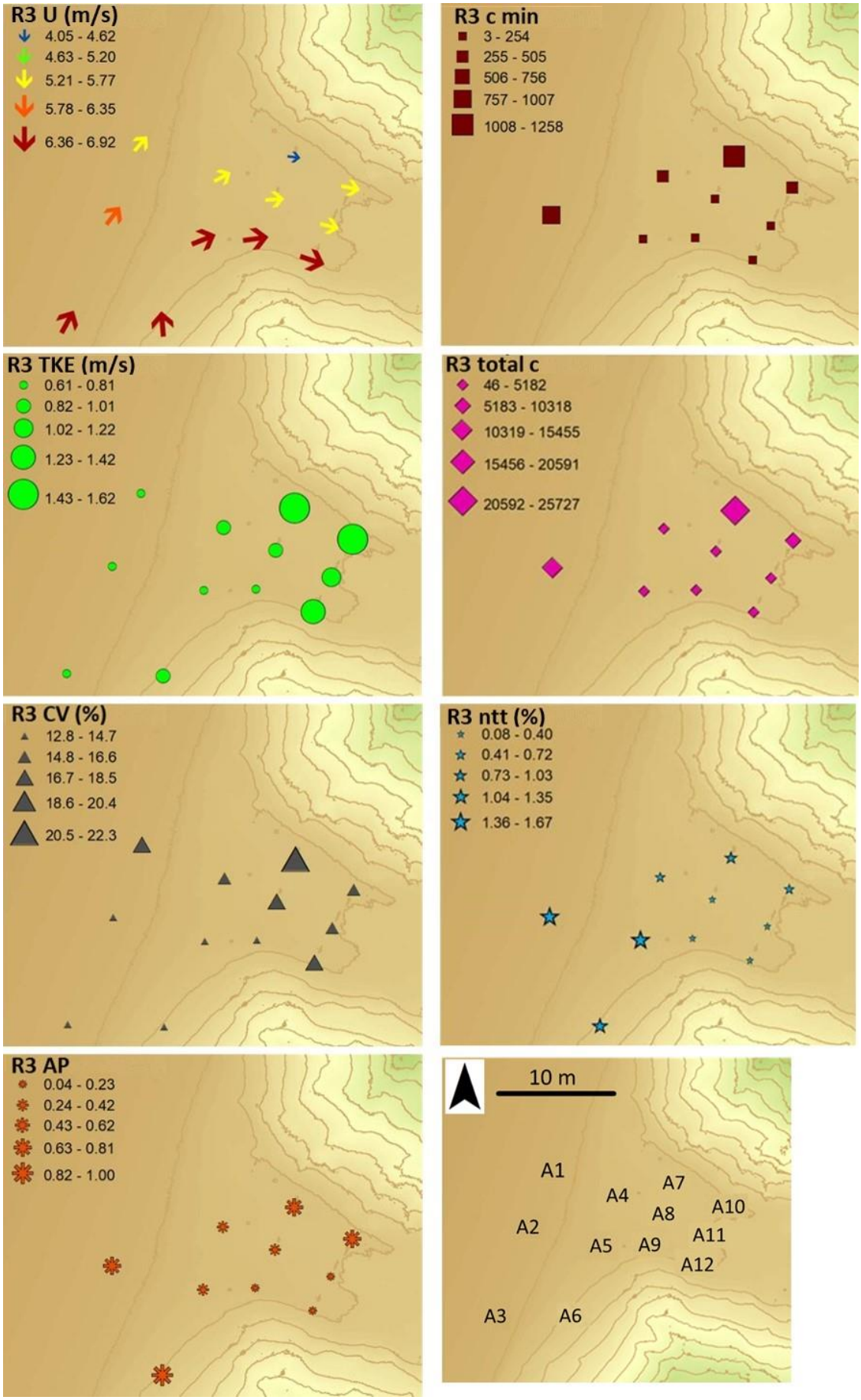

Figure 2.13: R3 wind patterns and sediment transport response.

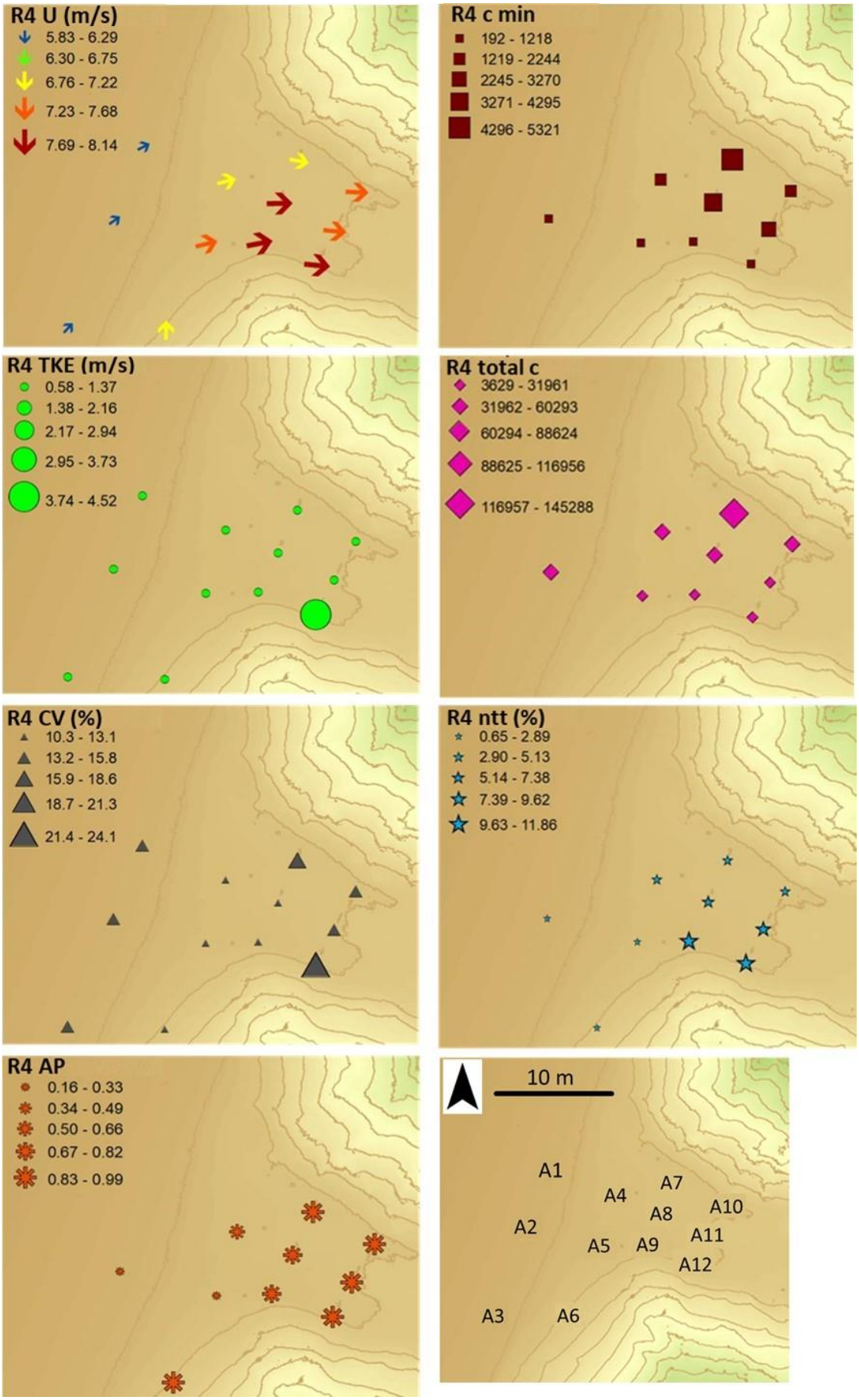

Figure 2.14: R4 wind patterns and sediment transport response.

R4 represented the 5 min period with the mostly strongly onshore A3 wind direction. As incident wind became more onshore directed, albeit still highly oblique (Figure 2.14), wind speeds inside the blowout increased and differentiated themselves most clearly from those recorded at the back beach (top-left figure). During R4 all trough locations experienced their highest positive wind speed differences to that of A3.

Normalised transport intensities also achieved maximum mean values throughout the trough. With the exception of A12, TKE within the trough reduced in comparison to R3. Similar to the spatial patterns observed during R3, transport was highest at locations where wind speeds where lowest (e.g., A7), and was lowest at locations where wind speeds where highest (e.g., A9 and A12). In general, AP increased markedly throughout the trough as the transport signal became less intermittent.

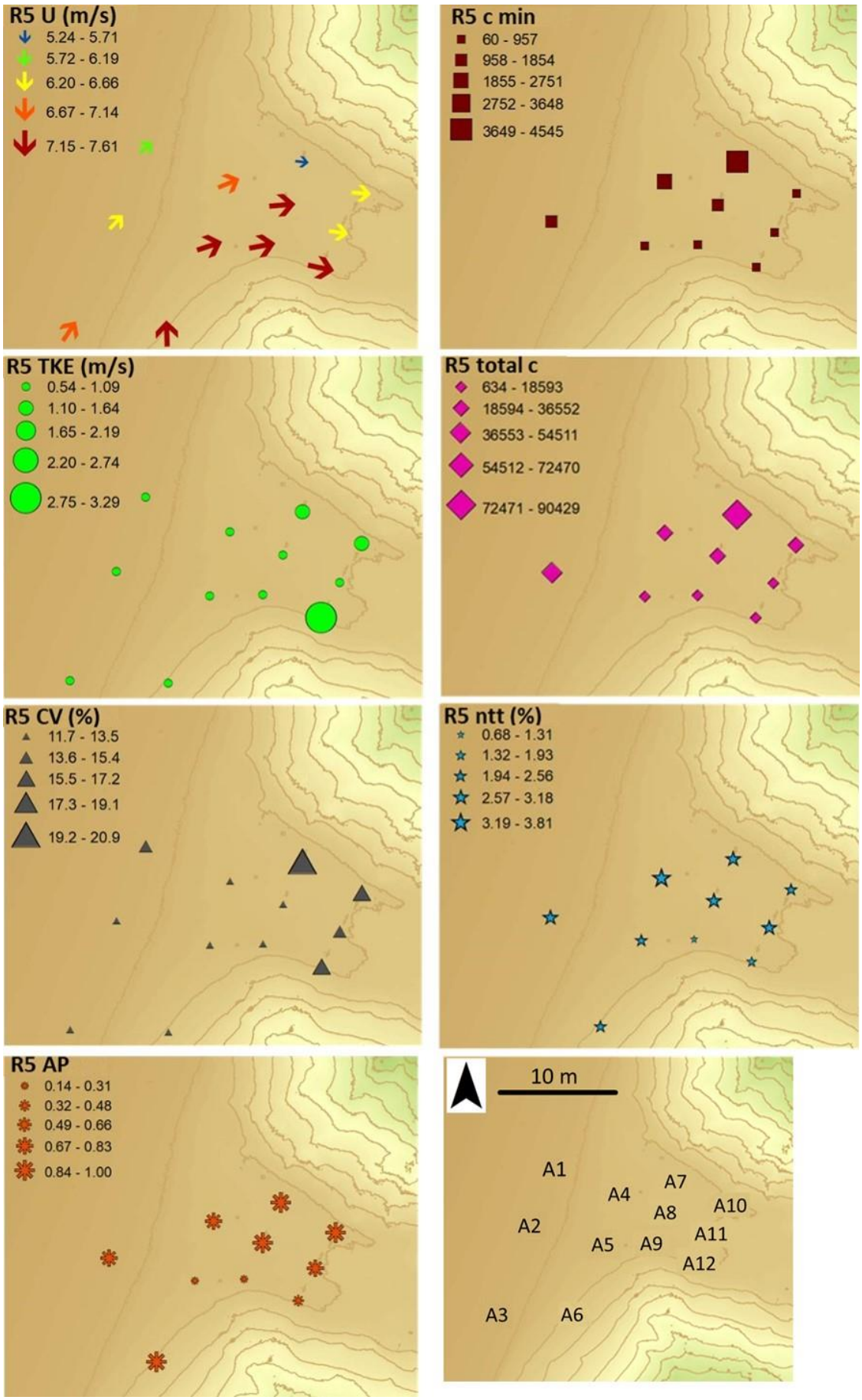

Figure 2.15: R5 wind patterns and sediment transport response.

R5, the transition run directionally between R3 and R4 (Figure 2.15) showed spatial patterns consistent with the previous runs, of relatively stronger winds

being associated with lower transport levels, and vice versa. A3 wind direction during R5 was approximately midway between that of R3 and R4, but importantly represented the maximum A3 mean wind speed for any 5 minute period during the 84 minutes of measurement. Mean A3 wind speed in R5 was 6.78 m s^{-1}, and 0.7 m s^{-1} higher than for R4. In R5 only three of the trough locations (A8, A9 and A12) showed increased wind speeds relative to that of A3.

All LPCs within the two most seaward rows experienced their maximum normalised transport intensities during R5. Despite higher wind speed at the A3 back-beach reference UA than that during R4, all locations within the trough showed lower normalised transport intensities (ntt), giving a clear indication of the importance of regional wind direction over wind speed. Similar to the other runs, transport intensity was strongest at A6, and most active, with AP ≈1.0. A7 and A10 AP values also demonstrated near continual transport activity. Although A5 was the closest LPC downwind of A6, and recorded some of the strongest winds, transport intensity and activity were negligible relative to other locations.

2.5 Discussion

2.5.1. Blowout airflow and transport patterns

Topographic modifications to airflow are characteristic of complex beach-dune landscapes. At reduced spatial scales, form-flow interactions specific to foredunes (e.g., Arens, 1996; Walker, *et al*. 2006), and to blowouts (e.g., Hesp, 1996; Smyth, *et al*. 2014) have perhaps received the greatest attention. More broadly, over several decades, the wealth of information gained from process based field studies has greatly advanced our knowledge of the ‘coherent flow structures’, and flow typologies associated with form-flow interactions (Bauer, *et al*. 2013). Often, distinct, localised flow modifications, and/or landform scale, turbulent flow

structures, are recognised to be strongly associated with particular coastal landforms, or to specific component features of their topography.

Extensive measurement and modelling, of event scale airflow patterns associated with a diversity of blowout geometries, and incident wind conditions, have allowed advanced characterisation of blowout airflow dynamics (e.g., Smyth, *et al*. 2012, 2013, 2014). The vast majority of understanding gained, is now well accepted. Having been heavily studied and documented, distinct flow modifications are often readily identifiable, and can frequently be explained with reference to the topographic setting of a point location. Knowledge of event scale sediment transport however remains scarce. This study, for the first time, measured synchronous, high frequency, instantaneous, airflow and sediment transport, across a systematic instrument grid, at the beach-dune interface of a foredune blowout.

Airflow and transport dynamics were found to be complex, and in particular, exhibited high responsiveness to even slight changes in incident wind direction. This study represents a first, early step towards understanding the nature of beach-dune sediment exchange, and instantaneous aeolian transport sediment transport in foredune blowout locations. Beyond gaining some important and fundamental insights in this respect, results were also informative in highlighting a number of potential future research pathways, likely to be of high relative value.

2.5.2. Weak relationships between airflow and sediment transport response

A recurrent theme of chapter one was the critical relationship between wind speed and aeolian sediment transport. The diversity of deterministic, aeolian sediment flux models in existence, are all exclusively based upon parameterising the

premise of wind speed being positively correlated with sand transport (e.g., Bagnold, 1941; Kawamura, 1951; Zingg, 1953; Owen, 1964; Hsu, 1971). Although widely applied, a persistent constraint of such models is their dependence on an unlimited supply of homogenous sediment, and idealised flow and surface conditions (Baas and Sherman, 2006; Sherman, *et al*. 2011; Bauer, *et al*. 2013). Progressive learning, through extensive field research, has identified a plethora of important environmental controls on transport, which to date render such models inadequate in resolving transport dynamics, particularly in coastal settings. The strong influence of surface form variability on aeolian dynamics determines sediment flux models to be wholly unsuitable for use in locations of high topographic complexity. With such complexity being a key characteristic of foredune blowouts, the need for construction of an empirical evidence base of field measurements was a primary motivation for this research.

An important finding of this study is the lack of relationship existing between airflow and transport dynamics, both in ‘at a point’ locations, and between proximal point locations, even within distances of just a few metres. For all runs explored here, spatio-temporal variability in flow and transport records were complex throughout the instrument grid, and cannot be explained using the ‘at a point’ measurements for each sensor location in isolation. In fact, even rudimentary interpretation of transport within the blowout trough is only possible by considering the entire beach-foredune-blowout context (sect. 2.5.3., 2.5.6., 3.4.7., and 3.4.8.).

In the trough, locations with the strongest, and therefore most transport capable winds, recorded the lowest transport magnitudes, and vice versa (i.e. relatively high transport magnitudes recorded in zones experiencing some of the weakest winds). A5, the closest sensor to the A6, foredune stoss slope location (where

transport intensities were continually highest), experienced the second highest mean wind speed of all locations. Despite this, LPC5 transport was particularly low (Fig. 2.9 and 3.3; Table 2.2). Low transport intensities at locations subject to strong winds can be explained by the local influence of supply limiting factors, or by the potential for sediment pathways and transport vectors being different to macro-scale airflow patterns.

Interestingly, the reversal of this occurrence is also evident. Locations such as A7 recorded extremely low relative wind speeds, but particularly high relative transport. The topographic setting of A7, at the foot of the elevated N blowout wall, together with markedly weaker winds in comparison to all other locations, strongly suggests this to be a zone of topographically induced flow stagnation. Other studies have attributed transport levels exceeding flow capabilities in zones of stagnation, to transport being maintained by turbulence. Wiggs (1996), linked this phenomenon to the destabilising effect of concave streamline curvature, which specifically occurs in dune toe locations. Although A7 turbulence (TKE) was relatively high, several pieces of evidence indicate turbulence may not have been the primary driver of high relative transport in this study.

In field settings, the strong disconnect between spatio-temporal patterns of flow with those of transport, is a recurrent characteristic of event scale dynamics which highlights the inadequacy of deterministic aeolian transport models. Saltation rather than suspension being the primary mode of transport in aeolian systems promotes this commonplace divergence between flow and transport vectors. In beach-dune settings characterised by complex topographic modifications to airflow, there is great potential for this divergence to be pronounced. Bauer, *et al*. (2013) stressed the importance of treating both flow and transport as vector rather than scalar properties. Further, that as aeolian sediment transport is almost

exclusively described in scalar terms, the direction of transport vectors are habitually assumed to simply mirror those of flow. Through reviewing the continual advancements in our understanding of ‘coherent flow structures’ they suggested that greater consideration of the now extensively documented flow signatures, and/or flow structures, associated with specific dune topographies, as being an alternative route, with perhaps the greatest prospects for resolving events of this nature.

Davidson-Arnott, *et al*. (2012) identified the transport signal of ‘at a point’ locations to evidently comprise both sediment entrained in the immediate vicinity of a point, and that which is ‘advected’ to the sensor locality, from the ‘far field’. As only ‘at a point’ transport is likely to show strong association with a co-located wind record, all things being equal, the strength of any flow-flux correlation is inversely related to the proportion of sediment transport derived from the far-field. Evidence suggesting the very poor, flow-flux relationship at A7 to be strongly influenced by the contribution of sediment from the far-field is offered from a number of sources, not least that the persistently low relative wind speeds at the location did not support an absolute grain count twice that of all grid locations other than A6.

A7 transport intensity sustaining levels which were largely more than double that of the two immediately seaward, upwind LPCs (A2 on the back-beach, and A4 at the beach-dune interface) further reduces the probability of the relatively high transport levels being associated with the maintenance of incoming saltation streamers by flow turbulence. It also points to the likelihood of transport vectors approaching the location from directions other than those aligned with landform scale patterns of airflow streamlines. If seeking to explain A7 transport intensities through sediment input from the ‘far field’, and with reference to the measured data of other grid locations, the only absolute grain count capable of supporting

the A7 transport signal, was A6, on the upwind S foredune, indicating the probable significance of this sediment pathway.

Beyond the empirical transport records available, continual bursts of sediment being propelled from the S foredune, across its entire elevation range, were visually observed throughout the event. Large volumes of grains, comprising the constant, high magnitude transport across the S foredune, were seen to follow ballistic trajectories towards the N wall, (and A7 locality), upon reaching the S foredune-blowout wall intersection. These 'jets' of saltating grains largely maintained their ballistic lines of flight, aligned with the foredune orientation, and were 'ejected' from dominant upwind streamlines at this juncture, on dune attached flow being steered landwards, along the S wall and into the trough. That is, absolute levels of transport at A7 appeared to be influenced significantly by S foredune derived sand supply, together with the dune aligned direction of the transport vector immediately upwind of S foredune terminus, at the blowout throat.

Delgado-Fernandez, *et al.* (2018) observed a similar phenomenon at the Devil's Hole, blowout-parabolic system in Sefton. Their study described sand being ejected from near-surface streamers, and over the upper edge of the blowout walls. These bursts of grains were observed to travel distances of tens of metres before landing back again on the blowout surface.

2.5.3. Temporal variability in transport, in association with wind direction, and topographic flow modifications

Two distinct transport regimes of differing character, were highly evident within the experiment duration (R1 & R2). That there was only negligible variance in mean wind speed (+0.05 m s^{-1}) at the A3 reference UA, strongly suggests local incident wind speed not to have been a significant function, in the forcing of these discrete

regimes. Smyth, *et al*. (2013) found that incident wind speed makes an inconsequential contribution to topographic flow modifications within blowouts, and that incident wind direction is the dominant control on the nature of turbulent flow structures. Given the pronounced, positive step change in transport intensities between the two ‘runs’, it appears that even small directional changes to incoming winds can subsequently result in topographically induced enhancements to flow, of sufficient magnitude to ‘turn on transport’ within the blowout.

At the event scale presented in this study, foredune configuration has been considered as a constant. It is also noteworthy that mean incident wind speed between the two regimes was also ‘constant’, or more specifically, of negligible difference. This facet of the airflow record was particularly fortunate. It allowed identification of strong dependencies for both airflow and transport dynamics inside the blowout trough, with the direction, and approach angle of incident winds. That the swift transition between the two diverse transport regimes coincided with an abrupt change in incident wind direction, strongly supports the assertion of blowout transport dynamics being primarily governed by wind direction.

In the absence of total coverage of the study area with airflow and transport sensors, in line with all experiments of this nature, event scale dynamics must be theorised, and then supported with the empirical evidence that is available. The suggestions included are well aligned with contemporary knowledge and understanding of airflow dynamics in coastal dune topography. Concerning wind direction, they propose the ‘how’, with regard to this parameter resulting in such a pronounced shift in transport patterns.

Previous studies have described wind direction, and dune slope orientation relative to incident direction, as primary factors which govern form-flow

interactions. They affirm relative flow direction to control both the proportion of incident wind, mass and momentum, that can be transferred across the foredune itself (e.g., Sweet and Kocurek, 1990; Bauer, *et al*. 2012), and more recently also the nature of macro flow structures and modifications within blowouts (Smyth, *et al*. 2012, 2013). This study supports a number of points suggesting transport inside the blowout is highly sensitive to even small directional changes in incident wind. Fluctuations in the direction of airflow at the A3 reference UA are assumed to be undoubtedly an expression of variance in regional winds.

Interactions between a regional wind field and foredune topography are accepted to be heavily dependent on wind approach angle relative to foredune orientation (Bauer, *et al*. 2012). As the directional range of airflow at the A3 reference UA is narrow in this event, we can assume that whilst always remaining highly oblique to the foredune, there was temporal variability in the angle of this obliquity. During R2, increasing transport intensities, wind speeds, and flow steadiness inside trough occurred in coincidence with negligible change to A3 mean wind speed. R2 characteristics being associated with flow compression offers the best explanation for these specific parameters to exhibit rapid change within the blowout. As topography and regional wind speed are '*constants*', flow compression is almost certainly the result of a greater volume of airflow entering the trough. It therefore follows, that the switch in regime relates to a greater proportion of regional wind mass and momentum is entering the blowout. In turn, that the marked alteration in flow/transport dynamics occurs in coincidence with a shift in regional wind direction, being the only notable change in key variables, offers a reasonable argument for this being the initial factor associated with increasing airflow entering the blowout, and the resultant compression of flow which follows.

Accepted theory on aeolian fluid dynamics determines that dune slope and orientation relative to wind approach angle, dictates the degree to which flow mass and momentum can be transferred across the dune surface (Walker, *et al*. 2006; Bauer, *et al*. 2012). Whilst steeper gradient slopes, and/or wind approach angles which are closer to dune perpendicular, promote flow refection or reversal, the increasing transfer of mass and momentum across a foredune surface, is positively correlated with increasing obliquity of airflow, relative to dune slope orientation (Walker, *et al*. 2017).

As the foredune represents a significant obstacle to boundary layer flow, incident wind is effectively compressed against the seaward stoss slope. The proportion of airflow mass and momentum that is transferred across the S foredune surface at any point in time, will be strongly attached, and deflected upwind towards the blowout (Sweet and Kocurek, 1990; Bauer, *et al*. 2012; Smyth and Hesp, 2016). At the foredune-blowout juncture, on elevated topography falling away to the east, airflow is steered landwards, and into the trough. With a greater proportion of the regional wind field being first deflected towards the blowout, and then steered landwards into the trough, which is geometrically constant, compression of airflow results in relative enhancements to blowout wind speeds. As detailed in chapter one, (section 1.5.1 and 1.5.2), local acceleration of airflow is a common mechanism associated with blowout genesis and evolution, as it promotes relative enhancements in the entrainment, and the maintenance of aeolian sediment transport (Hesp, 2002).

The shift in direction of A3 airflow, assumed to be an expression of some change in regional wind direction in this instance is suggested to have resulted in increasing obliquity of near-surface airflow with the S foredune, and therefore increasing blowout directed deflection of regional wind, mass and momentum. It is

the increased volume of airflow entering the trough in association with high magnitude foredune deflection which gives way to flow compression.

2.5.4. Event scale transport and longer term evolution

Measureable changes to topography were not detected during this short duration, moderate wind and sediment transport event. It is however known that even over limited time spans, events in similar topographic settings can produce geomorphic change of much greater magnitudes. As an example, research by Delgado-Fernandez, *et al.* (2018), at a nearby, inland blowout-parabolic dune complex in Sefton, recorded surface changes of up to 0.3 m in just a few hours. Furthermore, in their study, some specific surface changes were found to be dependent on wind direction, with geomorphic change on opposing walls of the blowout identified as occurring at differing times, dependent on incident flow approach angles during these respective periods.

The results of this study demonstrated highly complex transport and airflow dynamics, which were characterised by acute levels of spatio-temporal variability. As even over the short duration presented here, pronounced changes in transport intensity were recorded at multiple sensor locations, underlines that trends for longer term, sediment pathway, will be the product of episodic, short duration, and spatially variable transport events.

Investigations at Sefton, and other UK dune systems (Smyth, *et al*. 2020a, 2020b) explicitly stated that more work is necessary to understand meso-scale sediment transport pathways in blowouts. Further, that studies combining the measurement of both topographic changes, and instantaneous transport, at the event scale, would be of greatest value. Whilst not capturing geomorphic change, results here

did show a strong divergence in flow and transport vectors, through maximum transport in areas of weak flow, and minimum transport in high flow areas. Also, that quasi-instantaneous, spatially complex, airflow and transport responses were associated with minor changes in incident wind direction. Given this is a high frequency occurrence, it is most likely, that landform-scale patterns of geomorphic change will exhibit high spatial variability, both within, and between individual events.

Current research of secondary dune blowouts in Sefton (Smyth, *et al*. 2020a), identified a continual switching between erosion and deposition, was occurring at individual survey pin locations, within and independently of the longer term trend in geomorphic change. To the knowledge of the author, this longitudinal survey campaign of Smyth, *et al*. (2020a) is the first to provide a high frequency, topographic evidence base, which supports similar observations to those made by Jungerius and van der Meulen (1997), in an early, lower resolution study.

Following Delgado-Fernandez, *et al*. (2018), and Smyth, *et al*. (2020a), longer term geomorphic change associated with blowouts is acknowledged to result from sediment transport that occurs in multiple steps. Full resolution of this evolution therefore necessitates a comprehensive database of event scale, sediment transport studies, (which includes frequent repeat topographic surveys, and a wide range of incident wind conditions). Although, quantification of event scale topographic change was absent here, that pronounced changes in transport patterns were found to be associated with minor changes in incident wind direction, an occurrence of high frequency, is supportive of these contemporary theories on longer term evolution.

Finally on the links between event scale, foredune blowout, sediment transport, and coastal evolution. Until now, evidence concerning blowouts being involved in the landward transfer of sediment was largely anecdotal, and only supported by visual observations. High resolution measurement of processes in this study, in itself represents progress in this respect. Identification that topographic enhancements to airflow are associated with enhancements to the landward transfer of sediment via foredune blowout pathways, confirms their high potential to make significant contributions to longer term evolution.

2.5.5. Sediment transport pathways, potential controls, and their implications

Although at first view appearing characteristically distinct and chaotic, the complex transport dynamics within the trough appear strongly connected with conditions external to the blowout's internal geometry. Previous studies have identified that beach-dune interactions under highly oblique incident winds, can result in a decoupling of the transport regimes in operation on the back-beach and foredune stoss slope (e.g. Bauer, *et al*. 2012). That the nature of sediment transport on the foredune in this study, was notably decoupled from that on the beach, allowed greater insights into potential sediment pathways.

Foredune transport (A6), was orders of magnitude greater than elsewhere in the instrument grid (Table 2.2), and almost 9 times greater than measured transport at the back-beach (A2; Table 2.2). Further, AP values for A6 were ≈1.0 throughout data collection, and considerably higher than those recorded at the back-beach (Figures 2.13 - 2.15). Airflow deflected over the sparsely vegetated foredune generated sediment transport that was orders of magnitude greater than that across the back-beach surface, and were near continuous in delivering sediment to the blowout.

Aeolian transport across the lower slopes of foredunes on the deflection of oblique incident winds can be confirmed as a natural mechanism which feeds sediment to trough blowouts following wave scarping by storms. Such transport events could be strongly retarded on the gradual growth of vegetation, as following beach inputs, sediment retention by the foredune itself would be enhanced (Delgado-Fernandez, *et al*. 2019b). In this study, longshore transport across the seaward slope of the upwind foredune was identified as the primary pathway contributing to sediment delivery to the blowout. That incident winds must occur within a very narrow directional range to be perfectly aligned with foredune blowout orientations reduces their relative probability. This suggests that other than in cases where the wind regime is strongly uni-modal, (and blowout aligned), foredune deflected winds and transport, will be a primary control on blowout transport activity. It follows that longshore 'fetch' distances, of uninterrupted frontal dunes between blowouts, foredune geometry itself, together with its control on wind steering, and foredune/back-beach vegetation cover seem highly relevant for triggering different magnitude transport responses in coastlines dissected by trough blowouts.

Beyond knowledge concerning 'natural' beach-dune interactions, this insight is of particular relevance to coastal dune managers. Foredune 'notch cutting' is a primary intervention technique used by those adopting a 'dynamic restoration' management strategy (Arens, *et al*. 2004; Riksen, *et al*. 2016; Ruessink, *et al*. 2017). As the foredune, rather than the beach, appeared to be the main source of sediment for aeolian transport within the blowout interior during this study, the 'notching' of foredunes which are heavily vegetated, carries the risk of having relatively small impacts on the desired sediment transport, directly from the beach into the dune field. Although this intervention specifically targets foredunes which are 'over stabilised' by vegetation, caution should be taken when selecting sites.

This will likely be of particular importance in temperate climates, where the beach is frequently wet, and vegetation regrowth relatively quick, thus potentially reducing the magnitude and duration of the ecological benefits being targeted.

That findings in this study suggest longshore transport on the foredune stoss slope is a primary sediment pathway also raises questions about the potential impact of allowing foredunes to be artificially maintained in a sparsely vegetated state (e.g., by visitor trampling). In heavily degraded areas such as Formby point, human impact not only initiates and maintains foredune blowouts, but also limits vegetation coverage throughout the foredune itself. This occurs via multiple mechanisms which include, visitors sliding down, climbing up, and walking across the foredune stoss slope. Throughout wind conditions ranging from alongshore, to marginally onshore oblique, significant volumes of sand could be eroded through direct deflation of the foredune surface if not sufficiently protected by vegetation. With blowouts receiving sand derived from this source, and facilitating its landward transfer, such transport would be occurring at the expense of ‘denuding’ the foredunes themselves (rather than, or in addition to enhancing more direct, landward transfers of sediment from the seaward beach).

Elements of both this event scale study, and the decadal scale LiDAR analyses to follow (Chapter 4), provide the first empirical evidence in support of this occurrence. In Sefton, this increases the importance of further exploration. Airborne LiDAR data are now undertaken by the Environment Agency at near annual frequency. If complimented by concurrent photographic surveys of foredune vegetation, the importance of vegetation as a control on geomorphic change could be more fully understood, and its longer term consequences more readily quantified and forecast.

2.5.6. Cross-shore variability in forcing parameters of transport

Chapter 1 provided concise coverage of numerous factors additional to that of wind speed, which are capable of exerting significant control over aeolian sediment transport. Airflow turbulence, surface moisture, and topographically induced airflow modifications provide just a few examples. The relative importance of such factors on levels of instantaneous transport, typically exhibit high spatial and temporal variability. The grid based instrument deployment in this study, which spanned both the back-beach, foredune, and blowout interior, during a single event, allowed exploration of factors potentially contributing to recorded levels of sediment transport. Results highlighted well defined spatial variability in the relative importance of differing airflow characteristics, to sediment transport across the grid. Whilst numerous examples of this were displayed throughout the 84 min record, comparison between the transport responses during R4 and R5 offered the most compelling evidence (Table 2.3 and 2.4).

Table 2.3: Airflow and transport averages during R4.

	A2	A3	A4	A5	A6	A7	A8	A9	A10	A11	A12
Average *u* ($m\ s^{-1}$)	6.29	**6.09**	6.97	7.62	6.97	6.83	7.93	8.07	7.66	7.49	8.14
U Difference to A3 ($m\ s^{-1}$)	0.20	n/a	0.88	1.53	0.88	**0.74**	**1.84**	**1.98**	**1.57**	**1.40**	**2.05**
Average Direction (°)	235	**222.7**	255.2	256.2	182.1	280.5	269.1	258.9	272.0	275.8	275.4
Av. TKE ($m^2\ s^{-2}$)	0.59	0.67	0.71	0.68	0.72	0.80	0.58	0.81	0.90	0.81	4.52
Av. CV (%)	13.5	14.15	13.05	11.13	13.02	18.17	10.30	11.95	13.27	13.46	24.05
Av. ntt	0.65	n/a	3.39	1.42	1.34	**3.59**	**5.62**	**11.86**	**3.53**	**8.18**	**11.10**

Table 2.4: Airflow and transport averages during R5.

	A2	A3	A4	A5	A6	A7	A8	A9	A10	A11	A12
Average *u* ($m\ s^{-1}$)	6.57	**6.78**	6.74	7.55	7.23	5.24	7.14	7.61	6.63	6.55	7.48
U Difference to A3 ($m\ s^{-1}$)	-0.21	n/a	-0.04	0.77	0.45	**-1.54**	**0.36**	**0.83**	**-0.15**	**-0.23**	**0.70**
Average Direction (°)	223.2	**213.6**	247.2	251.3	178.1	276.2	265.2	259.2	274.7	277.5	282.0
Av. TKE ($m^2\ s^{-2}$)	0.54	0.67	0.69	0.65	0.76	1.17	0.72	0.71	1.30	1.02	3.29
Av. CV (%)	12.54	13.12	13.32	11.70	13.27	20.89	12.72	11.72	15.94	14.93	15.57
Av. ntt	**2.66**	n/a	**3.81**	**2.16**	**2.02**	3.06	3.15	0.68	2.03	3.08	1.85

During R4, the 5 min period when the A3 reference UA recorded oblique flow which was most strongly, onshore directed, maximum normalised transport intensities were experienced at all six blowout trough sensor locations. The unrivaled transport intensities occurring in this period coincided with an especially low A3 mean wind speed. Although analysis was constrained by absence of a high frequency regional wind record, the directional maximum of airflow on the back-beach, induced maximum positive increases in wind speed throughout the trough. During this period, transport intensities at all trough locations also exhibited a temporarily improved association with co-located wind records. Following Davidson-Arnott, *et al*. (2012), such phenomenon are known to signify an increase in the contribution of locally entrained sediment to a transport signal, relative to that delivered from the 'far field'. Enhancements to 'at a point' airflow with respect to incident wind, are typically indicative of localised flow compression, which in turn explains increased sediment entrainment in the immediate vicinity of a sensor. With the exception of A12, and only negligible difference for A9, (the two S blowout wall positions), abrupt suppression of CV and TKE values within the trough during R4 are additional indicators of the occurrence of flow compression (Smyth, *et al*. 2013).

Slope configuration and incident wind approach angle are known to be primary controls on the proportion of airflow mass and momentum which can be transferred across the surface of a dune (Sweet and Kocurek, 1990; Arens, *et al*. 1995; Bauer, *et al*. 2012). Numerous studies evidence this proportion being greatly increased under highly oblique conditions, and to then give compression induced enhancements, together with more strongly attached, and deflected secondary flow (e.g. Walker, *et al*. 2006). For this event, the absence of synchronous, high frequency, incident wind data, prevents comprehensive resolution of the influence of regional conditions on secondary airflow, and transport responses within the

blowout. Strongly compressed flow within the trough does however suggest incident wind direction as being the principle driver. That the proportion of the regional wind field being first deflected, and subsequently entering the blowout, is maximised on incident flow reaching an optimal approach angle, is well aligned with contemporary understanding of form-flow interactions.

In contrast, along the beach-dune interface, and back-beach, during R5, much greater correlation was shown between all transport signals and their co-located wind speed records, together with maximum intensities also all corresponding with this period of strongest, A3 mean wind speed. Despite the 0.7 m s^{-1} mean wind speed enhancement during this period, a 9°difference in A3 direction appears to have limited topographic enhancements to flow within the blowout, in some instances induced negative modifications, and at every trough location, resultant transport intensities were markedly lower than in R4. During R5, relative levels of TKE and CV within the blowout being generally higher than in R4 offers a further layer of evidence suggesting an absence of flow compression in this period.

As the relative magnitude of topographically induced airflow modifications are positively associated with terrain complexity, it is to be expected that their importance is generally less pronounced across beach topography, than across dunes. All things being equal, (and disregarding surface moisture), beach sediment transport was in the main, more strongly related to wind speed, than dune transport, as secondary airflow modifications across the beach are much less influential. Whilst this cross-shore variability was a general characteristic throughout the study, this identified contrast in dynamics was most strongly evident through comparison of R4 and R5 metrics.

Although confirmation would require measurement throughout a range of incident approach angles, it is reasonable to speculate that regional wind speeds are only most probable to play a dominant role in the magnitude of blowout transport, when incident directions align strongly with blowout trough orientations, thereby allowing the enhanced beach transport to more directly enter the blowout.

2.5.6. Observed complexities and methodological contributions

The data recorded during this short-term experiment allowed for in-depth analyses of spatio-temporal patterns of airflow and aeolian sediment transport. In Chapter 3, the absence, or existence and strength, of statistical relationships between all airflow and transport variables across the measuring grid are explored. These are presented in Chapter 3. Additional to the persistently evident horizontal trends reported in this chapter, visual observations, and measured data demonstrated the likelihood of variability in the divergence between airflow and transport vector directions, also occurring vertically, with height above the surface.

The most obvious example of such divergence was observed on the foredune at A6, a location of particular interest. The direction of continuous, high magnitude transport across the foredune, showed substantial disparity with that of the flow vector. Throughout the experiment, A6 transport, measured by the LPC in the very near-surface (20 mm), had a vector strongly aligned with foredune surface/orientation, whilst the airflow vector measured at 40 cm above the surface, was in general, approximately 20° obliquely offshore to foredune line. This scenario supports findings in other studies which point to the directional limitations of transport sensors (Ellis, *et al.* 2012; Walker, *et al.* 2017). For sensor arrays deployed in beach environments, LPC alignment with the current or expected direction of incoming winds, is ordinarily considered most appropriate. In complex

topography however, streamlines vary spatially, and over time, with optimal sensor alignment therefore being highly episodic and temporary.

Further, individually, the upwind ‘field of view’ for each sensor may be constrained or enhanced, dependent on its orientation relative to the temporarily variable direction of airflow and transport vectors, together with proximal upwind dune topography. Although quantitative results presented here matched visual observations during the experiment, the ‘field of view’ of sensors in the S wall (and to some degree, also throughout the grid), will have been impacted by their orientation in the field, and their relative proximity to elevated dune topography. An insight of particular significance in these findings came from the exceptional divergence exhibited by flow-flux vector directions, and highlighted the great potential importance of this logistical limitation. For future studies of similar design, this factor merits much greater attention than it is customarily afforded, and no more so than for experiments in topography where airflow/transport patterns are expected to be complex.

Finally, the lack of flow-flux correlation, both in ‘at a point’ signals, and between sensor locations, even over short distances of just metres, will to varying degrees be related to airflow modifications induced by sediment transport itself. Currently, understanding of the extent to which this factor may influence event scale dynamics is limited. Its specific importance is likely to be of greatest relevance for locations of high intensity transport, and/or where the presence of, terrain aligned, ballistic grain trajectories (such as those described in section 2.5.1 and 2.5.4), are prominent. Grains in saltation travel at lower mean velocities than their fluid flow, transport medium, which thereby creates a ‘drag’ effect, as the lower velocity grains extract momentum from airflow. Bauer, *et al.* (2013) theorised that this in itself may be sufficient to initiate secondary flow structures, due to the sharp

gradient which could be produced in the vertical wind profile, by high magnitude transport. At the foredune-blowout juncture, when flow and transport vectors diverge, as grains are 'ejected' to follow ballistic trajectories, this gradient ceases abruptly. The S wall of the blowout consistently experienced the strongest wind speeds but only low magnitude transport intensities. Aside from potential attachment and/or compression associated airflow enhancements, the removal of momentum extracting grains from flow streamlines, could theoretically have also led to additional ('non-topographic') increases in wind speed, and offer partial resolution of the observed higher relative mean wind speeds. The opposite could also be applicable for A7 at the foot of the N wall, which recorded high intensity transport, relative to low mean wind speeds. The considerable input of sand grains 'raining' into the location from above, having followed ballistic trajectories on ejection from the S foredune, may have further reduced wind speed, beyond that which might normally be attributed exclusively to flow stagnation.

2.6 Conclusions

For the first time, synchronous, quasi-instantaneous airflow and transport, were measured in high frequency, across a systematic, gridded deployment of instruments, at a foredune blowout location. Flow and transport dynamics were found to be highly complex. The structure of deterministic, sediment mass flux models are designed to parameterise positive, proportional relationships between wind speed and aeolian transport (Baas, *et al*. 2020). In this study, spatial patterns of wind speed, relative to transport intensity, demonstrated a strongly inverse relationship. This confirmed previous assertions (e.g. Baas and Sherman, 2006; Delgado-Fernandez and Davidson-Arnott, 2011; Sherman, *et al*. 2011), of such models being inadequate for predicting sediment transport within foredune blowouts, and more broadly, in coastal dune settings of comparable topographic complexity.

Strong directional divergence between airflow and transport vectors, further limits their application in resolving, the high frequency records of event scale field studies. Similar to airflow, transport exhibits high spatio-temporal variability. Maximum transport was measured on the stoss slope of the upwind foredune, whilst only moderate levels recorded on the back-beach, supporting the theory of considerable sediment being derived from the foredune, and the importance of this pathway to blowout transport. This additionally offered further validation of previous studies which identified a decoupling of back-beach and foredune transport regimes during highly oblique incident flow (Bauer, *et al*. 2012).

Wind direction at UA3, when compared with other sensor locations, and that recorded at the local met station, indicated oblique winds were being steered northwards and longshore. Both airflow and transport vectors were driven along the S foredune, and subsequently into the blowout via two distinct mechanisms. On reaching the blowout throat, sharp steering of foredune attached flow occurred, to give landward directed flow streamlines along the S trough wall. The ballistic trajectories of saltating grains on the S foredune, were however maintained. In remaining aligned with the orientation of the S foredune, grains were directed across the trough, to result in stronger relative levels of transport at the opposing N wall.

Marked variability in transport patterns exhibited significant dependency on spatio-temporal variability in topographically induced, airflow modifications. In turn, secondary airflow patterns were governed by fluctuations in incident wind direction. This suggests the landward transfer of sediment through foredune blowouts, is likely to occur via multiple incremental steps, during and between individual events. During this study, strong inter-dependencies between spatio-

temporal patterns of sediment transport, topographic flow modifications, and incident wind direction were very evident. A more comprehensive understanding of these associations were constrained by the absence of high frequency, incident wind data. Blowout configuration/orientation, foredune geometry, vegetation cover, and foredune orientation relative to the regional wind direction, all also appear to be of high potential influence on individual events. The strong, longshore deflection of regional winds for instance, which were of high significance in this study, would likely be far less pronounced for foredunes of lower amplitudes, or lower, stoss slope gradients.

The first initial steps made here have provided valuable, albeit, ‘broad brush’ insights into the character of foredune blowout, sediment transport dynamics. Assessment of the relative importance, and the degree of influence, that specific environmental factors may potentially have on foredune blowout transport events needs further exploration. Incremental progression along this theme would benefit from numerous additional field studies. Comprehensive characterisation of foredune blowout transport demands an evidence base of greater diversity. Studies which encompass differing wind approach angles, blowout configurations, foredune heights, and vegetative states, would all be of considerable benefit. Field measurement of airflow and sediment transport dynamics during directly onshore incident winds, or those which align perfectly with blowout trough orientations are likely to offer particularly important insights. The measurement of higher magnitude geomorphic events, for which short duration, responses in topography are more detectable, would also provide information of value with regard to sediment transport pathways.

CHAPTER 3 – STATISTICAL RELATIONSHIPS BETWEEN SEDIMENT TRANSPORT AND WIND FORCING UNDER COMPLEX AIRFLOW SCENARIOS

3.1. Introduction

Deterministic models of aeolian sediment transport are founded on the premise that higher wind speeds translate to higher levels of shear stress at the surface, and thus greater levels of sediment flux (e.g., Bagnold, 1941; Lettau and Lettau, 1977). Such models are based on airflow over idealised, flat, sandy surfaces, together with unlimited sediment supply. Increasing wind speeds in these 'transport-limited' scenarios, increase the potential for sediment transport. However, most natural settings are 'supply-limited', with actual transport often not reflecting increases in wind speeds, due to a diversity of sediment supply limiting factors (Nickling and Davidson-Arnott, 1990; Sherman, *et al*. 1998). Much progress has been made on the effect of supply-limiting conditions over the last few decades, including the role played by moisture, fetch, pebble lag development, etc., (Walker, *et al*. 2017). Although wind speed remains the control of primary interest in most reported experiments, flow turbulence and flow steadiness are also recognised as contributing factors.

During saltation, sand grains are entrained into the saltation clouds (or 'streamers'), to then follow ballistic trajectories. In complex, and abruptly changing dune topography, saltating grains can be ejected from the surface, to follow paths which diverge considerably from that of the main flow direction (Delgado-Fernandez, *et al*. 2018). As a result, in collecting synchronous, at-a-point airflow and transport records across a spatial grid, the spatio-temporal variability of

transport intensity at each location can be examined in association with the flow-flux records of all other sensors within the array, in addition to the airflow characteristics of the co-located anemometer, thereby providing an additional layer of information with which to resolve event scale dynamics. In this study, the approach has allowed an enhanced, and more 'nuanced' understanding of the flow/transport regimes associated with a foredune trough blowout. Results from Chapter 2 indicate that, in complex topographic scenarios, sensor locations with strong winds can experience limited levels of transport (and *vice versa*: sensor locations with weakest winds experienced high relative magnitudes of transport).

The lack of spatial relationships between main wind variables (U, TKE, and even CV), and sediment movement at particular locations, was associated to supply limited conditions, directional divergence of flow and transport vectors, and to complex modes of transport involving sand grains being ejected from dune edges, to then follow ballistic trajectories into other blowout locations. This chapter further investigates this complex event, and statistically analyses potential relationships between airflow and transport variables. The aim is to respond to questions such as *'if transport at A7 was not related with wind speed at its location, what was it related with?'*

Ultimately, two overriding, and highly desirable outcomes exist, for studies on aeolian geomorphic processes in complex topography. Firstly, to be able to explain and justify, the nature and extent of spatio-temporal variability in the airflow records, by relating observed values for flow parameters across the time-series, to probable topographically induced flow modifications that might be expected, or could be explained by the topographic setting of individual sensor locations. Secondly, and often subsequently, to be able to resolve or explain, relative and absolute spatio-temporal variability in the sediment transport records, by

comparison and analysis of at-a-point transport signals, in relation to the characteristics of airflow, together with the geographic location of individual sensors. Chapter 2 helped to characterise specific locations in respect of their topographic setting, and to assess spatio-temporal variability in geomorphic processes. This chapter comprises statistical interrogation of the dataset, to identify the presence and strength of any relationships which exist between the flow and transport parameters of a specific location, and with those of each of the other sensor locations within the array. This aids the identification and characterisation of any larger scale, 'coherent flow structures' which may be operating, and provides an additional level of detail in respect of location specific airflow or transport signals.

3.2. Methodology

3.2.1. Study site, instrument grid, and data analyses

The study site, experiment setup, and initial data analyses were described in detail in Chapter 2; hence only a summary is provided here. Airflow and sediment transport data were recorded at a foredune trough blowout in the Sefton Coast, NW England (Figure 3.1). The blowout consisted of a narrow throat, approximately 10 m longshore, flanked to the north and south, by steep, elevated foredunes (≈15 m). The trough was broadly oriented north-west to south-east, and expanded landwards at a near constant width for approximately 25 m. Longshore, the foredune was orientated SSW to NNE. The experiment was conducted on the 27th October 2016, during a moderate, broadly WSW wind event. A grid of instruments consisting of 12 3D Ultrasonic Anemometers (UAs) and 10 Laser Particle Counters (LPCs) were deployed at the back-beach, foredune, and blowout interior.

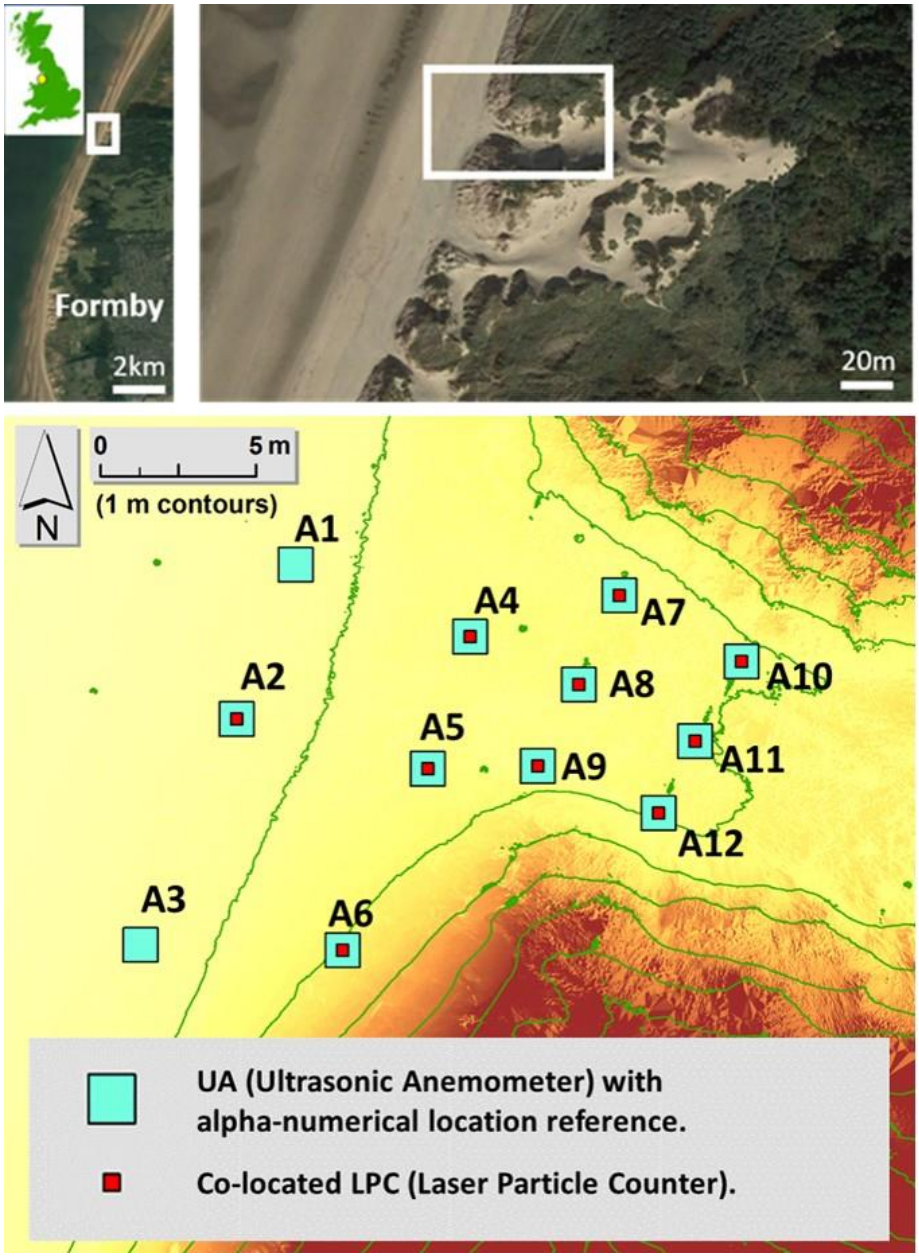

Figure 3.1: Location of study site, Sefton Coast, NW England, and aerial photograph of the blowout throat (above). Digital elevation model including 1 m contours and instrument locations (below).

Airflow data were sampled at 50 Hz, with 3D Gill HS-50 ultrasonic anemometers (UAs), mounted at an elevation of 0.4 m above the surface, with their UV plane positioned horizontally. No attempts to orientate sensors with local streamlines were made given the topographic complexity of the site, leading to largely non-logarithmic, vertical wind profiles. Near surface sediment transport was measured at 1 Hz with ©Wenglor, Laser Particle Counters (LPCs), co-located beneath UA sensors, with the beam positioned horizontally, 0.02 m above the surface. LPCs have no comparable 'between instrument' sensitivities, and that their signal is unaffected by individual grain momentum; they also permit rapid deployment and

are considered ideally suited for use in uneven terrain (Sherman, *et al*. 2011; Hugenholtz and Barchyn, 2011; Davidson-Arnott, *et al*. 2012; Bauer, *et al*. 2012; Chapman, *et al*. 2013; Delgado-Fernandez, *et al*. 2018).

UAs were positioned into four, shore normal rows of three, moving landwards cross-shore (Figure 3.1). During setup, significant transport was observed across the S foredune, with multiple streamers moving across the foredune stoss slope and towards the blowout throat. At the expense of an additional sensor location across the beach-dune interface of the blowout throat, as morphological processes were visibly of the highest magnitude across the S foredune, location A6 was positioned on the foredune stoss slope itself. All instrument locations were recorded via a Terrestrial Laser Scanner (TLS) survey (see Chapter 2, section 2.3.1 for additional details).

Total wind speed (U), wind direction (*a*), coefficient of variation (CV), and Turbulent Kinetic Energy (TKE) were derived from the three components of flow measured by the UAs, using equations (1-4) [Jackson, *et al.* 2011; Smyth, *et al.* 2014], where *u* is horizontal streamwise flow, *v* is horizontal spanwise flow, and *w* is the vertical component of flow.

$$\text{Total wind speed (U)} = \sqrt{u^2 + v^2 + w^2} \quad (1)$$

$$\text{Wind direction } (a) = atan2(u,v) - 180° \quad (2)$$

$$CV = (\sigma \text{ wind speed / mean wind speed}) \times 100 \quad (3)$$

$$TKE = \tfrac{1}{2}((\sigma u^2) + (\sigma v^2) + (\sigma w^2)) \quad (4)$$

Both CV and TKE are indicators of fluctuations to airflow characteristics and turbulence intensity. Sediment transport recorded by LPCs were expressed as average counts and normalised counts (section 2.3.2). The Activity Parameter

(AP) for each LPC was also calculated, with AP values ranging from 0.0 for no transport, up to 1.0 for continuous transport, (Davidson-Arnott, *et al.* 2012; Delgado-Fernandez, *et al*. 2018).

A frequent challenge in resolving sediment transport records, with the airflow patterns of aeolian geomorphic events, is the noise to signal ratio of high frequency data. A common pre-analysis procedure to mitigate this issue, is the use of an averaging period, to diminish the impact of short-term fluctuations within the time-series. Following Smyth, *et al*. (2014), throughout the analysis, transport intensity and AP, together with all airflow parameters, were represented as 1 minute averages. This helps suppress any temporal lags between wind forcing and transport which may exist, and may equally be spatially variable (Baas and Sherman, 2006; Davidson-Arnott, *et al.* 2012; Smyth, *et al.* 2014).

3.2.2. Normality tests and qualitative inspection of the time-series

An initial step in selecting appropriate statistical tests was to check whether data had a ‘normal distribution’, in other words, are the points of data populations evenly distributed about a mean value. Normality checks (Shapiro-Wilk test, SPSS) were performed on the data populations of every individual variable, albeit with a primary interest on sediment transport. Transport intensity was normally distributed in only 1 out of 10 locations, and this was at A6, on the S foredune, with the strongly longshore deflected/steered winds reported in the previous chapter (now also, section 3.3.1). As transport was the primary focus of the analysis, this lack of normality precluded use of the wide array of parametric statistical tests available to assess the absence, presence, and/or strength of relationships. Before conducting any kind of statistical analysis of transport intensity at each location, in relation to ‘at-a-point’ flow parameters, the data populations were plotted and visually inspected with the aim of:

- Investigating the reasons for the lack of normality in transport intensity data.
- Identifying visual trends in transport intensity and airflow parameters over the full time-series.
- Inspecting similarities or differences in flow and transport patterns to assist in the characterisation of specific locations, and/or clusters of data.
- Investigate relationships between extreme values in transport intensity *vs* the various flow parameters available.

(Appendix 1 for full details).

3.2.3. The 'transport run' method

Qualitative observations strongly suggested that the experiment encompassed two distinctly different geomorphic flow/transport regimes within the total 84 minute duration. There was therefore a need to split the time-series into these two separate periods prior to statistical analyses, to ensure that any relationships existing between flow and transport variables, would not be masked by a high noise to signal ratio, (caused by the inclusion of disparate data points from the other, incomparable 'regime').

In absolute terms, levels of transport varied between sensor locations, in some instances by orders of magnitude. This could be related to differing volumes in absolute sediment supply for each individual location, and/or to the orientation of the LPC laser path, relative to transport vector directions in the very near surface. That is, there could be instances where two sensors display considerable difference in absolute grain counts due to one of the sensors under-representing actual transport, as its orientation was less well aligned with the direction of saltation vectors. Despite differences in absolute transport values, visual inspection suggested similarities between the relative, underlying trends of

individual locations were frequent. In order to compare the behavior of sediment transport at different locations, counts per minute were ‘normalised’ by converting them to per minute percentages of the total grain count recorded by each of their respective sensors.

A simple technique was then designed to identify, (and delimit) the differing transport regimes, in a non-arbitrary way. At each sensor location, cumulative ‘normalised’ transport intensity (ntt) was plotted over the 84 minute duration of measurement. Whilst applying a minute averaging period to high frequency data smooths out ‘per second/shorter term’ fluctuations, a cumulative plotted time-series effectively smooths out ‘per minute’ fluctuations by ‘averaging’ transport over the full duration of the experiment. The value of this variable at any given point on the resultant ‘transport curve’ is simply the cumulative transport having occurred up to that point in the time-series, expressed as a percentage of total counts over the full duration. This cumulative transport curve was compared visually, and numerically, with a theoretical, linear transport curve, representing an idealised signal, had normalised transport intensity been perfectly constant throughout the entire measurement period (equating to 1.19% per min in each of the 84 minute total duration of the time-series). This allowed quantitative identification of a marked change in the transport regime by selecting the minute when the observed, cumulative transport curve, was the furthest away from the theoretical, linear transport curve (represented visually in section 3.3.2).

3.2.4. Statistical analyses

Statistical analysis allows highlighting the absence, presence, and/or strength of any relationships between sediment transport and flow parameters at each individual sensor location, and also between all transport and flow variables,

across all locations. This permits assessment of any spatial relationships in existence, which in turn may also be aligned with contemporary theories concerning geomorphic processes in similar topographic settings. With a few exceptions, data were not normally distributed across all the variables explored. Spearman's rho, (commonly termed 'rank'), and Kendall's tau b were performed to explore the existence, and nature of relationships between all airflow and transport parameters. These are the two most widely applied, non-parametric tests of correlation, which rank the values within data populations, thus making them distribution free. Spearman's rank is more easily computed and commonplace, and performs better with small populations. Kendall's Tau b holds a number of advantages, and provides improved understanding of the time-series, as its value can also inform the number of paired values within the population that are concordant. It is also more robust, in providing lower GME (gross mean error), in instances when the population includes equal values (which is relevant for the data here).

Statistical correlation analyses were conducted within all variables at each individual sensor location, and between each variable, at all other sensor locations. This was with the aim of exploring spatio-temporal relationships which may be present, and/or in association with potential, landform-scale flow structures.

3.3. Results

Transport activity had commenced prior to data loggers being launched and data recording coincided with low tide. With that, several hundred metres of the inter-tidal beach were exposed. Considerable levels of transport, in the form of streamers were observed across large areas of the beach, approaching the back-

beach from a broadly WSW bearing. This orientation on the beach being strongly aligned with the wind directional average recorded by the nearby station at Crosby (approximately 5 km to the South).

3.3.1 Description of transport and wind time series

Qualitative analyses of time-series suggested high levels of spatial and temporal variability across the instrument grid, even after having applied an averaging period to remove a proportion of the ‘noise’ associated with short-term fluctuations. Except for transport intensity at location A6, time series for all other locations were not normally distributed over the full duration of the experiment (Figure 3.2). In line with common explanations for the lack of normality, there were short periods of considerable positive and negative change in the magnitude of transport intensity relative to that occurring over the longer duration of data collection, thus resulting in a proportion of data points not being evenly distributed around the mean value of the whole population. For numerous sensor locations, this phenomena was observed in two ways: (i) most locations experienced incidents of very short-lived but extreme peaks in transport intensity relative to transport intensity experienced over the majority of time for which transport was recorded for; (ii) during approximately the final third of data collection, transport intensity increased and was sustained at a level higher than that which had been experienced throughout data collection until that point. A detailed description of all the time-series data recorded as part of the experiment has been included in Appendix 1.

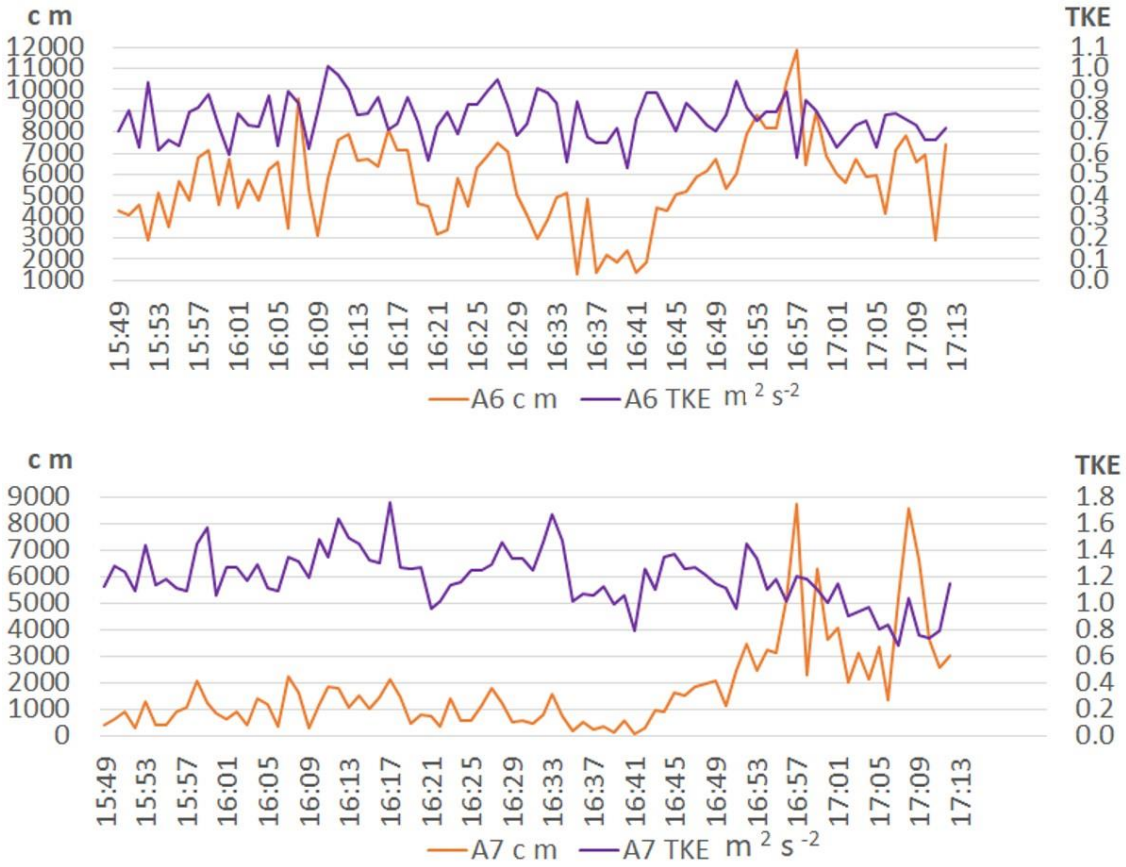

Figure 3.2: Example of time-series of transport intensity (c m) and TKE at a location with normally distributed transport (A6 – above), and a location where transport were not normally distributed around a mean (A7 – below).

In general terms, (as described in Chapter 2), locations A12, A9, and A5 registered the three highest mean wind speeds throughout the grid (Table 3.1). Whilst these three locations had the highest potential for sediment transport, actual total grain counts over the full 84 minute duration were the lowest. These sensors were in closest proximity to the S wall of the trough (Figure 3.1). Their combined total grain count was fewer than that of A11 alone, which had a total count of 29,627, and was the next lowest sensor for total absolute counts.

Table 3.1: Summary of key transport and wind speed metrics

	A2	A4	A5	A6	A7	A8	A9	A10	A11	A12
Total counts	53,015	56,863	13,494	469,583	148,306	58,787	8,861	40,308	29,627	3,858
Max. counts per min	2,942	4,939	1,198	11,835	8,736	5,871	1,514.7	1,828	3,704	726
Mean counts per min	631.13	676.94	160.64	5,590.27	1,765.55	699.85	105.49	479.86	352.7	45.93
CV (%) of counts per minute	75.61	137.44	141.94	36.82	97.58	151.56	260.19	73.83	188.04	256.81
Mean U m s^{-1}	6.29	6.01	6.89	6.76	4.71	6.3	6.81	6.05	5.97	6.91
Maximum U m s^{-1}	6.92	7.49	8.03	7.63	7.28	8.32	8.43	7.99	7.76	8.39
Mean CV (%) of U m s^{-1}	13.06	15.06	12.33	14.27	22.08	14.51	12.29	16.03	15.02	18.66
CV (%) 1 min mean U m s^{-1}	4.04	8.79	6.28	4.63	17.1	11.26	8.94	10.68	10.01	7.55

Transport intensity was highest at A6 (S foredune), and counts in total accounted for over half of all counts recorded during the experiment (Figure 3.3). Airflow at this location was relatively steady (4th lowest mean CV of wind speed), and this may have been a contributing factor to the exceptional steadiness in transport intensity (lowest CV of counts per minute throughout the grid; Table 3.1). Transport levels over the foredune (A6), were three times greater than for A7, the second highest count (inside the trough, proximal to N wall), and more than two orders of magnitude greater than for A12, the lowest of all locations. Total transport for A2, A4, and A8 were broadly comparable.

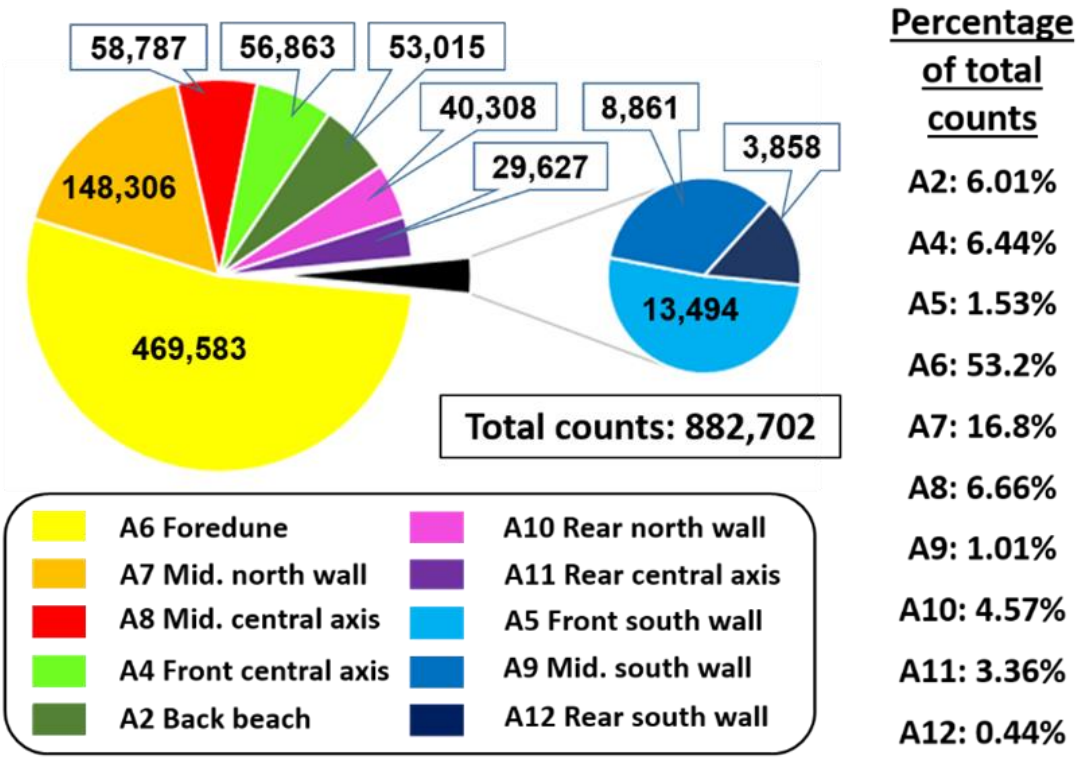

Figure 3.3: LPC count summary. (Fig. 3.1 for instrument locations).

Location A7, at 4.71 m s^{-1}, had the lowest mean wind speed of the grid. Chapter 2 discusses potential reasons for this, including airflow stagnation associated with its topographic location (dune toe area, at foot of the N wall of the trough). Additionally, flow was particularly unsteady at this location relative to all others, with both the average of 1 min CV, and the average CV for the entire period being the highest (22.08% and 17.10 %, respectively). However, this LPC registered the highest total grain count of all sensor locations inside the blowout, and its total was only second to that of A6 (on the S foredune).

3.3.2 'Transport run' method: Results

For multiple sensors, transport intensity increased and was sustained at a higher relative level towards the final third of the experiment, thus promoting the splitting of the total duration of the time-series into two separate periods, with differing lengths and characteristics. The 'transport-run' method was designed to

objectively delimit the time-series into these two distinctly different geomorphic flow/transport regimes.

Transport within the blowout trough

To varying degrees, transport intensity at all six sensor locations within the blowout trough (A7, A8, A9, A10, A11, and A12) exhibited a similar pattern, with the transport records clearly demonstrating the existence of two distinct transport regimes. The longer duration regime was of relatively lower magnitude, with lower overall transport intensity means, and lower magnitude fluctuations. The subsequent, shorter duration regime was characterised by higher transport levels, generally higher magnitude variability, and a number of extreme peaks in transport intensity which were multiple times greater than had been experienced during the longer duration preceding period. Chapter 1 summarised the most important factors additional to wind speed which may contribute to levels of aeolian sediment transport. Given the change in transport intensities between the two regimes, the potential changes in the control and forcing of transport are explored further within the discussion section to follow.

Transport intensity at A7 showed considerable fluctuations (Figure 3.2). When transport data, expressed as percentages of the total transport, are plotted against constant, linear transport (Figure 3.4-above), a portion of the time-series trends at a level below the mean transport value for that sensor (represented by the idealised line). Real time fluctuations above and below this mean transport value are exaggerated and more easily identified when the data is normalised, and plotted against the mean (Figure 3.4-middle).

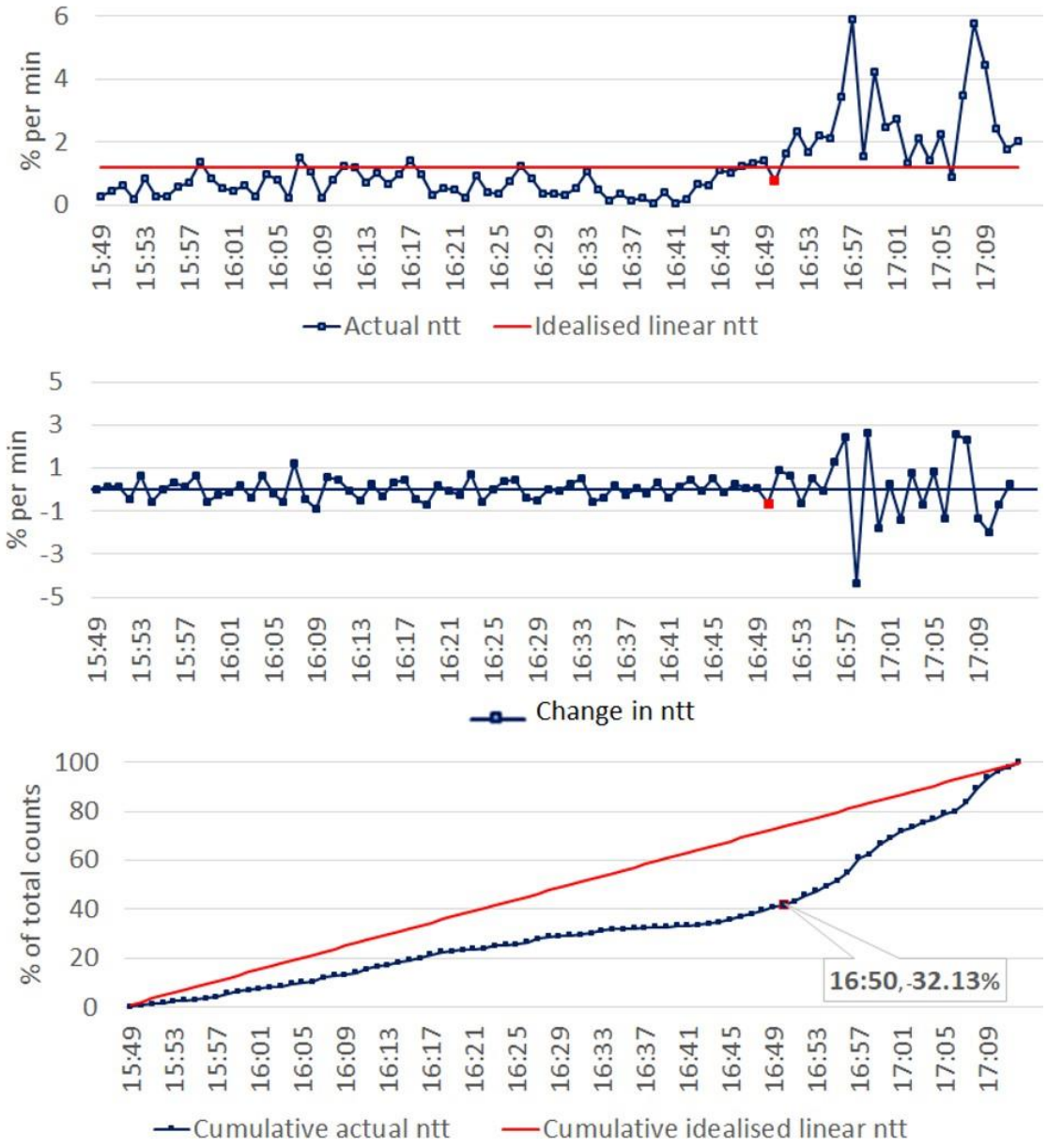

Figure 3.4: Example of 'transport-run' methodological steps and results for A7: transport time-series showing normalised counts per minute [ntt: expressed as percent of total counts] (above), change in ntt (middle), and transformation into a cumulative transport curve (below), that can be compared to cumulative 'idealised' transport to identify the furthest point between the 2 curves to objectively delimit the two transport regimes or 'transport runs' (R1 and R2).

Although positive and negative fluctuations are perfectly visible, their high frequency, in combination with varying magnitudes, results in longer term trends being less easily recognised, or assessed. The final step of plotting the data cumulatively, produced a smooth, gradually rising transport curve. That A7 cumulative transport is initially at a level much lower than the 'idealised' (84 minute, linear mean) is very visible evident (Fig. 3.4-below). The margin by which cumulative transport is lower than 'idealised' transport gradually increases from

outset, as the number of minutes with grain counts below idealised transport pass. The two lines (actual cumulative and idealised cumulative) were furthest apart at 16:50 (cumulative transport 32.13% lower than idealised transport). Beyond this point, real time, measured transport intensity increased leading to a decreasing margin between the two plotted lines (with this also occurring over a shorter period of time), until reaching zero in the final minute of the experiment.

The normalised transport record (Figure 3.4-middle) explains visually the pattern of cumulative transport (Figure 3.4-below). Until 16:50, actual transport in each minute rarely exceeds 1.19%, the level required each minute for transport to have been perfectly linear across the 84 minute duration. Transport intensity until 16:50 has a much lower mean value. Beyond this time, mean transport intensity is visibly higher, and in absolute grain counts, peaks reach levels several times greater than had been experienced up to this point.

An additional example of step-by-step results in the ‘transport-run’ method are shown for A8 (Fig. 3.5). The pattern is similar to that of A7 but changes in the cumulative curve are more pronounced. Cumulative transport falls further below cumulative ‘idealised’ transport (51.19% lower at ‘step change’), before the curve rises at a steeper gradient. In addition to explanation of the occurrence of two discrete transport regimes within the 84 minute duration (chapter 2), suggestions for the differing degrees of polarity between R1 and R2 trough locations, are explored within the discussion section to follow. On the transport-run method itself, this process was successful in differentiating between the two characteristically diverse transport regimes within the 84 minute event.

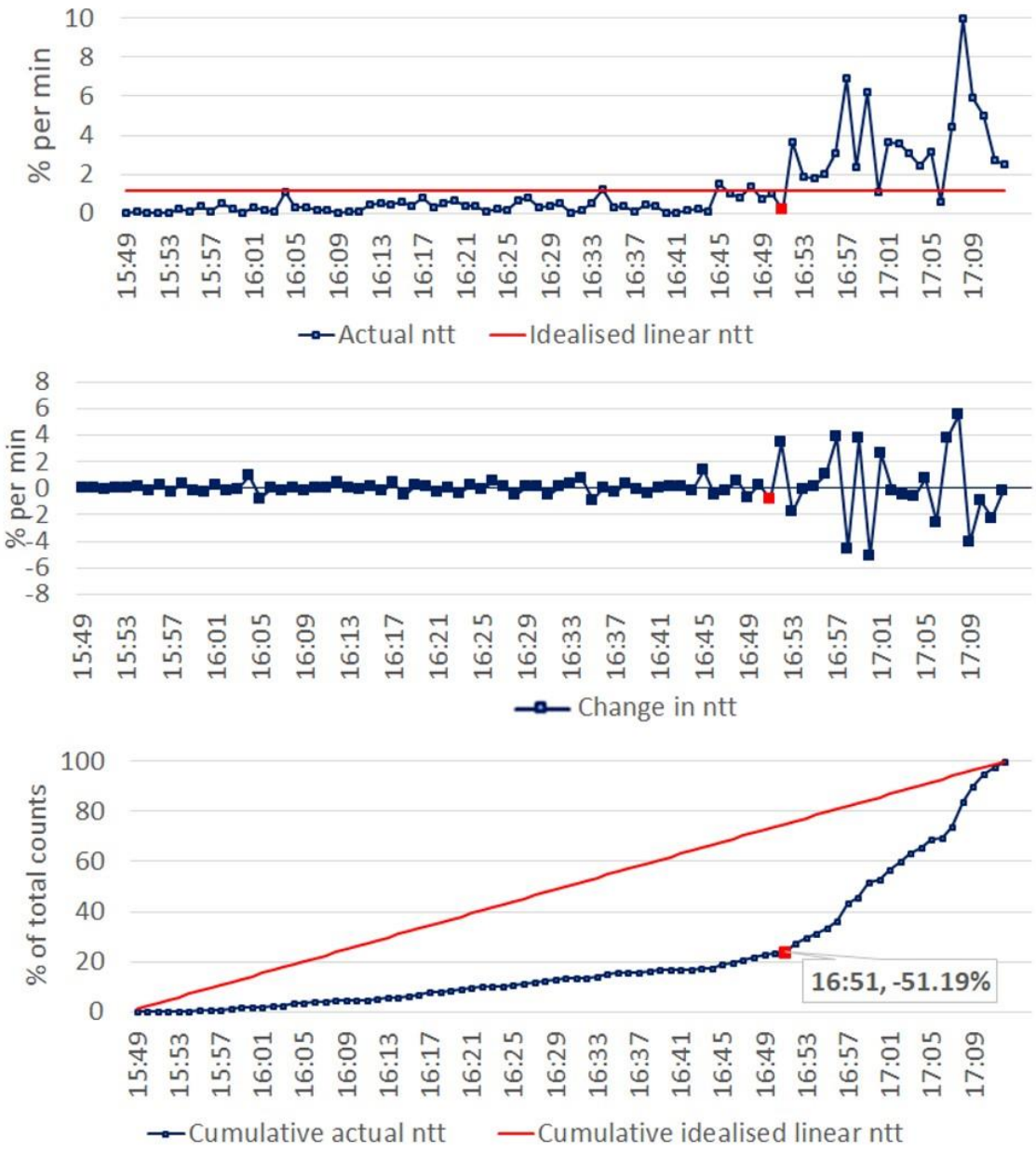

Figure 3.5: Example of 'transport-run' methodological steps and results for A8. transport time-series showing normalised counts per minute [ntt: expressed as percent of total counts] (above), change in ntt (middle), and transformation into a cumulative transport curve (below), that can be compared to cumulative 'idealised' transport to identify the furthest point between the 2 curves to objectively delimit the two transport regimes or 'transport runs' (R1 and R2).

Changes in the regime at the remaining locations within the blowout trough are displayed in Figure 3.6. At A9, the change between regimes was even more pronounced than for A8 and also occurred slightly later. For A10, the positive step change between the two regimes was less pronounced than for all other trough locations, occurred at 16:51, and actual cumulative transport was just 26.63% below idealised. The pronounced step change at A11 occurred at 16:51 when

actual cumulative transport was 61.76% lower than hypothetical linear transport. A12 exhibited the most pronounced change of all locations, due to largely only trace levels of transport being experienced in R1, up to this point (16:54). Finally, also worthy of note was that for A9 and A12, (the two sensors proximal to the S trough wall), the positive step change between the two regimes was staggered. After the initial increase in gradient of their actual cumulative transport curves, (at 16:56 and 16:54 respectively), the curves levelled out slightly, before then rising even more sharply during the final 10 minutes of measurement.

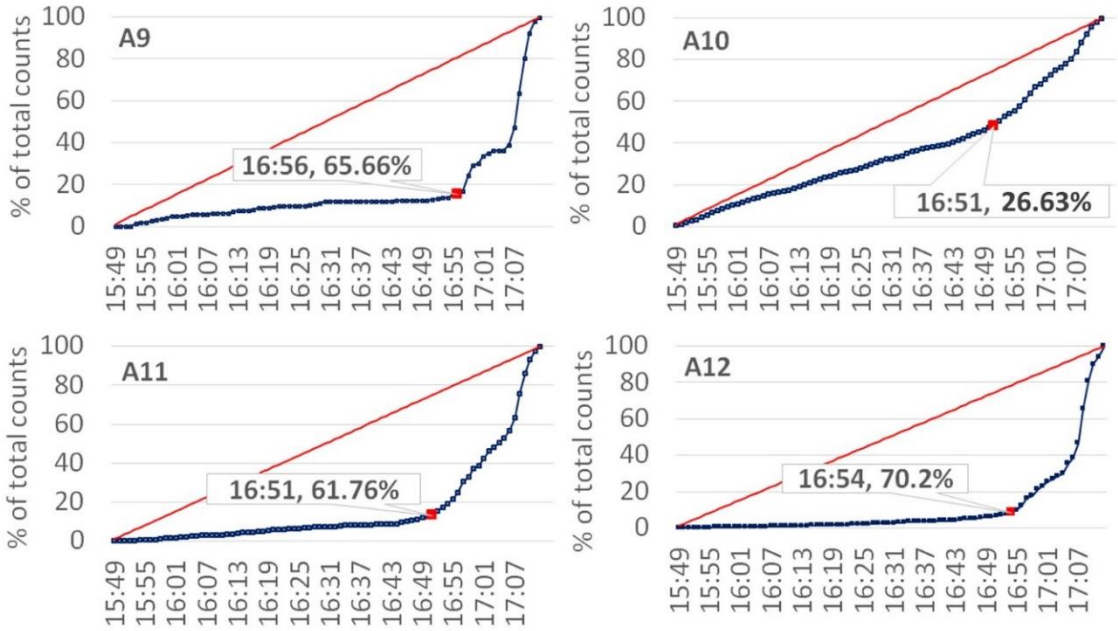

Figure 3.6: Cumulative percentage of total counts (blue line) vs. cumulative, idealised linear transport (red line) for locations A9, A10, A11, and A12, inside the blowout.

The timing of the ‘step-change’ between the two regimes varied spatially amongst the sensors in the trough, over a period of 6 minutes (Table 3.2).

Table 3.2. Timing of 'step-change' for locations within blowout trough

LPC Location	Minute
A7	16:50
A8	16:51
A9	16:56
A10	16:51
A11	16:51
A12	16:54

Transport outside the blowout

With the exception of location A4, transport magnitudes, and temporal patterns of intensity outside the blowout did not generally exhibit the same characteristics as for the blowout trough locations.

The total grain count at location A5 was just 13,494, whilst average wind speeds were relatively high (Chapter 2 and Appendix 1). The pattern of transport was highly variable throughout the experiment, and plotted cumulative transport was unlike that of any other sensor location. In consequence, the existence of two, distinct in character, differing transport regimes, was not evident at this sensor location. Several early spikes in transport relative to its total grain count (Figure 3.7-up), resulted in the plotted cumulative record exceeding idealised linear transport during R1 (Figure 3.7-below). Two short periods of negligible activity (Figure 3.7-middle) then resulted in the gradient of the actual cumulative transport curve, first reducing to thus converge with cumulative, idealised transport, and then levelling out completely to result in the actual cumulative transport curve falling below the idealised transport curve (Figure 3.7-below).

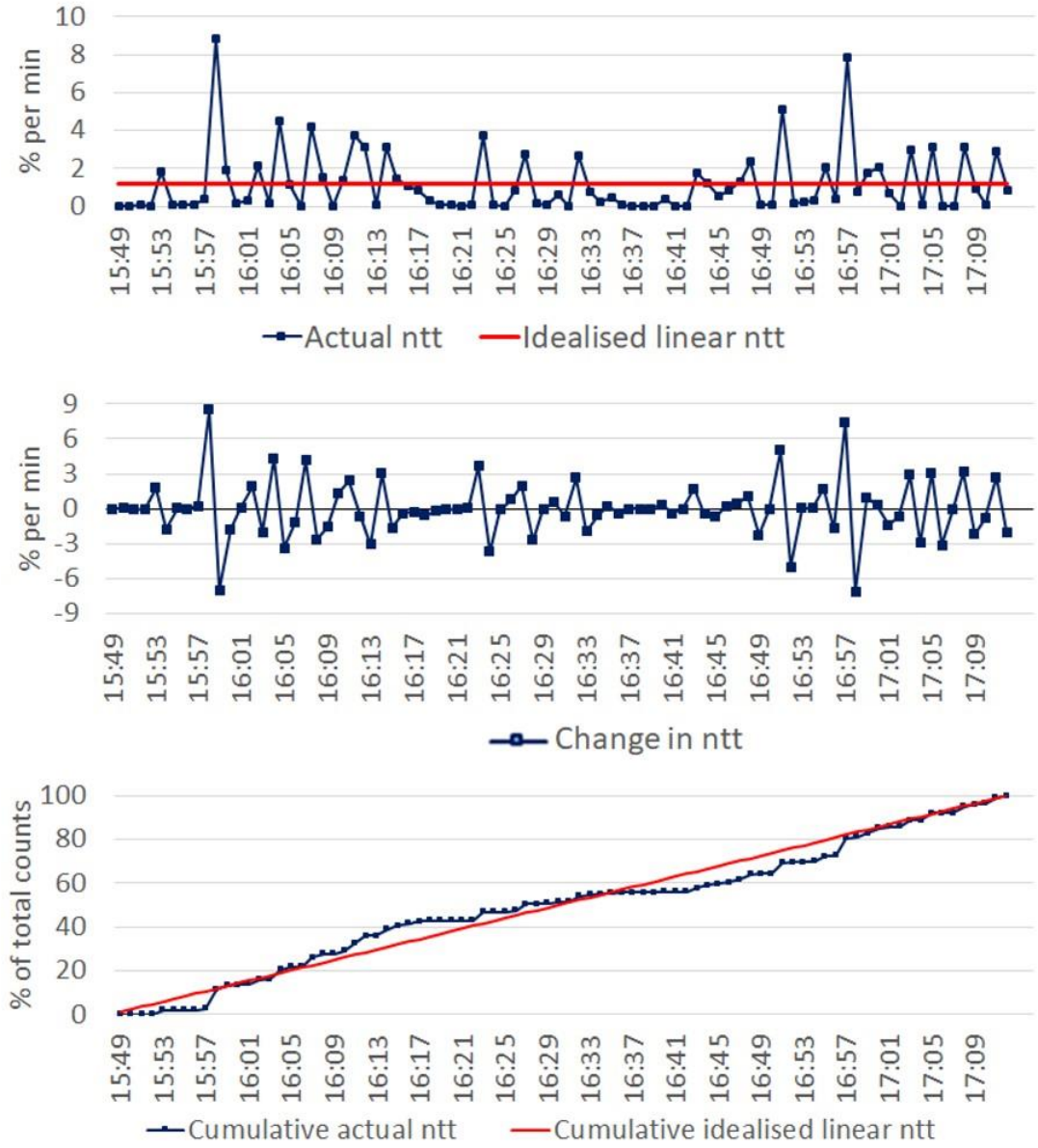

Figure 3.7: 'Transport-run' results for A5. Normalised transport intensity (above), change in normalised transport intensity (middle), and transformation into a cumulative transport curve plotted with a cumulative 'idealised' linear transport curve (below).

Over the full 84-minute duration, A6 transport intensity was the only normally distributed data population. Although fluctuating on a per minute basis, data points were evenly distributed about their mean value. As a result, when plotted, cumulative, normalised transport is highly linear. A linear trend line, plotted through the data has an R^2 value of 0.99 (Figure 3.8-below). The only period for which a margin of any note develops between idealised, cumulative transport, and actual cumulative transport, occurs at approximately the midway point in the time-series. This diversion is as a result actual normalised transport (transport intensity

as a percentage of the total grain count) falling below the perfectly linear percentage of 1.19% for a period of 18 continuous minutes.

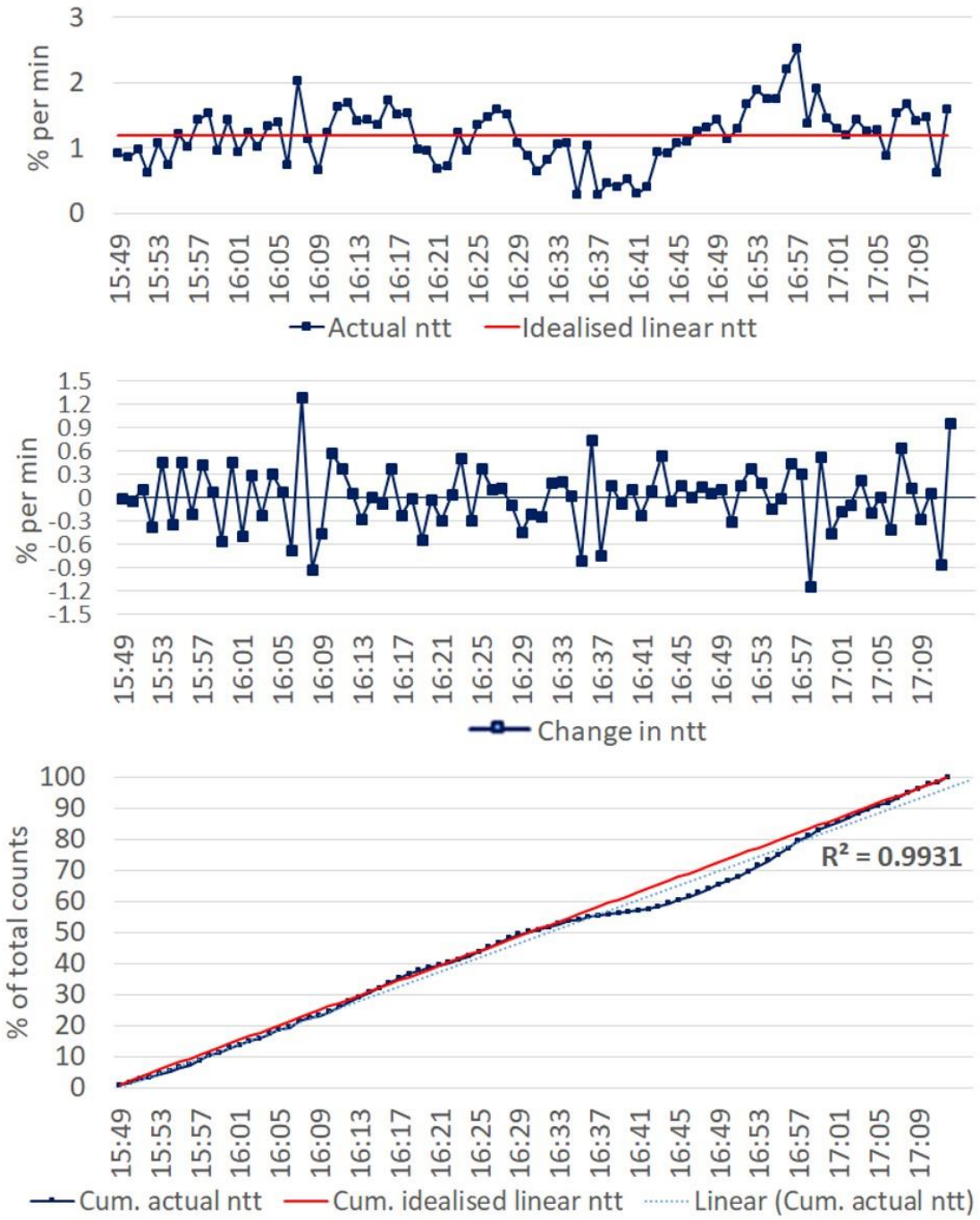

Figure 3.8: 'Transport-run' results for A6. Normalised transport intensity (above), change in normalised transport intensity (middle), and transformation into a cumulative transport curve, with linear trend line, and a cumulative 'idealised' linear transport curve (below).

Transport at A4, (in the centre of the throat at the beach-dune interface) exhibited similar trends to locations within the trough. The point furthest from cumulative, idealised linear transport however occurred earlier at 16:44 (-41.56%). Whilst there was a slight rise in cumulative actual transport at this point, it was not until 16:51

that cumulative transport curve began to rise rapidly, with several sharp increases in gradient highlighted in green, (Figure 3.9 - above).

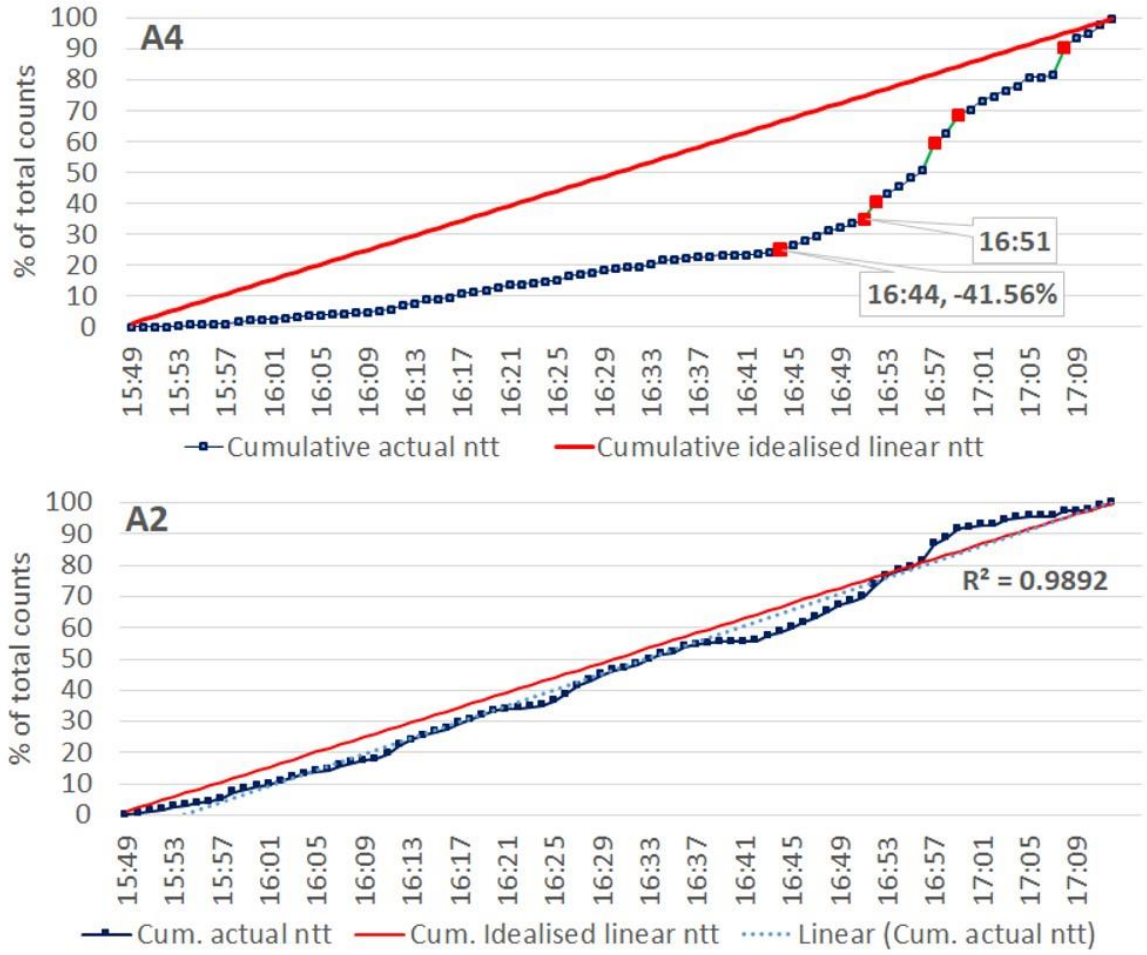

Figure 3.9: 'Transport-run' results for A4 (above) and A2 (below). Beyond the 16:44 regime change at A4, sharp increases in the cumulative transport curve are highlighted green. For A2, a linear trend line and R^2 value of actual cumulative normalised transport are included.

Plotted cumulative transport at A2, on the back-beach was relatively close to idealised linear transport. The time-series did however, potentially reflect two regimes, albeit markedly less pronounced than elsewhere, with actual cumulative transport intensity being below idealised linear for much of the experiment, before rising above idealised cumulative transport for only a short period towards the end of measurement (Figure 3.9-below). Although statistically, the data was not normally distributed, the pattern of cumulative actual transport intensity followed a similar pattern to that of A6 on the foredune.

3.3.3 Statistical results

The absence, presence, nature, changes in, and/or strength of statistical relationships for both transport, and flow parameters, between sensors deployed across a spatial grid, permits an improved evidence base to further resolve, and characterise, event-scale, sediment transport and airflow dynamics.

With the change between two characteristically distinct, transport regimes occurring at 16:51 for three of the locations, and for location A7, at 16:50, in order that the evident changes in airflow and sediment transport patterns could be explored in a consistent manner, 16:49 was selected as the cut-off point for R1, and 16:50 as the starting point for R2 in the statistical analysis. The change between the two regimes at A9 and A12 occurred a few minutes subsequent to this. As the changes were particularly pronounced for these locations, due to the two regimes appearing particularly polarised, that data points within their R2 populations include the final few minutes of the their initial ‘R1 regime’ which was characterised by highly limited transport activity for both sensors, the ‘noise’ associated with their inclusion will be mitigated to a greater extent by the relatively strong transport ‘signal’ of their subsequent R2 data populations.

All locations within the trough (A7 - A12) recorded higher total counts in the final 23 minutes of data collection (R2), than over the preceding 61 minute duration of R1. Statistical analysis was conducted across all variables, for the full duration of the experiment, and for the two ‘runs’. Basic, descriptive statistics are included in Appendix 2.

Results from the statistical tests for all variables are included in Appendix 3, in the form of large matrices consisting of coefficient/R values expressing the strength

and sign of correlations. In addition to numerical values, coefficients within the matrices, (and their statistical significance) are classified visually using the colour code/syntax displayed in Table 3.3. This allows for the presence, nature, strength, and temporal variability of statistical relationships, to be easily identified.

Table 3.3. Syntax/colour code used in the interpretation of statistical analyses.

*	Significant at 0.05
**	Significant at 0.01
	Not statistically significant
	0.1 to 0.1999
	0.2 to 0.2999
	0.3 to 0.3999
	0.4 to 0.4999
	0.5 to 0.5999
	0.6 to 0.6999
	0.7 to 0.7999
	0.8 to 0.8999
	0.9 to 0.9999

In general, the strongest and most pronounced relationships occurred during R2. Dependent on individual locations or variables, this manifested through either or both, an increasing number of correlations between existing, and/or often pronounced increases in the strength, or direction of relationships which were already in existence during R1. Following the onset of R2, multiple above medium correlations emerged or strengthened (e.g., increased correlations between incident wind direction at A3 and changes to transport variables within the blowout).

Another example worth highlighting concerned wind speed at A3. During R1, only one low and one medium correlation, (both positive), existed between A3 wind speed, with that of wind speed at the two other back-beach sensors. For A1, 0.185*, and for the closer A2 location, 0.49**. During R2, the A1 correlation strengthened marginally to become 0.202, but however became not statistically significant, whilst the correlation with A2, weakened slightly to 0.455**, and remained statistically significant (at a level of 0.01). Four positive and statistically

significant, (at a level of 0.01), medium correlations also existed between A3 wind speed with the wind speeds of sensor locations within the trough, (in R1). All of these values swung considerably during R2, changing sign to become negative, with three additionally becoming not statistically significant, and the significance level of the final correlation falling from 0.01 to 0.05. For A8, the R1 coefficient of 0.43** changed to a NSS (not statistically significant), -0.241, A10 from 0.385** to -0.312*, A11 from 0.507** to -0.289 NSS, and lastly A12, from 0.573** to -0.115 NSS. The general cross-location statistical trends concerning wind patterns, (and changes therein), both supported theoretical observations made in Chapter 2, which pointed to wind direction rather than wind speed having played a dominant role in event scale dynamics.

Numerous other examples of cross-instruments correlations can be found within the matrices. Those for wind speed at location A5 provide a further example of particular interest, in also being well aligned with the theories offered in Chapter 2, aimed at resolving airflow patterns. During R1 for instance, the strongest relationship with A5 wind speed, across all grid locations and variables, was a positive one of 0.757** with wind speed at A9. Further, the second highest ranked A5 correlation for wind speed, and also positive, was of 0.554** with wind speed at A6. Based on the general airflow patterns described in Chapter 2, these two locations are immediately, downwind, and upwind respectively, of A5's position.

The lack of correlations for certain variables or locations, were also of great interest in understanding the event. For example, the LPC located at A7 recorded the second highest total grain count of all locations throughout the grid, and which were only exceeded by exceptional transport activity recorded at A6 (on the upwind S foredune). The relationship between transport and wind speed however

was not statistically significant in either Run, and during R1, at 0.131 NSS was the lowest across the entire study site. During R1, A7 normalised transport, at 0.435** did however have the strongest ‘at-a-point’ correlation with TKE.

3.4. Discussion

3.4.1. Modelling and the resolution of aeolian sediment transport events in beach-dune environments

As discussed in Chapter 1 (e.g. sections, 1.8.1. and 1.8.5), an overarching motivation of coastal science is to arrive at a point where we can successfully model geomorphic change, and be able to do so across extended spatio-temporal scales. The relative importance of this has been further heightened by a better understanding of the effects of climate change, particularly with regard to sea level rise (section 1.1.3.). A pre-requisite in achieving this long term aim, is full resolution of event scale, aeolian transport field studies, (which are as a rule, logistically constrained in spatial extent). As a consequence, for several decades, the field measurement of processes has experienced massive growth. It is now wholly accepted, that in character, the airflow and transport dynamics of such events, exhibit high spatio-temporal variability (Davidson-Arnott, *et al*. 2003; Houser, 2009). Additionally, it is often the case for this variability to occur within temporal scales of just seconds or minutes, and across sub-metre distances (Walker, *et al*. 2017; Delgado-Fernandez, *et al*. 2018). This in itself continues to fuel new studies, necessitated by emerging requirements for further data, under differing environmental conditions, and at different topographic settings, or geographical locations.

Fundamentally, whilst the design of aeolian sediment transport, and/or coastal evolution models, may be theoretical, their validation is reliant on possession of a

comprehensive database of empirical evidence, gained through field measurement. The absence of field studies measuring synchronous, instantaneous airflow and sediment transport, at foredune blowout locations, was an initial knowledge gap to be addressed by this PhD research. Whilst this in itself is essential, equally important was being able to explain the data acquired, and to better understand the nature of such geomorphic events.

Current deterministic models of aeolian transport are based on assumptions of idealised environmental and surface conditions, together with an unlimited supply of homogenous sediment (Sherman, *et al*. 1996; Sherman, *et al*. 2013; Baas, *et al*. 2020). With this, application of these models have been repeatedly identified to be wholly unsuitable in coastal, beach-dune settings (Baas and Sherman, 2006; Sherman, *et al*. 2011; Baas, *et al*. 2020). Intrinsic to such models is surface sheer stress, (the force which drives transport), being derived from wind velocity at some height above the surface (Sherman, *et al*. 2011). This in itself, being based on the 'law of the wall', relies on a logarithmic, vertical wind profile. Characteristically, the vertical profile of airflow over complex dune topography is known to be non-logarithmic (Chapman, *et al*. 2013; Smyth, *et al*. 2014), and this further supported the need for measurement. Through statistical analysis, marked spatio-temporal variability was exhibited in the relationships between at-a-point, instantaneous transport intensities, with both airflow and transport variables across the study site. This undoubtedly reflects variability in the number, composition of, and relative influence made by, the environmental factors contributing to site specific transport activity at any given moment in time. Improvement of current aeolian transport models depends on better parameterisation of sediment transport influencing factors. Both the statistical information gained in this study, and the statistical approach adopted in the analysis, offer insights beneficial to characterising event scale transport events in complex dune topography.

3.4.2. Traditional methodologies and analytical approaches

Through both field studies and laboratory experiment, significant knowledge has been gained in respect of aeolian dynamics in beach-dune environments. Information around the diversity of important additional controls on sediment transport, and that concerning topographic modifications to airflow, are themes which perhaps benefit from the greatest recent advancements in understanding (Chapter 1). Typically, this knowledge has brought enhancements in our ability to formulate, and to support interpretations of complex field datasets. The description and analysis of event scale processes presented in Chapter 2, was heavily rooted in this approach.

Interrogation of spatio-temporal variability in airflow and transport signals, from co-located sensors, is a commonplace analytical technique (e.g., Wiggs and Weaver, 2012; Smyth, *et al*. 2014, Delgado-Fernandez, *et al*. 2018). Validating explanations for flow-flux variability, with reference to the geometry of topography, proximal to individual field sensors is also customary (e.g., Walker and Nickling, 2002; Chapman, *et al*, 2013). Despite incremental growth in understanding being gained, numerous logistical, methodological, and analytical issues continue to constrain the full potential value of this approach.

An important logistical problem associated with analysing the flow-flux records of co-located sensors, comes from our inability as yet, to measure these variables at truly ‘co-located’ positions. Acknowledged three dimensional variability, in the magnitude and direction, of both airflow and transport vectors, compounds this issue. Insightful discussions from Bauer, *et al*. (2013) were particularly influential in the acquisition and analysis of data for this study. These insights highlighted the limitations of sensors, the routine treatment of sediment transport as a scalar rather than vector property, and the customary assumption of transport vector

directions mirroring those of airflow, have all limited greater progress within the discipline. In light of the known directional divergence between flow-flux vectors, these suggestions have significant credibility. Bauer, *et al*. (2013), also called for novel, or more 'nuanced' approaches in process based studies, and identified our now well-developed understanding of topographically induced, airflow typologies and/or 'coherent flow structures', as offering some of the greatest potential for making significant scientific progression.

3.4.3. Statistical analysis of complex, aeolian transport events

Use of descriptive statistics in the analysis of aeolian sediment transport events is commonplace. A specific theme which continues to draw considerable attention concerns the diversity of deterministic, sediment transport models in existence. Many studies have tested the validity of such equations against measured data, assessed relative performance between models against measured data, and sought to either improve equations, or introduce additional variables within them (Belly, 1964; Lettau and Lettau, 1977; Hotta, *et al*. 1984; Anderson, *et al*. 1991; McEwan and Willetts, 1994; Lancaster, 1995; Sherman, *et al*. 1996; Dong, *et al*. 2003; Baas and Sherman, 2006; Liu, *et al*. 2006; Ellis, *et al*. 2009; Sherman, *et al*. 2013). Beyond this, for field studies, regression analysis of instantaneous transport, with co-located wind speed or wind turbulence is frequent (e.g. Smyth, *et al*. 2014). In coastal settings, poor relationships between at-a-point wind speed and sediment transport is a common finding. This is typically linked to a variety of local, supply limiting factors, the most important of which received coverage in Chapter 1.

Chapter 2 detailed that in this study, clear, at-a-point, positive relationships between wind speed and sediment transport were few in number. Further, at the landform scale, there was an exceptional, spatial pattern of inverse relationships

between the transport capabilities of airflow, with that of measured transport. In the main, locations with the strongest winds experienced the lowest transport intensities, and maximum transport intensities occurred at locations of weaker wind speeds. Directional divergence of flow-flux vectors, and contemporary knowledge of airflow modifications in complex topography featured heavily in the initial (Chapter 2) interpretation.

The remarkable nature of the event, and the initial, evidence based interpretation being primarily theoretical, demanded further exploration, through extensive statistical analysis. This analytical approach offered potential for both, a more informed understanding of the event, and an additional layer of evidence with which to support its interpretation. Insights from Bauer, *et al*. (2013), (in section 2.5.1.), strongly informed and validated development of the methods used. The grid based instrument deployment facilitated these methods, with this also being an important consideration during the experiment design.

3.4.4. Maximising current knowledge of airflow and sediment transport dynamics in complex beach-dune topography

Foredunes and coastal blowouts are strongly associated with topographically induced airflow modifications, and the development of distinct, coherent flow structures. At reduced spatial scales, discrete landform components, (for example, the dune toe or blowout wall), are also known to be characterised by specific flow typologies. The nature of these airflow modifications have been well documented, through extensive measurement and modelling (e.g., Arens, et al. 1995; Lynch, *et al*. 2010; Smyth, *et al*. 2012; Hesp and Walker, 2012; Hesp, *et al*. 2017). With this, airflow parameters at individual dune locations are often compared to synchronous, incident wind data, to identify differences. Moderation or enhancements to incident wind speed, or directional variance, are then typically

explained with reference to surrounding topography. Our now advanced understanding of form-flow interactions, indicates that the presence of spatial relationships between the signals of proximal, upwind and downwind locations should be expected. Given this, the conventional approach of comparing the specific airflow properties of an individual sensor location, exclusively with only co-located data, or often additionally, also with that of a reference anemometer, guarantees a considerable proportion of the (potentially, high value) information available, is routinely under-exploited. A decision was therefore made to statistically examine each of the flow-flux parameters available, both with all other at-a-point variables, and also with those of every other sensor location. This novel, analytical step proved of particular value, and should be strongly considered in future field studies of high complexity.

Beyond greater exploitation of both available data, and current *a posteriori* knowledge of topographic airflow modifications, this approach also offered potential opportunities to mitigate two confounding issues relating to sediment transport. Firstly, as saltation rather than suspension is the primary mode of aeolian transport, divergence between the direction of flow and transport vectors in complex terrain, is commonplace (Bauer, *et al*. 2013). Event scale, sediment transport pathways, are therefore likely to be poorly aligned with more easily recognised, landform-scale, air streamline patterns. Secondly, that the instantaneous transport signal of individual sensor locations are also known to potentially comprise both, sediment entrained in the immediate vicinity of the sensor, and also grains advected to the sensor, from the far field (Davidson-Arnott, *et al*. 2012). As yet, at-a-point instrument capabilities do not permit true identification of the direction of aeolian transport vectors. Although seldom acknowledged, implicitly, this fact largely validates the disregard for transport direction, or making the assumption of alignment with airflow streamlines, in the

large majority of studies (Bauer, *et al*. 2013). Here, examination of transport signals between sensor locations offered opportunities to account for these factors, for enhancements in event resolution, and additionally, further evidence to support the interpretations made.

3.4.5. The need for transport centric analysis and the 'transport run' method

The rationale for, and value in, examining correlations between every available, at-a-point variable, both within and across all sensor locations, was initially not borne out, when using the 84 minute data populations. Although some of the most evident trends discussed in Chapter 2 could be recognised, the strength or nature of many correlations added a confounding layer of complexity to the event, and constrained interpretation. Testing all data populations for normality, and visual inspection of plotted variables over the full time-series had strongly evidenced significant temporal variability in transport magnitudes (Chapter 2). The majority of locations shared a common similarity in evidencing the presence of two, characteristically distinct, 'transport regimes'. The first regime, (R1), from outset and lasting for a longer duration, exhibited relatively lower, less variable transport intensities. The second regime, (R2), and much shorter in duration, occurred in the final period of measurement. During this time, many locations experienced sharp increases in transport intensity, higher average magnitudes, and more pronounced fluctuations.

Chapter 1 detailed a multitude of factors which may exert control on aeolian transport activity at any given time or location. In the main, the presence, magnitude, and consequential influence of these factors exhibit high spatio-temporal variability. The number, composition, and relative contribution that each potential factor makes, to instantaneous transport activity at any specific location, therefore of course also experiences marked variability.

Most aeolian experiments result in time-series, of wind and transport records that are ordinarily sub-divided into ‘runs’ for further analyses. These sub-divisions are typically based on subjective choices made by researchers, e.g. by looking at the time-series and selecting a period for in-depth analyses, and these choices are almost exclusively based on periods of interest within the incident wind speed record (e.g. Delgado-Fernandez, *et al*. 2018). This practice is grounded on the premise that wind speed is persistently the factor which exerts dominant control on sediment transport, an assumption widely acknowledged not to be the case, and no more so than in complex beach-dune environments. Beyond wind speed being the primary driving force of sediment entrainment, it may be that our higher relative knowledge of airflow properties in complex terrain, further promotes this systematic but biased choice. Temporal variability in the nature of instantaneous transport however, undoubtedly reflects changes in the composition, and relative weight of its contributing factors.

In studies where understanding of sediment transport is paramount, it is logical to therefore explore ways in which shorter duration sections of a time-series can be delimited specifically using transport data. Objective, sub-division of the time-series based exclusively on measured transport data, (the outcome, or dependent variable), rather than wind speed, one of a potential multitude of influential factors, brought fundamental improvements in this analysis. The ‘transport run’ method provided a simple and rapid technique for identifying ‘cut-off’ points in a robust way. It based decisions on transport data trends, and allowed optimisation of the timing and duration of data ‘runs’ for subsequent statistical analyses. Additionally, normalising transport, as a percentage of the total grain count at each location, allowed for transport patterns to be visualised on comparable scales, independent of their absolute magnitudes. By being focused on the patterns of sediment transport, rather than absolute counts, the approach also offers opportunities to

mitigate the influence of under-representation of actual grain counts, when there may be temporal variability in the degree to which sensors are aligned with transport vectors.

3.4.6. Critical overview of the transport run statistical results

The ‘transport run’ method was effective in delimiting the two discrete transport regimes, and the output ‘runs’ gave considerable improvements to statistical correlations for the majority of sensors and variables (compare full statistics *vs*. Run 1 and R2 statistics; Appendix 3). The approach further proved useful in clustering transport behavior, not only temporally, but also spatially. Both increased inter-relationships, and spatial clustering of sensors, reflect actual flow and transport dynamics during the event. A further, and fundamental reason however was that correlation values derived from the full 84 minutes of measurement, were essentially the product of mixing two, often poorly related data populations. Beyond masking any relationships which potentially persisted throughout, even at first glance, a number of spurious correlations were visible.

3.4.7. Statistical overview and the importance of wind direction

Chapter 2 identified that there was negligible difference in reference, (A3) mean wind speed, between the two events. Further, that the timing of the change in regime coincided perfectly with a marked change in the direction of wind approach angle. This suggests incident wind direction, to be the dominant control on airflow modifications, and therefore also flow-flux dynamics throughout the event. This finding is well aligned with previous assertions that incident wind direction, not speed, governs the nature and structure of turbulent flow structures in complex dune topography (e.g. Smyth, *et al*. 2013). Interpretations of the event (Chapter 2) were founded on a number of interconnected, topographic flow modifications

having developed, as a result of a shift in wind approach angle. These theories were supported by contemporary understanding of form-flow interactions in beach-dune settings (Walker, *et al*. 2006, 2017; Bauer, *et al*. 2012, 2013).

In R2, the emergence of new, or strengthening directional correlations, both positive and negative, occurring between multiple sensor locations, is indicative of an increased spatial connectivity of airflow at the landform scale. The weight of statistical evidence which pointed towards the development of a more coherent structure to airflow patterns during R2 was compelling (e.g. [A3 statistical matrix], Table AP3.3: Appendix 3). The existence of such flow structures in complex dune topography, both over and across a foredune, and within coastal blowouts is well documented (Walker *et al*., 2017, Delgado-Fernandez, *et al*. 2018). However, this is the first systematic study in a foredune blowout, beach-dune system, which details their existence and nature, for both a variety of airflow and transport variables, and between multiple instrument locations.

As would be expected, whether negative or positive, directional correlations between proximal sensor locations were the most numerous. This characteristic was evident even using the full 84 minute data population which encompassed the two distinct regimes. Over the full 84 minutes, during R1, and also R2, the relatively strongest of these correlations throughout the instrument grid occurred between trough locations. Within the six blowout interior locations, the relative strength of between-sensor correlations also increased moving landwards. The more pronounced directional relationships present within the trough itself, reflects variability in the directional range of flow streamlines being topographically constrained by the steep blowout walls. Over any chosen time period, the relative strength of correlations moving landwards results from streamlines becoming increasing trough axis aligned, which is a frequent characteristic of trough blowout

airflow patterns (e.g., Hesp and Hyde, 1996; Fraser, *et al*. 1998; Hesp, *et al*. 2017; Delgado-Fernandez, *et al*. 2018).

For between-sensor relationships, beyond those which were exclusively wind direction based, correlations between wind direction at one location, and separate measured variables at other sensor locations, were the next greatest in number. The marked increase in transport intensities within the trough during R2 were largely attributed to wind speed enhancements as a result of flow compression (Chapter 2). In turn, compression of airflow within the trough was found to have resulted from a greater proportion of regional wind, mass and momentum entering the trough. The onset of this change in dynamics was initiated by a shift in incident wind approach angle, which increased the relative proportion of the wind field being transferred across the surface of the S foredune, to then become strongly attached, and steered towards the blowout throat.

The measurement of instantaneous sediment transport within blowouts of any type remains scarce. As a consequence, airflow enhancements which are frequently identified in ‘non-transport’, blowout studies, are often described in such terms as having the potential to likely also enhance transport frequency and magnitude (e.g., Hesp and Hyde, 1996; Smyth, *et al*. 2012). Until this point, it has only been well substantiated that the direction of incident wind is the primary factor which governs the nature and structure of airflow patterns within blowouts. The measurement and statistical analysis performed in this study has provided new empirical evidence, which demonstrates wind approach angle as therefore also being a primary control on instantaneous, blowout sediment transport.

The marked change in wind approach angle (at the A3 reference anemometer) resulted in pronounced changes to airflow and transport dynamics within the

blowout. During R2, multiple, medium to very strong correlations emerged between A3 wind direction, and flow-flux parameters within the trough. Wind speeds at all locations, other than A9, exhibited high strength relationships with the direction of incident flow at A3, (the most distal of all sensor locations). As the shift in wind approach angle induced flow compression within the blowout, directional changes in wind approach angle, a primary control on the proportion of the regional wind field being steered into the trough, were seen to adjust mutually with trough wind speeds. In consequence, enhanced blowout wind speeds produced higher magnitude transport intensity, thereby also resulting in multiple above medium positive correlations between wind approach angle and sediment transport.

3.4.8. Statistical analysis of sediment transport: Evidence and Insights

Poor relationships between co-located wind speeds and sediment transport are a common finding of coastal field studies. The reasons behind this received ample coverage in the first chapter. In this study, Chapter 2 described an exceptional spatial pattern of flow-flux dynamics, in that zones with the highest wind speeds experienced the lowest transport intensities, and highest relative transport activity occurred at locations of weaker winds. In consequence of these confounding spatial patterns, statistical analysis of transport with both at-a-point airflow parameters, and with all the available variables of every grid sensors proved insightful.

During R1, in the main, at-a-point relationships between wind speeds and transport intensity were below medium, very weak, or often not evident at all. At individual locations, multiple environmental factors will have, to varying degrees, contributed to the nature of these highly limited relationships. A non-exhaustive list

of potential reasons includes localised supply limiting factors, height differentials between measurement, directional divergence between airflow and transport vectors, the relative alignment of LPCs with transport vector directions, sediment input from the far field, and variable lag times between airflow forcing and sediment transport response. Proportional relationships between wind speeds and sediment transport can typically only be parameterised in idealised conditions (Sherman, *et al*. 2011). In complex topographic settings, the invalidity of deterministic transport models is often associated with such influences (Baas and Sherman, 2006; Sherman, *et al*. 2011; Baas, *et al*. 2020). During R1, throughout the instrument grid, the strongest, and at 0.543**, also the only above medium correlation, for transport intensity with co-located wind speed, was at location A2, on the back-beach. This is likely a consequence of the simplicity of its topographic setting, relative to all other sensor locations.

The lack of, or typically only weak, R1 statistical relationships existing between wind speed and transport intensity also reflects the nature of sediment transport in general, and specifically during this period. During R1, at most locations, transport activity was much more intermittent than in R2, airflow enhancements were limited, and wind speeds fluctuated slightly above threshold velocities. A proportion of the R1 data points for transport will thus have been influenced by pauses in saltation, and therefore mean values, will be less associated with wind speed due to the one minute averaging period. Temporal variability in lag times between wind forcing and transport response, that are associated with sporadic transport activity (Bauer, *et al*. 2013), will have also lessened any statistical relationships which existed.

During R2, with the exception of A7, correlations between at-a-point wind speed and transport intensity, either emerged, or greatly improved for all trough locations.

In the most landward row of sensors, weak R1 correlations for all three of these sensors transformed to become high strength. Airflow compression in R2 served to enhance wind speeds and flow steadiness within the trough. These factors contributed to higher transport intensities, reduced levels of transport intermittency, and likely the proportion of individual transport signals associated with near-field entrainment. Each of these characteristics are known to improve statistical relationships between wind speed and transport (Sherman, *et al*. 2011; Davidson-Arnott, *et al*. 2012; Barchyn, *et al*. 2014). As flow compression was associated with the blowout topography, the higher relative strength of correlations in this most landward row likely also benefitted from the influx of airflow from upwind positions, which will have been 'transport saturated' to a greater degree. In turn, the weak and medium strength correlations (of A9 and A8 respectively) were likely influenced by levels of saltation within airflow being relatively more 'fetch limited' in being more proximal to the blowout throat.

At 0.356*, the R2 flow-flux correlation for A9 was weak. Transport activity at this location was persistently intermittent, as evidenced by the lowest mean AP value of all blowout sensors, both in R1, and R2. Given mean wind speeds at this location were continually one of the most transport capable, supply limiting factors contributed to transport activity being low magnitude, and highly sporadic, relative to other grid positions. The topographic setting of A9 was an obvious influence, as proximity to the high elevation, S blowout wall, resulted in the 'field of view' of the LPC being particularly constrained. It was also closest to, and immediately downwind of the juncture between the S foredune terminus, and the S blowout wall. At this interface, flow streamlines veered landwards towards A9, whilst saltating grains continued on their ballistic trajectories, perpendicular to A9, and across the throat, thereby reducing 'far field' sediment input. In terms of transport intensity not fully reflecting the pronounced flow compression within the trough

during R2, of all the blowout sensors, A9 was ‘fetch-limited’ to the greatest extent. That all these factors potentially heightened the sporadic nature of transport activity at A9, whilst winds were persistently strong, allows explanation of its especially poor flow-flux relationship.

For A7, a statistically significant relationship of any strength, between wind speed and transport intensity, was absent during both transport regimes. Located at the foot of the N blowout wall, A7 was identified as a zone of flow stagnation, and experienced the lowest mean wind speeds of all sensors throughout the 84 minute duration. Despite this, its mean transport intensities, and total grain count, were only surpassed by A6, (on the S foredune). Further, transport levels at A7 were at least double, but more often, over treble those of all other sensors. Upwind divergence of airflow and transport vectors, together with considerable sediment input from the far field, offered the best explanations of the exceptional A7 transport activity (Chapter 2). At A6, on the S foredune, transport intensity was high magnitude, blowout directed, and near continuous for the full 84 minutes of measurement. Chapter 2 identified saltation across the S foredune as the principle transport pathway in this study, having played a dominant role in delivering sediment to the blowout. Further, that on saltating grains reaching the S foredune terminus, whilst wind streamlines veered landwards sharply, and into the blowout, grains in transport maintained their ballistic trajectories. In being aligned with the orientation of the S foredune, transport vectors were thereby also directed towards the N blowout wall, thus making a significant contribution to the A7 transport signal. In addition to being the most logical explanation for A7 transport activity greatly exceeding wind speed capabilities, the theories offered were well supported by contemporary scientific knowledge (Chapter 2).

Wiggs, *et al*. (1996) theorised that in dune toe locations, which are characterised by flow stagnation, streamline curvature of turbulent airflow has the potential to maintain sediment transport. The presence of a correlation, albeit weak, between transport intensity and TKE in R1, indicates this may have made some contribution to flow-flux dynamics at A7 in this period. A7 grain counts however, were more than treble those of A4, and almost double those of A2, the two sensors immediately seaward of A7 in a cross-shore direction. In this study, this limits the credibility of turbulence having maintained, beach derived streamers to thus make a significant contribution to the A7 transport signal.

Customarily, interrogation of flow-flux measurements is limited to analysis of variables at co-located sensors, or additionally with those of a reference anemometer. The inclusion of analysis for all flow-flux variables, between all sensor locations, yielded further statistical evidence in support of the initial resolution for the event. For A7 transport, at 0.672**, the strongest of all relationships present during R1, was with AP at A5, upwind of A7, and located at the foot of the S foredune/blowout interface. Further, the second highest correlation, of 0.622** was with normalised transport intensity (ntt), at A6, on the upwind S foredune itself. A7 transport being most strongly associated with transport signals of the two S foredune LPCs provides empirical evidence to validate theoretical explanations of the event. During R2, A7 transport became slightly less related to transport activity in the area of the upwind foredune. In coincidence, relationships with wind speed and transport variables at A8, the most proximal sensor located within the trough strengthened. As flow compression resulted in marked increases in transport intensities within the trough, this shift likely reflects foredune derived, ‘far field’ sediment input making a lesser contribution to the A7 transport signal, whilst the contribution of locally entrained grains increased.

Further, cross-location relationships provided additional layers of statistical evidence to support interpretation of the event. Abrupt divergence in the direction of flow and transport vectors at the foredune/blowout juncture were also visible within the correlations for airflow. As an example, during R1, at A9, beside the S trough wall, the highest wind speed relationship found across all locations, was with A5, a strong, positive correlation of 0.757**. Additionally, the second highest, also positive, was of 0.554** and with A6 wind speed (section 3.3.3). This provides further validity for longshore, foredune deflected airflow having being steered landwards at the point of divergence with the foredune aligned, transport vector.

3.4.9. Relationships in airflow properties

Whilst wind speeds within the blowout exhibited strong relationships with incident wind direction, correlations between at-a-point wind speeds, with those of other locations, were in the main much lower. In part this is a reflection of the complexity of the terrain. At-a-point wind speeds of individual locations were of course subject to variable, topographically induced modifications, (including both enhancement and stagnation). In addition to the modifications which were characteristic to each location, the relative strength of any modifications will have varied temporally, for example, as a result of even small fluctuations in at-a-point wind direction. During R1, wind speed relationships between sensor locations were in general weak, or in some cases non-existent. The exception to this, and of particular interest, were the medium to strong relationships between A5, A6, and A9 (section 3.3.3 and 3.4.8). A number of medium to strong, positive wind speed correlations did however emerge between all the trough locations during R2. This relates to all trough locations experiencing, quasi-synchronous wind speed enhancements as a result of flow compression during this period. Simultaneously, multiple at-a-point, and

between-sensor, negative, wind speed correlations also became evident, with both TKE and CV of wind speed. In Chapter 2, enhancements in trough wind speeds, to values above those of approach winds at A3 proved useful in identifying flow compression within the blowout. As compression is known to suppress turbulence, and enhance flow steadiness (Smyth, *et al*. 2013), the many inverse relationships which emerged via additional analytical steps, allowed initial interpretations to be underpinned with statistical evidence.

3.4.10. Temporal variability in sediment transport forcing and response

Typically, instantaneous transport responds to variability in the forces acting to promote, or inhibit saltation. Further inferences could be gained by considering the timing of the change in regime, and also the rate of positive changes to transport intensity. In other words, how pronounced the step change in regime appeared, relative to other locations. At individual trough locations, this may reflect spatio-temporal variability in topographically forced airflow modifications, and also the degree to which specific locations were influenced by both supply limiting factors, and/or sediment input from the far-field, (pre and post the change in airflow patterns).

As an example, for both A7 and A10, (both beside the N blowout wall), plotted cumulative transport indicated the change in regime was least pronounced in comparison to other trough locations. In relation to incoming airflow and sediment, these two locations were the least topographically constrained by the S foredune. In being more ‘open’ to incoming streamers from the beach or foredune, it is probable their R1 transport records benefitted from higher relative proportions of sediment input from the far field. In consequence, prior to R2, there was less of a deficit between cumulative, idealised linear transport, and actual cumulative transport, than for elsewhere in the trough (section 3.3.2). This reduced the

gradient of their respective, cumulative transport curves, between the timing of the step change, and the final minute of measurement.

Alternatively, at A9 and A12, proximity to the S wall was a significant topographic constraint which limited sediment supply. R1 transport at both locations, was low magnitude and highly intermittent. As a result, the deficits between cumulative, idealised linear transport, and actual cumulative transport curves were much greater (≈70%), thereby giving a much more pronounced, positive step change at the onset of R2. The timing of the change in regime also occurred later at both sensors, as their locations remained least advantageous for receiving 'far field' sediment input from elsewhere in the trough. Additional to this and of interest, unlike all other trough locations, the change in regime was also staggered. Whilst both experienced rising transport activity on the change in regime, peaks in transport intensities did not occur until some minutes after the initial, positive 'step change'. For both sensors, the delayed timing until the steepest rising gradient in their cumulative transport curves was related to wind direction. On their respective wind directions falling below a threshold at which flow approached almost directly from the S blowout wall, high magnitude bursts of transport began to occur. This is likely indicative of a reduction in supply limiting conditions, and the onset of additional sediment input to the LPCs directly from the trough wall.

Theoretically, subdivision of the time-series was necessary in this study, in order to better understand the two markedly distinct periods of differing flow-flux dynamics. Relationships of value to event interpretation would undoubtedly have been otherwise masked by a high noise-to-signal ratio, (had statistical analysis been based on the 84 minute data populations). A recent article by Baas, *et al*. (2020) found that sediment transport predictions improve when cumulative wind speeds (rather than time-averaged velocities) are used to predict saltation. While

their technique provided improved transport predictions, questions still exist with regards to the ‘ideal’ duration of the wind and transport ‘runs’. The transport run method employed in this analysis was effective in providing significant new insights and additional layers of evidence, together with improvements to identification and/or quantification of statistical, flow-flux relationships.

Extensive visual and numerical interrogation of data did however also identify a number of further challenges. The nature of which suggested that, although general trends for an experiment can provide important information, superficial analyses of time-series data can miss significant details. At a coarse level, observations here indicated two transport regimes which were clearly differentiated. The methods employed, delimited the two regimes in a robust manner, and enhanced their characterisation. Relatively speaking transport was lower during R1 at all locations, wind speeds were slightly lower in general, and both TKE and CV were slightly higher; during R2, transport increased at each location, winds were slightly higher, and TKE and CV were lower. However, more detailed analyses revealed that, during the two periods of time, transport was related with discrete wind properties in different ways. Many such peculiarities were also observed to occur, either sporadically, or for only short periods, within their longer duration ‘runs’. For example, at some locations (A7, A8) peaks in transport followed peaks in TKE within discrete periods of R1, but not at all during R2, suggesting that the predominant role played by wind variables changes over time (Appendix 3). The influence of wind direction falling below a threshold value at A9 and A12, during R2 was also seen to have a considerable impact on transport, but these changes were exhibited for even shorter durations, within the two delimited ‘regimes’. Advanced refinement of the ‘transport run’ method used in this study, to delimit, discrete, shorter duration periods of interest, or expansion of

statistical analysis from bivariate to multi-variate are two avenues which now demand further exploration.

Finally on temporal trends, and although not explored in great detail here, a time lag between transport intensity, and the potential forcing factors of, either wind speed, or TKE, was at times observed in sensor records. The existence of such time lags was only applicable to specific locations, and even at these locations, the presence of any lag was not continual, or varied in duration. Further studies involving the high-frequency measurement of aeolian processes could make use of wavelet analyses (Foufoula-Georgiou and Kumar, 1995; Lau and Weng, 1995; Torrence and Compo, 1998; Percival and Walden, 2000) to gain insights into potential lag responses, and their relative importance.

3.5. Conclusion

High frequency, quasi-instantaneous, airflow and sediment transport were recorded synchronously, for a duration of 84 minutes. The experiment design and instruments deployed permitted advancement in the understanding of event scale, geomorphological processes operating within a foredune blowout, and over its immediately seaward surroundings. To the knowledge of the author, this is the first study to encompass synchronised airflow and transport measurement on the beach, across the foredune, and within a blowout itself. Over recent decades, a substantial body of empirical data has been collected, and research conducted to examine the nature of form-flow interactions within blowouts, and across, on approach to, and over foredunes. This has provided an enhanced level of confidence in predicting the typical flow modifications which might be expected in discrete zones of a beach-dune environment, or at discrete component parts of specific dune landforms, largely based on topographic setting, dune geometry, surface roughness, and wind approach angle.

In respect of foredune blowouts, studies which include co-located measurement of transport remain scarce, and the understanding of transport activity, its spatio-temporal variability, and sediment transport pathways is extremely limited. In this respect, fundamental knowledge gaps were addressed through measurement. Further, the novel, analytical techniques adopted for this study allowed advanced insights and characterisation of foredune blowout, flow-flux dynamics, beyond those available through the customary approaches in current use.

The simple ‘transport-run’ method introduced in this chapter permits differentiation of characteristically diverse transport ‘regimes’. The method performs well, and provides a simple, rapid solution, for objectively selecting ‘runs’. The solution removes arbitrary, or imprecise decisions about ‘run’ durations based on visual analyses of wind speed records (the common approach), and yields significant improvements to the effectiveness of statistical analyses. The essential value of the technique comes from allowing characteristically distinct, shorter duration periods of transport dynamics, to be delimited within a longer time-series. In this study, factors contributing to sediment transport exhibited marked spatio-temporal variability. In the absence of using this approach, any selected ‘runs’ which partly spanned two differing regimes, would constrain identification of flow-flux relationships, and quantification of their respective strengths and nature.

It is likely, the technique will be most applicable to aeolian transport events in complex topographic settings, where strong divergence between airflow and transport vectors are commonplace. In respect of such events, Bauer, *et al*. (2013) identified a number of explicit principles, which it would be necessary to follow, if positive step changes are to be made in their resolution. Consideration of two of which, were prioritised in development of this approach. Namely, seeking to better

exploit current knowledge of topographically induced, coherent, flow structures or typologies, together with closer treatment of aeolian sediment transport, as a vector, rather than scalar property.

In agreement with Smyth, *et al*. (2012, 2013), 'landform scale' airflow patterns and topographic modifications, were found to be governed by incident wind approach angle. A shift in wind approach angle brought about flow enhancements within the blowout, which were of sufficient magnitude to induce a pronounced change in sediment transport activity. As yet, technological constraints limit the continual measurement of transport vector directions. In this study, current knowledge of airflow modifications in complex terrain, were used to locate probable points of marked divergence between flow and transport vectors, which were then further explored, and supported by statistical analysis of spatio-temporal variability in measured flow-flux data.

The strength, and temporal variability of at-a-point relationships, between wind speed and transport intensity, highlighted the likely influence of sediment input from the far field to individual transport signals. Between-sensor, exclusively transport based, statistical relationships, were additionally able to support theoretical interpretations concerning spatial patterns of airflow and sediment flux. The approach allows for advanced insights into the understanding of event scale, transport patterns, in future studies, together with opportunities for enhanced resolution of historic field data sets.

CHAPTER 4 – MESO-SCALE GEOMORPHIC CHANGE AT A RETREATING COASTLINE IN THE PRESENCE OF FOREDUNE BLOWOUTS

4.1 Introduction

Beach-dune systems provide a natural first line of defence against coastal flooding. A primary mechanism governing their geomorphic change, and therefore also the behavior of these systems is beach-dune sediment exchange (e.g., Short and Hesp, 1982; Pye, 1983; Psuty, 1988; Sherman and Bauer, 1993). Whilst these exchanges occur temporally at the 'event' scale, the cumulative magnitude, direction, and frequency of sediment exchange between cross-shore units of the system, result in fundamental changes to both form and morphodynamics, across the full spectrum of temporal scales. The seminal model proposed by Psuty (1988), determined that sediment exchange, specifically between the nearshore beach and foredune, exerts a primary control on the evolution of dune fringed coastlines (sections 1.6.2, 1.8.5 and 1.8.6).

A sediment budget approach is often adopted to understand the evolution of beach-dune systems across a range of spatial and temporal scales (Aagaard, 2011; Darke, *et al.* 2016; Lerma, *et al.* 2019; Psuty, *et al.* 2019; Rotnicka, *et al.* 2020). This approach assesses the volume of sediment or 'sediment budget' of predefined sub-units of the landscape, over fixed periods of time. Although the specific nature of beach-dune sediment exchanges are highly non-linear (e.g. Aagaard, *et al.* 2004; Houser, 2009), foredune sediment loss is often related to winter storms, and aeolian sediment input associated with wind events, of which we know relatively little (Walker, *et al*. 2017). Within these dynamic events, multiple exchanges, varying in magnitude, duration and frequency, occur as

sediment is ‘continually cycled between the beach and foredune sub-units. The resultant balance, or ‘net sediment budget’ of each, over any given period of time, may therefore be positive, negative or in quasi-equilibrium, with morphological responses being expressed in beach and dune topography. Typically, and also intuitively, positive dune sediment budgets are most often reflected in foredune growth, together with progradation.

The presence of blowouts within a foredune have the potential to limit or reverse this association by influencing the inputs and outputs of the foredune sediment budget. Blowouts, erosional dune landforms associated with enhanced levels of aeolian transport, are recognised as highly efficient transport corridors. Foredune blowouts may therefore reduce sediment input to the foredune budget by facilitating marked levels in throughput of sediment to the landward dune field, which would ordinarily accumulate within the frontal dunes. This transfer of sediment to the landward dune field, which in the absence of blowouts would ordinarily be cycled repeatedly between the beach and foredune, would also be expected to reduce beach levels, thus increasing the frequency of foredune sediment outputs via marine processes. Although knowledge is scarce, it might also be expected that foredunes fragmented by blowouts may be less robust, and/or resilient to the effects of marine processes, thus increasing the magnitude of foredune sediment losses as a result of more frequent wave scarping events.

Coastal erosion, or more specifically foredune retreat in the vicinity of Formby Point in Sefton, is strongly associated with marine processes. The principle mechanism of incremental retreat has been identified as continual wetting of the dune toe leading to ‘slumping’ or slope failure of the foredune face (Pye and Blott, 2016). Lower frequency, but higher magnitude foredune scarping has been linked to a variety of conditions associated with marine processes. Although the list in not

exhaustive, these include the coincidence of spring high tides with storm surges, the combination of wave run up and tide height exceeding specified elevation thresholds, the duration water levels remain above a specified threshold, total water levels exceeding a specified threshold on concurrent tides, and the width of the ‘backshore’ falling below a minimum distance (Pye and Neal, 1994; Esteves, *et al*. 2012; Dissanayake, *et al*. 2015; Pye and Blott, 2016).

At Sefton, and more widely, coastal erosion is customarily linked to marine processes only, with limited information on the role played by the presence of foredune blowouts, which fragment dune fringed coastlines (Pye and Neal, 1994; Esteves, *et al*. 2012; Mir-Gual, *et al*. 2015; Pye and Blott, 2016). It is not uncommon for coastal dune erosion to be solely associated with marine processes, and aeolian processes solely with dune ‘building’. While wave action is a principle driver of coastline change, the conservation state of foredunes is equally key, as coastal dunes act as a main physical barrier against large storm surges and flooding. Their coastal defence role depends on their ability to withstand erosion, which is a function of their overall size and volume, and the degree to which they are vegetated. Ultimately, it is the amount of sand stored over time within the dunes, and how this is bounded by vegetation, which makes foredunes strong, a characteristic that is largely dependent on the efficiency of aeolian transport from the seaward beach, and the overall preservation of dune vegetation (Davidson-Arnott, *et al.* 2019).

At the landscape scale, as blowouts are understood to experience heightened levels of aeolian transport (Hesp, 2002), it follows that coastline evolution may be enhanced in their localities, relative to longshore positions where they are absent. To date, evidence supporting this theory remains largely anecdotal. Further, the nature of coastline evolution associated with foredune blowouts has also received

limited research coverage. Finally, the occurrence of foredune blowouts directly influencing dune sediment budgets by allowing sand to bypass the frontal dunes, thereby decreasing the amount of sand deposited at the beach-dune interface, is a process that has not been quantified to date.

Whilst chapters 2 & 3 were concerned with the nature of aeolian beach-dune sediment exchange at the 'event' and 'landform' scale, the aim of this chapter is to examine foredune blowout transport over extended temporal scales, and to explore its potential role in coastal landscape evolution. Geomorphic change is assessed at the meso-scale, and dune sediment budgets calculated for longshore sections of the coast where foredune blowouts are present. In addition to exploring geomorphic change associated with foredune blowouts more generally, of particular interest is identification of whether these blowouts may be contributing to, or enhancing the rate of coastline retreat.

4.2 Methodology – Part 1

4.2.1 Study Site

Research was conducted at Sefton dunes, NW England (Figure 4.1), one of the largest dune fields in Britain, which extends 16 km longshore, and up to 4 km inland (Esteves, *et al.* 2012). The dunes have been recognised as an international hotspot for biodiversity (Smith, 2009), and constitute a text-book example of a coastal dune field acting as a buffer against coastal erosion and flooding. The dune field is currently retreating at a dramatic rate of 4 m per year at Formby Point, with Formby town, an urban settlement of approximately 25,000 residents located directly landwards (Figure 4.1). The ability of coastal dunes to cope with rising sea levels and climate change will determine the future of existing built infrastructure. The dunes have been subject to much research over the last

decade and thus important background information is available (e.g., Pye and Blott, 2008, 2010; Plater and Grenville, 2010; Pontee, 2011). Additionally the site benefits from considerable, freely available environmental data, aerial photography (15 mosaics dating back to 1945; see Delgado-Fernandez, *et al*. 2019b) and near yearly LiDAR survey data (starting in 1999).

Figure 4.1: Location of study area and approximate extent of landward urban settlement.

Sefton provided an ideal natural laboratory for the study for multiple reasons. The coast is macro-tidal (mean spring tidal range > 8 m), and consists of medium to fine grained, quartz rich sand. It is subject to an energetic wind regime promoting significant onshore aeolian transport, and favouring the formation of dunes under a variety of environmental conditions (different beach widths, fetch scenarios, etc.). Dune heights are > 20 m OD at several locations along the coast, with their shape

changing from linear foredunes and embryo dunes in Ainsdale, to three-dimensional, alongshore variable dune morphologies in Formby (Figure 4.2).

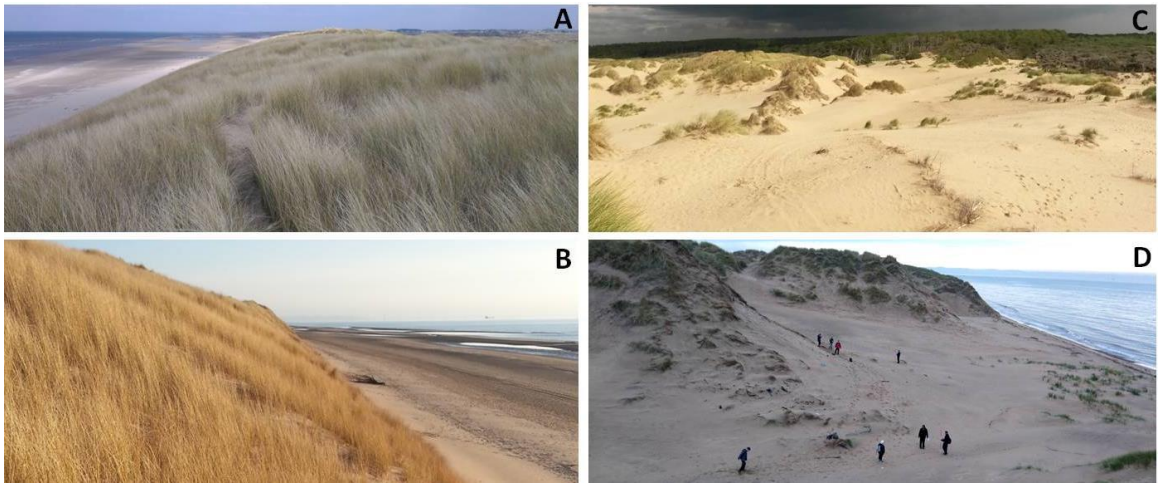

Figure 4.2: Diversity of coastal dune morphologies at the Sefton Coast. A-B) well-vegetated dunes towards the north, with low levels of human impact; C-D) sand sheet and blowouts around Formby Point, in the area selected for this study.

At a regional level, the Sefton coast is cuspate in configuration. The central and western-most section, has for many decades been experiencing a long term trend of coastline retreat. To both the north and the south, this zone of retreat is flanked by areas of sediment accretion, and as a result, foredune progradation. In consequence of this longshore variability in evolutionary trends, a gradual 'flattening' of the coastline configuration is ongoing. The central zone which is experiencing retreat, comprises multiple blowout, remnant knob, and parabolic dune landforms of different levels of topographic complexity (Figure 4.3). Visitor pressure is acknowledged in contributing to a diversity of dune landscapes along the coast (Delgado-Fernandez, *et al*. 2019b), with low levels of trampling favouring naturally vegetated dunes to the N (location 1 in Fig. 4.3), and high levels of human impact, for maintaining active foredune blowouts, (in addition to the initiation of new features; (location 2 in Fig. 4.3).

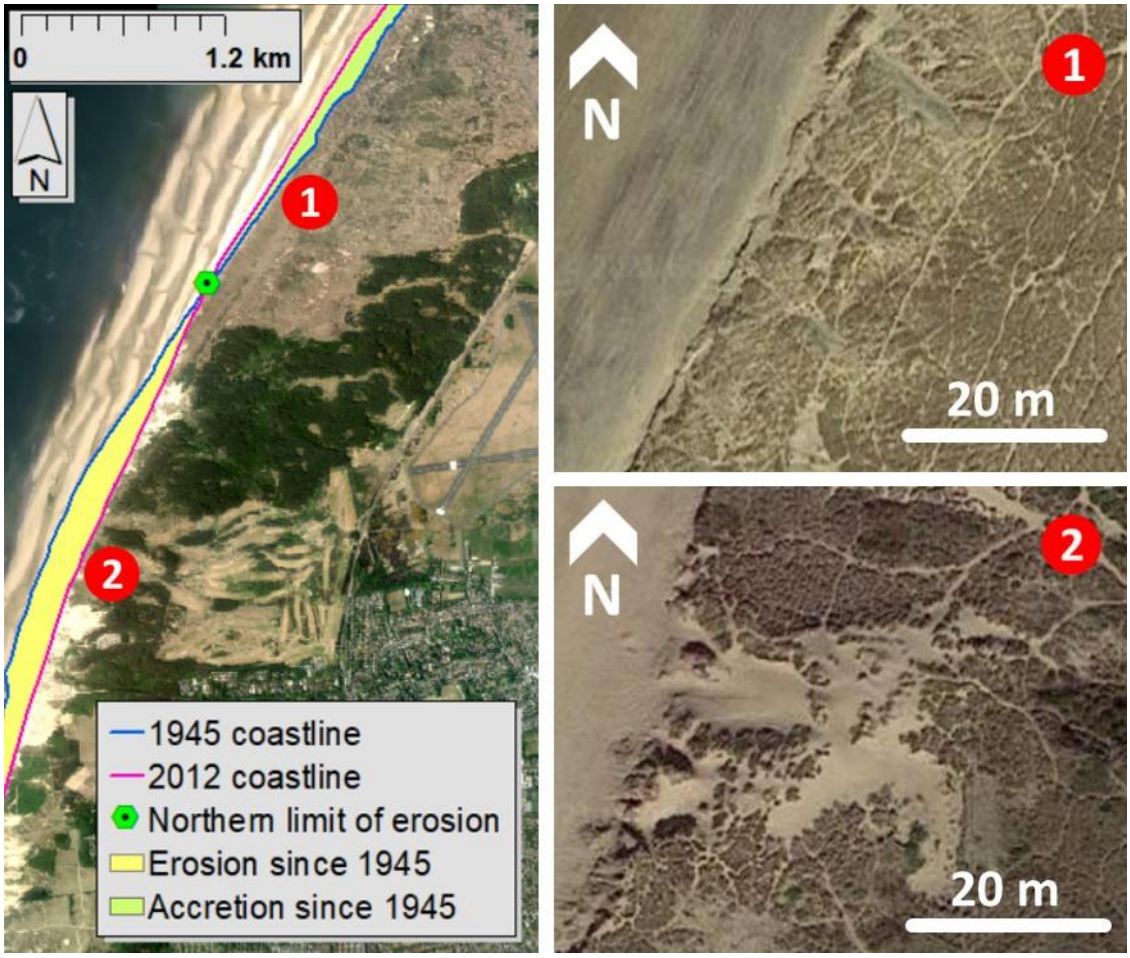

Figure 4.3: Erosion/accretion along the Sefton Coast. Right-hand side images show differences in vegetation cover and dune morphologies between sections of foredune retreat and progradation.

Despite its ideal physical characteristics and the substantial suite of remotely sensed data (spatial/temporal), only a few studies have made use of the available LiDAR and photographic datasets (e.g., Saye, *et al*. 2005; Pye and Blott, 2016; Delgado-Fernandez, *et al*. 2019b), with none exploring the evolution of the foredune in direct association with blowout transport, or its influence on dune sediment budgets within the zone of retreat, for longshore units which comprise major complexes of foredune blowouts. Such information is key for management and major custodians of the coastal landscape such as the National Trust (landowner of site 2, figure 4.3), and Natural England (landowner of site 1, figure 4.3), who will be direct end users to benefit from this research.

4.2.2 Description of remotely sensed data

Tables 4.1 summarises the aerial photo ortho-mosaics used in this study. Use of the aerial photography was constrained to delimiting the longitudinal extent of the area of interest (foredune experiencing retreat), and subsequently to aid interpretation of LiDAR derived analyses outputs. Table 4.2 details the Digital Terrain Models (DTMs) used to produce GIS outputs for analysis.

Table 4.1 Aerial photo ortho-mosaics (Courtesy of Sefton Council, ©Crown Copyright). Pixel resolution (PR) ranged between 0.25 and 1 m, and number of bands (NB) correspond to monochrome (1), RGB photos (3) and Compact Airborne Spectrographic Imager (CASI) flight (28).

Year	(PR) Pixel Resolution (m)	(NB) Number of Bands
1945	0.25	1
1961	0.25	1
1979	0.25	1
1982	0.12	1
1984	0.25	1
1989	0.25	3
1992	0.25	3
1996	0.43	3
1997	0.25	3
1999	0.25	3
2000	0.25	3
2002	0.25	3
2005	0.12	3
2010	0.25	3
2012	1	3
2015	1	28

4.2.3 Delimiting the longshore area of interest

All processing of remotely sensed data was conducted using ESRI ArcMap v10.5. Although exhibiting some variability annually, the approximate longshore limits of the central section of the coast experiencing foredune retreat are well known locally, and have been detailed in previous studies (Pye and Neal, 1994; Pye and Blott, 2016). To the south, the position has remained relatively stable and in close proximity to Lifeboat Road. The location of the northern longshore limit of retreat has gradually migrated northwards, and its current position is close to the Formby-Ainsdale ward boundary. Beyond these limits there is a transition from coastal

retreat to foredune progradation. Using the seaward vegetation line as a proxy for the beach-dune boundary, coastlines were digitised for each aerial photo ortho-mosaic in the time-series (Delgado-Fernandez, *et al*. 2019b). From 1945 to 2015, the most northern and southern limits of the central zone of retreat were in close agreement with those previously documented.

In the absence of a need for absolute precision, the northern and southern limits of the longshore area of interest were positioned arbitrarily. A MapitUK (2019) polygon (kml. file) of the Ainsdale-Formby electoral ward boundary marked the northern limit of the study site. The southern limit was positioned slightly north of Lifeboat Road solely to avoid inclusion of the Lifeboat Rd beach access path within the LiDAR analysis, (which would have otherwise introduced an unnecessary and additional anthropogenic influence). In 1999, the earliest date for which LiDAR was available, the approximate length of the beach-dune boundary exhibiting a long term trend of retreat was ≈ 4.7 km, and all analyses to follow fall within these longshore limits.

4.2.4 LiDAR pre-processing

The full catalogue of LiDAR data for Sefton dunes (Ordnance Survey grid tiles SD20NE and SD21SE) were sourced from the Environment Agency. Table 4.2 summarises only the LiDAR datasets from which results presented within the main body of the thesis were derived.

Digital Terrain Models (DTMs) were identified as the optimal data type for use in this analysis. Environment Agency LiDAR data comprise zipped folders containing all 2 km^2 tiles available for the respective Ordnance Survey grid reference, per survey year. For each year, all tiles were mosaicked into single, one band rasters, projected using the British National Grid coordinate system, and elevations

corrected to local chart datum (CD) for Formby. DTMs were selected for inclusion in analyses if they provided full coverage of the delimited area of interest. The sole exception to this was the 1999 DTM which only covered ≈ 83% of the retreating coastline, omitting the northernmost ≈ 750 m. The 1999 DTM was however included to maximise the temporal range of the study. Geomorphic change detection requires DTMs to have matching cell sizes, and maximising the number of surveys within analyses would also provide more informative results. Therefore, when necessary DTMs with a cell size which was finer than the coarsest (2 m) within the time-series, were resampled to the 2 m resolution. Resampling was performed via bilinear interpolation, as this outperformed cubic convolution, the alternative ESRI ArcMap operation that is also suitable for use with 'continuous' data.

Table 4.2 Digital Terrain Models (DTMs) used for analysis.

Survey year	Original pixel resolution (m)	Pixel resolution following resampling (m)
1999	2	n/a
2008	0.25	2
2010	1	2
2013	1	2
2014	2	n/a
2016	1	2
2017	1	2
2018	1	2

Full spatial coverage of the longshore zone of retreat was desirable as it would provide data for two blowout complexes of particular interest, one close to the northernmost extent of retreat, and one reaching its southernmost limit. To the south, a complex of high magnitude, foredune blowouts, extend northwards from the Lifeboat Road beach access path (Fig. 4.4), and the location of the blowout investigated in chapters 2 and 3 is located within a complex towards the northern limit of retreat.

It was decided that inclusion of the earliest DTM (1999), at the expense of forgoing the northernmost 0.75 km of coastline within the retreating section of coast, was

the preferred option for this final map output. Even without this northernmost section, the remaining ≈ 4 km of coastline was considered an acceptable spatial scale, and would be sufficiently informative.

4.2.5 Deriving decadal scale information on landscape evolution

An assessment of coastal geomorphic change at the maximum temporal scale (decadal in this study) was conducted by deriving a 'dynamic layer' from the multi-epoch time-series of LIDAR DTMs (Mitasova, *et al*. 2011; Holden, *et al*. 2014). 'Dynamic layers' provide the total range of elevation change within a time-series, on a cell by cell basis. This would allow confirmation of a study prerequisite, (in significant topographic change having occurred during the study period), together with quantification of its magnitude, and spatial distribution. Interpretation of the results would subsequently benefit from the rich suite of aerial photography available, and a detailed knowledge of the site, permitting enhanced characterisation of any locations identified to be areas of high relative, landscape dynamism. Many areas of 'bare sand' or sparse vegetation, visible within the aerial mosaics are known to be blowout locations which have persisted for the duration of the LiDAR time-series. Comparison of these with the 'dynamic layer' was aimed at confirming the potential relationships thought to exist between the magnitude of topographic change, together with its distribution, and the spatial distribution of foredune blowouts, (and/or the extent of 'bare sand' areas).

A 'core' and an 'envelope' layer were derived from the time-series using all 8 DTMs from 1999 to 2018. Although maximising the temporal range via inclusion of the 1999 DTM came with the expense of omitting the northernmost ≈ 0.75 km of retreating coastline, the ≈ 4 km of retreating coastline covered was deemed more than sufficient to inform on landscape scale change. The 'core' layer is a single

surface, with each individual cell containing the minimum elevation value present for its location throughout the time-series. This effectively represents a ground surface, below which the elevation has not fallen throughout the temporal range of the study. Conversely, the ‘envelope’ layer is a surface with individual cells containing the maximum value present for each cell location within the series. The ‘dynamic layer’, derived by subtracting the ‘core’ layer from the ‘envelope’, represents the absolute range, (or total magnitude), of elevation change within the time-series, on a ‘per cell’ basis.

Elevation change magnitude was categorised into 9 classes, all with a 2 m range, other than the maximum class of 16 m to 17.1 m. Although accounting for DTM ‘uncertainty’ is a requirement for robust sediment budget analysis (Wheaton, *et al*. 2010), and accurate geomorphic change detection, no attempt was made to incorporate ‘uncertainty’ within the ‘dynamic layer’. The typically sub-15 cm Root Mean Squared Error which is associated with individual DTMs, was considered to be of negligible significance, relative to the 17.1 m range of absolute elevation change, and the landscape scale of analysis, which further spanned an almost 20 year duration.

In addition to its intended purpose, visual inspection of the dynamic layer allowed the coastline to be partitioned into 3 discrete zones (Figure 4.4), facilitating more detailed analyses of change at a reduced spatial scale, for specific locations within two of the delimited zones.

4.3 Results – Part 1

4.3.1 Decadal Landscape Dynamism

Fig. 4.4 displays the resultant layer of 'landscape dynamism', together with a 2012 aerial photograph covering the same longshore extent.

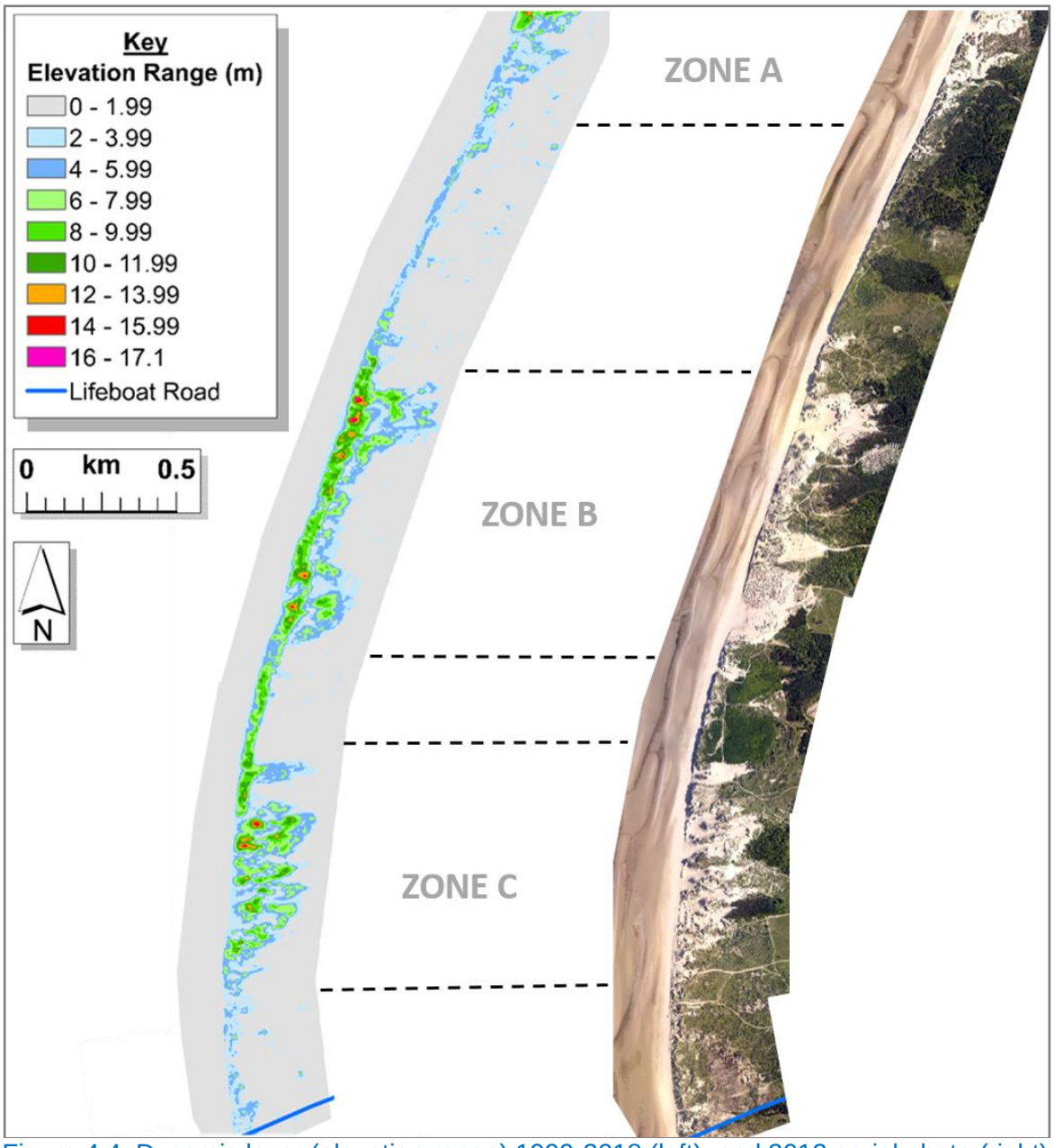

Figure 4.4: Dynamic layer (elevation range) 1999-2018 (left), and 2012 aerial photo (right).

The beach area of the dynamic layer is wholly composed of total elevation changes below 2 m. Moving landwards, the seaward boundary of the dune field is highly visible. This is primarily a result of the dunes being of greater amplitude than the beach, and due to coastline retreat having occurred throughout the study duration, thereby giving rise to variable, but markedly higher magnitude levels of

elevation change throughout the cross-shore ‘band’ that the retreating foredune has been positioned within.

A clear spatial relationship is visible between areas of higher magnitude topographic change, and the distribution of ‘bare sand’ in the aerial imagery. The spatial extent of areas having experienced elevation changes > 2 m, which extend landwards of the beach-dune boundary, also correspond strongly with the spatial extent of ‘bare sand’ areas. Irrespective of the topographic character of discrete areas of ‘bare sand’ visible in the aerial photo, and disregarding their potential coincidence with ‘blowouts’, this relationship was expected. That both vegetation coverage and composition, are primary controls on the relative mobility, (or stability) of dune fields is heavily documented (Hesp, *et al*. 2007; Jackson and Cooper, 2011; Delgado-Fernandez, et al. 2019a; Gao, *et al*. 2020). Beyond this, ‘bare sand’ localities which additionally, either wholly represent individual blowouts, or their overall area is partly comprised of blowouts, may also be expected to have experienced incrementally higher magnitude change than those where this is not the case. The potential for a relatively higher magnitude change, exceeding that of locations solely with a sparsity of vegetation cover, could be attributed to the topographically induced, near-surface modifications to airflow, which enhance the potential for transport and are associated with blowout landforms (e.g., Smyth, *et al*. 2012; Pease and Gares, 2013).

Based on the overall, ca. 17 m range of elevation change, ‘low’ magnitude change was deemed to be < 6 m, medium 6 - 12 m, and high, > 12 m. ‘High magnitude’ topographic changes were predominantly located toward the seaward edge of the dune field, and were largely found within the cross-shore band of elevation changes which clearly represent the zone through which there has been a net

landward migration of the foredune-beach interface. This ‘band’ can be seen to be quasi-continuous for the length of the coastline, and longshore variability in magnitude will in part be a function of antecedent longshore variability in foredune configuration.

The maximum, absolute elevation change value, throughout the dynamic layer measured ≈ 17.1 m. Whilst the relatively small scale areas of ‘high magnitude’ change occur in isolated or discrete patches, they almost exclusively occur within the seaward ‘band’ through which the foredune has migrated. Two exceptions to this are found within zone C. In one instance, an isolated spot is positioned marginally landward of the foredune ‘band’, and in the second example, a short, elongated area of high magnitude change can be seen to extend landwards of the frontal dune. The elongated example represents lateral expansion of a trough blowout. The isolated spot beyond the foredune ‘band’ is erosion of a remnant knob partially separating two trough blowout-like features, bringing considerable subjectivity to the landform classification of this feature, and is considered more fully in the subsequent analysis at the reduced spatial scale.

Typically, the longshore positions of higher magnitude ‘patches’ of elevation change also have wider, cross-shore areas, of medium magnitude change immediately landwards, which in some cases extend considerable distance inland. These locations correspond to known positions of foredune blowouts, and their landward extents are depositional environments, with sediment derived from the erosion of seaward area, that has been deposited downwind in blowout lobes and/or the leading edge of parabolic dune configurations.

4.4 Methods – Part 2

4.4.1 Zone Selection

At the landscape scale, the ‘dynamic layer’ (Fig. 4.4) indicated that longshore positions of ‘bare sand’, many of which are known to be foredune blowout locations, were associated with relatively higher magnitude elevation changes, which further, also extended landwards over greater spatial extents. Fully understanding this heightened geomorphic change necessitated investigation at a reduced spatial scale. Although the vast majority of ‘quasi’ individual blowouts which can be identified in 1999 aerial photos, and the DTMs, have persisted throughout the time-series, all have experienced varying levels of temporary, or permanent, connectivity with adjacent longshore features. The potential for both cross-shore, and longshore sediment exchanges within the dune system constrained the possibility to delimit, and then resolve sediment budgets on an individual, ‘blowout by blowout’ basis.

Three areas of significant topographic change in the dynamic layer all extended considerably landwards of the immediate foredunes. These three areas corresponded with expanses of ‘bare sand’ in the aerial imagery, were highly visible, and could be considered discrete. This allowed the coast to be compartmentalised into three longshore zones, with their arbitrary longshore boundaries detailed in figure 4.4. Two of these zones were to be selected for more detailed analysis, and their spatial extents were more objectively refined prior to ‘per cell’ GIS analyses.

Rather than attempting to delimit and classify multiple blowouts which have exhibited acute spatial and temporal variability, grouping areas of relatively greater landscape dynamism into three ‘zones’, allowed comparison between longshore stretches of either no blowouts, small scale blowouts, or only ephemeral blowout

features, with the evolution of areas characterised by the presence of large scale, blowout complexes. Future research will investigate volumetric and shape changes to the highly complex and diverse collection of erosional landforms 'nested' across multiple spatial scales.

4.4.2 Zone A

Located towards the northern limit of dune field retreat, this first zone chosen for analysis is the least accessible to visitors, and therefore the most natural stretch of foredunes in the larger study area. At the terminus of the 'Fisherman's Path', two blowout complexes bisect the frontal dunes to promote enhanced beach-dune sediment exchange. Although the 1999 DTM only provides partial coverage of the blowout systems, thus reducing the temporal range of zone A analyses, knowledge of event scale processes within this zone, (detailed in chapters 2 and 3), offered enhanced opportunities for interpretation of geomorphic change, and potentially also for bridges to be made across the temporal scales. Figure 2.2 details the beach-dune interface of the blowout within this zone, where 'event' scale geomorphic processes were measured.

4.4.3 Zone B

Zone B is located centrally within the longshore stretch of coastline experiencing retreat. The 'dynamic layer' indicated this zone experienced the highest magnitude elevation changes throughout the study site, and it further included sections of medium to high elevation change, which of the three zones, also extended the greatest distance landwards of the beach-dune interface. It has however been subject to a diverse range of intense anthropogenic influences throughout the study duration, which constrain interpretation of natural geomorphic change. Primary drivers of landscape evolution in this zone include intense visitor pressure, and multiple management interventions aimed at mitigating human impacts. The

National Trust visitor car park at Victoria Road (Fig. 4.5 (3)), is located immediately landward of the single foredune ridge, and has experienced continual encroachment by sand as the foredune retreats, leading to temporary reductions in car parking spaces (Fig. 4.6). North of Victoria Road and also sited within the dune field, is a permanent caravan park (Fig. 4.5 (4)). The sole access road to this caravan park has also been repeatedly inundated with blown sand by the large scale, transgressive sand sheet complex to its west (Fig. 4.5 (1)). As a result, the use of plant machinery to remove and redistribute large volumes of sand has been a management intervention for many years, (thus preventing accurate quantification of natural sediment exchanges using sediment budget analysis).

The physical characteristics of the two large areas of bare sand within zone B are also less well aligned with the landforms under investigation. Although smaller scale, ephemeral blowouts can be found superimposed on zone B ‘bare sand’ areas, acute levels of vegetation trampling (Fig 4.7 (A)), have led to progressive development of larger scale landforms which are more representative of ‘sand sheets’. Large scale planting and fencing interventions aimed at promoting stability and/or dune building have also occurred intermittently over the time-series duration, further masking the natural processes under investigation. Finally, at the beach-dune interface of zone B, south of the Victoria Road beach access path, the seaward face of the frontal dune comprises a matrix of sand and anthropogenic waste (Fig. 4.6 (6)) and 4.7 (B)). Repeated sequences of wave scarping events and slope failures have given way to large volumes of masonry, plumbing and electrical waste being deposited in the back-beach/dune toe area (Fig. 4.7 (B)), which impede natural beach-dune sediment exchange, a primary focus of this thesis. These materials are associated with the historic location of residential and tourist facilities, previously overcome by the retreating dune field. Figure 4.5

broadly locates all these key factors of anthropogenic influence within zone B,

(which justified its omission from further analysis).

Figure 4.5: Zone B Anthropogenic Locations; Sand sheets (1 and 2), Victoria Road and National Trust carpark (3), permanent caravan site (4), sole caravan site access road (5), and foredune exposure of anthropogenic waste (6).

Figure 4.6: Sand encroachment requiring removal and redistribution. National Trust carpark, Victoria Rd, Formby, 2015.

Figure 4.7: Zone B Human Impacts; A) Vegetation trampling, B) Anthropogenic waste at beach-dune interface (2019).

4.4.4 Zone C

Occupying the southern extent of retreating coastline, zone C houses a series of relatively well defined, large scale trough blowouts, all of which exhibit marked levels of deposition in their landward reaches. Multiple ‘breaches’, and/or blowout throats within the foredune extend down to the back-beach level, and range in width from ≈ 10 to > 50 m, providing considerable connectivity between the beach and dunes, thus promoting occurrence of the enhanced beach-dune sediment exchanges that are being targeted in this research. Visually, these blowout features exhibit all the characteristics of being ‘corridors of high sediment transport’. In refining the area of interest for analyses, the most northern blowout trough in this zone was excluded from the analysis as a result of it not being representative of typical foredune blowouts found in sandy coastlines. Immediately

adjacent to this blowout, the northern stretch of foredune is composed of a composite of both sand and ageing tobacco waste (Fig. 4.8). Although this varies temporally, the tobacco waste greatly increases the cohesiveness of sediment comprising this foredune. Over time, as new material on the seaward face of this section of foredune is exposed by erosion, the nature of the dune face experiences periods of being solid, or semi-solid in structure. During such periods, the physical structure of this section of dune therefore impedes beach-dune sediment exchanges, and in particular aeolian processes, which justified exclusion of this blowout from zone C analyses.

Figure 4.8: Tobacco waste in Zone C; (A) The blowout flanked by tobacco waste and excluded from further analysis, (B & C) differing degrees of cohesiveness in foredune structure north of the blowout throat.

Whilst the entirety of zone B was omitted from the investigation due to extreme anthropogenic influence, zones A and C both contained sections of coastal dunes which provided ideal physical characteristics for the study. Areas within each zone were further refined and delimited prior to ‘per cell’ analysis.

4.4.5 DTM (Digital Elevation Model) uncertainty analysis

For the past few decades, much of the work aimed at quantification and mapping of coastal geomorphic change has been based on the creation of DoDs (DEMs of Difference), from repeat topographic survey data (e.g., Saye, *et al.* 2005; James, *et al.* 2012; Pye and Blott, 2016; Guisado-Pintado, *et al.* 2019). As models, all DEMs are accepted to contain levels of ‘error’, (or alternatively ‘uncertainty’), relative to how accurately each individual DEM represents the actual terrain surveyed. DEM errors can be derived from a diversity of sources. A non-

exhaustive set of examples could include, instrument precision, sampling technique, complexity of terrain, influence of vegetation cover, point registration, and interpolation methods used for DEM surface creation. As DoDs are a GIS product derived through the differencing of two individual DEMs, inherent uncertainty in each of the input DEMs, is propagated (and potentially enhanced), within the resultant DoD (Wheaton, *et al*. 2010). In the absence of assessing input DEM uncertainty, the levels of geomorphic change expressed in the resultant DoD, (and the volumes derived from this change), cannot be portioned into that which may simply be a product of DEM uncertainty, and that which can be confidently attributed to 'real' morphological change.

Prior to their use in DoD creation, LiDAR data was therefore subject to uncertainty analyses. It is commonplace for organisations involved in the collection or distribution of remotely sensed data, to offer estimations of quality for specific surveys and/or digital formats. In line with this, the Environment Agency (EA) publishes levels of accuracy, (or ranges of error) for the data they distribute, and these have simply been accepted, or just routinely declared in previous studies for Sefton (e.g., Saye, *et al.* 2005; Esteves, *et al*. 2012; Smyth, *et al*. 2020a). An increasingly critical view of this practice (Wheaton, *et al*. 2010), together with an acknowledgement of the presence of errors within the Sefton LiDAR, potentially beyond those declared by the EA (Pye and Blott, 2016), encouraged further assessment of actual levels of uncertainty. The use of a wider range of survey years in this study heightened this need. Preliminary uncertainty analyses revealed marked variability in error magnitudes between survey years.

Fiducial surfaces from multiple locations along the Sefton coast were therefore sampled (in total 325 points), with point elevations of all DTMs in the time-series, compared initially to those of the 2018 DTM. Selection of the (most recent) 2018

DTM as a proxy for ‘ground truth’ elevation data was based on the broad assumption that the accuracy of LiDAR datasets has generally improved over time, in line with advancements in technology and LiDAR processing ‘best practice’.

To provide clarity in respect of abbreviations, as the acronym DTM is seemingly being used interchangeably with DEM in this section, it is worth differentiating the two terms. The term DEM describes any continuous, surface elevation model which exists in digital format. For the purpose of specificity, and as the EA provide elevation data in a variety of structures, the definitive product utilised in this research, (DTM) is explicitly stated when necessary. A DTM (Digital Terrain Model) is simply a DEM which represents the ground surface. Prior to DTM creation, all LiDAR returns within the full survey identified as being associated with vegetation, (or anthropogenic features) existing above the bare ground, are first filtered out of the ‘raw’ point cloud data, prior to the continuous surface being interpolated. To qualify this further, DSM (Digital Surface Model), sometimes termed a ‘first return’ surface, is an alternative EA DEM product. The individual cell values of the DSM format represents the elevation of the bare ground, plus the height of any vegetation or artificial features existing above the surface.

Mean error differences and RMSE of residuals were calculated, and residual values additionally visualised using boxplots. In being markedly high, levels of uncertainty for the 2008 DTM were exceptional, relative to all other survey years. These discrepancies were viewed as beyond an acceptable level, and the 2008 DTM was hence excluded from any further analyses. Subsequent availability of newly released ‘ground truth data’ by the EA in 2020 facilitated a re-run of uncertainty analyses, with 279 additional, measured ‘ground truth’ points. This identified the 2017 DTM (1 m resolution), as having the lowest level of uncertainty

in the time-series (< 0.03 m mean difference), and therefore surface values which are most representative of the true ground elevations for the area surveyed.

As ‘per cell’ analysis is dependent on the use of DTMs with matching resolutions, uncertainty analysis was performed on each 2 m resolution DTM. For some, this was their original resolution, and for others the cell size chosen for newly created DTMs (via re-sampling). Using all 604 ‘ground truth’ sample points (279 EA points surveyed with high precision, and the 325 selected from fiducial surfaces, with the 2017 1 m DTM, elevation values taken to be ‘real’. RMSEs were calculated for each 2 m DTM, and used to calculate propagated errors in DoDs produced for sediment budget analysis.

4.4.6 Delimiting zone boundaries for ‘per cell’ analysis

Limiting the extent of analysis in each zone solely to the area of the dune field housing foredune blowouts, permits improvement of the signal to noise ratio of GIS outputs, by removing areas with limited connectivity to blowouts at the beach-dune interface, (which would otherwise dilute trends in sediment exchange). The seaward boundary of each zone was delimited using a ‘dune toe’ file associated with the earliest DTM within their respective time-series (2010 for zone A, and 1999 for zone C). The position of the ‘dune toe’ at Sefton exhibits extreme spatio-temporal variability. A sparsity of lower foredune vegetation, visitor pressure, regular foredune interactions with tidal waters, and high frequency onshore directed aeolian transport events, all contribute to this variability. The resultant accumulation of sediment between the ‘dune toe’ and the typically steep, ‘cliffed’ face of the foredune, which could be termed the ‘foot’ of the dune, also varies greatly in size, configuration and residence time. Even following repeated phases of accretion, when the foredune ‘foot’ is relatively large, the volume of sediment it holds only represents a minor proportion of the overall dune sediment budget.

Recognising this, Pye and Blott (2016) suggested that the cliffed face of the foredune might be a more appropriate choice of beach-dune boundary, when undertaking analysis of foredune position, or dune sediment budgets. In this study however, the dune toe itself provided the least parsimonious option, and over the extended duration of analysis, in understanding its location has only limited influence on the total dune budget, a high level of precision in its position was not required, (nor could it be obtained at a 2 m spatial resolution).

The northern and southern limits of each area of analysis were positioned arbitrarily, just beyond the approximate longshore boundaries of each zone's blowout system. Incremental thresholding of the lower class ranges of elevation change in the 'dynamic layer' provided an objective tool to then delimit the landward boundary of each zone. The desirable threshold would be the minimum level possible, which provided an optimal balance between, maximising the spatial extent of dune field experiencing geomorphic change, whilst limiting the occurrence of isolated patches of elevation change above the threshold, but being positioned beyond the landward boundary. A 1.5 m minimum level of elevation change produced the most advantageous results and was manually digitised.

4.4.7 'Per cell' geomorphic change detection and sediment budget analysis

Elevation variability

'Cell by cell' assessment of variability in elevation values within a LiDAR time-series allows the location of areas having experienced relatively higher magnitude, and/or more frequent geomorphic change. Whilst Holden, *et al.* (2014) propose the use of a standard deviation (SD) for this purpose, a limitation of SD comes from the measure being influenced by the absolute scale of elevation values within the population. Ultimately this prevents individual cell SD values, from being truly

comparable. Over extended time periods, blowout evolution is typically expressed by the presence of two spatially coherent zones. An upwind area dominated by erosion, and a downwind area by deposition (Hesp, 2002). Variability assessment permits identification of locations where there has been higher magnitude variability in topography, but importantly, potentially also, locations having experienced higher frequency phases of elevation change which may have opposed longer term trends. Smyth, *et al.* (2020a) found locations with this characteristic in a study of blowout evolution, and their identification can provide insights on sediment pathways within blowouts, for which understanding to date is limited.

Here 'per cell' variability was assessed using Coefficient of Variation (CV), as this provides a measure for each individual cell, on a single scale, (in this case percentage), by normalising SD using the mean value of data populations, thus permitting cell by cell comparison. CV was computed as;

SD/mean X 100

As measures of SD are also influenced by population size, and in only providing partial coverage, the 1999 DTM needed to be omitted from the zone A time-series. In consequence, direct comparisons of variability between zones could not be made.

Spatial trends

Associating each individual cell within the zone, to the time-series survey date of its minimum and maximum elevation value, can provide information on longer term trends in dune field evolution across broad spatial scales (Holden, *et al.* 2014). Time at minimum, and time at maximum rasters were derived from the time-series

of each zone using the ‘local’ function of the ESRI ‘spatial analyst’ toolbox. As outputs are based solely on rank (rather than actual elevation values), RMSE measures of individual DTM uncertainty were not considered. This was deemed only a minor limitation as the vast majority of DTM values of uncertainty were likely to be far lower in magnitude, relative to the absolute elevation changes in topography having occurred between survey years in an ‘active’ dune field.

DoD creation and sediment budget analysis

All differencing of DEMs was performed using GCD (Geomorphic Change Detection), v7, (Riverscapes Consortium, 2018), an ArcMap plug-in. The 2018 DTM (2 m) was used as the most recent survey for both zones. For each zone, to maximise temporal range of the analysis, the earliest available DEM with full coverage was deducted to derive each DoD (2010 for Zone A, and 1999 for Zone C).

Although DEM differencing can be performed solely using ArcMap, GCD software holds numerous advantages. The first being it provides two sets of outputs for each operation; the simple ‘raw’ DoD, and a second, thresholded DoD which accounts for any known uncertainty associated with the input DEMs. Additionally, the propagation of errors (from the DEMs into the DoD) is automated, with output metrics provided for both area and volume. The RMSE for each DTM, quantified in section 4.5.5, were propagated using the following equation;

$$\delta u\ DoD\ \sqrt{(\delta z\ new)^2 + (\delta z\ old)^2}$$

Where δ*u* is the propagated error in the DoD, with δ*z new,* and *δz old,* being the errors for the individual, input DEMs. Table 4.3 details the individual RMSE of each DTM used, and the resultant propagated error for each DoD.

Table 4.3: DTM and DoD Uncertainty

Zone A	RMSE	Propagated Error
2018 DTM	0.053 m	0.0927 m
2010 DTM	0.076 m	
Zone C		
2018 DTM	0.053 m	0.104 m
1999 DTM	0.089 m	

For both DoDs, uncertainty was assumed to be spatially uniform across the zone, and a simple minimum level of detection was applied, to threshold out all elevation changes, (positive or negative), up to the level of the propagated error.

4.5 Results – Part 2

4.5.1 Zone A

Elevation change magnitude

The earliest and most recent DTMs with full coverage had survey dates of March 2010, and September 2018 respectively. Zone area measured 78,671 m^2 and its 2010 seaward boundary 656 m. Figure 4.9 details elevation change magnitude during the 8.5 year temporal range.

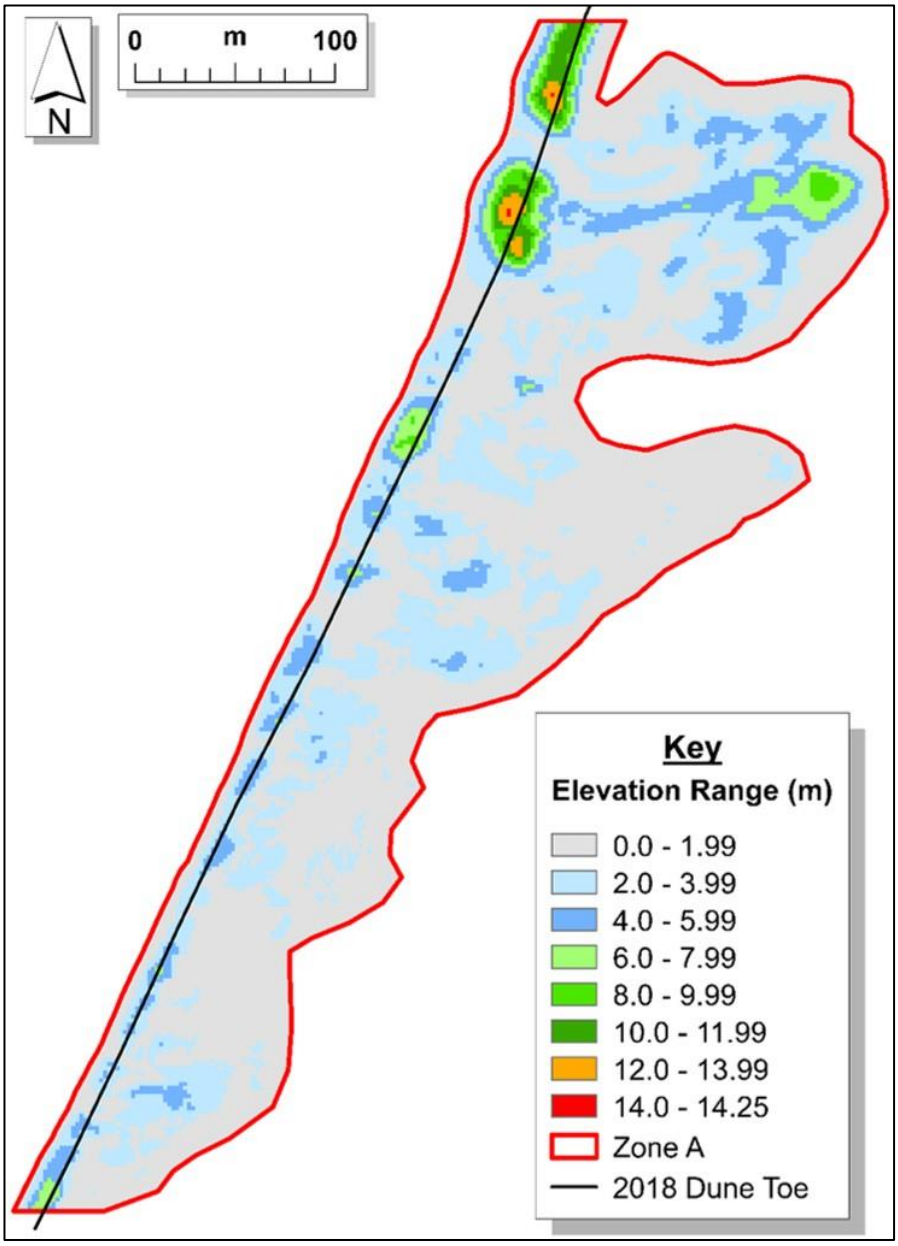

Figure 4.9: Zone A, Dynamic Layer, Elevation Change Magnitude 2010 to 2018.

Zone A is dominated spatially by elevation changes of < 2 m. Medium to higher magnitude elevation change are concentrated along the seaward boundary, largely within a cross-shore area through which the foredune has retreated. All elevation changes > 10 m are related to the initial foredune line. Two prominent clusters of the highest magnitude change (up to the 14.25 m maximum in zone A), occur in the north, and are associated with erosion of the N and S foredunes which flank the throat of the blowout examined in chapters 2 and 3.

Patches of low magnitude change along the seaward boundary are associated specifically with the presence of blowout throats, and additionally, more minor

fragmentation of the foredune, (where blowouts have not fully developed, or small gaps have subsequently been consumed by retreat). The multiple isolated patches of 2 - 6 m elevation change which occur landward of the initial dune crest are largely aligned with either blowout throats, (which have persisted throughout the term), or smaller scale, ephemeral gaps in the foredune.

A prominent cluster of > 4 m patches of elevation change occur in the NE, and are landward of the two highest magnitude blowout throats, which bisect the foredune. Finally, within this cluster, there is a peak of > 8 m elevation change, which occurs ≈ 150 m landward of beach-dune interface.

Elevation variability

'Per cell' variability in elevation, (measured by CV), is detailed in Fig. 4.10. The spatial distribution of variability exhibits very similar patterns to that of elevation change magnitude. The lowest category of < 5% CV has the greatest areal coverage. Medium to high CV is clearly visible and concentrated in the seaward band through which the foredune has retreated, with maximum variability (> 35% CV) relating to foredune erosion immediately N and S of the most northern blowout throat (examined in chapters 2 and 3). The numerous patches of 5 - 10 % CV which occur landward of the foredune crest, in the main appear to be aligned with foredune blowout throats. Additionally, relative to other output layers, these foredune gaps were found to be most easily identified through the use of CV. An isolated patch of medium to high CV corresponds with the most landward peak of elevation change (identified in Fig. 4.9.).

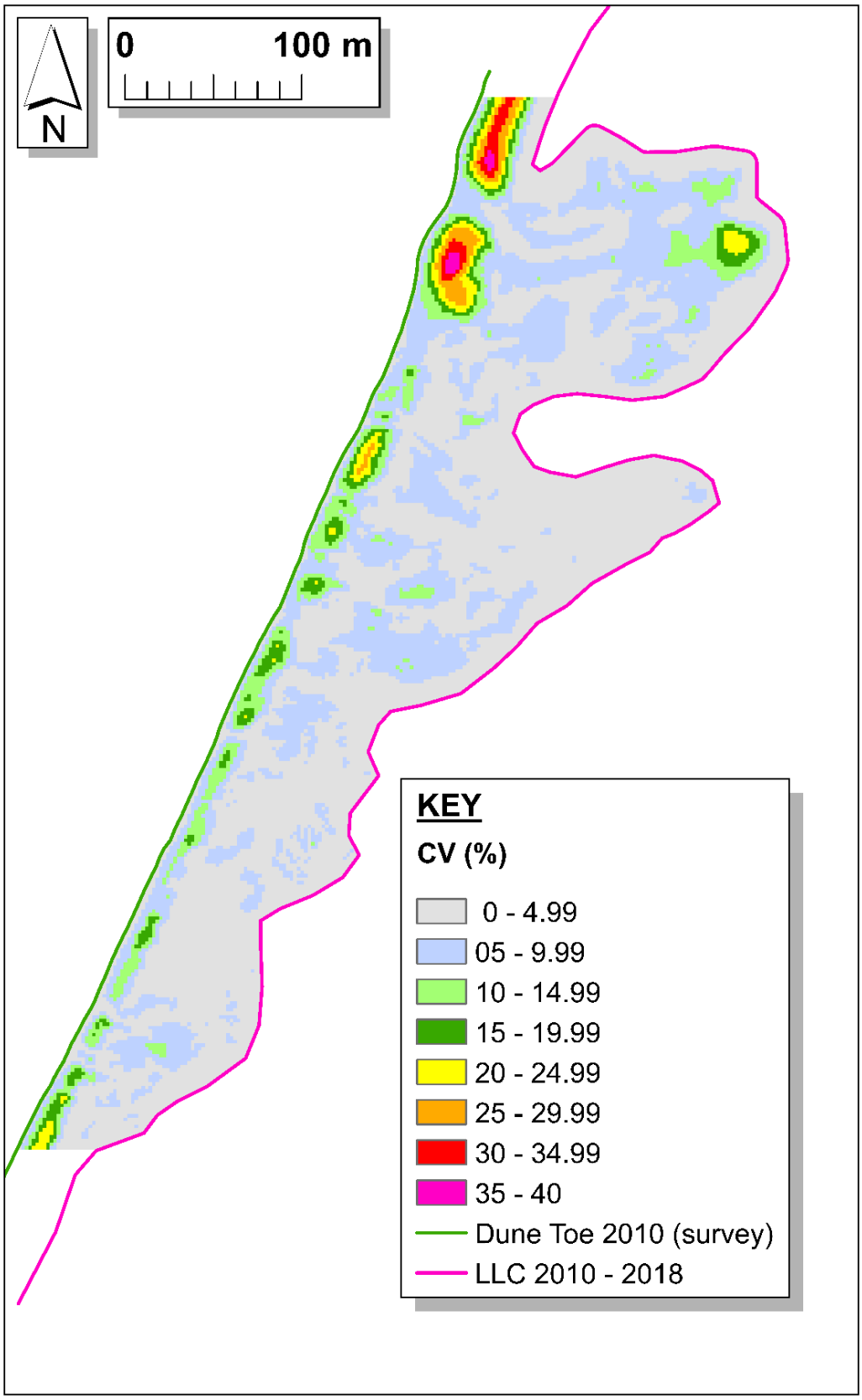

Figure 4.10: Zone A, CV of elevation 2010 to 2018.

Temporal Trends

Coastline retreat is the trend in landscape evolution most evident on assigning individual cells with the survey year, of maximum, and minimum elevation values, throughout the time-series (Figure 4.11).

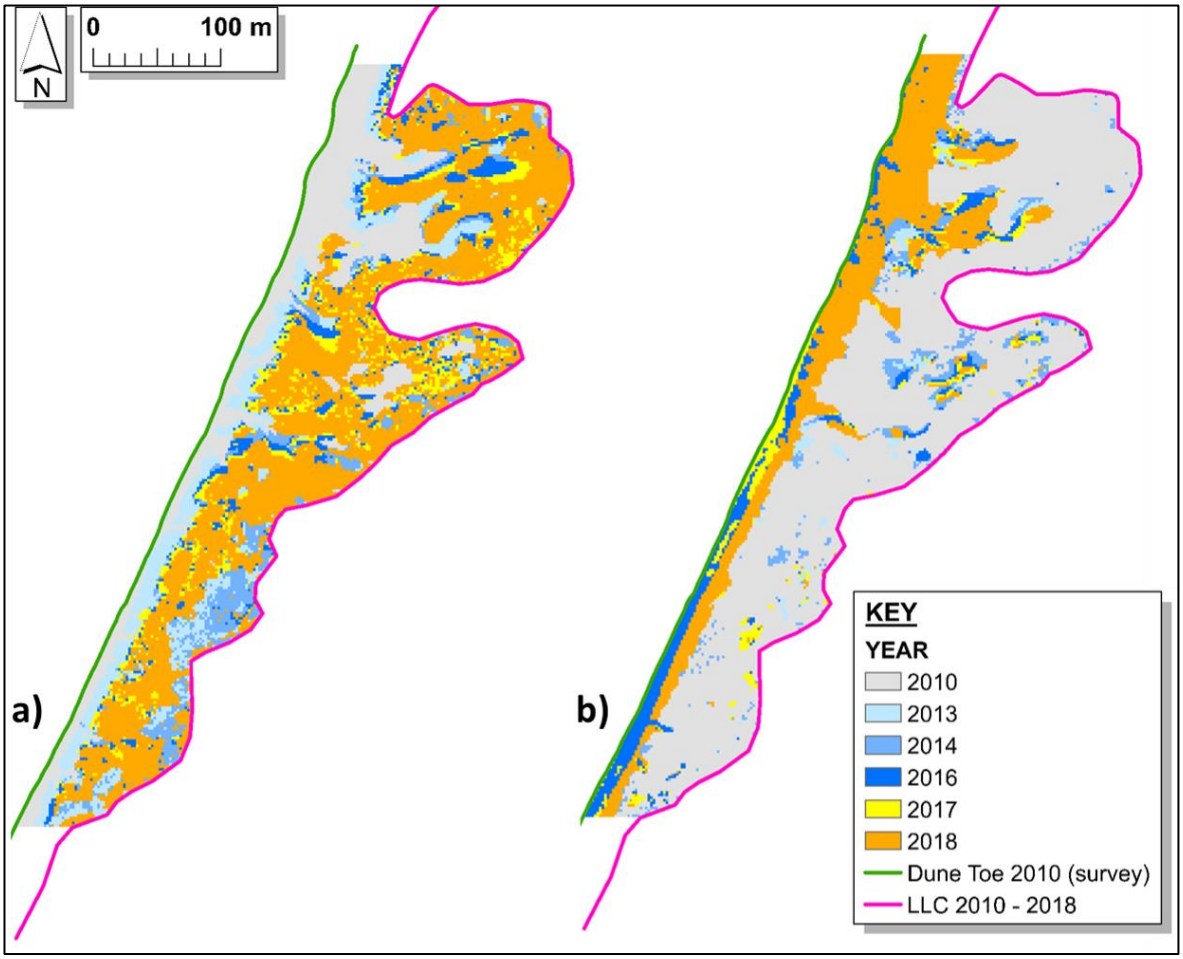

Figure 4.11: Zone A, Time at Maximum Elevation (a), and Time at Minimum Elevation (b).

Throughout zone A, the seaward boundary experienced maximum elevations during the earliest year of 2010, which have since lowered as a result of frontal dune retreat. The cross-shore width of this band of maximum elevations in 2010, which stretches the full length of the zone, remains relatively uniform. The exceptions to this are two sizeable areas in the north of zone A, which extend landwards between ≈ 100 to 140 m from the 2010 dune toe position. Both of these distensions evidence the lateral and landward expansion of well-developed foredune blowouts located in each of their positions. East of the zone through which foredune retreat has progressed, zone A is dominated by maximum elevations during 2018. Maximum elevation values occurring in 2018 across the majority of land area to the east of the migrating line of frontal dunes is most likely associated with incremental, landward directed sediment transfers throughout the term, to give maximum elevations in the final year of the time-series.

Landwards of the frontal dune line, over 90% of the land area for the time at minimum elevation (Fig. 4.11 (b)) is associated with 2010, (the earliest year of the time-series), and demonstrates net sediment deposition. The reversal of the trend exhibited for maximum elevations further evidences, incremental net landwards transfers of sediment having occurred over the term. Also mirroring the pattern for maximum elevations, the two areas of minimum elevations associated with 2018, extending landward of the frontal dune indicate progressive erosion of these blowout troughs. In addition to the two well developed troughs in the far north, two much narrower, elongated patches of minimum elevations during 2018, extend landwards, perpendicular to the frontal dune line, and are associated with progressive deflation of two blowout troughs in earlier stages of development (the most southern of the pair is approximately central to the zone).

A final point of interest relating to this group of four, varying magnitude trough blowouts, is that three of the features display narrow stretches of maximum elevations in 2016, along their southern trough walls (Fig. 4.11 (b)). It is unclear if these represent an epoch where significant, temporary deposition has occurred, or that the onset of erosion of their S trough walls did not commence until post the 2016 survey date at each of these locations.

Geomorphic Change Detection and Sediment Budget Analysis

GCD outputs provide DoDs with all elevation changes, (both positive and negative), subsequent to thresholding out the propagated error, otherwise termed the ‘minimum level of detection’. Figure 4.12 details zone A elevation changes greater than ±0.0927 m, occurring between 2010 and 2018.

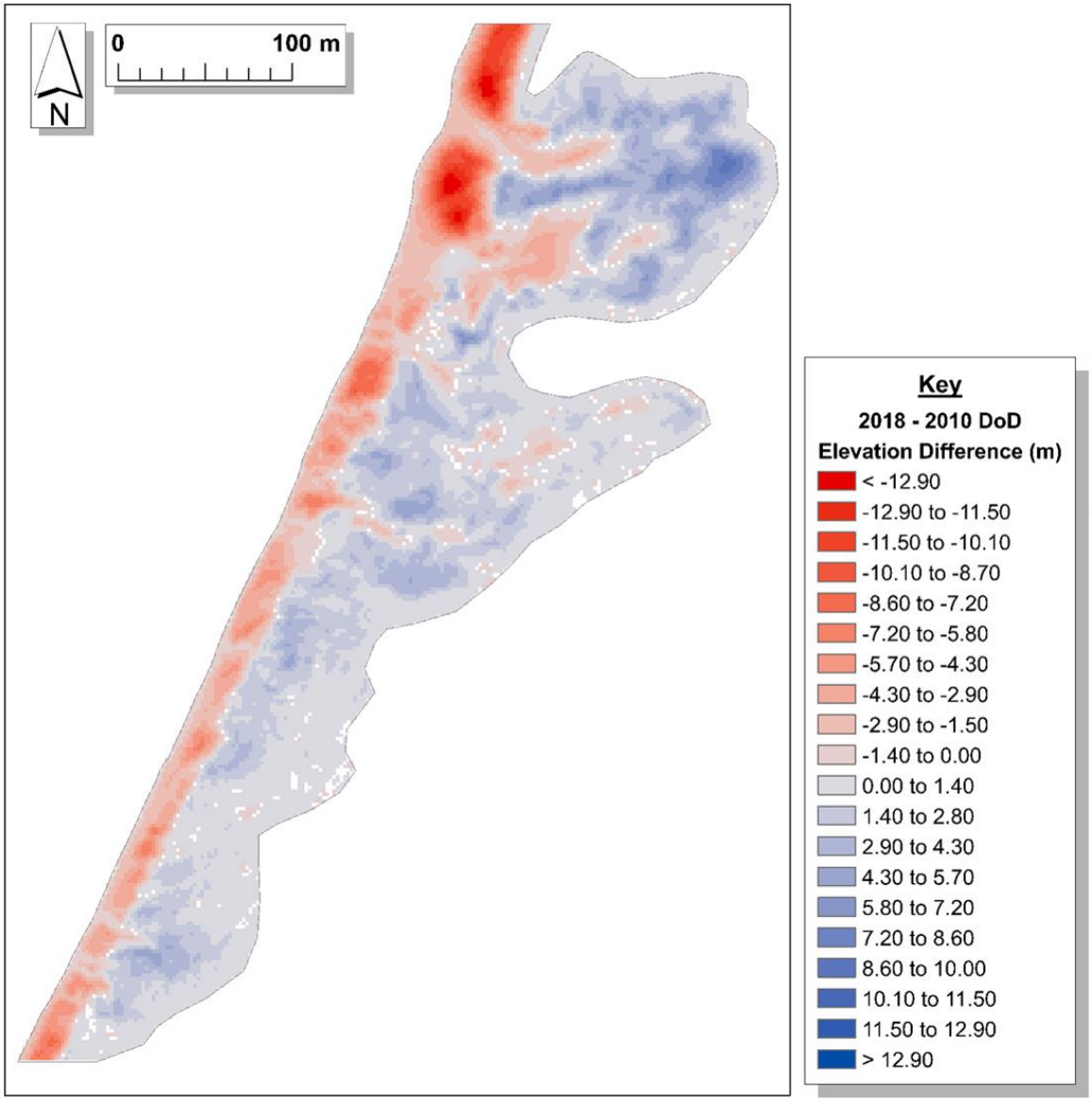

Figure 4.12: Zone A DoD, 2010 to 2018, thresholded by propagated error.

Decreases in elevation largely occur along the seaward boundary of zone A, and are associated with erosion of the foredune as the coastline has retreated. The width of this band of erosion, which stretches the full length of zone A is relatively uniform. Exceptions to this, where elevation decreases are seen to protrude landwards from the frontal dune line, are all associated with gaps in the foredune, where trough blowouts, at varying stages of progressive evolution are located. In total, six instances of foredune blowouts resulting in erosion extending landwards of the area occupied by the frontal dune crest are visible. The two largest scale examples occur in the far north. In both cases, lateral and landward expansion of the troughs has created the largest spatial areas of elevation decreases, beyond

but with connectivity to the foredune line, and the erosional portion of these landforms also stretch the farthest distance inland. Negative elevation changes in this locality are the highest magnitude throughout zone A, with areas of foredune flanking both sides of the northernmost blowout trough having experienced decreases of just over 14 m.

Two troughs in the centre of zone A, where elevation decreases extend landwards of the foredune line, have reduced spatial areas, and their landward extensions are also of a shorter distance. Finally, two relatively low magnitude blowout troughs can also be seen in the far south of zone A. Both of which extend only a short distance landwards of the frontal dune line.

Although there are a few examples of isolated patches of lower magnitude, negative elevation change occurring landwards, and also disconnected to the longshore band of foredune erosion, the land east of the band through which the foredune has retreated is dominated by positive change, indicating a largely depositional environment. After thresholding out changes up to the level of DoD uncertainty, 97.75% of zone A experienced elevation change. At 52,300 m^2, the area experiencing deposition was more than double that of the, 24,536 m^2 area which experienced erosion (Table 4.4). Zone A areas which experienced the highest relative levels of sediment deposition are aligned, in landward positions of trough blowouts which breach the foredune line. The area of zone A, where both its spatial extent, and the magnitude of positive elevation change, combine to give the sector of greatest deposition, is positioned landward of the two largest, most fully developed troughs. In this area, approximately 165 m landwards of the 2010 dune toe position, and in close proximity to the eastern boundary of zone A, the height of positive elevation change peaks at 9.29 m.

Table 4.4: Zone A, Geomorphic Change Detection Metrics (2010 - 2018)

Attribute	Raw	Thresholded	Error Volume
AREAL (m^2)			
Area of Surface Lowering	25,264	24,536	
Area of Surface Raising	53,344	52,300	
Area of Detectable Change	n/a	76,836	
Area of Interest	78,608	n/a	
Percent of Area of Interest With Detectable Change	n/a	97.75%	
VOLUMETRIC (m^3)			
Volume of Surface Lowering	76,123	76,089	± 2,273
Volume of Surface Raising	93,684	93,635	± 4,846
Volume of Difference	169,807	169,724	± 7,119
Total Net Volume Difference	17,561	17,545	± 5,353
VERTICAL AVERAGES (m)			
Average Depth of Surface Lowering	3.01	3.10	± 0.09
Average Depth of Surface Raising	1.76	1.79	± 0.09
Av. Total Thickness of Difference for Area of Interest	2.16	2.16	± 0.09
Av. Net Thickness Difference for Area of Interest	0.22	0.22	± 0.07
Av. Total Thickness of Difference for Area with Detectable Change	n/a	2.21	± 0.09
Av.Net Thickness Difference for Area with Detectable Change	n/a	0.23	± 0.07
PERCENTAGES (By Volume)			
Percent Elevation Lowering	44.83%	44.83%	
Percent Surface Raising	55.17%	55.17%	
Percent Imbalance (departure from equilibrium)	5.17%	5.17%	
Net to Total Volume Ratio	10.34%	10.34%	

After thresholding out DOD uncertainty, the total volume of sediment loss between 2010 and 2018 is 76,089 m^3, and of sediment gain, 93,684 m^3. This results in a positive, net sediment budget of 17,545 m^3, (all error bars detailed in Table 4.4). This is a positive departure of 5.17% from equilibrium. The positive budget is indicative of Zone A having received sediment input from, either or both of, the beach, and the longshore stretches of foredune flanking the zone.

Although the total area of deposition is more than twice that of the area of erosion, the positive increase in volume is a much smaller ratio, as a result of mean negative changes in elevation per m^2, being far greater than mean positive changes. A contributing factor to this difference in the mean values for positive and negative change is that zone A erosion has been concentrated at the frontal dune line in which crest heights of the eroding foredune exceed 10 m above beach

level, at multiple longshore positions. Using the dune toe positions as a marker, average coastline retreat in Zone A has been 15.75 m or 1.85 m pa (8.5 year term), and the cross-shore band through which retreat has occurred is characterised by high amplitude foredunes.

4.5.2 Zone C

Elevation change magnitude

Zone C spatial extent measures 144,799 m^2, and analysis covered a 19.5 year term.

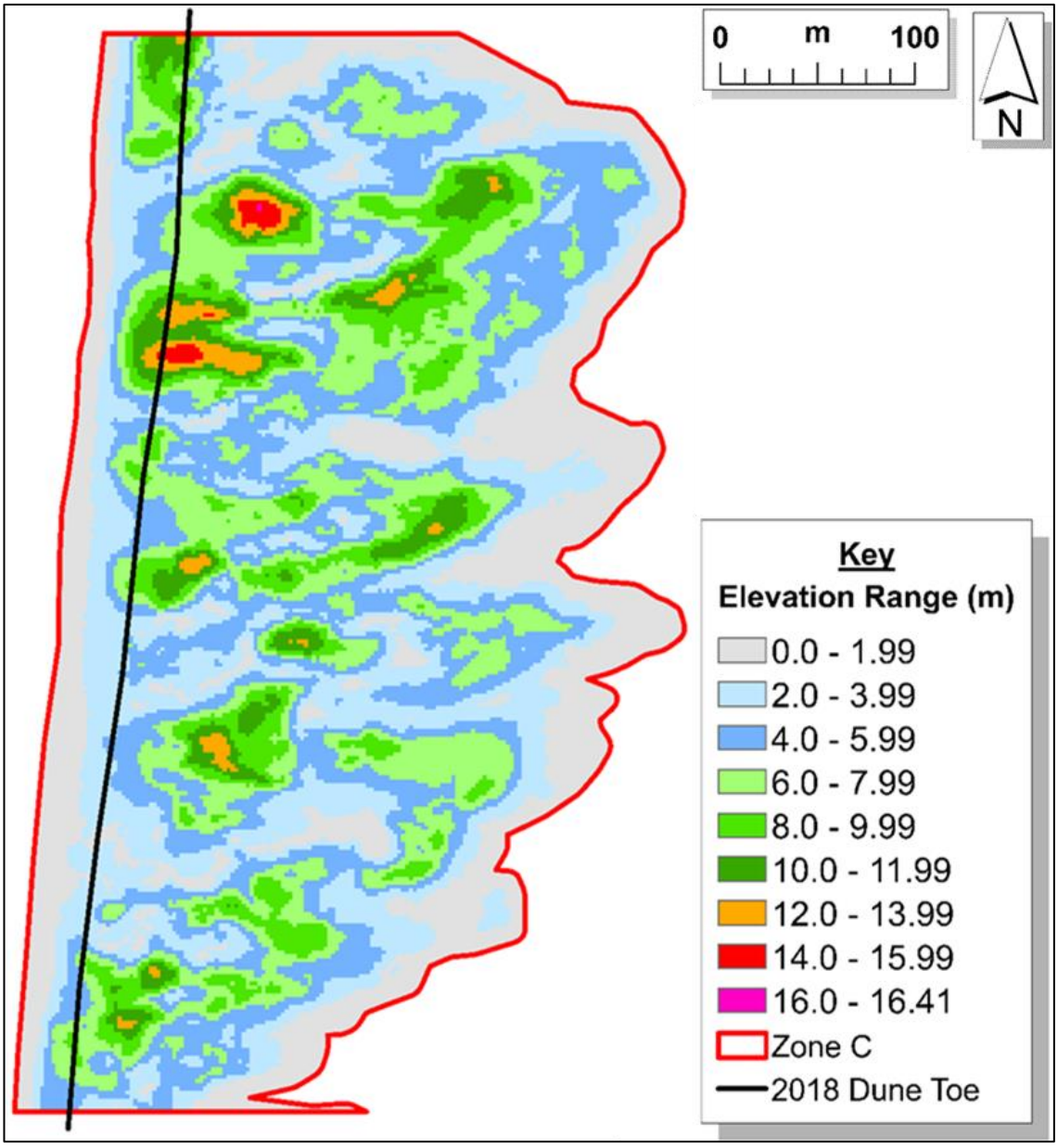

Figure 4.13: Zone C, Dynamic Layer, Elevation Change Magnitude 1999 to 2018.

Unlike for zone A, no single category dominated elevation change magnitude, with change therefore being distributed more evenly across the absolute range of elevation. The ‘dynamic layer’ identified zone C as an area which has experienced ‘high’ magnitude geomorphic change (Figure 4.13), and these changes have occurred across a relatively broad, longshore and cross-shore, spatial extent. The majority of medium to high magnitude change (6 m up to the 16.41 m maximum), occurred landward of the western ‘band’ through which the dune toe has retreated.

Within the area of coastline retreat, low magnitude (0 - 6 m) elevation change is most prevalent, in part as a result of the frontal dune line already being highly fragmented, and partly composed of remnant knobs, or isolated, short stretches of discontinuous ‘foredune’, already having experienced varying degrees of erosion prior to 1999. Two large scale protrusions of low magnitude change extend landward of the seaward boundary in the southern half of zone C. Each of these are associated with large scale, foredune blowouts, which were already at mature stages of development in 1999.

Multiple ‘discrete’ patches of the highest magnitude elevation changes which have occurred in zone C are positioned within ≈ 70 m of the 2018 dune toe, and relate to the erosion of existing topography over the ≈ 20 year term. Patches of medium to higher magnitude elevation change, which are positioned landward to this, are largely occurring in environments which are at present, strongly depositional, and exhibit strong, cross-shore alignment with foredune blowouts to their west.

Elevation variability

The minimum elevation CV throughout zone C, was 0.31%, and 38.77% the maximum. In combination, the lower magnitude (0 - 4.99% and 5 - 9.99%) CV

classes, account for over two thirds of zone C area. Figure 4.14 includes aerial photos, as many discrete patches of raised CV correspond to highly visible, landscape features.

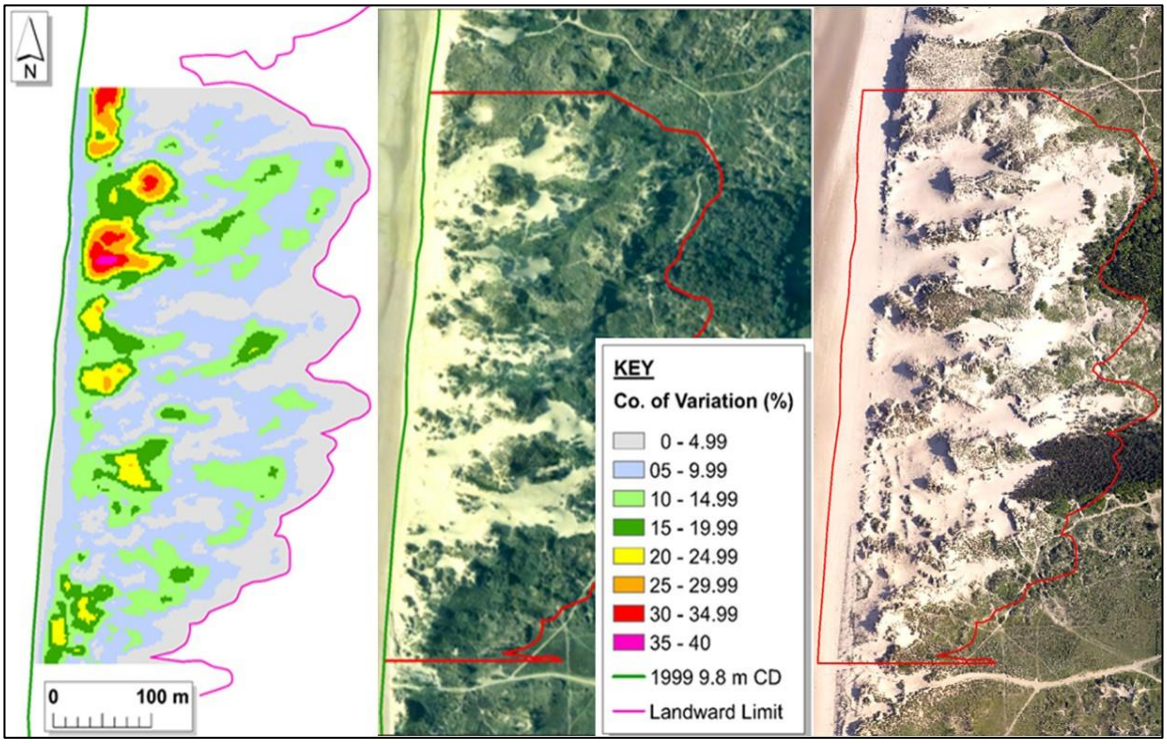

Figure 4.14: Zone C, CV of elevation, 1999 to 2038 (left), 1999 aerial photo (centre), and 2012 (right).

All areas of the highest magnitude CV (> 20%), are located toward the seaward boundary of zone C. These patches of high variability occur in association with the removal and erosion of the 'foredune', which even at the beginning of the time-series (in 1999), is highly fragmented. Other than for a short stretch of ≈ 70 m of continuous foredune, in the northernmost section, the beach-dune boundary of zone C can be seen to consist of a series of remnant knobs. Each of the five, discrete patches of >20% CV, in longshore positions S of the northern foredune, can be linked to sections of dune, or isolated 'remnant' knobs which are visible in 1999. These remnant knobs, generally elongated in shape, and extending landward, are in the main also representative of the lateral walls of trough blowouts, (at various points in the time-series over which this complex of erosive features has evolved).

In the main, a clear spatial coherence is evident, between areas of high magnitude CV in the seaward extent, and separate patches of raised CV that are aligned in cross-shore, landward positions. The majority of these landward patches, likely represent areas having experienced the deposition of sediment, transported eastwards/downwind, by the net onshore directed prevailing winds. The 2012 image illustrates many of these patches as being in the depositional lobe areas of foredune, trough blowouts, or within the transgressing, parabolic dune crests which are developing.

Finally, the largest spatial area of medium scale CV (10 - 20%), east of the frontal dunes, is strongly aligned with the two seaward patches of highest magnitude CV. This landward area appears to have been a location of both erosion and deposition. The obvious coherence between these discrete, cross-shore ‘patches’ is perhaps the best representation of a transport corridor being visible through the use of CV. Orientated in a southwest to northeast direction, the central, narrower section of this feature, appears to be the location where a breach has occurred, in the section of elevated dune topography, which had been separating two individual blowouts until this point. CV here identifies the coalescing of two previously more ‘discrete’, individual blowouts, towards what could now be considered, more of a singular, larger scale landform (post the lateral wall breach).

Temporal Trends

Figure 4.15 (a) illustrates maximum cell values are dominated by just two years, 1999 and 2018. The entire western area of zone C, up to a minimum cross-shore distance of 50 m, was at its maximum elevation in 1999. This area of maximum elevation in 1999, also extended landwards at numerous longshore positions, by up to ≈ 175 m. These areas of maximum elevations, extending cross-shore during

the year 1999, represent elevated dune topography, which can be seen to have been vegetated to a much greater extent in 1999 aerial imagery (Fig. 4.14).

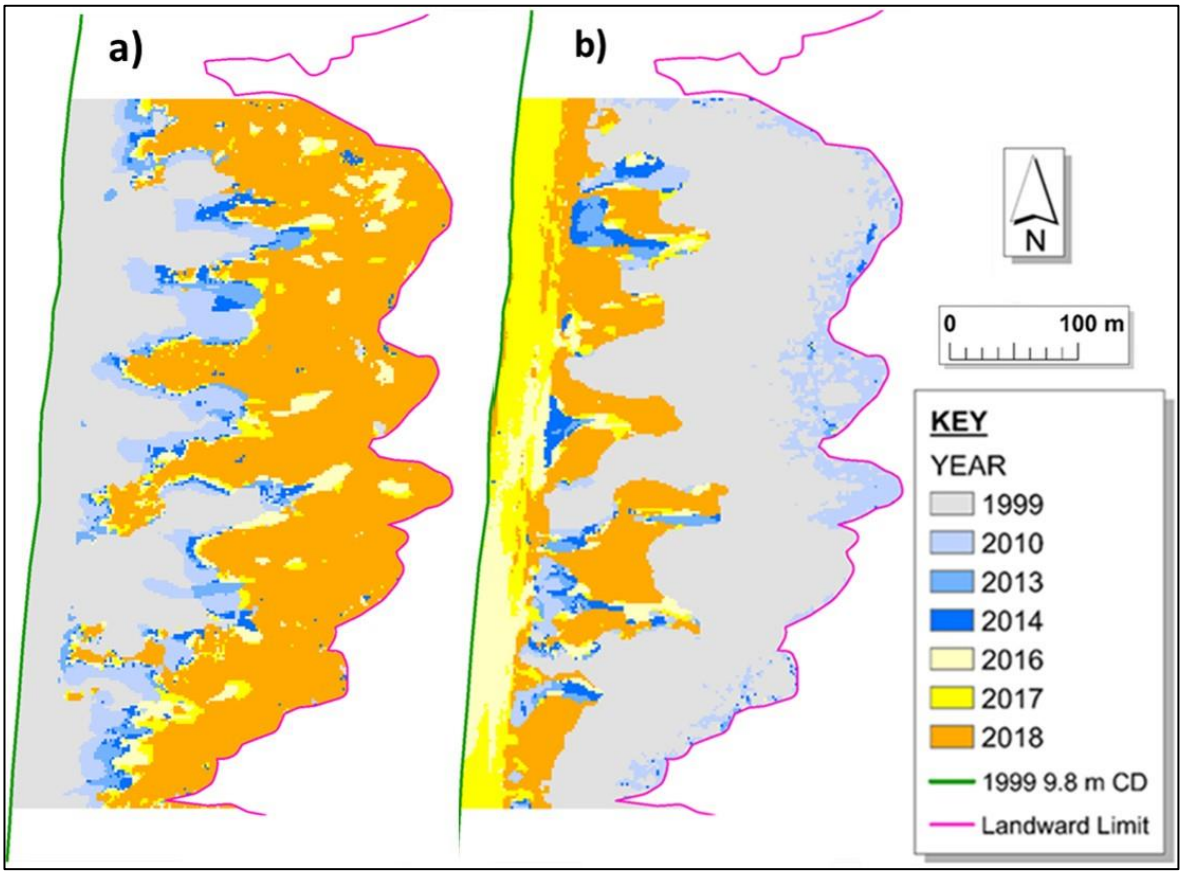

Figure 4.15: Zone C, Time at Maximum Elevation (a) and Time at Minimum Elevation (b).

The entire western sector of zone C (Fig. 4.15 (a)), held maximum elevations during the first year of the time-series. This demonstrates that the entire spatial extent coloured grey, has experienced net erosion, and reductions in elevation over the time-series. The geomorphological evolution of the landscape which has given way to these net decreases in elevation since 1999 comprise a number of mechanisms; 1) erosion of the fragmented 'foredune', 2) erosion of larger, elevated sections of vegetated dune topography which extended east of the beach-dune boundary, down towards collections of isolated remnant knobs by recent years, and 3) both lateral, and cross-shore expansion of blowout troughs.

Figure 4.15 (b), time at minimum, displays the vast majority of the eastern and larger sector of zone C, as having minimum elevations during 1999, thereby

demonstrating net sediment deposition over time. The vertical yellow band, at the seaward boundary of the zone, exhibits the long term trend of foredune retreat experienced over the time-series, and is in the main composed of 2016 and 2017 cell values. As this section of coastline has experienced continual retreat, it was expected that this 'band' might consist mainly of 2018 cells. That it comprises 2017 and 2016 values may be indicative of short term deposition having occurred soon before the timing of the 2018 survey. At first glance, this serves to partially mask the strongly erosional trend of longer term evolution. Both the 2016 and 2017 surveys were collected during April of their respective years, whilst the timing of the 2018 survey was late September. At Sefton, (NW England), the 'summer' months are characterised as periods of less frequent, low pressure weather systems, fewer storms, and lower water levels relative to those of 'winter' months. With respect to the acknowledged trend of continual coastline retreat, this anomaly in the 'time at minimum' layer most likely relates to seasonal variability in patterns of beach-dune sediment exchange, and highlights a period of temporary foredune growth/recovery.

Multiple, irregularly shaped, (orange) features, composed of 2018 cells, can be seen to extend landwards from the beach-dune boundary (Fig. 4.15 (b)), each broadly comparable with similar shaped grey features in Fig. 4.15 (a). These features demonstrate continued erosion of both, blowout trough floors, and the elongated remnant knobs, (which in part take the form of blowout trough, side walls. The two principle processes exhibited in Fig. 5.15, are coastline retreat, and the progressive development of blowouts by wind erosion. In turn, both mechanisms have undoubtedly resulted in the downwind deposition of sediment eroded from upwind, seaward locations. Given the particularly 'open' nature of the

zone C seaward boundary, the throughput of beach sediment may also make a significant contribution to the net landward transfer of sediment which is evident.

Geomorphic Change Detection and Sediment Budget Analysis

Figure 4.16 details zone C elevation changes, which are greater than the DoD uncertainty level (±0.104 m), that have occurred between 1999 and 2018.

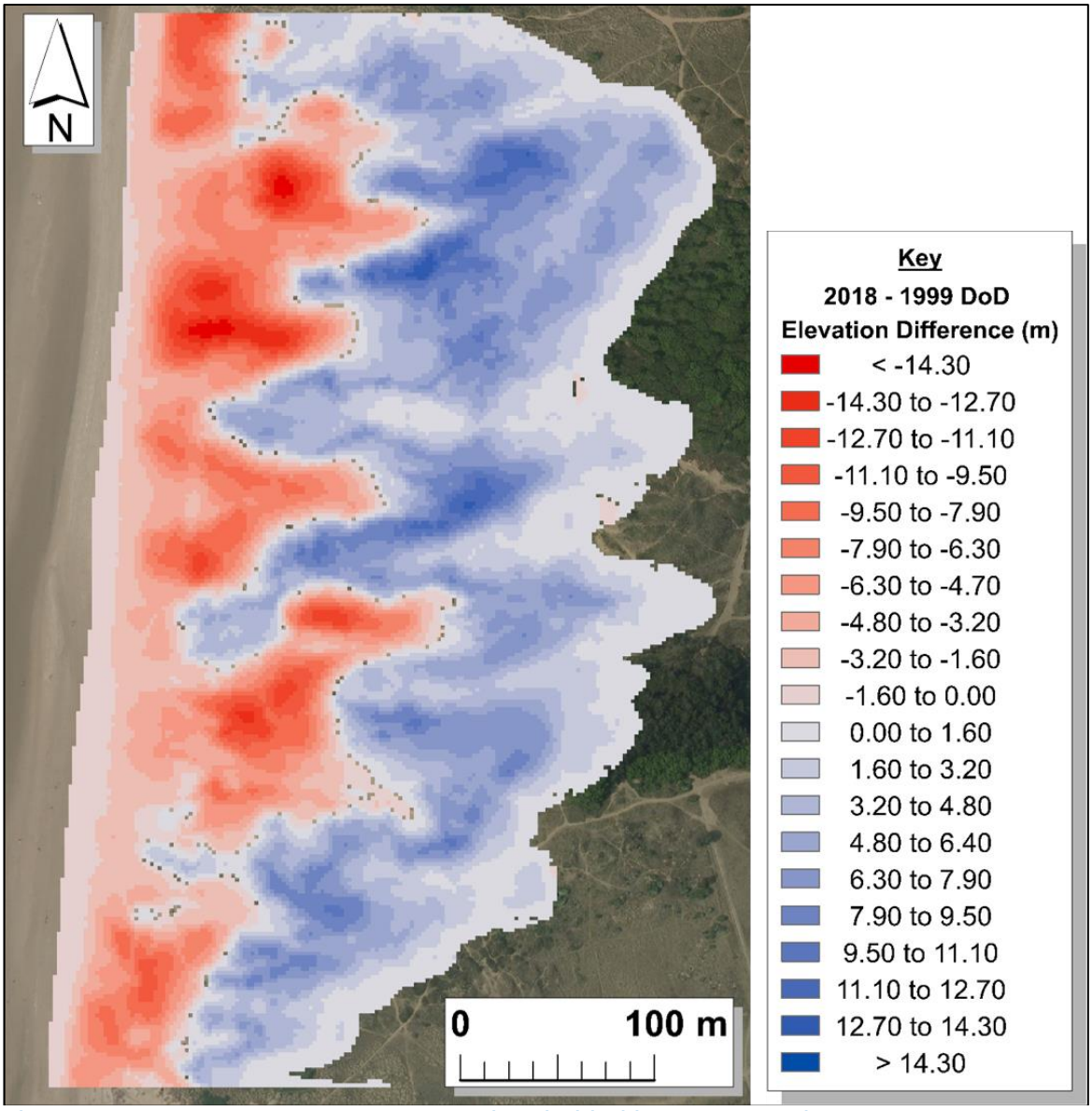

Figure 4.16: Zone C DoD 1999 to 2018 thresholded by propagated error.

The entire seaward boundary of zone C has experienced elevation decreases. Maximum elevation loss in zone C was -15.83 m, and the two highest magnitude concentrations, both of > 15 m decreases, are visible toward the north of zone C.

The northernmost of the two, is located approximately 80 m landwards of the 1999 dune toe, with the second, to the south, and in a slightly more seaward position. Both these features are associated with the ongoing erosion of what was already, highly fragmented foredune topography in 1999. Whilst zone A evidenced maximum decreases in its most seaward extent, zone C has a seaward band (with a cross-shore width of ≈ 10-20 m), of lower level elevation decreases, prior to sharp increases in the magnitude of erosion, immediately landwards. This reflects the zone C frontal dune line already being heavily degraded at the start of the time-series.

The two concentrations of highest magnitude elevation increase (> 14 m), are both immediately landward of peaks in erosion. Throughout zone C, multiple blowouts, of varying complexity, can be seen to extend inland from the beach-dune boundary, with elevation decreases evidencing their progressive erosion, and expansion. These landward protrusions are all flanked laterally, and also beyond their eastern extents, by pronounced levels of deposition. To varying degrees, these bands of deposition, which envelope each ‘discrete’ blowout trough, have shore-normal, ‘u-shaped’ configurations, and are parabolic in nature. The larger scale trend evidenced by the DoD, is of seaward erosion, in conjuncture with downwind deposition, thus illustrating a net landwards transfer of sediment. The clear pattern of strong deposition at the eastern terminus of troughs is exhibited multiple times throughout the zone, and provides clear evidence of blowouts being corridors of high sediment transport at Sefton.

Zone C is broadly split into an erosional, seaward area of elevation decrease, and a landward, depositional area, of elevation increase. Each of these areas exhibit, near-continuous spatial coverage of their respective trends. Only very negligible, isolated patches of low magnitude erosion occur within the depositional area, and

just a sole, small scale example of deposition within the seaward, erosional sector is visible. After thresholding out changes up to the level of DoD uncertainty (±0.104 m), 99.41% of zone C experienced elevation change over the term. Proportionately, with 57,600 m^2 experiencing surface lowering, and 86,196 m^2 elevation increases, there is a 40% to 60% split between the areal extents of erosion and deposition (Table 4.5).

Table 4.5: Zone C, Geomorphic Change Detection Metrics (1999 - 2018)

Attribute	Raw	Thresholded	Error Volume
AREAL (m^2)			
Area of Surface Lowering	57,968	57,600	
Area of Surface Raising	53,344	86,196	
Area of Detectable Change	n/a	143,796	
Area of Interest	144,644	n/a	
Percent of Area of Interest With Detectable Change	n/a	99.41%	
VOLUMETRIC (m^3)			
Volume of Surface Lowering	273,518	273,497	± 5,967
Volume of Surface Raising	348,422	348,398	± 8,929
Volume of Difference	621,940	621,895	± 14,895
Total Net Volume Difference	74,904	74,901	± 10,739
VERTICAL AVERAGES (m)			
Average Depth of Surface Lowering	4.72	4.75	± 0.10
Average Depth of Surface Raising	4.02	4.04	± 0.10
Av. Total Thickness of Difference for Area of Interest	4.30	4.30	± 0.10
Av. Net Thickness Difference for Area of Interest	0.52	0.52	± 0.07
Av. Total Thickness of Difference for Area with Detectable Change	n/a	4.32	± 0.10
Av.Net Thickness Difference for Area with Detectable Change	n/a	0.52	± 0.07
PERCENTAGES (By Volume)			
Percent Elevation Lowering	43.98%	43.98%	
Percent Surface Raising	56.02%	56.02%	
Percent Imbalance (departure from equilibrium)	6.02%	6.02%	
Net to Total Volume Ratio	12.04%	12.04%	

Above the DoD threshold for uncertainty, the total volume of sediment loss between 1999 and 2018 is 273,497.41 m^3, and of sediment gain, 348,397.97 m^3. This gives a net, positive sediment budget, of 74,900.56 m^3 (error bars detailed in Table 4.5). This represents a positive departure of 6.02% from equilibrium. The positive budget for zone C is indicative of the landward depositional area, having received sediment input from either, or both of, the beach, and the adjacent

foredunes to the north and south, in addition to that derived directly through the erosion of its initial dune topography.

Although the (19.5 year) zone C time-series duration, is more than double that of zone A, at 6.02%, the increase in budget is just 0.85% greater. Mean coastline retreat in zone C totals 37.05 m, which equates to ≈1.9 m pa. Positive sediment budgets are typically associated with dune building, and foredune progradation, and coastline retreat with net sediment losses. Both sections of coastal dunes examined here exhibit positive values in sediment budgets, whilst experiencing a longer term trend of retreat. In each zone, spatial patterns of geomorphic change have provided a diversity of evidence indicative of foredune blowouts being landforms characterised by heightened levels of morphological change. Additionally, results here demonstrate these landforms as also being facilitators for the enhanced landward transfers of sediment. At the landscape scale, blowouts positioned at the beach-dune interface showed strong spatial coherence with higher magnitude elevation changes, with such changes typically also extending across greater spatial extents, particularly in a cross-shore direction.

4.6 Discussion

4.6.1 Meso-scale, geomorphic change associated with foredune blowouts

Coastal, beach-dune environments are landscape scale systems, composed of a multitude of diverse, smaller scale geomorphic features. Dune blowouts are aeolian dune landforms, or '*landscape sub-units'* (Gregory and Lewin, 2014), and as such, potential component parts of these larger scale systems. Foredune blowouts, and more generally all blowouts, whether coastal or continental, are widely acknowledged as landscape features associated with high relative levels of

aeolian sediment transport, and in consequence, also geomorphic change (Carter, *et al*. 1990; Hesp, 2002).

Two primary reasons for this are accepted to be; 1) the relative sparsity of vegetation cover in 'active' blowout interiors, which increases the susceptibility of their surface to erosion (Hesp, 2002), and 2), the known propensity of their topographic form to induce airflow enhancements capable of promoting the initiation, or maintenance of aeolian sediment transport (e.g. Carter, *et al.* 1990; Smyth, *et al*. 2014). Research in this chapter first sought to assess the validity of this assertion concerning heightened levels of geomorphic, process-form response activity, and to produce empirical evidence in its support. The study was conducted at a retreating beach-dune system that encompasses multiple foredune blowouts, geomorphic change was quantified and characterised, over the meso-scale. Both the sedimentary structure, and the coastal setting of beach-dune systems, are promotional of higher frequency, short duration, transport events, in comparison to landscapes composed of more stable materials, or which are located in less 'process-rich' environments. Over the longer term, spatial patterns of elevation change provide a valid and recognised proxy measure, of cumulative sediment transport (Hugenholtz and Wolfe, 2005, 2006; Hugenholtz, *et al*, 2009; Mitasova, *et al*. 2011). The 'dynamic layer' derived from the multi-epoch, 19.5 year, LiDAR time-series (Mitasova, *et al*. 2011; Holden, *et al*. 2014), assessed spatial patterns of elevation change, and therefore also the cumulative effect of multi-directional, sediment transport events over the period.

Figure 4.4., displays the magnitude, and spatial distribution of elevation changes having occurred within the retreating section of the coastline at Sefton. An undeniable, and pronounced coherence is evident, between the distribution and

spatial extents of areas experiencing higher relative levels of topographic change, with the locations, and the geometry of foredune blowouts. Excluding the narrow, cross-shore band through which the foredune has retreated landwards, all patches of medium to high elevation change are associated with foredune blowout localities. In longshore sections of the coast where foredune blowouts are absent, elevation changes > 2 m are constrained spatially within the 'band' of foredune retreat. The dynamic layer allowed confirmation that foredune blowouts experience heightened levels of sediment transport, and as a consequence, also geomorphic change. Foredune blowout locations were seen to mirror all discrete areas of highest magnitude elevation change. The longshore positions of foredune blowout throats also showed full correspondence with locations where patches of elevation change exceeding 2 m, had the most substantial areal coverage, and additionally often extended the greatest distances inland. Study findings therefore provide a valuable evidence base in support of widely held (but largely anecdotal) perceptions concerning these landforms.

4.6.2 Foredune blowouts as 'transport corridors'

Blowouts are frequently described using terminology such as highly 'efficient', 'active', or 'effective', transport corridors, or sediment pathways (e.g., Carter, *et al*. 1990; Gares and Nordstrom, 1995; Hesp, 2002; Anderson and Walker, 2006). This in part is as a result of extensive research having been conducted on blowout evolution. With this comes appreciation, that the deposition of sediment in downwind areas, is most commonly derived from surface erosion in upwind areas of their interior, and that this plays a principle role in their progressive development (section 1.5.2). In addition to this mode of geomorphic change, 'open system' blowouts facilitate the throughput of sediment, surplus to that eroded from the host dune of individual landscape features (Carter, *et al*. 1990). Perhaps no more so,

than for foredune trough blowouts, which are commonly fronted by extensive beach systems, and therefore, the sizeable, additional sediment source they represent.

In this chapter, all of the analytical measures used to either quantify, or characterise geomorphic change, demonstrated foredune blowouts to be effective transport corridors/sediment pathways. Throughout the entire longshore section of coastline retreat, without exception, every landscape feature identified as a foredune blowout, exhibited a cross-shore pattern of upwind erosion in their seaward area, together with marked sediment deposition, in their landward, (downwind) reaches. Often, the magnitude of surface lowering in the seaward area of individual blowout locations, was also reflected in the magnitude and/or spatial extent of downwind deposition. Foredune blowouts were thus confirmed to be playing a lead role in the landward transfer of sediment, and in many cases were seen to facilitate deposition of sediment, several hundred metres inland of the beach-dune interface. The positive sediment budgets of both zone A, and zone C (Tables 4.4 and 4.5), also demonstrated their role, specifically as ‘transport corridors’, through their respective volumes of downwind deposition, exceeding that which had been eroded from upwind dune topography.

4.6.3 Implications for coastal evolution

The longshore stretch of the Sefton coast explored in this chapter has experienced a continual, and ongoing trend of coastline retreat for over a century (Gresswell, 1937, 1953; Pye and Blott, 2016). In this analysis, multiple layers of evidence identified foredune blowouts to be a significant and direct contributor to this retreat. A ubiquitous feature, throughout the ≈ 4 km zone of retreat, was the explicit involvement of foredune blowouts in the landward transfer of sediment. Whilst the conservation of sediment by a coastline experiencing retreat, can be associated

with episodes of vertical foredune growth, as the beach-dune boundary gradually migrates upwards and landwards through ‘rollover’ (Pye, 1990; Saye, *et al*. 2005), the principle mechanism of retreat at Sefton is very clearly, by aeolian sediment transport, via foredune blowout corridors. This assertion is supported not only by being highly visible in numerous GIS outputs, but also through the lack of significant geomorphic change in the dune hinterland, landwards of the band through which the foredune has retreated, at longshore positions where foredune blowouts are absent (e.g. Fig. 4.4).

A theoretical cornerstone of this research was that foredune blowouts may potentially augment an evolutionary trend of coastline retreat. The findings of this study have identified that large volumes of sediment have been transferred landwards via these pathways. In their absence, such transfers would be limited to minor volumes of sediment (relative to the total dune budget), which could be transported up and over the foredune, (by high magnitude wind events), direct deflation of foredune crests, the transport of sediment from the finer fraction of grain size (at elevations allowing direct transfer above foredune crest heights), and that associated with very gradual landward migration via slope processes. The only logical conclusion which can be drawn through the identification of blowout transport, rather than foredune ‘rollover’, as the most significant contributor to landward sediment transfers, is that foredune blowouts do in fact heighten rates of coastline retreat at Sefton. Sediment involved in these transfers, is in the main derived from the vicinity of the beach-dune interface, with deposition sometimes occurring over great distances, and often reaching the most landward limits of the secondary dune system, which can still be considered ‘mobile’. Importantly, and in addition to this overarching pattern, the positive sediment budgets of both zone A and zone C, demonstrate these landward transfers also encompass sediment from seaward areas, which is surplus to the initial volume of existing dune topography.

Beyond the landward transfer of sediment via blowouts being instrumental to observed coastline retreat at Sefton, this process must logically have multiple indirect consequences, which further enhance this long term trend. Section 1.6.2 of the thesis detailed seminal works on which contemporary understanding of coastal evolution are based. It is widely understood, that sediment exchanges between the foredune and nearshore beach, are critical to the evolution of beach-dune systems (e.g. Psuty, 1988; Nickling and Davidson-Arnott, 1990; Pye, 1990; Sherman and Bauer, 1993; Hesp, 2002; Walker, *et al*. 2017). In turn, across the full spectrum of spatio-temporal scales, mutual adjustments between geomorphic processes and form, continually influence coastal behavior, together with all subsequent sediment exchanges, and beach-dune interactions (Wright and Thom, 1977; Short and Hesp, 1982).

Saye, *et al*. (2005) identified that steep, elevated foredunes in Sefton are a characteristic, specifically associated with longshore sections of the dune field experiencing retreat. In turn, this has been theorised to limit the occurrence of aeolian sediment transport up, and over the foredune crest (Pye, 1990, Saye, *et al*. 2005; Pye and Blott, 2016). Figure 4.4 provides empirical evidence to validate these suggestions, as in longshore positions where foredune blowouts are absent, elevation change in the secondary dune field is almost exclusively constrained within the lowest category of magnitude (0-2 m). However, where blowouts are present, the landward transfer of large volumes of sediment to secondary dunes is evident, and high magnitude geomorphic change can be observed, in some instances, reaching hundreds of metres landward of the beach-dune boundary, through the enhanced connectivity with the beach-dune interface that blowouts provide.

Without the presence of foredune blowout ‘transport corridors’, it is therefore reasonable to deduce that landward transfers of sediment would be significantly less. In turn also, that this sediment would therefore initially accumulate in frontal dunes, and over time, likely be repeatedly cycled between ‘sub-units’ of the cross-shore profile, (which are seaward of the secondary dune field). *Ceteris paribus*, the sizeable landward sediment transfers which Sefton blowouts facilitate, must result in increased foredune budget losses, as well as reduced inputs from the nearshore beach, (through sediment bypassing frontal dunes via blowouts, rather than accumulating within them).

At present, coastal erosion at Sefton is largely attributed to seaward directed, foredune sediment losses, in association with wave scarping events, and slope failures caused by continual wetting, or submergence of the dune toe (Section 1.8.7; Esteves, *et al*. 2012; Pye and Blott, 2016). These mechanisms are directly governed by the heights of waves, still water, and/or wave ‘run-up’, relative to back-beach and dune toe elevations. Additionally, also to periods of time when the width of the ‘backshore’ or ‘back-beach’, immediately seaward of the dune toe, falls below a minimum threshold. At which point, foredune erosion is understood to accelerate (Gresswell, 1937, 1953; Pye and Blott, 2016). All things being equal with regards to marine conditions, (and trends in SLR), decreases in beach elevations, (as a consequence of landward directed, foredune blowout transfers), must undoubtedly result in increases to the frequency and the magnitude of offshore directed sediment losses, and foredune erosion by marine processes.

The combined net sediment gain of the two zones in this study measured 92,445 m^3 in total. Although purely hypothetical, it is worth contextualising this volumetric gain in relation to beach elevations. In the absence of landward transfers via blowouts, over time, varying proportions of this sediment would be stored within

the nearshore beach and foredune budgets. For simplicity, this disregards, sediment losses to longshore, or offshore areas. It must further be acknowledged, that in reality, the areal distribution of such a potential sediment 'gain', would not be confined to a discrete, cross-shore section of the beach. Nethertheless, if it were to be evenly distributed, specifically across the minimum width threshold (≈ 60 m) of the backshore beach defined by Gresswell (1937, 1953), and also over the entire longshore stretch of coastline experiencing retreat (≈ 4700 m), this sediment 'unit' would provide an approximate rise in 'backshore' beach elevation, of 0.33 m. A surface rising of this order would of course reduce the frequency of foredune sediment losses resulting from wave-dune interactions by reducing both their frequency and magnitude. Whilst greatly over simplified, beyond their direct involvement in landward sediment transfers at Sefton, this conceptual scenario does provide a useful example of how, in all probability, their presence must indirectly, also amplify marine induced erosion.

Dune toe position is fundamentally determined by the net balance of repeated cycles of beach-dune sediment exchange. Subsequent to episodic foredune sediment losses from the combined effects of wave scarping events and/or submergence by tidal waters, foredune recovery depends largely on inputs from the nearshore beach, via aeolian sediment transport. Under 'healthy' foredune conditions, over time, sediment delivered through this process will be fixed in place by vegetation, resulting in dune building and foredune recovery. In the presence of foredune blowouts however, rather than sediment accumulating at the beach-dune interface to give frontal dune growth, in acting as conduits for landward sediment transfers, foredune blowouts impede recovery. Over extended time frames, the balance between beach-foredune sediment exchanges will become increasingly promotional of a negative foredune budget, amplifying the effects of erosional events, and accelerating the rate of coastline retreat. The observed trends in dune

toe positions, and budget analysis of longshore zones which house foredune blowouts, is well aligned with the evolutionary model of Davidson-Arnott (2005). Contrary to the Bruun model (1962) of coastline responses to SLR, Davidson-Arnott (2005) theorises that landward sediment transfers occur mutually, with the upward and landward migration of the dune toe. At the landscape scale, conservation of sediment within the dune field, promotes the terms 'coastal erosion', and 'coastline retreat' being more strongly distinguished. Further, that coastal 'squeeze' (Pontee, 2011), rather than the retreat itself, should be of primary concern.

4.6.4 Coastline retreat in association with visitor pressure and vegetation cover

To date, factors beyond a variety of marine related processes or conditions, have not been considered of great influence to the longer term, evolutionary trend of coastal retreat at Sefton. In this study, analysis of geomorphic change, and dune sediment budgets, identify aeolian processes to be making a significant contribution to retreat, and specifically, sediment transport via foredune blowouts to be a key mechanism. In recognition of this, it must additionally be acknowledged that coastline retreat is therefore also a function of human impact. At Sefton, aeolian processes, blowout development, blowout transport activity, and visitor pressure are intrinsically linked.

Dune vegetation cover is known to exert a variety of controls on aeolian sediment transport. A non-exhaustive list of examples include in; 1) providing a protective barrier between airflow and surficial sediment, 2) increasing cohesion between surface grains to bind sediment in place, 3) increasing the shear stress threshold necessary for entrainment, 4) directly trapping grains in transport to remove them from airflow, and 5) as a surface roughness element, inducing airflow stagnation

(section 1.3.3.6). In this knowledge, climate-vegetation indices are often employed to better understand dune field mobility (section 1.6.2). For coastal dunes specifically, vegetation cover and composition, are accepted to be critical controls on foredune evolution (sections 1.6.1 and 1.6.2). Localised decreases in vegetation cover, both generally, and explicitly at Sefton, are additionally a frequent cause of blowout genesis (section 1.5.1), and further, exert considerable influence on the degree to which their evolution is progressive, or cyclical (section 1.5.2).

Vegetation trampling and footpath erosion are two major impacts of intense visitor pressure at the Sefton coast, and both these anthropogenic processes are heavily involved in the initiation, and the maintenance of blowouts throughout the coast. In a recent study of human disturbance at Sefton, Delgado-Fernandez, *et al*. (2019b) demonstrated that the extents, and distribution of 'bare sand' areas, many of which represented blowouts, showed exceptional spatial coherence with visitor pressure. As foredune blowout transport can be seen to make key contributions to landward sediment transfers at Sefton, by propagating more frequent and higher magnitude aeolian transport events, coastline retreat must be attributed to visitor pressure also.

Research directly linking pedestrian traffic to blowout initiation, their progressive expansion, and/or their maintenance at Sefton is constrained by a number of logistical considerations. Not least the longevity of the largest scale, and most active blowout features present, as many pre-date the earliest aerial surveys. Although simply snapshots in time, examples throughout the coast can however be found to demonstrate this association, across the full range of spatial scales, and stages of maturity (Fig. 4.17).

Figure 4.17: Blowout evolution associated with visitor pressure, footpath erosion and vegetation trampling, at Sefton. Initiation (top-left), progressive development (clockwise).

The individual, ‘anthropogenic’ foredune blowouts in Figure 4.17 were selected to encompass examples throughout the broad ‘continuum’ of their progressive development. All of the examples included are associated with dune field footpaths, beach access points, and high relative densities of visitor footprints.

Although short of being conclusive evidence to demonstrate the strong interdependencies which exist between visitor pressure, dune blowouts, and aeolian transport, it is difficult to argue otherwise. To support the assertion that blowouts, and therefore human impact must be considered as a contributing factor in coastline retreat, it is useful here to also offer a complementary example, for an individual blowout at Sefton (Figure 4.18). In this case, blowout initiation and progressive expansion has occurred in association with visitor pressure, and within the temporal range of the aerial ortho-photos available.

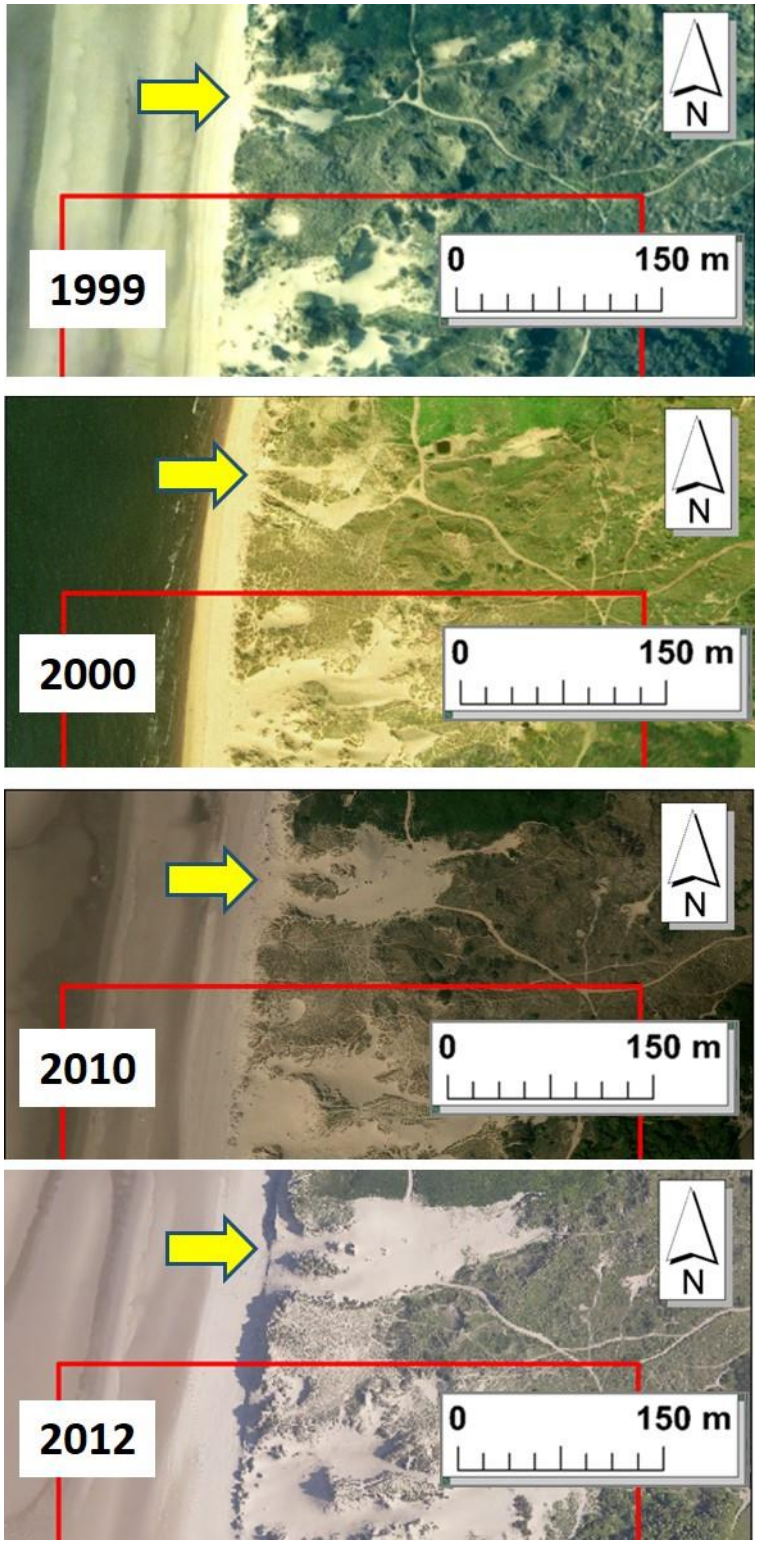

Figure 4.18: Foredune blowout, initiation and expansion in association with visitor pressure, 1999 - 2012.

Prior to refinement of its spatial extent, an isolated foredune blowout can be identified towards the northern boundary of zone C's initial longshore limit (Fig. 4.4). Figure 4.18 displays the genesis and evolution of this feature between 1999 and 2012. *Inconsequential to the purpose of the figure, the red line visible on each image represents a 'clipping' boundary used during the GIS refinement of zone C's*

spatial domain. The yellow arrow in each image indicates the longshore position of the blowout. Initiation and expansion of this feature is associated with visitor pressure and vegetation trampling, on the convergence of multiple dune field footpaths in proximity to a beach access point.

In addition to direct involvement with blowout genesis and maintenance, visitor pressure is also known to impact the vegetative state of foredunes (Figures 4.17 and 4.7 (A)), and therefore also the trapping, and fixing in place of sediment at the beach-dune interface during periods of foredune recovery. Ephemeral deposits of loose sediment, accumulating at the foot of frontal dunes in these periods therefore remain highly susceptible to removal by wind. Pye and Neal (1994) noted the frequent occurrence of such deposits being driven alongshore by winds, until reaching foredune blowouts, to then be transferred landwards.

4.6.5 Longshore variability in blowout evolution and sediment transport

The attributes of 'discrete' depositional units, located in the landward extents of blowouts exhibited marked longshore variability, (both within zones, and between them). Examples of this variability were expressed in elevation peaks, distances from the beach-dune boundary, areal scale, and volumetric storage. In general, albeit subjectively, clear spatial clustering and cross-shore alignment can be seen, between the longshore positions of quasi-discrete patches of landward surface raising, the inter-connecting blowout troughs, and the seaward throats which bisect the foredune. Despite this, full resolution of the variability in landward deposition, or the potential 'closing' of sediment budgets' for individual blowouts remains constrained. The exceptional complexity of dune field evolution, and the extended time frames of analysis, both contribute to this limitation. Over shorter durations, frequent examples of longshore sediment exchanges can be identified. Typically these relate to the erosion of remnant knobs in the throat area, lateral

blowout growth due to the breaching of trough sides walls leading to the coalescence of ‘individual’ blowouts, and the union of depositional units, via cross-shore, radial expansion.

Having said this, and through being a fundamental factor in their evolution (Carter, *et al*. 1990; Hesp, 2002), the dimensions of the host dunes through which blowouts have progressively expanded, clearly exerted significant influence on the nature of downwind deposition. In the more seaward areas of each zone, (where erosion was the dominant process), the principle control on the magnitude of surface lowering, was the geometry of existing dune topography. This was most visible in geomorphic change detected within the seaward section of zone A, with the magnitude of change being a very obvious expression of longshore variability in antecedent foredune characteristics.

As a consequence, comprehensive interpretation of longshore variability in blowout evolution, and blowout transport over extended time frames, includes two essential elements. Resolution of longshore variability in antecedent foredune configuration, together with explanation of spatio-temporal variability in sediment transport over the full time-series duration. Research concerning longshore variability in foredune characteristics has received considerable coverage from the scientific community. A vast and diverse range of contributing factors are acknowledged, and with varying degrees of success, have been used to resolve such foredune variability for specific study locations. Frequent, potential factors cited include longshore differences in sediment supply, beach width, beach slope, grain size, coastline orientation, wind direction, resultant fetch distances, wave energy, beach moisture, vegetation cover, storm impacts and anthropogenic influence (Pye, 1990; Hesp, 2002; Aagaard, *et al*. 2004; Miot da Silva and Hesp,

2010; Delgado-Fernandez and Davidson-Arnott, 2011; Anthony, 2013; Walker, *et al*. 2017; Guisado-Pintado and Jackson, 2018; Strypsteen, *et al*. 2019). The highly non-linear nature of beach-dune transport events, and the strong inter-dependencies between many of the contributing factors, continues to confound this subject. Irrespective of assessing the relative importance of individual components, an insightful conclusion from Houser (2009), described foredune sediment supply, and therefore foredune growth, as being fundamentally dependent of the frequency and duration, of periods for which transport potential, and back-shore sediment availability, are synchronous. In light of this, both the comprehensive resolution of longshore variability in antecedent foredune characteristics, and hindcasting nearshore sediment supply to foredunes with real confidence, remain just beyond our reach.

The composition and relative weight to which possible contributing factors impact longer term transport activity at individual blowouts, likely varies temporally in nature, and also spans a range of spatial scales. Topographic enhancements in wind speed and flow steadiness are two elements recognised to promote increased transport capacity (Sherman, *et al*. 1996). Further, both these airflow modifications translated into increased transport intensity, at the event scale for this study (chapters 2 and 3). In both being associated with flow compression (Hesp, 2002; Smyth, *et al*. 2013), the degree to which blowout geometry, particularly trough width and side wall height (Smyth, *et al*. 2020b), promote the occurrence of flow compression, should be expected to have a contribution to, the total transport record of a blowout over the longer term. Airflow patterns within blowouts are strongly dependent on both foredune, and blowout orientation, relative to incident wind direction (e.g., Hesp, 2002; Bauer, *et al*. 2012; Smyth, *et al*. 2013), and will therefore exhibit high variability between individual events. Over

the longer term, the frequency of events involving airflow modifications, together with the relative magnitudes of any airflow enhancements experienced, should therefore show a degree of association with the modality of regional wind direction, and as such, this demands further investigation.

Given the complexity of this geomorphic conundrum, again at the landform scale, it is likely useful to exclude consideration of event scale sediment supply from the nearshore beach, when examining the transport activity of individual blowouts. If solely assessing the potential for sediment transport in respect of the characteristics of dune topography most proximal to the blowout trough, the absolute volume of sediment available for transport, and its erodibility, are likely to be key factors. In turn, the size, configuration, and vegetative state of both the blowout interior, and the foredunes which are immediately adjacent to the throat will govern this.

Over the full durations of their time-series, both of the zones explored in this study were found to have positive sediment budgets. This raises rudimentary questions around the provenance of each surplus, and the dominant sediment transport pathways of their respective locations. Ultimately any net budget gain, surplus to that eroded from the initial, antecedent dune topography within the zone, is derived from the beach. This may have passed directly from beach into blowout, or alternatively have first been delivered to adjacent back-beach/dune toe areas, and then driven longshore to blowout throat locations with each zone.

Although limited within a narrow range of wind approach angle, the transport signal across the foredune in ‘event’ scale investigations (chapters 2 and 3), were orders of magnitude greater than that on the back-beach. This suggested transport

along the face of the upwind foredune to be a principle pathway by which sediment was delivered to the throat during the event. Visual observation of the relative magnitude of this sediment flux, and of upwind streamers arriving from the beach, to then be diverted longshore at the dune toe, demanded an LPC be re-located to the lower slope of the S foredune during the minutes prior to commencement of measurement. Regardless of incident wind direction, the exchange of sediment (in transport across the beach), directly into the blowout, is definitively limited to a cross-shore swath width, approximately equal to that of the blowout throat (Figure. 4.19). During oblique onshore incident winds, recognition must therefore be given to the much greater potential sediment supply which can be derived from the foredune aligned, longshore transport pathway.

Figure 4.19 details a conceptual model of longshore blowout sediment supply, during oblique incident winds. Upon arriving to the dune toe area, flow deflection results in transport vectors becoming broadly foredune aligned, with sediment being driven longshore and downwind. Whilst any proportion of oblique incident flow driven up the foredune is known to become increasingly crest normal with height, at the base of the dune, airflow is deflected in a longshore direction most strongly, to thereby promote transport vectors which are aligned with foredune orientation (Bauer, *et al*. 2013). The decoupling of the beach and dune transport regimes, in association with foredune form-flow interactions is a common observation (e.g., Bauer, *et al*. 2012, 2013; Davidson-Arnott, *et al*. 2012, Walker, *et al*. 2017). As a result, in the schematic (Fig. 4.19), the number of ‘sediment units’ which may potentially contribute to beach-dune sediment exchange via this throat directed, longshore pathway, becomes controlled the length and ‘continuity’ of the upwind foredune.

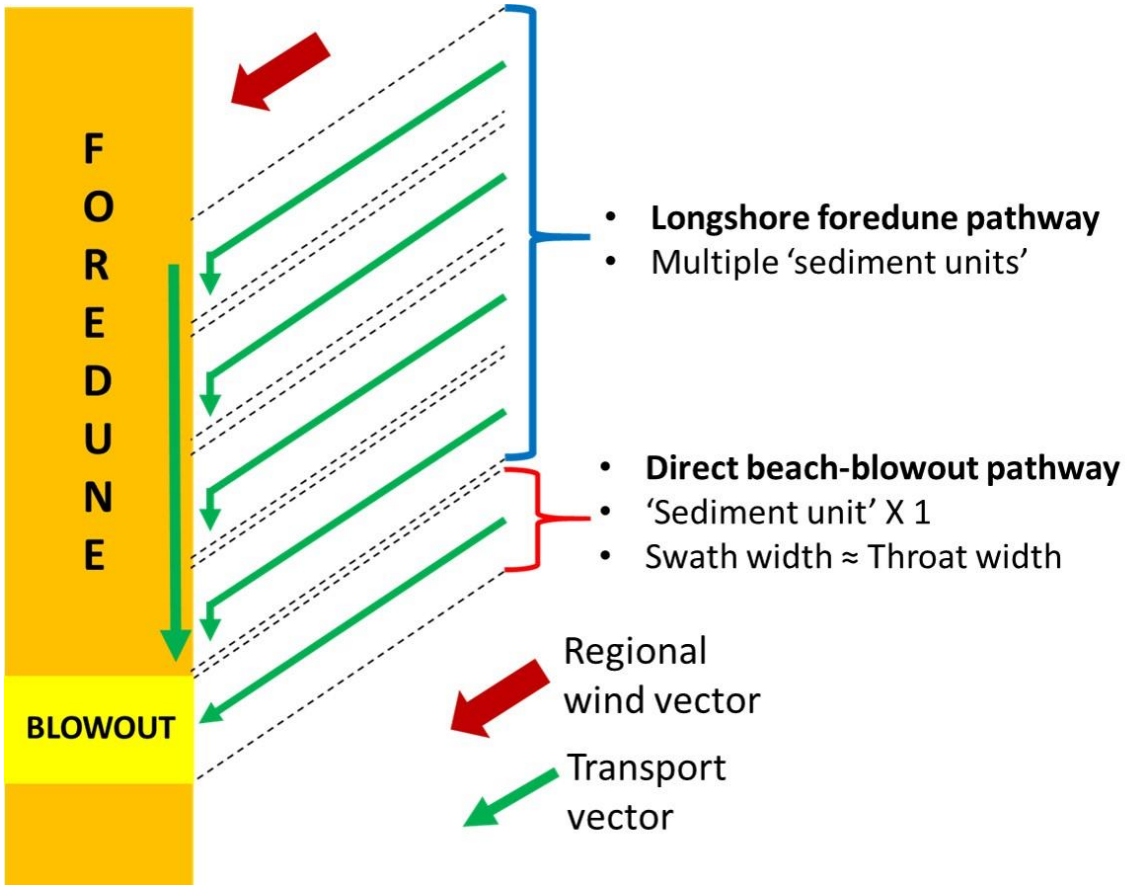

Figure 4.19: Sediment pathway potential during oblique incident winds.

In addition to the greater potential source of sediment supply derived through longshore deflection, airflow modifications to oblique incident winds will likely also enhance airflow transport capabilities. Whilst incident winds close to perfectly onshore directed, are known to be most greatly stagnated by the foredune (Wiggs, *et al*. 1996; Bauer, *et al*. 2013), should the obliquity of approach angle promote longshore deflection, topographically steered flow is acknowledged to become 'dune' attached, and to some degree, also compressed against the foredune surface, as this topographic obstacle in the lower boundary layer may cause the 'piling up' of air mass against it (Walker, *et al*. 2006). In this scenario of strongly deflected winds, at any given point along the lower slope of the foredune, the measured airflow vector can therefore be considered to have two discrete components. In addition to a proportion of the vector being associated with the deflection of at-a-point incident wind streamlines, longshore directed airflow mass, arriving to the same point from upwind areas (via foredune deflection), can make a

significant contribution. This specific property of foredune deflected flow is understood to give pronounced enhancements in flow steadiness (Walker, *et al*. 2009; Davidson-Arnott, *et al*. 2012), which in turn also enhances transport capacity. This potentially transport enhancing feature, associated with near-surface airflow vectors on the foredune, being enhanced by the supplementary component from upwind deflected air mass, was intermittently expressed in the transport signals of the event scale study. Whilst the transport signals of back-beach LPCs were highly responsive to the gustiness of incident flow, the longshore deflected component of airflow on the foredune was during analysis, theorised to be maintaining the exceptionally steady transport observed at the A6 LPC (Fig. 2.3), or alternatively, at times extending the 'lag' response of transport intensity, to the high frequency, negative fluctuations, observed in the A3, wind speed record.

Conceptually, these theories concerning the likely importance of the foredune as a sediment transport pathway, are of relevance to the large majority of beach-dune systems. The exception being for graded shorelines, with a uni-modal wind regime, where the prevailing wind direction is onshore, and perpendicular to a highly linear foredune. Irrespective of coastline shape, the probability of strongly crest normal, onshore directed winds, are also constrained to a very narrow directional range. For Sefton specifically, the coast possesses a number of characteristics which promote the longshore deflection of airflow, and sediment transport vectors.

Firstly, at the landscape scale, the coastline has a distinctly cuspate configuration (Pye and Blott, 2008). With this, during any individual event, the occurrence of regional wind vectors resulting in perfectly onshore directed flow, perpendicular to

the foredune line, are constrained spatially to only short, longshore segments of the larger coastline. To compound this, Sefton's multi-modal wind regime (Pye and Blott, 2016) means that incident winds across a wide directional range, will result in a much greater frequency of foredune oblique, approach angles.

Finally, Saye, *et al*. (2005) identified the high amplitude, steep gradient foredunes at Sefton, (and in coastal dune fields more broadly), to show strong association, with retreating sections of coast. Both these characteristics are known to inhibit transport up and over the frontal dune (Pye and Blott, 2016), and to promote the longshore deflection of airflow (Parsons, *et al*. 2004; Bauer, *et al*. 2013; Walker, *et al*. 2017). Over extended time frames, the cumulative effect of the greater supply potential of longshore directed transport vectors, may therefore be a key factor in determining the volumetric levels of transport experienced at individual blowouts, which exceeds that of the host dune.

The net sediment gains for zone A and zone C represented positive departures from equilibrium, of 6.02% and 5.17% respectively. Whilst comparable, the increase for zone A was gained in just 8.5 years, an 11 year shorter duration than that of zone C. Figure 4.20 illustrates that the foredune sediment pathways, both north and south of zone C are highly limited. To the north, zone C is flanked by a large scale blowout, whilst the foredune to the south is highly fragmented by beach access paths, and small scale blowouts. Although frontal dunes to the north of zone A are also interrupted, to the south, the foredune stretches 214 m longshore before the the occurrence of a small scale breach, and then a further 381 m before reaching the first, large scale sand sheet, at the National Trust site.

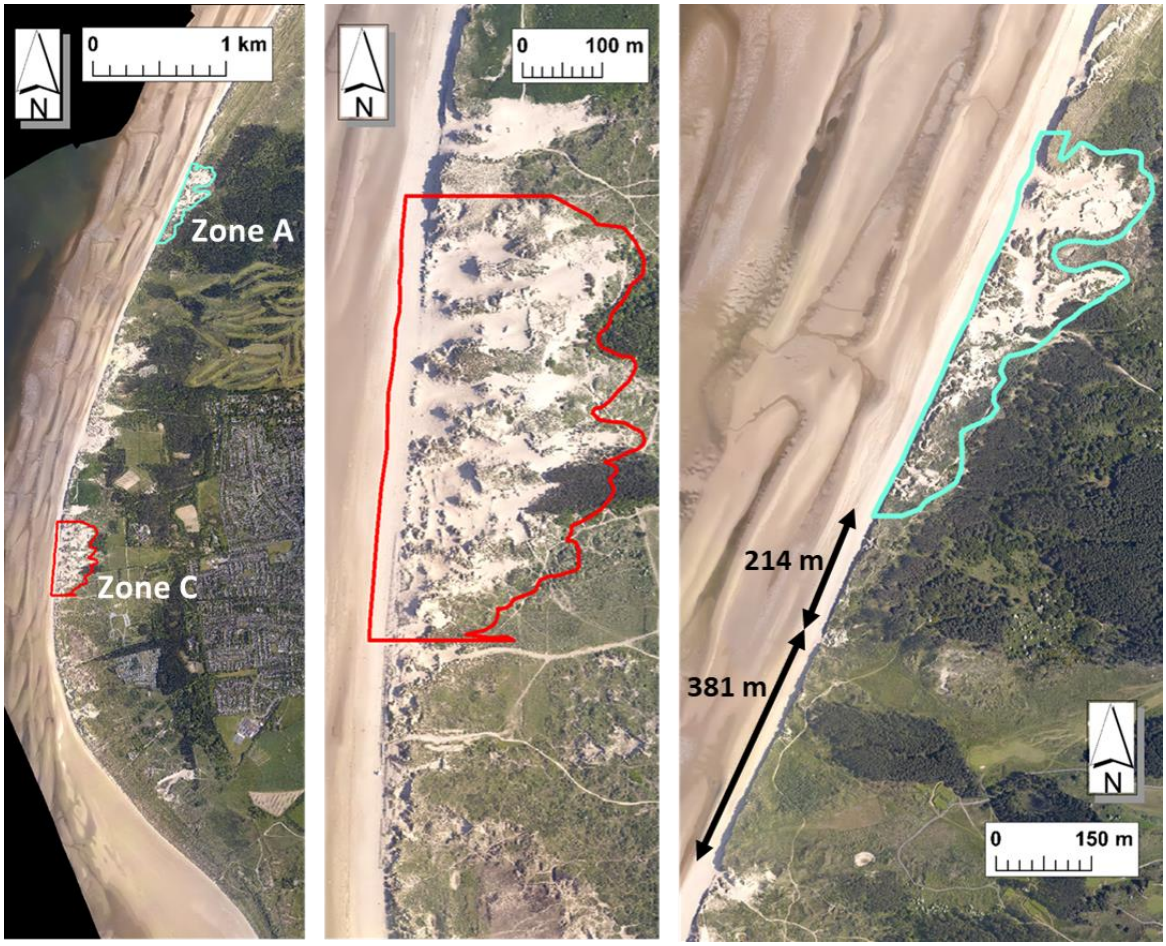

Figure 4.20: Longshore positions and zone A, foredune fetch distance (2012 aerial photo).

In the context of topographic setting, zone A could therefore be considered to have much greater potential for sediment supply from the adjacent foredune to the south. The orientation of this stretch of the coast in relation to the most frequently occurring, westerly and south-westerly winds, will also offer greater potential for more frequent deflection of airflow and transport vectors towards its blowouts. Whilst a number of important additional factors require analysis, not least the inter-tidal beach width at each location, the relative contribution of transport along the foredune offers one probable explanation for marked variability in the magnitude of each zone's respective rate of sediment gain.

The relative significance of these observations concerning foredune deflection is amplified by established knowledge regarding the behaviour of Sefton's littoral sediment cell. At the macro scale, (encompassing the full longshore and cross-shore boundaries), the Sefton coast, beach-dune system, is known to have a

positive budget. This is as a result of net, onshore directed sediment input from the offshore zone, seaward of the depth of closure (Pye and Blott, 2016). Despite this, within the central stretch of coastline experiencing retreat, although showing longshore variability, trends in the beach sediment budget, range between strongly negative, to showing only marginal losses (Saye, *et al.* 2005; Pye and Blott, 2016). These erosional trends in beach volume transition from negative to positive with increasing longshore distance, north of the northern limit of coastal retreat, and south of the southern limit (Pye and Blott, 2016). This spatial variability is attributed to a splitting of the littoral cell at the apex of the 'coastline scale', cuspate configuration. As a result of directional divergence around this point, (also quasi-central to the retreating sector), to the north, the net direction of longshore sediment transport is northwards, and to the south, southwards (Plater and Grenville, 2010; Pye and Blott, 2010). In consequence, the dominant direction of longshore sediment transfers for zone A is northbound, and for zone C, southbound. With this, the significant breach in the foredune immediately N of zone C, serves to 'cut off' the foredune transport pathway with the greatest potential, sediment supply. Conversely, for zone A, the dominant direction of longshore transport, also benefits from fetch enhancements associated with the uninterrupted foredune to its S. The influence of foredune continuity, and therefore also fetch distance, together with the dominant directions of longshore transport vectors, offer strong possibilities to resolve the differing rates of sediment gains between the two zones.

Finally on this point, additional to divergence in the direction of longshore transport, in scalar terms, there is considerable known disparity between the proportion of littoral sediment being directed northwards, with that directed towards the south. Pye and Blott (2016) approximate the northbound fraction of longshore

transport being limited to just one third, with the remainder being transferred in the opposite direction to the south. The distribution of skewness in this ratio is therefore contrary to the nature of the imbalance in rates of sediment budget gains for the northern zone A, and zone C to the south. There now exists a diversity of evidence which suggests, that through deflection, in all probability, foredune aligned, longshore transport is a primary pathway by which sediment is delivered to the throats of foredune blowouts. That the magnitudes of northbound and southbound directed longshore transport, oppose the rates of sediment gains in their destinations, is to some extent also supportive of the theory, that longshore variability in foredune characteristics may well be a critical factor in resolving the transport records of individual blowouts.

4.6.6 Insights and potential future applications for coastal dune managers

Through these findings, some important, initial and necessary steps have been made in understanding the mechanisms of foredune blowout transport, together with its implications for coastal evolution in relation to blowouts. Foredune sediment supply from the nearshore beach is a fundamental control on the evolution of coastal dune systems (Psuty, 1988; Sherman and Bauer, 1993). Discussions around the potential modelling or hindcasting of longshore variability in foredune configuration (or growth), are therefore typically dominated by the resolution of longshore variability foredune sediment supply (Hesp, 2002; Aagaard, *et al*. 2004; Houser, 2009; Delgado-Fernandez and Davidson-Arnott, 2011; Anthony, 2013; Wernette, *et al*. 2016; Strypsteen, *et al*. 2019). When conceptualised at large spatial scales, in the nearshore beach being the ‘sub-unit’ directly seaward of the foredune in the coastal profile, the transport vector of foredune sediment input becomes most strongly perceived as cross-shore directed. As blowout sediment supply appears to be dominated by longshore

directed transport vectors, this raises the importance of giving greater consideration to actual longshore variability in the foredunes adjacent to blowouts, as opposed, or in addition to, the potential causes of this variability.

In assessing the role of aeolian processes and specifically of foredune blowouts, on longer term coastal evolution, the contribution of longshore sediment transport, and therefore also longshore variability in foredune characteristics, has been seen to demand much greater consideration. Beyond this, models of coastal evolution would further benefit from more explicit inclusion of cross-shore sediment transfers to the secondary dune field. In Sefton, foredune sediment 'losses' via landward transfers to the secondary dune field were sizable. Whilst the sediment budget approach of Psuty (1988) is widely utilised, that the model focuses solely on sediment exchanges between the foredune and the nearshore beach, but gives little consideration to landward foredune losses to the secondary dune field is a limitation. This dependency hinders full resolution of coastal evolution at many sites, and gaining insights of the highest value is constrained to beach-dune systems which are relatively 'closed' in nature, with landward sediment losses therefore being negligible relative to the total budget (e.g.' Aagaard, *et al*. 2004; Anthony, 2013). The global trend of coastal dune field 'sealing' in association with biotic processes, will to some extent mitigate this limitation of the Psuty (1988) model, given the effects of vegetation on aeolian transport and dune field mobility (Kocurek and Lancaster, 1999; Hesp, 2013; Delgado-Fernandez, *et al*. 2019b). For coastlines which are characterised by high visitor pressure however, vegetation trampling, blowouts, parabolics, and aeolian sediment transport to secondary dunes can be significant (Pye, 1983, 1990; Hesp, 2002, Ruz, *et al*. 2005; Mir-Gual, *et al*. 2015; Delgado-Fernandez, *et al*. 2019b).

If focussed explicitly on longshore transport, when seeking to explain foredune blowout transport, the foredune orientation, and that of the blowout trough, relative to regional wind approach angle likely becomes a critical factor. These parameters are known to exert control on the frequency of longshore transport, and also the magnitude of any wind speed enhancements within the blowout interior (Gares and Nordstrom, 1995; Fraser, *et al*. 1998; Hesp, 2002; Bauer, *et al*. 2013; Smyth and Hesp, 2016). Temporal variability in the strength of correlations between incoming wind direction, with trough wind speeds, were explored in chapter 3. Although variability in near-surface incoming wind at the A3 reference anemometer was a clear expression of incident wind variability (section 2.5.2), the absence of a high frequency wind record was a major constraint of this study. Re-runs of the event scale experiment, throughout a range of wind approach angles, and for different blowout/foredune orientations therefore offers a number of opportunities. Peaks in the strength of correlations, between wind approach angle, with either or both of, trough wind speeds, and blowout transport intensities, would be particularly informative. Results could be used to identify optimal foredune/blowout orientations relative to the incident wind directions. With this, analysis of wind regimes at individual sites might reveal further new knowledge concerning the frequency or magnitude of airflow enhancements at specific blowouts, and about the associated transport response during singular events. If definitive wind directions, or even finite ranges of approach angle, could be enlightening in respect associated responses in sediment transport, progression towards the forecasting, or hindcasting of longer term geomorphic change might be conceivable.

In addition to advancing our understanding of evolution at beach-dune systems characterised by ‘naturally’ occurring foredune blowouts, this type of knowledge would directly inform the specifics of foredune ‘notching’ management

interventions. Presently, the longshore positioning of artificial ‘notches’ appears in the main, to be determined by identification of locations where potential ecological benefits are estimated to be greatest. As a caveat to this, as promotion of sediment transfers beyond frontal dunes is the primary objective, current guidance for coastal managers planning ‘dynamic restorations’, is to ensure there is a plentiful supply of sand on the beach/inter-tidal zone (UKCEH, *et al*. 2021). This implies decisions around sand supply are focussed on the cross-shore characteristics of longshore positions, with the potential high relevance of the foredune sediment pathway and longshore transport, a lesser consideration. On ‘notch’ orientation, the UKCEH, *et al*. (2021) does highlight oblique rather than shore normal notch orientations, proved more successful for projects in the Netherlands, but limiting guidance on this point to just one comment suggests much of the current knowledge around form-flow interactions has likely been underexploited.

Finally on specific ‘best practice’ recommendations for ‘notch cutting’, the assertion that ‘in most cases, bigger is better’ (UKCEH, 2021:54), and potentially ‘longer lasting’, deserves considerable qualification. In this investigation, the beach-dune interface of zone C was characterised by frequent, high magnitude throats, with relatively broad ‘troughs’. Although requiring a much wider evidence base, the relative ‘openness’ of this terrain may have been a contributing factor to the relatively lower rate of gain for the zone C sediment budget. The event scale analysis in this study identified wind speed enhancements, induced by topographic compression of airflow, to be a critical influence on transport intensity in the blowout interior (chapters 2 and 3). The magnitude of any such enhancements, are of course strongly governed by the degree to which airflow is compressed by surrounding blowout topography. Over time, the lateral expansion of blowout form, (through continued deflation), typically results in broader, lower gradient

geometries. Current knowledge on blowout evolution suggests such terrain is promotional of flow expansion, and as a consequence, reductions in wind speeds, increasing vegetation cover, and lower magnitude transport activity (Gares and Nordstrom, 1995). Therefore, contrary to the intended purpose, increasing the spatial scale of foredune notches may in fact inhibit levels of transport, and reduce notch/blowout longevity.

A second point worthy of discussion around the potential benefits of 'bigger' notch geometries, and equally, also their positioning, concerns possible negative impacts in longshore locations. The effects of sediment starvation that are associated with beach groyne installations, is now well documented (e.g., Brown, *et al*. 2011; Simm, *et al*. 2020). Given their intended purpose, increasing the spatial scale of foredune notches, may potentially introduce heightened disruption to longshore sediment transport regimes. At the planning stage of such interventions, there is likely some value in widening the scope of current decision making processes. Volumetric estimations of the desired beach sediment inputs to dune hinterlands, at individual longshore locations, is an obvious consideration which could inform notch design. In turn, improved understanding of the relationships between notch size and transport magnitude, would allow interventions to be more targeted. In addition to greater focus on at-a-point specifics, the effects of resultant sediment 'losses', to the wider system, could potentially be assessed using estimates of transport, on a 'notch' by 'notch' basis.

Lastly, on the influence of longshore transport to geomorphic change at foredune blowouts. The width of blowout throats, (and equally, artificial notches) will exert some control on longer term transport records. On foredune deflected airflow and saltation reaching blowout throats from upwind areas, flow expansion, and divergence of the flow-flux vectors, will promote the ejection of grains across the

throat, together with raised levels of sediment deposition. Dependent on throat width, (or alternatively distance to the downwind foredune, and therefore recommencement of topographic enhancements to flow-flux vectors), levels of longshore directed transport may recover to varying degrees. Bitton and Byrne (2002) identified a tendency for sediment deposition in the blowout throat area, and such occurrences may be strongly governed by throat width. Additionally, Gares and Nordstrom (1995) also eluded to the importance of this parameter, in their cyclical model of blowout evolution, as did Hesp (2002) with reference to incipient foredune development. Such occurrences would serve to limit landward directed airflow and sediment transport. Throat width, potential dune building, and/or sediment deposition in the throat locality, all likely influence whether blowout evolution is progressive or cyclical. Further investigation of the inter-dependencies of throat geometry, flow-flux divergence, and throat sedimentation, would permit improved estimations of blowout 'life expectancies', and therefore longer term volumes of transport.

4.6.7 Human perceptions of coastal erosion

To conclude on a less discussed theme. The implications of foredune blowouts over the longer term, to the evolution of dune fringed coastlines, and also coastal management more broadly, remains heavily influenced by human perception. Section 1.8.7 suggested that at Sefton, the contribution of aeolian activity, relative to that of marine processes, may be underestimated. In part and importantly, this may be as a potential consequence of the general visibility of each. High magnitude foredune erosion via wave scarping, typically occurs over short durations, and is also focussed at the beach-dune interface. Irrespective of the nature of any geomorphic change occurring in this 'narrow', cross-shore section, which stretches from the dune toe to the foredune crest, visually this is a

prominent and easily identified location of the coastal landscape. The cumulative effects of landward sediment transfers via aeolian transport however, are generally the result of lower magnitude, higher frequency events. Further, depositional areas landward of the beach-dune interface, in the main also have relatively large spatial extents. These characteristics were reflected in both zone A and zone B. Although both had positive sediment budgets, the average height of surface lowering in each zone was much greater than that that of surface raising (Tables 4.4 and 4.5). This facet is a direct function of erosion being spatially constrained within the seaward boundary of each zone, whilst deposition occurs across much broader areas of dune hinterland, landward of the foredune line, (and also over extended time frames). As a result, incremental surface raising is often imperceptible.

In this chapter, the DoDs for each zone (Figs. 4.12 and 4.16), allowed this characteristic of longer term evolution to be easily visualised. Further, the vast majority of geomorphic change occurring landward of the beach-dune interface, and within the secondary dune field, clearly relates specifically to aeolian activity. Despite this, aeolian sediment transport occurring in beach-dune environments remains most strongly associated with foredune growth, and embryo dune/sand ramp formation, (also at the beach-dune interface). The conceptual simplicity of DoDs permits improved awareness of aeolian processes, and promotes greater engagement with aeolian science. It is hoped, that over time, further dissemination of findings from similar studies, will adjust current perceptions around the nature and importance of aeolian processes at Sefton.

4.7 Conclusions

Decadal scale results demonstrated heightened geomorphic change to be associated with the location of foredune blowouts throughout the Sefton coast,

with the positions of foredune blowouts exclusively corresponding to greater amplitude topographic change, and also change which extended over greater spatial extents, particularly landwards. Findings also suggested that foredune blowouts were contributing to coastline retreat at the site. Detected geomorphic change demonstrated strong spatial coherence between seaward erosion and landward deposition at all blowout locations. Findings demonstrated that foredune blowouts at the site were contributing to coastline retreat both directly and indirectly. Directly, this was through the landward deposition of sediment derived from erosion of upwind areas of the blowout's host dune. Indirectly, positive sediment budgets for both of the zones investigated in detail, evidenced landward deposition to be surplus that of sediment derived from the 'in situ' foredune topography, demonstrating blowouts to also be effective transport corridors for additional sediment from the beach or foredunes adjacent to the blowouts themselves. In the absence of foredune blowouts facilitating this landward transfer, this additional sediment would ordinarily contribute to foredune recovery or increased beach elevations, in being repeatedly cycled between the two via natural beach-dune sediment exchanges.

The initiation and maintenance of blowouts at Sefton is strongly linked to visitor pressure. Numerous examples of evidence can be found for this in landscape morphology, and from daily visual observations during site visits. As blowouts are making significant contributions to coastal erosion and retreat at the site, human impact can also be considered as an important contributing factor to this erosion and retreat. Up to these findings being presented, the fundamental causes of coastal erosion and retreat have been solely attributed to marine processes, and a variety of marine conditions.

The characteristics of the foredunes were also found to likely exert important controls on transport levels within individual blowouts. In addition to the geometry of the blowout's host dune having a direct influence on landward deposition, longshore sediment transport across adjacent foredunes appears to play an important role. As such, the geometry and vegetative state of adjacent foredunes undoubtedly influence the sediment supply to individual blowouts.

Sediment delivery to blowouts via longshore sediment transport pathways was also found to be of importance in the findings of event scale investigations (in chapters 2 and 3). For making decisions on future management interventions related to controlling the landward transfer of sediment occurring at specific blowouts, both the amplitude and vegetation coverage of adjacent foredunes needs to be a specific consideration. Although further research is needed, the longshore length of the upwind foredune will therefore also be a controlling factor (in controlling 'fetch'), as will the prevailing wind directions in relation to the orientation of the frontal dune line, in that these facets will determine the frequency of longshore deflected airflow and transport.

The creation of 'artificial' foredune blowouts (or 'notches') is a management strategy currently employed to enhance the landward transfer of beach sediments, (when desirable to promote ecological benefits). The findings of this research may also inform project decisions regarding their optimal, longshore locations, particularly with reference to prevailing wind direction, foredune orientation, foredune characteristics, and the dominant direction of longshore sediment transport, at given positions within the littoral cell.

CHAPTER 5 – CONCLUSIONS

5.1. Introduction

Essentially, the aim of this research was to enhance understanding of aeolian sediment transport in beach-dune environments, and specifically, that associated with foredune blowout landforms. This was to encompass the nature of instantaneous transport in foredune blowout localities, and the implications of such transport events, in relation to longer term, coastal landscape evolution. The study is primarily positioned within the discourse of aeolian geomorphology. Irrespective of this 'sub-discipline', an overarching motivation behind all coastal science, is to improve our capacity to resolve geomorphic change. In this concern, a principle objective being, to arrive at a point where the evolution of coastal systems can be definitively modelled.

5.2. Thesis relevance and wider context.

A generic and fundamental requirement of doctorate studies, is to introduce new contributions to knowledge, of material value within their particular discipline. The knowledge gaps identified in this thesis, are in the main specific to foredune blowout landforms, and the research questions formulated to address them were defined with precision. In this way, the research conducted is highly specialised, and intrinsically 'niche', relative to the wider discourse it is positioned within. Beyond the incremental and 'niche' contributions this thesis makes academically, the findings directly progress a broader scientific objective, of much greater urgency.

As a result of climate change, for an extended period, there has been a continual rising of global mean sea level, and over recent decades this trend is recognised to be accelerating (Lindsey, 2021). Two primary impacts of this phenomena are

heightened levels of coastal erosion and flooding. As a consequence, increasingly, SLR is accepted to represent a credible threat to the existence of humankind. Further, the potential effects of these hazards are exacerbated due to the high relative concentrations of both human settlement, and resources, in coastal zones globally. It is estimated, that by the turn of the century, approximately half the Earth's population and assets, will be exposed to significant risk from flood waters (Kirezci, *et al*. 2020). Although specificity is a quality of this research, the findings offer small, gradual steps towards the resolution of coastal change more broadly. It is hoped, that the piecemeal contributions made here, and by similar studies, progress achieving competency in the accurate modelling of coastal geomorphology, to then permit improved capacity to manage and mitigate the risks associated with climate change.

5.3 The relevance of foredune blowouts

Blowouts are dune landforms associated with heightened levels of aeolian transport, and are recognised to be particularly efficient sediment transport pathways. Beach-dune sediment exchanges are considered to be a primary control on the form and behaviour of dune-fringed coastlines. As, foredune blowouts, landforms known for enhanced levels of sediment transport and geomorphic change, are additionally positioned at a critical point in the beach-dune cross-shore profile, and must therefore be of high importance to dune field evolution.

5.4. Thesis substance in the context of scale

Review of the existing body of literature concerning beach-dune systems, and prioritisation of the many knowledge gaps identified, dictated that the thesis be comprised of two substantial, but also semi-discrete component parts. The spatio-temporal scale of each element, is the definitive characteristic by which they can

be distinguished. Importantly, the concept of scale is an ever-present and essential facet of all geomorphological research. An elemental premise for the discipline, is that adjustments to the morphology of the Earth's surface, understood to be a process-response system (Walker, *et al*. 2017), are in simple terms, a product of the material composition of the landscape, together with the processes which act upon it (Huggett, 2017). Ordinarily, individual geomorphological studies are in the main confined within the limits of a well-defined, singular, spatio-temporal scale (Sherman, 1995; Bauer and Sherman, 1999; Walker, *et al*. 2017). In character, contemporary studies which examine coastal geomorphic processes, typically involve the instrumentation of field locations. The nature of such processes, and the logistical constraints of this approach, determine that field experiments have confined spatial extents, and must usually be executed over relatively short durations. Walker, *et al*. (2017) categorise these studies spatially as being 'plot' scale, and define the temporal scale as 'event'. In contrast, assessment of evolving coastal morphology is most often undertaken at the 'landscape' scale, and over extended time frames. Widely acknowledged discontinuities between spatio-temporal scales, dictate this common protocol. A number of seminal works within the discipline have however asserted a pressing need for much greater research attempting to tackle a diversity of scale related issues (Sherman, 1995; Bauer and Sherman, 1999; Walker, *et al*. 2017). That this thesis constitutes the amalgamation of material from two distinct spatio-temporal scales, addresses their demands, was in part a deliberate choice, and is an important particularity of the research. The relevance of scale is thus given due consideration throughout this concluding chapter.

5.5. Critical review of thesis responses to research questions

The three research chapters of the thesis (chapters 2, 3, and 4), together with the research questions, defined in section 1.7.2., provide a structural basis from which

conclusions are initially drawn. The research process and findings can be most easily categorised into three distinct classes; 1), event scale research, 2), meso-scale research, and 3), methodological research. Chapters 2 and 3, wholly positioned within the event scale, primarily addressed research question 1, and also made partial contributions towards research question 4. These two chapters were associated with an event scale field study, and concerned, instantaneous, sediment transport, and airflow dynamics, at a foredune blowout location. Section 5.4.1., considers event scale knowledge contributions, the validity of the research process, and how the findings relate to, and advance existing work.

5.5.1. Characterisation of event scale, foredune blowout sediment transport and airflow dynamics.

Research question 1

What are the characteristics of event scale, aeolian sediment transport, and airflow dynamics in foredune blowouts?

To address this question, event scale, instantaneous sediment transport and airflow dynamics, were measured in high frequency during a field study, at a foredune blowout location. In chapter 2, the data were then presented, described and analysed, to allow aeolian process dynamics to be characterised. The development of novel analytical techniques, described in chapter 3, allowed the initial interpretation of the event to be further expanded, and additionally, better supported. Although derived from the findings of both chapter 2 and 3, discussion here solely concerns the characteristics of event scale processes. Critical assessment of the analytical approaches developed in chapter 3, concern the second research question, and are covered in section 5.4.3. Here, in examining event scale dynamics, contributions to the fourth research question are also made;

Research question 4

Which environmental factors appear to be of primary importance to the frequency or magnitude of foredune blowout transport events?

Event scale contributions

Whilst our understanding of airflow dynamics in complex blowout topography is well advanced, knowledge of aeolian sediment transport is scarce, particularly with regard to foredune blowouts. Fundamentally, the changing morphological form of beach-dune systems, is an expression of sediment transport events. Therefore, understanding of sediment transport processes is critical. Although, research question 1 encompasses both airflow and transport dynamics, the knowledge gaps being targeted, specifically concern, instantaneous sediment transport, of which we know relatively little. As transport results from fluid forcing by airflow, advancing our understanding of event scale transport, necessitated also, the inclusion and examination of airflow dynamics during the event.

Both airflow and sediment transport patterns were complex in nature, and exhibited acute levels of spatio-temporal variability during the event. The instrument grid encompassed locations on the back-beach, the upwind foredune, and within the blowout interior. Throughout this grid, airflow patterns fully conformed to contemporary knowledge of form-flow interactions in complex beach-dune topography (e.g., Arens, *et al*. 1995; Walker, *et al*. 2006, 2009, 2017; Jackson, *et al*. 2011; Smyth, *et al*. 2012, 2013, 2014; Delgado-Fernandez, *et al*. 2018). Despite aeolian sediment transport being fundamentally a product of surface shear stress, (associated with wind speed), in coastal environments generally, and particularly so over complex terrain, aeolian transport typically shows poor association with wind speed (Baas and Sherman, 2006). Overall, at-a-

point transport exhibited this expected characteristic and was in agreement with current knowledge.

In the main, our existing understanding attributes this weak relationship of transport with wind speed, to sediment supply limiting conditions, and thus results in actual levels of transport typically being less than the transport capability of the airflow fluid forcing. In this study, divergence between the direction of airflow and transport vectors, together with at-a-point sediment input from the far field, were two major contributors to the poor wind speed *vs* transport relationships. Within the blowout trough, these factors produced an exceptional pattern of flow-flux dynamics, whereby the areas of strongest winds experienced the lowest levels of transport, and zones of weaker winds were associated with higher levels of transport. This inverse spatial relationship between at-a-point wind speed and transport within the trough, confirmed aeolian sediment transport in foredune blowouts cannot be modelled, and validated the approach of undertaking field measurements. It also questioned the value in the commonplace practice of identifying points, zones, or corridors of high potential sediment transport within blowouts, based solely on either measured or modelled airflow parameters (e.g., Smyth, et al. 2012, 2013; Hesp, *et al*. 2016). Further, that with this, there is a need for foredune blowout transport to be extensively measured, if progress is to be made in understanding it.

Despite this confounding characteristic of transport in individual point locations, the relative importance of wind speed, and of other potential factors contributing to transport activity requires to be considered in the context of scale. Blowout geometry is recognised to often induce topographic modifications to airflow, and in particular those which enhance incident winds (Hesp, 2002). Smyth, *et al*. (2013) postulated that incident wind direction rather than wind speed, governed the

nature of turbulent flow structures in blowout topography. The findings of this study supported their theory. In this research, a change in incident wind direction resulted in all locations within the blowout trough experiencing flow enhancements, via the topographic compression of airflow. Overall, this resulted in a general increase in trough wind speeds and flow steadiness, together with suppression of flow turbulence, and irrespective of the weak at-a-point flow-flux relationships, had the effect of giving relative increases to sediment transport intensity throughout the blowout interior. Topographic enhancements to airflow are thus a principle factor in determining foredune blowout transport, and the nature of the topographic modifications which occur are controlled by incident wind direction. That ultimately, wind direction is a dominant factor in regulating transport, in addition to airflow dynamics, advances existing knowledge of aeolian processes in foredune blowouts.

A route towards fully understanding foredune blowout sediment transport, is to identify the dominant controls on the transport system, in order that they can be isolated, and better parameterised in future experiments. Statistical analysis identified that the primary controls on sediment transport can differ between sensor locations, even across only short distances of just metres, and further, that the dominant controls at individual point locations can show temporal variability over short durations. This questions the logic of attempting to forecast transport over extended time frames, using deterministic models which are based on constant proportional relationships between wind speed, shear stress, and saltation.

Across the instrument grid as a whole, the complexity of topography was seen to exert significant control over transport dynamics. This confounds the establishing of correlations between instantaneous saltation and wind speed. The abruptly

changing topography was a root cause of divergence between the direction of airflow and transport vectors, no more so than at the juncture of the upwind foredune and the blowout throat. This divergence resulted in the A7 sensor location recording transport far above the capability of at-a-point airflow (via sediment input from the far field), whilst locations A9 and A12 experienced transport much below wind speed capabilities (as grains following ballistic trajectories had been 'ejected' from airflow upwind of these locations, on airflow streamlines being steered landwards). Although Hesp and Hyde (1996) alluded to the potential of flow-flux divergence, and a 're-setting of fetch' at the blowout throat, this was a theorised interpretation, and actual transport was not measured. Whilst the influence of topography on aeolian sediment transport is well documented (e.g., Baas and Sherman, 2006), in this study there was a pronounced increasing gradient in the control exerted by surface form and topographic setting, moving landwards over the cross-shore profile. The location where the effects of surface form were minimal, occurred at the most seaward location on the back-beach, (with the lowest topographic complexity), and where transport intensity was therefore best associated with wind speeds. Meanwhile, topographic complexity induced flow-flux divergence at the beach-dune interface, to then result in A9 and A12 transport being least associated with wind speed (two of the most landward positions). Finally of relevance to transport *vs* wind speed relationships; as a consequence of flow compression within the blowout trough, increasing trough wind speeds and reducing proportions of far field input to at-a-point transport signals, the transport-wind speed correlations were seen to strengthen, this agreeing with previous assertions from Davidson-Arnott, *et al*. (2012).

Beyond characterising foredune blowout transport, research question 4 sought identification of environmental factors of importance to the frequency or magnitude of events. The chaotic nature of flow-flux dynamics across the instrument grid, and spatial and temporal variability in the factors of greatest importance to sediment transport, constrains comprehensively characterising foredune blowout transport. In this study however, throughout measurement, sediment transport along the upwind foredune was orders of magnitude greater than all other grid locations, and was constant for the full 84 minute duration. Identifying longshore transport across the foredune as the primary sediment transport pathway, which dominated sediment delivery to the blowout was an important finding. That Pye and Neal (1994) had observed the frequent occurrence of sediment being driven along frontal dunes, prior to being directed landwards at foredune blowouts was a partial motivation for the study. Conceptual frameworks for foredune evolution based around the Psuty model (1988), are however focussed on sediment transfers to foredune blowouts being cross-shore directed, and cross-shore transport is also strongly implied to be dominant for beach-dune sediment exchanges in recent management guidance on foredune notching (section 4.6.6.). Walker, *et al*. (2017) did however promote the inclusion of longshore deflected airflow and transport in beach-dune evolutionary models, and this finding supports their suggestions.

As well as longshore foredune transport playing the lead role in delivering sediment to the blowout, airflow-foredune interactions, and the resultant increase in foredune attached/deflected flow, was identified as critical to transport dynamics during measurement. With this, insights were gained from existing knowledge into important foredune characteristics which are likely to make significant contributions to foredune blowout transport dynamics during individual events. The elevation, steepness, general geometry of the foredune, its continuity (or ‘fetch’ length), and its orientation relative to incident winds, will all therefore be of high

potential influence to event scale blowout transport dynamics, and to the frequency/magnitude of foredune deflection itself (Arens, 1996; Fraser, *et al*. 1998; Walker, *et al*. 2006, 2009, 2017; Bauer, *et al*. 2012, 2013; Davidson-Arnott, *et al*. 2012; Smyth and Hesp, 2016). The size of the foredune, together with the coverage and composition of vegetation will further influence the levels of sediment delivered to blowouts via this pathway at the event scale (Walker, *et al*. 2006; Miot da Silva and Hesp, 2010; Davidson-Arnott, *et al*. 2012; Hesp, *et al*. 2017).

5.5.2. The influence of foredune blowout transport events on meso-scale coastal evolution.

Assessment of the influence of foredune blowouts on meso-scale evolution primarily involved analysis of LiDAR time-series. Through this, in addition to addressing research question 3, further contributions were also made to the fourth research question.

Research question 3

What influence do foredune blowout transport events have on the medium to longer term evolution of coastal dune systems?

Meso-scale contributions

A ubiquitous descriptor of blowouts is that they are landforms which experience heightened relative levels of aeolian sediment transport, and therefore also geomorphic change (e.g., Carter, et al. 1990; Hesp, 2002; Smyth, et al. 2013, 2014). Two common blowout attributes in particular promote this characteristic. Firstly, that their internal surface is typically more susceptible to erosion due to a relative sparsity of vegetation cover, and secondly, that their topographic form has a propensity to induce airflow enhancements which promote aeolian sediment transport (Gares and Nordstrom, 1995; Hesp and Hyde, 1996; Hesp, 2002; Smyth,

et al. 2013). This study strongly supported these assertions for foredune blowouts. Findings demonstrated that across a > 4 km longshore stretch of coastline, foredune blowouts were found to be locations of considerably higher magnitude geomorphic change, and that this heightened change also extended over much greater spatial extents, particularly landwards.

In addition to enhanced deflation of *in situ* sediment, blowouts are frequently also associated with the throughput of sediment, beyond that which is eroded from their host dune. Implicit to this, additional terminology used to describe them are often along the lines of ‘efficient transport corridors’ or ‘effective sediment transport pathways’ (e.g., Gares, 1992; Hesp, 2002; Smyth and Hesp, 2016; Delgado-Fernandez, *et al*. 2018). Such descriptions are largely anecdotal and based on perception, as quantification of blowout sediment budgets is rare. This characteristic is especially relevant to foredune blowouts as they are fronted by beaches, which represent a significant supplemental source of sediment. Both zones examined in chapter 4 were found to have positive dune sediment budgets. This study therefore advances current knowledge with empirical evidence to confirm foredune blowouts are corridors specifically for the throughput of sediment, by quantifying net dune sediment gains volumetrically.

Current understanding of evolutionary trends specifically at Sefton dunes, attribute erosion and shoreline recession, exclusively to a diverse range of marine conditions, with aeolian processes seldom being considered. Pye and Neal (1994) assessed aeolian transport as not fundamental to recession, but of potential importance in enhancing an established trend. The findings of this thesis, and the conceptual framework which underpins it, in part contest this assertion. Sediment transport via foredune blowouts was found to be the primary mechanism by which beach sediment was transferred landwards. The significant volumes of sediment

transferred to the landward dune field demonstrated foredune blowout processes were a direct cause of retreat. It also needs to be qualified here that the findings of the thesis are in agreement with the suggestion that aeolian processes do additionally enhance the long term trend of retreat, but that the mechanisms by which this occurs must also be considered as fundamental. In erosion being wholly attributed to wave scarping and/or continual submergence of the dune toe, as dune sediment budgets were positive, relative decreases in beach elevations will have increased both the frequency and magnitude of these events.

A criticism of conceptual models which adopt a sediment budget approach to resolve beach-dune evolution, is that they do not adequately account for sediment 'leakage', whether this be to the offshore zone, or to the secondary dune field (e.g., Sherman, 1995; Bauer and Sherman, 1999). The positive net gains for both zones in this study support these criticisms, and in quantifying landward transfers to be sizeable, demonstrate a key limitation of the Psuty model (1988), which in the main disregards net sediment losses to the secondary dune field. The thesis therefore highlights opportunities to further improve models which base coastal evolution solely on sediment exchanges between the nearshore beach and the foredune. No more so than for systems which are characterised by foredune blowouts and/or parabolic dunes.

Meso-scale analysis of geomorphic change identified significant longshore variability. In longshore positions where foredune blowouts were present, medium-high magnitude change was observed to have larger spatial areas, and often to extend hundreds of metres inland. In the absence of foredune blowouts however, for geomorphic change of similar magnitude, the cross-shore extent was typically limited to just tens of metres. A fundamental feature of models which explain coastal evolution specifically in relation to sea level, is that beach-dune systems

respond to SLR through vertical and landward migration of the dune toe. The most prominent and enduring model of this type was developed by Bruun (1962) and associates dune toe migration with proportional sediment losses to the offshore zone. Although including the same dune toe response as Bruun, the alternative model of Davidson-Arnott (2005), determines recession will occur in coincidence with sediment conservation by the beach-dune system, and maintenance of the cross-shore profile during retreat. As foredune blowouts have been identified as facilitating landward transfers even surplus to foredune losses via wave scarping, these findings are supportive of the 'RD-A' theoretical model of Davidson-Arnott (2005). In recognising that foredune blowouts can be a direct cause of coastline retreat, whilst also allowing sediment to be conserved, greater consideration needs to be given to 'coastal squeeze' and accommodation space, for beach-dune systems characterised by frontal dunes fragmented by blowouts.

At Sefton, the thesis provides examples which demonstrated visitor pressure to be strongly associated with foredune blowout initiation, evolution, and maintenance (section 4.6.4). This association has been acknowledged further in a number of previous studies at the site (e.g., Pye and Neal, 1994; Delgado-Fernandez, *et al*. 2019ab). Through identifying aeolian transport via foredune blowouts to be a primary and direct mechanism of shoreline recession, human impact can be explicitly linked to coastal erosion and retreat. This is an important new contribution of the thesis, and it is believed by the author, one of significant public interest. Whilst the ecological benefits of dynamic restoration are well reasoned, and supported by scientific evidence, the potential implications of creating foredune 'notches', (essentially artificial foredune blowouts), demands much greater consideration and discussion.

Over the meso-scale, foredune blowouts were found to result in accelerated and higher magnitude geomorphic change. This change was consistently expressed through a spatial coherence between surface lowering (erosion) in their seaward areas, together with surface raising (deposition) towards their landward extents. This pattern of the landward (and downwind) deposition, of sediment eroded from upwind (seaward) locations, wholly conforms to accepted knowledge on blowout evolution (e.g., Carter, *et al*. 1990; Gares and Nordstrom, 1995; Hesp, 2002), and demonstrates their direct involvement in the landward transfer of beach and foredune sediment. Throughout the coast, a clear proportional relationship was visible at individual foredune blowouts, between the combined spatial extent and magnitude of positive elevation changes in depositional areas of the secondary dune field, with the volumes of sediment removed from their seaward zone of erosion. Additionally, in the 'band' through which the foredune had retreated, a marked longshore variability was exhibited in the magnitude of negative elevation change associated with shoreline recession. This was recognised to be an obvious expression of antecedent foredune topography, in the knowledge that the host dune configuration of a blowout exerts a fundamental control on absolute geomorphic change (Carter, *et al*. 1999; Hesp, 2002). It was therefore apparent that the configuration of the foredunes immediately adjacent to blowout throats had exerted significant control on overall meso-scale geomorphic change at individual blowouts. Comprehensive explanation of geomorphic change is therefore in part dependent on resolution of longshore variability in foredune configuration, a topic which continues to attract considerable interest (e.g., Davidson-Arnott and Law, 1990; Aagaard, *et al*. 2004; Houser, 2009; Delgado-Fernandez and Davidson-Arnott, 2009, 2011; Anthony, 2013).

As is customary, absolute, meso-scale geomorphic change was expressed in this thesis using DoDs. These visual representations of change have both a start point

together with an end point, and the geomorphic change exhibited in the DoD, describes the cumulative outcome of all geomorphic transport events having occurred over the time-series duration. This will encompass a great diversity of events in terms of magnitude, duration, and transport direction. These findings confirmed that foredune blowouts both accelerate and enhance the morphological evolution of coastal dune fields over the meso-scale. The influence of foredune blowout transport events on the meso-scale evolution of the system will therefore be partially governed by their longshore frequency. Longshore variability in foredune configuration has been identified as a further influence on the nature and extent of longer term geomorphic change. The maximum potential magnitude of geomorphic change associated with foredune blowouts will therefore depend not just on their longshore frequency, and the foredune geometry, but also on the degree to which individual blowouts occur in coincidence with longshore positions of higher magnitude foredunes. Whilst this suggestion is based on a spatial coherence between landform location, (i.e., the blowout) and sediment availability (i.e., foredune geometry), parallels can be drawn with Houser's (2009) theories on synchronicity. He determined that ultimately, sediment supply to foredunes depended not on the cumulative transport capability of the wind regime, (based on the frequency, magnitude, direction, and duration of all wind events), but on the degree to which they occurred in synchronicity with sediment availability on the back-beach.

Although the positive dune sediment budgets for the two zones examined were comparable in size, zone A's net surplus was gained at approximately double the rate. The cross-shore transfer of sediment directly from the beach into a foredune blowout is fundamentally limited by the blowout's throat width, and also incrementally reduced further, by the degree to which event scale incident winds

are oblique. In a multi-modal wind regime such as Sefton's, ultimately this limits both the frequency and the magnitude of direct beach-dune transfers. Both existing discourse (section 4.6.5), and the data analysis herein, highlighted the importance of foredune deflected airflow and sediment transport. A number of plausible, foredune related factors were theorised to have contributed to the marked divergence in rates of surplus sediment transport between the two zones. These included the continuity (or alternatively, 'fetch' distance) of foredunes adjacent to individual blowouts, foredune orientation relative to prevailing winds, foredune configuration, its vegetative state, and longshore position relative to the dominant direction of longshore littoral cell transport. The conflated impact of these factors was of seen to have exerted some level of control over the influence that each foredune blowout system (zone A and zone B), had on meso-scale evolution. Importantly, that their relevance is expressed in longer term evolution, strongly suggests they must equally have been of importance during the individual events from which meso-scale change is derived, and therefore their identification also makes further contributions in response to research question 4.

5.5.3. Methodological advancement in the resolution of aeolian sediment transport events.

Whilst the outcomes of the research steps detailed in chapter 3 greatly enhanced interpretation of field data, and characterisation of event scale dynamics, it is the development and effectiveness of the approaches adopted which address the second research question.

Research question 2

Can improvements be made in respect of traditional analytical approaches for event scale, aeolian sediment transport data?

Methodological contributions

Although aeolian geomorphology is now a thriving, advanced, and respected division within the geo-sciences on a ‘stand-alone’ basis, it is not far into the distant past that it was perceived as a marginal curiosity, alongside more established disciples (Bauer, 2009). Technological advancements, particularly in field instrumentation and remote sensing techniques, have facilitated rapid progress over recent decades, but a diversity of methodological and logistical issues mean aeolian science remains far less developed relative to other sub-disciplines, (e.g., fluvial geomorphology). Many of these constraints revolve around; 1) an inability to measure surface shear stress, 2) a dependency on the use of wind speed as a proxy for shear stress, 3) differences between the heights at which airflow and saltation are measured, and 4) the implications of the marked disparity between the fluid density of water and air relative to sand (Baas and Sherman, 2005, 2006; Bauer, 2009; Bauer, *et al*. 2013; Walker, *et al*. 2017).

At a planetary scale, coastal science exists geographically at the interface of the marine, terrestrial, biological and atmospheric earth systems. With this, the number and diversity of processes in play bring great complexity to morphological systems, together with many logistical challenges (Davidson-Arnott, *et al*. 2019). To overcome the acute spatio-temporal variability of airflow and aeolian sediment transport dynamics in coastal environments, over the past few decades, there has been a growing trend of increasingly dense instrument arrays being deployed for field studies in beach-dune settings (e.g., Baas, 2003; Bauer, *et al*. 2012; Smyth, *et al*. 2014; Delgado-Fernandez, *et al*. 2018). In the expectation of complex airflow and transport dynamics, the experiment for this field study was designed in this fashion. Initial inspection and interrogation of the data collected, revealed extraordinary levels of complexity and seemingly chaotic flow-flux patterns. Despite there now being an advanced appreciation of the many environmental

factors which exert control over sediment transport, ultimately validation of any interpretations formed are customarily related back to wind speed, the elemental component of all sediment flux models (e.g., Bagnold, 1941; Kawamura, 1951; Zingg, 1953; Owen, 1964; Belly, 1964; Hsu, 1971; Lettau and Lettau, 1977; Hotta, *et al*. 1984). To offer just a singular example which confounded early resolution of the event; sensors were clustered spatially into locations which recorded high wind speeds but negligible transport, and those experiencing weaker winds but relatively higher magnitude transport.

A speculative, trial and error approach to data interrogation was adopted, on having exhausted conventional analysis methods, whilst failing to adequately resolve event dynamics. The original contributions to knowledge in respect of research question 2 come from the successful application of novel analytical steps for the treatment and interpretation of aeolian process data. The three practical but innovative elements of the research methods followed (see chapter 3), which differentiate this work from traditional studies are defined here;

1) The use of transport data itself to compartmentalise the time-series.
2) The use of a cumulative derivative of instantaneous transport, to identify and delimit the discrete, shorter duration transport regimes, present within the overall time-series.
3) Undertaking bivariate statistical analysis of all at-a-point variables, both between each other, and then also with all of the variables measured, at each other sensor locations within the grid.

On appearance, all of these analytical steps are somewhat unremarkable in nature, and individually no one contribution could be considered especially ground-breaking. For this study however, their consecutive application was hugely

beneficial to data analysis and interpretation. In the absence of these steps, several important event characteristics would have gone unnoticed, some of the initial theories which did eventually transpire to be correct would have been either partially based on conjecture, or less well evidenced, and a number of incorrect insights which were expressed in the outputs of conventional analytical techniques would have wrongly formed part of the thesis findings.

Both the topographic setting, and the character of event scale dynamics for this study, necessitated development of a bespoke research process. With this, the eventual value gained was maximised. For application in future field studies, it is likely that the potential benefits of this methodology will be positively correlated with increasing topographic and/or general surface complexity. Irrespective of potential beneficial outcomes, (which will be study specific), the conceptual framework which underpins the steps taken, offer insights to at least inform 'best practice'. Despite being particularly primitive and axiomatic in nature, it is the opinion of the author that the third analytical step represents a glaring opportunity for scientific progression, if adopted more broadly within the discipline. All three methodological contributions are unconventional, especially so for the first two which were developed experimentally. As such, they are not strongly associated with any specific thread of existing literature. Contemporary, commonplace practice is therefore also used to provide context.

Use of transport data to compartmentalise the time-series

In character, instantaneous sediment transport exhibits high spatio-temporal variability. This is in consequence to comparable variability in the multitude of environmental factors which exert control on transport. Of all the potential factors contributing to aeolian transport, wind speed and wind direction are viewed to be of greatest importance (Sherman, 1995). Routinely, longer duration aeolian

process time-series data are sub-divided into shorter duration ‘runs’ for in depth analysis. Typically, the timing and duration of such ‘runs’ are determined by researchers in an arbitrary and subjective way, with reference to incident wind speed or direction (e.g., Jackson, *et al*. 2011; Delgado-Fernandez, *et al*. 2018; Garcia-Romero, *et al*. 2019). To use wind direction as an example, ‘runs’ which comprise periods of time for which incident winds differ (e.g., onshore, oblique-onshore, or offshore) are useful to examine. Through this, insights can be gained about relationships between incident wind direction, and airflow or transport dynamics across an instrument grid. To build on this methodological framework, it might be further desirable that the ‘runs’ only comprise periods of time for which incident wind speeds were quasi-steady, and of comparable magnitude. Through this, the influence of wind direction on aeolian dynamics can be better isolated, as the potential influence of wind speed on the resultant dynamics is reduced. Equally, ‘runs’ of steady wind directions and differing speeds offer better opportunities to understand the impacts of wind speed.

Inherent within these choices is an assumption of either of these two factors being the principle control on transport, something that we know is often not the case (section 1.3.3). The findings of this study for instance found that the transport signal of A7 was often best associated with either airflow turbulence or sediment transport from an upwind location (via far field sediment input). In statistical terminology, the assumption also implies transport to be a dependent variable, and either wind direction or wind speed to be the principle independent variable. If understanding sediment transport is the overarching objective of a study, it is argued here that the timing of any sub-divisions made to the time-series, should be based on sediment transport itself. In doing so this analytical step removes an unnecessary and potentially incorrect assumption. With this, any issues associated with temporal variability in the primary controls on transport, and also

any lag times that might exist between wind forcing and sediment transport response.

Use of a cumulative derivative of transport intensity, to identify and delimit discrete sections of a time-series.

To the knowledge of the author this method has not been used in aeolian science previously. The only example of a cumulative derivative of any kind being used in data analysis which could be found, came from Baas, *et al*. (2020). In their study however, the cumulative derivative was of wind speeds above threshold velocity, which was shown to be better associated to sediment transport, than 1 minute averaged wind speed records. The use of cumulative transport intensity in this study, to delimit characteristically distinct transport regimes, proved to be a successful and objective method. It further removes research subjectivity from the analytical process.

Bivariate statistical analysis of all at-a-point variables; between each other, and also with all variables measured, at all instrument grid locations.

Common practice for field studies which examine both instantaneous airflow and sediment transport, is to perform regression analysis between at-a-point sediment transport, and at-a-point airflow parameters (such as wind speed, direction, steadiness, or turbulence). This can be to improve our understanding of which airflow parameters are best associated with transport (e.g., Smyth, *et al*. 2014), or to test the performance of deterministic transport models, and typically make interpretations of why actual transport differs from model predictions (e.g., Sherman, *et al*. 1996, 2011, 2013). In beach-dune environments, especially those which encompass foredunes and/or blowouts, at-a-point wind speed and direction are often also compared with synchronous incident wind records. This allows differences between incident winds, and airflow at sensor locations to be resolved

with reference to their surrounding topography and fluid dynamics theory (e.g., Smyth, *et al*. 2012, 2013, 2014; Delgado-Fernandez, *et al*. 2018). For studies which encompass spatial grids of instruments, by limiting statistical testing of relationships to these two themes, it means that much of the data collected is being routinely under-exploited.

It was found in this research that these conventional methods could not adequately explain event scale sediment transport. The analytical process followed in this thesis was therefore forced, but also directly responded to a paper from Bauer, *et al*. (2013) concerning coherent flow structures. Having identified that progress within the discipline was being constrained by traditional methodological practice, they called for novel techniques to be developed which would allow more 'nuanced' interpretations of event scale dynamics to be gained. In particular, Bauer, *et al*. (2013) identified that our now advanced appreciation of landform scale, turbulent airflow structures, and of flow typologies generated by complex dune topographies, offered the greatest potential for progress. Specifically, they also demanded that at-a-point transport needed to be treated more closely as a vector rather than scalar property, and with this much greater understanding could be gleaned in respect of sediment transport pathways.

The statistical analysis undertaken allowed directional divergence between airflow and transport vectors to be identified with reference to topographic modifications to airflow, and demonstrated that at times, instantaneous airflow or transport can be better explained in association with processes at other grid locations, than by the time-series of any at-a-point airflow or transport parameter. Temporal variability in the nature and strength of relationships between transport and at-a-point airflow properties, and that at-a-point transport was sometimes best associated with transport at another grid location, proved critical to analysis. These insights could

not have been recognised without this new analytical approach. At present, the capabilities of sensors do not yet allow aeolian sediment transport to be truly measured as a vector property, but establishing links in transport activity between different grid locations moved a step closer to doing so. Further, the improved awareness of sediment transport vector directions, allowed variability in the strength of at-a-point wind speed and transport relationships to be resolved in association with temporal variability of the proportion of a transport signal which was made up by far field sediment input.

Although termed ‘novel’, this analytical approach is grounded in practicality. By simply ensuring all available data is fully exploited, it allows for more ‘nuanced’ insights to be gained. With this, it provides opportunities to revisit historic datasets, to either validate, or to further improve previous interpretations. It is suggested here that this methodological step be routinely applied for future field studies which use spatial grids of instruments in complex topography.

5.6. Relevance of scale to knowledge contributions, thesis limitations, and thoughts on future research

Despite the heavily documented scale discontinuities within the discipline, several review papers have stressed the need for a greater number of studies which encompass work at differing spatio-temporal scales (Sherman and Bauer, 1993; Sherman, 1995; Bauer and Sherman, 1999; Walker, *et al*. 2017). Although the thesis containing two major components of differing spatio-temporal scales was initially driven by prioritising gaps in knowledge, it must also be stated doing so directly addresses this requirement. In terms of connections between the two temporal scales of the thesis, it needs to be acknowledged that there are many constraints on the degree to which the event scale and meso-scale finding can be directly linked.

Morphological change and behaviour of beach-dune systems is strongly governed by cross-shore transfers of materials and energy (Short and Hesp, 1982; Psuty, 1988). Sherman and Bauer (1993) identified that the forcing of sediment transport is associated with individual waves and gusts of wind, with these occurring over time-frames of just seconds or minutes. It is also acknowledged that at any given moment in time and/or space, the potential factors contributing to transport, and their relative weight, exhibit high variability (Baas and Sherman, 2006; Walker, *et al*. 2017). As a consequence, the findings of event scale sediment transport studies cannot be up-scaled in a linear way (Sherman, 1995; Houser, 2009; Delgado-Fernandez and Davidson-Arnott, 2009, 2011). Even if it were possible, the nature and effectiveness of geomorphic processes are strongly controlled by system topography, and this is an important variable for which we cannot assume constancy (Sherman, 1995; Sherman and Bauer, 1993). These assertions were borne out in this study by the high spatio-temporal variability in transport activity over just 84 minutes, and even more so by the acute temporal variability in the factors of most influence to transport, at individual point locations.

With these limitations being wholly accepted as unavoidable, adopting a synoptic approach has been identified as a method by which they can be mitigated to some extent, and scale related discontinuities be partially bridged (Sherman, 1995; Sherman and Bauer, 1999). In terms of event scale work, this demands establishing a process climatology (Sherman, 1995; Sherman and Bauer, 1999), and enhanced specification of the dominant controls on sediment transport over short durations. Even in doing so, it remains the case that it is impossible to measure all potential environmental controls during field studies (Sherman, 1995; Bauer and Sherman, 1999). Beach moisture and a more comprehensive assessment of transport across the inter-tidal beach are two examples of data which would have been of particular benefit to the field study of this thesis. The

reality is that there are a diversity of further data which would have given additional insights, but limitations of this nature are applicable to all such work at the ‘plot’ scale and simply have to be accepted; and equally, although field studies represent just a vignette, financial and logistical constraints prohibit attempts to instrument beach-dune field sites over extended time frames (Walker, *et al*. 2017).

An interesting insight from the field study was that scale discontinuities can be seen to exist even across confined spatial scales, and over short durations. Whilst wind speed on the beach showed reasonable statistical association with instantaneous transport throughout the event, wind direction together with resultant airflow modifications, demonstrated significant control over transport within the blowout, only tens of metres landwards. Further, that the airflow properties which dominated sediment transport intensity at specific point locations across the grid, were seen to also exhibit marked temporal variability during the 84 minutes of measurement. This feature of event scale dynamics in itself is a characteristic which conforms to current understanding of longer term blowout evolution, and could also be seen in findings of the meso-scale study. Over the period of measurement, two characteristically distinct transport ‘regimes’ were identified, and even within each of these periods, marked variability in transport was observed. Smyth, *et al*. (2020a) demonstrated that geomorphic change over the meso-scale is the product of a multitude of episodic transport events that are also highly diverse in magnitude. The sporadic nature of at-a-point transport activity and intensity during this short study is well aligned with this suggestion. Further, such patterns must result in specific locations across a site alternating between being points of erosion or deposition, with this occurring independently of any longer term tendency. Irrespective of the longer term trends of geomorphic change which could be seen in the DoDs (chapter 4, figures, 4.12 and 4.16), CV of elevation demonstrated foredune blowouts to have higher frequency variability

occurring within the trend over their fixed temporal limits, and their ‘end state’ condition.

Beyond identification of the environmental controls which are most prevalent during short duration events, the partial bridging of scale discontinuities rely on the synthesis of information from differing spatio-temporal scales (Sherman, 1995). Although few in number, the potential to do so is a particular advantage of research which tackles the issue through inclusion of scale distinctive components (Walker, *et al*. 2017). They assert that spatially confined, event scale studies, promote consideration of the longer term implications to landscape scale evolution, and further, that through landscape scale characterisation of beach-dune systems, insights are gained concerning how large scale system attributes, must exert influence on event scale processes. If such synergy can be achieved, the total benefits of the research project can then become greater than the sum of its component parts.

A number of specific commonalities in the findings from the two scale distinct elements of the thesis demonstrate this valuable feature. At the event scale, foredune deflected airflow and longshore foredune transport, were the primary mechanism by which sediment was delivered to the blowout. Further, in respect of airflow, foredune deflection was recognised to induce airflow modifications within the blowout trough, giving marked enhancement of *in situ* deflation. With this, a number of foredune related attributes were acknowledged as undoubtedly exerting significant control over event scale dynamics. Supported by existing knowledge, specifically these included foredune volume, amplitude, longshore continuity, vegetative state, orientation relative to incident wind approach angle, and the degree to which foredune configuration promoted airflow enhancements (Arens, *et al*. 1995; Walker, *et al*. 2006, 2009, 2017; Miot da Silva and Hesp, 2010; Jackson,

et al. 2011; Bauer, *et al*. 2012, 2013; Davidson-Arnott, *et al*. 2012). At the meso-scale, all these characteristics were also seen to exert control over longer term geomorphic change at the landscape scale, and on volumetric levels of landward sediment transfers at individual blowouts. Despite being factors which were prevalent to event scale dynamics, meso-scale evolution ultimately reflects the frequency, magnitude, and sequencing of transport events over any given period of time (Sherman, 1995; Walker, *et al*. 2017). Whilst a constraint of short duration field studies is that, in essence they provide only a snapshot of event characteristics, as these same characteristics were expressed over the longer term, it demonstrates a tendency for them to be of particularly high relative influence, and/or also for this to be the case relatively more often than not. Despite an inability for links to be made in a direct and linear way, the nature of these insights, and of the findings from the thesis in themselves, illustrate the existence of bridges between spatio-temporal scales, together with the relative importance of foredune blowouts on dune fringed coastlines (i.e., short duration, landform scale transport events can be seen to have considerable implications to longer term, landscape scale evolution, and large scale system morphology can further be recognised to influence event scale dynamics).

To understand meso-scale morphological change in beach-dune systems, researchers typically adopt a sediment budget approach, with this being further improved through assessment of dune form chronologies (Sherman and Bauer, 1993; Sherman, 1995). The foredune evolution model of Psuty (1988) model has, and continues to be, most widely applied (e.g., Aagaard, *et al*. 2004; Delgado-Fernandez and Davidson-Arnott, 2011; Anthony, 2013; Strypsteen, *et al*. 2019). This model explains evolution, and system behaviour, via assessment of the relative balance of sediment budgets, following exchanges specifically between

the nearshore beach and the foredune. Two limitations, one practical and one conceptual, are associated with this methodology. A practical constraint of the Psuty (1988) approach is that sediment leakage from the combined total budget of the nearshore beach and foredune budget is disregarded. This means comprehensive resolution of evolution, and closure of the sediment budgets, is restricted to instances where there has been negligible sediment leakage from the beach-foredune system (e.g., Aagaard, *et al*. 2004). In this research, budget analysis incorporated areas of the secondary dune field which foredune blowout troughs extended landwards through. The landward directed 'losses' of sediment to this zone were found to be significant, and therefore the thesis supports assertions from Sherman (1995) who stated sediment 'leakage' needed to be better incorporated into meso-scale budget analyses. Conceptually, the Psuty (1988) model must also be considered a 'static' or 'fixed' state tool. Although if can often successfully explain meso-scale change in system, it relies on a fixed start and end date to a system which is highly dynamic, and therefore does not provide adequate insights of the system mechanisms between these two points (Houser, 2009). The inclusion of process based, event scale research in this thesis partially mitigates this constraint.

Thesis specific limitations

Two non-generic, primary constraints specific to the thesis concern the event scale, field study. The first being that as the event was relatively short in duration, and winds moderate, topographic change was also moderate. Throughout the thesis, the tendency of event scale studies to be centred on geomorphic processes, and meso-scale studies on morphological change has been given coverage. In doing so, the customary research process augments a recognised scale discontinuity, as beach-dune environments are process-form response systems (Walker, et al. 2017). Studies which link event scale process, to

morphological responses over the same time frame, provide the logical first step in addressing this issue (e.g., Delgado-Fernandez, *et al*. 2018). This study sought to capture event scale elevation changes through pre and post event, TLS surveys. As detectable changes were of a similar scale of magnitude to 'uncertainty' within the resultant DoD, they could not be confidently attributed to 'real' event scale geomorphic change (Wheaton, *et al*. 2010), and thus omitted. Despite this, the capture of TLS surveys proved invaluable by providing a high resolution, current topographic surface model for interpretation of form-flow interactions, which were of significant influence to airflow, and sediment transport dynamics during the event.

The second limitation of consequence also relates to the event scale field study. Namely, the failure of the data-logger linked to the mast-mounted anemometer. This resulted in the study lacking a high frequency record of incident winds with which to interpret airflow modifications. To overcome this, interpretation of the event utilised the time-series of the most upwind anemometer at location A3. It must be acknowledged that in being positioned 40 cm above the bed on the back-beach, airflow is within the boundary layer, and therefore already subject to the influence of topographic modification. Despite this, it did provide a high frequency record of near-surface airflow approaching the blowout. That variability in wind speeds and direction, undoubtedly reflect respective variability in the regional wind, made this a preferable option to using less frequent wind data from a local weather station some distance from the field site. Had a record of high frequency incident flow at the site been available, the study would have benefitted from a more precise understanding of relationships between wind approach angle, foredune deflection, resultant airflow enhancements within the blowout trough, and also the associated increases in sediment transport intensities.

Future research

Thoughts on future research which would build upon the finding of this thesis revolve around relationships between incident wind direction, foredune airflow deflection, and resultant sediment transport responses within foredune blowouts. The findings of this research agreed with thoughts from Walker, *et al*. (2017) in respect of foredune flow deflection and longshore transport. Conceptual models of beach-dune evolution (Short and Hesp, 1982; Psuty, 1988) are strongly biased towards relationships and sediment exchanges between cross-shore units of the coastal profile, and demand much greater inclusion of longshore directed processes. It is apparent from this research that the nature, frequency, and magnitude of flow-flux deflection by the foredune, plays an important role in coastal evolution, and that the longshore spacing of foredune blowouts has implications to the volumes of sediment being transferred through blowouts, as this controls foredune fetch distances. For Sefton and other dune systems characterised by foredune blowouts, it is likely that assessment of long term wind records, in relation to longshore variability in foredune geometry, orientation, and vegetation, may help progress resolution of meso-scale, foredune blowout geomorphic change.

The statistical analysis of chapter three identified variability in the existence, nature, and relative strength of relationships between airflow and transport parameters throughout the instrument grid. With a synchronous, high frequency record of incident flow, there would be opportunities to identify more precisely the relationships between incident wind approach angles, with subsequent airflow modifications, and the associated responses in sediment dynamics. Information around this would be of value not just for coastal managers at sites characterised by foredune blowouts, but also to inform on the optimal locations and notch configurations used in dynamic restoration management projects.

More generally, the thesis confirmed that relationships between at-a-point wind speeds and sediment transport are particularly weak in foredune blowouts. Directional divergence between airflow and transport vectors was further found to be a prominent cause. This confounds the use of conventional sediment flux models in relation to foredune blowout transport. As such, given the importance of these landforms on longer term evolution, these is a real need for much further measure via event scale field studies.

5.7. Concluding remarks

Pye and Neal (1994), observed that at Sefton, sediment was frequently blown along the frontal dunes to be subsequently transferred landwards through foredune blowouts, and this in part motivated the choice of research topic. Essentially this thesis concerned the nature of foredune blowout transport events, and the implications of them to the longer term evolution of beach-dune systems. The contributions to knowledge made by the research were summarised in this final thesis chapter, along with how they related to the existing body of literature, and current practice.

REFERENCES

AAGAARD, T., 2011. Sediment transfer from beach to shoreface: the sediment budget of an accreting beach on the Danish North Sea coast. *Geomorphology*. 135 pp.143-157.

AAGAARD, T., DAVIDSON-ARNOTT, R.G.D., GREENWOOD, B. and NIELSEN, J., 2004. Sediment supply from shoreface to dunes: linking sediment transport measurements and long-term morphological evolution. *Geomorphology*. 60 pp.205-224.

ABER, J.S., MARZOLFF, I., RIES, J.B. and ABER, S.E.W., 2019. Chapter 3 - Principles of Photogrammetry. In: ABER, J.S., MARZOLFF, I., RIES, J.B. and ABER, S.E.W. (Eds.). *Small-Format Aerial Photography and UAS Imagery* (Second Edition). London: Academic Press. pp. 19-38.

ABHAR, K.C., WALKER, I.J., HESP, P.A. and GARES, P.A., 2015. Spatial–temporal evolution of aeolian blowout dunes at Cape Cod. *Geomorphology*, *236*, pp.148-162.

ABUODHA, J.O.Z., 2003. Grain size distribution and composition of modern dune and beach sediments, Malindi Bay coast, Kenya. *Journal of African Earth Sciences*. 36 pp.41-54.

AHNERT, F., 1998. *Introduction to Geomorphology*. London: Arnold.

ALLABY, M., 2020. *A Dictionary of Geology and Earth Sciences*. 5th ed. Oxford: Oxford University Press.

ANDERSON, J.L. and WALKER, I.J., 2006. Airflow and sand transport variations within a backshore-parabolic dune complex: NE Graham Island, British Colombia, Canada. *Geomorphology.* 77 pp. 17-34.

ANDERSON, R.S., SORENSON, M. and WILLETTS, B.B., 1991. A review of recent progress in our understanding of aeolian sediment transport. *Acta Mechanica*. (Supp.1) pp.1-19.

ANDREWS, B.D., GARES, P.A. and COLBY, J.D., 2002. Techniques for GIS modelling of coastal dunes. *Geomorphology*. 48 pp.289-308.

ANTHONY, E., 2013. Storms, shoreface morphodynamics, and accretion and erosion of coastal dune barriers in the southern North Sea. *Geomorphology*. 199 pp.8-21.

ANTHONY, E.J., RUZ, M-H., and VANHÉE, S., 2009. Aeolian sediment transport over complex intertidal bar-trough topography. *Geomorphology*. 105 pp.95-105.

ARENS, S.M., 1996. Patterns of sand transport on vegetated foredunes. *Geomorphology*. 17 pp.339-350.

ARENS, S.M., van KAAM-PETERS, H.M.E. and van BOXEL, J.H., 1995. Air flow over foredunes and implications for sand transport. *Earth Surface Processes and Landforms.* (20) pp.315-332.

ARENS, S.M., van BOXEL, J.H. and ABUODHA, J.O.Z., 2002. Changes in grain size of sand in transport over a foredune. *Earth Surface processes and Landforms*. 27 pp.1163-1175.

ARENS, S.M., SLINGS, Q. and de VRIES, C.N., 2004. Mobility of a remobilised parabolic dune in Kennemerland, The Netherlands' *Geomorphology.* (59) pp.175-188.

ARENS, S.M., de VRIES, S., GEELEN, L.H.W.T., RUESSINK, G., van der HAGEN, H.G.J.M. and GROENENDIJK, D., 2020. Comment on 'is 're-mobilisation' nature restoration or nature destruction? A commentary' by I. Delgado-Fernandez, R.G.D. Davidson-Arnott & P.A. Hesp. Journal of Coastal Conservation 24:17. [online]. Available from: https://doi.org/10.1007/s11852-020-00731-1 [Accessed 13 Mar 2021].

ASH, J.E. and WASSON, R.J., 1983. Vegetation and sand mobility in the Australian dunefield. *Z. Geomorphology*. N.F. Suppl. 45 pp.7-25.

AVIS, A.M., 1989. A review of coastal dune stabilization in the Cape Province of South Africa. *Landscape Urban Planning*. 18 pp.55-68.

BAAS, A.C.W., 2006. Wavelet power spectra of aeolian sand transport by boundary layer turbulence. *Geophysical Research Letters*. 33 (L05403) pp.1-4 [online]. Available from: https://agupubs.onlinelibrary.wiley.com/doi/full/10.1029/2005GL025547 [Accessed 13 Mar 2021].

BAAS, A.C.W. and SHERMAN, D.J., 2005. *Formation and behavior of aeolian streamers*. Journal of Geophysical Research. 110 (F3011) pp.1-15.

BAAS, A.C.W. and SHERMAN, D.J., 2006. Spatiotemporal variability of aeolian sand transport in a coastal dune environment. *Journal of Coastal Research*. 22 (5) pp.1198-1205.

BAAS, A.C.W., JACKSON, D.W.T., DELGADO-FERNANDEZ, I., LYNCH, K. and COOPER, J.A.G., 2020. Using wind run to predict sand drift. *Earth Surface Processes and Landforms*. 45 (8) pp.1817-1827.

BAGNOLD, R.A., 1941. *The Physics of Blown Sand and Desert Dunes*. London: Marrow.

BARBOSA, L.M. and DOMINGUEZ, J.M.L., 2004. Coastal dune fields at the São Francisco River strandplain, northeastern Brazil: morphology and environmental controls. *Earth Surface Processes and Landforms.* 29 (4) pp.443-456.

BARCHYN, T.E. and HUGENHOLTZ, C.H., 2013. Reactivation of supply-limited dune fields from blowouts: A conceptual framework for state characterization. *Geomorphology*. 201. pp.172-182.

BARCHYN, T.E., HUGENHOLTZ, C.H., BAILING, LI., MCKEENA-NEUMAN, C. and SANDERSON, R.S., 2014. From particle counts to flux: Wind tunnel testing and calibration of the 'Wenglor' aeolian sediment transport sensor. *Aeolian Research*. 15 pp.311-318.

BARRINEAU, C.P. and ELLIS, J.T., 2013. Sediment transport and wind flow around hummocks. *Aeolian Research* 8 pp.19-27.

BATE, G. and FERGUSON, M., 1996. Blowouts in coastal foredunes. *Landscape and Urban Planning*, *34*(3-4), pp.215-224.

BAUER, B.O., 2009. Contemporary research in aeolian geomorphology. Geomorphology. 105. pp. 1-5.

BAUER, B.O. and DAVIDSON-ARNOTT, R.G.D., 2002. A general framework for modelling sediment supply to coastal dunes including wind angle, beach geometry, and fetch effects. *Geomorphology*. 49 (1–2) pp.89-108.

BAUER, B.O. and SHERMAN, D.J., 1999. Coastal dune dynamics: problems and prospects. In: GOUDIE, A.S., LIVINGSTONE, I. and STOKES, S. (Eds.). *Aeolian Environments, Sediments and Landforms.* Chichester: Wiley. pp. 71-104.

BAUER, B.O., SHERMAN, D.J., NORDSTROM, K.F. and GARES, P.A., 1990. Aeolian transport measurement and prediction across a beach and dune at Castroville, California. In: NORDSTROM, K.F., PSUTY, N.P. and CARTER, R.W.G. (Eds.). *Coastal Dunes - Form and Process*. Chichester: Wiley. pp. 39-55.

BAUER, B.O., DAVIDSON-ARNOTT, R.G.D., HESP, P.A., NAMIKAS, S.L., OLLERHEAD, J. and WALKER, I.J., 2009. Aeolian sediment transport on a beach: Surface moisture, wind fetch, and mean transport. *Geomorphology*. 105 pp.106-116.

BAUER, B.O., DAVIDSON-ARNOTT, R.G.D., WALKER, I.J., HESP, P.A., and OLLERHEAD, J., 2012. Wind direction and complex sediment transport response across a beach-dune system. *Earth Surface Processes & Landforms.* (37) pp.1661-1677.

BAUER, B.O., WALKER, I.J., BAAS, A.C.W., JACKSON, D.W.T., MCKENNA-NEUMAN, C., WIGGS, G.F.S. and HESP, P.A., 2013. Critical reflections on the coherent flow structures paradigm in aeolian geomorphology. In: VENDITTI, J.G., BEST, J.L., CHURCH, M. and HARDY, R.J. (Eds.). Coherent Flow Structures at Earth's Surface. London: Wiley. pp. 111-134.

BELLY, P.Y., 1964. *Sand Movement by Wind*. US Army Corps of Engineers. CERC. Technical Memorandum 1.

BERTONI, D., BIAGIONI, C., SARTI, G., CICCARELLI, D. and RUOCCO, M., 2014. The role of sediment grain-size, mineralogy, and beach morphology on plant communities of two Mediterranean coastal dune systems. *Italian Journal of Geosciences.* 133 (2) pp.271–281.

BEYERS, M., JACKSON, D., LYNCH, K., COOPER, A., BAAS, A., DELGADO-FERNANDEZ, I. and DALLAIRE, P.O., 2010. Field testing and CFD LES simulation of offshore wind flows over coastal dune terrain in Northern Ireland. In: *The Fifth International Symposium on Computational Wind Engineering (CWE2010)*. International Association for Wind Engineering. Available from: https://pure.ulster.ac.uk/ws/portalfiles/portal/11251664/PaperID126_Beyers.pdf [Accessed 23 Mar 2021].

BIAUSQUE, M., GROTTOLI, E., JACKSON, D.W.T. and COOPER, J.A.G., 2020. Multiple intertidal bars on beaches: A review. Earth-Science Reviews. 210. 103358 [online]. Available from: https://reader.elsevier.com/reader/sd/pii/S0012825220304049?token=4164B2285AE533DB75C6D76275919DA874EAC9099E3FF7CA228DE27D647455E0A5E3C9A13F8093E1E849E9E3327BE161 [Accessed 17 Mar 2021].

BIRD, E.C.F., 1985. *Coastline Changes: A Global Review*. Hoboken, NJ: Wiley-Blackwell.

BITTON, M.C. and BYRNE, M.L., 2002. A volumetric analysis of coastal dune blowout morphology change, Pinery Provincial Park. *Proceedings of the Parks Research Forum of Ontario (PRFO) Annual Meeting.* pp. 221-230.

BLANCO, P.D., ROSTAGNO, C.M., DEL VALLE, H.F., BEESKOW, A.M. and WIEGAND, T., 2008. Grazing impacts in vegetated dune fields: predictions from spatial pattern analysis. *Rangeland Ecology & Management*. 61 (2), pp.194-203.

BLOTT, S.J. and PYE, K., 2001. GRADISTAT: A grain size distribution and statistics package for the analysis of unconsolidated sediments. *Earth Surface Processes and Landforms*. 26 pp.1237-1248.

BROCK, J.C. and PURKIS, S.J., 2009. The emerging role of lidar remote sensing in coastal research and resource management. *Journal of Coastal Research Online*. 10053 pp.1-5. [online]. Available from: https://pubs.er.usgs.gov/publication/70035339 [Accessed 17 Mar 2021].

BROWN, S., BARTON, M. and NICHOLLS, R.J., 2010. Coastal retreat and/or advance adjacent to defences in England and Wales. *Journal of Coastal Conservation*. 15(4) pp. 659-670.

BROWN, S., NICHOLLS, R.J., WOODROFFE, C.D., HANSON, S., HINKEL, J., KEBEDE, A.S., NEUMANN, S. and VAFEIDIS, A.T., 2013. Sea-Level rise impacts and responses: A Global Perspective. FINKL, C.W. ed. Coastal Hazards. Dordrecht, NL: Springer. pp. 117-149.

BRUUN, P., 1962. Sea level rise as a cause of shore erosion. *Journal of Waterways and Harbors Division*. 88 (1) pp.117–130.

BULLARD, J.E., THOMAS, D.S.G., LIVINGSTONE, I. and WIGGS, G.F.S., 1997. Dune field activity and interactions with climatic variability in the Southwest Kalahari Desert. Earth Surface Processes and Landforms. 22 pp.165-174.

BURKLEY, K., HOCKING, A., HOWELL, B., MEDEMA, E., NEWSWANGER, J., THORNE, C. and TIEMEYER, A., 2014. Blowouts and Unmanaged Trails in Hoffmaster State Park, Michigan. Available from: https://calvin.edu/academics/departments-programs/fyres/files/research-reports/FYRES_2014Report11_Burkley.pdf [Accessed 17 Mar 2021].

BURRI, K., GROMKE, C., LEHNING, M. and GRAF, F., 2011. Aeolian sediment transport over vegetation canopies: a wind tunnel study with live plants. *Aeolian Research*. 3 pp.205–213.

BYRNE, M.L., 1997. Seasonal sand transport through a trough blowout at Pinery Provincial Park, Ontario. *Canadian Journal of Earth Sciences.* 34 (11) pp.1460-1466.

CARNEIRO, M., RASMUSSEN, K. and HERRMANN, H., 2015. Bursts in discontinuous Aeolian saltation. *Scientific Reports* 5 11109 pp.1-8 [online]. Available from: https://www.nature.com/articles/srep11109.pdf [Accessed 13 Mar 2021].

CARTER, R.W.G., 1988. *Coastal Environments*. London: Academic Press.

CARTER, R.W.G., 1990. The morphology of coastal dunes in Ireland. In: BAKKER, T.W.M., JUNGERIUS, P.D. and KLIJN, J.A. *Dunes of the European Coasts*. Catena. 18 pp.31-41. (50)

CARTER, R.W.G. and WILSON, P., 1990. The geomorphological, ecological and pedological development of coastal foredunes at Magilligan Point, Northern Ireland. In: NORDSTORM, K.F., PSUTY, N. and CARTER, R.W.G. (Eds.). *Coastal Dunes: Form and Process*. Chichester: Wiley. pp. 129-155.

CARTER, R.W.G., HESP, P. A. and NORDSTROM, K. F. 1990. Erosional landforms in coastal dunes. In: NORDSTORM, K.F., PSUTY, N. and CARTER, R.W.G. (Eds.) *Coastal Dunes: Form and Process*. Chichester: Wiley. pp. 217-250.

CARTER, R.W.G., CURTIS, T.G.F. and SHEEHY-SKEFFINGTON, M.J. (Eds.). 1992. *Coastal Dunes: Geomorphology, Ecology and Management for Conservation*. Rotterdam, NL: Balkema.

CATTO, N., MacQUARRIE, K. and HERMANN, M., 2002. Geomorphic response to Late Holocene climate variation and anthropogenic pressure, northeastern Prince Edward Island, Canada. *Quaternary International.* 87 pp.101-117.

CHAPMAN, C., WALKER, I.J., HESP, P.A., BAUER, B.O., DAVIDSON-ARNOTT, R.G.D. and OLLERHEAD, J., 2013. Reynolds stress and sand transport over a foredune. *Earth Surface Processes and Landforms*. 38 (14) pp.1735-1747.

CHAPMAN, D.M., 1990. Aeolian sand transport - an optimized model. *Earth Surface Processes and Landforms.* 15 pp.751-760.

CHATERJEE, S.K., 2013. Fundamental Physics: An Introduction. Oxford: Alpha Science International.

CHEPIL, W.S. and MILNE, R.A., 1939. Comparative Study of Soil Drifting in the Field and in a Wind Tunnel. *Scientific Agriculture*. 19 (5) p.249.

CHEPIL, W.S. and WOODRUFF, N.P., 1963. The Physics of Wind Erosion and Its Control. *Advances in Agronomy*. 15 pp.211-302.

CHORLEY, R.J., 1962. Geomorphology and General Systems Theory. *US Geological Survey Professional Paper 500-B.* [online]. pp.1-9. Available from: https://pubs.usgs.gov/pp/0500b/report.pdf [Accessed 27 Feb 2021].

CLEMMENSEN, L.B., MURRAY, A., HEINEMEIER, J. and DE JONG, R., 2009. The evolution of Holocene coastal dunefields, Jutland, Denmark: A record of climate change over the past 5000 years. *Geomorphology*. 105 pp.303-313.

COHN, N., RUGGIERO, P., DE VRIES, S. and KAMINSKY, G.M., 2018. New insights on coastal foredune growth: The relative contributions of marine and aeolian processes. *Geophysical Research Letters.* 45(10) pp.4965-4973.

COOKE. R., WARREN, A. and GOUDIE, A., 1993. Anchored and Stabilized Dunes. In: COOKE. R., WARREN, A. and GOUDIE, A. (Eds.). *Desert Geomorphology.* London: UCL Press. pp.353-367.

COOPER, J.A.G. and JACKSON, D.W.T., 2020. Dune Gardening? A Critical View of the Contemporary Coastal Dune Management Paradigm. *Area.* 12692 pp.1-8.

COOPER, W.S., 1958. *Coastal sand dunes of Oregon and Washington* (Vol. 72). Geological Society of America. P.169.

CORNELIS, W.M. and GABRIELS, D., 2003. The effect of surface moisture on the entrainment of dune sand by wind: an evaluation of selected models. *Sedimentology*. 50 (4) pp.771-790.

CREER, J., LITT, E., RATCLIFFE, J., REES, S., THOMAS, N. and SMITH, P., 2020. A comment on some of the conclusions made by Delgado-Fernandez et al. (2019). "Is 're-mobilisation' nature conservation or nature destruction? A commentary". Journal of Coastal Conservation. 24:29. [online]. Available from: https://doi.org/10.1007/s11852-020-00745-9 [Accessed 27 Feb 2021].

DARKE, I.B., EARNER, J.B.R., BEAUGRAND, H.E.R. and WALKER, I.J., 2013. Monitoring considerations for a dynamic dune restoration project: Pacific Rim National Park Reserve, British Columbia, Canada. *Earth Surface Processes and Landforms*. 38 pp.983-993.

DARKE, I.B., WALKER, I.J. and HESP, P.A. 2016., Beach–dune sediment budgets and dune morphodynamics following coastal dune restoration, Wickaninnish Dunes, Canada. *Earth Surface Processes and Landforms*. 41 (10) pp.1370-1385.

DAVIDSON-ARNOTT, R.G.D., 2005. Conceptual Model of the Effects of Sea Level Rise on Sandy Coasts. *Journal of Coastal Research*. 21(6) pp. 1166-1172.

DAVIDSON-ARNOTT, R.G.D. and LAW, M.N., 1990. Seasonal patterns and controls on sediment supply to coastal foredunes, Long Point, Lake Erie. In: NORDSTROM, K.F., PSUTY, N.P. and CARTER, R.W.G. (Eds.). *Coastal Dunes - Form and Process*. Chichester: Wiley. pp. 177-200.

DAVIDSON-ARNOTT, R.G.D., WHITE, D.C. and OLLERHEAD, J., 1997. The effect of artificial pebble concentrations on eolian sand transport on a beach. *Canadian Journal of Earth Science*. 34 (11) pp.1499-1508.

DAVIDSON-ARNOTT, R.G.D., OLLERHEAD, J., HESP, P.A. and WALKER, I.J., 2003. Spatial and temporal variability in intensity of aeolian transport on a beach and foredune. In: DAVIS, R.A., SALLENGER, A. and HOWD, P. *Coastal Sediments 2003*, 18-23 May 2003. Clearwater Beach, FL [online]. Hackensack, NJ: World Scientific Publishing Inc. pp.1-12. Available from: https://citeseerx.ist.psu.edu/viewdoc/download?doi=10.1.1.585.7992&rep=rep1&type=pdf [Accessed 22 Feb 2021].

DAVIDSON-ARNOTT, R.G.D., MACQUARRIE, K. and AAGAARD, T., 2005. The effect of wind gusts, moisture content and fetch length on sand transport on a beach. *Geomorphology*. 68 pp.115-129.

DAVIDSON-ARNOTT, R.G.D., BAUER, B.O., WALKER, I.J., HESP, P.A., OLLERHEAD, J., DELGADO-FERNANDEZ, I., 2009. Instantaneous and mean aeolian sediment transport rate on beaches: an intercomparison of measurements from two sensor types. *Journal of Coastal Research*. SI (56) pp.297-301.

DAVIDSON-ARNOTT, R.G.D., BAUER, B.O., WALKER, I.J., HESP, P.A., OLLERHEAD, J. & CHAPMAN, C., 2012. High-frequency sediment transport responses on a vegetated foredune. *Earth Surface Processes and Landforms*. 37 pp.1227-1241.

DAVIDSON-ARNOTT, R.G.D., BAUER, B. and HOUSER, C. (Eds.). 2019. *Introduction to coastal processes and geomorphology.* 2nd ed. Cambridge: Cambridge University Press.

De JONG, B., KEIJSERS, J.G.S., RIKSEN, M.J.P.M., KROL and SLIM, P.A., 2014. Soft Engineering vs a Dynamic Approach in Coastal Dune Management: A case Study on the North Sea Barrier Island of Ameland, The Netherlands. *Journal of Coastal Research.* 30 (4) pp.670-684.

DE VRIES, S., SOUTHGATE, H., KANNING, W. and RANASINGHE, R., 2012. Dune behavior and aeolian transport on decadal timescales. *Coastal Engineering*. 67 pp.41-53.

DE VRIES, S., VAN THIEL DE VRIES, J.S.M., VAN RIJN, L.C., ARENS, S.M. and RANASINGHE, R., 2014. Aeolian sediment transport in supply limited situations. *Aeolian Research*. 12 pp.75-85.

DEKIMPE, N. M., DOLAN, R. and HAYDEN, B.P., 1991. Predicted dune recession on the Outer Banks of North Carolina, USA. *Journal of Coastal Research* (7) pp.451-463.

DELGADO-FERNANDEZ, I. and DAVIDSON-ARNOTT, R.G.D. 2009. Sediment input to foredunes: description and frequency of transport events at Greenwich Dunes, Prince Edward Island, Canada. *Journal of Coastal Research*. SI 56 pp.302-306.

DELGADO-FERNANDEZ, I. and DAVIDSON-ARNOTT, R.G.D., 2011. Meso-scale aeolian sediment input to coastal dunes: The nature of aeolian transport events. *Geomorphology*. 125 pp.217-232.

DELGADO-FERNANDEZ, I., SMYTH, T.A.G., JACKSON, D.W.T., SMITH, A.B. and DAVIDSON-ARNOTT, R.G.D., 2018. Event-Scale Dynamics of a Parabolic Dune and Its Relevance for Mesoscale Evolution. *Journal of Geophysical Research: Earth Surface*. (123) pp.3084-3100.

DELGADO-FERNANDEZ, I., DAVIDSON-ARNOTT, R.G.D. and HESP, P.A. (a), 2019. Is 're-mobilisation' nature restoration or nature destruction? A commentary. Journal of Coastal Conservation. 23. Pp.1093-1103.

DELGADO-FERNANDEZ, I., O'KEEFFE, N. and DAVIDSON-ARNOTT, R.G. (b), 2019. Natural and human controls on dune vegetation cover and disturbance. *Science of the Total Environment.* 672 pp. 643-656.

DISSANAYAKE, P., BROWN, J. and KARUNARATHNA, H., 2010. Modelling storm- induced beach/dune evolution: Sefton Coast, Liverpool Bay, UK. *Marine Geology.* 357. pp.225-242.

DISSANAYAKE, P., BROWN, J. and KARAUNARATHNA, H., 2015. Impacts of storm chronology on the morphological changes of the Formby beach and dune system, UK. *Natural Hazards and Earth System Sciences.* (15) pp.1533-1543.

DOLAN, R., HAYDEN, B.P. and HEYWOOD, J., 1978. A new photo-grammetric method for determining shoreline erosion. *Coastal Engineering*. 2 (1) pp.21-39.

DONG, Z., LIU, X., WANG, H. and WANG, X., 2003. Aeolian sand transport: a wind tunnel model. *Sedimentary Geology*. 161 pp. 71-83.

DONG, Z., LUO, W., QIAN, G. and LU, P., 2008. Wind tunnel simulation of the three-dimensional airflow patterns around shrubs. *Journal of Geophysical Research*. 113 (F2) pp.1-12 [online]. Available from: https://agupubs.onlinelibrary.wiley.com/doi/pdf/10.1029/2007JF000880 [Accessed 21 Mar 2021].

DUARTE-CAMPOS, L., WIJNBERG, K.M. and HULSCHER, S.J.M.H., 2021. Field test of the accuracy of laser particle counters to measure aeolian sediment flux. *Aeolian Research*. 50 pp.1-9.

DUNLOP, S., 2008. *A Dictionary of Weather*. 2nd ed. Oxford: Oxford University Press.

DUPONT, S., BERGAMETTI, G. and SIMOENS, S., 2014. Modelling aeolian erosion in presence of moisture. *Journal of Geophysical Research: Earth Surface*. 119 pp.168-187.

ELLIS, J.T., LI, B., FARRELL, E.J. and SHERMAN, D.J., 2009. Protocols for characterizing aeolian mass-flux profiles. *Aeolian Research*, 1 (1-2) pp.19-26.

ELLIS, J.T., SHERMAN, D.J., FARRELL, E.J. and BAILANG, L., 2012. Temporal and spatial variability of aeolian sand transport: Implications for field measurements. *Aeolian Research*. 3 pp.379-387.

ESTEVES, L.S., BROWN, J.M., WILLIAMS, J.J. and LYMBERY, G., 2012. Quantifying thresholds for significant dune erosion along Sefton Coast, Northwest England. *Geomorphology.* (143-144) pp.52-61.

EVANS, I.S., 2012. Geomorphometry and landform mapping: What is a landform? *Geomorphology*. 137 pp.94-106.

FARRELL, E.J. and SHERMAN, D.J., 2015. A new relationship between grain size and fall (settling) velocity in air. *Progress in Physical Geography: Earth and Environment*. 39 (3) pp.361-387.

FÉCAN, F., MARTICORENA, B. and BERGAMETTI, G., 1999. Parametrization of the increase of the aeolian erosion threshold wind friction velocity due to soil moisture for arid and semi-arid areas. *Annales Geophysicae*. 17 pp.149-157.

FESER, F., BARCIKOWSKA, M., KRUEGER, O., SCHENK, F., WEISSE, R. and XIA, L., 2014. Storminess over the North Atlantic and northwestern Europe - A review. *Quarterly Journal of the Royal Meteorological Society*. 141 (687) pp.350-382.

FOUFOULA-GEORGIOU, E. and KUMAR, P. (Eds.)., 1994. *Wavelets in Geophysics, Volume 4, 1st Edition.* Cambridge, MA: Academic Press.

FRASER, G.S., BENNETT, S.W., OLYPHANT, G.A., BAUCH, N.J., FERGUSON, V., GELLASCH, C.A., MILLARD, C.L., MUELLER, B., O'MALLEY, P.J., WAY, J.N. and WOODFIELD, M.C., 1998. Windflow Circulation Patterns in a Coastal Dune Blowout, South Coast of Lake Michigan. *Journal of Coastal Research.* 14 (2) pp.451-460. (100)

FREDERIKSE, T., LANDERER, F., CARON, L., ADHIKARI, S., PARKES, D., HUMPHREY, N.W., DANGENDORF, S., HOGARTH, P., ZANNA, L., CHENG, L. and WU, E-H., 2020. The causes of sea-level rise since 1900. *Nature.* 584 pp.393–397.

FRYBERGER, S.G. and DEAN, G. 1979. Dune Forms and Wind Regime. In: MCKEE, E.D. (ed.). *A Study of Global Sand Seas.* Professional Paper 1052. Washington: US Geological Survey pp. 137-169.

FRYER, J., MITCHELL, H. and CHANDLER, J. (Eds.)., 2007. Applications of 3d measurement from images. Dunbeath, Scotland: Whittles Publishing.

GAO, J., KENNEDY, D.M. and KONLECHNER, T.M., 2020. Coastal dune mobility over the past century: A global review. *Progress in Physical Geography: Earth and Environment.* p.0309133320919612 [Online]. Available from: https://journals.sagepub.com/doi/10.1177/0309133320919612 [Accessed 30 Dec 2020].

GARCÍA-ROMERO, L., DELGADO-FERNANDEZ, I., HESP, P.A., HERNÁNDEZ-CALVENTO, L., VIERA-PÉREZ, M., HERNÁNDEZ-CORDERO, A.I., CABRERA-GÁMEZ, J. and DOMÍNGUEZ-BRITO, A.C., 2019. Airflow dynamics, vegetation and aeolian erosive processes in a shadow zone leeward of a resort in an arid transgressive dune system. *Aeolian Research*. 38 pp.48-59.

GARES, P.A., 1992. Topographic changes associated with coastal dune blowouts at Island Beach State Park, New Jersey. *Earth Surface Processes and Landforms.* 17 pp.589-604.

GARES, P. A. and NORDSTROM, K. F., 1988. Creation of dune depressions by foredune accretion. *Geographical Review* 78 (2) Thematic Issue: Coastal Geomorphology. pp. 194-204.

GARES, P.A. and NORDSTROM, K.F., 1995. A cyclic model of foredune blowout evolution for a leeward coast: Island Beach, New Jersey. *Annals of the Association of American Geographers*, *85*(1), pp.1-20.

GILLIES, J.A., NIELD, J.M. and NICKLING, W.G., 2014. Wind speed and sediment transport recovery in the lee of a vegetated and denuded nebkha within a nebkha dune field. *Aeolian Research*. 12 pp.135-141.

GONZÁLEZ-VILLANUEVA, R., COSTAS, S., DUARTE, H., PÉREZ-ARLUCEA, M. and ALEJO, I., 2011. Blowout evolution in a coastal dune: using GPR, aerial imagery and core records. *Journal of Coastal Research*, pp.278-282.

GOOSSENS, D., OFFER, Z. and LONDON, G., 2000. Wind tunnel and field calibration of five aeolian sand traps. *Geomorphology*. 35 pp.233-252.

GRASS, A.J., 1983. The influence of boundary layer turbulence on the mechanics of sediment transport. In: SUMER, B.M. and MÜLLER, A. (Eds.). Euromech 156: Mechanics of Sediment Transport. Istanbul: Balkema. pp3-18. [online]. Available from: https://1lib.uk/book/6037459/9a3108?regionChanged=&redirect=219148454 [Accessed 11 March 2021].

GREGORY, K.J. and LEWIN, J., 2014. The Basics of Geomorphology: Key Concepts. London: Sage.

GRESSWELL, R.K., 1937. The geomorphology of the south-west Lancashire coast-line. *Geographical Journal.* 90 pp.335-348.

GRESSWELL, R.K., 1953. *Sandy shores in south Lancashire: The geomorphology of south-west Lancashire*. University Press. pp. 194

GRILLIOT, M.J., WALKER, I.J. and BAUER, B.O., 2019. Aeolian sand transport and deposition patterns within a large woody debris matrix fronting a foredune. *Geomorphology*. 338 (1) pp.1-15.

GUISADO-PINTADO, E., JACKSON, D.W. and ROGERS, D., 2019. 3D mapping efficacy of a drone and terrestrial laser scanner over a temperate beach-dune zone. *Geomorphology* 328 pp.157-172.

GUNARATNA, A., SUZUKI, T. and YANAGISHIMA, C., 2019. Cross-shore grain size and sorting patterns for the bed profile variation at a dissipative beach: Hasaki Coast, Japan. Marine Geology. 407 pp.111-120.

GUTIERREZ-ELORZA, M., DESIR, G., GUITIERREZ-SANTOLALLA, F. and MARIN, C., 2005. Origin and evolution of playas and blowouts in the semiarid zone of Tierra de Pinares (Duero Basin, Spain). *Geomorphology*. 72 pp.177-192.

HAARSMA, R.J., HAZELEGER, W., SEVERIJNS, C., DE VRIES, H., STERL, A., BINTANJA, R., VAN OLDENBORGH, G.J. and VAN DER BRINK, H.W., 2013. More hurricanes to hit western Europe due to global warming. *Geophysical Research Letters*. 40 (9) pp.1783-1788.

HANSEN, E., DEVRIES-ZIMMERMAN, S., VAN DIJK, D. and YURK, B., 2009. Patterns of wind flow and aeolian deposition on a parabolic dune on the southeastern shore of Lake Michigan. *Geomorphology*. 105 (1-2) pp.147-157.

HARDIN, E., MITASOVE, H., TATEOSIAN, L.G. and OVERTON, M., 2014. *GIS-based Analysis of Coastal Lidar Time-Series*. New York: Springer. pp. 27-34.

HASLETT, S.K., 2016. *Coastal Systems*. 3rd Ed. Cardiff; University of Wales Press.

HATTAM, C., ATKINS, J.P., BEAUMONT, N., BÖRGER, T., BÖHNKE-HENRICHS, A., BURDON, D., DE GROOT, R., HOEFNAGEL, E., NUNES, P.A., PIWOWARCZYK, J. and SASTRE, S., 2015. Marine ecosystem services: linking indicators to their classification. *Ecological Indicators.* 49 pp.61-75.

HESP, P.A., 1981. The formation of shadow dunes. *Journal of Sedimentary Petrology*. 51 pp.101-112.

HESP, P.A., 1983. Morphodynamics of incipient foredunes in New South Wales, Australia. In: BROOKFIELD, M.E. and AHLBRANDT, T.S. (Eds.). *Eolian Sediments and Processes*. Amsterdam: Elsevier. pp. 325-342.

HESP, P.A., 1989. A review of biological and geomorphological processes involved in the initiation and development of incipient foredunes. In: GIMINGHAM, C.H., RITCHIE, W., WILLETTS, B.B. and WILLIS, A.J. (Eds.). *Coastal Sand Dunes. Proceedings of Royal Society of Edinburgh*. 96B pp. 181–201.

HESP, P.A., 1991. Ecological Processes and Plant Adaptations on Coastal Dunes. *Journal of Arid Environments*. 21 (2) pp.165-191.

HESP, P.A., 1996. Flow dynamics in a trough blowout. *Boundary-Layer Meteorology*. (77) pp.305-330.

HESP, P.A., 1999. The beach backshore and beyond. In: SHORT, A.D. (Ed.) *Handbook of Beach and Shoreface Morphodynamics*. London: Wiley. pp. 145-170.

HESP, P.A., 2001. The Manawatu Dunefield: Environmental changes and human impacts. *New Zealand Geographer*. 57 (2) pp.33-40.

HESP, P.A., 2002. Foredunes and blowouts: initiation, geomorphology and dynamics *Geomorphology* 48 (1-3) pp.245-268.

HESP, P.A., 2013. Conceptual models of the evolution of transgressive dune field systems. *Geomorphology*. (138) pp.138-149.

HESP, P.A. and HYDE, R., 1996. Flow dynamics and geomorphology of a trough blowout. *Sedimentology.* 43 pp.505- 525.

HESP, P.A. and PRINGLE, A., 2001. Wind Flow and Topographic Steering Within a Trough Blowout. *Journal of Coastal Research.* SI (34) pp.597-601.

HESP. P.A. and SMYTH. T.A.G., 2017. Nebkha flow dynamics and shadow dune formation. *Geomorphology*. 282 pp.27-38.

HESP. P.A. and WALKER, I.J., 2012. Three-dimensional aeolian dynamics within a bowl blowout during offshore winds: Greenwich dunes, Prince Edward Island, Canada. Aeolian Research. 3 (4) pp.389-399.

HESP P.A. and WALKER I.J., 2013. Coastal Dunes. In: SHRODER, J.F. (Ed.). *Treatise on Geomorphology.* Volume 11 pp.328-355. San Diego: Academic Press.

HESP, P.A., ABREU DE CASTILHOS, J., MIOT DA SILVA, G., DILLENBURG, S., MARTINHO, T.M., AGUIAR, D., FONARI, M., FONARI, M. and ATUNES, G., 2007. Regional wind fields and dunefield migration, southern Brazil. *Earth Surface Processes and Landforms*. 32 pp.561-573.

HESP, P.A., HILTON, M. and KONLECHER, T., 2017. Flow and sediment transport dynamics in a slot and cauldron blowout and over a foredune, Mason Bay, Stewart Island (Rakiura), NZ. *Geomorphology*. 295 pp.598-610

HESP, P.A., HERNÁNDEZ-CALVENTO, GALLEGO-FERNÁNDEZ, J.B., MIOT DA SILVA, G., HERNÁNDEZ-CORDERO, A.I., RUZ, M.H. and GARCIA-ROMERO, L.G., 2021. Nebkha or not? - Climate control on foredune mode. *Journal of Arid Environments.* 187 (104444).

HORTON, B.P., KHAN, N.S., CAHILL, N., LEE, J.S.H., SHAW, T.A., GARNER, A.J., KEMP, A.C., ENGELHART, S.E. and RAHMSTORF, S., 2020. Estimating global mean sea-level rise and its uncertainties by2100 and 2300 from an expert survey. *npj Climate and Atmospheric Science*. 3 (18) pp.1-8.

HOTTA, S., KUBOTA, S., KATORI, S. and HORIKAWA, K., 1984. Sand transport by wind on a wet sand surface. *Coastal Engineering*. 29th Jan 1984. Houston, TX. New York:

ASCE. Available from: https://icce-ojs-tamu.tdl.org/icce/index.php/icce/article/view/3867 [Accessed 19 Mar 2021].

HOUSER, C., 2009. Synchronization of transport and supply in beach-dune interaction. *Progress in Physical Geography*. 33 (6) pp.733-746.

HOUSTON, J., EDMONDSON, S.E. and ROONEY, P. (Eds.)., 2001. *Coastal Dune Management, Shared Experience of European Conservation Practice*. Liverpool: Liverpool University Press.

HSU, S-A., 1971. Wind stress criteria in eolian sand transport. Journal of Geophysical Research. 76 pp.8684-8686.

HUANG, H-J., 2020. Modelling the effect of saltation on surface layer turbulence. *Earth Surface Processes and Landforms*. 45 (15) pp.3943-3954.

HUGENHOLTZ, C. H., WOLFE, S.A., WALKER, I.J., and MOORMAN, B.J., 2009. Spatial and temporal patterns of aeolian sediment transport on an inland parabolic dune, Bigstick Sand Hills, Saskatchewan, Canada. *Geomorphology*. (105) pp.158-170.

HUGENHOLTZ, C.H. and WOLFE, S.A., 2006. Morphodynamics and climate controls of two aeolian blowouts on the northern Great Plains, Canada. *Earth Surface Processes and Landforms: The Journal of the British Geomorphological Research Group*, 31 (12) pp.1540-1557.

HUGENHOLTZ, C.H. and BARCHYN, T.E., 2011. Laboratory and field performance of a laser particle counter for measuring aeolian sand transport. *Journal of Geophysical Research: Earth Surface.* 116 (F1). Available from: https://agupubs.onlinelibrary.wiley.com/doi/epdf/10.1029/2010JF001822 [Accessed 23 Mar 2021].

HUGENHOLTZ, C.H. and WOLFE, S.A., 2005. Recent stabilization of active sand dunes on the Canadian prairies and relation to recent climate variations. *Geomorphology*. 68 pp.131-147.

HUGGETT, R.J., 2017. Fundamentals of Geomorphology. 4th ed. Abingdon: Routledge.

JACKSON, D.W.T. and COOPER, J.A.G., 2011. Coastal dune fields in Ireland: rapid regional response to climatic change. *Journal of Coastal Research*. SI 64 pp.293-297.

JACKSON, N.L. and NORDSTROM, K.F., 1997. Effects of time-dependent moisture content of surface sediments on aeolian transport rates across a beach, Wildwood, New Jersey, USA. *Earth Surface Processes and Landforms*. 26 pp.611-621. (150)

JACKSON, D.W.T., BEYERS, J.H.M., LYNCH, K., COOPER, J.A.G., BAAS, A.C.W. and DELGADO-FERNANDEZ, I., 2011. Investigation of three-dimensional wind flow behaviour over coastal dune morphology under offshore winds using computational fluid dynamics (CFD) and ultrasonic anemometry. *Earth Surface Processes and Landforms.* 36 (8) pp.1113-1124.

JACKSON, R.G., 1976. Sedimentological and fluid-dynamic implications of the turbulent bursting phenomenon in geophysical flows. *Journal of Fluid Mechanics*. 77 pp.531-569.

JAMES, L.A., HODGSON, M.E., GHOSHAL, S. and LATIOLAIS, M.M., 2012. Geomorphic change detection using historic maps and DEM differencing: The temporal dimension of geospatial analysis. *Geomorphology.* 137(1) pp.181-198.

JAMES, M.R. and QUINTON, J.N., 2013. Ultra-rapid topographic surveying for complex environments: the hand-held mobile laser scanner (HMLS). *Earth Surface Processes and Landforms* [online]. Available from: https://www.lancaster.ac.uk/staff/jamesm/software/James%20&%20Quinton%202013.pdf [Accessed 19 Feb 2021].

JEFFERIES, R.L., DAVY, A.J. and RUDMIK, T., 1979. The growth strategies of coastal halophytes. In: JEFFERIES, R.L. and DAVY, A.J. (Eds.). *Ecological processes in coastal environments*. Oxford: Blackwell. pp. 243-268.

JEWELL, M., HOUSER, C. and TRIMBLE, S., 2014. Initiation and evolution of blowouts within Padre Island National Seashore, Texas. *Ocean & Coastal Management.* 95 pp.156-164.

JUNGERIUS, P.D. and van der MEULEN, F., 1989. The Development of Dune Blowouts, as measured with erosion pins and sequential aerial photos. *Catena* 16 pp.369-376.

JUNGERIUS, P.D., VERHEGGEN, A.J.T. and WIGGERS, A.J., 1981. The development of blowouts in 'De Blink', a coastal dune area near Noordwijkerhout, the Netherlands. *Earth Surface Processes and Landforms*. 6 pp.375-396.

JUNGERIUS, P.D., WITTER, J.V. and VAN BOXEL, J.H., 1991. The effects of changing wind regimes on the development of blowouts in the coastal dunes of The Netherlands. *Landscape Ecology.* 6 (1-2), pp.41-48.

KAWAMURA, R., 1951. *Study of sand movement by wind, University of California Hydraulics Engineering Laboratory Report HEL 2 - 8*. Berkeley, CA: University of California.

KÄYHKÖ, J., 2007. Aeolian blowout dynamics in subarctic Lapland based on decadal levelling investigations. *Geografiska Annaler*, Series A: *Physical Geography*. 89 (1) pp.65-81.

KEIJSERS, J.G.S., DE GROOT, A.V. and RIKSEN, M.J.P.M., 2015. Vegetation and sedimentation on coastal foredunes. *Geomorphology.* 228 pp.723-734.

KELLER, E.A., DEVECCHIO, D.E. and BLODGETT, R.H., 2019. *Natural Hazards: Earth's Processes as Hazards, Disasters, and Catastrophes.* 5th ed. London: Routledge.

KEMP, D., 1998. The Environment Dictionary. London: Taylor and Francis.

KING, C.A.M., 1972. *Beaches and Coasts.* 2nd Ed. London: Edward Arnold.

KIREZCI, E., YOUNG, I.R., RANASINGHE, R., MUIS, S., NICHOLLS, R.J., LINCKE, D. and HINKEL, J., 2020. Projections of global-scale extreme sea levels and resulting episodic coastal flooding over the 21st century. *Scientific Reports*. 10 (11629) pp.1-12.

KISH, S.A. and DONOGHUE, J.F., 2013. Coastal Response to Storms and Sea-Level Rise: Santa Rosa Island, Northwest Florida, U.S.A. *Journal of Coastal Research*. SI (63) pp.131-140.

KLINE, S.J., REYNOLDS, W.C., SCHRAUB, F.A. and RUNDSTADLER, P.W., 1967. The structure of turbulent boundary layers. *Journal of Fluid Mechanics*. 30 pp.741-773.

KOCUREK, G. and LANCASTER, N., 1999. Aeolian system sediment state: theory and Mojave Desert Kelso dune field example. *Sedimentology*. 46 pp.505-515.

LAING, C.C., 1954. *The ecological life history of the Ammophila breviligulata community on Lake Michigan dunes* (Doctoral dissertation, University of Chicago).

LANCASTER, N., 1986. Dynamics of deflation hollows in the Elands Bay area, Cape Province, South Africa. *Catena* 13 pp.139-153.

LANCASTER, N., 1988. Development of linear dunes in the southwestern Kalahari, southern Africa. *Journal of the Arid Environment*. 14 pp.233-244.

LANCASTER, N., 1995. *Geomorphology of Desert Dunes*. London: Routledge.

LAU, K, -M. and WENG, H., 1995. Climate Signal Detection Using Wavelet Transform: How to Make a Time Series Sing. *Bulletin of the American Meteorological Society.* 76 (12) pp. 2391-2402.

LEE, Z.S. and BAAS, A.C., 2012. Streamline correction for the analysis of boundary layer turbulence. *Geomorphology.* 171 pp.69-82.

LEEGE, L.M. and KILGORE, J.S., 2014. Recovery of foredune and blowout habitats in a freshwater dune following removal of invasive Austrian pine (Pinus nigra). *Restoration Ecology*. 22 pp.641-648.

LEEMING, D., 2006. *The Oxford Companion to World Mythology* [online]. Oxford: Oxford University Press. Available from: https://www-oxfordreference-com.edgehill.idm.oclc.org/view/10.1093/acref/9780195156690.001.0001/acref-9780195156690-e-27?rskey=dkClRN&result=27 [Accessed 10 Mar 2021].

LERMA, A.N., AYACHE, B., ULVOAS, B., PARIS, F., BERNON, N., BULTEAU, T. and MALLET, C., 2019. Pluriannual beach-dune evolutions at regional scale: Erosion and recovery sequences analysis along the aquitaine coast based on airborne LiDAR data. *Continental Shelf Research*. 189 103974. Available from: https://www.sciencedirect.com/science/article/pii/S0278434319303577?via%3Dihub [Accessed 10 Mar 2021].

LETTAU, K. and LETTAU, H., 1977. Experimental and micrometeorological field studies of dune migration. In: LETTAU, K. and LETTAU, H. (eds.) *Exploring the World's Driest Climate*. Madison, WI. University of Wisconsin Press. IES Report 101. Pp.110-147.

LINDELL, J., FREDRIKSSON, C and HANSON, H., 2017. Impact of dune vegetation on wave and wind erosion. *Journal of Water Management and Research*. 73 pp.39-48.

LINDSEY, R., 2021. *Climate Change: Global Sea Level, NOAA* [online]. Available from: https://www.climate.gov/news-features/understanding-climate/climate-change-global-sea-level [Accessed 3 March 2021].

LIU, X., DONG, Z. and WANG, X., 2006. Wind tunnel modelling and measurements of the flux of wind-blown sand. *Journal of Arid Environments*. 66 pp.657-672.

LIVINGSTONE, I. and WARREN, A., 1996. *Aeolian Geomorphology: An Introduction*. Harlow: Longman.

LUNA, M.D., PARTELI, M.D., DURÁN, O. and HERRMANN, H.J., 2011. Model for the genesis of coastal dune fields with vegetation. *Geomorphology.* 129 pp.215-224.

LUNA, M.C.M.D., PARTELI, E.J.R. and HERRMANN, H.J., 2012. Model for a dune field with an exposed water table. *Geomorphology* (159-160) pp.169-177.

LYNCH, K., JACKSON, D.W. and COOPER, J.A.G., 2008. Aeolian fetch distance and secondary airflow effects: the influence of micro-scale variables on meso-scale foredune development. *Earth Surface Processes and Landforms.* 33 (7) pp.991-1005.

LYNCH, K., JACKSON, D.W.T. and COOPER, J.A.G., 2010. Coastal foredune topography as a control on secondary airflow regimes under offshore winds'. *Earth Surface Processes & Landforms.* (35) pp. 344-353.

MACLACHLIN, A., 1991. Ecology of coastal dune fauna. *Journal of Arid Environments*. 21 pp.229-243.

MAPITUK., 2020. Ainsdale ward boundary shapefile. Available from: https://mapit.mysociety.org/ [Accessed 02 Feb 2019].

MARSTON, R.A., 1986. Maneuver-caused wind erosion impacts, South Central, New Mexico. In: NICKLING, W.G. (Ed.). *Aeolian Geomorphology*. The Binghampton Series in Geomorphology. London: Allen and Unwin. Pp.275-290.

MARTÍNEZ, M.L., INTRALAWAN, A., VÁZQUEZ, G., PÉREZ-MAQUEO, O., SUTTON, P. and LANDGRAVE, R., 2007. The coasts of our world: Ecological, economic and social importance. *Ecological economics*, *63*(2-3), pp.254-272.

MASHHADI, N., AHMADI, H., EKHTESASI, M.R., FEIZNIA, S. and FENGHHI, G., 2007. Analysis of sand dunes to determine wind direction and detect sand source site (case study: Khartooran Erg, Iran). *Biaban* (*Desert Journal*). 12 pp.69-75.

MASSELINK, G., 2012. Coasts. In: Holden, J. (Ed.) *An Introduction to Physical Geography and the Environment.* 3rd ed. Harlow: Pearson. pp. 426-466.

MASSELINK, G. and ANTHONY, E.J., 2001. Location and size of intertidal bars on ridge and runnel beaches. *Earth Surface Processes and Landforms*. 26 pp.759–774.

MASSELINK, G., HUGHES, M.G. and KNIGHT, J., 2011. Introduction to Coastal Processes and Geomorphology. 2nd Ed. Abingdon: Routledge.

MATHEW, S., DAVIDSON-ARNOTT, R.G.D. and OLLERHEAD, J., 2009. Evolution of a beach-dune system following a catastrophic storm overwash event: Greenwich Dunes, Prince Edward Island, 1936-2005. *Canadian Journal of Earth Science*. 47 pp.1-18.

MAUN, M.A., 1994. Adaptations enhancing survival and establishment of seedlings on coastal dune systems. *Vegetatio*. 111 pp.59-70.

MAUN, M.A., 2009. *The Biology of Coastal Sand Dunes*. Oxford: Oxford University Press.

MAYAUD, J.R., WIGGS, G.F.S. and BAILEY, R.M., 2016. Characterizing turbulent wind flow around dryland vegetation. *Earth Surface Processes and Landforms.* 41 pp.1421-1436.

MAZZULLO, J., SIMS, D. and CUNNINGHAM, D., 1986. The effects of eolian sorting and abrasion upon the shapes of fine quartz sand grains. *Journal of Sedimentary Petrology*. 56 (1) pp.45-56.

MCEWAN, I.K. and WILLETTS, B.B., 1994. On the prediction of bed-load sand transport rate in air. Sedimentology. 41 pp.1241-1251.

MCKENNA, W., 2007. *An Evolutionary Model of Parabolic Dune Develop: From Blowout to mature parabolic, Padre Island National Seashore, Texas*. MSc thesis. Baton Rouge, LA.: Louisiana State University. Available from: https://digitalcommons.lsu.edu/cgi/viewcontent.cgi?article=5152&context=gradschool_theses [Accessed 3 April 2021].

MCKENNA-NEUMAN, C. and NICKLING, W.G., 1989. A theoretical and wind Tunnel investigation of the effect of capillarity water on the entrainment of sediment by wind. *Canadian Journal of Soil Science.* 69 pp.79-96.

MCTAINISH, G.H., LYNCH, A.W. and BURGESS, R.C., 1990. Wind erosion in eastern Australia. *Australian Journal of Soil Research*. 28 pp.323-339.

MELTON, F.A., 1940. A tentative classification of sand dunes: its application to dune history in the southern High Plains. *Journal of Geology*. 48 pp.113-174.

MENTASCHI, L., VOUSDOUKAS, M.I., PEKEL, J.F., VOUKOUVALAS, E. and FEYEN, L., 2018. Global long-term observations of coastal erosion and accretion. *Scientific Reports*. 8 (12876) pp.1-11. (200)

MIOT DA SILVA, G. and HESP, P.A., 2010. Coastline orientation, aeolian sediment transport and foredune and dunefield dynamics of Moçambique Beach, Southern Brazil. *Geomorphology*. 120 pp.258-278.

MIOT DA SILVA, G., MOUSAVI, S.M.S. and JOSE, F., 2012. Wave-driven sediment transport and beach-dune dynamics in a heartland bay beach. *Marine Geology*. 323-325 pp.29-46.

MIOT da SILVA, G., MARTINHO, C.T., HESP, P.A., KEIM, B. and FERLING, Y., 2013. Changes in dunefield geomorphology and vegetation cover as a response to local and regional climate variations. *Journal of Coastal Research*. SI 65, pp. 1307-1312.

MIR-GUAL, M. and PONS, G.X., 2011. Coast sandy strip fragmentation of a protected zone in the N of Mallorca, Spain (Western Mediterranean). *Journal of Coastal Research*. (SI 64) pp.1367-1371.

MIR-GUAL, M., PONS, G.X., MARTÍN-PRIETO, J.Á., ROIG-MUNAR, F.X. and RODRÍGUEZ-PEREA, A., 2013. Geomorphological and ecological features of blowouts in a western Mediterranean coastal dune complex: a case study of the Es Comú de Muro beach-dune system on the island of Mallorca, Spain. *Geo-Marine Letters.* 33 (2-3) pp.129-141.

MIR-GUAL, M., PONS, G.X., DELGADO-FERNANDEZ, I., GELABERT, B., MARTÍN-PRIETO, J.A. and RODRÍGUEZ-PEREA, A., 2015. La importancia de la primera línea de duna para el estado de conservación de los sistemas de dunas costeras. *Geo-temas.* (15) pp.41-44.

MITASOVA, H., HARDIN, E., STAREK, M., HARMON, R.S. and OVERTON, M., 2011. Landscape dynamics from LiDAR data time series. *Geomorphometry 2011*. Redlands, CA. 7-11 Sept. 2011. pp. 3-6. [Online]. Available from: https://geomorphometry.org/landscape-dynamics-from-lidar-data-time-series/ [Accessed 18 Mar 2019].

MOUNTNEY, N.P. and RUSSELL, A.J., 2009. Aeolian dune-field development in a water table controlled system – Skeiðarársandur, Southern Iceland. *Sedimentology.* 56 (7) pp.2107-2131.

MUHS, D.R. and MAAT, P.B., 1993. The potential response of eolian sands to Greenhouse Warming and precipitation reduction on the Great Plains of the United States. Journal of the Arid Environment. 25 pp.351-361.

MUSILA, W.N., 1998. Composition, structure and distribution of coastal dune vegetation between Malindi and Mambrui. In: HOORWEG, J. (ed.) *Dunes, groundwater, mangroves and birdlife in coastal Kenya*. Nairobi, KE: Acts Press. pp. 17-39 [online]. Available from: https://www.oceandocs.org/bitstream/handle/1834/8871/ktf00585.pdf?sequence=1&isAllowed=y [Accessed 13 Mar 2021].

NICKLING, W.G., 1994. Aeolian sediment transport and deposition. In PYE, K. (ed.). *Sediment Transport and Depositional Processes*. Oxford: Blackwell

NICKLING, W.G. and DAVIDSON-ARNOTT, R.G.D., 1990. Aeolian sediment transport on beaches and coastal sand dunes. In: DAVIDSON-ARNOTT, R.G.D. (Ed.). *Proceedings of the Symposium on Coastal Sand Dunes*. National Research Council of Canada. pp. 1-35.

NICKLING, W.G. and MCKENNA-NEUMAN, C., 1997. Wind tunnel evaluation of a wedge-shaped aeolian sediment trap. *Geomorphology*. 18 pp.333-345.

NIELD, J.M. and WIGGS, G.F.S., 2011. The application of terrestrial laser scanning to aeolian saltation cloud measurement and its response to changing surface moisture. *Earth Surface Processes and Landforms*. 36 pp.273-278.

NIELD, J.M., WIGGS, G.F.S. and SQUIRREL, R.S., 2011. Aeolian sand strip mobility and protodune development on a drying beach: examining surface moisture and surface roughness patterns measured by terrestrial laser scanning. *Earth Surface Processes and Landforms*. 36 pp.513-522.

NORDSTORM, K.F., PSUTY, N. and CARTER, R.W.G. (Eds.). 1990. *Coastal Dunes: Form and Process*. Chichester: Wiley.

NORDSTROM, K.F., JACKSON, N.L. and KOROTKY, K.H., 2011. Aeolian sediment transport across beach wrack. *Journal of Coastal Research*. 59 pp.211-217.

OLIVIER, M.J. and GARLAND, G.G., 2003. Short-term monitoring of foredune formation on the east coast of South Africa. *Earth Surface Processes and Landforms.* 28 pp. 1143 – 1155.

OLSON, J.S., 1958. Lake Michigan dune development 2. Plants as agents and tools in geomorphology. *The Journal of Geology*, 66 (4) pp.345-351.

OWEN, P.R., 1964. Saltation of Uniform Grains in Air. *Journal of Fluid Mechanics*. 20 pp.225-242.

PANARIO, D. and PINEIRO, G., 1997. Vulnerability of oceanic dune systems under wind pattern change scenarios in Uruguay. *Climate Research*. 9 pp.67-72.

PARSONS, D.R., WALKER, I.J. and WIGGS, G.F., 2004. Numerical modelling of flow structures over idealized transverse aeolian dunes of varying geometry. *Geomorphology.* 59 (1-4) pp.149-164.

PEASE, P. and GARES, P.A., 2013. The influence of topography and approach angles on local deflections of airflow within a coastal blowout. *Earth Surface Processes and Landforms.* 38 (10) pp.1160-1169.

PERCIVAL, D.B. and WALDEN, A.T., 2000. *Wavelet methods for time series analysis*. Cambridge: Cambridge University Press

PLATER, A.J. and GRENVILLE, J.S., 2010. Liverpool Bay: linking the eastern Irish Sea to the Sefton coast. In: WORSLEY, A.T., LYMBERY, G., HOLDEN, V.J.C. and NEWTON, M.

(Eds.). *Sefton's Dynamic Coast*. Ainsdale-on-Sea: Coastal Defence: Sefton MBC Technical Services Department. pp. 28-54.

PLUIS, J.L.A., 1992. Relationships between deflation and near surface wind velocity in a coastal dune blowout. *Earth Surface Processes and Landforms*. 17 (7) pp.663-673.

PONTEE, N.I., 2011. Reappraising coastal squeeze: a case study from north-west England. Proceedings of the Institution of Civil Engineers. *Maritime Engineering.* 164 pp. 127-138.

PREOTEASA, L. and VESPREMEANU-STROE, A., 2010. Grain-Size Analysis of the Beach-Dune Sediments and the Geomorphological Significance. *Revisita de Geomorfologie*. 12 pp.73-79.

PROVOOST, S., LAURENCE, M. and EDMONDSON, S.E., 2011. Changes in landscape and vegetation of coastal dunes in northwest Europe: a review. *Journal of Coastal Research*. 15 pp.207-226.

PSUTY, N.P., 1988. Sediment budget and dune/beach interaction. In: PSUTY, N.P. (Ed.). *Journal of Coastal Research*. SI (3) Florida: C.E.R.F. pp.1-4.

PSUTY, N.P., AMES, K., HABECK, A. and LIU, G., 2019. Sediment Budget and Geomorphological Evolution of the Estuarine Dune-Beach System on Three Nourished Beaches, Delaware Bay, New Jersey. *Geosciences 2019*. 9 (1) 16. Available from: https://www.mdpi.com/2076-3263/9/1/16 [Accessed 10 March 2021].

PYE, K., 1983. Coastal Dunes. *Progress in Physical Geography*. 7 pp.531-557.

PYE, K., 1990. Physical and human influences on coastal dune development between the Ribble and Mersey estuaries, north-west England. In: Nordstrom, K.F., PSUTY, N.P. and CARTER, R.W.G.
(Eds.). *Coastal Dunes: Form and Process*. Chichester: Wiley. pp. 339-359.

PYE, K. and BLOTT, S.J., 2008. Decadal scale variation in dune erosion and accretion rates: An investigation of the significance of changing storm tide frequency and magnitude on the Sefton coat, UK. Geomorphology. 102 (3-4) pp.652-666.

PYE, K. and BLOTT, S.J., 2010. Geomorphology of the Sefton Coast sand dunes. In: WORSLEY, A.T., LYMBERY, G., HOLDEN, V.J.C. and NEWTON, M. (Eds.). *Sefton's Dynamic Coast*. Southport: Sefton Council. pp. 131-160.

PYE, K. and BLOTT, S.J., 2016. Assessment of beach and dune erosion and accretion using LIDAR: Impact of the stormy 2013-14 winter and longer term trends on the Sefton Coast, UK. *Geomorphology.* 266. pp.39-56.

PYE, K. and BOWMAN, G.M., 1984. The Holocene marine transgression as a forcing function in episodic dune activity on the eastern Australian coast. In: THOM, B.G. (Ed.). *Coastal geomorphology in Australia*. Sydney: Academic Press. pp. 179-196.

PYE, K. and NEAL, A., 1994. Coastal dune erosion at Formby Point, north Merseyside, England: Causes and mechanisms. *Marine Geology*. 119 pp.39-56.

PYE, K., SAYE, S., and BLOTT, S.J., 2007. Sand dune processes and management for flood and coastal defence. Part 1: Project overview and recommendations. Technical Report FD1302/TR. Department for Environment, Food and Rural Affairs. [online]. Available from: http://sciencesearch.defra.gov.uk/Document.aspx?Document=FD1302_5395_TRP.pdf [Accessed 13 Mar 2021].

PYE, K., BLOTT, S.J. and HOWE, M.A., 2014. Coastal dune stabilisation in Wales and requirements for rejuvenation. *Journal of Coastal Conservation.* 18 pp.27-54.

PYE, K., BLOTT, S.J. and FORBES, N., 2020. Geomorphological and ecological change in a coastal foreland dune system, Sandscale haws, Cumbria, UK: the management challenges posed by climate change. *Journal of Coastal Conservation.* 24**:**64. [online]. Available from: https://doi.org/10.1007/s11852-020-00781-5 [Accessed 13 Mar 2021].

RÄDLER, A.T., GROENEMEIJER, P.H., FAUST, E., SAUSEN, R. and PÚČIK, T., 2019. Frequency of severe thunderstorms across Europe expected to increase in the 21st century due to rising instability. npj *Climate and Atmospheric Science*. 2 (30) pp.1-5.

RHIND, P.M., BLACKSTOCK, T.H. HARDY, H.S., JONES, R.E. and SANDISON, W., 2001. The evolution of Newborough warren dune system with particular reference to the past four decades. In: HOUSTON, J., EDMONDSON, S.E. and ROONEY, P. (Eds.). *Coastal Dune Management, Shared Experience of European Conservation Practice*. Liverpool: Liverpool University Press. pp. 345-379.

RIKSEN, M.J.P.M., GOOSSENS, D., HUISKES, R.H.P.J., KROL, J. and SLIM, P.A., 2016. Constructing notches in foredunes: Effect on sediment dynamics in the dune hinterland. *Geomorphology*. 253 (2016) pp.340-352.

RITCHIE, W., 1972. The evolution of coastal sand dunes. *Scottish Geographical Magazine.* 88 pp.19-35.

RIVERSCAPES CONSORTIUM. 2018*. GCD v7. Download*. [Online]. Available from: https://gcd.riverscapes.xyz/Download/ [Accessed 30 Mar 2018].

ROTNICKA, J., DŁUŻEWSKI, M., DABSKI, M., MIROSŁAW, R., WOJCIECH, W. and ZMARZ, A., 2020. Accuracy of the UAV-Based DEM of Beach–Foredune Topography in Relation to Selected Morphometric Variables, Land Cover, and Multi-temporal Sediment Budget. *Estuaries and Coasts*. 43 pp.1939-1955. Available from: https://link.springer.com/article/10.1007/s12237-020-00752-x#citeas [Accessed 10 Mar 2021].

RUESSINK, B.J., ARENS, S.M., KUIPERS, M. and DONKER, J.A.A., 2017. Coastal dune dynamics in response to excavated foredune notches. *Aeolian Research.* 31 (A) pp.3-17.

RUZ, M-H., ANTHONY, E. and FAUCON, L., 2005. Coastal dune evolution on a shoreline subject to strong human pressure: the Dunkirk area, northern France. In: HERRIER, J-L., MEES, J., SALMAN, A., SEYS, J., VAN NIEUWENHUYSE, H. and DOBBELAERE, J. (Eds.). *Proceedings 'Dunes and Estuaries 2005' International Conference in Natural Restoration Practices in European Coastal Habitats*. Koksijde, Belgium, 19-23 Sept 2005. Available from: https://www.bing.com/search?q=Coastal+dune+evolution+on+a+shoreline+subject+to+strong+human+pressure%3A+the+Dunkirk+area%2C+northern+France&form=ANSPH1&refig=60025b6ff7834d0fb4cd4761c8a9d1aa&pc=U531 [Accessed 7 Feb 2021].

SARRE, R.D., 1989. The morphological significance of vegetation and relief on coastal foredune processes. *Zietschrift für Geomorphologie*. Supplement 73 pp.17-31.

SAWAKUCHI, A.O., KALCHGRUBER, R., GIANNINI, P.C.F., NASCIMENTO, J. D.R., GUEDED, C.C.F. & UNISEDO, N.K., 2008. The development of blowouts and foredunes in the Ilha Comprida barrier (Southeastern Brazil): the influence of Late Holocene climate changes on coastal sedimentation. *Quaternary Science Reviews.* 27 (21-22) pp.2076-2090.

SAYE, S. E., van der WAL, D., PYE, K. and BLOTT, S.J., 2005. Beach-dune morphological relationships and erosion/accretion: An investigation at five sites in England and Wales using LIDAR data. *Geomorphology*. 72 pp.128-155.

SCHATZ, V. and HERMANN, H. J., 2006. Flow separation in the lee side of transverse dunes: A numerical investigation. *Geomorphology*. 81 pp.207-216.

SEELIGER, U., CORDAZZO, C.V., OLIVIERA, C.P. and SEELIGER, M., 2000. Long-term changes of coastal foredunes in the Southwest Atlantic. Journal of Coastal Research. 16 (4) pp.1068-1072.

SEPPALA, M., 1995. Deflation and redeposition of sand dunes in Finnish Lapland. *Quaternary Science Reviews.* 14 (95) pp.799–809.

SHERMAN, D.J., 1995. Problems of scale in the modelling and interpretation of coastal dunes. *Marine Geology*. 1124 (1-4) pp.339-349.

SHERMAN, D.J. and BAUER, B.O., 1993. Dynamics of beach-dune systems. *Progress in Physical Geography.* 17 (4) pp.413-447.

SHERMAN, D.J. and HOTTA, S., 1990. Aeolian sediment transport: theory and measurement. In: NORDSTORM, K.F., PSUTY, N. & CARTER, R.W.G. (eds.) *Coastal Dunes: Form and Process*. Chichester: Wiley. pp. 17–37.

SHERMAN, D.J., BAUER, B.O., GARES, P.A. and JACKSON, D.W.T., 1996. Wind blown sand at Castroville, California. *Coastal Engineering Proceedings*, *1*(25) pp. 4212-4226. Available from: https://icce-ojs-tamu.tdl.org/icce/index.php/icce/article/view/5542/5216 [Accessed 07 Feb 2021].

SHERMAN, D.J., JACKSON, D.W.T., NAMIKAS, S.L. and WANG, J., 1998. Wind-blown sand on beaches: an evaluation of models. *Geomorphology*. 22 pp.113-133.

SHERMAN, D.J., BAILANG, LI., FARRELL, E.J., ELLIS, J.T., COX, W.D. and MAIA, L.P., 2011. Measuring Aeolian Saltation: A Comparison of Sensors. *Journal of Coastal Research.* SI 59 pp.280-290.

SHERMAN, D.J., BAILANG, L., ELLIS, J.T., FARRELL, E.J., PARENTE MAIA, L. and GRANJA, H., 2013. Recalibrating aeolian sand transport models. *Earth Surface Processes and Landforms*. 38 pp.169-178.

SHORT, A.D. and HESP, P.A., 1982. Wave, beach and dune interactions in south-east Australia. *Marine Geology*. 48 pp.259-284.

SIMM, J., ORSINI, A., BLANCO B., LEE, A., SANDS, P., WILLIAMS, J., CAMILLERI, A. and SPENCER, R., 2020. *Groynes in coastal engineering. Guide to design, monitoring and maintenance of narrow footprint groynes (C793F).* CIRIA. [online]. Available from: https://www.ciria.org/ItemDetail?iProductCode=C793F&Category=FREEPUBS&WebsiteKey=3f18c87a-d62b-4eca-8ef4-9b09309c1c91 [Accessed 4 Jul 2020].

SLAYMAKER, O., 2009. The Future of Geomorphology. *Geography Compass*. 1/3 pp.329-349.

SMALL, C. and NICHOLLS, R., 2003. A global analysis of human settlement in coastal zones. *Journal of Coastal Research*. 19 (3) pp.584-599

SMITH, M.W., 2015. Section 2.1.5. Direct acquisition of elevation data: Terrestrial Laser Scanning. In: COOK, S.J., CLARKE, L.E. and NIELD, J.M. (Eds.). *Geomorphological Techniques*. (Online Edition) London, UK. ISSN: 2047-0371. Available from: https://www.geomorphology.org.uk/sites/default/files/chapters/2.1.5_TLS_0.pdf [Accessed 7 Feb 2021]

SMITH, P.H., 2009. *The Sands of Time Revisited – An introduction to the sand dunes of the Sefton Coast*. Stroud: Amberley

SMITH, P.H., 2014. Personal account. (E-Mail communication on 16 Mar 2014).

SMITH, P.H. and LOCKWOOD, P.A., 2013. *Changing flora of a sand-dune blow-out on the Sefton Coast, Merseyside.* (draft) Unpublished Report.

SMYTH, T.A.G. and HESP, P. A., 2016. Numerical Modelling of Turbulent Flow Structures in a Trough Blowout. *Journal of Coastal Research.* SI 75 pp.328-332.

SMYTH, T. A. G., JACKSON, D. W. T. and COOPER, J. A. G., 2012. High resolution measured and modelled three-dimensional airflow over a coastal bowl blowout. *Geomorphology.* (177-178) pp.62-73.

SMYTH, T. A. G., JACKSON, D. W. T. and COOPER, J. A. G., 2013. Three dimensional airflow patterns within a coastal trough-bowl blowout during fresh breeze to hurricane force winds. *Aeolian Research.* (9) pp.111-123.

SMYTH, T.A.G., JACKSON, D.W.T. and COOPER, J.A.G., 2014. Airflow and aeolian sediment transport patterns within a coastal trough blowout during lateral wind conditions. *Earth Surface Processes and Landforms*. 39 (4) pp.1847-1854.

SMYTH, T.A.G., THORPE, E. and ROONEY, P., 2020a. Blowout evolution between 1999 and 2015 in Ainsdale Sand Dunes, National Nature Reserve, England. *North West Geography*. 20 (1) pp.1-13.

SMYTH, T.A.G., DELGADO-FERNANDEZ, I., JACKSON, D.W.T., YURK, B. and ROONEY, P., 2020b. Greedy parabolics: wind flow direction within the deflation basin of parabolic dunes is governed by deflation basin width and depth. *Progress in Physical Geography: Earth and Environment*. 44 (5) pp.643-660.

STERK, G., JACOBS, A.F.G. and van BOXEL, J.H., 1998. The effect of turbulent flow structures on saltation sand transport in the atmospheric boundary layer. *Earth Surface Processes and Landforms.* 23 pp.877-887.

STRAHLER, A.N., 1950. Equilibrium theory of erosional slopes, approached by frequency distribution analysis. *American Journal of Science.* 248 pp. 673-96 and 800-14.

STRAHLER, A.N., 1952. Dynamic basis of geomorphology. *Bulletin of the Geological Society of America.* 63 pp. 923-38.

STRAHLER, A.N., 1980. Systems theory in physical geography. *Physical Geography.* 1 pp.1-27.

STRYPSTEEN, G., HOUTHUYS, R. and RAUWOENS, P., 2019. Dune volume change at decadal timescales and its relation with potential aeolian transport. *Journal of Marine Science and Engineering*. (7) 357 pp.1-24.

SUN, Y., HASI, E., LIU, M, H., DU., H., GUAN, C. and TAO, B., 2016. Airflow and sediments movement within an inland blowout in Hulun Buir sandy grassland, Inner Mongolia, China. *Aeolian Research,* 22 pp. 13-22.

SUN, Y., ZHONG, Z., LI, T., YI, L., HU, Y., WAN, H., CHEN, H., LIAO, Q., MA, C. and LI, Q., 2017. Impact of Ocean Warming on Tropical Cyclone Size and Its Destructiveness. *Scientific Reports*. 7 (8154) pp.1-10.

SUTER-BURRI, K., GROMKE, C., LEONARD, K.C. and GRAF, F., 2013. Spatial patterns of aeolian sediment deposition in vegetation canopies: Observations from wind tunnel experiments using colored sand. *Aeolian Research*. 8 pp.65-73.

SWEET, M.L. and KOCUREK, G., 1990. An empirical model of aeolian dune lee-face airflow. *Sedimentology*. 37 pp.1023-1038.

TAHERKHANI, M., VITOUSEK, S., BARNARD, P., FRAZER, N., ANDERSON, T.R. and FLETCHER, C.H., 2020. Sea-level rise exponentially increases coastal flood frequency. *Scientific Reports*. 10 (6466) pp.1-17.

THOM, B., HESP, P. and BRYANT, E., 1994. Last glacial "coastal" dunes in Eastern Australia and implications for landscape stability during the Last Glacial Maximum. *Palaeogeography, Palaeoclimatology, Palaeoecology*. 111 (3-4) pp.229-248.

THORNTON, E.B., HUMISTON, R.T. and BIRKEMEIER, W., 1996. Bar/trough generation on a natural beach. *Journal of Geophysical Research: Oceans*. 101 (C5) pp.12097-12110.

TORRENCE, C. and COMPO, G.P., 1998. A practical guide to wavelet analysis. *Bulletin of the American Meteorological Society*. 79 pp.61-78.

TSOAR, H., 2005. Sand dunes mobility and stability in relation to climate. *Physica A*: Stat. Mech. Appl. 357 (1) pp.50-56.

UDO, K., KURIYANA, Y. and JACKSON, D.W.T., 2008. Observations of wind-blown sand under various meteorological conditions at a beach. *Journal of Geophysical Research*. 113 (F4) pp.1-15 [online]. Available from: https://agupubs.onlinelibrary.wiley.com/doi/epdf/10.1029/2007JF000936 [Accessed 19 Mar 2021].

UKCEH, UK Sand Dune and Shingle Network and Dynamic Dunescapes partners., 2021. *The Sand Dune Managers Handbook*. Version 1, June 2021. Produced for the Dynamic Dunescapes (DuneLIFE) project: LIFE17 NAT/UK/000570; HG-16-08643. [online]. Available from: https://dynamicdunescapes.co.uk/ [Accessed 12 July 2021].

VAN BOXEL, J.H., JUNGERIUS, P.D., KIEFFER, N. and HAMPELE, N., 1997. Ecological effects of reactivation of artificially stabilized blowouts in coastal dunes. *Journal of Coastal Conservation.* 3 pp.57-62.

VAN DER WAL, D., 1998. Effects of fetch and surface texture on aeolian sand transport on two nourished beaches. *Journal of Arid Environments*. 39 (3) pp.533-547.

VERSTAPPEN, H.T., 1968. On the origins of longitudinal (seif) dunes. *Zeitschrift fur Geomorphologie*. N.F. 12 pp.200-220.

VITOUSEK, S., BARNARD, P., FLETCHER, C., FRAZER, N., ERIKSON, L. and STORLAZZI, C.D., 2017. Doubling of coastal flooding frequency within decades due to sea-level rise. *Scientific Reports*. 7 (1399) pp.1-9.

VON KARMAN, T.H., 1931. *Mechanical Similitude and Turbulence, Technical Memorandum 611*. [online]. Washington DC: National Advisory Committee for Aeronautics. Available from: https://authors.library.caltech.edu/47900/1/19930094805.pdf [Accessed 27 Mar 2021].

WAKES, S.J., MAEGLI, T., DICKINSON, K.J. and HILTON, M.J., 2010. Numerical modelling of wind flow over a complex topography. *Environmental Modelling & Software*. 25 (2) pp.237-247.

WALKER, I.J., 1999. Secondary airflow and sediment transport in the lee of a reversing dune. *Earth Surface Processes and Landforms.* 24 (5) pp.437-448.

WALKER, I.J., 2005. Physical and logistical considerations of using ultrasonic anemometers in aeolian sediment transport research. *Geomorphology*. 68 pp.57-76.

WALKER, I.J. and NICKLING, W.G., 2002. Dynamics of secondary airflow and sediment transport over and in the lee of transverse dunes. *Progress in Physical Geography.* 26 (1) pp.47-75.

WALKER, I.J., HESP, P.A., DAVIDSON-ARNOTT, R.G.D. and OLLERHEAD, J., 2006. Topographic steering of alongshore airflow over a vegetated foredune: Greenwich Dunes, Prince Edward Island, Canada. *Journal of Coastal Research*. 22 (5) pp.1278-1291.

WALKER, I.J., HESP, P.A., DAVIDSON-ARNOTT, R.G.D. and OLLERHEAD, J., 2009. Response of three-dimensional flow to variations in the angle of incident flow and profile form of dunes: Greenwich Dunes, Prince Edward Island, Canada. *Geomorphology*. 105 pp.127–138.

WALKER, I.J., DAVIDSON-ARNOTT, R.G.D., BAUER, B.O., HESP, P.A., DELGADO-FERNANDEZ, I., OLLERHEAD, J. and SMYTH, T.A.G., 2017. Scale dependent perspectives on the geomorphology and evolution of beach-dune systems. *Earth Science Reviews*. 171 pp.220-253.

WANG, X., EERDUN, H., ZHOU, Z. and LIU, X., 2007. Significance of variations in the wind energy environment over the past 50 years with respect to dune activity and desertification in arid and semiarid northern China. *Geomorphology*, 86 (3-4) pp.252-266.

WERNETTE, P., HOUSER, C. and BISHOP, M.P., 2016. An automated approach for extracting Barrier Island morphology from digital elevation models. *Geomorphology*. 262 pp.1-7.

WHEATON, J.M., BRASINGTON, J., DARBY, S.E. and SEAR, D.A., 2010. Accounting for uncertainty in DEMs from repeat topographic surveys: improved sediment budgets. *Earth surface processes and landforms.* 35 (2) pp.136-156.

WIGGS, G.F.S. and WEAVER, C.M., 2012. Turbulent flow structures and aeolian sediment transport over a barchan sand dune. *Geophysical Research Letters*. 39 (5) pp.1-7.

WIGGS, G.F.S., LIVINGSTONE, I. and WARREN, A., 1996. The role of streamline curvature in sand dune dynamics: evidence from the field and wind tunnel measurements. *Geomorphology*. 17 pp.29-46.

WIGGS, G.F.S., ATHERTON, R.J. and BAIRD, A.J., 2004. Thresholds of aeolian sand transport: establishing suitable values. Sedimentology. 51 (1) pp.95-108.

WILLETTS, B.B., RICE, M.A. and SWAINE, S.E., 1982. Shape effects in aeolian grain transport. *Sedimentology*. 29 (3) pp.409-417.

WILLIAMS, G.W., 1964. Some aspects of the eolian saltation load. *Sedimentology*. 3 pp.257-287.

WOLFE, S.A. and NICKLING, W.G., 1993. The protective role of sparse vegetation in wind erosion. Progress in Physical Geography. 17 pp.50-68.

WRIGHT, L.D. and THOM, B.G., 1977. Coastal depositional landforms: a morphodynamics approach. *Progress in Physical Geography*. 1 pp. 412-459.

YANG, Y. and DAVIDSON-ARNOTT, R.G.D., 2005. Rapid measurement of surface moisture content on a beach. *Journal of Coastal Research*. 21 (3) pp.447-452.

ZINGG, A. W., 1953. Wind tunnel studies of the movement of sedimentary material. *Proceedings of the 5th Hydraulic Conference*. Bulletin 34 Institute of Hydraulics. pp. 111-135.

APPENDICES

APPENDIX 1 - Full description of time-series

Key

c m: counts per minute

U: mean wind speed (m s^{-1})

Dir: wind direction (° degrees)

TKE: turbulent kinetic energy (m^2 s^{-2})

CV: coefficient of variation of U (%)

ntt: normalised transport intensity (%)

AP: activity parameter (scale of 0 to 1 per minute)

A map of instrument locations is included to facilitate reading of Appendix.

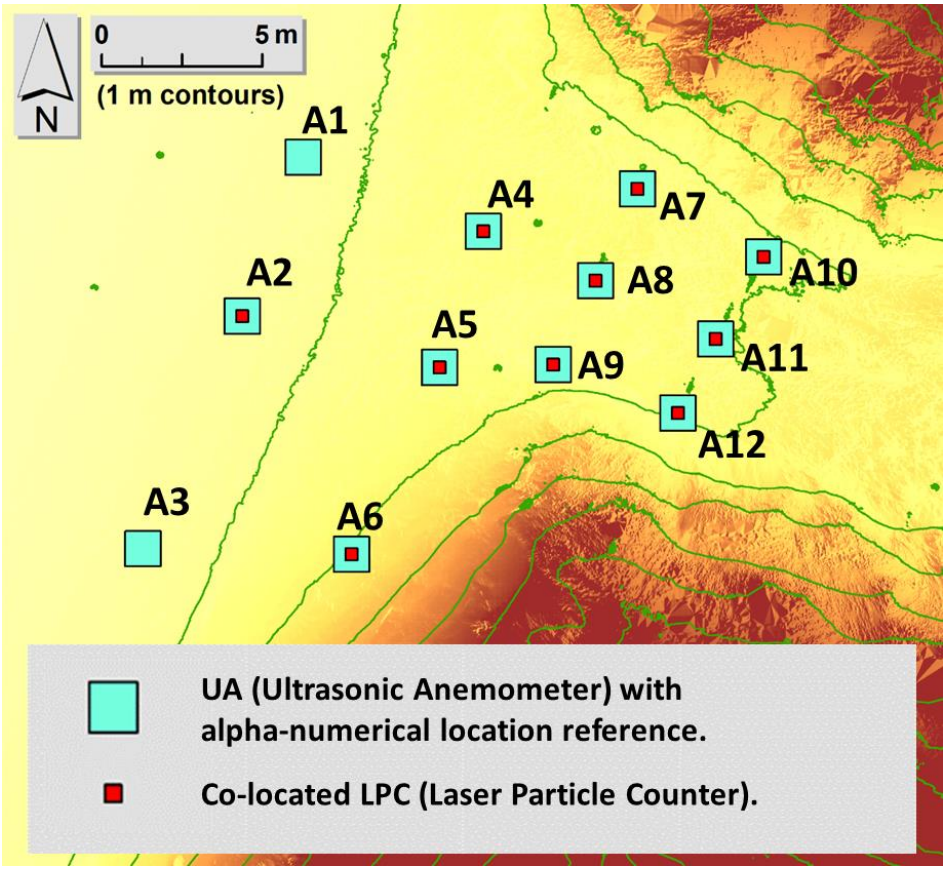

Figure AP1.1: Instrument grid

A2 transport and airflow (full time-series)

Total transport at A2 was the fifth highest of all locations, with a total count of 56,863. Visually the plotted time-series of transport intensity had a closer resemblance to the plotted time-series of total wind speed, than for any other

location. Although some of the peaks and troughs in either time-series varied in magnitude, almost all increases, and decreases in wind speed, were reflected in matching changes in transport intensity. This location appearing to have the closest relationship between wind speed and transport intensity, likely relates to its topographic setting. Located on the beach, upwind of the more complex dune topography, means its surface topography is closer to the 'idealised' flat surface upon which deterministic transport models are based. Each of the five highest peaks in transport intensity over the 84 minutes of measurement, occurred during one of the five minutes when winds speeds were also at their highest (Table AP1).

Table AP1.1: Peak values in A2 counts and mean total wind speeds.

Minute	Actual counts	Rank in time-series	Mean total *u* (m s^{-1})	Rank in time-series
16:57	2,942	1st	6.92	1st
16:52	2,000	2nd	6.9	2nd
16:53	1,636	3rd	6.78	4th
16:59	1,565	4th	6.89	3rd
16:27	1,474	5th	6.72	5th

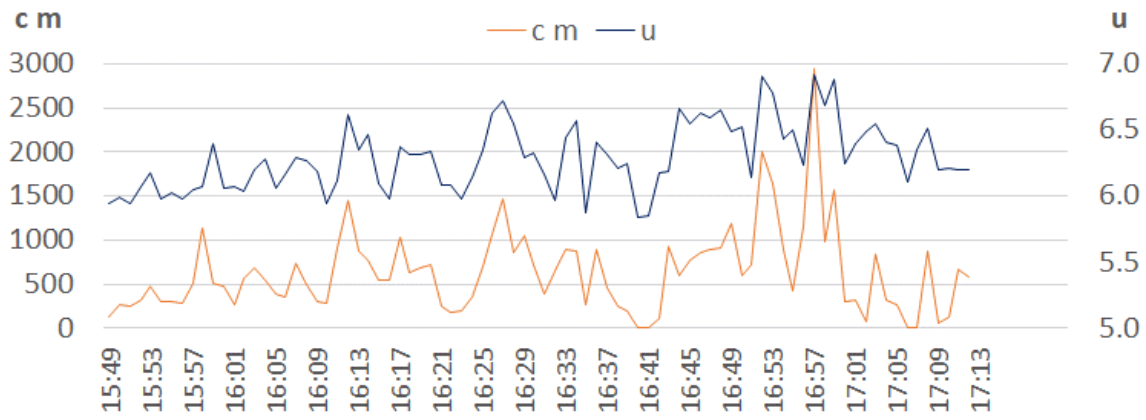

Figure AP1.2: A2 transport intensity and mean wind speed

The σ of wind speed (0.25) was the lowest of all locations where transport was recorded, as was the CV of wind speed at 4%. The maximum mean wind speed of 6.92 m s^{-1} during minute 16:57, was also the lowest maximum mean wind speed

for any location where transport was also measured. Although there are two noticeable peaks in the transport record (ca. 16:52 and 16:57, Fig. AP2), both are less prominent than peaks in transport at other locations. An explanation for this again is topographic setting. A2 is located on the back-beach. All other locations with LPC sensors were either within the trough, or near elevated dune topography. Such locations have an increased potential for enhancements to incident wind speed (via flow compression, or acceleration of attached/steered flow).

On occasions, peaks and/or troughs in the TKE time-series, coincided with peaks or troughs in transport intensity. Visually the relationship between TKE and transport intensity was far less evident at A2, than the relationship between wind speed and transport intensity (Fig. AP3).

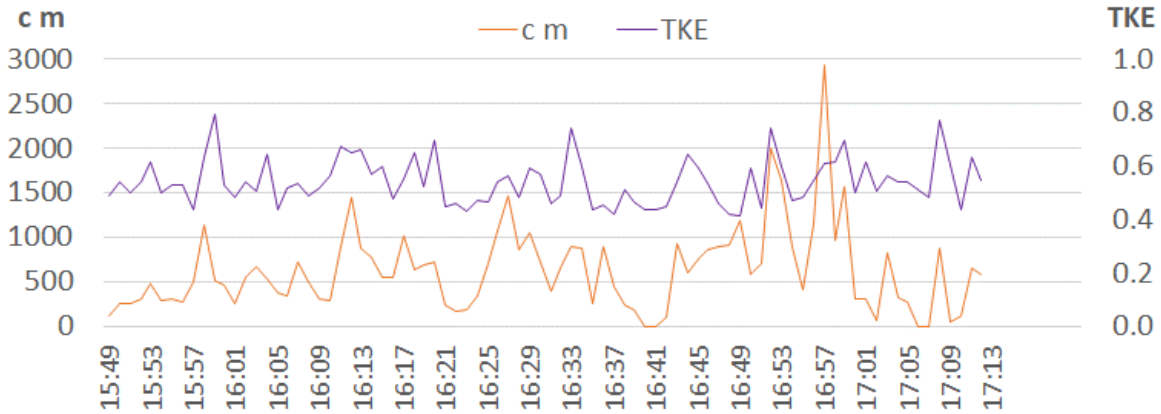

Figure AP1.3: A2 transport intensity and TKE

Of all sensor locations where LPCs were positioned, mean wind direction at A2 had the highest directional range (of 20.5°), and also the highest σ of direction at 4.6. A2, located in an upwind position, on the back-beach, has the most 'open' topographic setting. Fluctuations in wind direction at more landward locations will to varying degrees, be suppressed through proximity to dune topography (via flow steering, attachment of flow, and/or flow compression), reducing the potential range of wind direction, and σ of direction in the time-series. The main point of interest in relation to wind direction and transport at A2, is the occurrence of clear

divergence between direction of the transport, and airflow vectors. The LPC laser path was orientated perpendicular to orientation of the incoming streamers traversing the inter-tidal beach. This orientation was approximately 250° at outset, also being strongly aligned with the hourly mean wind direction, recorded at the local meteorological station in Crosby. During the first hour of the time-series, although there is considerable fluctuation, the wind direction recorded at A2 (40 cm above the surface), is approximately 189°. The transport vector, estimated visually from field observations, and presumably the very near-surface flow vector within the transport zone, therefore differed from the measured airflow vector, at 40 cm above the surface, by approximately 60°.

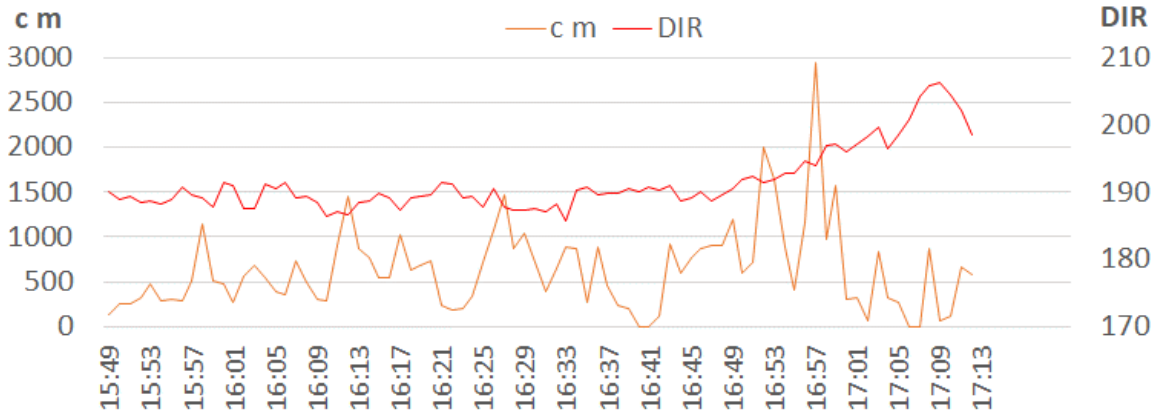

Figure AP1.4: A2 transport intensity and wind direction

Following the two pronounced peaks in transport intensity at 16:52 and 16:57, from 17:01 onwards there is a marked reduction in transport intensity that coincides with a change in wind direction from 196° 206.2°. The change in wind direction could have resulted in a change in near-surface airflow, and as a consequence, It could be therefore, that during this period, the measured transport intensity is under-representative of actual transport, as the laser pathway of the LPC becomes less well aligned with the orientation of incoming streamers.

No relationship between the mean CV of wind speed, and transport intensity at A2 was evident on visually inspection (Fig. AP5). This location had the third lowest

mean CV of wind speed, and the lowest CV of 1 min mean wind speed values, suggesting steadier flow. Being in the location, least proximal to dune topography, may indicate that heightened levels of CV elsewhere in the grid, are derived topographically, i.e., topography enhances lower magnitude fluctuations present in upwind incident flow on the back-beach.

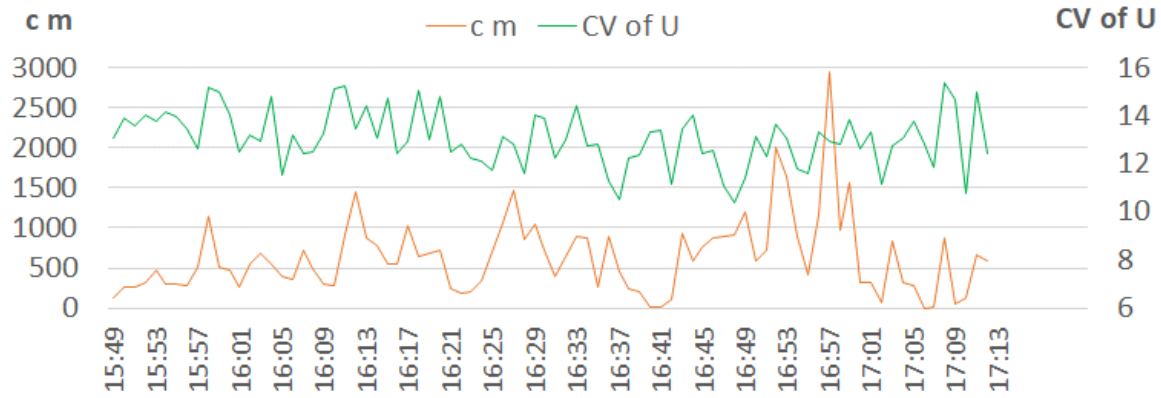

Figure AP1.5: A2 transport intensity and CV of wind speed.

A4 transport and airflow (full time-series)

Total grain counts at A4 was the 4th highest of all locations at 56,863. Its location was on the central axis of the trough at the beach-dune interface. The pattern of at-a-point wind is very similar to that of sediment transport intensity, especially during the first 70 minutes of the time-series. Transport intensity increased with wind speed from approximately 16:40 to 17:00. This was followed by a few minutes of relatively low transport, diverging from high wind speeds, until the highest peak in wind speed was registered at 17:07, and generated a pronounced peak in transport at ca. 17:08. An obvious trend within the transport time-series was a 1 minute lag time, with marked peaks in transport tending to occur 1-2 minutes following wind speed peaks. The five highest peaks in transport activity provides an example (Table AP2).

Table AP1.2: A4 ranked minutes of peaks in transport intensity and wind speed.

Minute	Actual counts	Rank in time-series	Preceding minute	Mean total *u* (m s^{-1})	Rank in time-series
17:08	4,939	1st	17:07	7.49	1st
16:57	4,913	2nd	16:56	7.12	3rd
16:59	3,510	3rd	16:58	7.16	2nd
16:52	3,111	4th	16:51	6.92	6th
17:09	1,927	5th	17:08	7.05	4th

Transport intensity fluctuated at very low levels for the majority of data collection, and then rose considerably, during the final thirty minutes, (additionally including some extreme peaks during this final period). These two highly contrasting transport regimes were therefore the cause of a lack of normality for the full 84 minute data population.

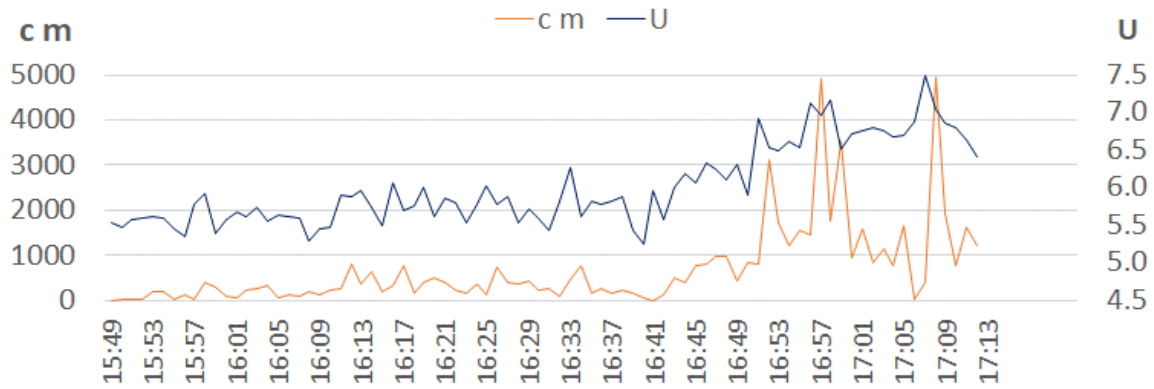

Figure AP1.6: A4 transport intensity and wind speed2

Mean and maximum values of TKE were slightly higher at A4, than on the back-beach. Occasionally TKE peaks preceded peaks in transport but this tended to occur more towards the end of the time series and visually the plotted time series of TKE was far less similar to transport than the plotted total wind speed series.

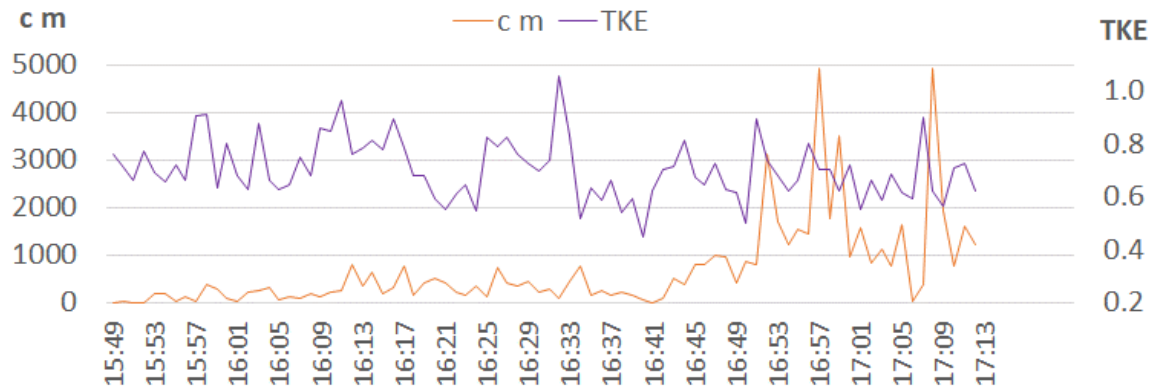

Figure AP1.7: A4 transport intensity and TKE

Again, similar to at A2, there appeared to be a marked divergence between the direction of the transport vector, and wind direction, measured at 40 cm above the surface. The laser path of the LPC at A4 was ca. perpendicular to the regional wind direction recorded at Crosby, and to streamers approaching the blowout across the inter-tidal beach (~250°). The mean wind direction measured at 40 cm above the bed, for the first 70 minutes, was however 213°, with the vector therefore almost perfectly aligned with the orientation of the foredune. As wind direction began to shift from alongshore to very oblique onshore, transport intensity began to increase (Fig. AP8). This shift in wind direct coincided with an overall trend of slightly decreasing, and lower magnitude fluctuations in TKE, increasing wind speed, and decreasing CV of wind speed.

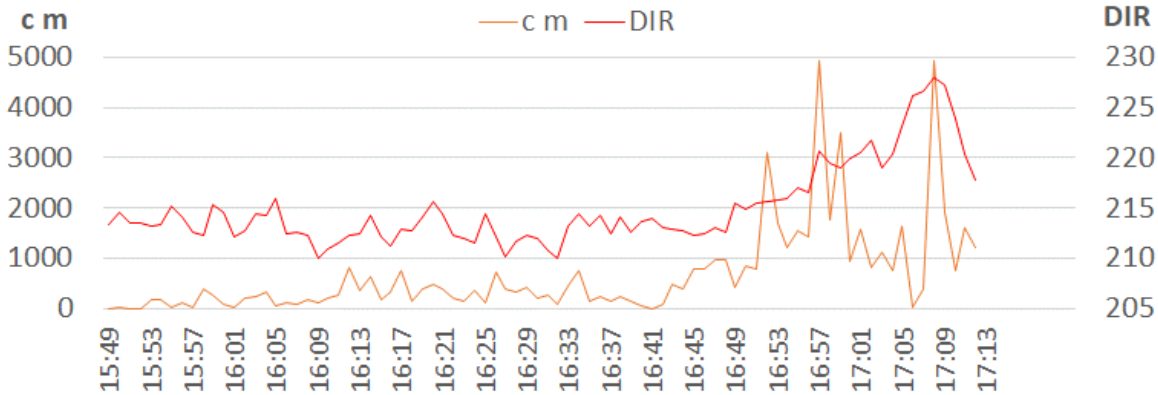

Figure AP1.8: A4 transport intensity and wind direction

At A4 there was no obvious relationship between minute by minute oscillations in CV, and transport intensity (Fig. AP9). However, CV of mean wind speed continually decreased, experienced its lowest level during the final 30 minutes, and this coincided with the highest levels of transport.

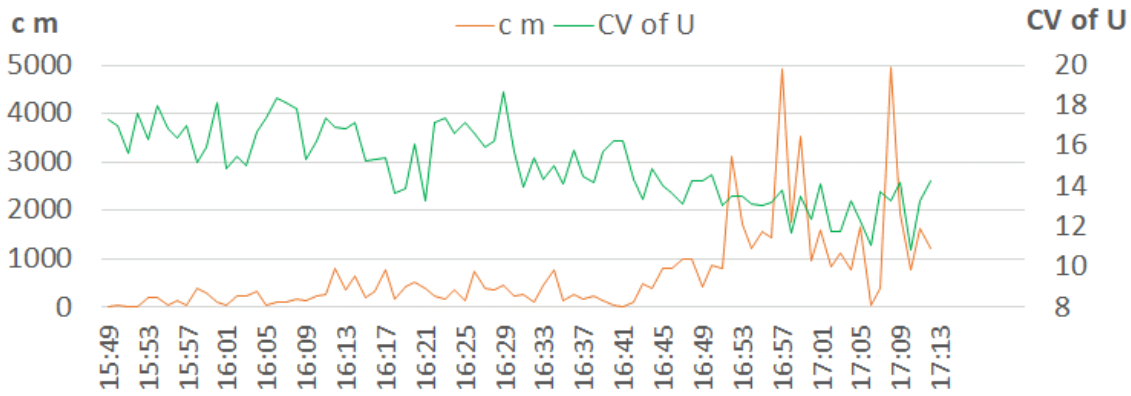

Figure AP1.9: A4 transport intensity and CV of wind speed

A5 transport and airflow (full time-series)

A5 had the second highest mean wind speed of all sensors, and the 4th highest maximum mean wind speed in any one minute, but the total grain count of 13,494 was the third lowest of all sensors. Located at the foot of the foredune-blowout entrance, the high magnitude transport being driven along the foredune towards A5, measured at the upwind location of A6, appears to have bypassed this LPC. It is also possible that although well aligned with incoming streamers from the beach, the sensors 'field-of-view' may have been partially obstructed by the micro-topography of the foredune toe and back-beach. However, a similar trend is observed at A9 and A12, suggesting that if the sensor orientation played a role in this low measurement, it is likely to have been a secondary factor.

The A5 transport regime was intermittent, and grain counts frequently drop to zero, or only trace levels. There is no obvious relationship between wind speed and transport intensity during the time-series. In fact, the majority of the higher peaks

in transport intensity occur early in the time-series, whilst wind speeds are markedly higher towards the end (Figure AP10).

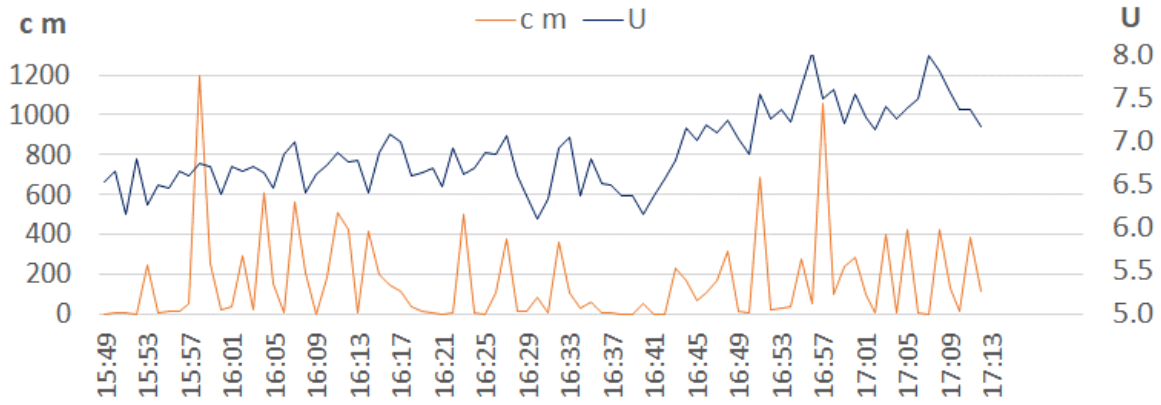

Figure AP1.10: A5 transport intensity and wind speed

Absolute values of TKE were the lowest of all non-beach sensors. The highest peak in grain counts, of 1,198, coincided with maximum TKE of 0.92 m^{-2} s^{-2} at 15:58. The second highest transport occurred at 16:57, in the minute following the third highest TKE peak, whilst the third highest transport occurred at 16:52, in the minute after the second highest TKE. There is however no obvious visual trend between TKE and transport intensity over the full time-series duration.

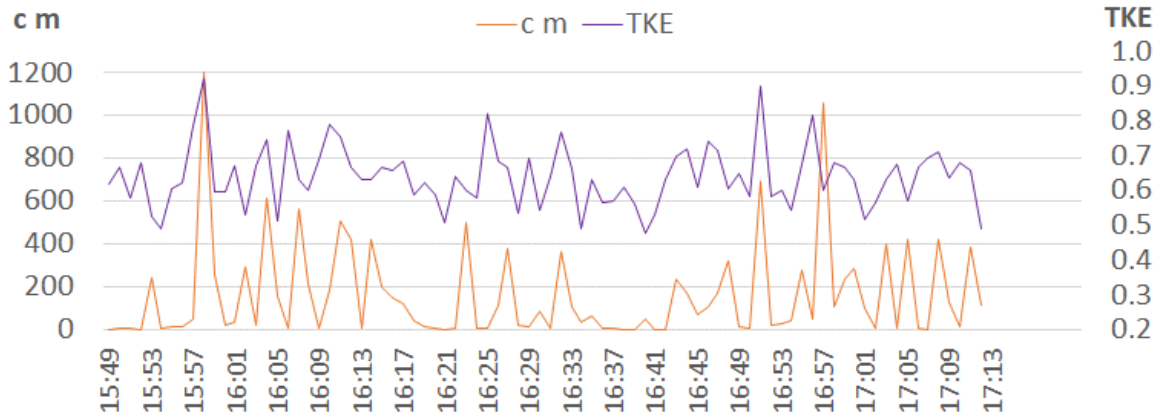

Figure AP1.11: A5 transport intensity and TKE

The mean wind direction of A5 over the 84 minutes, was just over 5° greater than at A4, the immediately downwind/longshore sensor. At the centre of the throat, airflow at A4 was closer to alongshore, whilst at the southern edge of the throat (A5), airflow was in general, more landward directed. In the final 20-30 minutes of

measurement, in addition to airflow at both sensors becoming more onshore directed, the near constant difference between them in degrees, narrowed to the point that directions were almost perfectly aligned at both sensors. Whilst the patterns of wind direction fluctuations were close to identical, fluctuations at A4, a few metres further from the foredune, were slightly greater in magnitude (Fig. AP12).

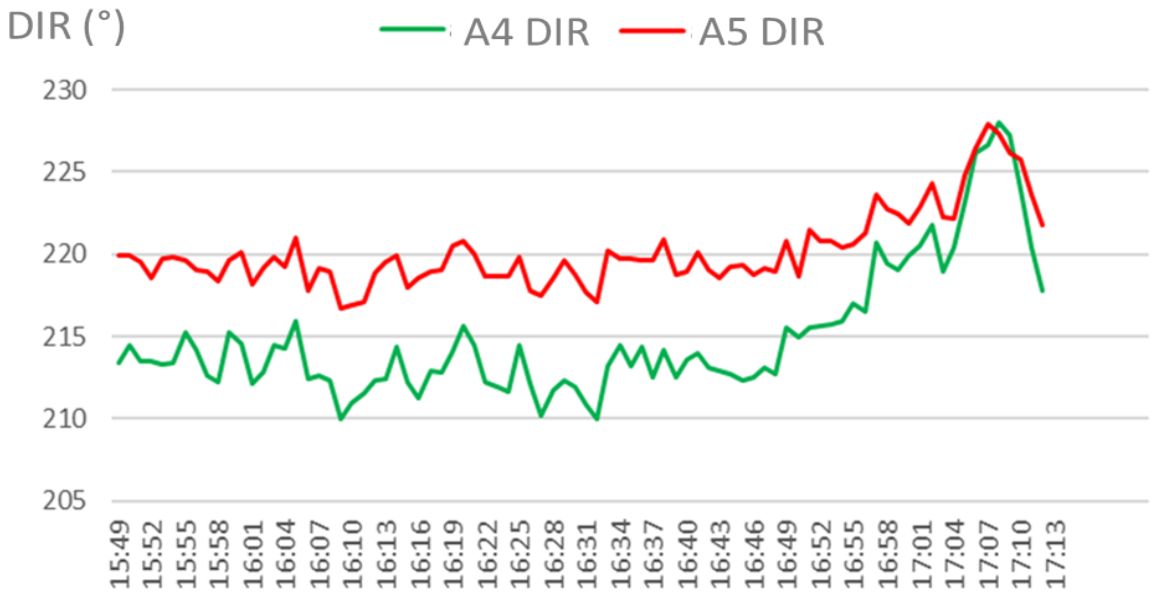

Figure AP1.12: A4 and A5 wind direction

The plotted times-series of transport intensity and wind direction showed no visible similarities throughout the duration of measurement (Fig. AP13).

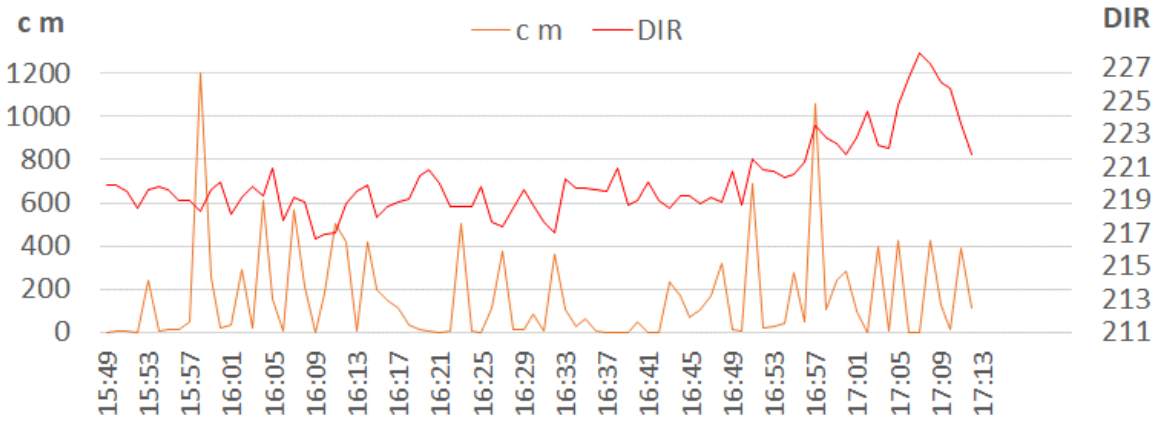

Figure AP1.13: A5 transport intensity and wind direction

The plotted times series of transport and CV of wind speed at A5 showed no visible similarities for the duration of measurement (Fig. AP14). A5 had the second

lowest mean CV of wind speed over the 84 minutes, (and the third lowest CV of the 84 individual, 1 min mean values for CV of wind speed). CV of wind speed at A5 made slight fluctuations about its mean value for the first circa 60 minutes of the time-series, before still fluctuating but reducing to a lower mean level for the remainder of the experiment.

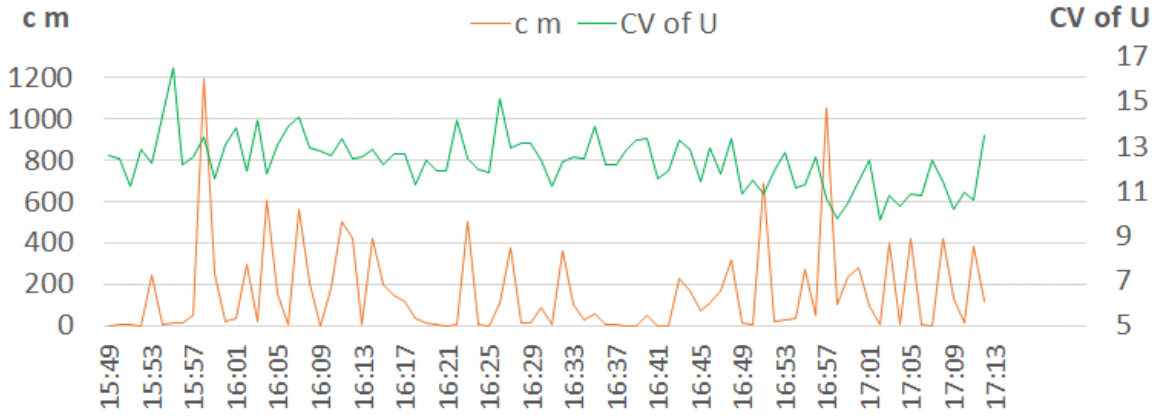

Figure AP1.14: A5 transport intensity and CV of wind speed

A6 transport and airflow (full time-series)

A6 recorded the highest magnitude transport intensity throughout the grid, for the entire duration of the experiment. A clear positive relationship can be seen between mean wind speed and transport intensity (Fig. AP15). Although higher wind speeds generally result in higher magnitude transport intensity, and reduced wind speeds with lower magnitude transport, the degree to which this is proportional, is variable throughout the 84 minutes.

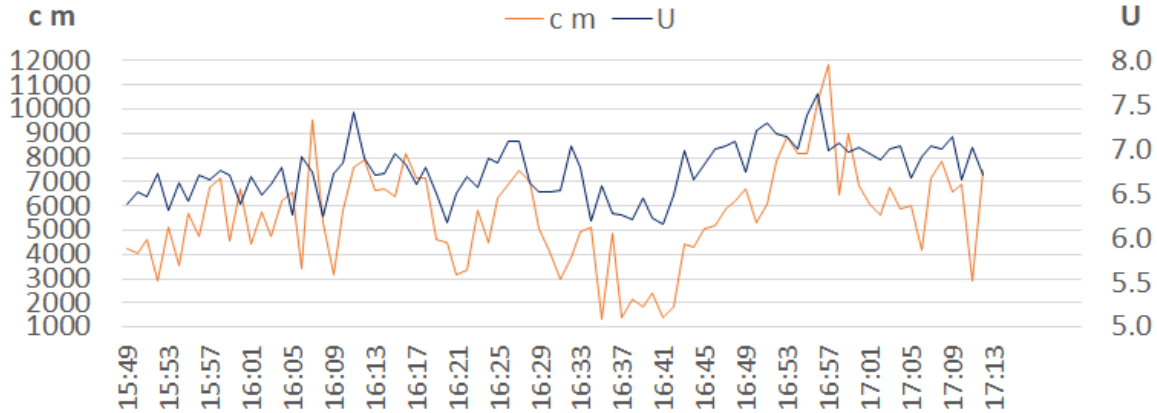

Figure AP1.15: A6 transport intensity and wind speed

A generally positive relationship can be seen between transport intensity and TKE, with a 1 minute lag often present, between TKE peaks occurring, and subsequently the peaks in transport intensity (Fig.AP16).

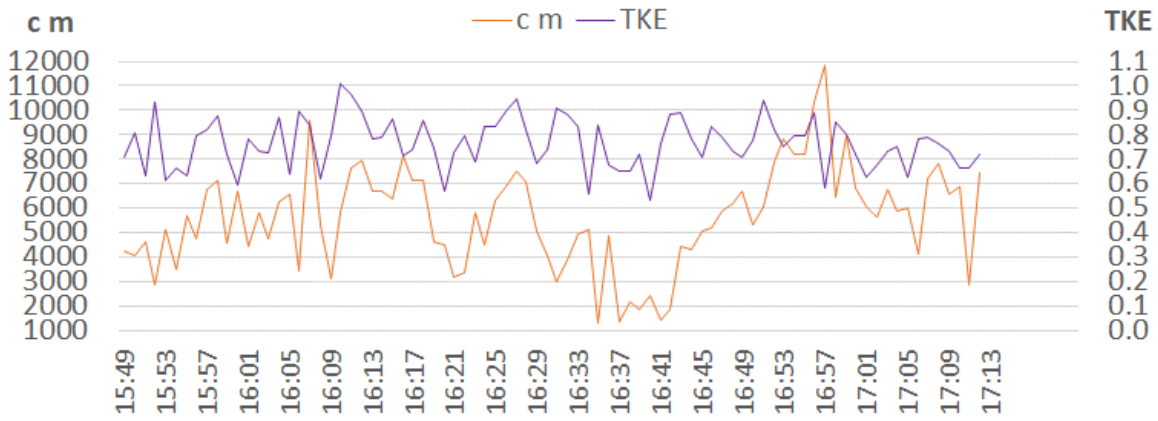

Figure AP1.16: A6 transport intensity and TKE

As a proportion of incident flow is steered downwind, and alongshore, in the very near surface (again evidenced by observed saltation), airflow from upwind positions on the foredune is arriving to the sensor location. Whilst incident flow will be broadly similar at upwind locations on the foredune, for the proportion of airflow being deflected longshore, gusts of higher wind speeds within this flow have a travel time before they arrive at the sensor location, as too will streamers being driven along the foredune. The transport signal at the sensor location will therefore comprise instantaneous saltation, associated with the at-a-point wind field in that moment, plus potentially pulses of sediment from upwind locations associated with preceding gusts.

For now the transport signal at A6 remains unresolved. There are multiple potential factors influencing flow and sediment transport here – some of which may be in the immediate vicinity of the sensor, whilst others will be associated with airflow and transport dynamics upwind, both on the foredune, and on the beach. Further layers of evidence in subsequent steps may provide additional clues. It is likely wind direction will play a key role. Airflow approaching the foredune more

directly is likely to experience greater levels of reflection, which in turn may also be associated with heightened turbulence, and potentially could also play a role in influencing at-a-point entrainment. For flow approaching more obliquely, a greater proportion of mass and momentum will be transferred onto and across the foredune surface. This is of course going to influence near surface flow characteristics and transport dynamics at the point, with these processes subsequently influencing locations downwind along the foredune. Short term fluctuations in wind direction upwind will influence wind speed and turbulence in the immediate location of interacting with the foredune, and thus have instantaneous implications to sediment transport, but as the proportions of airflow reflection, and deflection associated with the transfer of mass and momentum will be in continuous flux, so too will time lags in relation to downwind areas. This may confound fully resolving transport dynamics at A6. Rather than offer suggestions grounded in aeolian science but based on limited evidence, A6 airflow and transport will be re-visited if further clues are identified.

Wind direction and transport intensity at A6 appear unrelated (Fig. AP17). A key preliminary finding of data analysis was that this sensor location provided very clear evidence of pronounced divergence between the direction of the airflow vector, with that of the transport vector. The LPC laser pathway was orientated perpendicular to the orientation of the foredune, and was mounted with its horizontal plane parallel to the underlying topography. The instruments deployed at A6 on the foredune were re-located from another position shortly before data-logging commenced, as the seaward face of the foredune was visibly the area of maximum transport activity. Dense saltation streamers were evident across much of the foredune, and were passing through the laser pathway whilst deploying the instrument, and prior to launching the data logger.

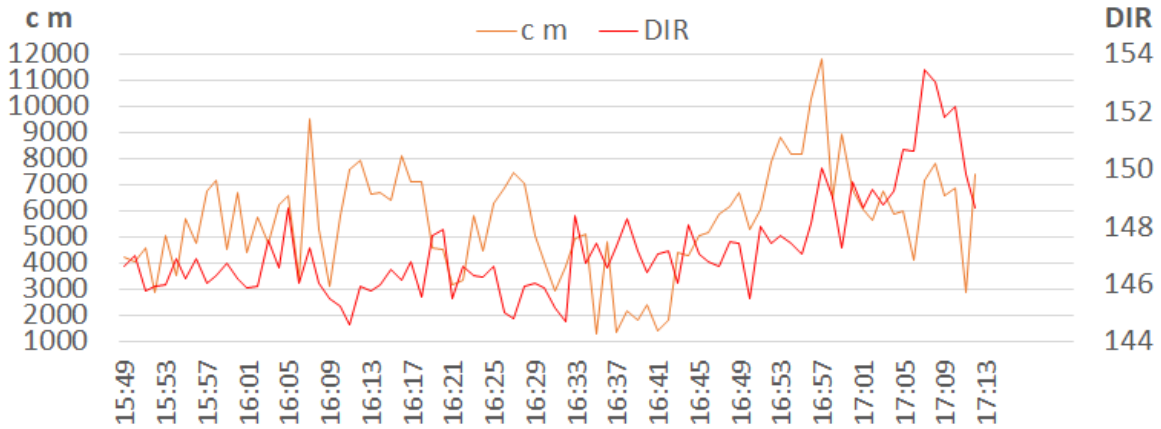

Figure AP1.17: A6 transport intensity and wind direction

Whilst in the very near-surface sediment transport was observed throughout a range of elevations across the foredune surface, (and therefore aligned with the orientation of the foredune), to be northward directed, and thus moving towards the blowout, airflow measured at 40 cm above the surface by the co-located anemometer, was slightly offshore directed for the duration of the experiment. In relation to the orientation of the foredune, wind direction was offshore directed to a greater extent during the first approximately 60 minutes of data collection, before the obliquity of the offshore direction began to increase (i.e., the angle separating the orientation of the foredune, to the A6 offshore vector direction began to decrease).

The considerable difference in direction of the very near-surface transport vector (and associated near-surface airflow direction, measured at 40 cm above the surface), was a highlight of the preliminary findings. In observing and measuring transport, a greater understanding of airflow has been achieved. The divergence in direction (and likely also wind speed) over just 40 cm in elevation, highlights one of the key challenges associated with aeolian studies in complex dune topography. Reducing the vertical distance between the height at which transport is measured, with that at which airflow is measured, would no doubt improve flow-flux statistical relationships. An appreciation of transport vectors not mirroring flow vectors in aeolian systems, due to grains in saltation following ballistic trajectories rather than

being advected into the flow vector direction (Bauer, *et al*. 2013) complicates resolution of flow-flux relationships. That divergence is likely to be enhanced in complex topographic settings, and that evident differences in flow parameters within the vertical wind profile likely also exhibit spatio-temporal variability, further complicates analyses.

Outside of the pronounced directional divergence, between the airflow and transport vectors at A6, some of the characteristics of measured airflow relative to other locations seem well suited to the topographic setting. The standard deviation of wind direction over the full time-series was the third lowest of all sensor locations. At 8.9°, the range of wind direction was also the third lowest. Flow deflection and topographic steering by the foredune, together with proximity to topography constraining the directional range of airflow approach, will all suppress temporal variability in direction.

The A6, mean value for CV of wind speed, at 14.27% was the 4th lowest of all locations where transport was also measured (Table AP3). The CV of the 84 mean values of CV of wind speed for each minute of the time series, was also the 2nd lowest across the grid. This supports the suggestion that a proportion of airflow becomes attached and deflected longshore, as this would of course result in a steadier flow regime, with a relatively lower CV of total wind speed.

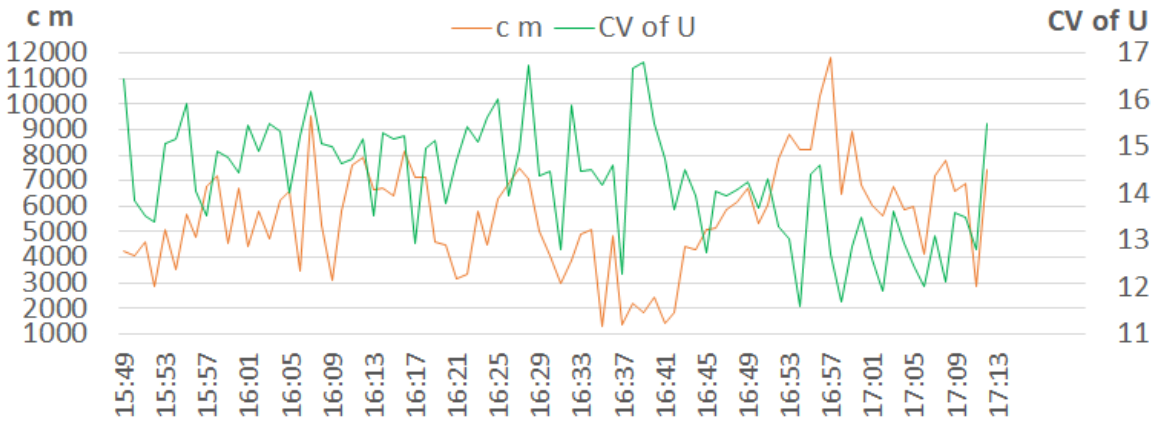

Figure AP1.18: A6 transport intensity and CV of wind speed

It is unclear from the plotted time-series of A6, CV of wind speed and transport intensity, if there is an association between the two variables (Fig.AP18). On occasions (e.g. 16:39), a peak in CV of wind speed, and thus less steady flow, coincides with a pronounced trough in transport intensity as might be expected, but there are also instances, (e.g. 16:07), when peaks in flow variability also coincide with peaks in transport. This likely relates to whether fluctuations in wind speed are upward or downward trending, as transport intensity will be a function of absolute wind speed to a much greater extent, with the magnitude of fluctuations within the record being secondary factor.

A7 transport and airflow (full time-series)

At 4.71 m s^{-1}, A7 had the lowest mean wind speed of any location where transport was measured. Its mean wind speed maximum for any individual minute was also the second lowest at 7.28 m s^{-1}. Its total grain count of 148,306 however, was the second highest of any location, and more than double that of the nest highest ranked location, with almost 90,000 counts more. The exceptionally low absolute wind speeds at A7 is most likely due to flow stagnation in association with being positioned at the foot of the northern blowout wall.

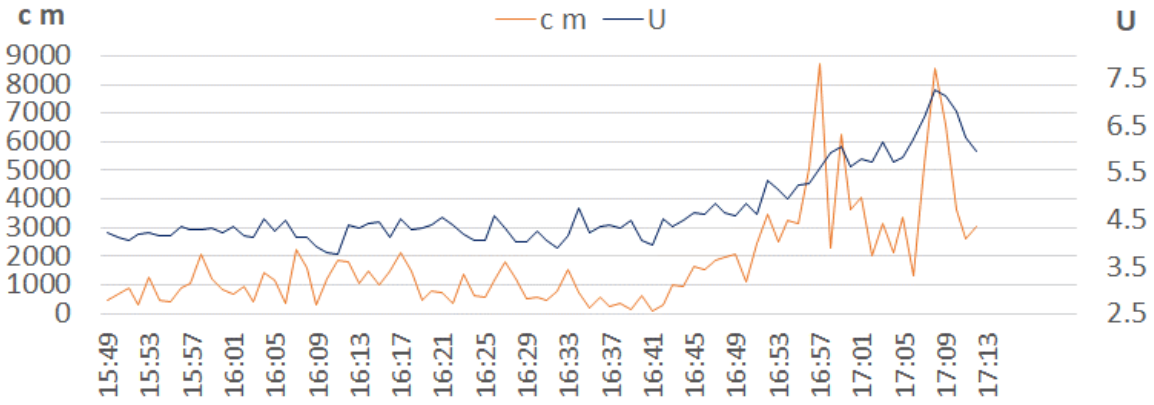

Figure AP1.19: A7 transport intensity and wind speed

A general trend evident over the full 84 minutes, is that higher levels of transport intensity occurred during the final quarter of the experiment, during a period when mean total wind speeds were also relatively stronger. Although some of the individual transport intensity peaks coincide with high wind speeds, others coincided with relatively low wind speeds, suggesting poor association between wind speed and transport intensity. Table AP3 illustrates that of the top 10 ranked, individual minutes of peak transport intensities, only five of these minutes corresponded with minutes within the top ten peaks for wind speed.

Table AP1.3: A7 highest ranking peaks in transport intensity and wind speed

Actual grain count	Minute in time-series	Transport intensity rank	Mean wind speed (m s^{-1})	Wind speed rank
8,736	16:57	1st	5.61	16th
8,583	17:08	2nd	7.28	1st
6,605	17:09	3rd	7.14	2nd
6,268	16:59	4th	6.06	8th
5,176	17:07	5th	6.67	4th
5,103	16:56	6th	5.26	18th
4,071	17:01	7th	5.8	12th
3,644	17:00	8th	5.63	15th
3,635	17:10	9th	6.82	3rd
3,448	16:52	10th	5.35	17th

Generally, the two most probable explanations for poor relationships between wind speed and transport intensity, are ‘supply limiting’ factors (e.g. moisture, vegetation, fetch distances, etc.), or sediment input from the ‘far-field’. Transport intensity being high, relative to intensities associated with relative wind speeds at other grid locations, points towards the A7 sensor experiencing higher levels of sediment input from the ‘far-field’. The topographic setting of A7 also supports this suggestion, with the position of A7 being the most topographically ‘open’, both to sediment input from the beach, and/or from the upwind foredune.

Table AP1.4: Transport peaks which were poorly correlated to A7 at-a-point wind speed, compared to transport intensity ranks of upwind sensor locations

Minute	Rank in A7 transport series	A7 wind speed rank	A2 (beach) transport rank	A4 (beach-dune interface) transport rank	A6 (upwind foredune) transport rank
16:57	1st	16th	1st	2nd	1st
16:56	6th	18th	8th	12th	2nd
17:01	7th	12th	23rd	10th	37th
17:00	8th	15th	60th	18th	22nd
16:52	10th	17th	2nd	4th	10th

Minutes 16:57, 16:56 and 16:52 rank highly for transport intensity at upwind locations, which supports the theory that some transport peaks at A7 may be associated with 'far field' sediment input, in association with high transport intensities at upwind locations (chapter 3). A possible explanation for the A7 transport peak in minute 17:00, is a potential lag response time with 'at-a-point' wind speed, as 16:59 at A7 was the 4th highest ranking minute for A7 mean wind speed. There is no definitive explanation for high transport intensity at A7 in the subsequent minute of 17:01.

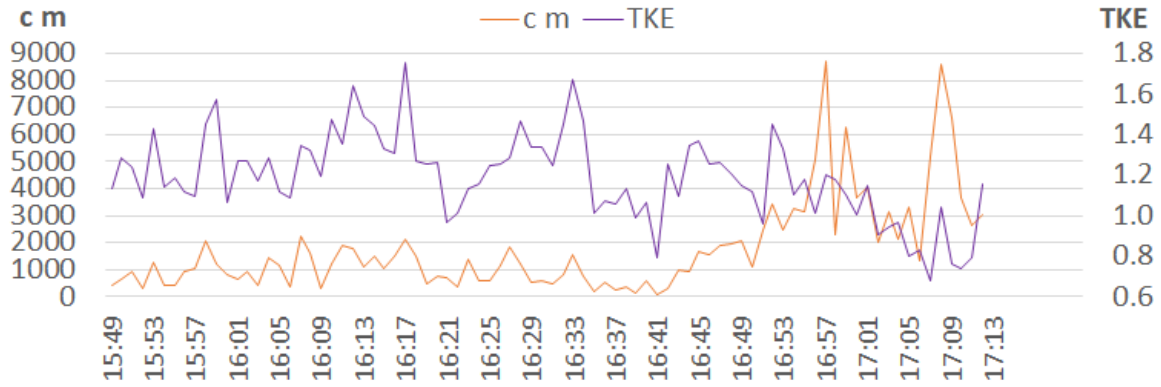

Figure AP1.30: A7 transport intensity and TKE

Many peaks in A7 TKE corresponded to peaks in transport intensity. Pronounced troughs in TKE also typically related to very low transport intensity values. Although continually fluctuating, it is very clear from the plotted time-series, that the mean values for TKE are lower in the second half of the time-series than

during the first. In the second half of the experiment, the final, or fourth quarter of measurement also has a noticeably lower mean than the third quarter. The most pronounced peaks in transport intensity occur during the final ‘quarter’ of the experiment, which although often coinciding with peaks in TKE, these TKE peaks towards the end of data recording are relatively low in comparison to those early in the experiment (which also coincided with low magnitude transport. TKE does appear somewhat associated with transport intensity. The relationship does however appear to be chaotic, and it may be that the importance of TKE to sediment transport varies temporally, and perhaps the relative importance of the various potential factors contributing to the transport signal may be episodic.

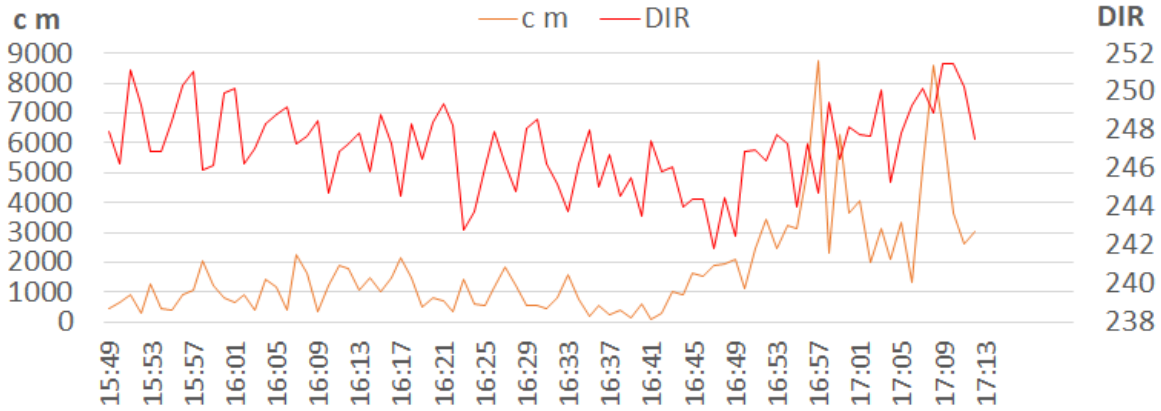

Figure AP1.21: A7 transport intensity and wind direction

Visually, A7 wind direction and transport intensity appear unrelated.

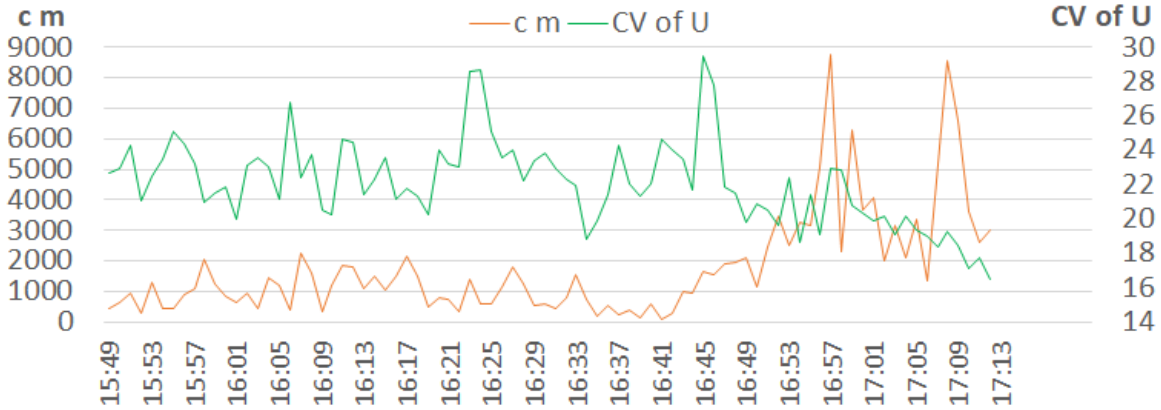

Figure AP1.22: A7 transport intensity and CV of wind speed

At 17.1%, the CV of the 84 individual mean wind speed values was the highest of all locations. The plotted CV of wind speed at A7 shows a marked decreasing

trend towards the end of the experiment, indicating airflow becoming steadier at this location. During the same period, all the major peaks in transport intensity occur. Looking at individual peaks and troughs of both variables, throughout the time-series, there is no obvious relationship present.

A8 transport and airflow (full time-series)

Based on the full 84 minutes of measurement, A8 had the 4th highest average wind speed, and also the 3rd highest maximum mean wind speed for any one individual minute.

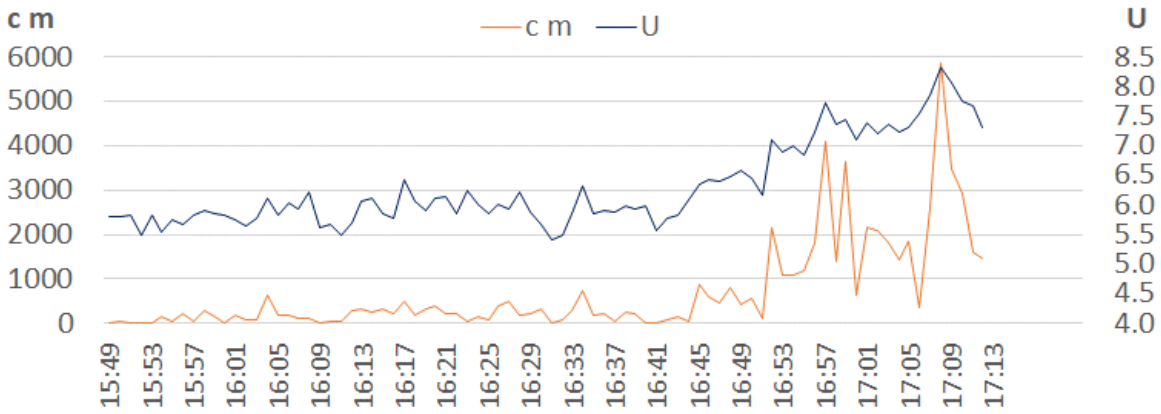

Figure AP1.23: A8 transport intensity and wind speed

Similar to other locations, transport intensity was relatively low for the first ca. three quarters of the time-series, before increasing, and for this location, to levels 5 or 6 times greater in the ca. final quarter of the time-series. As a result, transport intensity data was not normally distributed evenly about a mean value. Although fluctuating around a mean for much of the experiment, there is a clear trend of increasing wind speeds towards the final ca. third/quarter of the time-series. There is also an evident trend for higher wind speeds to result in higher transport intensity. Many of the peaks in wind speed are reflected in the transport intensity plotted series. The degree to which peaks in wind speed result in peaks in transport intensity however, varies over time. During the early part of the

experiment, some of the lower magnitude peaks in wind speed, did not result in relative 'bursts' of transport. This may be associated with a minimum threshold for entrainment, or supply limiting factors, both of which will vary temporally. Although not perfect in ranking, the link between high wind speeds, and transport intensity peaks, seemed to improve towards the end of the time-series. Of the ten highest minutes for grain count, seven were in the top ten ranking minutes for mean wind speed also (Table AP5).

Table AP1.5: A8 highest ranked minutes for transport intensity with corresponding ranks for wind speed.

Minute	Grain count	Transport series rank	Mean wind speed m s^{-1}	Wind speed series rank
17:08	5,871	1	8.32	1st
16:57	4,088	2	7.71	5th
16:59	3,644	3	7.45	8th
17:09	3,489	4	8.08	2nd
17:10	2,934	5	7.75	4th
17:07	2,612	6	7.85	3rd
17:01	2,167	7	7.39	9th
16:52	2,148	8	7.11	17th
17:02	2,095	9	7.21	16th
17:05	1,852	10	7.3	12th

Plotted TKE fluctuates considerably. Many of these fluctuations are not reflected in the transport series. The mean level of TKE is visibly lower in the second half of the experiment than the first. Although transport also increases during this period, the peaks and troughs of the two variables rarely match, and the two variables appear poorly related.

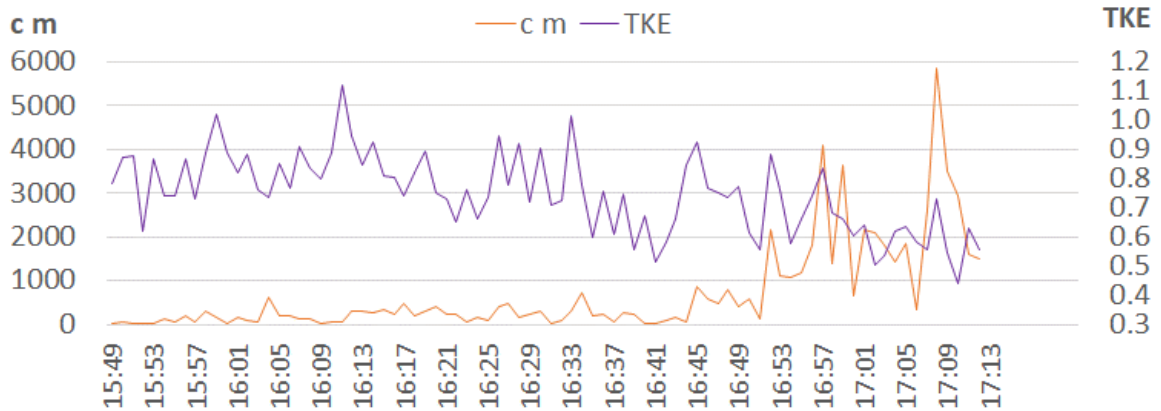

Figure AP1.24: A8 transport intensity and TKE

At just 6.8°, A8 had the second lowest range in wind direction. Although continually fluctuating throughout the experiment, during the first three quarters of the time-series, wind direction decreases marginally, before then rising by a much greater extent (to become more onshore), during the ca. final quarter of the experiment. Although this increasing wind direction coincides with higher levels of transport intensity, no obvious relationships exists between the two plotted time-series.

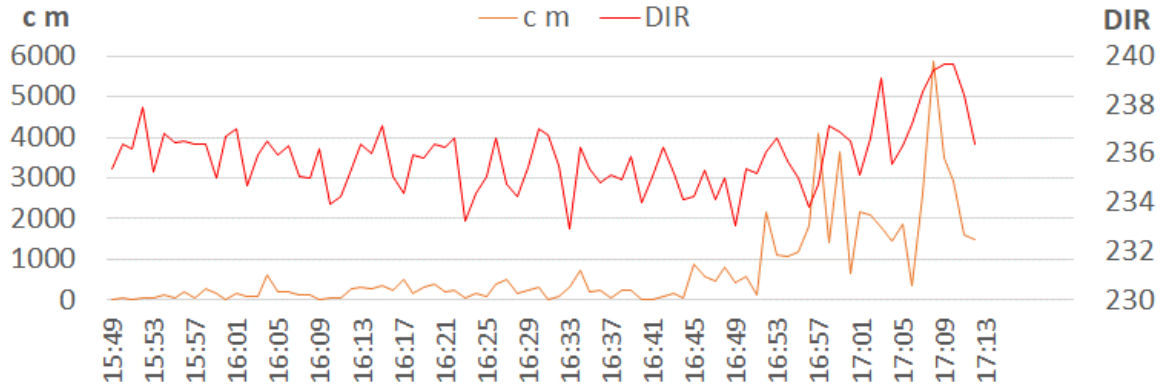

Figure AP1.25: A8 transport intensity and wind direction

At A8, the most visible trend in CV of wind speed is that it shows a marked continual decrease over the final third of the time-series. This decrease, indicating flow becoming steadier at A8, coincides with increasing transport intensity. Whilst CV of wind speed continually fluctuates, there is no obvious relationship between the peaks and troughs of flow steadiness, with those of transport intensity.

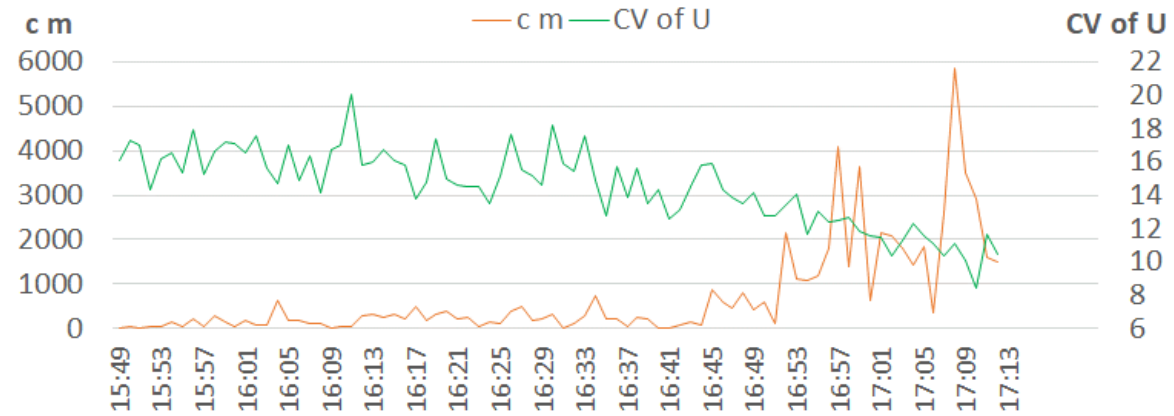

Figure AP1.26: A8 transport intensity and CV of wind speed

A9 transport and airflow (full time-series)

At 6.81 m s^{-1}, A9 had the third highest mean wind speed (over the full 84 mins). A9 also registered the highest mean wind speed (8.43 m s^{-1}), in any individual minute. Despite this, transport intensity was the second lowest, with a total grain count of 8,861, and for the majority of measurement, transport remained at 'trace' levels. This low level of transport likely reflects sediment supply being topographically constrained. The 'field of view' of the LPC is limited by the close proximity of the southern blowout wall. Streamers approaching the blowout obliquely, from upwind areas of the inter-tidal beach, are also obstructed by the foredune and blowout wall. The high levels of transport recorded on the foredune itself will follow ballistic trajectories, thus being ejected from the near surface of the foredune, to travel across the throat/trough of the blowout, rather than being steered landwards towards the A9 sensor position, as flow streamlines are theorised to do.

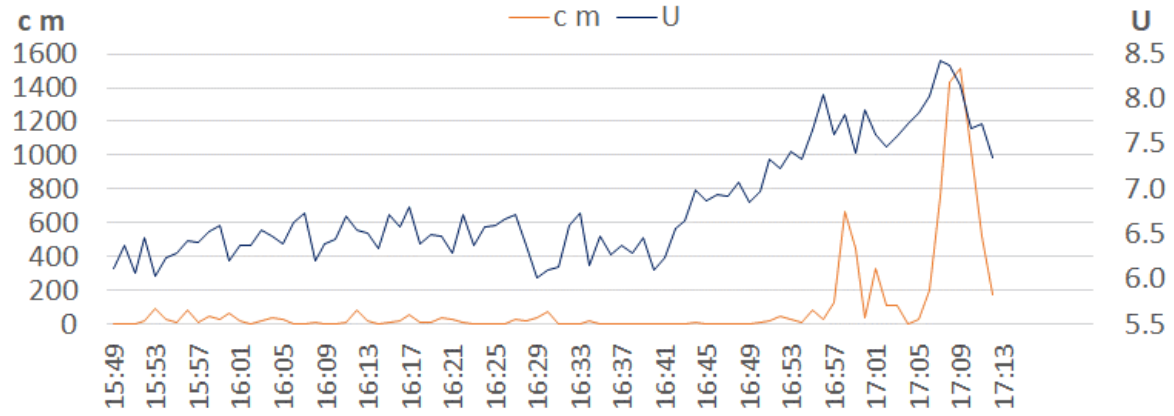

Figure AP1.27: A9 transport intensity and wind speed

In addition to having generally higher absolute wind speeds throughout, like a number of other locations, there is a marked increase in wind speed towards the end of the experiment. There are just three prominent peaks in transport during the time-series, all of which occur in the minute, or two minutes, subsequent to peaks in wind speed. There may therefore be an association between the two variables, at least during this final stage of the experiment. Due to the very low levels of transport prior to this, any association is undiscernible.

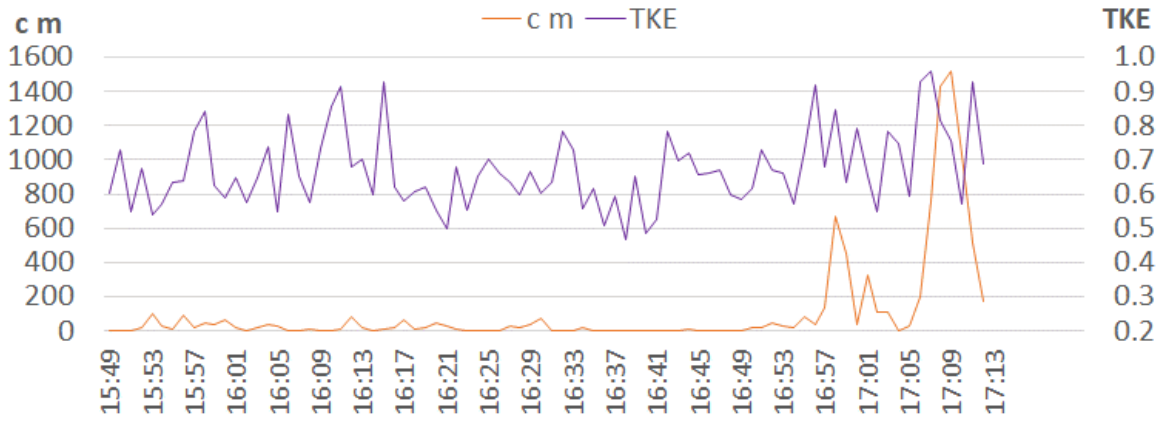

Figure AP1.28: A9 transport intensity and TKE

At 0.67, TKE was the third lowest mean across all locations where transport was also measured. As TKE is in part a product of mean wind speed, as visible in Figure AP28, the three noticeable peaks in transport intensity all occur subsequent to peaks of varying magnitude in TKE. Other than for these three potential associations, the frequent and varying magnitude fluctuations in TKE throughout the experiment show no association with the transport record.

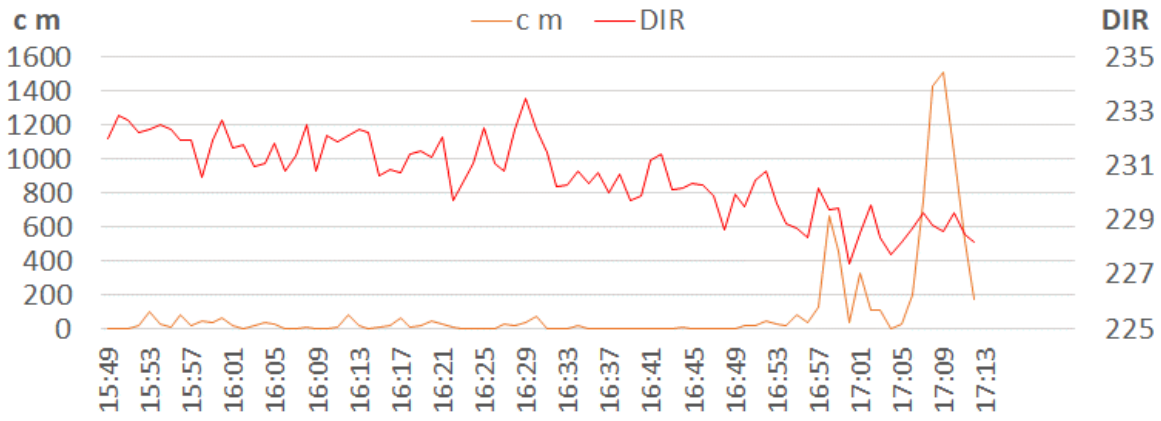

Figure AP1.29: A9 transport intensity and wind direction

Wind direction at A9 has the lowest range throughout the grid (6°). Fluctuations visible in the plotted time-series are therefore of lower magnitude than for other locations. The trend most evident is that wind direction gradually decreases (to become less onshore), over the course of the experiment, with this decrease being most pronounced in the final ca. third of the time-series. There may potentially be a threshold influencing the association of wind direction and transport intensity at A9. Other than trace levels, transport of note does occur above a wind direction of ca. 230°. Given the proximity of the sensor to the southern wall of the trough, these low wind directions have flow approaching the sensor from the wall/foredune topography.

A9 had the lowest CV of wind speed for any of the six sensors within the trough. This reflects airflow being relatively steadier here. Most like this is associated with airflow attachment to the proximal blowout wall/foredune lee topography. There is an overall trend of CV of wind speed gradually decreasing over time, denoting an already steady flow becoming increasingly steadier. There is no obvious relationship present at any time between CV of wind speed and transport intensity.

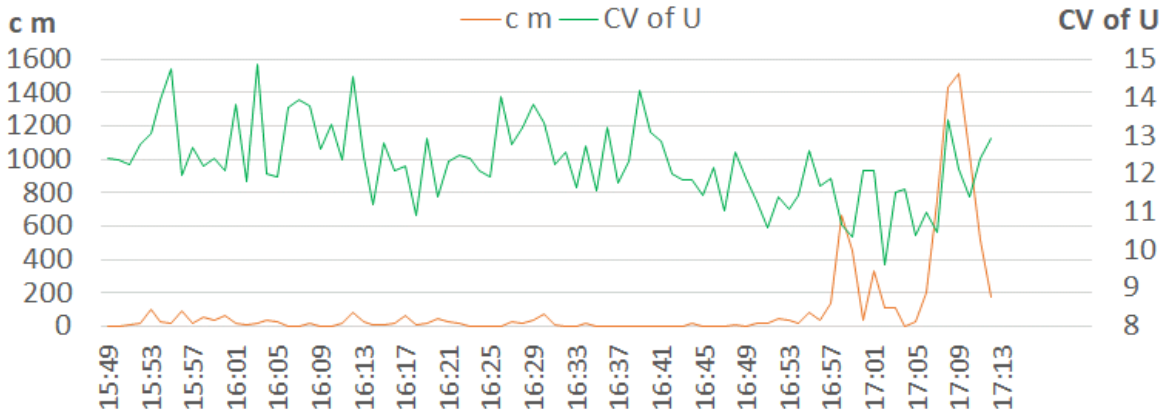

Figure AP1.30: A9 transport intensity and CV of wind speed

A10 transport and airflow (full time-series)

At 6.05 m s^{-1}, mean wind speed was the third lowest of all sensors where transport was also recorded. This may also be associated with some degree of flow

stagnation, similar but to a lesser extent to that evidenced at A7, the upwind sensor also located in proximity to the foot of the northern wall of the blowout. Mean wind speeds show a similar pattern to other locations within the trough. For the first ca. two thirds of the experiment there are minor fluctuations around a lower mean value. In the final 'third' of the time series there is a marked increase in wind speed. This overall trend is reflected in transport intensity. Many of the fluctuations in wind speed are mirrored by matching fluctuations in sediment transport. The association does appear to be stronger towards the end of the time-series but this may simply be a due to the greater visibility of the more pronounced peaks in both variables.

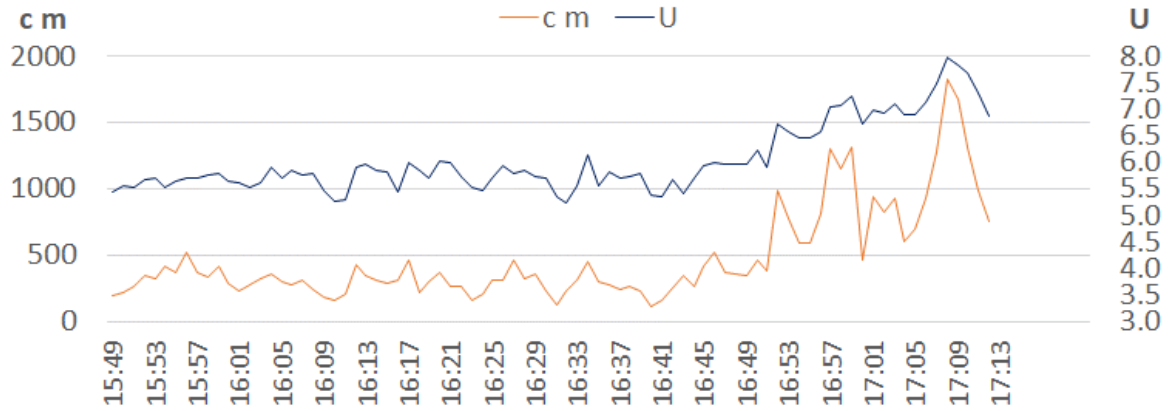

Figure AP1.31: A10 transport intensity and wind speed

Mean TKE at A10 was the second highest at 1.29, and the maximum mean TKE in any one minute of the experiment was also the second highest at 1.84. There is a noticeable decline in TKE towards the end of measurement, and although fluctuating throughout, the magnitude of fluctuations are lower during the second half of the experiment, as is mean TKE. It may be that as a greater proportion of airflow enters the trough, both flow compression and steering increase. Both these events may potentially supress turbulence/TKE. Although the highest magnitude peaks in transport occur towards the end of the experiment, whilst TKE is at its lowest levels, a strong association between the two variables is not immediately evident.

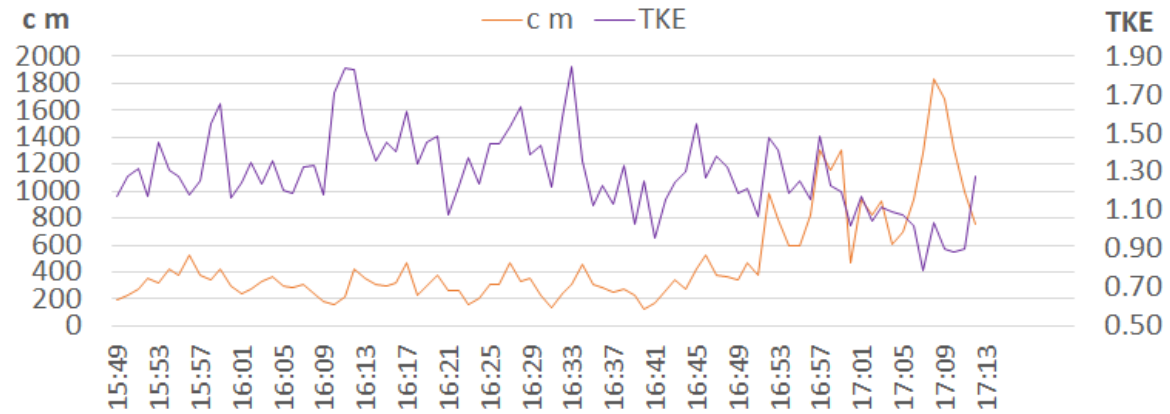

Figure AP1.32: A10 transport intensity and TKE

At 12.3°, the range of wind direction at A10 is the greatest of all locations within the trough. Mean wind direction is visibly higher during the first half of the experiment, than the second. Wind direction, although fluctuating is broadly at a similar direction during the first half of the time-series. Beyond this, whilst continuing to fluctuate, there is a marked decrease in direction, with airflow becoming less onshore directed, and therefore then approaching the sensor more directly from the area of southern blowout wall. This trend is also evident in the two other locations within the most landward row of trough sensors. Although there is no obvious trend between peaks and troughs in wind direction, with the peaks and troughs of transport intensity, the most pronounced peaks in transport occur when wind direction has dropped to its lowest level. This provides some evidence that transport here may be associated with a negative threshold in direction.

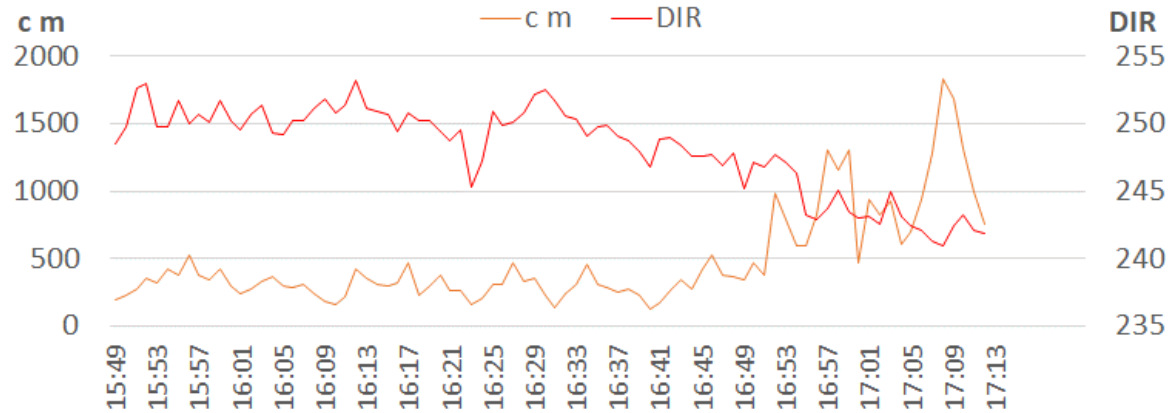

Figure AP1.33: A10 transport intensity and wind direction

Similar to other locations within the trough, CV of wind speed showed a marked decrease towards the end of the experiment, with this indicating airflow becoming

steadier. Transport intensity exhibited a pattern similar to at numerous other locations, of fluctuating at a low level for much of the time-series before rising considerably towards the end of the experiment. Major peaks in transport intensity therefore coincide with decreasing levels of CV of wind speed. Looking at individual peaks and troughs within the plotted time-series, peaks in transport appear sometimes to be associated with peaks in CV of wind speed, and on other occasions with troughs. Other than the general trend of higher overall levels of transport when CV reduced, there was no clear relationships between the two variables.

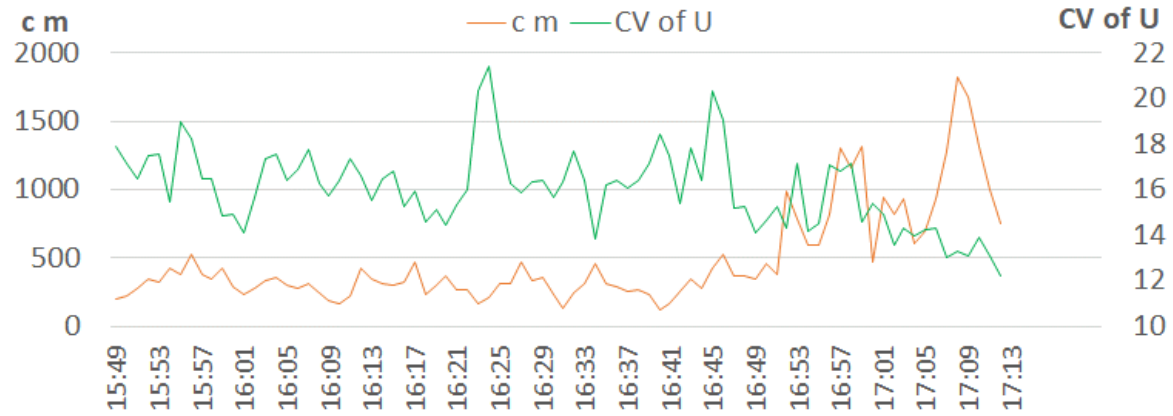

Figure AP1.44: A10 transport intensity and CV of wind speed

A11 transport and airflow (full time-series)

At 5.97 m s^{-1}, A11 had the second lowest mean wind speed of all sensor locations. Its total grain count of 29,627, was the fourth lowest throughout the grid. Transport remained at 'trace' levels for the first ca. 'two thirds' of the experiment, before rising sharply, and incorporating two pronounced peaks towards the end of the time-series. This pattern is similar to that of numerous other locations. Similarities can also been seen between the plotted time-series of the two variables. Due to the very low levels of transport occurring in the early stages of measurement, visibly, the strength of this relationship is unclear during the first two-thirds of the time-series. In the final third of the experiment, increasing and decreasing trends within both variables are mirrored.

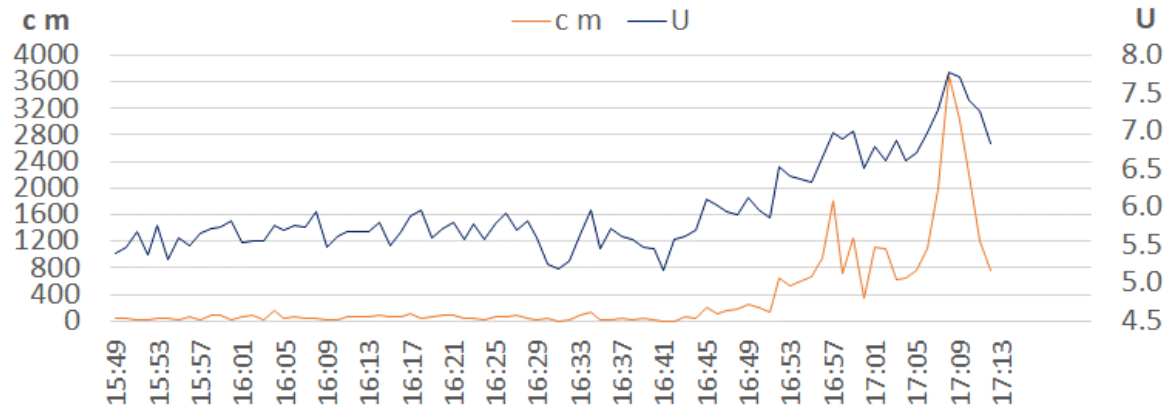

Figure AP1.35: A11 transport intensity and wind speed

TKE values have a slightly lower mean value in the second half of the experiment than the first. This lower TKE towards the end of measurement, coincides with higher transport intensity. TKE however fluctuates greatly throughout the experiment at A11, and no obvious relationships exists between the two variables.

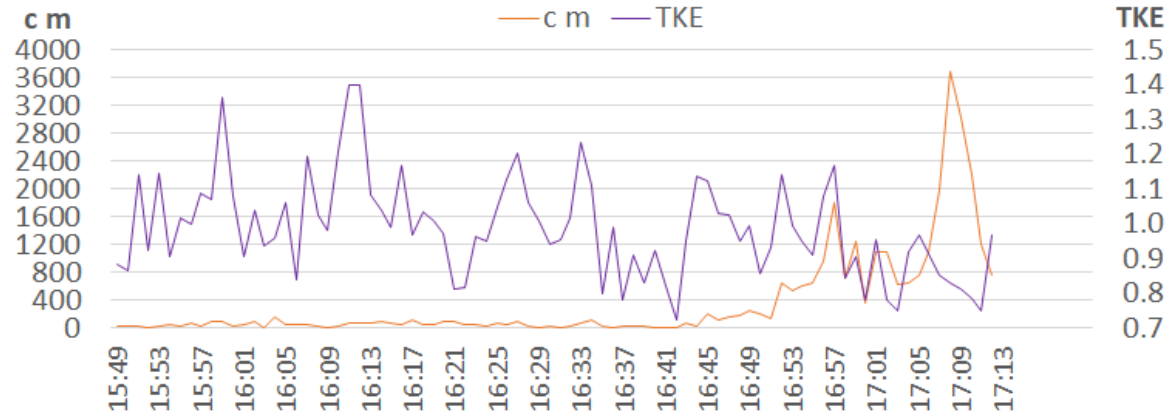

Figure AP1.36: A11 transport intensity and TKE

Wind direction at A11 follows a very similar pattern to that of A10. Fluctuating about a relatively higher mean value during the first half of the experiment, which is therefore more directly onshore, before a steady decrease. For A11, over the final ca. 20 minutes of measurement, fluctuations become lower in magnitude, and wind direction ‘plateaus’ to an extent. The wind direction during this final period suggests airflow is approaching the sensor from the centre of the trough, and the southern blowout wall/foredune lee slope. It may be that transport here is associated with wind direction falling below a certain threshold value. Although transport towards the end of the experiment clearly has some positive relationship

with mean wind speed (Fig. AP35), winds approaching more directly from the central and southern area of the trough, (and therefore with a greater potential for sediment supply), may play a role in resultant levels of transport.

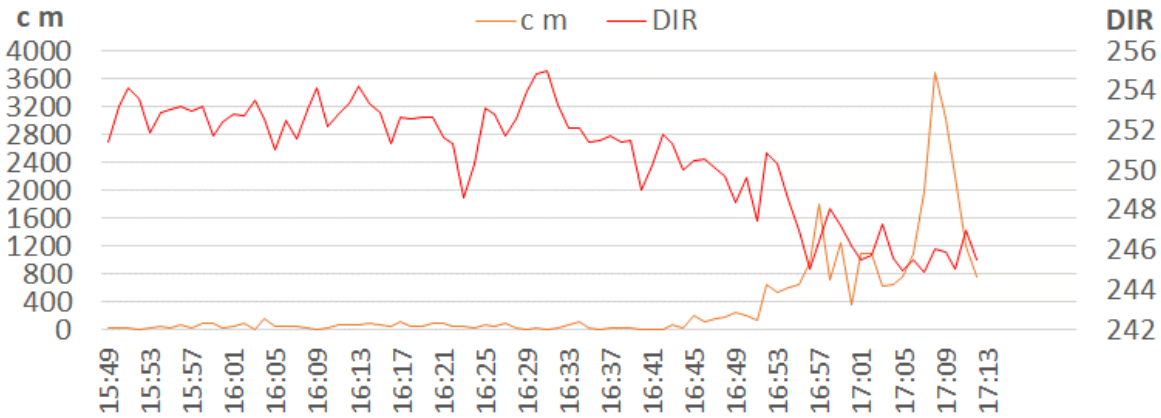

Figure AP1.37: A11 transport intensity and wind direction

CV of wind speed fluctuates for the duration of the experiment. There is an overall trend of CV decreasing, and therefore airflow becoming steadier towards the end of the time-series. This increase in flow steadiness coincides with transport intensity increasing but there is no obvious association between the fluctuations of the two plotted variables.

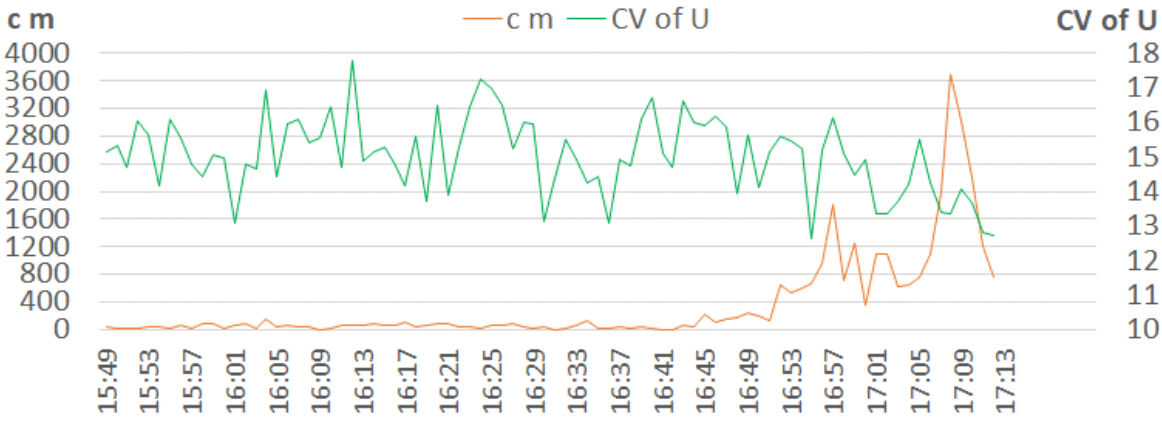

Figure AP1.38: A11 transport intensity and CV of wind speed

A12 transport and airflow (full time-series)

A12's time-series is very similar to the other sensor locations within the trough, particularly those in the most landward row. At 6.91 m s^{-1}, mean wind speed was the highest of all locations. At 8.39 m s^{-1}, A12 also had the second highest mean wind speed in any one individual minute. Nevertheless, the total grain count at

A12, of 3,858, was by far, the lowest throughout the grid. The exceptionally low transport, relative to high wind speeds, most likely reflects supply limiting factors associated with proximity to topography. The location is shielded by the southern blowout wall from incoming transport from the beach. High magnitude saltation on the upwind foredune, will follow ballistic trajectories, and grains travel across the trough, rather than becoming landward, (and A12 directed) at the foredune-blowout juncture (as 'potentially' a proportion of airflow does). Finally, the 'field of view' of this LPC is particularly constrained by topography, relative to the other sensors within the trough.

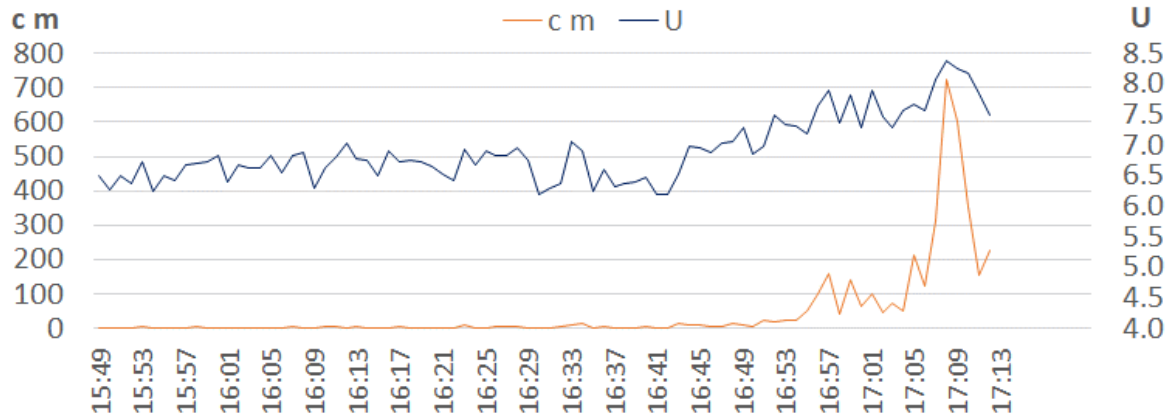

Figure AP1.39: A12 transport intensity and wind speed

A12 wind speed fluctuates about a lower mean value for the first circa 'three quarters' of the time-series before rising steadily. Transport intensity follows a similar pattern, initially with only minimal 'trace' levels of transport, followed by a sharp increase in intensity during the final third of the experiment. Towards the end of measurement, peaks in wind speed can be seen to correspond with peaks in transport intensity. It is unclear if this is the case before hand due to the scale of transport occurring. Based on the transport signals of other sensors, A12 wind speeds throughout measurement remained 'transport capable', suggesting the influence of supply limiting conditions reduced at this location towards the end of the experiment.

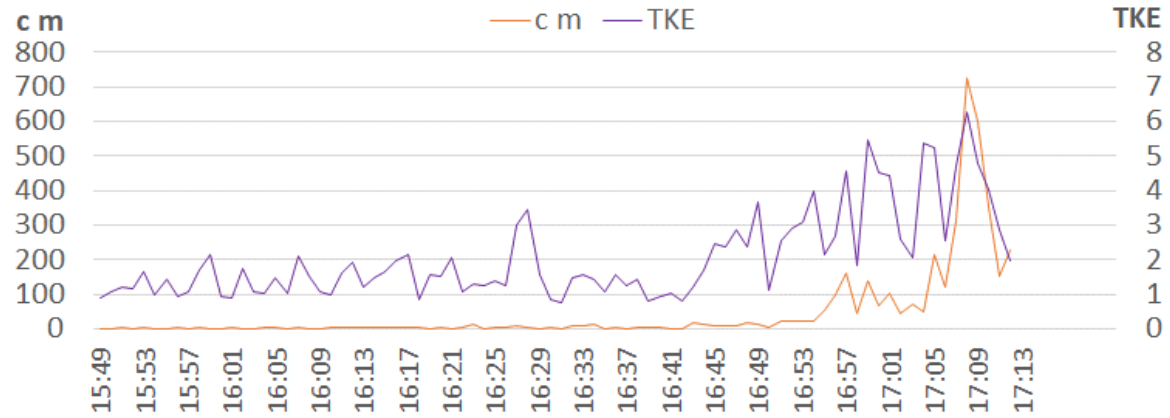

Figure AP1.40: A12 transport intensity and TKE

A12 had the highest TKE values of all locations. A mean of 20.07% (over 84 minutes), and a maximum in any one minute of 6.26%. TKE values follow a similar pattern to wind speeds at A12, as might be expected with TKE being in part a product of total wind speed. To varying degrees, some of the peaks in TKE correspond to varying peaks in transport intensity. Transport begins to occur sometime subsequent to the rise in TKE, suggesting there may be a threshold of some kind relating to transport at this location, and/or that wind speed, or another flow parameter is of greater importance to transport than turbulence.

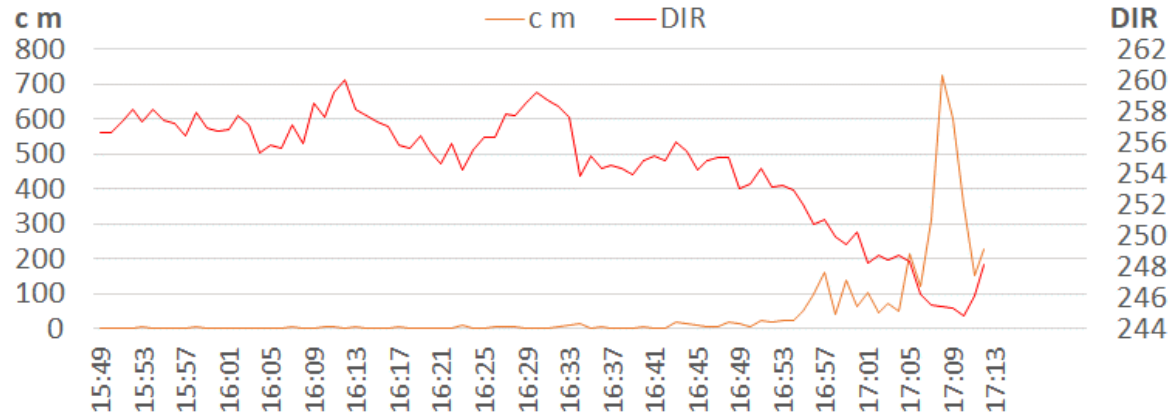

Figure AP1.51: A12 transport intensity and wind direction

Wind direction follows a similar pattern to the other two sensors in the most landward row of the trough. Direction initially fluctuates about a higher mean, which is more aligned with the orientation of the trough, before reducing sharply, resulting in airflow at A12 approaching directly off the southern blowout wall.

Again, there appears to be a threshold in place. Irrespective of high relative wind speeds, transport does not commence until direction reduces below a certain level.

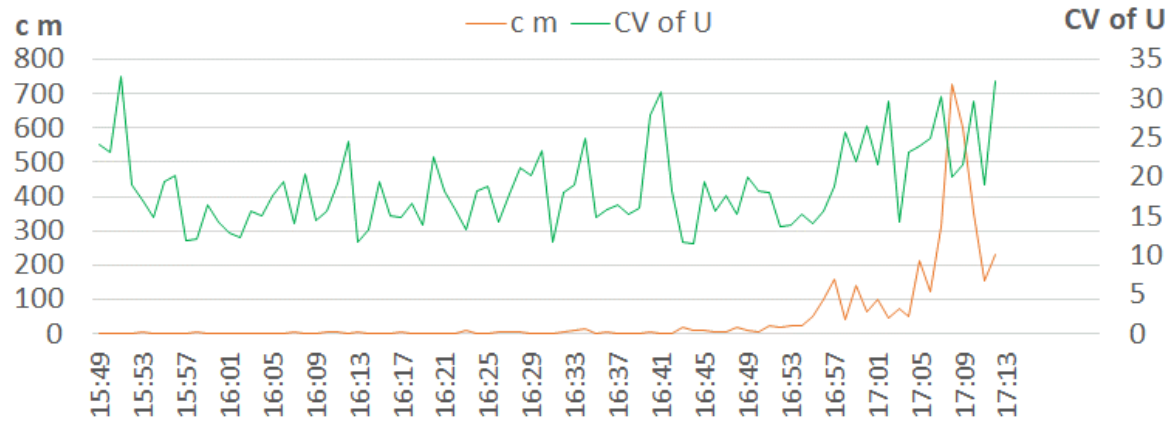

Figure AP1.42: A12 transport intensity and CV of wind speed

CV of wind speed levels were highly variable throughout the duration of measurement, and appear to be poorly associated with transport intensity.

Appendix 2: Basic descriptive statistics

Table AP2.1: Full time-series (84 minutes)

	A1	A2	A3	A4	A5	A6	A7	A8	A9	A10	A11	A12
Av. u	5.56	6.29	6.34	6.01	6.89	6.76	4.71	6.30	6.81	6.05	5.97	6.91
Max u	6.10	6.92	7.13	7.49	8.03	7.63	7.28	8.32	8.43	7.99	7.76	8.39
σ u	0.25	0.25	0.26	0.53	0.43	0.31	0.81	0.71	0.61	0.65	0.60	0.52
CV u	4.6	4.0	4.1	8.8	6.3	4.6	17.1	11.3	8.9	10.7	10.0	7.5
Av. TKE	0.61	0.54	0.64	0.70	0.64	0.76	1.19	0.75	0.67	1.29	0.99	2.07
Max TKE	0.93	0.79	0.96	1.06	0.92	1.01	1.76	1.12	0.96	1.84	1.40	6.26
σ TKE	0.11	0.09	0.09	0.11	0.09	0.10	0.21	0.13	0.11	0.21	0.14	1.29
CV TKE	17.8	15.9	14.5	15.9	13.8	13.4	17.8	17.9	16.7	16.4	14.5	62.2
Av. DIR	195.9	191.5	182.3	215	220.2	147.2	247.1	235.8	230.7	248.2	250.7	254.5
σ DIR	6.0	4.6	3.7	4.0	2.3	1.8	2.1	1.4	1.4	3.2	2.8	3.8
Range DIR	25.8	20.5	17.0	18.0	11.2	8.9	9.7	6.8	6.0	12.3	10.2	10.2
Total count	n/a	53015	n/a	56863	13494	469583	148306	58787	8861	40308	29627	3858
Av. c m	n/a	631	n/a	677	161	5590	1766	700	106	480	353	46
Av. ntt	n/a	1.19	n/a	1.19	1.19	1.19	1.19	1.19	1.19	1.19	1.19	1.19
Min. ntt	n/a	0.00	n/a	0.00	0.00	0.28	0.05	0.00	0.00	0.30	0.00	0.00
Max. ntt	n/a	5.55	n/a	8.69	8.88	2.52	5.89	9.99	17.09	4.54	12.50	18.82
Range ntt	n/a	5.55	n/a	8.69	8.88	2.24	5.84	9.99	17.09	4.24	12.50	18.82
σ c m	n/a	477.1	n/a	930.3	228.0	2058.3	1722.8	1060.6	274.4	354.2	663.2	117.9
CV c m	n/a	76	n/a	137	142	37	98	152	259	74	188	257

Table AP2.2: Run 1 (61 minutes)

	A1	A2	A3	A4	A5	A6	A7	A8	A9	A10	A11	A12
Av. u	5.47	6.23	6.33	5.74	6.68	6.65	4.29	5.92	6.48	5.70	5.65	6.65
Max u	5.85	6.72	6.83	6.32	7.24	7.42	4.84	6.58	7.08	6.13	6.12	7.29
σ u	0.19	0.23	0.24	0.26	0.27	0.27	0.23	0.26	0.25	0.21	0.21	0.26
CV u	3.6	3.7	3.8	4.5	4.0	4.1	5.3	4.4	3.8	3.6	3.7	3.9
Av. TKE	0.61	0.53	0.64	0.72	0.64	0.77	1.25	0.79	0.65	1.35	1.02	1.51
Max TKE	0.93	0.79	0.96	1.06	0.92	1.01	1.76	1.12	0.93	1.84	1.40	3.69
σ TKE	0.11	0.08	0.09	0.12	0.09	0.11	0.18	0.12	0.10	0.19	0.14	0.64
CV TKE	18.1	15.8	14.7	16.1	13.8	14.1	14.4	14.8	15.2	14.1	13.9	42.2
Av. DIR	192.9	189.2	180.5	213.0	219.1	146.5	246.7	235.5	231.3	249.8	252.2	256.4
σ DIR	1.7	1.4	1.4	1.4	1.0	0.9	2.1	1.1	1.0	1.7	1.4	1.6
Range DIR	7.3	5.8	5.7	5.9	4.3	4.0	9.3	5.0	5.0	8.1	6.7	7.0
Total count	n/a	35697	n/a	18222	8667	307443	30511	13322	1104	18656	3581	230
Av. c m	n/a	585	n/a	299	142	5040	995	218	18	306	59	4
Av. ntt	n/a	1.10	n/a	0.53	1.05	1.07	0.67	0.37	0.20	0.76	0.20	0.10
Min. ntt	n/a	0.00	n/a	0.00	0.00	0.28	0.05	0.00	0.00	0.30	0.00	0.00
Max. ntt	n/a	2.78	n/a	1.73	8.88	2.04	1.51	1.49	1.11	1.31	0.84	0.44
Range ntt	n/a	2.78	n/a	1.73	8.88	1.76	1.46	1.49	1.11	1.02	0.84	0.44
σ c m	n/a	340	n/a	252.1	212.5	1842.6	585.8	202.9	0.27	90.16	50.08	4.11
CV c m	n/a	58	n/a	84	150	37	59	93	1	29	85	109

Table AP2.3: Run 2 (23 minutes)

	A1	A2	A3	A4	A5	A6	A7	A8	A9	A10	A11	A12
Av. u	5.82	6.45	6.38	6.75	7.44	7.04	5.84	7.32	7.68	6.97	6.80	7.60
Max u	6.10	6.92	7.13	7.49	8.03	7.63	7.28	8.32	8.43	7.99	7.76	8.39
σ u	0.21	0.25	0.32	0.31	0.27	0.22	0.70	0.48	0.36	0.50	0.48	0.39
CV u	3.6	3.9	4.9	4.6	3.6	3.1	11.9	6.6	4.7	7.2	7.1	5.2
Av. TKE	0.60	0.57	0.65	0.67	0.64	0.75	1.02	0.63	0.73	1.13	0.91	3.55
Max TKE	0.79	0.77	0.84	0.90	0.90	0.94	1.45	0.88	0.96	1.49	1.17	6.26
σ TKE	0.10	0.09	0.09	0.10	0.09	0.09	0.20	0.11	0.12	0.18	0.12	1.40
CV TKE	17.2	15.5	14.0	14.8	14.1	11.5	19.2	16.6	17.0	16.1	12.8	39.6
Av. DIR	204.1	197.6	187.1	220.2	223.0	149.3	248.0	236.7	229.0	243.8	246.8	249.3
σ DIR	5.8	4.6	3.7	4.0	2.4	2.0	2.0	1.7	0.8	2.0	1.7	2.9
Range DIR	18.7	14.8	12.7	13.1	9.2	8.0	7.5	5.9	3.4	6.7	6.0	9.5
Total count	n/a	17318	n/a	38641	4827	162140	87619	45465	7757	21652	26045	3628
Av. c m	n/a	753	n/a	1680	210	7050	3810	1977	337	941	1132	158
Av. ntt	n/a	1.42	n/a	2.95	1.56	1.5	2.57	3.36	3.81	2.34	3.82	4.09
Min. ntt	n/a	0.00	n/a	0.06	0.07	0.61	0.76	0.18	0.03	0.94	0.48	0.13
Max. ntt	n/a	5.55	n/a	8.69	7.84	2.52	5.89	9.99	17.09	4.54	12.50	18.82
Range ntt	n/a	5.55	n/a	8.63	7.77	1.91	5.13	9.80	17.06	3.59	12.03	18.69
σ c m	n/a	722.7	n/a	1282	263.6	1912.8	2061.1	1335.9	453.1	380.3	881.7	185.6
CV c m	n/a	96	n/a	76	126	27	54	68	134	40	78	118

APPENDIX 3.3 – CORRELATION TEST MATRICES

The A3 matrices below use the following syntax/color code:

*	Significant at 0.05
**	Significant at 0.01
	Not statistically significant
	0.1 to 0.1999
	0.2 to 0.2999
	0.3 to 0.3999
	0.4 to 0.4999
	0.5 to 0.5999
	0.6 to 0.6999
	0.7 to 0.7999
	0.8 to 0.8999
	0.9 to 0.9999

Table AP3.1: Location **A1**.

	FULL (84mins)				Run1: 15.49 to 16.49 inc. (61mins)				Run2: 16.50 to 17.12 inc. (23mins)			
	a1u	a1tke	a1dir	a1CV	a1u	a1tke	a1dir	a1CV	a1u	a1tke	a1dir	a1CV
a1u		.231**	.268**	-0.049		.284**	-0.055	0.033		.399**	-0.154	0.170
a1tke	.231**		-.158*	.671**	.284**		-.277**	.690**	.399**		-0.028	.739**
a1dir	.268**	-.158*		-.243**	-0.055	-.277**		-.224*	-0.154	-0.028		0.012
a1CV	-0.049	.671**	-.243**		0.033	.690**	-.224*		0.170	.739**	0.012	
a2u	.333**	.179*	0.076	-0.006	.258**	.231**	-0.167	0.082	0.194	0.146	-.360*	0.043
a2tke	.282**	.373**	-0.114	.211**	.240**	.410**	-.405**	.277**	.320*	.304*	-0.012	0.154
a2dir	.319**	-0.126	.794**	-.224**	0.037	-.211*	.631**	-.180*	-0.123	-0.075	.858**	-0.051
a2CV	0.059	.194**	-.182*	.163*	0.059	.209*	-.287**	.204*	.296*	0.186	0.028	0.036
a2ntt	.262**	.278**	-.170*	0.128	.283**	.256**	-.295**	0.119	.407**	.328*	-.478**	0.194
a2AP	-0.007	.272**	-.371**	.230**	.175*	.233**	-.274**	0.131	0.213	.301*	-.414**	0.189
a3u	.159*	.197**	-.176*	0.108	.185*	.230**	-.269**	0.151	0.202	0.170	-.557**	0.083
a3tke	0.138	.255**	-0.061	.157*	.217*	.302**	-.210*	.184*	-0.146	0.186	0.059	0.194
a3dir	.268**	-0.121	.675**	-.207**	-0.046	-.220*	.425**	-0.165	-0.130	0.028	.818**	0.051
a3CV	-0.030	.149*	-0.063	0.142	0.101	.217*	-0.071	0.167	-0.225	0.059	0.265	0.099
a4u	.365**	0.039	.430**	-0.131	0.103	0.089	0.027	0.001	0.091	0.012	.312*	-0.091
a4tke	-0.037	.151*	-.279**	.172*	0.046	.217*	-.349**	.209*	-0.028	0.051	-0.059	-0.020
a4dir	.219**	-0.011	.517**	-0.090	-0.141	-0.002	0.140	0.068	-0.154	-0.028	.668**	-0.004
a4CV	-.288**	0.056	-.429**	.192**	-0.034	0.026	-0.111	0.092	0.123	0.202	-0.115	0.146
a4ntt	.449**	0.123	.280**	-0.059	.246**	0.140	-0.116	0.044	.372*	.444**	-0.079	0.277
a4AP	.353**	.154*	.164*	-0.007	.281**	.189*	-0.078	0.076	0.092	0.252	-0.268	0.212
a5u	.337**	0.056	.376**	-0.112	0.062	0.120	-0.042	0.042	0.043	-0.004	0.138	-0.138
a5tke	0.004	-0.020	-0.061	-0.048	-0.004	0.038	-0.150	0.034	-0.004	-0.115	0.075	-0.249
a5dir	.240**	0.007	.479**	-0.095	-0.072	0.032	0.123	0.049	-0.154	-0.012	.636**	-0.004
a5CV	-.232**	0.020	-.295**	0.137	0.008	-0.046	0.011	0.009	-0.059	0.099	-0.170	0.091
a5ntt	.169*	.222**	0.005	0.135	0.136	.269**	-0.146	.205*	0.067	0.123	0.012	0.083
a5AP	.185*	.236**	-0.065	0.113	0.171	.249**	-.205*	0.161	0.170	0.186	-0.162	0.032
a6u	.347**	0.080	.209**	-0.074	0.139	0.131	-0.116	0.068	0.233	-0.004	-.368*	-0.154
a6tke	0.033	0.045	-.150*	-0.001	0.093	0.103	-0.157	0.048	0.138	-0.099	-0.273	-0.233
a6dir	.186*	-0.046	.526**	-0.138	-0.129	-0.084	.274**	-0.073	-0.146	0.028	.597**	0.051
a6CV	-.270**	0.080	-.302**	.182*	-0.026	0.128	0.008	0.139	-0.154	-0.123	-0.091	-0.115
a6ntt	.346**	.232**	0.116	0.087	.246**	.306**	-.175*	.238**	0.178	0.225	-0.217	0.091
a6AP	0.110	0.145	-0.092	0.091	0.091	.227*	-.288**	0.188	-0.105	-0.182	-0.278	-0.105
a7u	.411**	0.006	.604**	-.158*	.212*	0.021	.281**	-0.067	-0.091	0.036	.794**	0.028
a7tke	-0.053	.334**	-.508**	.318**	.208*	.370**	-.410**	.242**	0.217	.328*	-.542**	0.257
a7dir	.243**	0.072	.186*	0.002	.202*	0.081	0.028	0.039	0.099	0.099	.589**	0.107
a7CV	-.279**	0.033	-.365**	0.143	-0.086	-0.011	-0.022	0.031	0.059	0.043	-.478**	-0.043
a7ntt	.422**	0.138	.317**	-0.033	.207*	.232**	-0.129	0.144	0.209	0.178	0.146	0.028
a7AP	.407**	0.088	.309**	-0.064	.213*	0.171	-0.073	0.123	.314*	0.143	0.045	-0.020
a8u	.386**	-0.003	.537**	-0.144	0.158	-0.007	.188*	-0.048	-0.012	0.130	.605**	0.091
a8tke	-0.075	.274**	-.444**	.292**	.183*	.326**	-.267**	.249**	0.233	0.265	-.352*	0.115
a8dir	.240**	0.017	.262**	-0.030	0.172	0.017	0.085	0.000	0.043	0.075	.565**	0.067
a8CV	-.234**	.148*	-.591**	.220**	0.104	.230**	-.280**	0.166	0.130	0.115	-.739**	0.028
a8ntt	.481**	0.073	.419**	-0.128	.359**	0.112	0.047	-0.047	0.107	0.170	.344*	0.083
a8AP	.436**	0.136	.339**	-0.059	.288**	0.137	0.011	-0.005	0.277	.430**	0.036	.325*
a9u	.337**	0.049	.434**	-0.104	0.058	0.125	0.000	0.063	-0.036	-0.099	.470**	-0.154
a9tke	.159*	0.063	0.093	-0.001	0.060	0.116	-0.151	0.092	0.028	-0.083	0.202	-0.123
a9dir	-.250**	0.119	-.519**	.258**	0.039	0.132	-.250**	.202*	0.170	.312*	-0.273	0.225
a9CV	-.182*	0.039	-.328**	0.129	0.021	-0.007	-.175*	0.024	0.099	0.178	0.146	0.170
a9ntt	.416**	.194*	.291**	0.059	.289**	.295**	-0.143	.232*	0.063	0.206	.586**	0.166
a9AP	.451**	.207**	.343**	0.052	.302**	.320**	-0.103	.253**	0.136	0.184	.567**	0.128
a10u	.486**	0.068	.468**	-0.114	.350**	0.128	0.047	0.010	0.012	0.091	.676**	0.051
a10tke	-0.058	.302**	-.518**	.302**	.204*	.332**	-.435**	.230**	0.138	0.217	-.557**	0.162
a10dir	-.245**	0.145	-.722**	.238**	0.066	.211*	-.545**	.185*	0.249	0.186	-.636**	0.099
a10CV	-.310**	0.020	-.324**	.146*	-.255**	-0.063	-0.024	0.033	0.233	0.170	-.478**	0.036
a10ntt	.421**	0.096	.378**	-0.059	.205*	0.162	-0.093	0.095	0.162	0.273	.462**	0.186
a10AP	.383**	0.051	.416**	-0.094	0.132	0.097	-0.018	0.058	0.117	0.061	.444**	-0.014
a11u	.399**	0.084	.456**	-0.057	.186*	0.152	0.027	0.115	0.004	0.162	.652**	0.107
a11tke	-0.045	.320**	-.425**	.313**	0.152	.391**	-.387**	.326**	0.012	0.170	-.399**	0.130
a11dir	-.229**	0.116	-.621**	.211**	0.079	0.143	-.377**	0.123	.360*	0.265	-.478**	0.178
a11CV	-.161*	0.041	-.242**	0.108	-0.084	-0.028	-0.028	0.022	0.273	0.209	-.360*	0.075
a11ntt	.419**	0.102	.483**	-0.076	.216*	.193*	0.078	0.084	-0.004	0.154	.581**	0.115
a11AP	.442**	0.118	.446**	-0.076	.241**	.221*	0.059	0.093	0.189	0.173	0.245	0.044
a12u	.410**	.154*	.376**	-0.011	.201*	.285**	-0.093	.198*	0.036	0.194	.494**	0.123
a12tke	.359**	0.101	.252**	-0.065	0.141	.195*	-.192*	0.109	0.115	0.067	0.194	-0.099
a12dir	-.238**	0.122	-.711**	.213**	0.105	.207*	-.482**	0.169	0.138	0.028	-.858**	-0.028
a12CV	0.081	-0.035	.162*	-0.068	0.016	-0.004	-0.046	-0.015	-.375*	-0.123	.510**	0.028
a12ntt	.381**	0.026	.452**	-0.146	0.156	0.062	0.002	-0.041	-0.166	0.055	.626**	0.048
a12AP	.391**	0.034	.453**	-0.144	0.165	0.075	-0.002	-0.034	-0.100	0.084	.649**	0.044

Table AP3.2: Location **A2**.

	FULL (84mins)						Run1: 15.49 to 16.49 inc. (61mins)						Run2: 16.50 to 17.12 inc. (23mins)					
	a2u	a2tke	a2dir	a2CV	a2ntt	a2AP	a2u	a2tke	a2dir	a2CV	a2ntt	a2AP	a2u	a2tke	a2dir	a2CV	a2ntt	a2AP
a1u	.333**	.282**	.319**	0.059	.262**	-0.007	.258**	.240**	0.037	0.059	.283**	.175*	0.194	.320*	-0.123	.296*	.407**	0.213
a1tke	.179*	.373**	-0.126	.194**	.278**	.272**	.231**	.410**	-.211*	.209*	.256**	.233**	0.146	.304*	-0.075	0.186	.328*	.301*
a1dir	0.076	-0.114	.794**	-.182*	-.170*	-.371**	-0.167	-.405**	.631**	-.287**	-.295**	-.274**	-.360*	-0.012	.858**	0.028	-.478**	-.414**
a1CV	-0.006	.211**	-.224**	.163*	0.128	.230**	0.082	.277**	-.180*	.204*	0.119	0.131	0.043	0.154	-0.051	0.036	0.194	0.189
a2u		.279**	0.096	-0.103	.477**	.297**		.233**	-0.137	-0.130	.543**	.478**		.336*	-.312*	0.091	.534**	.558**
a2tke	.279**		-0.040	.552**	.323**	0.145	.233**		-.272**	.572**	.320**	.183*	.336*		0.051	.628**	.360*	0.269
a2dir	0.096	-0.040		-0.107	-0.146	-.355**	-0.137	-.272**		-0.154	-.257**	-.247**	-.312*	0.051		0.091	-.415**	-.390*
a2CV	-0.103	.552**	-0.107		0.073	-0.017	-0.130	.572**	-0.154		0.038	-0.088	0.091	.628**	0.091		0.194	0.092
a2ntt	.477**	.323**	-0.146	0.073		.571**	.543**	.320**	-.257**	0.038		.643**	.534**	.360*	-.415**	0.194		.759**
a2AP	.297**	0.145	-.355**	-0.017	.571**		.478**	.183*	-.247**	-0.088	.643**		.558**	0.269	-.390*	0.092	.759**	
a3u	.434**	.212**	-.177*	-0.047	.478**	.472**	.490**	.219*	-.275**	-0.066	.487**	.490**	.455**	0.138	-.542**	0.020	.510**	.598**
a3tke	.330**	.310**	-0.052	0.073	.282**	.268**	.372**	.337**	-.195*	0.079	.365**	.363**	0.170	0.217	0.091	0.130	0.146	0.213
a3dir	.182*	0.009	.755**	-0.121	-0.125	-.329**	0.008	-.204*	.572**	-.191*	-.229**	-.227*	-0.209	0.154	.850**	0.130	-.312*	-0.253
a3CV	0.034	0.129	-0.046	0.080	0.031	0.061	0.091	.211*	-0.038	0.104	0.088	0.068	-0.051	0.012	0.265	0.020	-0.059	0.036
a4u	.332**	0.100	.424**	-0.117	.195**	-0.072	.298**	0.019	0.014	-0.148	.347**	.259**	-0.178	-0.083	.312*	-0.075	-0.186	-0.245
a4tke	-0.045	0.093	-.295**	0.114	.187*	.177*	0.036	.233**	-.370**	.215*	.251**	0.165	-0.059	-0.123	-0.138	-0.178	0.138	0.020
a4dir	.165*	0.084	.554**	-0.011	-0.063	-.238**	-0.015	-0.028	.205*	0.028	-0.095	-0.025	-0.202	0.020	.684**	0.107	-.447**	-.406**
a4CV	-.264**	-0.027	-.403**	.154*	-0.066	.179*	-.175*	0.046	-0.059	0.162	-0.102	-0.018	0.123	.296*	-0.130	0.273	0.225	0.189
a4ntt	.538**	.268**	.261**	-0.023	.387**	0.096	.549**	.221*	-0.155	-0.057	.527**	.389**	.404**	.562**	-0.063	.459**	.475**	.463**
a4AP	.572**	.182*	.157*	-0.118	.409**	.272**	.594**	0.170	-0.091	-0.131	.553**	.526**	.428**	0.156	-0.276	-0.012	.380*	.508**
a5u	.307**	.147*	.359**	-0.060	.197**	-0.082	.245**	0.114	-0.081	-0.039	.326**	.214*	-0.178	-0.083	0.170	-0.012	-0.043	-0.092
a5tke	0.016	0.084	-0.052	0.105	.151*	0.032	0.078	0.169	-0.145	0.148	.226*	0.115	-0.130	-0.083	0.170	-0.028	-0.028	-0.100
a5dir	.165*	0.069	.480**	-0.033	-0.054	-.186*	0.023	-0.043	0.117	-0.016	-0.075	0.049	-0.186	0.067	.684**	0.154	-.399**	-.374*
a5CV	-.178*	-0.074	-.287**	0.042	0.024	.178*	-0.055	-0.020	0.031	0.044	0.033	0.012	-0.028	-0.043	-0.202	-0.051	0.091	0.149
a5ntt	.148*	.258**	-0.014	0.145	.319**	.157*	0.144	.271**	-.188*	0.137	.364**	.274**	0.036	0.187	0.060	0.226	0.234	0.133
a5AP	.188*	.266**	-0.071	0.147	.390**	.259**	.187*	.276**	-.225*	0.140	.420**	.336**	0.089	0.202	-0.105	0.242	.331*	0.287
a6u	.309**	.199**	.197**	0.034	.287**	-0.002	.219*	.177*	-0.142	0.074	.356**	.192*	0.091	0.028	-.352*	0.099	0.209	0.108
a6tke	0.019	0.077	-0.137	0.094	.166*	0.076	0.055	0.151	-0.136	0.136	0.153	0.043	0.075	-0.083	-0.241	-0.028	0.225	0.157
a6dir	.173*	-0.005	.486**	-0.118	-0.069	-.220**	0.082	-0.145	.200*	-0.169	-0.072	-0.032	-0.241	-0.067	.581**	0.067	-.391**	-.366*
a6CV	-.254**	-0.116	-.295**	-0.005	-0.072	0.070	-0.121	-0.056	0.023	-0.043	-0.123	-0.113	-0.202	-0.123	-0.091	-0.083	0.028	0.028
a6ntt	.312**	.220**	0.106	-0.009	.395**	.232**	.234**	.249**	-.199*	0.063	.468**	.414**	0.289	0.020	-0.202	-0.067	.439**	.526**
a6AP	0.156	.179*	-0.078	0.095	.233**	0.156	0.146	.273**	-.260*	.236*	.347**	.244*	0.067	-.355*	-0.316	-.393*	-0.086	0.010
a7u	.395**	0.144	.628**	-0.096	0.101	-.149*	.410**	0.054	.320**	-0.145	.186*	0.121	-0.186	0.194	.842**	0.170	-0.273	-0.245
a7tke	0.127	.309**	-.548**	.163*	.348**	.469**	.277**	.493**	-.480**	.217*	.394**	.339**	.470**	0.281	-.573**	0.067	.542**	.566**
a7dir	-.186*	0.061	.270**	.180*	-.199**	-.225**	-.267**	0.052	.188*	.227**	-.193*	-0.130	-.328*	-0.012	.589**	0.043	-.352*	-.422**
a7CV	-0.104	-0.055	-.353**	0.022	0.032	.151*	-0.020	0.007	-0.002	-0.015	-0.042	-0.105	.470**	0.107	-.478**	-0.012	.336*	0.269
a7ntt	.343**	.243**	.293**	0.009	.289**	0.041	.278**	.247**	-.181*	0.057	.460**	.386**	0.099	0.178	0.194	0.202	0.123	0.116
a7AP	.368**	.175*	.295**	-0.069	.274**	0.079	.285**	0.151	-0.109	-0.059	.402**	.384**	0.151	0.118	0.110	0.127	0.118	0.224
a8u	.415**	0.118	.530**	-0.124	0.140	-0.073	.433**	-0.009	0.162	-.208*	.242**	.245**	-0.107	0.289	.684**	0.265	-0.162	-0.157
a8tke	0.043	.255**	-.427**	.226**	.265**	.436**	.177*	.404**	-.236**	.240**	.264**	.273**	.423**	.455**	-.336*	.399**	.510**	.502**
a8dir	-0.056	0.113	.325**	.161*	-.162*	-.255**	-.177*	0.087	.210*	.210*	-0.149	-.183*	-0.115	0.075	.549**	0.067	-0.249	-0.237
a8CV	-.183*	0.099	-.558**	.205**	0.067	.278**	-0.052	.337**	-.223*	.310**	0.078	0.085	.336*	0.162	-.692**	0.091	.486**	.406**
a8ntt	.471**	.239**	.433**	-0.048	.252**	0.013	.472**	.182*	0.070	-0.079	.416**	.327**	0.170	.312*	.375*	0.241	0.036	0.076
a8AP	.506**	.227**	.346**	-0.056	.335**	0.117	.541**	0.161	0.026	-0.118	.422**	.405**	0.253	0.285	0.020	0.205	.325*	.420**
a9u	.343**	.151*	.415**	-0.066	.167*	-0.114	.323**	0.101	-0.035	-0.081	.321**	.201*	-0.257	-0.020	.455**	0.130	-.312*	-.317*
a9tke	0.044	.220**	0.099	.187*	0.100	-0.119	0.031	.223*	-0.140	.221*	0.124	-0.011	-0.178	0.091	0.202	0.115	-0.012	-0.197
a9dir	-.238**	0.013	-.488**	.168*	-0.031	.234**	-0.161	0.158	-.193*	.237**	-0.090	0.022	.344*	0.091	-0.241	-0.059	0.289	0.253
a9CV	-.196**	-0.048	-.287**	0.101	-0.049	0.094	-0.077	-0.015	-0.090	0.059	-0.064	-0.021	-0.138	0.178	0.099	0.186	0.059	0.060
a9ntt	.178*	.287**	.302**	0.142	0.088	-0.072	0.060	.268**	-0.123	.238**	0.150	0.176	-0.071	0.246	.586**	0.127	-0.135	-0.161
a9AP	.208**	.284**	.365**	0.119	0.113	-0.072	0.077	.273**	-0.069	.228*	0.165	0.180	-0.048	.311*	.615**	0.168	-0.104	-0.130
a10u	.476**	.204**	.506**	-0.068	.197**	-0.033	.539**	0.154	0.113	-0.102	.357**	.329**	-0.051	0.249	.723**	0.194	-0.217	-0.213
a10tke	0.122	.283**	-.535**	.175*	.374**	.467**	.251**	.448**	-.468**	.243**	.417**	.305**	.502**	0.281	-.542**	0.020	.573**	.639**
a10dir	-.163*	0.061	-.640**	.190*	0.089	.322**	-0.023	.283**	-.388**	.298**	0.134	.175*	.439**	0.012	-.636**	-0.091	.447**	.414**
a10CV	-.196**	-0.052	-.330**	0.054	0.019	0.129	-.177*	-0.007	-0.042	0.026	-0.116	-0.151	0.281	0.059	-.462**	0.004	.368*	0.269
a10ntt	.372**	.254**	.394**	0.010	.237**	-0.019	.326**	.230**	-0.068	0.036	.406**	.323**	0.099	.399**	.494**	0.281	0.012	0.020
a10AP	.367**	0.142	.409**	-0.101	.196**	0.021	.311**	0.049	-0.032	-0.149	.331**	.400**	0.033	0.136	.453**	0.126	-0.089	-0.009
a11u	.415**	.181*	.486**	-0.078	.202**	-0.004	.430**	0.110	0.078	-0.121	.354**	.372**	-0.107	0.289	.700**	0.249	-0.130	-0.125
a11tke	0.110	.251**	-.399**	.165*	.351**	.454**	.243**	.383**	-.339**	.188*	.383**	.351**	0.107	0.075	-.399**	0.099	.304*	.382*
a11dir	-.184*	0.057	-.581**	.194**	0.069	.272**	-0.064	.250**	-.296**	.285**	0.086	0.078	.407**	0.202	-.494**	0.067	.462**	.357*
a11CV	0.001	0.045	-.227**	0.100	0.110	.176*	0.077	0.122	0.004	0.096	0.019	-0.052	0.241	0.020	-.391**	0.075	.344*	.333*
a11ntt	.385**	.243**	.464**	-0.012	.213**	-0.066	.379**	.246**	0.041	0.015	.385**	.261**	-0.099	0.202	.581**	0.209	-0.154	-0.108
a11AP	.400**	.268**	.436**	-0.016	.249**	-0.021	.364**	.294**	0.033	0.024	.417**	.304**	0.116	0.149	0.285	0.060	0.036	0.159
a12u	.411**	.196**	.353**	-0.071	.263**	0.047	.427**	0.161	-0.141	-0.104	.461**	.457**	-0.107	0.225	.526**	.328*	-0.115	-0.100
a12tke	.380**	.149*	.252**	-0.096	.275**	0.068	.361**	0.127	-.201*	-0.125	.453**	.406**	0.067	0.115	0.241	0.265	-0.036	-0.020
a12dir	-.223**	0.063	-.698**	.214**	0.089	.273**	-0.104	.322**	-.456**	.355**	0.154	0.102	.328*	-0.083	-.858**	-0.107	.399**	.374*
a12CV	-0.007	0.002	.190*	-0.006	-.182*	-.263**	-0.039	-0.004	0.015	0.020	-0.084	-0.085	-.328*	-0.186	.431**	-0.209	-.462**	-.390*
a12ntt	.345**	.155*	.437**	-0.065	.207**	-0.087	.330**	0.097	-0.036	-0.081	.388**	.242**	-0.277	0.087	.681**	0.174	-0.253	-0.201
a12AP	.357**	.159*	.435**	-0.068	.221**	-0.072	.358**	0.103	-0.037	-0.078	.418**	.281**	-.323*	0.116	.633**	0.131	-0.275	-0.263

Table AP3.3: Location **A3**.

	FULL (84mins)				Run1: 15.49 to 16.49 inc. (61mins)				Run2: 16.50 to 17.12 inc. (23mins)			
	a3u	a3tke	a3dir	a3CV	a3u	a3tke	a3dir	a3CV	a3u	a3tke	a3dir	a3CV
a1u	.159*	0.138	.268**	-0.030	.185*	.217*	-0.046	0.101	0.202	-0.146	-0.130	-0.225
a1tke	.197**	.255**	-0.121	.149*	.230**	.302**	-.220*	.217*	0.170	0.186	0.028	0.059
a1dir	-.176*	-0.061	.675**	-0.063	-.269**	-.210*	.425**	-0.071	-.557**	0.059	.818**	0.265
a1CV	0.108	.157*	-.207**	0.142	0.151	.184*	-0.165	0.167	0.083	0.194	0.051	0.099
a2u	.434**	.330**	.182*	0.034	.490**	.372**	0.008	0.091	.455**	0.170	-0.209	-0.051
a2tke	.212**	.310**	0.009	0.129	.219*	.337**	-.204*	.211*	0.138	0.217	0.154	0.012
a2dir	-.177*	-0.052	.755**	-0.046	-.275**	-.195*	.572**	-0.038	-.542**	0.091	.850**	0.265
a2CV	-0.047	0.073	-0.121	0.080	-0.066	0.079	-.191*	0.104	0.020	0.130	0.130	0.020
a2ntt	.478**	.282**	-0.125	0.031	.487**	.365**	-.229**	0.088	.510**	0.146	-.312*	-0.059
a2AP	.472**	.268**	-.329**	0.061	.490**	.363**	-.227*	0.068	.598**	0.213	-0.253	0.036
a3u		.326**	-0.133	-0.059		.395**	-.199*	-0.020		0.194	-.486**	-0.059
a3tke	.326**		-0.010	.535**	.395**		-0.142	.538**	0.194		0.194	.589**
a3dir	-0.133	-0.010		-0.033	-.199*	-0.142		-0.032	-.486**	0.194		.320*
a3CV	-0.059	.535**	-0.033		-0.020	.538**	-0.032		-0.059	.589**	.320*	
a4u	0.106	0.089	.414**	-0.077	.212*	0.068	0.021	-0.091	-0.186	0.036	0.241	0.115
a4tke	0.039	.153*	-.332**	.184*	0.052	.186*	-.432**	.211*	0.059	0.107	-0.130	0.138
a4dir	-0.028	0.051	.569**	-0.029	-0.012	-0.027	.254**	-0.017	-.383*	0.217	.644**	.296*
a4CV	-0.027	-0.034	-.435**	0.054	-0.064	-0.030	-0.142	0.024	0.194	0.241	-0.075	0.051
a4ntt	.325**	.236**	.338**	0.001	.467**	.296**	-0.011	0.039	.317*	.309*	0.071	0.150
a4AP	.404**	.280**	.199**	0.023	.538**	.325**	-0.020	0.055	.484**	0.244	-0.148	0.028
a5u	0.103	.161*	.345**	0.031	.191*	.198*	-0.085	0.103	-0.123	0.051	0.130	0.209
a5tke	-0.029	0.085	-0.055	.150*	0.022	0.114	-0.130	0.172	-0.138	0.036	0.115	0.178
a5dir	-0.008	0.067	.503**	-0.071	0.052	-0.024	.176*	-0.130	-.415**	0.186	.660**	0.249
a5CV	-0.041	0.003	-.294**	0.090	-0.110	-0.040	-0.004	0.059	0.138	0.217	-0.146	0.107
a5ntt	.164*	.290**	-0.078	.177*	.249**	.346**	-.292**	.200*	-0.012	0.099	0.036	0.242
a5AP	.279**	.347**	-0.132	.151*	.337**	.378**	-.334**	0.155	0.202	0.259	-0.089	0.275
a6u	.161*	0.123	.161*	-0.007	.183*	.207*	-.188*	0.160	0.209	-0.202	-.407**	-0.233
a6tke	0.015	0.044	-.164*	0.065	-0.016	0.102	-0.170	0.146	0.146	-0.123	-0.265	-0.138
a6dir	-0.075	0.036	.515**	-0.063	-0.042	-0.072	.266**	-0.132	-.423**	0.130	.557**	.304*
a6CV	-0.048	-0.065	-.339**	0.058	-0.061	-0.070	-0.062	0.012	-0.051	-0.067	-0.146	0.043
a6ntt	.351**	.405**	0.040	.189*	.414**	.451**	-.317**	.238**	.391**	.375*	-0.178	0.233
a6AP	.292**	.198*	-0.102	0.084	.308**	.255*	-.282**	0.144	0.278	-0.048	-.355*	-0.086
a7u	0.055	.172*	.682**	0.057	0.144	.210*	.423**	0.152	-.431**	0.202	.929**	.296*
a7tke	.388**	.314**	-.477**	0.120	.426**	.463**	-.377**	0.172	.573**	0.194	-.423**	-0.059
a7dir	-.347**	-0.075	.194**	0.074	-.303**	-0.064	0.052	0.138	-.589**	-0.146	.549**	0.059
a7CV	0.044	-0.102	-.321**	-0.021	-0.030	-0.134	0.042	-0.098	.415**	0.004	-.439**	-0.028
a7ntt	.286**	.357**	.248**	0.104	.489**	.484**	-.254**	.195*	0.091	.455**	0.202	.328*
a7AP	.320**	.287**	.269**	0.045	.468**	.352**	-0.142	0.132	0.265	.306*	0.078	0.094
a8u	.222**	.169*	.560**	-0.062	.430**	.187*	.230**	-0.074	-0.241	.296*	.708**	0.265
a8tke	.310**	.377**	-.425**	.240**	.331**	.550**	-.258**	.330**	.510**	.368*	-0.217	0.083
a8dir	-.343**	-0.076	.324**	0.088	-.316**	-0.130	.184*	0.090	-.518**	-0.043	.636**	0.115
a8CV	0.052	0.144	-.531**	.217**	0.036	.344**	-.199*	.348**	.439**	-0.020	-.605**	-0.178
a8ntt	.212**	.243**	.498**	0.029	.348**	.266**	.178*	0.060	0.020	.478**	.431**	.320*
a8AP	.301**	.297**	.409**	0.037	.435**	.340**	0.142	0.074	.309*	.366*	0.084	0.173
a9u	0.087	.162*	.409**	0.043	.193*	.211*	-0.024	0.127	-.296*	0.083	.399**	0.289
a9tke	-0.112	0.090	0.101	0.117	-0.075	0.099	-0.133	.192*	-0.265	-0.028	0.194	0.036
a9dir	0.039	-0.006	-.476**	0.067	0.026	0.042	-.189*	0.067	0.289	0.020	-0.186	-0.170
a9CV	-0.084	-0.011	-.263**	0.109	-0.064	-0.045	-0.063	0.046	-0.036	0.107	0.138	0.107
a9ntt	-0.022	.175*	.272**	0.114	0.044	0.177	-.183*	.201*	-0.293	0.230	.657**	0.246
a9AP	0.019	.202**	.298**	0.111	0.082	.227*	-.196*	.231*	-0.232	0.279	.639**	0.232
a10u	.193**	.225**	.563**	0.028	.385**	.299**	.213*	0.095	-.312*	0.225	.810**	0.257
a10tke	.397**	.271**	-.458**	0.076	.432**	.381**	-.352**	0.087	.636**	0.178	-.391**	-0.075
a10dir	0.064	0.016	-.619**	0.083	0.070	0.129	-.377**	0.119	.431**	-0.138	-.534**	-.312*
a10CV	0.001	-0.103	-.326**	-0.044	-0.139	-0.117	-0.042	-0.087	.368*	-0.059	-.470**	-0.123
a10ntt	0.124	.197**	.430**	0.028	.224*	.229**	0.002	0.095	-0.083	.344*	.581**	0.249
a10AP	0.132	.187*	.401**	0.038	.246**	.217*	-0.035	0.107	-0.136	0.276	.472**	0.257
a11u	.260**	.253**	.473**	0.031	.507**	.345**	0.054	0.097	-0.289	0.281	.771**	.296*
a11tke	.396**	.375**	-.423**	.181*	.386**	.489**	-.391**	.258**	.557**	.304*	-.328*	0.067
a11dir	-0.010	-0.024	-.520**	0.071	-0.052	0.059	-.215*	0.095	0.241	-0.217	-.360*	-.344*
a11CV	0.135	-0.033	-.232**	-0.042	0.054	-0.047	-0.020	-0.079	.391**	0.012	-.336*	-0.099
a11ntt	.188*	.287**	.473**	0.084	.360**	.405**	0.067	.200*	-0.138	.368*	.621**	.304*
a11AP	.227**	.296**	.440**	0.074	.386**	.421**	0.049	.203*	0.149	.333*	.301*	0.173
a12u	.310**	.293**	.329**	0.030	.573**	.393**	-.180*	0.080	-0.115	.423**	.565**	.360*
a12tke	.277**	.303**	.263**	0.076	.462**	.373**	-0.168	0.103	0.059	.360*	0.249	.407**
a12dir	0.018	0.013	-.717**	0.103	-0.011	0.138	-.502**	0.156	.478**	-0.170	-.834**	-.296*
a12CV	-0.064	0.018	.229**	-0.006	0.067	-0.049	0.098	-0.131	-.336*	0.154	.360*	.344*
a12ntt	.177*	.219**	.440**	0.000	.375**	.273**	-0.015	0.005	-.333*	.333*	.665**	.491**
a12AP	.200**	.235**	.444**	-0.005	.411**	.306**	-0.006	0.014	-0.275	.323*	.641**	.363*

Table AP3.4: Location **A4**.

	FULL (84mins)						Run1: 15.49 to 16.49 inc. (61mins)						Run2: 16.50 to 17.12 inc. (23mins)					
	a4u	a4tke	a4dir	a4CV	a4ntt	a4AP	a4u	a4tke	a4dir	a4CV	a4ntt	a4AP	a4u	a4tke	a4dir	a4CV	a4ntt	a4AP
a1u	.365**	-0.037	.219**	-.288**	.449**	.353**	0.103	0.046	-0.141	-0.034	.246**	.281**	0.091	-0.028	-0.154	0.123	.372*	0.092
a1tke	0.039	.151*	-0.011	0.056	0.123	.154*	0.089	.217*	-0.002	0.026	0.140	.189*	0.012	0.051	-0.028	0.202	.444**	0.252
a1dir	.430**	-.279**	.517**	-.429**	.280**	.164*	0.027	-.349**	0.140	-0.111	-0.116	-0.078	.312*	-0.059	.668**	-0.115	-0.079	-0.268
a1CV	-0.131	.172*	-0.090	.192**	-0.059	-0.007	0.001	.209*	0.068	0.092	0.044	0.076	-0.091	-0.020	-0.004	0.146	0.277	0.212
a2u	.332**	-0.045	.165*	-.264**	.538**	.572**	.298**	0.036	-0.015	-.175*	.549**	.594**	-0.178	-0.059	-0.202	0.123	.404**	.428**
a2tke	0.100	0.093	0.084	-0.027	.268**	.182*	0.019	.233**	-0.028	0.046	.221*	0.170	-0.083	-0.123	0.020	.296*	.562**	0.156
a2dir	.424**	-.295**	.554**	-.403**	.261**	.157*	0.014	-.370**	.205*	-0.059	-0.155	-0.091	.312*	-0.138	.684**	-0.130	-0.063	-0.276
a2CV	-0.117	0.114	-0.011	.154*	-0.023	-0.118	-0.148	.215*	0.028	0.162	-0.057	-0.131	-0.075	-0.178	0.107	0.273	.459**	-0.012
a2ntt	.195**	.187*	-0.063	-0.066	.387**	.409**	.347**	.251**	-0.095	-0.102	.527**	.553**	-0.186	0.138	-.447**	0.225	.475**	.380*
a2AP	-0.072	.177*	-.238**	.179*	0.096	.272**	.259**	0.165	-0.025	-0.018	.389**	.526**	-0.245	0.020	-.406**	0.189	.463**	.508**
a3u	0.106	0.039	-0.028	-0.027	.325**	.404**	.212*	0.052	-0.012	-0.064	.467**	.538**	-0.186	0.059	-.383*	0.194	.317*	.484**
a3tke	0.089	.153*	0.051	-0.034	.236**	.280**	0.068	.186*	-0.027	-0.030	.296**	.325**	0.036	0.107	0.217	0.241	.309*	0.244
a3dir	.414**	-.332**	.569**	-.435**	.338**	.199**	0.021	-.432**	.254**	-0.142	-0.011	-0.020	0.241	-0.130	.644**	-0.075	0.071	-0.148
a3CV	-0.077	.184*	-0.029	0.054	0.001	0.023	-0.091	.211*	-0.017	0.024	0.039	0.055	0.115	0.138	.296*	0.051	0.150	0.028
a4u		-0.033	.407**	-.535**	.525**	.406**		0.062	-0.028	-.286**	.361**	.396**		0.233	.439**	-0.281	-0.087	-.332*
a4tke	-0.033		-.239**	0.109	-0.094	-0.062	0.062		-.269**	0.083	-0.015	0.029	0.233		-0.091	-0.115	-0.079	-0.060
a4dir	.407**	-.239**		-.356**	.301**	.178*	-0.028	-.269**		0.023	-0.075	-0.058	.439**	-0.091		-0.130	-0.016	-0.180
a4CV	-.535**	0.109	-.356**		-.442**	-.324**	-.286**	0.083	0.023		-.272**	-.258**	-0.281	-0.115	-0.130		0.238	0.292
a4ntt	.525**	-0.094	.301**	-.442**		.658**	.361**	-0.015	-0.075	-.272**		.703**	-0.087	-0.079	-0.016	0.238		.305*
a4AP	.406**	-0.062	.178*	-.324**	.658**		.396**	0.029	-0.058	-.258**	.703**		-.332*	-0.060	-0.180	0.292	.305*	
a5u	.648**	0.053	.320**	-.441**	.486**	.367**	.404**	.219*	-0.156	-0.139	.274**	.326**	.605**	0.249	0.233	-0.138	0.055	-.340*
a5tke	.149*	.437**	-0.101	-0.048	0.035	0.020	.191*	.475**	-.230**	0.002	0.094	0.131	.415**	.375*	0.123	-0.249	-0.087	-0.244
a5dir	.461**	-.203**	.777**	-.350**	.312**	.193**	0.102	-.246**	.658**	0.013	-0.009	0.018	.470**	0.004	.826**	-0.162	0.000	-0.220
a5CV	-.315**	.165*	-.364**	.417**	-.273**	-.200**	-0.035	0.131	-0.123	.220*	-0.056	-0.059	-0.178	0.099	-0.202	0.281	-0.032	0.068
a5ntt	0.138	0.128	-0.008	-0.069	.284**	.222**	0.090	.199*	-.179*	0.014	.256**	.228*	0.083	0.020	0.044	-0.036	.398**	0.084
a5AP	.153*	.225**	-0.056	-0.048	.274**	.267**	0.169	.289**	-.203*	-0.002	.272**	.271**	0.032	0.113	-0.081	0.137	.458**	0.245
a6u	.427**	.165*	0.091	-.306**	.413**	.316**	.262**	.328**	-.327**	-0.073	.268**	.262**	0.004	0.202	-.399**	0.146	0.048	-0.076
a6tke	0.019	.320**	-.253**	0.006	-0.018	-0.044	0.120	.337**	-.333**	-0.043	0.060	0.047	0.036	0.217	-.336*	-0.059	-0.032	-0.084
a6dir	.450**	-.187*	.598**	-.387**	.300**	.174*	0.132	-.255**	.383**	-0.116	0.035	0.041	.462**	0.107	.755**	-0.154	-0.071	-0.276
a6CV	-.372**	0.075	-.349**	.383**	-.337**	-.242**	-0.126	-0.014	-0.052	0.164	-0.140	-0.103	-0.146	0.115	-.312*	0.233	-0.127	-0.028
a6ntt	.295**	.173*	.169*	-0.114	.377**	.390**	0.131	.295**	-0.086	0.130	.235**	.328**	0.012	0.178	-0.154	0.170	.333*	.396**
a6AP	0.157	.178*	0.046	-0.042	.196*	.184*	0.133	.264**	-0.049	0.062	.242*	.213*	-0.067	-0.105	-0.240	-0.029	-0.259	0.019
a7u	.535**	-.211**	.519**	-.504**	.542**	.423**	.235**	-.209*	0.151	-.262**	.358**	.398**	0.281	-0.107	.636**	-0.083	0.079	-0.172
a7tke	-.251**	.278**	-.377**	.251**	-0.013	0.086	0.032	.329**	-.179*	-0.017	.302**	.296**	-0.265	-0.020	-.447**	0.289	.380*	.412**
a7dir	0.020	-0.006	.192**	0.000	-0.101	-.193**	-.236**	0.048	0.060	.231**	-.338**	-.296**	0.281	-0.028	.415**	-0.209	-0.063	-.380*
a7CV	-.325**	0.068	-.377**	.388**	-.265**	-.230**	-0.013	-0.050	-0.080	.187*	-0.032	-0.102	-0.091	0.043	-0.273	0.051	0.222	0.196
a7ntt	.484**	0.037	.338**	-.343**	.558**	.444**	.173*	.181*	-0.104	-0.032	.357**	.386**	0.233	0.083	0.273	0.249	.364*	0.172
a7AP	.442**	-0.041	.345**	-.284**	.478**	.457**	0.143	0.061	-0.023	0.039	.310**	.413**	0.290	0.045	0.225	0.176	0.205	0.223
a8u	.519**	-.219**	.484**	-.427**	.570**	.471**	.192*	-.230**	0.080	-0.132	.401**	.474**	.391**	-0.043	.684**	0.012	0.190	-0.084
a8tke	-.290**	.243**	-.306**	.324**	-0.114	-0.036	-0.020	.234**	-0.034	0.091	0.143	0.143	-0.091	0.123	-0.178	0.241	.507**	0.228
a8dir	0.049	-0.026	.228**	-0.108	0.008	-0.050	-.251**	0.052	0.045	0.121	-.215*	-.195*	0.146	-0.067	.407**	-0.202	-0.024	-0.156
a8CV	-.469**	.235**	-.441**	.426**	-.341**	-.238**	-0.118	.243**	-0.030	0.119	-0.040	-0.070	-.304*	0.162	-.549**	0.123	0.230	0.196
a8ntt	.552**	-.167*	.393**	-.432**	.658**	.540**	.325**	-0.116	-0.014	-.211*	.562**	.573**	0.225	0.012	.455**	0.178	.404**	0.228
a8AP	.481**	-0.136	.359**	-.351**	.628**	.585**	.294**	-0.098	0.050	-0.137	.537**	.639**	0.036	0.036	0.044	0.221	.507**	.305*
a9u	.631**	0.003	.375**	-.473**	.509**	.372**	.378**	0.157	-0.119	-.189*	.307**	.340**	.510**	0.138	.581**	-0.138	0.000	-.428**
a9tke	.234**	.318**	0.015	-0.128	0.116	-0.006	0.083	.439**	-.287**	0.034	0.012	0.013	.368*	0.265	0.154	-0.043	-0.048	-.460**
a9dir	-.514**	.193**	-.313**	.545**	-.424**	-.285**	-.294**	0.148	0.120	.389**	-.212*	-.206*	0.036	0.138	-0.162	0.067	0.150	.340*
a9CV	-.372**	0.055	-.310**	.401**	-.275**	-.201**	-.238**	0.035	-0.141	.261**	-0.169	-0.160	-0.083	-0.075	0.083	0.249	0.198	0.092
a9ntt	.280**	-0.012	.387**	-.196*	.350**	.222**	-0.117	0.123	0.053	0.171	0.124	0.104	.309*	-0.032	.523**	-0.016	0.218	-0.088
a9AP	.315**	-0.009	.418**	-.218**	.387**	.266**	-0.110	0.146	0.049	.187*	0.129	0.154	0.279	-0.080	.519**	0.016	0.244	-0.057
a10u	.499**	-.185*	.506**	-.404**	.569**	.483**	0.165	-0.158	0.127	-0.081	.407**	.499**	.352*	-0.051	.660**	-0.075	0.150	-0.084
a10tke	-.213**	.239**	-.380**	.267**	0.001	0.092	0.105	.278**	-.185*	0.019	.322**	.299**	-.344*	-0.067	-.478**	0.273	.364*	.412**
a10dir	-.516**	.278**	-.480**	.480**	-.385**	-.244**	-.215*	.349**	-0.094	.232**	-0.105	-0.097	-0.249	-0.004	-.589**	0.020	0.103	.348*
a10CV	-.310**	.153*	-.325**	.355**	-.314**	-.321**	-0.083	0.077	-0.049	.220*	-.183*	-.229*	0.020	0.028	-.336*	-0.091	0.158	0.044
a10ntt	.518**	-0.067	.523**	-.371**	.555**	.428**	.208*	0.053	.188*	-0.034	.356**	.378**	.296*	0.004	.494**	0.043	.364*	0.068
a10AP	.498**	-0.092	.498**	-.388**	.476**	.393**	0.144	0.018	0.140	-0.037	.223*	.341**	.472**	-0.079	.491**	-0.136	0.187	-0.166
a11u	.533**	-0.117	.487**	-.383**	.556**	.470**	.222*	-0.040	0.094	-0.042	.378**	.476**	.360*	-0.012	.636**	-0.020	0.190	-0.108
a11tke	-0.132	.285**	-.251**	.243**	-0.030	0.066	0.109	.321**	-0.089	0.078	.204*	.234**	-0.059	0.043	-0.241	0.257	0.190	0.268
a11dir	-.530**	.268**	-.460**	.454**	-.379**	-.257**	-.239**	.329**	-0.074	.181*	-0.114	-0.122	-.296*	-0.036	-.494**	0.067	0.222	.300*
a11CV	-.235**	0.099	-.248**	.274**	-0.141	-0.123	-0.085	0.011	-0.067	.191*	0.012	-0.020	0.059	0.130	-0.217	-0.004	0.166	0.036
a11ntt	.574**	-0.119	.489**	-.435**	.611**	.484**	.300**	-0.047	0.088	-0.146	.471**	.484**	.304*	-0.020	.628**	0.067	0.230	0.036
a11AP	.555**	-0.120	.478**	-.422**	.591**	.476**	.267**	-0.033	0.104	-0.127	.428**	.440**	.333*	-0.036	.382*	0.076	.298*	0.191
a12u	.571**	-0.025	.431**	-.335**	.570**	.469**	.301**	0.113	-0.002	0.022	.404**	.465**	.296*	0.036	.636**	0.154	0.238	0.020
a12tke	.533**	-0.032	.361**	-.377**	.527**	.476**	.339**	0.042	-0.014	-0.128	.410**	.455**	0.107	0.036	.368*	0.154	0.230	0.172
a12dir	-.482**	.346**	-.567**	.476**	-.372**	-.269**	-0.139	.460**	-.236**	.214*	-0.063	-0.113	-0.265	0.123	-.684**	0.067	0.048	0.204
a12CV	0.099	-.158*	.252**	-0.071	0.025	-0.049	-0.125	-0.160	0.134	0.115	-0.108	-0.131	0.217	0.036	.399**	-0.130	-0.269	-0.276
a12ntt	.579**	-0.063	.367**	-.478**	.556**	.432**	.295**	0.050	-0.160	-.212*	.382**	.414**	0.277	-0.032	.642**	0.048	0.131	-0.120
a12AP	.604**	-0.065	.382**	-.467**	.562**	.453**	.335**	0.041	-0.143	-.197*	.405**	.449**	.331*	0.028	.681**	0.108	0.032	-0.125

Table AP3.5: Location **A5**.

	FULL (84mins)						Run1: 15.49 to 16.49 inc. (61mins)						Run2: 16.50 to 17.12 inc. (23mins)					
	a5u	a5tke	a5dir	a5CV	a5ntt	a5AP	a5u	a5tke	a5 dir	a5CV	a5ntt	a5AP	a5u	a5tke	a5 dir	a5CV	a5ntt	a5AP
a1u	.337**	0.004	.240**	-.232**	.169*	.185*	0.062	-0.004	-0.072	0.008	0.136	0.171	0.043	-0.004	-0.154	-0.059	0.067	0.170
a1tke	0.056	-0.020	0.007	0.020	.222**	.236**	0.120	0.038	0.032	-0.046	.269**	.249**	-0.004	-0.115	-0.012	0.099	0.123	0.186
a1dir	.376**	-0.061	.479**	-.295**	0.005	-0.065	-0.042	-0.150	0.123	0.011	-0.146	-.205*	0.138	0.075	.636**	-0.170	0.012	-0.162
a1CV	-0.112	-0.048	-0.095	0.137	0.135	0.113	0.042	0.034	0.049	0.009	.205*	0.161	-0.138	-0.249	-0.004	0.091	0.083	0.032
a2u	.307**	0.016	.165*	-.178*	.148*	.188*	.245**	0.078	0.023	-0.055	0.144	.187*	-0.178	-0.130	-0.186	-0.028	0.036	0.089
a2tke	.147*	0.084	0.069	-0.074	.258**	.266**	0.114	0.169	-0.043	-0.020	.271**	.276**	-0.083	-0.083	0.067	-0.043	0.187	0.202
a2dir	.359**	-0.052	.480**	-.287**	-0.014	-0.071	-0.081	-0.145	0.117	0.031	-.188*	-.225*	0.170	0.170	.684**	-0.202	0.060	-0.105
a2CV	-0.060	0.105	-0.033	0.042	0.145	0.147	-0.039	0.148	-0.016	0.044	0.137	0.140	-0.012	-0.028	0.154	-0.051	0.226	0.242
a2ntt	.197**	.151*	-0.054	0.024	.319**	.390**	.326**	.226*	-0.075	0.033	.364**	.420**	-0.043	-0.028	-.399**	0.091	0.234	.331*
a2AP	-0.082	0.032	-.186*	.178*	.157*	.259**	.214*	0.115	0.049	0.012	.274**	.336**	-0.092	-0.100	-.374*	0.149	0.133	0.287
a3u	0.103	-0.029	-0.008	-0.041	.164*	.279**	.191*	0.022	0.052	-0.110	.249**	.337**	-0.123	-0.138	-.415**	0.138	-0.012	0.202
a3tke	.161*	0.085	0.067	0.003	.290**	.347**	.198*	0.114	-0.024	-0.040	.346**	.378**	0.051	0.036	0.186	0.217	0.099	0.259
a3dir	.345**	-0.055	.503**	-.294**	-0.078	-0.132	-0.085	-0.130	.176*	-0.004	-.292**	-.334**	0.130	0.115	.660**	-0.146	0.036	-0.089
a3CV	0.031	.150*	-0.071	0.090	.177*	.151*	0.103	0.172	-0.130	0.059	.200*	0.155	0.209	0.178	0.249	0.107	0.242	0.275
a4u	.648**	.149*	.461**	-.315**	0.138	.153*	.404**	.191*	0.102	-0.035	0.090	0.169	.605**	.415**	.470**	-0.178	0.083	0.032
a4tke	0.053	.437**	-.203**	.165*	0.128	.225**	.219*	.475**	-.246**	0.131	.199*	.289**	0.249	.375*	0.004	0.099	0.020	0.113
a4dir	.320**	-0.101	.777**	-.364**	-0.008	-0.056	-0.156	-.230**	.658**	-0.123	-.179*	-.203*	0.233	0.123	.826**	-0.202	0.044	-0.081
a4CV	-.441**	-0.048	-.350**	.417**	-0.069	-0.048	-0.139	0.002	0.013	.220*	0.014	-0.002	-0.138	-0.249	-0.162	0.281	-0.036	0.137
a4ntt	.486**	0.035	.312**	-.273**	.284**	.274**	.274**	0.094	-0.009	-0.056	.256**	.272**	0.055	-0.087	0.000	-0.032	.398**	.458**
a4AP	.367**	0.020	.193**	-.200**	.222**	.267**	.326**	0.131	0.018	-0.059	.228*	.271**	-.340*	-0.244	-0.220	0.068	0.084	0.245
a5u		.277**	.280**	-.238**	.237**	.244**		.409**	-.201*	0.075	.249**	.308**		.526**	0.249	0.043	0.210	0.218
a5tke	.277**		-0.116	0.017	0.142	.213**	.409**		-.290**	0.109	.182*	.254**	.526**		0.202	-0.115	0.020	0.065
a5dir	.280**	-0.116		-.366**	-0.020	-0.051	-.201*	-.290**		-0.162	-.205*	-.219*	0.249	0.202		-0.217	0.028	-0.040
a5CV	-.238**	0.017	-.366**		-0.019	0.015	0.075	0.109	-0.162		0.104	0.097	0.043	-0.115	-0.217		-0.067	0.024
a5ntt	.237**	0.142	-0.020	-0.019		.747**	.249**	.182*	-.205*	0.104		.785**	0.210	0.020	0.028	-0.067		.649**
a5AP	.244**	.213**	-0.051	0.015	.747**		.308**	.254**	-.219*	0.097	.785**		0.218	0.065	-0.040	0.024	.649**	
a6u	.603**	.336**	0.029	-.166*	.266**	.298**	.554**	.463**	-.396**	0.084	.325**	.364**	0.273	0.257	-.383*	0.091	-0.028	0.073
a6tke	.149*	.448**	-.308**	0.074	0.083	0.139	.340**	.474**	-.437**	0.043	0.150	0.175	0.178	.368*	-0.209	0.059	-0.123	0.000
a6dir	.409**	-0.032	.668**	-.245**	0.025	-0.022	0.079	-0.123	.460**	0.002	-0.115	-0.154	.336*	0.194	.771**	-0.115	0.052	-0.073
a6CV	-.320**	-0.020	-.329**	.405**	0.008	0.005	-0.068	-0.045	-0.054	.205*	0.071	0.012	0.107	0.154	-.296*	0.273	0.052	0.154
a6ntt	.358**	0.121	0.143	-0.080	.376**	.469**	.233**	0.164	-0.101	0.051	.473**	.551**	0.154	0.043	-0.202	0.273	0.163	.396**
a6AP	.216*	0.129	0.007	-0.076	.203*	.270**	.244*	0.192	-0.089	-0.045	.319**	.359**	-0.144	-0.182	-0.259	0.067	-0.270	-0.118
a7u	.505**	0.037	.460**	-.343**	0.098	0.063	.201*	0.030	0.086	-0.085	0.033	0.027	0.186	0.170	.668**	-0.154	0.044	-0.057
a7tke	-.152*	0.053	-.330**	.194**	.204**	.267**	.190*	.185*	-0.106	-0.063	.387**	.426**	-0.138	-0.249	-.462**	0.233	0.075	0.202
a7dir	0.031	0.022	.167*	-0.054	-0.103	-0.143	-.198*	-0.026	0.011	0.075	-0.136	-0.148	0.217	0.138	.462**	-0.091	-0.036	-0.186
a7CV	-.320**	-0.007	-.344**	.176*	-0.055	-0.056	-0.025	-0.002	-0.059	-0.082	-0.025	-0.069	-0.012	0.020	-0.273	-0.099	0.147	0.178
a7ntt	.555**	0.107	.322**	-.273**	.428**	.477**	.307**	0.153	-0.103	-0.034	.570**	.672**	0.265	0.075	0.225	0.146	0.290	.558**
a7AP	.475**	0.081	.317**	-.269**	.258**	.322**	.222*	0.091	-0.055	-0.035	.354**	.437**	0.208	0.135	0.200	0.086	-0.103	0.138
a8u	.483**	-0.008	.469**	-.309**	0.141	0.129	0.154	-0.052	0.103	-0.032	0.111	0.144	0.233	0.170	.700**	-0.123	0.091	0.024
a8tke	-.207**	0.014	-.262**	.236**	.176*	.252**	0.097	0.037	0.015	0.014	.325**	.364**	0.115	0.020	-0.162	0.186	0.131	.299*
a8dir	0.072	0.046	.193**	-0.102	-0.112	-.189*	-.187*	0.026	-0.028	0.093	-.173*	-.232**	0.067	0.178	.455**	-0.178	-0.075	-0.178
a8CV	-.406**	0.014	-.391**	.301**	0.013	0.043	-0.047	0.039	0.015	0.016	0.157	0.155	-0.036	0.043	-.534**	0.067	0.099	0.145
a8ntt	.523**	0.037	.388**	-.280**	.172*	.177*	.301**	0.086	0.027	-0.032	.180*	.207*	0.067	0.020	.439**	-0.067	0.139	0.275
a8AP	.494**	0.094	.344**	-.233**	.203**	.219**	.315**	0.126	0.078	-0.032	.186*	.219*	0.084	0.068	0.044	0.116	0.069	0.292
a9u	.830**	.232**	.321**	-.266**	.198**	.191*	.757**	.367**	-0.168	0.054	.216*	.257**	.573**	.368*	.534**	-0.083	0.036	0.000
a9tke	.384**	.515**	-0.020	-0.049	.149*	.158*	.344**	.614**	-.356**	0.084	0.111	0.150	.526**	.415**	0.233	0.012	0.083	0.016
a9dir	-.544**	-0.055	-.276**	.241**	-0.139	-0.096	-.334**	-0.089	0.126	-0.026	-0.103	-0.101	-0.107	0.036	-0.051	-0.067	-0.115	-0.008
a9CV	-.315**	-0.025	-.326**	.410**	-0.020	-0.025	-0.169	-0.024	-.186*	.336**	-0.046	-0.050	0.170	-0.020	-0.043	0.162	.313*	0.267
a9ntt	.278**	-0.004	.366**	-.210**	.166*	0.115	-0.098	-0.036	0.030	0.041	0.142	0.100	0.230	0.190	.539**	-0.135	0.040	0.004
a9AP	.333**	0.033	.381**	-.235**	.185*	0.150	-0.053	0.028	0.004	0.029	0.171	0.147	0.176	0.152	.543**	-0.096	0.016	0.033
a10u	.468**	0.010	.469**	-.328**	0.105	0.095	0.138	-0.016	0.106	-0.059	0.057	0.092	0.194	0.194	.708**	-0.209	0.036	-0.040
a10tke	-0.145	0.038	-.334**	.195**	.248**	.321**	.209*	0.168	-0.125	-0.043	.438**	.487**	-0.217	-0.281	-.462**	0.154	0.083	0.178
a10dir	-.439**	0.060	-.474**	.318**	-0.063	-0.018	-0.083	0.163	-0.141	0.055	0.042	0.061	-0.217	-0.138	-.526**	0.028	0.004	0.081
a10CV	-.255**	0.094	-.338**	.268**	0.001	0.016	-0.001	0.142	-0.118	0.069	0.057	0.015	0.115	0.051	-.320*	0.091	0.123	0.202
a10ntt	.523**	0.082	.464**	-.271**	.171*	0.142	.240**	0.114	0.118	0.044	.179*	0.161	0.170	0.186	.526**	-0.186	0.012	0.057
a10AP	.541**	0.039	.441**	-.305**	0.123	0.111	.259**	0.040	0.074	-0.026	0.078	0.088	0.266	0.145	.509**	-0.136	0.056	0.105
a11u	.503**	0.039	.461**	-.330**	.203**	.211**	.195*	0.034	0.089	-0.066	.231**	.304**	0.217	0.186	.684**	-0.154	0.075	-0.008
a11tke	-0.104	0.059	-.220**	.164*	.262**	.370**	0.154	0.138	-0.059	-0.047	.427**	.496**	-0.043	-0.123	-0.225	.312*	-0.004	0.194
a11dir	-.480**	0.063	-.452**	.294**	-0.111	-0.077	-0.168	0.163	-0.115	0.015	-0.059	-0.052	-0.186	-0.107	-.431**	-0.051	0.075	0.081
a11CV	-0.130	0.092	-.265**	.149*	0.039	0.092	0.113	.177*	-0.133	0.010	0.075	0.090	0.012	-0.051	-0.202	0.004	0.052	0.170
a11ntt	.593**	0.065	.439**	-.348**	.243**	.216**	.366**	0.087	0.050	-0.094	.312**	.302**	0.162	0.130	.597**	-0.130	0.020	0.057
a11AP	.585**	0.066	.428**	-.317**	.249**	.250**	.355**	0.098	0.068	-0.051	.342**	.360**	0.181	0.125	.349*	-0.028	-0.060	0.148
a12u	.567**	0.074	.443**	-.290**	.262**	.298**	.319**	0.099	0.056	-0.011	.340**	.440**	0.170	0.091	.605**	-0.043	0.012	0.089
a12tke	.541**	0.050	.380**	-.278**	.262**	.279**	.360**	0.048	0.035	-0.045	.311**	.331**	0.075	0.075	0.289	-0.075	0.131	0.267
a12dir	-.399**	0.082	-.526**	.361**	0.007	0.040	-0.011	.187*	-.220*	0.127	0.158	0.157	-0.123	-0.091	-.636**	0.107	0.004	0.129
a12CV	0.062	-0.124	.235**	-.228**	-0.130	-0.142	-0.154	-.197*	0.103	-0.167	-0.165	-0.157	-0.020	0.043	.399**	-0.154	-0.163	-0.226
a12ntt	.575**	0.072	.350**	-.277**	.286**	.291**	.302**	0.091	-0.154	0.030	.350**	.417**	0.246	0.103	.618**	-0.008	0.215	0.158
a12AP	.587**	0.076	.370**	-.276**	.273**	.293**	.322**	0.093	-0.122	0.035	.353**	.441**	0.251	0.163	.626**	-0.028	0.028	0.049

Table AP3.6: Location **A6**.

	FULL (84mins)						Run1: 15.49 to 16.49 inc. (61mins)						Run2: 16.50 to 17.12 inc. (23mins)					
	a6u	a6tke	a6dir	a6CV	a6ntt	a6AP	a6u	a6tke	a6dir	a6CV	a6ntt	a6AP	a6u	a6tke	a6dir	a6CV	a6ntt	a6AP
a1u	.347**	0.033	.186*	-.270**	.346**	0.110	0.139	0.093	-0.129	-0.026	.246**	0.091	0.233	0.138	-0.146	-0.154	0.178	-0.105
a1tke	0.080	0.045	-0.046	0.080	.232**	0.145	0.131	0.103	-0.084	0.128	.306**	.227*	-0.004	-0.099	0.028	-0.123	0.225	-0.182
a1dir	.209**	-.150*	.526**	-.302**	0.116	-0.092	-0.116	-0.157	.274**	0.008	-.175*	-.288**	-.368*	-.273	.597**	-0.091	-0.217	-0.278
a1CV	-0.074	-0.001	-0.138	.182*	0.087	0.091	0.068	0.048	-0.073	0.139	.238**	0.188	-0.154	-0.233	0.051	-0.115	0.091	-0.105
a2u	.309**	0.019	.173*	-.254**	.312**	0.156	.219*	0.055	0.082	-0.121	.234**	0.146	0.091	0.075	-0.241	-0.202	0.289	0.067
a2tke	.199**	0.077	-0.005	-0.116	.220**	.179*	.177*	0.151	-0.145	-0.056	.249**	.273**	0.028	-0.083	-0.067	-0.123	0.020	-.355*
a2dir	.197**	-0.137	.486**	-.295**	0.106	-0.078	-0.142	-0.136	.200*	0.023	-.199*	-.260*	-.352*	-0.241	.581**	-0.091	-0.202	-0.316
a2CV	0.034	0.094	-0.118	-0.005	-0.009	0.095	0.074	0.136	-0.169	-0.043	0.063	.236*	0.099	-0.028	0.067	-0.083	-0.067	-.393*
a2ntt	.287**	.166*	-0.069	-0.072	.395**	.233**	.356**	0.153	-0.072	-0.123	.468**	.347**	0.209	0.225	-.391**	0.028	.439**	-0.086
a2AP	-0.002	0.076	-.220**	0.070	.232**	0.156	.192*	0.043	-0.032	-0.113	.414**	.244*	0.108	0.157	-.366*	0.028	.526**	0.010
a3u	.161*	0.015	-0.075	-0.048	.351**	.292**	.183*	-0.016	-0.042	-0.061	.414**	.308**	0.209	0.146	-.423**	-0.051	.391**	0.278
a3tke	0.123	0.044	0.036	-0.065	.405**	.198*	.207*	0.102	-0.072	-0.070	.451**	.255*	-0.202	-0.123	0.130	-0.067	.375*	-0.048
a3dir	.161*	-.164*	.515**	-.339**	0.040	-0.102	-.188*	-0.170	.266**	-0.062	-.317**	-.282**	-.407**	-0.265	.557**	-0.146	-0.178	-.355*
a3CV	-0.007	0.065	-0.063	0.058	.189*	0.084	0.160	0.146	-0.132	0.012	.238**	0.144	-0.233	-0.138	.304*	0.043	0.233	-0.086
a4u	.427**	0.019	.450**	-.372**	.295**	0.157	.262**	0.120	0.132	-0.126	0.131	0.133	0.004	0.036	.462**	-0.146	0.012	-0.067
a4tke	.165*	.320**	-.187*	0.075	.173*	.178*	.328**	.337**	-.255**	-0.014	.295**	.264**	0.202	0.217	0.107	0.115	0.178	-0.105
a4dir	0.091	-.253**	.598**	-.349**	.169*	0.046	-.327**	-.333**	.383**	-0.052	-0.086	-0.049	-.399**	-.336*	.755**	-.312*	-0.154	-0.240
a4CV	-.306**	0.006	-.387**	.383**	-0.114	-0.042	-0.073	-0.043	-0.116	0.164	0.130	0.062	0.146	-0.059	-0.154	0.233	0.170	-0.029
a4ntt	.413**	-0.018	.300**	-.337**	.377**	.196*	.268**	0.060	0.035	-0.140	.235**	.242*	0.048	-0.032	-0.071	-0.127	.333*	-0.259
a4AP	.316**	-0.044	.174*	-.242**	.390**	.184*	.262**	0.047	0.041	-0.103	.328**	.213*	-0.076	-0.084	-0.276	-0.028	.396**	0.019
a5u	.603**	.149*	.409**	-.320**	.358**	.216*	.554**	.340**	0.079	-0.068	.233**	.244*	0.273	0.178	.336*	0.107	0.154	-0.144
a5tke	.336**	.448**	-0.032	-0.020	0.121	0.129	.463**	.474**	-0.123	-0.045	0.164	0.192	0.257	.368*	0.194	0.154	0.043	-0.182
a5dir	0.029	-.308**	.668**	-.329**	0.143	0.007	-.396**	-.437**	.460**	-0.054	-0.101	-0.089	-.383*	-0.209	.771**	-.296*	-0.202	-0.259
a5CV	-.166*	0.074	-.245**	.405**	-0.080	-0.076	0.084	0.043	0.002	.205*	0.051	-0.045	0.091	0.059	-0.115	0.273	0.273	0.067
a5ntt	.266**	0.083	0.025	0.008	.376**	.203*	.325**	0.150	-0.115	0.071	.473**	.319**	-0.028	-0.123	0.052	0.052	0.163	-0.270
a5AP	.298**	0.139	-0.022	0.005	.469**	.270**	.364**	0.175	-0.154	0.012	.551**	.359**	0.073	0.000	-0.073	0.154	.396**	-0.118
a6u		.362**	0.098	-.182*	.363**	.271**		.548**	-.221*	0.020	.294**	.310**		.462**	-.312*	.407**	0.107	0.048
a6tke	.362**		-.221**	0.062	0.099	0.058	.548**		-.249**	-0.013	0.108	0.051	.462**		-.296*	0.123	0.170	0.125
a6dir	0.098	-.221**		-.298**	0.088	-0.096	-.221*	-.249**		-0.043	-0.170	-.247*	-.312*	-.296*		-0.194	-0.162	-0.259
a6CV	-.182*	0.062	-.298**		-0.128	-0.082	0.020	-0.013	-0.043		0.028	-0.089	.407**	0.123	-0.194		0.099	0.182
a6ntt	.363**	0.099	0.088	-0.128		.362**	.294**	0.108	-0.170	0.028		.414**	0.107	0.170	-0.162	0.099		0.144
a6AP	.271**	0.058	-0.096	-0.082	.362**		.310**	0.051	-.247*	-0.089	.414**		0.048	0.125	-0.259	0.182	0.144	
a7u	.316**	-0.074	.481**	-.417**	.239**	0.060	0.087	-0.015	.200*	-.198*	0.046	-0.012	-.336*	-0.209	.549**	-0.138	-0.123	-0.336
a7tke	-0.027	0.136	-.341**	.182*	0.123	.181*	.225*	0.138	-0.145	-0.021	.361**	.293**	0.178	0.162	-.502**	0.028	.328*	0.144
a7dir	-0.014	-0.040	0.067	-0.130	0.014	0.031	-0.121	-0.001	-.190*	-0.028	-0.023	0.056	-0.162	-0.178	.518**	-0.075	-0.233	-0.259
a7CV	-.175*	0.092	-.330**	.218**	-.169*	-0.019	0.047	0.062	-0.059	-0.011	-0.030	0.019	0.241	0.146	-.312*	-0.036	0.123	0.221
a7ntt	.443**	0.003	.303**	-.317**	.605**	.300**	.329**	0.102	-0.085	-0.081	.622**	.394**	-0.083	-0.130	0.186	0.020	.447**	-0.105
a7AP	.382**	-0.058	.282**	-.312**	.599**	.304**	.216*	-0.051	-0.072	-0.071	.597**	.350**	0.053	0.053	0.151	-0.045	.461**	0.129
a8u	.284**	-.153*	.479**	-.334**	.319**	0.090	0.030	-0.150	.195*	-0.039	.178*	0.038	-.304*	-0.273	.581**	-0.170	0.004	-0.316
a8tke	-0.089	0.065	-.315**	.205**	0.126	.193*	0.152	0.040	-0.116	0.002	.395**	.341**	0.225	0.130	-0.202	-0.083	.328*	-0.144
a8dir	0.046	-0.006	0.127	-.209**	-0.008	0.009	-0.067	0.067	-0.131	-0.066	-0.110	0.023	-0.265	-0.123	.415**	-0.146	-0.162	-0.278
a8CV	-.224**	0.091	-.457**	.296**	-0.100	0.099	0.054	0.038	-0.166	-0.013	.196*	.291**	.470**	.312*	-.510**	0.115	0.162	0.086
a8ntt	.388**	-0.064	.408**	-.335**	.359**	0.160	.254**	0.049	0.131	-0.082	.222*	0.164	-0.233	-0.265	.320*	-0.115	0.233	-0.182
a8AP	.374**	-0.027	.343**	-.279**	.396**	.175*	.213*	0.004	0.138	-0.063	.246**	0.181	0.020	0.044	0.012	-0.004	.510**	-0.058
a9u	.575**	0.131	.467**	-.340**	.328**	0.160	.532**	.349**	0.160	-0.063	.200*	0.152	-0.012	-0.059	.589**	-0.099	-0.036	-0.221
a9tke	.454**	.411**	0.091	-0.098	0.139	0.079	.473**	.537**	-0.144	-0.015	0.097	0.130	0.225	0.209	0.289	0.091	-0.051	-0.297
a9dir	-.364**	0.048	-.446**	.277**	-0.129	0.054	-.181*	-0.050	-.226**	0.008	0.109	.214*	0.115	0.194	-0.138	-0.130	0.154	0.105
a9CV	-.213**	-0.013	-.290**	.391**	-0.134	-.173*	-0.060	-0.008	-.173*	.278**	-0.021	-0.060	0.091	-0.178	0.059	0.225	0.130	-.355*
a9ntt	.172*	-0.136	.250**	-.282**	.320**	.268**	-0.077	-0.102	-0.134	-0.070	.244**	.365**	-0.174	-0.150	.420**	-0.071	0.016	-0.298
a9AP	.222**	-0.109	.284**	-.296**	.387**	.245**	-0.032	-0.087	-0.117	-0.054	.319**	.323**	-0.216	-0.128	.407**	-0.088	0.048	-0.271
a10u	.309**	-0.109	.428**	-.382**	.341**	0.124	0.077	-0.066	0.102	-0.121	.234**	0.100	-.296*	-0.265	.589**	-0.194	-0.099	-0.336
a10tke	-0.003	0.112	-.350**	.214**	.158*	.254**	.274**	0.123	-0.162	0.026	.414**	.381**	0.146	0.115	-.565**	0.091	.328*	0.278
a10dir	-.235**	.153*	-.542**	.295**	-0.144	0.062	0.057	0.160	-.325**	0.001	0.120	.225*	0.289	0.194	-.518**	0.043	0.154	0.336
a10CV	-0.112	.154*	-.253**	.298**	-0.137	-0.054	0.097	0.137	0.007	0.168	-0.043	-0.049	0.273	0.194	-.328*	0.028	0.217	0.316
a10ntt	.368**	-0.076	.442**	-.393**	.378**	.219*	.176*	-0.029	0.148	-0.157	.279**	.263*	-0.178	-0.146	.407**	-0.170	0.130	-0.278
a10AP	.330**	-0.058	.430**	-.401**	.398**	.213*	0.115	-0.004	0.116	-0.161	.297**	.217*	-.332*	-0.089	.444**	-0.201	0.182	0.057
a11u	.343**	-0.124	.391**	-.369**	.439**	.200*	0.140	-0.103	0.025	-0.108	.409**	.234*	-0.289	-0.225	.581**	-0.138	0.004	-0.336
a11tke	0.017	0.079	-.272**	0.138	.298**	.294**	.235**	0.067	-.181*	-0.050	.558**	.367**	0.099	0.130	-0.202	0.059	.344*	0.297
a11dir	-.257**	.147*	-.535**	.270**	-.184*	0.033	0.004	0.140	-.325**	-0.036	0.046	.205*	.352*	0.273	-.423**	-0.004	0.091	-0.029
a11CV	-0.013	.157*	-.215**	.208**	-0.022	0.035	.204*	0.141	-0.063	0.144	0.071	0.052	0.154	0.186	-0.130	-0.107	0.162	0.336
a11ntt	.433**	-0.055	.423**	-.341**	.400**	.227**	.296**	0.025	0.093	-0.054	.325**	.278**	-0.233	-0.217	.478**	-0.115	0.043	-0.297
a11AP	.428**	-0.047	.391**	-.352**	.458**	.256**	.279**	0.021	0.071	-0.068	.398**	.309**	-0.141	-0.036	0.237	-0.149	.349*	-0.049
a12u	.391**	-0.085	.406**	-.324**	.511**	.254**	.240**	-0.024	0.040	-0.036	.533**	.326**	-0.273	-0.273	.549**	-0.154	0.083	-0.297
a12tke	.354**	-0.080	.377**	-.305**	.413**	.242**	.204*	-0.038	0.066	-0.037	.351**	.295**	-0.162	-0.178	.312*	-0.217	0.130	-0.163
a12dir	-.168*	.207**	-.578**	.336**	-0.116	0.101	.181*	.247**	-.386**	0.060	.175*	.297**	.399**	.320*	-.549**	0.091	0.186	0.297
a12CV	-0.034	-.178*	.185*	-0.111	-0.033	-0.051	-0.128	-0.141	0.017	0.035	-0.097	-0.104	-.462**	-0.225	.391**	-0.170	-0.186	0.067
a12ntt	.413**	-0.049	.402**	-.338**	.385**	.193*	.279**	0.041	0.003	-0.072	.293**	.220*	-.356*	-0.293	.594**	0.016	0.055	-0.279
a12AP	.421**	-0.056	.409**	-.356**	.403**	.194*	.280**	0.027	0.016	-0.095	.328**	.224*	-0.267	-0.267	.586**	-0.020	0.012	-0.280

Table AP3.7: Location **A7**.

	FULL (84mins)						Run1: 15.49 to 16.49 inc. (61mins)						Run2: 16.50 to 17.12 inc. (23mins)					
	a7u	a7tke	a7dir	a7CV	a7ntt	a7AP	a7u	a7tke	a7dir	a7CV	a7ntt	a7AP	a7u	a7tke	a7dir	a7CV	a7ntt	a7AP
a1u	.411**	-0.053	.243**	-.279**	.422**	.407**	.212*	.208*	.202*	-0.086	.207*	.213*	-0.091	0.217	0.099	0.059	0.209	.314*
a1tke	0.006	.334**	0.072	0.033	0.138	0.088	0.021	.370**	0.081	-0.011	.232**	0.171	0.036	.328*	0.099	0.043	0.178	0.143
a1dir	.604**	-.508**	.186*	-.365**	.317**	.309**	.281**	-.410**	0.028	-0.022	-0.129	-0.073	.794**	-.542**	.589**	-.478**	0.146	0.045
a1CV	-.158*	.318**	0.002	0.143	-0.033	-0.064	-0.067	.242**	0.039	0.031	0.144	0.123	0.028	0.257	0.107	-0.043	0.028	-0.020
a2u	.395**	0.127	-.186*	-0.104	.343**	.368**	.410**	.277**	-.267**	-0.020	.278**	.285**	-0.186	.470**	-.328*	.470**	0.099	0.151
a2tke	0.144	.309**	0.061	-0.055	.243**	.175*	0.054	.493**	0.052	0.007	.247**	0.151	0.194	0.281	-0.012	0.107	0.178	0.118
a2dir	.628**	-.548**	.270**	-.353**	.293**	.295**	.320**	-.480**	.188*	-0.002	-.181*	-0.109	.842**	-.573**	.589**	-.478**	0.194	0.110
a2CV	-0.096	.163*	.180*	0.022	0.009	-0.069	-0.145	.217*	.227**	-0.015	0.057	-0.059	0.170	0.067	0.043	-0.012	0.202	0.127
a2ntt	0.101	.348**	-.199**	0.032	.289**	.274**	.186*	.394**	-.193*	-0.042	.460**	.402**	-0.273	.542**	-.352*	.336*	0.123	0.118
a2AP	-.149*	.469**	-.225**	.151*	0.041	0.079	0.121	.339**	-0.130	-0.105	.386**	.384**	-0.245	.566**	-.422**	0.269	0.116	0.224
a3u	0.055	.388**	-.347**	0.044	.286**	.320**	0.144	.426**	-.303**	-0.030	.489**	.468**	-.431**	.573**	-.589**	.415**	0.091	0.265
a3tke	.172*	.314**	-0.075	-0.102	.357**	.287**	.210*	.463**	-0.064	-0.134	.484**	.352**	0.202	0.194	-0.146	0.004	.455**	.306*
a3dir	.682**	-.477**	.194**	-.321**	.248**	.269**	.423**	-.377**	0.052	0.042	-.254**	-0.142	.929**	-.423**	.549**	-.439**	0.202	0.078
a3CV	0.057	0.120	0.074	-0.021	0.104	0.045	0.152	0.172	0.138	-0.098	.195*	0.132	.296*	-0.059	0.059	-0.028	.328*	0.094
a4u	.535**	-.251**	0.020	-.325**	.484**	.442**	.235**	0.032	-.236**	-0.013	.173*	0.143	0.281	-0.265	0.281	-0.091	0.233	0.290
a4tke	-.211**	.278**	-0.006	0.068	0.037	-0.041	-.209*	.329**	0.048	-0.050	.181*	0.061	-0.107	-0.020	-0.028	0.043	0.083	0.045
a4dir	.519**	-.377**	.192**	-.377**	.338**	.345**	0.151	-.179*	0.060	-0.080	-0.104	-0.023	.636**	-.447**	.415**	-0.273	0.273	0.225
a4CV	-.504**	.251**	0.000	.388**	-.343**	-.284**	-.262**	-0.017	.231**	.187*	-0.032	0.039	-0.083	0.289	-0.209	0.051	0.249	0.176
a4ntt	.542**	-0.013	-0.101	-.265**	.558**	.478**	.358**	.302**	-.338**	-0.032	.357**	.310**	0.079	.380*	-0.063	0.222	.364*	0.205
a4AP	.423**	0.086	-.193**	-.230**	.444**	.457**	.398**	.296**	-.296**	-0.102	.386**	.413**	-0.172	.412**	-.380*	0.196	0.172	0.223
a5u	.505**	-.152*	0.031	-.320**	.555**	.475**	.201*	.190*	-.198*	-0.025	.307**	.222*	0.186	-0.138	0.217	-0.012	0.265	0.208
a5tke	0.037	0.053	0.022	-0.007	0.107	0.081	0.030	.185*	-0.026	-0.002	0.153	0.091	0.170	-0.249	0.138	0.020	0.075	0.135
a5dir	.460**	-.330**	.167*	-.344**	.322**	.317**	0.086	-0.106	0.011	-0.059	-0.103	-0.055	.668**	-.462**	.462**	-0.273	0.225	0.200
a5CV	-.343**	.194**	-0.054	.176*	-.273**	-.269**	-0.085	-0.063	0.075	-0.082	-0.034	-0.035	-0.154	0.233	-0.091	-0.099	0.146	0.086
a5ntt	0.098	.204**	-0.103	-0.055	.428**	.258**	0.033	.387**	-0.136	-0.025	.570**	.354**	0.044	0.075	-0.036	0.147	0.290	-0.103
a5AP	0.063	.267**	-0.143	-0.056	.477**	.322**	0.027	.426**	-0.148	-0.069	.672**	.437**	-0.057	0.202	-0.186	0.178	.558**	0.138
a6u	.316**	-0.027	-0.014	-.175*	.443**	.382**	0.087	.225*	-0.121	0.047	.329**	.216*	-.336*	0.178	-0.162	0.241	-0.083	0.053
a6tke	-0.074	0.136	-0.040	0.092	0.003	-0.058	-0.015	0.138	-0.001	0.062	0.102	-0.051	-0.209	0.162	-0.178	0.146	-0.130	0.053
a6dir	.481**	-.341**	0.067	-.330**	.303**	.282**	.200*	-0.145	-.190*	-0.059	-0.085	-0.072	.549**	-.502**	.518**	-.312*	0.186	0.151
a6CV	-.417**	.182*	-0.130	.218**	-.317**	-.312**	-.198*	-0.021	-0.028	-0.011	-0.081	-0.071	-0.138	0.028	-0.075	-0.036	0.020	-0.045
a6ntt	.239**	0.123	0.014	-.169*	.605**	.599**	0.046	.361**	-0.023	-0.030	.622**	.597**	-0.123	.328*	-0.233	0.123	.447**	.461**
a6AP	0.060	.181*	0.031	-0.019	.300**	.304**	-0.012	.293**	0.056	0.019	.394**	.350**	-0.336	0.144	-0.259	0.221	-0.105	0.129
a7u		-.303**	0.130	-.364**	.460**	.438**		-0.040	-0.068	-0.035	0.131	0.157		-.431**	.557**	-.415**	0.257	0.143
a7tke	-.303**		-.271**	.208**	0.001	-0.043	-0.040		-.181*	-0.094	.435**	.301**	-.431**		-.462**	.494**	-0.020	0.029
a7dir	0.130	-.271**		-0.111	0.008	0.064	-0.068	-.181*		0.069	-.207*	-0.066	.557**	-.462**		-.447**	0.083	0.045
a7CV	-.364**	.208**	-0.111		-.326**	-.269**	-0.035	-0.094	0.069		-0.051	0.032	-.415**	.494**	-.447**		-0.083	-0.159
a7ntt	.460**	0.001	0.008	-.326**		.699**	0.131	.435**	-.207*	-0.051		.611**	0.257	-0.020	0.083	-0.083		.510**
a7AP	.438**	-0.043	0.064	-.269**	.699**		0.157	.301**	-0.066	0.032	.611**		0.143	0.029	0.045	-0.159	.510**	
a8u	.686**	-.232**	0.006	-.357**	.567**	.561**	.439**	0.072	-.283**	-0.038	.316**	.358**	.779**	-.320*	.447**	-.320*	.431**	.372*
a8tke	-.309**	.570**	-0.135	.242**	-0.032	-0.071	-0.035	.463**	0.021	-0.054	.395**	.264**	-0.194	.526**	-.336*	.383*	0.186	0.167
a8dir	.267**	-.236**	.574**	-.178*	0.021	0.045	0.085	-0.120	.554**	0.005	-.263**	-0.171	.660**	-.407**	.628**	-.344*	0.059	0.045
a8CV	-.513**	.437**	-0.071	.320**	-.308**	-.340**	-0.157	.262**	.174*	-0.064	0.130	0.004	-.581**	.502**	-.486**	.518**	-0.170	-0.118
a8ntt	.670**	-0.122	0.056	-.345**	.552**	.522**	.502**	.201*	-0.136	-0.083	.292**	.299**	.470**	-0.091	0.138	-0.107	.597**	.429**
a8AP	.608**	-0.039	0.004	-.324**	.522**	.525**	.504**	.252**	-.177*	-0.117	.308**	.344**	0.141	0.173	-0.012	-0.004	.534**	.515**
a9u	.581**	-.197**	0.021	-.321**	.546**	.467**	.286**	0.151	-.255**	0.016	.290**	.202*	.439**	-.328*	.391**	-0.186	0.265	0.225
a9tke	.167*	0.010	0.101	-0.100	.178*	0.114	-0.013	.197*	0.014	0.045	0.045	-0.022	0.249	-0.138	0.217	-0.138	0.043	0.020
a9dir	-.539**	.332**	0.061	.361**	-.369**	-.293**	-.296**	0.123	.348**	0.094	-0.046	0.031	-0.178	0.225	-0.162	0.225	-0.020	0.127
a9CV	-.321**	.162*	0.010	.192**	-.295**	-.230**	-0.162	-0.004	0.156	0.027	-0.161	-0.020	0.130	0.138	0.004	-0.146	0.194	0.078
a9ntt	.403**	-0.087	.370**	-.281**	.402**	.398**	0.062	.229*	.336**	-0.035	0.142	.195*	.697**	-0.222	.475**	-0.238	.317*	0.229
a9AP	.450**	-0.101	.367**	-.319**	.464**	.487**	0.087	.250**	.339**	-0.040	.184*	.288**	.711**	-0.232	.479**	-0.287	.391**	.318*
a10u	.770**	-.201**	.151*	-.350**	.520**	.557**	.589**	0.137	-0.026	-0.033	.249**	.371**	.866**	-.360*	.518**	-0.281	.296*	0.249
a10tke	-.302**	.730**	-.295**	.282**	0.013	-0.033	-0.050	.658**	-.193*	0.012	.456**	.310**	-.399**	.794**	-.542**	.478**	-0.036	0.045
a10dir	-.596**	.422**	0.034	.355**	-.382**	-.339**	-.325**	.252**	.330**	0.022	-0.007	0.004	-.510**	.447**	-.320*	.431**	-0.162	-0.020
a10CV	-.406**	.189*	-.176*	.541**	-.273**	-.280**	-.190*	-0.070	-0.091	.379**	-0.036	-0.071	-.431**	.431**	-0.209	.589**	-0.036	-0.045
a10ntt	.601**	-.154*	.151*	-.318**	.544**	.571**	.303**	.192*	0.004	0.011	.276**	.371**	.652**	-0.130	.352*	-0.194	.399**	.429**
a10AP	.549**	-.199**	.159*	-.323**	.537**	.607**	.224*	0.119	0.011	0.007	.254**	.429**	.528**	-0.210	.360*	-0.229	.453**	.473**
a11u	.639**	-.169*	0.078	-.344**	.645**	.641**	.342**	.189*	-0.153	-0.009	.474**	.518**	.842**	-.304*	.478**	-.352*	.352*	0.290
a11tke	-.255**	.528**	-.189*	.149*	0.099	0.084	-0.081	.483**	-0.062	-0.054	.486**	.381**	-.320*	.415**	-.399**	0.162	0.107	0.249
a11dir	-.531**	.398**	0.053	.368**	-.428**	-.372**	-.226**	.198*	.352**	0.057	-0.096	-0.048	-.352*	.447**	-0.209	.368*	-0.178	-0.151
a11CV	-.243**	.194**	-.177*	.353**	-0.137	-0.099	-0.037	0.011	-0.108	.235**	0.067	0.075	-.328*	0.217	-0.202	.312*	0.067	0.192
a11ntt	.687**	-0.137	0.054	-.348**	.654**	.575**	.457**	.255**	-.176*	-0.021	.477**	.384**	.644**	-0.265	0.281	-0.265	.407**	.355*
a11AP	.647**	-0.099	0.069	-.359**	.681**	.624**	.424**	.291**	-0.122	-0.061	.518**	.436**	.357*	-0.036	0.125	-0.133	.542**	.618**
a12u	.517**	-0.109	0.005	-.358**	.703**	.658**	0.163	.290**	-.256**	-0.050	.562**	.522**	.589**	-0.257	0.273	-0.289	.462**	.437**
a12tke	.442**	-0.064	-0.047	-.281**	.618**	.591**	0.160	.295**	-.270**	-0.008	.454**	.442**	0.273	-0.162	0.067	-0.036	.526**	.355*
a12dir	-.654**	.453**	-0.043	.360**	-.352**	-.374**	-.377**	.316**	.223*	0.013	0.063	-0.037	-.826**	.510**	-.526**	.510**	-0.209	-0.143
a12CV	0.131	-.187*	.159*	-0.031	0.092	0.116	-0.085	-0.004	0.067	.215*	-0.071	0.012	.352*	-.352*	0.257	-0.225	-0.028	-0.151
a12ntt	.557**	-.151*	-0.038	-.410**	.663**	.535**	.207*	.258**	-.370**	-0.122	.473**	.314**	.657**	-.364*	.372*	-.364*	.436**	0.229
a12AP	.565**	-0.149	-0.038	-.414**	.679**	.567**	.219*	.263**	-.369**	-0.123	.506**	.356**	.649**	-.363*	.339*	-.394**	.402**	.333*

Table AP3.8: Location **A8**.

	FULL (84mins)						Run1: 15.49 to 16.49 inc. (61mins)						Run2: 16.50 to 17.12 inc. (23mins)					
	a8u	a8tke	a8dir	a8CV	a8ntt	a8AP	a8u	a8tke	a8dir	a8CV	a8ntt	a8AP	a8u	a8tke	a8dir	a8CV	a8ntt	a8AP
a1u	.386**	-0.075	.240**	-.234**	.481**	.436**	0.158	.183*	0.172	0.104	.359**	.288**	-0.012	0.233	0.043	0.130	0.107	0.277
a1tke	-0.003	.274**	0.017	.148*	0.073	0.136	-0.007	.326**	0.017	.230**	0.112	0.137	0.130	0.265	0.075	0.115	0.170	.430**
a1dir	.537**	-.444**	.262**	-.591**	.419**	.339**	.188*	-.267**	0.085	-.280**	0.047	0.011	.605**	-.352*	.565**	-.739**	.344*	0.036
a1CV	-0.144	.292**	-0.030	.220**	-0.128	-0.059	-0.048	.249**	0.000	0.166	-0.047	-0.005	0.091	0.115	0.067	0.028	0.083	.325*
a2u	.415**	0.043	-0.056	-.183*	.471**	.506**	.433**	.177*	-.177*	-0.052	.472**	.541**	-0.107	.423**	-0.115	.336*	0.170	0.253
a2tke	0.118	.255**	0.113	0.099	.239**	.227**	-0.009	.404**	0.087	.337**	.182*	0.161	0.289	.455**	0.075	0.162	.312*	0.285
a2dir	.530**	-.427**	.325**	-.558**	.433**	.346**	0.162	-.236**	.210*	-.223*	0.070	0.026	.684**	-.336*	.549**	-.692**	.375*	0.020
a2CV	-0.124	.226**	.161*	.205**	-0.048	-0.056	-.208*	.240**	.210*	.310**	-0.079	-0.118	0.265	.399**	0.067	0.091	0.241	0.205
a2ntt	0.140	.265**	-.162*	0.067	.252**	.335**	.242**	.264**	-0.149	0.078	.416**	.422**	-0.162	.510**	-0.249	.486**	0.036	.325*
a2AP	-0.073	.436**	-.255**	.278**	0.013	0.117	.245**	.273**	-.183*	0.085	.327**	.405**	-0.157	.502**	-0.237	.406**	0.076	.420**
a3u	.222**	.310**	-.343**	0.052	.212**	.301**	.430**	.331**	-.316**	0.036	.348**	.435**	-0.241	.510**	-.518**	.439**	0.020	.309*
a3tke	.169*	.377**	-0.076	0.144	.243**	.297**	.187*	.550**	-0.130	.344**	.266**	.340**	.296*	.368*	-0.043	-0.020	.478**	.366*
a3dir	.560**	-.425**	.324**	-.531**	.498**	.409**	.230**	-.258**	.184*	-.199*	.178*	0.142	.708**	-0.217	.636**	-.605**	.431**	0.084
a3CV	-0.062	.240**	0.088	.217**	0.029	0.037	-0.074	.330**	0.090	.348**	0.060	0.074	0.265	0.083	0.115	-0.178	.320*	0.173
a4u	.519**	-.290**	0.049	-.469**	.552**	.481**	.192*	-0.020	-.251**	-0.118	.325**	.294**	.391**	-0.091	0.146	-.304*	0.225	0.036
a4tke	-.219**	.243**	-0.026	.235**	-.167*	-0.136	-.230**	.234**	0.052	.243**	-0.116	-0.098	-0.043	0.123	-0.067	0.162	0.012	0.036
a4dir	.484**	-.306**	.228**	-.441**	.393**	.359**	0.080	-0.034	0.045	-0.030	-0.014	0.050	.684**	-0.178	.407**	-.549**	.455**	0.044
a4CV	-.427**	.324**	-0.108	.426**	-.432**	-.351**	-0.132	0.091	0.121	0.119	-.211*	-0.137	0.012	0.241	-0.202	0.123	0.178	0.221
a4ntt	.570**	-0.114	0.008	-.341**	.658**	.628**	.401**	0.143	-.215*	-0.040	.562**	.537**	0.190	.507**	-0.024	0.230	.404**	.507**
a4AP	.471**	-0.036	-0.050	-.238**	.540**	.585**	.474**	0.143	-.195*	-0.070	.573**	.639**	-0.084	0.228	-0.156	0.196	0.228	.305*
a5u	.483**	-.207**	0.072	-.406**	.523**	.494**	0.154	0.097	-.187*	-0.047	.301**	.315**	0.233	0.115	0.067	-0.036	0.067	0.084
a5tke	-0.008	0.014	0.046	0.014	0.037	0.094	-0.052	0.037	0.026	0.039	0.086	0.126	0.170	0.020	0.178	0.043	0.020	0.068
a5dir	.469**	-.262**	.193**	-.391**	.388**	.344**	0.103	0.015	-0.028	0.015	0.027	0.078	.700**	-0.162	.455**	-.534**	.439**	0.044
a5CV	-.309**	.236**	-0.102	.301**	-.280**	-.233**	-0.032	0.014	0.093	0.016	-0.032	-0.032	-0.123	0.186	-0.178	0.067	-0.067	0.116
a5ntt	0.141	.176*	-0.112	0.013	.172*	.203**	0.111	.325**	-.173*	0.157	.180*	.186*	0.091	0.131	-0.075	0.099	0.139	0.069
a5AP	0.129	.252**	-.189*	0.043	.177*	.219**	0.144	.364**	-.232**	0.155	.207*	.219*	0.024	.299*	-0.178	0.145	0.275	0.292
a6u	.284**	-0.089	0.046	-.224**	.388**	.374**	0.030	0.152	-0.067	0.054	.254**	.213*	-.304*	0.225	-0.265	.470**	-0.233	0.020
a6tke	-.153*	0.065	-0.006	0.091	-0.064	-0.027	-0.150	0.040	0.067	0.038	0.049	0.004	-0.273	0.130	-0.123	.312*	-0.265	0.044
a6dir	.479**	-.315**	0.127	-.457**	.408**	.343**	.195*	-0.116	-0.131	-0.166	0.131	0.138	.581**	-0.202	.415**	-.510**	.320*	0.012
a6CV	-.334**	.205**	-.209**	.296**	-.335**	-.279**	-0.039	0.002	-0.066	-0.013	-0.082	-0.063	-0.170	-0.083	-0.146	0.115	-0.115	-0.004
a6ntt	.319**	0.126	-0.008	-0.100	.359**	.396**	.178*	.395**	-0.110	.196*	.222*	.246**	0.004	.328*	-0.162	0.162	0.233	.510**
a6AP	0.090	.193*	0.009	0.099	0.160	.175*	0.038	.341**	0.023	.291**	0.164	0.181	-0.316	-0.144	-0.278	0.086	-0.182	-0.058
a7u	.686**	-.309**	.267**	-.513**	.670**	.608**	.439**	-0.035	0.085	-0.157	.502**	.504**	.779**	-0.194	.660**	-.581**	.470**	0.141
a7tke	-.232**	.570**	-.236**	.437**	-0.122	-0.039	0.072	.463**	-0.120	.262**	.201*	.252**	-.320*	.526**	-.407**	.502**	-0.091	0.173
a7dir	0.006	-0.135	.574**	-0.071	0.056	0.004	-.283**	0.021	.554**	.174*	-0.136	-.177*	.447**	-.336*	.628**	-.486**	0.138	-0.012
a7CV	-.357**	.242**	-.178*	.320**	-.345**	-.324**	-0.038	-0.054	0.005	-0.064	-0.083	-0.117	-.320*	.383*	-.344*	.518**	-0.107	-0.004
a7ntt	.567**	-0.032	0.021	-.308**	.552**	.522**	.316**	.395**	-.263**	0.130	.292**	.308**	.431**	0.186	0.059	-0.170	.597**	.534**
a7AP	.561**	-0.071	0.045	-.340**	.522**	.525**	.358**	.264**	-0.171	0.004	.299**	.344**	.372*	0.167	0.045	-0.118	.429**	.515**
a8u		-.274**	0.068	-.573**	.643**	.615**		0.003	-.261**	-.296**	.433**	.493**		-0.036	.486**	-.455**	.565**	.317*
a8tke	-.274**		-.216**	.652**	-.198**	-0.128	0.003		-0.067	.620**	0.077	0.103	-0.036		-.328*	.518**	0.115	.349*
a8dir	0.068	-.216**		-0.128	.192**	0.096	-.261**	-0.067		0.143	0.011	-0.071	.486**	-.328*		-.478**	0.225	0.044
a8CV	-.573**	.652**	-0.128		-.411**	-.372**	-.296**	.620**	0.143		-0.055	-0.101	-.455**	.518**	-.478**		-.304*	0.020
a8ntt	.643**	-.198**	.192**	-.411**		.750**	.433**	0.077	0.011	-0.055		.734**	.565**	0.115	0.225	-.304*		.446**
a8AP	.615**	-0.128	0.096	-.372**	.750**		.493**	0.103	-0.071	-0.101	.734**		.317*	.349*	0.044	0.020	.446**	
a9u	.540**	-.250**	0.084	-.461**	.572**	.513**	.213*	0.058	-.209*	-0.091	.357**	.344**	.455**	-0.028	0.273	-.320*	0.209	0.044
a9tke	0.092	-0.058	.160*	-0.107	.147*	.159*	-0.143	0.064	0.108	0.093	0.034	0.036	0.217	0.067	0.130	-0.067	-0.059	-0.084
a9dir	-.506**	.414**	-0.036	.534**	-.467**	-.383**	-.251**	.234**	.247**	.295**	-.235**	-.174*	-0.051	0.146	-0.075	0.233	0.083	0.213
a9CV	-.315**	.193**	-0.015	.264**	-.268**	-.225**	-0.161	0.023	0.156	0.056	-0.112	-0.089	0.146	0.123	-0.067	-0.059	0.091	0.181
a9ntt	.332**	-0.106	.394**	-.235**	.401**	.351**	-0.067	.207*	.292**	.207*	0.114	0.101	.665**	-0.063	.531**	-.404**	.451**	.314*
a9AP	.396**	-0.128	.366**	-.289**	.440**	.413**	-0.014	.206*	.265**	0.169	0.126	0.149	.719**	-0.048	.511**	-.415**	.551**	.381*
a10u	.757**	-.236**	.242**	-.497**	.717**	.666**	.573**	0.081	0.042	-0.146	.574**	.600**	.834**	-0.091	.605**	-.494**	.542**	0.197
a10tke	-.210**	.552**	-.295**	.435**	-0.096	-0.028	0.106	.425**	-.189*	.263**	.239**	.267**	-.304*	.462**	-.439**	.534**	-0.059	0.181
a10dir	-.591**	.420**	-0.055	.573**	-.455**	-.369**	-.326**	.238**	.243**	.291**	-0.152	-0.099	-.447**	0.225	-0.265	.534**	-0.217	0.076
a10CV	-.344**	.207**	-.247**	.281**	-.386**	-.354**	-0.093	-0.067	-0.102	-0.047	-.216*	-.261**	-.304*	.368*	-.375*	.470**	-0.217	0.076
a10ntt	.550**	-.208**	.237**	-.414**	.645**	.575**	.200*	0.106	0.056	-0.017	.425**	.400**	.731**	0.107	.470**	-.296*	.676**	.462**
a10AP	.540**	-.212**	.200**	-.435**	.559**	.540**	.198*	0.116	-0.002	-0.042	.287**	.349**	.631**	-0.005	.388*	-.397*	.491**	.385*
a11u	.769**	-.166*	0.099	-.465**	.585**	.575**	.581**	.212*	-.214*	-0.087	.325**	.418**	.905**	-0.067	.549**	-.486**	.534**	.301*
a11tke	-.186*	.581**	-.314**	.419**	-0.127	-0.054	0.025	.541**	-.183*	.366**	0.079	0.110	-0.194	.399**	-.486**	.344*	-0.012	0.165
a11dir	-.579**	.379**	0.049	.581**	-.432**	-.367**	-.321**	0.149	.413**	.304**	-0.112	-0.095	-.368*	0.241	-0.075	.502**	-0.233	0.036
a11CV	-.146*	.182*	-.239**	.147*	-.225**	-0.141	0.126	-0.047	-0.141	-0.152	-0.058	-0.001	-0.202	.312*	-0.225	.336*	-0.036	0.108
a11ntt	.661**	-.157*	0.133	-.392**	.707**	.648**	.396**	.228**	-0.127	0.056	.541**	.547**	.755**	0.004	.368*	-.431**	.684**	.374*
a11AP	.641**	-0.128	0.143	-.362**	.709**	.665**	.389**	.267**	-0.085	0.089	.540**	.533**	.526**	0.108	0.189	-0.293	.647**	.600**
a12u	.663**	-0.094	0.002	-.391**	.565**	.553**	.417**	.321**	-.352**	0.028	.286**	.378**	.763**	0.059	.296*	-.375*	.660**	.382*
a12tke	.543**	-0.099	-0.060	-.346**	.516**	.497**	.340**	.217*	-.388**	-0.008	.312**	.368**	.352*	0.107	0.107	-0.170	.439**	0.197
a12dir	-.690**	.443**	-0.088	.637**	-.489**	-.439**	-.463**	.280**	.232**	.383**	-0.170	-.192*	-.700**	0.289	-.534**	.692**	-.407**	-0.116
a12CV	.158*	-.179*	0.103	-.239**	0.137	0.080	-0.019	0.003	-0.058	-0.080	-0.015	-0.019	0.241	-.336*	0.265	-.518**	0.091	-0.141
a12ntt	.635**	-.206**	0.056	-.439**	.589**	.502**	.355**	0.163	-.285**	-0.009	.343**	.294**	.705**	-0.143	.349*	-.531**	.507**	0.241
a12AP	.659**	-.198**	0.046	-.436**	.601**	.521**	.389**	0.176	-.300**	-0.006	.364**	.329**	.761**	-0.100	.323*	-.506**	.482**	0.223

Table AP3.9: Location **A9**.

	FULL (84mins)						Run1: 15.49 to 16.49 inc. (61mins)						Run2: 16.50 to 17.12 inc. (23mins)					
	a9u	a9tke	a9dir	a9CV	a9ntt	a9AP	a9u	a9tke	a9dir	a9CV	a9ntt	a9AP	a9u	a9tke	a9dir	a9CV	a9ntt	a9AP
a1u	.337**	.159*	-.250**	-.182*	.416**	.451**	0.058	0.060	0.039	0.021	.289**	.302**	-0.036	0.028	0.170	0.099	0.063	0.136
a1tke	0.049	0.063	0.119	0.039	.194*	.207**	0.125	0.116	0.132	-0.007	.295**	.320**	-0.099	-0.083	.312*	0.178	0.206	0.184
a1dir	.434**	0.093	-.519**	-.328**	.291**	.343**	0.000	-0.151	-.250**	-.175*	-0.143	-0.103	.470**	0.202	-0.273	0.146	.586**	.567**
a1CV	-0.104	-0.001	.258**	0.129	0.059	0.052	0.063	0.092	.202*	0.024	.232*	.253**	-0.154	-0.123	0.225	0.170	0.166	0.128
a2u	.343**	0.044	-.238**	-.196**	.178*	.208**	.323**	0.031	-0.161	-0.077	0.060	0.077	-0.257	-0.178	.344*	-0.138	-0.071	-0.048
a2tke	.151*	.220**	0.013	-0.048	.287**	.284**	0.101	.223*	0.158	-0.015	.268**	.273**	-0.020	0.091	0.091	0.178	0.246	.311*
a2dir	.415**	0.099	-.488**	-.287**	.302**	.365**	-0.035	-0.140	-.193*	-0.090	-0.123	-0.069	.455**	0.202	-0.241	0.099	.586**	.615**
a2CV	-0.066	.187*	.168*	0.101	0.142	0.119	-0.081	.221*	.237**	0.059	.238**	.228*	0.130	0.115	-0.059	0.186	0.127	0.168
a2ntt	.167*	0.100	-0.031	-0.049	0.088	0.113	.321**	0.124	-0.090	-0.064	0.150	0.165	-.312*	-0.012	0.289	0.059	-0.135	-0.104
a2AP	-0.114	-0.119	.234**	0.094	-0.072	-0.072	.201*	-0.011	0.022	-0.021	0.176	0.180	-.317*	-0.197	0.253	0.060	-0.161	-0.130
a3u	0.087	-0.112	0.039	-0.084	-0.022	0.019	.193*	-0.075	0.026	-0.064	0.044	0.082	-.296*	-0.265	0.289	-0.036	-0.293	-0.232
a3tke	.162*	0.090	-0.006	-0.011	.175*	.202**	.211*	0.099	0.042	-0.045	0.177	.227*	0.083	-0.028	0.020	0.107	0.230	0.279
a3dir	.409**	0.101	-.476**	-.263**	.272**	.298**	-0.024	-0.133	-.189*	-0.063	-.183*	-.196*	.399**	0.194	-0.186	0.138	.657**	.639**
a3CV	0.043	0.117	0.067	0.109	0.114	0.111	0.127	.192*	0.067	0.046	.201*	.231*	0.289	0.036	-0.170	0.107	0.246	0.232
a4u	.631**	.234**	-.514**	-.372**	.280**	.315**	.378**	0.083	-.294**	-.238**	-0.117	-0.110	.510**	.368*	0.036	-0.083	.309*	0.279
a4tke	0.003	.318**	.193**	0.055	-0.012	-0.009	0.157	.439**	0.148	0.035	0.123	0.146	0.138	0.265	0.138	-0.075	-0.032	-0.080
a4dir	.375**	0.015	-.313**	-.310**	.387**	.418**	-0.119	-.287**	0.120	-0.141	0.053	0.049	.581**	0.154	-0.162	0.083	.523**	.519**
a4CV	-.473**	-0.128	.545**	.401**	-.196*	-.218**	-.189*	0.034	.389**	.261**	0.171	.187*	-0.138	-0.043	0.067	0.249	-0.016	0.016
a4ntt	.509**	0.116	-.424**	-.275**	.350**	.387**	.307**	0.012	-.212*	-0.169	0.124	0.129	0.000	-0.048	0.150	0.198	0.218	0.244
a4AP	.372**	-0.006	-.285**	-.201**	.222**	.266**	.340**	0.013	-.206*	-0.160	0.104	0.154	-.428**	-.460**	.340*	0.092	-0.088	-0.057
a5u	.830**	.384**	-.544**	-.315**	.278**	.333**	.757**	.344**	-.334**	-0.169	-0.098	-0.053	.573**	.526**	-0.107	0.170	0.230	0.176
a5tke	.232**	.515**	-0.055	-0.025	-0.004	0.033	.367**	.614**	-0.089	-0.024	-0.036	0.028	.368*	.415**	0.036	-0.020	0.190	0.152
a5dir	.321**	-0.020	-.276**	-.326**	.366**	.381**	-0.168	-.356**	0.126	-.186*	0.030	0.004	.534**	0.233	-0.051	-0.043	.539**	.543**
a5CV	-.266**	-0.049	.241**	.410**	-.210**	-.235**	0.054	0.084	-0.026	.336**	0.041	0.029	-0.083	0.012	-0.067	0.162	-0.135	-0.096
a5ntt	.198**	.149*	-0.139	-0.020	.166*	.185*	.216*	0.111	-0.103	-0.046	0.142	0.171	0.036	0.083	-0.115	.313*	0.040	0.016
a5AP	.191*	.158*	-0.096	-0.025	0.115	0.150	.257**	0.150	-0.101	-0.050	0.100	0.147	0.000	0.016	-0.008	0.267	0.004	0.033
a6u	.575**	.454**	-.364**	-.213**	.172*	.222**	.532**	.473**	-.181*	-0.060	-0.077	-0.032	-0.012	0.225	0.115	0.091	-0.174	-0.216
a6tke	0.131	.411**	0.048	-0.013	-0.136	-0.109	.349**	.537**	-0.050	-0.008	-0.102	-0.087	-0.059	0.209	0.194	-0.178	-0.150	-0.128
a6dir	.467**	0.091	-.446**	-.290**	.250**	.284**	0.160	-0.144	-.226**	-.173*	-0.134	-0.117	.589**	0.289	-0.138	0.059	.420**	.407**
a6CV	-.340**	-0.098	.277**	.391**	-.282**	-.296**	-0.063	-0.015	0.008	.278**	-0.070	-0.054	-0.099	0.091	-0.130	0.225	-0.071	-0.088
a6ntt	.328**	0.139	-0.129	-0.134	.320**	.387**	.200*	0.097	0.109	-0.021	.244**	.319**	-0.036	-0.051	0.154	0.130	0.016	0.048
a6AP	0.160	0.079	0.054	-.173*	.268**	.245**	0.152	0.130	.214*	-0.060	.365**	.323**	-0.221	-0.297	0.105	-.355*	-0.298	-0.271
a7u	.581**	.167*	-.539**	-.321**	.403**	.450**	.286**	-0.013	-.296**	-0.162	0.062	0.087	.439**	0.249	-0.178	0.130	.697**	.711**
a7tke	-.197**	0.010	.332**	.162*	-0.087	-0.101	0.151	.197*	0.123	-0.004	.229*	.250**	-.328*	-0.138	0.225	0.138	-0.222	-0.232
a7dir	0.021	0.101	0.061	0.010	.370**	.367**	-.255**	0.014	.348**	0.156	.336**	.339**	.391**	0.217	-0.162	0.004	.475**	.479**
a7CV	-.321**	-0.100	.361**	.192**	-.281**	-.319**	0.016	0.045	0.094	0.027	-0.035	-0.040	-0.186	-0.138	0.225	-0.146	-0.238	-0.287
a7ntt	.546**	.178*	-.369**	-.295**	.402**	.464**	.290**	0.045	-0.046	-0.161	0.142	.184*	0.265	0.043	-0.020	0.194	.317*	.391**
a7AP	.467**	0.114	-.293**	-.230**	.398**	.487**	.202*	-0.022	0.031	-0.020	.195*	.288**	0.225	0.020	0.127	0.078	0.229	.318*
a8u	.540**	0.092	-.506**	-.315**	.332**	.396**	.213*	-0.143	-.251**	-0.161	-0.067	-0.014	.455**	0.217	-0.051	0.146	.665**	.719**
a8tke	-.250**	-0.058	.414**	.193**	-0.106	-0.128	0.058	0.064	.234**	0.023	.207*	.206*	-0.028	0.067	0.146	0.123	-0.063	-0.048
a8dir	0.084	.160*	-0.036	-0.015	.394**	.366**	-.209*	0.108	.247**	0.156	.292**	.265**	0.273	0.130	-0.075	-0.067	.531**	.511**
a8CV	-.461**	-0.107	.534**	.264**	-.235**	-.289**	-0.091	0.093	.295**	0.056	.207*	0.169	-.320*	-0.067	0.233	-0.059	-.404**	-.415**
a8ntt	.572**	.147*	-.467**	-.268**	.401**	.440**	.357**	0.034	-.235**	-0.112	0.114	0.126	0.209	-0.059	0.083	0.091	.451**	.551**
a8AP	.513**	.159*	-.383**	-.225**	.351**	.413**	.344**	0.036	-.174*	-0.089	0.101	0.149	0.044	-0.084	0.213	0.181	.314*	.381*
a9u		.384**	-.605**	-.324**	.275**	.338**		.366**	-.407**	-0.167	-0.138	-0.079		.462**	-.312*	0.154	.356*	.327*
a9tke	.384**		-.189*	-0.029	0.114	.153*	.366**		-0.063	0.019	-0.063	-0.002	.462**		-0.186	0.217	0.206	0.160
a9dir	-.605**	-.189*		.297**	-0.114	-.165*	-.407**	-0.063		.186*	.338**	.296**	-.312*	-0.186		-.320*	0.016	0.040
a9CV	-.324**	-0.029	.297**		-0.106	-.154*	-0.167	0.019	.186*		0.107	0.090	0.154	0.217	-.320*		0.143	0.072
a9ntt	.275**	0.114	-0.114	-0.106		.879**	-0.138	-0.063	.338**	0.107		.854**	.356*	0.206	0.016	0.143		.876**
a9AP	.338**	.153*	-.165*	-.154*	.879**		-0.079	-0.002	.296**	0.090	.854**		.327*	0.160	0.040	0.072	.876**	
a10u	.530**	0.130	-.418**	-.262**	.468**	.524**	.199*	-0.072	-0.089	-0.048	.182*	.225*	.431**	0.209	-0.059	0.059	.721**	.743**
a10tke	-.185*	-0.022	.299**	.166*	-0.105	-0.116	.178*	0.152	0.063	0.021	.193*	.217*	-.423**	-0.233	0.241	0.043	-0.253	-0.248
a10dir	-.497**	-0.086	.620**	.342**	-.191*	-.230**	-0.125	0.168	.425**	.230**	.279**	.271**	-.581**	-.312*	.399**	-0.257	-.333*	-.343*
a10CV	-.269**	0.012	.259**	.185*	-.356**	-.372**	0.030	0.152	-0.017	0.078	-.228*	-.224*	-0.138	0.020	0.194	-0.146	-0.222	-0.224
a10ntt	.538**	.176*	-.347**	-.267**	.543**	.592**	.232**	0.026	0.009	-0.057	.318**	.346**	.328*	0.123	0.154	0.051	.729**	.790**
a10AP	.547**	.151*	-.345**	-.302**	.475**	.517**	.231**	-0.026	0.053	-0.094	.232*	.239*	.444**	0.145	-0.070	-0.107	.450**	.533**
a11u	.538**	0.124	-.398**	-.324**	.420**	.492**	.214*	-0.090	-0.051	-.175*	0.098	0.168	.439**	0.249	-0.051	0.115	.729**	.767**
a11tke	-0.128	-0.017	.283**	0.096	-0.075	-0.037	0.141	0.108	0.138	-0.021	0.177	.244**	-0.154	-0.107	0.130	0.012	-0.277	-0.208
a11dir	-.542**	-0.063	.627**	.332**	-.174*	-.226**	-.227**	.184*	.443**	.184*	.291**	.257**	-.470**	-0.123	.383*	-0.036	-0.206	-0.216
a11CV	-0.126	0.029	.193**	0.059	-.293**	-.255**	0.156	.191*	-0.050	0.012	-0.173	-0.130	-0.115	-0.099	0.249	-0.281	-0.269	-0.208
a11ntt	.615**	.181*	-.460**	-.366**	.450**	.509**	.355**	0.029	-0.169	-.249**	0.156	.199*	.415**	0.115	0.004	0.138	.673**	.727**
a11AP	.588**	.153*	-.440**	-.355**	.437**	.493**	.331**	0.006	-0.157	-.222*	0.159	.191*	0.269	-0.052	0.165	0.068	.475**	.556**
a12u	.580**	.174*	-.398**	-.296**	.395**	.473**	.302**	0.017	-0.062	-0.125	0.079	0.156	.423**	0.138	-0.036	0.115	.539**	.615**
a12tke	.540**	0.092	-.390**	-.268**	.316**	.369**	.338**	-0.062	-0.131	-0.108	0.059	0.089	.296*	-0.036	-0.083	0.020	0.111	0.176
a12dir	-.483**	-0.046	.581**	.330**	-.207**	-.272**	-0.103	.232**	.368**	.192*	.299**	.243**	-.455**	-0.202	0.257	-0.178	-.602**	-.615**
a12CV	0.099	-0.017	-0.102	-0.044	0.145	0.147	-0.132	-0.093	0.125	0.084	-0.016	-0.009	0.265	0.043	-0.225	-0.107	0.277	0.224
a12ntt	.601**	.193*	-.571**	-.296**	.334**	.376**	.308**	0.025	-.355**	-0.128	-0.071	-0.057	.491**	0.198	-0.230	0.230	.575**	.572**
a12AP	.613**	.191*	-.572**	-.301**	.329**	.375**	.324**	0.011	-.357**	-0.141	-0.081	-0.062	.530**	0.275	-0.195	0.251	.567**	.579**

Table AP3.10: Location **A10**.

	FULL (84mins)						Run1: 15.49 to 16.49 inc. (61mins)						Run2: 16.50 to 17.12 inc. (23mins)					
	a10u	a10tke	a10dir	A10CV	a10ntt	a10AP	a10u	a10tke	a10dir	a10CV	a10ntt	a10AP	a10u	a10tke	a10dir	a10CV	a10ntt	a10AP
a1u	.486**	-0.058	-.245**	-.310**	.421**	.383**	.350**	.204*	0.066	-.255**	.205*	0.132	0.012	0.138	0.249	0.233	0.162	0.117
a1tke	0.068	.302**	0.145	0.020	0.096	0.051	0.128	.332**	.211*	-0.063	0.162	0.097	0.091	0.217	0.186	0.170	0.273	0.061
a1dir	.468**	-.518**	-.722**	-.324**	.378**	.416**	0.047	-.435**	-.545**	-0.024	-0.093	-0.018	.676**	-.557**	-.636**	-.478**	.462**	.444**
a1CV	-0.114	.302**	.238**	.146*	-0.059	-0.094	0.010	.230**	.185*	0.033	0.095	0.058	0.051	0.162	0.099	0.036	0.186	-0.014
a2u	.476**	0.122	-.163*	-.196**	.372**	.367**	.539**	.251**	-0.023	-.177*	.326**	.311**	-0.051	.502**	.439**	0.281	0.099	0.033
a2tke	.204**	.283**	0.061	-0.052	.254**	0.142	0.154	.448**	.283**	-0.007	.230**	0.049	0.249	0.281	0.012	0.059	.399**	0.136
a2dir	.506**	-.535**	-.640**	-.330**	.394**	.409**	0.113	-.468**	-.388**	-0.042	-0.068	-0.032	.723**	-.542**	-.636**	-.462**	.494**	.453**
a2CV	-0.068	.175*	.190*	0.054	0.010	-0.101	-0.102	.243**	.298**	0.026	0.036	-0.149	0.194	0.020	-0.091	0.004	0.281	0.126
a2ntt	.197**	.374**	0.089	0.019	.237**	.196**	.357**	.417**	0.134	-0.116	.406**	.331**	-0.217	.573**	.447**	.368*	0.012	-0.089
a2AP	-0.033	.467**	.322**	0.129	-0.019	0.021	.329**	.305**	.175*	-0.151	.323**	.400**	-0.213	.639**	.414**	0.269	0.020	-0.009
a3u	.193**	.397**	0.064	0.001	0.124	0.132	.385**	.432**	0.070	-0.139	.224*	.246**	-.312*	.636**	.431**	.368*	-0.083	-0.136
a3tke	.225**	.271**	0.016	-0.103	.197**	.187*	.299**	.381**	0.129	-0.117	.229**	.217*	0.225	0.178	-0.138	-0.059	.344*	0.276
a3dir	.563**	-.458**	-.619**	-.326**	.430**	.401**	.213*	-.352**	-.377**	-0.042	0.002	-0.035	.810**	-.391**	-.534**	-.470**	.581**	.472**
a3CV	0.028	0.076	0.083	-0.044	0.028	0.038	0.095	0.087	0.119	-0.087	0.095	0.107	0.257	-0.075	-.312*	-0.123	0.249	0.257
a4u	.499**	-.213**	-.516**	-.310**	.518**	.498**	0.165	0.105	-.215*	-0.083	.208*	0.144	.352*	-.344*	-0.249	0.020	.296*	.472**
a4tke	-.185*	.239**	.278**	.153*	-0.067	-0.092	-0.158	.278**	.349**	0.077	0.053	0.018	-0.051	-0.067	-0.004	0.028	0.004	-0.079
a4dir	.506**	-.380**	-.480**	-.325**	.523**	.498**	0.127	-.185*	-0.094	-0.049	.188*	0.140	.660**	-.478**	-.589**	-.336*	.494**	.491**
a4CV	-.404**	.267**	.480**	.355**	-.371**	-.388**	-0.081	0.019	.232**	.220*	-0.034	-0.037	-0.075	0.273	0.020	-0.091	0.043	-0.136
a4ntt	.569**	0.001	-.385**	-.314**	.555**	.476**	.407**	.322**	-0.105	-.183*	.356**	.223*	0.150	.364*	0.103	0.158	.364*	0.187
a4AP	.483**	0.092	-.244**	-.321**	.428**	.393**	.499**	.299**	-0.097	-.229*	.378**	.341**	-0.084	.412**	.348*	0.044	0.068	-0.166
a5u	.468**	-0.145	-.439**	-.255**	.523**	.541**	0.138	.209*	-0.083	-0.001	.240**	.259**	0.194	-0.217	-0.217	0.115	0.170	0.266
a5tke	0.010	0.038	0.060	0.094	0.082	0.039	-0.016	0.168	0.163	0.142	0.114	0.040	0.194	-0.281	-0.138	0.051	0.186	0.145
a5dir	.469**	-.334**	-.474**	-.338**	.464**	.441**	0.106	-0.125	-0.141	-0.118	0.118	0.074	.708**	-.462**	-.526**	-.320*	.526**	.509**
a5CV	-.328**	.195**	.318**	.268**	-.271**	-.305**	-0.059	-0.043	0.055	0.069	0.044	-0.026	-0.209	0.154	0.028	0.091	-0.186	-0.136
a5ntt	0.105	.248**	-0.063	0.001	.171*	0.123	0.057	.438**	0.042	0.057	.179*	0.078	0.036	0.083	0.004	0.123	0.012	0.056
a5AP	0.095	.321**	-0.018	0.016	0.142	0.111	0.092	.487**	0.061	0.015	0.161	0.088	-0.040	0.178	0.081	0.202	0.057	0.105
a6u	.309**	-0.003	-.235**	-0.112	.368**	.330**	0.077	.274**	0.057	0.097	.176*	0.115	-.296*	0.146	0.289	0.273	-0.178	-.332*
a6tke	-0.109	0.112	.153*	.154*	-0.076	-0.058	-0.066	0.123	0.160	0.137	-0.029	-0.004	-0.265	0.115	0.194	0.194	-0.146	-0.089
a6dir	.428**	-.350**	-.542**	-.253**	.442**	.430**	0.102	-0.162	-.325**	0.007	0.148	0.116	.589**	-.565**	-.518**	-.328*	.407**	.444**
a6CV	-.382**	.214**	.295**	.298**	-.393**	-.401**	-0.121	0.026	0.001	0.168	-0.157	-0.161	-0.194	0.091	0.043	0.028	-0.170	-0.201
a6ntt	.341**	.158*	-0.144	-0.137	.378**	.398**	.234**	.414**	0.120	-0.043	.279**	.297**	-0.099	.328*	0.154	0.217	0.130	0.182
a6AP	0.124	.254**	0.062	-0.054	.219*	.213*	0.100	.381**	.225*	-0.049	.263*	.217*	-0.336	0.278	0.336	0.316	-0.278	0.057
a7u	.770**	-.302**	-.596**	-.406**	.601**	.549**	.589**	-0.050	-.325**	-.190*	.303**	.224*	.866**	-.399**	-.510**	-.431**	.652**	.528**
a7tke	-.201**	.730**	.422**	.189*	-.154*	-.199**	0.137	.658**	.252**	-0.070	.192*	0.119	-.360*	.794**	.447**	.431**	-0.130	-0.210
a7dir	.151*	-.295**	0.034	-.176*	.151*	.159*	-0.026	-.193*	.330**	-0.091	0.004	0.011	.518**	-.542**	-.320*	-0.209	.352*	.360*
a7CV	-.350**	.282**	.355**	.541**	-.318**	-.323**	-0.033	0.012	0.022	.379**	0.011	0.007	-0.281	.478**	.431**	.589**	-0.194	-0.229
a7ntt	.520**	0.013	-.382**	-.273**	.544**	.537**	.249**	.456**	-0.007	-0.036	.276**	.254**	.296*	-0.036	-0.162	-0.036	.399**	.453**
a7AP	.557**	-0.033	-.339**	-.280**	.571**	.607**	.371**	.310**	0.004	-0.071	.371**	.429**	0.249	0.045	-0.020	-0.045	.429**	.473**
a8u	.757**	-.210**	-.591**	-.344**	.550**	.540**	.573**	0.106	-.326**	-0.093	.200*	.198*	.834**	-.304*	-.447**	-.304*	.731**	.631**
a8tke	-.236**	.552**	.420**	.207**	-.208**	-.212**	0.081	.425**	.238**	-0.067	0.106	0.116	-0.091	.462**	0.225	.368*	0.107	-0.005
a8dir	.242**	-.295**	-0.055	-.247**	.237**	.200**	0.042	-.189*	.243**	-0.102	0.056	-0.002	.605**	-.439**	-0.265	-.375*	.470**	.388*
a8CV	-.497**	.435**	.573**	.281**	-.414**	-.435**	-0.146	.263**	.291**	-0.047	-0.017	-0.042	-.494**	.534**	.534**	.470**	-.296*	-.397*
a8ntt	.717**	-0.096	-.455**	-.386**	.645**	.559**	.574**	.239**	-0.152	-.216*	.425**	.287**	.542**	-0.059	-0.217	-0.217	.676**	.491**
a8AP	.666**	-0.028	-.369**	-.354**	.575**	.540**	.600**	.267**	-0.099	-.261**	.400**	.349**	0.197	0.181	0.076	0.076	.462**	.385*
a9u	.530**	-.185*	-.497**	-.269**	.538**	.547**	.199*	.178*	-0.125	0.030	.232**	.231**	.431**	-.423**	-.581**	-0.138	.328*	.444**
a9tke	0.130	-0.022	-0.086	0.012	.176*	.151*	-0.072	0.152	0.168	0.152	0.026	-0.026	0.209	-0.233	-.312*	0.020	0.123	0.145
a9dir	-.418**	.299**	.620**	.259**	-.347**	-.345**	-0.089	0.063	.425**	-0.017	0.009	0.053	-0.059	0.241	.399**	0.194	0.154	-0.070
a9CV	-.262**	.166*	.342**	.185*	-.267**	-.302**	-0.048	0.021	.230**	0.078	-0.057	-0.094	0.059	0.043	-0.257	-0.146	0.051	-0.107
a9ntt	.468**	-0.105	-.191*	-.356**	.543**	.475**	.182*	.193*	.279**	-.228*	.318**	.232*	.721**	-0.253	-.333*	-0.222	.729**	.450**
a9AP	.524**	-0.116	-.230**	-.372**	.592**	.517**	.225*	.217*	.271**	-.224*	.346**	.239*	.743**	-0.248	-.343*	-0.224	.790**	.533**
a10u		-.197**	-.449**	-.406**	.658**	.635**		0.136	-0.069	-.212*	.404**	.385**		-.360*	-.391**	-.312*	.739**	.565**
a10tke	-.197**		.407**	.229**	-0.137	-.215**	0.136		.230**	-0.025	.218*	0.076	-.360*		.478**	.399**	-0.130	-0.173
a10dir	-.449**	.407**		.291**	-.367**	-.391**	-0.069	.230**		-0.024	0.065	0.027	-.391**	.478**		.462**	-0.257	-0.276
a10CV	-.406**	.229**	.291**		-.317**	-.354**	-.212*	-0.025	-0.024		-0.065	-0.150	-.312*	.399**	.462**		-0.194	-0.070
a10ntt	.658**	-0.137	-.367**	-.317**		.665**	.404**	.218*	0.065	-0.065		.441**	.739**	-0.130	-0.257	-0.194		.556**
a10AP	.635**	-.215**	-.391**	-.354**	.665**		.385**	0.076	0.027	-0.150	.441**		.565**	-0.173	-0.276	-0.070	.556**	
a11u	.724**	-.157*	-.488**	-.368**	.602**	.578**	.502**	.203*	-0.132	-0.136	.293**	.271**	.881**	-0.289	-.447**	-.320*	.763**	.631**
a11tke	-.173*	.558**	.315**	.194**	-0.071	-0.110	0.070	.502**	.208*	0.003	.228**	0.144	-.328*	.462**	0.194	0.241	-0.083	-0.042
a11dir	-.426**	.354**	.798**	.274**	-.364**	-.398**	-0.049	0.133	.677**	-0.031	0.053	0.017	-0.249	.368*	.636**	0.273	-0.146	-.341*
a11CV	-.199**	.252**	.172*	.465**	-.189*	-.172*	0.031	0.084	-0.085	.381**	0.027	0.027	-0.225	.296*	.391**	.470**	-0.091	0.136
a11ntt	.676**	-0.099	-.512**	-.378**	.654**	.568**	.433**	.321**	-0.167	-0.155	.392**	.263**	.700**	-0.265	-.455**	-.296*	.771**	.509**
a11AP	.649**	-0.084	-.486**	-.358**	.654**	.572**	.417**	.315**	-0.164	-0.137	.410**	.262**	.438**	-0.052	-0.165	-0.116	.631**	.584**
a12u	.596**	-0.076	-.457**	-.317**	.580**	.562**	.307**	.345**	-0.084	-0.050	.284**	.265**	.660**	-0.257	-.415**	-0.273	.652**	.491**
a12tke	.517**	-0.032	-.375**	-.281**	.541**	.540**	.302**	.349**	-0.044	-0.056	.349**	.334**	.328*	-0.178	-0.225	-0.130	0.289	0.294
a12dir	-.571**	.427**	.741**	.317**	-.397**	-.438**	-.242**	.273**	.583**	0.015	0.060	-0.032	-.708**	.494**	.605**	.462**	-.510**	-.435**
a12CV	.192**	-.180*	-.177*	-0.096	.149*	.179*	0.046	0.010	0.017	0.095	-0.016	0.020	0.249	-.368*	-.447**	-0.289	0.130	0.248
a12ntt	.555**	-0.112	-.576**	-.286**	.519**	.475**	.218*	.316**	-.259**	0.032	0.159	0.081	.618**	-.333*	-.602**	-.349*	.515**	.478**
a12AP	.572**	-0.111	-.583**	-.309**	.516**	.483**	.241**	.327**	-.267**	-0.007	0.147	0.092	.641**	-.371*	-.626**	-.363*	.538**	.476**

Table AP3.11: Location **A11**.

	FULL (84mins)						Run1: 15.49 to 16.49 inc. (61mins)						Run2: 16.50 to 17.12 inc. (23mins)					
	a11u	a11tke	a11dir	a11CV	a11ntt	a11AP	a11u	a11tke	a11dir	a11CV	a11ntt	a11AP	a11u	a11tke	a11dir	a11CV	a11ntt	a11AP
a1u	.399**	-0.045	-.229**	-.161*	.419**	.442**	.186*	0.152	0.079	-0.084	.216*	.241**	0.004	0.012	.360*	0.273	-0.004	0.189
a1tke	0.084	.320**	0.116	0.041	0.102	0.118	0.152	.391**	0.143	-0.028	.193*	.221*	0.162	0.170	0.265	0.209	0.154	0.173
a1dir	.456**	-.425**	-.621**	-.242**	.483**	.446**	0.027	-.387**	-.377**	-0.028	0.078	0.059	.652**	-.399**	-.478**	-.360*	.581**	0.245
a1CV	-0.057	.313**	.211**	0.108	-0.076	-0.076	0.115	.326**	0.123	0.022	0.084	0.093	0.107	0.130	0.178	0.075	0.115	0.044
a2u	.415**	0.110	-.184*	0.001	.385**	.400**	.430**	.243**	-0.064	0.077	.379**	.364**	-0.107	0.107	.407**	0.241	-0.099	0.116
a2tke	.181*	.251**	0.057	0.045	.243**	.268**	0.110	.383**	.250**	0.122	.246**	.294**	0.289	0.075	0.202	0.020	0.202	0.149
a2dir	.486**	-.399**	-.581**	-.227**	.464**	.436**	0.078	-.339**	-.296**	0.004	0.041	0.033	.700**	-.399**	-.494**	-.391**	.581**	0.285
a2CV	-0.078	.165*	.194**	0.100	-0.012	-0.016	-0.121	.188*	.285**	0.096	0.015	0.024	0.249	0.099	0.067	0.075	0.209	0.060
a2ntt	.202**	.351**	0.069	0.110	.213**	.249**	.354**	.383**	0.086	0.019	.385**	.417**	-0.130	.304*	.462**	.344*	-0.154	0.036
a2AP	-0.004	.454**	.272**	.176*	-0.066	-0.021	.372**	.351**	0.078	-0.052	.261**	.304**	-0.125	.382*	.357*	.333*	-0.108	0.159
a3u	.260**	.396**	-0.010	0.135	.188*	.227**	.507**	.386**	-0.052	0.054	.360**	.386**	-0.289	.557**	0.241	.391**	-0.138	0.149
a3tke	.253**	.375**	-0.024	-0.033	.287**	.296**	.345**	.489**	0.059	-0.047	.405**	.421**	0.281	.304*	-0.217	0.012	.368*	.333*
a3dir	.473**	-.423**	-.520**	-.232**	.473**	.440**	0.054	-.391**	-.215*	-0.020	0.067	0.049	.771**	-.328*	-.360*	-.336*	.621**	.301*
a3CV	0.031	.181*	0.071	-0.042	0.084	0.074	0.097	.258**	0.095	-0.079	.200*	.203*	.296*	0.067	-.344*	-0.099	.304*	0.173
a4u	.533**	-0.132	-.530**	-.235**	.574**	.555**	.222*	0.109	-.239**	-0.085	.300**	.267**	.360*	-0.059	-.296*	0.059	.304*	.333*
a4tke	-0.117	.285**	.268**	0.099	-0.119	-0.120	-0.040	.321**	.329**	0.011	-0.047	-0.033	-0.012	0.043	-0.036	0.130	-0.020	-0.036
a4dir	.487**	-.251**	-.460**	-.248**	.489**	.478**	0.094	-0.089	-0.074	-0.067	0.088	0.104	.636**	-0.241	-.494**	-0.217	.628**	.382*
a4CV	-.383**	.243**	.454**	.274**	-.435**	-.422**	-0.042	0.078	.181*	.191*	-0.146	-0.127	-0.020	0.257	0.067	-0.004	0.067	0.076
a4ntt	.556**	-0.030	-.379**	-0.141	.611**	.591**	.378**	.204*	-0.114	0.012	.471**	.428**	0.190	0.190	0.222	0.166	0.230	.298*
a4AP	.470**	0.066	-.257**	-0.123	.484**	.476**	.476**	.234**	-0.122	-0.020	.484**	.440**	-0.108	0.268	.300*	0.036	0.036	0.191
a5u	.503**	-0.104	-.480**	-0.130	.593**	.585**	.195*	0.154	-0.168	0.113	.366**	.355**	0.217	-0.043	-0.186	0.012	0.162	0.181
a5tke	0.039	0.059	0.063	0.092	0.065	0.066	0.034	0.138	0.163	.177*	0.087	0.098	0.186	-0.123	-0.107	-0.051	0.130	0.125
a5dir	.461**	-.220**	-.452**	-.265**	.439**	.428**	0.089	-0.059	-0.115	-0.133	0.050	0.068	.684**	-0.225	-.431**	-0.202	.597**	.349*
a5CV	-.330**	.164*	.294**	.149*	-.348**	-.317**	-0.066	-0.047	0.015	0.010	-0.094	-0.051	-0.154	.312*	-0.051	0.004	-0.130	-0.028
a5ntt	.203**	.262**	-0.111	0.039	.243**	.249**	.231**	.427**	-0.059	0.075	.312**	.342**	0.075	-0.004	0.075	0.052	0.020	-0.060
a5AP	.211**	.370**	-0.077	0.092	.216**	.250**	.304**	.496**	-0.052	0.090	.302**	.360**	-0.008	0.194	0.081	0.170	0.057	0.148
a6u	.343**	0.017	-.257**	-0.013	.433**	.428**	0.140	.235**	0.004	.204*	.296**	.279**	-0.289	0.099	.352*	0.154	-0.233	-0.141
a6tke	-0.124	0.079	.147*	.157*	-0.055	-0.047	-0.103	0.067	0.140	0.141	0.025	0.021	-0.225	0.130	0.273	0.186	-0.217	-0.036
a6dir	.391**	-.272**	-.535**	-.215**	.423**	.391**	0.025	-.181*	-.325**	-0.063	0.093	0.071	.581**	-0.202	-.423**	-0.130	.478**	0.237
a6CV	-.369**	0.138	.270**	.208**	-.341**	-.352**	-0.108	-0.050	-0.036	0.144	-0.054	-0.068	-0.138	0.059	-0.004	-0.107	-0.115	-0.149
a6ntt	.439**	.298**	-.184*	-0.022	.400**	.458**	.409**	.558**	0.046	0.071	.325**	.398**	0.004	.344*	0.091	0.162	0.043	.349*
a6AP	.200*	.294**	0.033	0.035	.227**	.256**	.234*	.367**	.205*	0.052	.278**	.309**	-0.336	0.297	-0.029	0.336	-0.297	-0.049
a7u	.639**	-.255**	-.531**	-.243**	.687**	.647**	.342**	-0.081	-.226**	-0.037	.457**	.424**	.842**	-.320*	-.352*	-.328*	.644**	.357*
a7tke	-.169*	.528**	.398**	.194**	-0.137	-0.099	.189*	.483**	.198*	0.011	.255**	.291**	-.304*	.415**	.447**	0.217	-0.265	-0.036
a7dir	0.078	-.189*	0.053	-.177*	0.054	0.069	-0.153	-0.062	.352**	-0.108	-.176*	-0.122	.478**	-.399**	-0.209	-0.202	0.281	0.125
a7CV	-.344**	.149*	.368**	.353**	-.348**	-.359**	-0.009	-0.054	0.057	.235**	-0.021	-0.061	-.352*	0.162	.368*	.312*	-0.265	-0.133
a7ntt	.645**	0.099	-.428**	-0.137	.654**	.681**	.474**	.486**	-0.096	0.067	.477**	.518**	.352*	0.107	-0.178	0.067	.407**	.542**
a7AP	.641**	0.084	-.372**	-0.099	.575**	.624**	.518**	.381**	-0.048	0.075	.384**	.436**	0.290	0.249	-0.151	0.192	.355*	.618**
a8u	.769**	-.186*	-.579**	-.146*	.661**	.641**	.581**	0.025	-.321**	0.126	.396**	.389**	.905**	-0.194	-.368*	-0.202	.755**	.526**
a8tke	-.166*	.581**	.379**	.182*	-.157*	-0.128	.212*	.541**	0.149	-0.047	.228**	.267**	-0.067	.399**	0.241	.312*	0.004	0.108
a8dir	0.099	-.314**	0.049	-.239**	0.133	0.143	-.214*	-.183*	.413**	-0.141	-0.127	-0.085	.549**	-.486**	-0.075	-0.225	.368*	0.189
a8CV	-.465**	.419**	.581**	.147*	-.392**	-.362**	-0.087	.366**	.304**	-0.152	0.056	0.089	-.486**	.344*	.502**	.336*	-.431**	-0.293
a8ntt	.585**	-0.127	-.432**	-.225**	.707**	.709**	.325**	0.079	-0.112	-0.058	.541**	.540**	.534**	-0.012	-0.233	-0.036	.684**	.647**
a8AP	.575**	-0.054	-.367**	-0.141	.648**	.665**	.418**	0.110	-0.095	-0.001	.547**	.533**	.301*	0.165	0.036	0.108	.374*	.600**
a9u	.538**	-0.128	-.542**	-0.126	.615**	.588**	.214*	0.141	-.227**	0.156	.355**	.331**	.439**	-0.154	-.470**	-0.115	.415**	0.269
a9tke	0.124	-0.017	-0.063	0.029	.181*	.153*	-0.090	0.108	.184*	.191*	0.029	0.006	0.249	-0.107	-0.123	-0.099	0.115	-0.052
a9dir	-.398**	.283**	.627**	.193**	-.460**	-.440**	-0.051	0.138	.443**	-0.050	-0.169	-0.157	-0.051	0.130	.383*	0.249	0.004	0.165
a9CV	-.324**	0.096	.332**	0.059	-.366**	-.355**	-.175*	-0.021	.184*	0.012	-.249**	-.222*	0.115	0.012	-0.036	-0.281	0.138	0.068
a9ntt	.420**	-0.075	-.174*	-.293**	.450**	.437**	0.098	0.177	.291**	-0.173	0.156	0.159	.729**	-0.277	-0.206	-0.269	.673**	.475**
a9AP	.492**	-0.037	-.226**	-.255**	.509**	.493**	0.168	.244**	.257**	-0.130	.199*	.191*	.767**	-0.208	-0.216	-0.208	.727**	.556**
a10u	.724**	-.173*	-.426**	-.199**	.676**	.649**	.502**	0.070	-0.049	0.031	.433**	.417**	.881**	-.328*	-0.249	-0.225	.700**	.438**
a10tke	-.157*	.558**	.354**	.252**	-0.099	-0.084	.203*	.502**	0.133	0.084	.321**	.315**	-0.289	.462**	.368*	.296*	-0.265	-0.052
a10dir	-.488**	.315**	.798**	.172*	-.512**	-.486**	-0.132	.208*	.677**	-0.085	-0.167	-0.164	-.447**	0.194	.636**	.391**	-.455**	-0.165
a10CV	-.368**	.194**	.274**	.465**	-.378**	-.358**	-0.136	0.003	-0.031	.381**	-0.155	-0.137	-.320*	0.241	0.273	.470**	-.296*	-0.116
a10ntt	.602**	-0.071	-.364**	-.189*	.654**	.654**	.293**	.228**	0.053	0.027	.392**	.410**	.763**	-0.083	-0.146	-0.091	.771**	.631**
a10AP	.578**	-0.110	-.398**	-.172*	.568**	.572**	.271**	0.144	0.017	0.027	.263**	.262**	.631**	-0.042	-.341*	0.136	.509**	.584**
a11u		-0.054	-.512**	-.160*	.693**	.681**		.280**	-.202*	0.096	.457**	.470**		-0.225	-.304*	-0.202	.739**	.502**
a11tke	-0.054		.231**	.263**	-0.094	-0.054	.280**		0.066	0.093	.199*	.251**	-0.225		0.004	.439**	-0.123	0.004
a11dir	-.512**	.231**		.155*	-.497**	-.471**	-.202*	0.066		-0.103	-0.157	-0.135	-.304*	0.004		0.233	-.360*	-0.197
a11CV	-.160*	.263**	.155*		-.203**	-.178*	0.096	0.093	-0.103		0.020	0.045	-0.202	.439**	0.233		-0.209	-0.052
a11ntt	.693**	-0.094	-.497**	-.203**		.876**	.457**	.199*	-0.157	0.020		.823**	.739**	-0.123	-.360*	-0.209		.639**
a11AP	.681**	-0.054	-.471**	-.178*	.876**		.470**	.251**	-0.135	0.045	.823**		.502**	0.004	-0.197	-0.052	.639**	
a12u	.755**	0.072	-.517**	-0.111	.668**	.667**	.596**	.481**	-.204*	0.162	.416**	.454**	.731**	-0.020	-.415**	-0.075	.787**	.534**
a12tke	.582**	0.039	-.443**	-0.131	.580**	.554**	.424**	.336**	-.179*	0.019	.405**	.364**	0.289	0.059	-0.225	0.115	.344*	.325*
a12dir	-.592**	.349**	.714**	.199**	-.510**	-.474**	-.281**	.260**	.552**	-0.055	-0.127	-0.106	-.700**	.320*	.510**	.407**	-.628**	-.301*
a12CV	.153*	-.175*	-.188*	-0.047	0.136	0.115	-0.033	-0.054	0.015	0.126	-0.063	-0.077	0.273	-0.225	-.526**	-0.233	0.233	0.076
a12ntt	.636**	-0.049	-.572**	-.165*	.638**	.633**	.359**	.296**	-.265**	0.106	.355**	.395**	.689**	-0.158	-.539**	-0.277	.681**	.394**
a12AP	.664**	-0.036	-.587**	-.179*	.659**	.652**	.405**	.314**	-.292**	0.080	.381**	.421**	.713**	-0.092	-.554**	-0.259	.753**	.441**

Table AP3.12: Location **A12**.

	FULL (84mins)						Run1: 15.49 to 16.49 inc. (61mins)						Run2: 16.50 to 17.12 inc. (23mins)					
	a12u	a12tke	a12dir	a12CV	a12ntt	a12AP	a12u	a12tke	a12dir	a12CV	a12ntt	a12AP	a12u	a12tke	a12dir	a12CV	a12ntt	a12AP
a1u	.410**	.359**	-.238**	0.081	.381**	.391**	.201*	0.141	0.105	0.016	0.156	0.165	0.036	0.115	0.138	-.375*	-0.166	-0.100
a1tke	.154*	0.101	0.122	-0.035	0.026	0.034	.285**	.195*	.207*	-0.004	0.062	0.075	0.194	0.067	0.028	-0.123	0.055	0.084
a1dir	.376**	.252**	-.711**	.162*	.452**	.453**	-0.093	-.192*	-.482**	-0.046	0.002	-0.002	.494**	0.194	-.858**	.510**	.626**	.649**
a1CV	-0.011	-0.065	.213**	-0.068	-0.146	-0.144	.198*	0.109	0.169	-0.015	-0.041	-0.034	0.123	-0.099	-0.028	0.028	0.048	0.044
a2u	.411**	.380**	-.223**	-0.007	.345**	.357**	.427**	.361**	-0.104	-0.039	.330**	.358**	-0.107	0.067	.328*	-.328*	-0.277	-.323*
a2tke	.196**	.149*	0.063	0.002	.155*	.159*	0.161	0.127	.322**	-0.004	0.097	0.103	0.225	0.115	-0.083	-0.186	0.087	0.116
a2dir	.353**	.252**	-.698**	.190*	.437**	.435**	-0.141	-.201*	-.456**	0.015	-0.036	-0.037	.526**	0.241	-.858**	.431**	.681**	.633**
a2CV	-0.071	-0.096	.214**	-0.006	-0.065	-0.068	-0.104	-0.125	.355**	0.020	-0.081	-0.078	.328*	0.265	-0.107	-0.209	0.174	0.131
a2ntt	.263**	.275**	0.089	-.182*	.207**	.221**	.461**	.453**	0.154	-0.084	.388**	.418**	-0.115	-0.036	.399**	-.462**	-0.253	-0.275
a2AP	0.047	0.068	.273**	-.263**	-0.087	-0.072	.457**	.406**	0.102	-0.085	.242**	.281**	-0.100	-0.020	.374*	-.390*	-0.201	-0.263
a3u	.310**	.277**	0.018	-0.064	.177*	.200**	.573**	.462**	-0.011	0.067	.375**	.411**	-0.115	0.059	.478**	-.336*	-.333*	-0.275
a3tke	.293**	.303**	0.013	0.018	.219**	.235**	.393**	.373**	0.138	-0.049	.273**	.306**	.423**	.360*	-0.170	0.154	.333*	.323*
a3dir	.329**	.263**	-.717**	.229**	.440**	.444**	-.180*	-0.168	-.502**	0.098	-0.015	-0.006	.565**	0.249	-.834**	.360*	.665**	.641**
a3CV	0.030	0.076	0.103	-0.006	0.000	-0.005	0.080	0.103	0.156	-0.131	0.005	0.014	.360*	.407**	-.296*	.344*	.491**	.363*
a4u	.571**	.533**	-.482**	0.099	.579**	.604**	.301**	.339**	-0.139	-0.125	.295**	.335**	.296*	0.107	-0.265	0.217	0.277	.331*
a4tke	-0.025	-0.032	.346**	-.158*	-0.063	-0.065	0.113	0.042	.460**	-0.160	0.050	0.041	0.036	0.036	0.123	0.036	-0.032	0.028
a4dir	.431**	.361**	-.567**	.252**	.367**	.382**	-0.002	-0.014	-.236**	0.134	-0.160	-0.143	.636**	.368*	-.684**	.399**	.642**	.681**
a4CV	-.335**	-.377**	.476**	-0.071	-.478**	-.467**	0.022	-0.128	.214*	0.115	-.212*	-.197*	0.154	0.154	0.067	-0.130	0.048	0.108
a4ntt	.570**	.527**	-.372**	0.025	.556**	.562**	.404**	.410**	-0.063	-0.108	.382**	.405**	0.238	0.230	0.048	-0.269	0.131	0.032
a4AP	.469**	.476**	-.269**	-0.049	.432**	.453**	.465**	.455**	-0.113	-0.131	.414**	.449**	0.020	0.172	0.204	-0.276	-0.120	-0.125
a5u	.567**	.541**	-.399**	0.062	.575**	.587**	.319**	.360**	-0.011	-0.154	.302**	.322**	0.170	0.075	-0.123	-0.020	0.246	0.251
a5tke	0.074	0.050	0.082	-0.124	0.072	0.076	0.099	0.048	.187*	-.197*	0.091	0.093	0.091	0.075	-0.091	0.043	0.103	0.163
a5dir	.443**	.380**	-.526**	.235**	.350**	.370**	0.056	0.035	-.220*	0.103	-0.154	-0.122	.605**	0.289	-.636**	.399**	.618**	.626**
a5CV	-.290**	-.278**	.361**	-.228**	-.277**	-.276**	-0.011	-0.045	0.127	-0.167	0.030	0.035	-0.043	-0.075	0.107	-0.154	-0.008	-0.028
a5ntt	.262**	.262**	0.007	-0.130	.286**	.273**	.340**	.311**	0.158	-0.165	.350**	.353**	0.012	0.131	0.004	-0.163	0.215	0.028
a5AP	.298**	.279**	0.040	-0.142	.291**	.293**	.440**	.331**	0.157	-0.157	.417**	.441**	0.089	0.267	0.129	-0.226	0.158	0.049
a6u	.391**	.354**	-.168*	-0.034	.413**	.421**	.240**	.204*	.181*	-0.128	.279**	.280**	-0.273	-0.162	.399**	-.462**	-.356*	-0.267
a6tke	-0.085	-0.080	.207**	-.178*	-0.049	-0.056	-0.024	-0.038	.247**	-0.141	0.041	0.027	-0.273	-0.178	.320*	-0.225	-0.293	-0.267
a6dir	.406**	.377**	-.578**	.185*	.402**	.409**	0.040	0.066	-.386**	0.017	0.003	0.016	.549**	.312*	-.549**	.391**	.594**	.586**
a6CV	-.324**	-.305**	.336**	-0.111	-.338**	-.356**	-0.036	-0.037	0.060	0.035	-0.072	-0.095	-0.154	-0.217	0.091	-0.170	0.016	-0.020
a6ntt	.511**	.413**	-0.116	-0.033	.385**	.403**	.533**	.351**	.175*	-0.097	.293**	.328**	0.083	0.130	0.186	-0.186	0.055	0.012
a6AP	.254**	.242**	0.101	-0.051	.193*	.194*	.326**	.295**	.297**	-0.104	.220*	.224*	-0.297	-0.163	0.297	0.067	-0.279	-0.280
a7u	.517**	.442**	-.654**	0.131	.557**	.565**	0.163	0.160	-.377**	-0.085	.207*	.219*	.589**	0.273	-.826**	.352*	.657**	.649**
a7tke	-0.109	-0.064	.453**	-.187*	-.151*	-0.149	.290**	.295**	.316**	-0.004	.258**	.263**	-0.257	-0.162	.510**	-.352*	-.364*	-.363*
a7dir	0.005	-0.047	-0.043	.159*	-0.038	-0.038	-.256**	-.270**	.223*	0.067	-.370**	-.369**	0.273	0.067	-.526**	0.257	.372*	.339*
a7CV	-.358**	-.281**	.360**	-0.031	-.410**	-.414**	-0.050	-0.008	0.013	.215*	-0.122	-0.123	-0.289	-0.036	.510**	-0.225	-.364*	-.394**
a7ntt	.703**	.618**	-.352**	0.092	.663**	.679**	.562**	.454**	0.063	-0.071	.473**	.506**	.462**	.526**	-0.209	-0.028	.436**	.402**
a7AP	.658**	.591**	-.374**	0.116	.535**	.567**	.522**	.442**	-0.037	0.012	.314**	.356**	.437**	.355*	-0.143	-0.151	0.229	.333*
a8u	.663**	.543**	-.690**	.158*	.635**	.659**	.417**	.340**	-.463**	-0.019	.355**	.389**	.763**	.352*	-.700**	0.241	.705**	.761**
a8tke	-0.094	-0.099	.443**	-.179*	-.206**	-.198**	.321**	.217*	.280**	0.003	0.163	0.176	0.059	0.107	0.289	-.336*	-0.143	-0.100
a8dir	0.002	-0.060	-0.088	0.103	0.056	0.046	-.352**	-.388**	.232**	-0.058	-.285**	-.300**	.296*	0.107	-.534**	0.265	.349*	.323*
a8CV	-.391**	-.346**	.637**	-.239**	-.439**	-.436**	0.028	-0.008	.383**	-0.080	-0.009	-0.006	-.375*	-0.170	.692**	-.518**	-.531**	-.506**
a8ntt	.565**	.516**	-.489**	0.137	.589**	.601**	.286**	.312**	-0.170	-0.015	.343**	.364**	.660**	.439**	-.407**	0.091	.507**	.482**
a8AP	.553**	.497**	-.439**	0.080	.502**	.521**	.378**	.368**	-.192*	-0.019	.294**	.329**	.382*	0.197	-0.116	-0.141	0.241	0.223
a9u	.580**	.540**	-.483**	0.099	.601**	.613**	.302**	.338**	-0.103	-0.132	.308**	.324**	.423**	.296*	-.455**	0.265	.491**	.530**
a9tke	.174*	0.092	-0.046	-0.017	.193*	.191*	0.017	-0.062	.232**	-0.093	0.025	0.011	0.138	-0.036	-0.202	0.043	0.198	0.275
a9dir	-.398**	-.390**	.581**	-0.102	-.571**	-.572**	-0.062	-0.131	.368**	0.125	-.355**	-.357**	-0.036	-0.083	0.257	-0.225	-0.230	-0.195
a9CV	-.296**	-.268**	.330**	-0.044	-.296**	-.301**	-0.125	-0.108	.192*	0.084	-0.128	-0.141	0.115	0.020	-0.178	-0.107	0.230	0.251
a9ntt	.395**	.316**	-.207**	0.145	.334**	.329**	0.079	0.059	.299**	-0.016	-0.071	-0.081	.539**	0.111	-.602**	0.277	.575**	.567**
a9AP	.473**	.369**	-.272**	0.147	.376**	.375**	0.156	0.089	.243**	-0.009	-0.057	-0.062	.615**	0.176	-.615**	0.224	.572**	.579**
a10u	.596**	.517**	-.571**	.192**	.555**	.572**	.307**	.302**	-.242**	0.046	.218*	.241**	.660**	.328*	-.708**	0.249	.618**	.641**
a10tke	-0.076	-0.032	.427**	-.180*	-0.112	-0.111	.345**	.349**	.273**	0.010	.316**	.327**	-0.257	-0.178	.494**	-.368*	-.333*	-.371*
a10dir	-.457**	-.375**	.741**	-.177*	-.576**	-.583**	-0.084	-0.044	.583**	0.017	-.259**	-.267**	-.415**	-0.225	.605**	-.447**	-.602**	-.626**
a10CV	-.317**	-.281**	.317**	-0.096	-.286**	-.309**	-0.050	-0.056	0.015	0.095	0.032	-0.007	-0.273	-0.130	.462**	-0.289	-.349*	-.363*
a10ntt	.580**	.541**	-.397**	.149*	.519**	.516**	.284**	.349**	0.060	-0.016	0.159	0.147	.652**	0.289	-.510**	0.130	.515**	.538**
a10AP	.562**	.540**	-.438**	.179*	.475**	.483**	.265**	.334**	-0.032	0.020	0.081	0.092	.491**	0.294	-.435**	0.248	.478**	.476**
a11u	.755**	.582**	-.592**	.153*	.636**	.664**	.596**	.424**	-.281**	-0.033	.359**	.405**	.731**	0.289	-.700**	0.273	.689**	.713**
a11tke	0.072	0.039	.349**	-.175*	-0.049	-0.036	.481**	.336**	.260**	-0.054	.296**	.314**	-0.020	0.059	.320*	-0.225	-0.158	-0.092
a11dir	-.517**	-.443**	.714**	-.188*	-.572**	-.587**	-.204*	-.179*	.552**	0.015	-.265**	-.292**	-.415**	-0.225	.510**	-.526**	-.539**	-.554**
a11CV	-0.111	-0.131	.199**	-0.047	-.165*	-.179*	0.162	0.019	-0.055	0.126	0.106	0.080	-0.075	0.115	.407**	-0.233	-0.277	-0.259
a11ntt	.668**	.580**	-.510**	0.136	.638**	.659**	.416**	.405**	-0.127	-0.063	.355**	.381**	.787**	.344*	-.628**	0.233	.681**	.753**
a11AP	.667**	.554**	-.474**	0.115	.633**	.652**	.454**	.364**	-0.106	-0.077	.395**	.421**	.534**	.325*	-.301*	0.076	.394**	.441**
a12u		.635**	-.474**	.149*	.673**	.698**		.479**	-0.086	-0.033	.429**	.465**		.478**	-.589**	0.178	.673**	.729**
a12tke	.635**		-.372**	.156*	.544**	.564**	.479**		-0.028	0.016	.310**	.345**	.478**		-0.241	0.099	.356*	.371*
a12dir	-.474**	-.372**		-.204**	-.517**	-.537**	-0.086	-0.028		-0.042	-0.126	-0.158	-.589**	-0.241		-.415**	-.689**	-.713**
a12CV	.149*	.156*	-.204**		0.145	0.137	-0.033	0.016	-0.042		-0.064	-0.076	0.178	0.099	-.415**		.333*	0.291
a12ntt	.673**	.544**	-.517**	0.145		.947**	.429**	.310**	-0.126	-0.064		.936**	.673**	.356*	-.689**	.333*		.758**
a12AP	.698**	.564**	-.537**	0.137	.947**		.465**	.345**	-0.158	-0.076	.936**		.729**	.371*	-.713**	0.291	.758**	